

TWO TEST LEVEL 4 BRIDGE RAILING AND TRANSITION SYSTEMS FOR TRANSVERSE GLUE-LAMINATED TIMBER DECKS

Submitted by

Karla A. Polivka, M.S.M.E., E.I.T. ¹
Research Associate Engineer

Michael A. Ritter, P.E. ²
Project Leader

Michael D. Fowler, M.S.C.E., E.I.T. ¹
Former Graduate Research Assistant

Ronald K. Faller, Ph.D., P.E. ¹
Research Assistant Professor

Barry T. Rosson, Ph.D., P.E. ¹
Associate Professor

Eric A. Keller, B.S.M.E., E.I.T. ¹
Research Associate Engineer

MIDWEST ROADSIDE SAFETY FACILITY ¹

University of Nebraska-Lincoln
1901 "Y" Street, Building "C"
Lincoln, Nebraska 68588-0601
(402) 472-6864

U.S. DEPARTMENT OF AGRICULTURE ²

Forest Service
Forest Products Laboratory
Engineered Wood Products and Structures
One Gifford Pichot Dr.
Madison, Wisconsin 53705
(608) 231-9229

MwRSF Research Report No. TRP-03-71-01

January 30, 2002

Technical Report Documentation Page

1. Report No.	2.	3. Recipient's Accession No.	
4. Title and Subtitle Two Test Level 4 Bridge Railing and Transition Systems for Transverse Glue-Laminated Timber Decks		5. Report Date January 30, 2002	6.
7. Author(s) Polivka, K.A., Faller, R.K., Rosson, B.T., Ritter, M.A., Fowler, M.D., and Keller, E.A.		8. Performing Organization Report No. TRP-03-71-01	
9. Performing Organization Name and Address Midwest Roadside Safety Facility (MwRSF) University of Nebraska-Lincoln 1901 Y St., Bldg. C Lincoln, NE 68588-0601		10. Project/Task/Work Unit No.	11. Contract © or Grant (G) No. FP-95-RJVA-2630
12. Sponsoring Organization Name and Address U.S. Department of Agriculture Forest Service Forest Products Laboratory One Gifford Pinchot Drive Madison, Wisconsin 53705		13. Type of Report and Period Covered Draft Report 1995-2001	
14. Sponsoring Agency Code		15. Supplementary Notes Prepared in cooperation with U.S. Department of Transportation, Federal Highway Administration	
16. Abstract (Limit: 200 words) <p style="margin: 0;">Two bridge railing and approach guardrail transition systems for use on bridges with transverse glue-laminated timber decks were developed and crash tested for use on high volume or high speed roadways. The bridge railing and transition systems were subjected to full-scale crash tests in accordance with the Test Level 4 (TL-4) safety performance criteria presented in NCHRP Report No. 350, <i>Recommended Procedures for the Safety Performance Evaluation of Highway Features</i>. The first railing system was constructed with glulam timber components, whereas the second railing system was configured with steel hardware. Eight full-scale crash tests were performed, and the bridge railing and transition systems were acceptable according to current safety standards.</p>			
17. Document Analysis/Descriptors Highway Safety, Longitudinal Barrier, Bridge Railings, Approach Guardrail Transition		18. Availability Statement No restrictions. Document available from: National Technical Information Services, Springfield, Virginia 22161	
19. Security Class (this report) Unclassified	20. Security Class (this page) Unclassified	21. No. of Pages 493	22. Price

DISCLAIMER STATEMENT

The contents of this report reflect the views of the authors who are responsible for the facts and the accuracy of the data presented herein. The contents do not necessarily reflect the official views or policies of the Federal Highway Administration nor the United States Department of Agriculture, Forest Service, Forest Products Laboratory. This report does not constitute a standard, specification, or regulation.

ACKNOWLEDGMENTS

The authors wish to acknowledge several sources that made a contribution to the success of this research project: (1) John Foreman, Alamo Wood Products, Inc., Albert Lea, MN, for all your cooperation and supplying the glulam materials at a very competitive price; (2) Matthew Smith, Laminated Concepts Inc., Elmira, NY, for completing the bridge deck design and preparing standard plans; (3) MwRSF personnel for constructing the bridge structure and barrier systems as well as conducting the crash tests; (4) Daniel Mushett, Highway Timber Products Co. - a division of Cox Industries for donating wood guardrail posts and blockouts; and (5) the Office of Sponsored Programs and the Center for Infrastructure Research, University of Nebraska-Lincoln, Lincoln, NE for matching support.

A special thanks is also given to the following individuals who made a contribution to the completion of this research project.

Federal Highway Administration

Sheila R. Duwadi, P.E., Turner-Fairbank Highway Research Center

Midwest Roadside Safety Facility

D.L. Sicking, Ph.D., P.E., Professor and MwRSF Director
J.R. Rohde, Ph.D., P.E., Associate Professor
B.G. Pfeifer, Ph.D., P.E., Former Research Associate Engineer
J.C. Holloway, M.S.C.E., E.I.T., Research Associate Engineer
K.L. Krenk, B.S.M.A., Shop Manager
M.L. Hanau, Laboratory Mechanic I
Undergraduate and Graduate Assistants

Dunlap Photography

James Dunlap, President and Owner

TABLE OF CONTENTS

	Page
TECHNICAL REPORT DOCUMENTATION PAGE	i
DISCLAIMER STATEMENT	ii
ACKNOWLEDGMENTS	iii
TABLE OF CONTENTS	iv
List of Figures	ix
List of Tables	xviii
1 INTRODUCTION	1
1.1 Problem Statement	1
1.2 Objective	2
1.3 Scope	2
2 LITERATURE REVIEW	4
2.1 Bridge Railings for Timber Deck Bridges	4
3 TEST REQUIREMENTS AND EVALUATION CRITERIA	6
3.1 Test Requirements	6
3.2 Evaluation Criteria	7
4 TEST SITE PREPARATION	10
4.1 Bridge Construction	10
4.1.1 Test Pit	10
4.1.2 Bridge Substructure	10
4.1.3 Bridge Superstructure	18
5 TEST CONDITIONS	22
5.1 Test Facility	22
5.2 Vehicle Tow and Guidance System	22
5.3 Test Vehicle	22
5.3.1 Wood System	22
5.3.2 Steel System	23
5.3.3 Center-of-Mass Determination, Vehicle Targets, and Alignment	35
5.4 Data Acquisition Systems	49
5.4.1 Accelerometers	49
5.4.2 Rate Transducer	50
5.4.3 High-Speed Photography	50
5.4.4 Pressure Tape Switches	59
5.4.5 Bridge Railing Instrumentation	59

5.4.5.1 Strain Gauges	59
5.4.5.2 String Potentiometers	65
6 WOOD SYSTEM DEVELOPMENT	67
6.1 Background	67
6.2 Design Issues	67
7 WOOD SYSTEM DESIGN DETAILS	75
7.1 Wood Bridge Railing	75
7.2 Approach Guardrail Transition	83
8 COMPUTER SIMULATION	98
8.1 Introduction	98
8.2 BARRIER VII Results	98
8.2.1 Bridge Railing Results	98
8.2.2 Approach Guardrail Transition Results	99
9 CRASH TEST NO. 1 (WOOD SYSTEM - BRIDGE RAILING)	101
9.1 Test TRBR-1	101
9.2 Test Description	101
9.3 Bridge Rail Damage	102
9.4 Vehicle Damage	103
9.5 Occupant Risk Values	103
9.6 Discussion	104
9.7 Barrier Instrumentation Results	104
10 CRASH TEST NO. 2 (WOOD SYSTEM - BRIDGE RAILING)	119
10.1 Test TRBR-2	119
10.2 Test Description	119
10.3 Bridge Rail Damage	120
10.4 Vehicle Damage	120
10.5 Occupant Risk Values	121
10.6 Discussion	121
10.7 Barrier Instrumentation Results	122
11 CRASH TEST NO. 3 (WOOD SYSTEM - APPROACH GUARDRAIL TRANSITION)	136
11.1 Test TRBR-3	136
11.2 Test Description	136
11.3 Bridge Rail and Approach Guardrail Transition Damage	138
11.4 Vehicle Damage	139
11.5 Occupant Risk Values	140

11.6 Discussion	140
12 CRASH TEST NO. 4 (WOOD SYSTEM - APPROACH GUARDRAIL TRANSITION)	154
12.1 Test TRBR-4	154
12.2 Test Description	154
12.3 Bridge Rail and Approach Guardrail Transition Damage	156
12.4 Vehicle Damage	157
12.5 Occupant Risk Values	158
12.6 Discussion	158
13 SUMMARY AND CONCLUSIONS - WOOD SYSTEM	171
14 STEEL SYSTEM DEVELOPMENT	174
14.1 Background	174
14.2 Design Issues	175
15 STEEL SYSTEM DESIGN DETAILS	181
15.1 Steel Bridge Railing	181
15.2 Approach Guardrail Transition	192
16 COMPUTER SIMULATION	206
16.1 Introduction	206
16.2 BARRIER VII Results	206
16.2.1 Bridge Railing Results	206
16.2.2 Approach Guardrail Transition Results	207
17 CRASH TEST NO. 1 (STEEL SYSTEM - BRIDGE RAILING)	209
17.1 Test STTR-1	209
17.2 Test Description	209
17.3 Bridge Rail Damage	210
17.4 Vehicle Damage	211
17.5 Occupant Risk Values	212
17.6 Discussion	212
17.7 Barrier Instrumentation Results	213
18 CRASH TEST NO. 2 (STEEL SYSTEM - BRIDGE RAILING)	229
18.1 Test STTR-2	229
18.2 Test Description	229
18.3 Bridge Rail Damage	230
18.4 Vehicle Damage	231
18.5 Occupant Risk Values	232
18.6 Discussion	232
18.7 Barrier Instrumentation Results	233

19 CRASH TEST NO. 3 (STEEL SYSTEM - APPROACH GUARDRAIL TRANSITION)	247
19.1 Test STTR-3	247
19.2 Test Description	247
19.3 Bridge Rail and Approach Guardrail Terminal Damage	248
19.4 Vehicle Damage	250
19.5 Occupant Risk Values	251
19.6 Discussion	251
20 CRASH TEST NO. 4 (STEEL SYSTEM - APPROACH GUARDRAIL TRANSITION)	266
20.1 Test STTR-4	266
20.2 Test Description	266
20.3 Bridge Rail and Approach Guardrail Transition Damage	267
20.4 Vehicle Damage	269
20.5 Occupant Risk Values	269
20.6 Discussion	270
21 SUMMARY AND CONCLUSIONS - STEEL SYSTEM	284
22 RECOMMENDATIONS - STEEL SYSTEM	287
23 REFERENCES	288
24 APPENDICES	292
APPENDIX A - Strain Gauge Locations – Test STTR-1	293
APPENDIX B - Strain Gauge Locations – Test STTR-2	300
APPENDIX C - BARRIER VII Computer Models - Wood System	309
APPENDIX D - Typical BARRIER VII Input Data Files - Wood System	314
APPENDIX E - Accelerometer Data Analysis - Test TRBR-1	325
APPENDIX F - Strain Gauge Data Analysis - Test TRBR-1	332
APPENDIX G - String Potentiometer Data Analysis - Test TRBR-1	343
APPENDIX H - Accelerometer Data Analysis - Test TRBR-2	349
APPENDIX I - Rate Transducer Data Analysis - Test TRBR-2	356
APPENDIX J - Accelerometer Data Analysis - Test TRBR-3	358
APPENDIX K - Rate Transducer Data Analysis - Test TRBR-3	365
APPENDIX L - Accelerometer Data Analysis - Test TRBR-4	367
APPENDIX M - Rate Transducer Data Analysis - Test TRBR-4	374
APPENDIX N - BARRIER VII Computer Models - Steel System	376
APPENDIX O - Typical BARRIER VII Input Data Files - Steel System	379
APPENDIX P - Accelerometer Data Analysis - Test STTR-1	390
APPENDIX Q - Rate Transducer Data Analysis - Test STTR-1	397
APPENDIX R - Strain Gauge Data Analysis - Test STTR-1	399

APPENDIX S - Accelerometer Data Analysis - Test STTR-2	426
APPENDIX T - Rate Transducer Data Analysis - Test STTR-2	433
APPENDIX U - Strain Gauge Data Analysis - Test STTR-2	435
APPENDIX V - Accelerometer Data Analysis - Test STTR-3	476
APPENDIX W - Rate Transducer Data Analysis - Test STTR-3	483
APPENDIX X - Accelerometer Data Analysis - Test STTR-4	485
APPENDIX Y - Rate Transducer Data Analysis - Test STTR-4	492

List of Figures

	Page
1. Bridge Substructure Details - Profile View	11
2. Bridge Substructure Details - Plan and Elevation Views	12
3. Bridge Substructure Details - Abutment Supports	13
4. Bridge Substructure Details - Pier Supports	14
5. Bridge Substructure Construction	15
6. Bridge Substructure and Retaining Walls	17
7. Bridge Superstructure Construction	19
8. Bridge Superstructure Construction	20
9. Bridge Superstructure Construction	21
10. Test Vehicle, Test TRBR-1	24
11. Vehicle Dimensions, Test TRBR-1	25
12. Test Vehicle, Test TRBR-2	26
13. Vehicle Dimensions, Test TRBR-2	27
14. Test Vehicle, Test TRBR-3	28
15. Vehicle Dimensions, Test TRBR-3	29
16. Test Vehicle, Test TRBR-4	30
17. Vehicle Dimensions, Test TRBR-4	31
18. Test Vehicle, Test STTR-1	32
19. Vehicle Dimensions, Test STTR-1	33
20. Test Vehicle, Test STTR-2	34
21. Vehicle Dimensions, Test STTR-2	36
22. Test Vehicle, Test STTR-3	37
23. Vehicle Dimensions, Test STTR-3	38
24. Test Vehicle, Test STTR-4	39
25. Vehicle Dimensions, Test STTR-4	40
26. Vehicle Target Locations, Test TRBR-1	41
27. Vehicle Target Locations, Test TRBR-2	42
28. Vehicle Target Locations, Test TRBR-3	43
29. Vehicle Target Locations, Test TRBR-4	44
30. Vehicle Target Locations, Test STTR-1	45
31. Vehicle Target Locations, Test STTR-2	46
32. Vehicle Target Locations, Test STTR-3	47
33. Vehicle Target Locations, Test STTR-4	48
34. Location of High-Speed Cameras, Test TRBR-1	51
35. Location of High-Speed Cameras, Test TRBR-2	52
36. Location of High-Speed Cameras, Test TRBR-3	53
37. Location of High-Speed Cameras, Test TRBR-4	54
38. Location of High-Speed Cameras, Test STTR-1	55
39. Location of High-Speed Cameras, Test STTR-2	56
40. Location of High-Speed Cameras, Test STTR-3	57
41. Location of High-Speed Cameras, Test STTR-4	58

42. Strain Gauge and String Potentiometer Locations, Test TRBR-1	60
43. Strain Gauge and String Potentiometer Locations, Test TRBR-2	61
44. Strain Gauge Locations, Test STTR-1	63
45. Strain Gauge Locations, Test STTR-2	64
46. Wood Bridge Railing System	71
47. Wood Bridge Railing System	72
48. Wood Bridge Railing System - Bridge Posts	73
49. Wood Bridge Railing System - Rail Splices	74
50. Overall Layout of Wood Bridge Railing System	78
51. General Configuration of Wood Bridge Railing System	79
52. Bridge Railing Design Details - Wood System	80
53. Rail Splice Design Details - Wood System (Note - (a) upper rail and (b) lower curb rail) ..	81
54. Miscellaneous Design Details	82
55. Approach Guardrail Transition - Front View	87
56. Approach Guardrail Transition - Back View	88
57. Approach Guardrail Transition - Parallel View	89
58. Connection to Wood Bridge Railing System	90
59. Overall Layout of Approach Guardrail Transition System - Wood System	91
60. General Configuration of Approach Guardrail Transition System - Wood System	92
61. Transition Connection Details - Wood System	93
62. Transition Scupper Block, Curb Transition, and Curb Transition Block - Wood System ..	94
63. Curb Transition Splice Plate and Rail Transition Plate - Wood System	95
64. Curb Transition and Rail Transition Boring Details	96
65. Transition Post Configurations (6 views of posts embedded in soil)	97
66. Summary of Test Results and Sequential Photographs, Test TRBR-1	105
67. Additional Sequential Photographs, Test TRBR-1	106
68. Additional Sequential Photographs, Test TRBR-1	107
69. Documentary Photographs, Test TRBR-1	108
70. Documentary Photographs, Test TRBR-1	109
71. Documentary Photographs, Test TRBR-1	110
72. Impact Locations, Test TRBR-1	111
73. Final Vehicle Position, Test TRBR-1	112
74. Barrier Damage, Test TRBR-1	113
75. Typical Top of Post and Rail Damage, Test TRBR-1	114
76. Vehicle Damage, Test TRBR-1	115
77. Front and Rear Wheel Assembly Damage, Test TRBR-1	116
78. Damage to Truck Box Attachment Hardware, Test TRBR-1	117
79. Summary of Test Results and Sequential Photographs, Test TRBR-2	123
80. Additional Sequential Photographs, Test TRBR-2	124
81. Additional Sequential Photographs, Test TRBR-2	125
82. Documentary Photographs, Test TRBR-2	126
83. Documentary Photographs, Test TRBR-2	127
84. Documentary Photographs, Test TRBR-2	128
85. Impact Locations, Test TRBR-2	129

86. Final Vehicle Position, Test TRBR-2	130
87. Barrier Damage, Test TRBR-2	131
88. Steel Plate Deformations at Post No. 6, Test TRBR-2	132
89. Vehicle Damage, Test TRBR-2	133
90. Front and Rear Wheel Assembly Damage, Test TRBR-2	134
91. Occupant Compartment Deformations, Test TRBR-2	135
92. Summary of Test Results and Sequential Photographs, Test TRBR-3	141
93. Additional Sequential Photographs, Test TRBR-3	142
94. Additional Sequential Photographs, Test TRBR-3	143
95. Documentary Photographs, Test TRBR-3	144
96. Documentary Photographs, Test TRBR-3	145
97. Impact Locations, Test TRBR-3	146
98. Final Vehicle Position, Test TRBR-3	147
99. Barrier Damage, Test TRBR-3	148
100. Thrie Beam Rail Damage, Test TRBR-3	149
101. Permanent Set Deflections, Test TRBR-3	150
102. Vehicle Damage, Test TRBR-3	151
103. Front Wheel Assembly Damage, Test TRBR-3	152
104. Occupant Compartment Deformations, Test TRBR-3	153
105. Summary of Test Results and Sequential Photographs, Test TRBR-4	160
106. Additional Sequential Photographs, Test TRBR-4	161
107. Additional Sequential Photographs, Test TRBR-4	162
108. Documentary Photographs, Test TRBR-4	163
109. Documentary Photographs, Test TRBR-4	164
110. Impact Locations, Test TRBR-4	165
111. Final Vehicle Position, Test TRBR-4	166
112. Barrier Damage, Test TRBR-4	167
113. Permanent Set Deflections, Test TRBR-4	168
114. Vehicle Damage, Test TRBR-4	169
115. Vehicle Damage, Test TRBR-4	170
116. Steel Bridge Railing System	178
117. Steel Bridge Railing System	179
118. Steel Bridge Railing System - Bridge Posts	180
119. Overall Layout of Steel Bridge Railing System	183
120. General Configuration of Steel Bridge Railing System	184
121. Bridge Railing Design Details - Steel System	185
122. Tube Rail Connection and Tube Rail Splice Design Details	186
123. Upper Tube Rails	187
124. Rail Splice Tube and Mounting Angle Details	188
125. Top and Bottom Plate Assemblies	189
126. Bridge Post Assembly Details	190
127. Post Stiffener, Post Plate Washer, and Spacer Block Details	191
128. Approach Guardrail Transition - Front View	195
129. Approach Guardrail Transition - Back View	196

130. Approach Guardrail Transition - Parallel View	197
131. Connection to Steel Bridge Railing System	198
132. Overall Layout of Approach Guardrail Transition System - Steel System	199
133. General Configuration of Approach Guardrail Transition System - Steel System	200
134. Tube Rail Transition Details - Steel System	201
135. Tube Transition Rails and Transition Splice Tube Details - Steel System	202
136. Tube Rail Terminator Details - Steel System	203
137. Transition Post Nos. 1 through 5 Configurations	204
138. Transition Post Nos. 6 through 13 Configurations	205
139. Summary of Test Results and Sequential Photographs, Test STTR-1	214
140. Additional Sequential Photographs, Test STTR-1	215
141. Additional Sequential Photographs, Test STTR-1	216
142. Documentary Photographs, Test STTR-1	217
143. Documentary Photographs, Test STTR-1	218
144. Impact Locations, Test STTR-1	219
145. Final Vehicle Position, Test STTR-1	220
146. Barrier Damage, Test STTR-1	221
147. Post No. 6 Deformations, Test STTR-1	222
148. Permanent Set Deformations, Test STTR-1	223
149. Typical Post and Blockout Deformations, Test STTR-1	224
150. Vehicle Damage, Test STTR-1	225
151. Vehicle Damage, Test STTR-1	226
152. Occupant Compartment Deformations, Test STTR-1	227
153. Summary of Test Results and Sequential Photographs, Test STTR-2	234
154. Additional Sequential Photographs, Test STTR-2	235
155. Additional Sequential Photographs, Test STTR-2	236
156. Impact Locations, Test STTR-2	237
157. Final Vehicle Position, Test STTR-2	238
158. Barrier Damage, Test STTR-2	239
159. Post No. 6 Deformations, Test STTR-2	240
160. Permanent Set Deformations, Test STTR-2	241
161. Vehicle Damage, Test STTR-2	242
162. Truck Box and Frame Damage, Test STTR-2	243
163. Occupant Compartment Deformations, Test STTR-2	244
165. Summary of Test Results and Sequential Photographs, Test STTR-3	253
166. Additional Sequential Photographs, Test STTR-3	254
167. Additional Sequential Photographs, Test STTR-3	255
168. Documentary Photographs, Test STTR-3	256
169. Documentary Photographs, Test STTR-3	257
170. Impact Locations, Test STTR-3	258
171. Final Vehicle Position, Test STTR-3	259
172. Barrier Damage, Test STTR-3	260
173. Barrier Damage, Test STTR-3	261
174. Permanent Set Deformations, Test STTR-3	262

175. Vehicle Damage, Test STTR-3	263
176. Vehicle Damage, Test STTR-3	264
177. Occupant Compartment Deformations, Test STTR-3	265
178. Summary of Test Results and Sequential Photographs, Test STTR-4	271
179. Additional Sequential Photographs, Test STTR-4	272
180. Additional Sequential Photographs, Test STTR-4	273
181. Documentary Photographs, Test STTR-4	274
182. Documentary Photographs, Test STTR-4	275
183. Documentary Photographs, Test STTR-4	276
184. Impact Locations, Test STTR-4	277
185. Final Vehicle Position, Test STTR-4	278
186. Barrier Damage, Test STTR-4	279
187. Barrier Damage, Test STTR-4	280
188. Permanent Set Deformations, Test STTR-4	281
189. Vehicle Damage, Test STTR-4	282
190. Vehicle Damage, Test STTR-4	283
A-1. Strain Gauge Nos. 1 through 7 Locations, Test STTR-1	294
A-2. Strain Gauge No. 8 Location, Test STTR-1	295
A-3. Strain Gauge Nos. 9 and 10 Locations, Test STTR-1	296
A-4. Strain Gauge Nos. 11 through 17 Locations, Test STTR-1	297
A-5. Strain Gauge No. 18 Location, Test STTR-1	298
A-6. Strain Gauge Nos. 19 and 20 Locations, Test STTR-1	299
B-1. Strain Gauge Nos. 1 through 3 Locations, Test STTR-2	301
B-2. Strain Gauge No. 4 Location, Test STTR-2	302
B-3. Strain Gauge Nos. 5, 6, 9, and 11 through 14 Locations, Test STTR-2	303
B-4. Strain Gauge Nos. 7 and 8 Locations, Test STTR-2	304
B-5. Strain Gauge No. 10 Location, Test STTR-2	305
B-6. Strain Gauge Nos. 15 through 17 Locations, Test STTR-2	306
B-7. Strain Gauge No. 18 Location, Test STTR-2	307
B-8. Strain Gauge Nos. 19 and 20 Locations, Test STTR-2	308
C-1. Model of the Wood Bridge Railing System	310
C-2. Model of the Approach Guardrail System attached to the Wood Bridge Railing	311
C-3. Idealized Finite Element, 2 Dimensional Vehicle Model for the 2,000-kg Pickup Truck	312
C-4. Idealized Finite Element, 2 Dimensional Vehicle Model for the 8,000-kg Straight Truck	313
E-1. Graph of Longitudinal Deceleration, Test TRBR-1	326
E-2. Graph of Longitudinal Occupant Impact Velocity, Test TRBR-1	327
E-3. Graph of Longitudinal Occupant Displacement, Test TRBR-1	328
E-4. Graph of Lateral Deceleration, Test TRBR-1	329
E-5. Graph of Lateral Occupant Impact Velocity, Test TRBR-1	330
E-6. Graph of Lateral Occupant Displacement, Test TRBR-1	331
F-1. Graph of Post No. 3 Bolt Load, Test TRBR-1	333
F-2. Graph of Post No. 4 Bolt Load, Test TRBR-1	334

F-3. Graph of Post No. 5 Bolt Load, Test TRBR-1	335
F-4. Graph of Post No. 6 Bolt Load, Test TRBR-1	336
F-5. Graph of Post No. 7 Bolt Load, Test TRBR-1	337
F-6. Graph of Post No. 8 Bolt Load, Test TRBR-1	338
F-7. Graph of Traffic-Side Top Splice Plate at Post No. 6 Stress, Test TRBR-1	339
F-8. Graph of Back-Side Top Splice Plate at Post No. 6 Stress, Test TRBR-1	340
F-9. Graph of Back-Side Curb Rail Splice Plate at Midspan Between Post Nos. 5 and 6 Stress, Test TRBR-1	341
F-10. Graph of Back-Side Wood Rail at Midspan Between Post Nos. 5 and 6 Stress, Test TRBR-1	342
G-1. Graph of Deflection at Midspan of Timber Rail No. 1, Test TRBR-1	344
G-2. Graph of Deflection at $\frac{3}{4}$ -point of Timber Rail No. 1, Test TRBR-1	345
G-3. Graph of Deflection at $\frac{7}{8}$ -point of Timber Rail No. 1, Test TRBR-1	346
G-4. Graph of Deflection at Point Between Timber Rail Nos. 1 and 2, Test TRBR-1	347
G-5. Graph of Deflection at $\frac{1}{4}$ -point of Timber Rail No. 2, Test TRBR-1	348
H-1. Graph of Longitudinal Deceleration, Test TRBR-2	350
H-2. Graph of Longitudinal Occupant Impact Velocity, Test TRBR-2	351
H-3. Graph of Longitudinal Occupant Displacement, Test TRBR-2	352
H-4. Graph of Lateral Deceleration, Test TRBR-2	353
H-5. Graph of Lateral Occupant Impact Velocity, Test TRBR-2	354
H-6. Graph of Lateral Occupant Displacement, Test TRBR-2	355
I-1. Graph of Roll, Pitch, and Yaw Angular Displacements, Test TRBR-2	357
J-1. Graph of Longitudinal Deceleration, Test TRBR-3	359
J-2. Graph of Longitudinal Occupant Impact Velocity, Test TRBR-3	360
J-3. Graph of Longitudinal Occupant Displacement, Test TRBR-3	361
J-4. Graph of Lateral Deceleration, Test TRBR-3	362
J-5. Graph of Lateral Occupant Impact Velocity, Test TRBR-3	363
J-6. Graph of Lateral Occupant Displacement, Test TRBR-3	364
K-1. Graph of Roll, Pitch, and Yaw Angular Displacements, Test TRBR-3	366
L-1. Graph of Longitudinal Deceleration, Test TRBR-4	368
L-2. Graph of Longitudinal Occupant Impact Velocity, Test TRBR-4	369
L-3. Graph of Longitudinal Occupant Displacement, Test TRBR-4	370
L-4. Graph of Lateral Deceleration, Test TRBR-4	371
L-5. Graph of Lateral Occupant Impact Velocity, Test TRBR-4	372
L-6. Graph of Lateral Occupant Displacement, Test TRBR-4	373
M-1. Graph of Roll, Pitch, and Yaw Angular Displacements, Test TRBR-4	375
N-1. Model of the Steel Bridge Railing System	377
N-2. Model of the Approach Guardrail System attached to the Steel Bridge Railing	378
P-1. Graph of Longitudinal Deceleration, Test STTR-1	391
P-2. Graph of Longitudinal Occupant Impact Velocity, Test STTR-1	392
P-3. Graph of Longitudinal Occupant Displacement, Test STTR-1	393
P-4. Graph of Lateral Deceleration, Test STTR-1	394
P-5. Graph of Lateral Occupant Impact Velocity, Test STTR-1	395
P-6. Graph of Lateral Occupant Displacement, Test STTR-1	396

Q-1. Graph of Roll, Pitch, and Yaw Angular Displacements, Test STTR-1	398
R-1. Graph of Post No. 6 Upstream-Side Bolt Strain, Test STTR-1	401
R-2. Graph of Post No. 6 Upstream-Side Bolt Stress, Test STTR-1	402
R-3. Graph of Post No. 6 Downstream-Side Bolt Strain, Test STTR-1	403
R-4. Graph of Post No. 6 Downstream-Side Bolt Stress, Test STTR-1	404
R-5. Graph of Top Plate Post No. 6 - Downstream and Perpendicular to Rail - Strain, Test STTR-1	405
R-6. Graph of Top Plate Post No. 6 - Downstream and Perpendicular to Rail - Stress, Test STTR-1	406
R-7. Graph of Top Plate Post No. 6 - Downstream and Parallel to Rail - Strain, Test STTR-1	407
R-8. Graph of Top Plate Post No. 6 - Downstream and Parallel to Rail - Stress, Test STTR-1	408
R-9. Graph of Bottom Plate Post No. 6 - Middle and Perpendicular to Rail - Strain, Test STTR-1	409
R-10. Graph of Bottom Plate Post No. 6 - Middle and Perpendicular to Rail - Stress, Test STTR-1	410
R-11. Graph of Traffic-Side Flange Post No. 6 Strain, Test STTR-1	411
R-12. Graph of Back-Side Flange Post No. 6 Strain, Test STTR-1	412
R-13. Graph of Back-Side Flange Post No. 6 Stress, Test STTR-1	413
R-14. Graph of Post No. 7 Upstream-Side Bolt Strain, Test STTR-1	414
R-15. Graph of Post No. 7 Upstream-Side Bolt Stress, Test STTR-1	415
R-16. Graph of Post No. 7 Downstream-Side Bolt Strain, Test STTR-1	416
R-17. Graph of Post No. 7 Downstream-Side Bolt Stress, Test STTR-1	417
R-18. Graph of Top Plate Post No. 7 - Middle and Perpendicular to Rail - Strain, Test STTR-1	418
R-19. Graph of Top Plate Post No. 7 - Middle and Perpendicular to Rail - Stress, Test STTR-1	419
R-20. Graph of Bottom Plate Post No. 7 - Middle and Perpendicular to Rail - Strain, Test STTR-1	420
R-21. Graph of Bottom Plate Post No. 7 - Middle and Perpendicular to Rail - Stress, Test STTR-1	421
R-22. Graph of Traffic-Side Flange Post No. 7 Strain, Test STTR-1	422
R-23. Graph of Traffic-Side Flange Post No. 7 Stress, Test STTR-1	423
R-24. Graph of Back-Side Flange Post No. 7 Strain, Test STTR-1	424
R-25. Graph of Back-Side Flange Post No. 7 Stress, Test STTR-1	425
S-1. Graph of Longitudinal Deceleration, Test STTR-2	427
S-2. Graph of Longitudinal Occupant Impact Velocity, Test STTR-2	428
S-3. Graph of Longitudinal Occupant Displacement, Test STTR-2	429
S-4. Graph of Lateral Deceleration, Test STTR-2	430
S-5. Graph of Lateral Occupant Impact Velocity, Test STTR-2	431
S-6. Graph of Lateral Occupant Displacement, Test STTR-2	432
T-1. Graph of Roll, Pitch, and Yaw Angular Displacements, Test STTR-2	434
U-1. Graph of Post No. 5 Upstream-Side Bolt Strain, Test STTR-2	438

U-2. Graph of Post No. 5 Upstream-Side Bolt Stress, Test STTR-2	439
U-3. Graph of Post No. 5 Downstream-Side Bolt Strain, Test STTR-2	440
U-4. Graph of Post No. 5 Downstream-Side Bolt Stress, Test STTR-2	441
U-5. Graph of Top Plate Post No. 5 - Middle and Perpendicular to Rail - Strain, Test STTR-2	442
U-6. Graph of Top Plate Post No. 5 - Middle and Perpendicular to Rail - Stress, Test STTR-2	443
U-7. Graph of Bottom Plate Post No. 5 - Middle and Perpendicular to Rail - Strain, Test STTR-2	444
U-8. Graph of Bottom Plate Post No. 5 - Middle and Perpendicular to Rail - Stress, Test STTR-2	445
U-9. Graph of Post No. 6 Upstream-Side Bolt Strain, Test STTR-2	446
U-10. Graph of Post No. 6 Upstream-Side Bolt Stress, Test STTR-2	447
U-11. Graph of Post No. 6 Downstream-Side Bolt Strain, Test STTR-2	448
U-12. Graph of Post No. 6 Downstream-Side Bolt Stress, Test STTR-2	449
U-13. Graph of Traffic-Side Flange Post No. 6 Strain, Test STTR-2	450
U-14. Graph of Back-Side Flange Post No. 6 Strain, Test STTR-2	451
U-15. Graph of Back-Side Flange Post No. 6 Stress, Test STTR-2	452
U-16. Graph of Top Plate Post No. 6 - Middle and Perpendicular to Rail - Strain, Test STTR-2	453
U-17. Graph of Top Plate Post No. 6 - Middle and Perpendicular to Rail - Stress, Test STTR-2	454
U-18. Graph of Bottom Plate Post No. 6 - Middle and Perpendicular to Rail - Strain, Test STTR-2	455
U-19. Graph of Top Plate Post No. 6 - Upstream and Perpendicular to Rail - Strain, Test STTR-2	456
U-20. Graph of Top Plate Post No. 6 - Upstream and Perpendicular to Rail - Stress, Test STTR-2	457
U-21. Graph of Top Plate Post No. 6 - Downstream and Perpendicular to Rail - Strain, Test STTR-2	458
U-22. Graph of Top Plate Post No. 6 - Downstream and Perpendicular to Rail - Stress, Test STTR-2	459
U-23. Graph of Top Plate Post No. 6 - Middle Upstream and Perpendicular to Rail - Strain, Test STTR-2	460
U-24. Graph of Top Plate Post No. 6 - Middle Upstream and Perpendicular to Rail - Stress, Test STTR-2	461
U-25. Graph of Top Plate Post No. 6 - Middle Downstream and Perpendicular to Rail - Strain, Test STTR-2	462
U-26. Graph of Top Plate Post No. 6 - Middle Downstream and Perpendicular to Rail - Stress, Test STTR-2	463
U-27. Graph of Post No. 7 Upstream-Side Bolt Strain, Test STTR-2	464
U-28. Graph of Post No. 7 Upstream-Side Bolt Stress, Test STTR-2	465
U-29. Graph of Post No. 7 Downstream-Side Bolt Strain, Test STTR-2	466
U-30. Graph of Post No. 7 Downstream-Side Bolt Stress, Test STTR-2	467

U-31. Graph of Top Plate Post No. 7 - Middle and Perpendicular to Rail - Strain, Test STTR-2	468
U-32. Graph of Top Plate Post No. 7 - Middle and Perpendicular to Rail - Stress, Test STTR-2	469
U-33. Graph of Bottom Plate Post No. 7 - Middle and Perpendicular to Rail - Strain, Test STTR-2	470
U-34. Graph of Bottom Plate Post No. 7 - Middle and Perpendicular to Rail - Stress, Test STTR-2	471
U-35. Graph of Back-Side Steel Tube Rail at Midspan Between Post Nos. 6 and 7 Strain, Test STTR-2	472
U-36. Graph of Back-Side Steel Tube Rail at Midspan Between Post Nos. 6 and 7 Stress, Test STTR-2	473
U-37. Graph of Bottom-Side Steel Tube Rail at Midspan Between Post Nos. 6 and 7 Strain, Test STTR-2	474
U-38. Graph of Bottom-Side Steel Tube Rail at Midspan Between Post Nos. 6 and 7 Stress, Test STTR-2	475
V-1. Graph of Longitudinal Deceleration, Test STTR-3	477
V-2. Graph of Longitudinal Occupant Impact Velocity, Test STTR-3	478
V-3. Graph of Longitudinal Occupant Displacement, Test STTR-3	479
V-4. Graph of Lateral Deceleration, Test STTR-3	480
V-5. Graph of Lateral Occupant Impact Velocity, Test STTR-3	481
V-6. Graph of Lateral Occupant Displacement, Test STTR-3	482
W-1. Graph of Roll, Pitch, and Yaw Angular Displacements, Test STTR-3	484
X-1. Graph of Longitudinal Deceleration, Test STTR-4	486
X-2. Graph of Longitudinal Occupant Impact Velocity, Test STTR-4	487
X-3. Graph of Longitudinal Occupant Displacement, Test STTR-4	488
X-4. Graph of Lateral Deceleration, Test STTR-4	489
X-5. Graph of Lateral Occupant Impact Velocity, Test STTR-4	490
X-6. Graph of Lateral Occupant Displacement, Test STTR-4	491
Y-1. Graph of Roll, Pitch, and Yaw Angular Displacements, Test STTR-4	493

List of Tables

	Page
1. NCHRP Report No. 350 Test Levels, Crash Test Conditions, and Evaluation Criteria for Longitudinal Barriers	8
2. Relevant NCHRP Report No. 350 Evaluation Criteria	9
3. Strain Gauge and String Potentiometer Results, Test TRBR-1	118
4. NCHRP Report No. 350 TL-4 Evaluation Results - Wood System (Bridge Railing and Transition)	173
5. Strain Gauge Results, Test STTR-1	228
6. Strain Gauge Results, Test STTR-2	245
7. Strain Gauge Results, Test STTR-2 (continued)	246
8. NCHRP Report No. 350 TL-4 Evaluation Results - Steel System (Bridge Railing and Transition)	286

1 INTRODUCTION

1.1 Problem Statement

Over the past 30 years, numerous bridge railing systems have been developed and evaluated according to established vehicular crash testing standards. Most of the bridge railings previously crash tested have consisted of concrete, steel, and aluminum railings attached to concrete bridge decks. It is well known that a growing number of timber bridges with transverse and longitudinal timber bridge decks are being constructed throughout the country. Therefore, the demand for crashworthy railing systems has become more evident with the increasing use of timber decks located on secondary highways, county roads, and local roads. Over the past thirteen years, several crashworthy bridge railing systems have been developed for use on longitudinal timber decks. In addition, these railing systems were developed for multiple service levels, ranging from low-speed, low-volume roads to higher service level roadways. However, little research has been conducted to develop crashworthy bridge railing systems for transverse timber bridge decks, and those that have been developed are for use on low to medium service level roadways. For timber to be a viable and economical alternative in the construction of transverse timber decks, additional vehicular bridge railing systems must be developed and crash tested for timber decks located on higher service level roadways where none existed before.

In recognition of the need to develop bridge railing systems for this higher service level, the United States Department of Agriculture (USDA) Forest Service, Forest Product Laboratory (FPL), in cooperation with the Midwest Roadside Safety Facility (MwRSF) and the Federal Highway Administration (FHWA), undertook the task of developing two higher service level bridge railings and approach guardrail transitions.

1.2 Objective

The primary objective of this research project was to develop and evaluate two new bridge railings and approach guardrail transitions for use with transverse glue-laminated (glulam) timber deck bridges located on higher service level roadways. The bridge railing and transitions systems were developed to meet the Test Level 4 (TL-4) evaluation criteria described in the National Cooperative Highway Research Program (NCHRP) Report No. 350, *Recommended Procedures for the Safety Performance Evaluation of Highway Features* (1). The first bridge railing was a wood system constructed using an upper rail, a lower curb rail, scupper blocks, posts, and blockouts all manufactured from glulam timber. The second bridge railing was a steel system constructed using three beam rail, a structural tube rail, and wide-flange posts and blockouts.

The secondary objective of the research project was to determine the actual forces imparted to the key components of the bridge railing systems. A knowledge of these force levels would allow bridge researchers and designers to make minor modifications to the crash tested designs without additional full-scale crash testing and provide insight into the design of future systems.

1.3 Scope

The research objectives were accomplished by performing several tasks. First, a literature review was performed on existing higher performance level bridge railings, as well as bridge railings developed for timber deck bridges. Second, an analysis and design phase was performed on all structural members and connections. Third, computer simulation modeling was conducted using BARRIER VII to aid in the analysis and design of the bridge railing and approach guardrail transition systems. Fourth, static component testing was performed on selected bridge components that were instrumented and used to obtain calibration factors and static stiffness properties. Fourth,

a total of eight full-scale vehicle crash tests were performed using $\frac{3}{4}$ -ton pickup trucks and single-unit trucks - two crash tests on each bridge railing and transition. Finally, the test results were analyzed, evaluated, and documented. Conclusions and recommendations were then made that pertain to the safety performance of each bridge railing and transition system.

2 LITERATURE REVIEW

2.1 Bridge Railings for Timber Deck Bridges

Over the past eleven years, MwRSF and FPL engineers have designed and developed several bridge railings and transitions for use on longitudinal glulam timber deck bridges. Nine bridge railings have been developed for several design impact conditions, including American Association of State Highway and Transportation Officials (AASHTO) Performance Levels 1 and 2 (PL-1 and PL-2) (2), NCHRP Report No. 350 TL-1 and TL-4 (1), as well as for very low-speed, low-volume roadways (3-13). The bridge railing systems developed for timber decks include: (1) an AASHTO PL-1 Glulam Rail with Curb bridge railing (3-7); (2) an AASHTO PL-1 Glulam Rail without Curb bridge railing (3-7); (3) an AASHTO PL-1 Steel Thrie-Beam Rail bridge railing (3-7); (4) an AASHTO PL-2 Steel Thrie-Beam with top-mounted Channel Rail bridge railing (4-8); (5) a NCHRP Report No. 350 TL-4 Glulam Rail with Curb bridge railing (4-8); (6) a Low-Height Curb-Type Sawn Timber bridge railing for low-speed, low-volume roads (9-10); (7) a NCHRP Report No. 350 TL-1 low-cost Breakaway W-Beam bridge railing (9,11); (8) a NCHRP Report No. 350 TL-1 Curb-Type Glulam Rail bridge railing (9,12); and (9) a NCHRP Report No. 350 TL-1 Top-Mounted W-Beam bridge railing (9,13).

Two other research programs conducted in the United States provide information on the crashworthiness of bridge railings for use on timber deck bridges. The first program was performed at Southwest Research Institute (SwRI) in the late 1980's in which crash tests were conducted according to AASHTO PL-1 conditions on a glulam rail with a curb bridge railing system attached to a spike-laminated longitudinal timber bridge deck (14). In 1993, a second research project was conducted by the Constructed Facilities Center (CFC) at West Virginia University with crash testing

performed by the Texas Transportation Institute (TTI). Crash tests were performed according to AASHTO PL-1 conditions on three bridge railing systems and one transition system attached to a transverse glulam timber deck (15-18).

3 TEST REQUIREMENTS AND EVALUATION CRITERIA

3.1 Test Requirements

Longitudinal barriers, such as bridge railings and approach guardrail transitions, must satisfy the requirements provided in NCHRP Report No. 350 to be accepted for use on new construction projects or as a replacement for existing barrier designs not meeting current safety standards. The recently published NCHRP Report No. 350 provides for six test levels for evaluating longitudinal barriers, as shown in Table 1. Although this document does not contain objective criteria for the conditions under which each test level is to be used, safety hardware developed to meet the lower test levels are generally intended for use on lower service level roadways while higher test level hardware is intended for use on higher service level roadways.

According to TL-4 of NCHRP Report No. 350, longitudinal barriers must be subjected to three full-scale vehicle crash tests: (1) an 820-kg small car impacting at a speed of 100.0 km/hr and at an angle of 20 degrees; (2) a 2,000-kg pickup truck impacting at a speed of 100.0 km/hr and at an angle of 25 degrees; and (3) an 8,000-kg single-unit truck impacting at a speed of 80.0 km/hr and at an angle of 15 degrees.

For this research project, the two bridge railing and approach guardrail transition systems were crash tested using only the pickup truck and single-unit truck impact conditions. Although the small car test is used to evaluate the overall performance of the length-of-need section and occupant risk problems arising from snagging or overturing of the vehicle, it was deemed unnecessary for several reasons. First, during the design and development phase of both barrier systems, special attention was given to prevent geometric incompatibilities that would cause the small car tests to fail due to excessive snagging or overturning. Second, the structural adequacy of the higher service level

barrier systems is not a concern for the small car test due to the relatively minor impact severity when compared to the impact severity for the pickup truck and single-unit truck impact conditions. The impact severity for the pickup truck test is approximately 270% greater than that provided by the small car test. Fourth, a small car crash test was successfully conducted on a similar wood bridge railing system by SwRI (14). Finally, three beam barriers struck by small cars have been shown to meet safety performance standards and to be essentially rigid (19-21), with no significant potential for occupant risk problems arising from snagging or overturning. For these reasons, the 820-kg small car crash test was considered unnecessary for each bridge railing and approach guardrail transition system developed under this research project. The test conditions for the required test matrix are shown in Table 1.

3.2 Evaluation Criteria

Evaluation criteria for full-scale vehicle crash testing are based on three appraisal areas: (1) structural adequacy; (2) occupant risk; and (3) vehicle trajectory after collision. Criteria for structural adequacy are intended to evaluate the ability of the barrier to contain, redirect, or allow controlled vehicle penetration in a predictable manner. Occupant risk evaluates the degree of hazard to occupants in the impacting vehicle. Vehicle trajectory after collision is a measure of the potential for the post-impact trajectory of the vehicle to cause subsequent multi-vehicle accidents. It is also an indicator of the potential safety hazard for the occupants of the other vehicles or the occupants of the impacting vehicle when subjected to secondary collisions with other fixed objects. These three evaluation criteria are defined in Table 2. The full-scale vehicle crash tests were conducted and reported in accordance with the procedures provided in NCHRP Report No. 350.

Table 1. NCHRP Report No. 350 Test Levels, Crash Test Conditions, and Evaluation Criteria for Longitudinal Barriers

Test Level	Test Designation	Test Vehicle	Impact Conditions		Evaluation Criteria
			Speed (km/hr)	Angle (degrees)	
TL-1	1-10	Small Car	50	20	A,D,F,H,I,K,M
	1-11	Pickup Truck	50	25	A,D,F,K,L,M
TL-2	2-10	Small Car	70	20	A,D,F,H,I,K,M
	2-11	Pickup Truck	70	25	A,D,F,K,L,M
TL-3	3-10	Small Car	100	20	A,D,F,H,I,K,M
	3-11	Pickup Truck	100	25	A,D,F,K,L,M
TL-4	4-10	Small Car	100	20	A,D,F,H,I,K,M
	4-11	Pickup Truck	100	25	A,D,F,K,L,M
	4-12	Single-Unit Truck	80	15	A,D,G,K,M
TL-5	5-10	Small Car	100	20	A,D,F,H,I,K,M
	5-11	Pickup Truck	100	25	A,D,F,K,L,M
	5-12	Tractor/Van Trailer	80	15	A,D,G,K,M
TL-6	6-10	Small Car	100	20	A,D,F,H,I,K,M
	6-11	Pickup Truck	100	25	A,D,F,K,L,M
	6-12	Tractor/Tank Trailer	80	15	A,D,G,K,M

Table 2. Relevant NCHRP Report No. 350 Evaluation Criteria (1)

Structural Adequacy	A. Test article should contain and redirect the vehicle; the vehicle should not penetrate, underide, or override the installation although controlled lateral deflection of the test article is acceptable.
Occupant Risk	D. Detached elements, fragments or other debris from the test article should not penetrate or show potential for penetrating the occupant compartment, or present an undue hazard to other traffic, pedestrians, or personnel in a work zone. Deformations of, or intrusions into, the occupant compartment that could cause serious injuries should not be permitted.
	F. The vehicle should remain upright during and after collision although moderate roll, pitching and yawing are acceptable.
	G. It is preferable, although not essential, that the vehicle remain upright during and after collision.
	H. Longitudinal and lateral occupant impact velocities should fall below the preferred value of 9 m/s, or at least below the maximum allowable value of 12 m/s.
Vehicle Trajectory	I. Longitudinal and lateral occupant ridedown accelerations should fall below the preferred value of 15 G's, or at least below the maximum allowable value of 20 G's.
	K. After collision it is preferable that the vehicle's trajectory not intrude into adjacent traffic lanes.
	L. The occupant impact velocity in the longitudinal direction should not exceed 12 m/s and the occupant ridedown acceleration in the longitudinal direction should not exceed 20 G's.
	M. The exit angle from the test article preferably should be less than 60 percent of test impact angle, measured at time of vehicle loss of contact with test device.

4 TEST SITE PREPARATION

4.1 Bridge Construction

A full-size simulated timber bridge deck system was constructed at the MwRSF outdoor test site for use in the development of the two new bridge railing and approach guardrail transition systems. The full-size system was selected to ensure that the research results were representative of actual bridge site conditions. In the following sections, site details are provided that pertain to the construction of the test pit, bridge substructure, and bridge superstructure. It is noted that the bridge system described below was used for both the wood and steel bridge railing systems.

4.1.1 Test Pit

A test pit was constructed in the existing concrete tarmac by cutting out a rectangular shape slab of concrete, measuring 60.96-m long by 6.10-m wide. The 60.96-m length was required to accommodate the 36.58-m long bridge and a 22.86-m long bridge approach section and attached guardrail. The pit was then excavated to a depth of approximately 2.13-m to provide clearance for constructing the bridge substructure and to provide the necessary clearance to allow personnel to stand upright and work below the bridge deck. Following the soil excavation, retaining walls were constructed on three sides of the test pit to prevent erosion of the subgrade soils located below the concrete tarmac.

4.1.2 Bridge Substructure

After the soil was excavated from the test pit, four reinforced concrete bridge supports were constructed on the bottom of the test pit. Design details are shown in Figures 1 through 4. Photographs of the concrete support construction as well as the completed supports and retaining wall are shown in Figure 5. The supports were founded at the necessary elevations with respect to

11

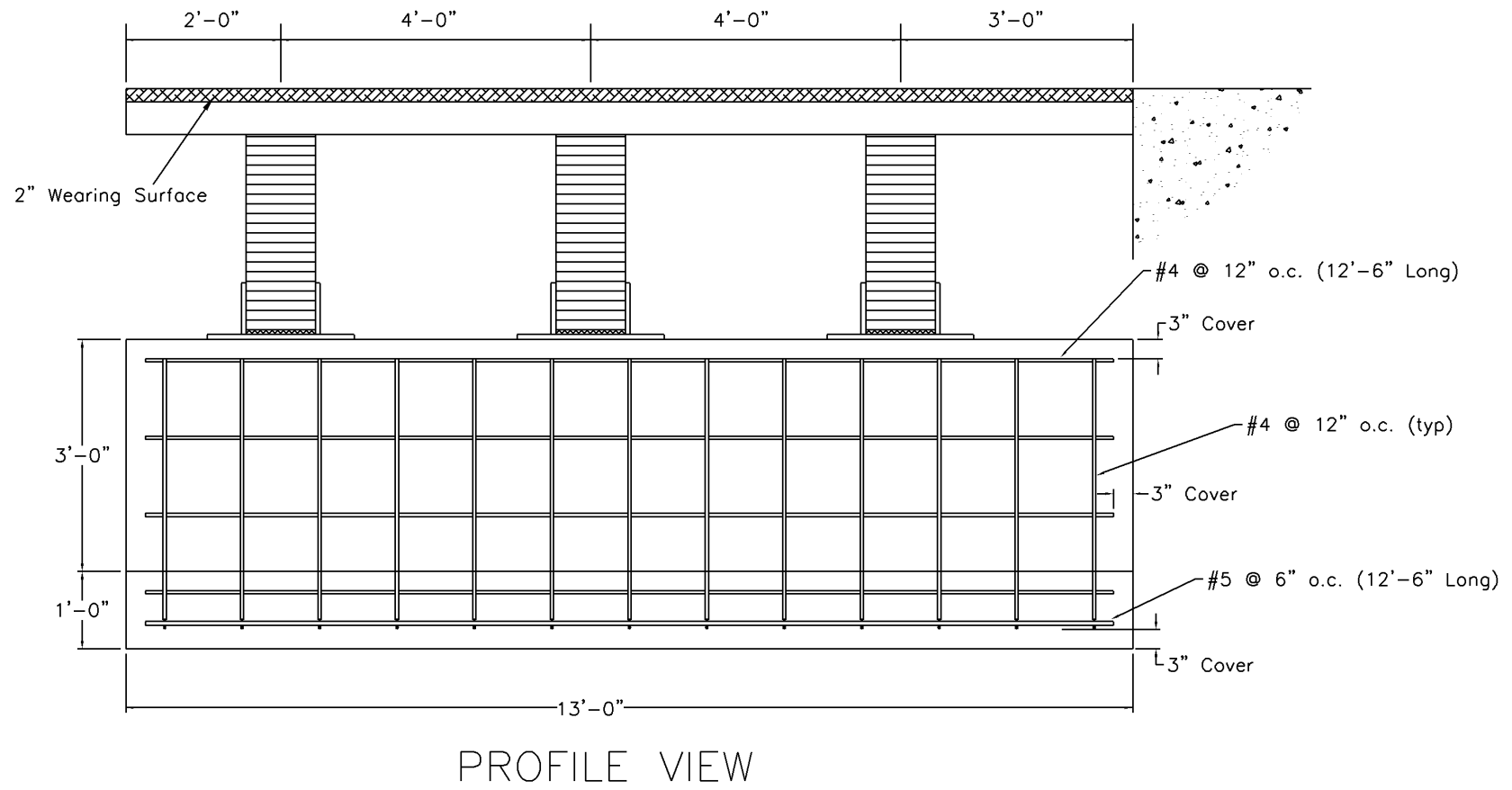
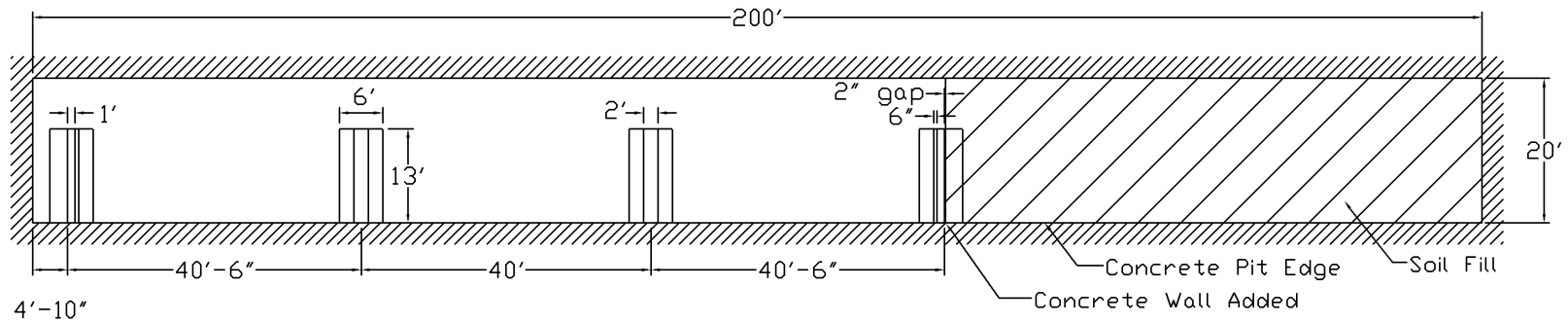
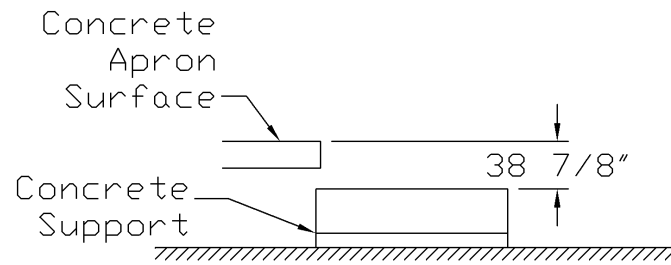


Figure 1. Bridge Substructure Details - Profile View



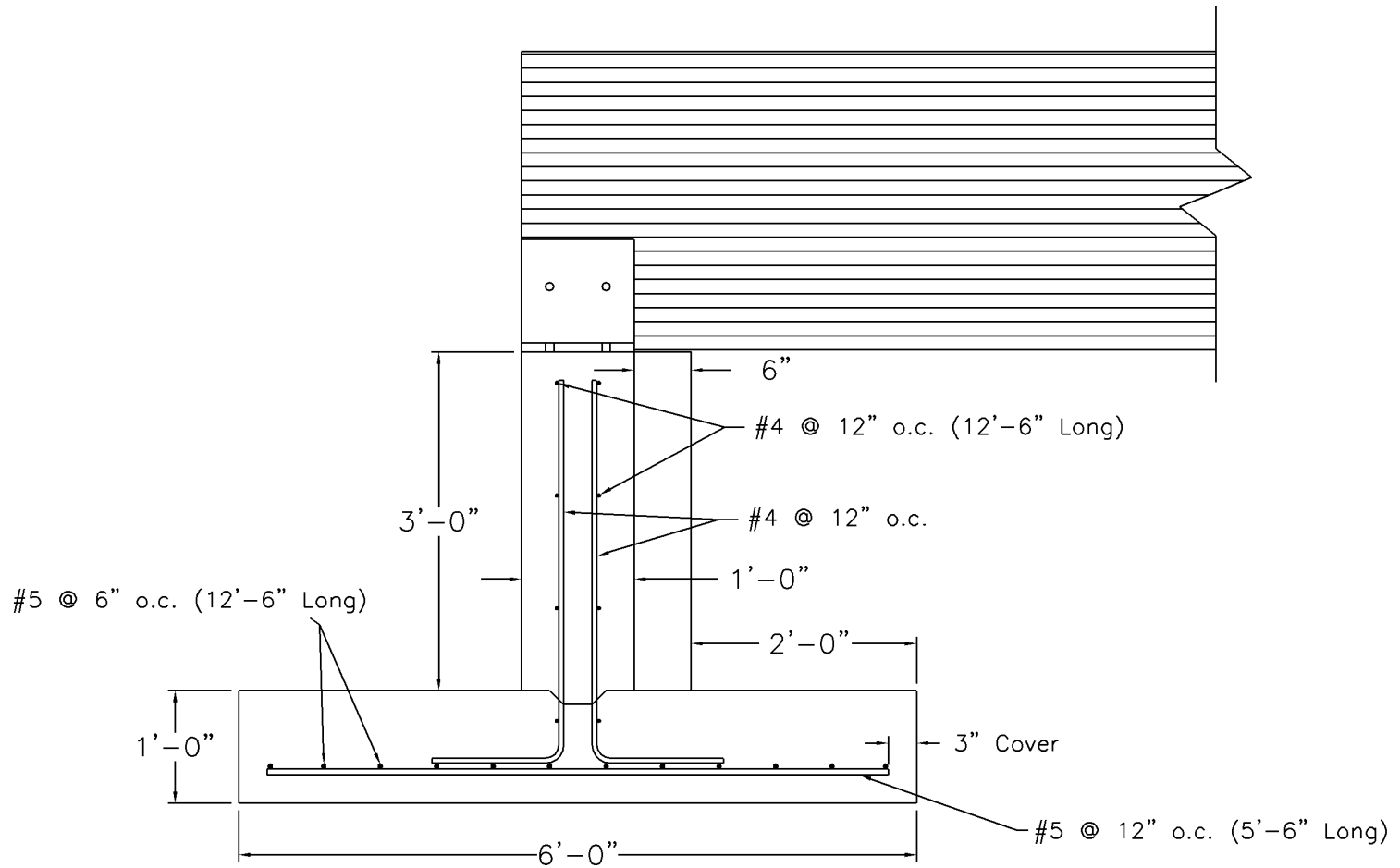
PLAN VIEW

12



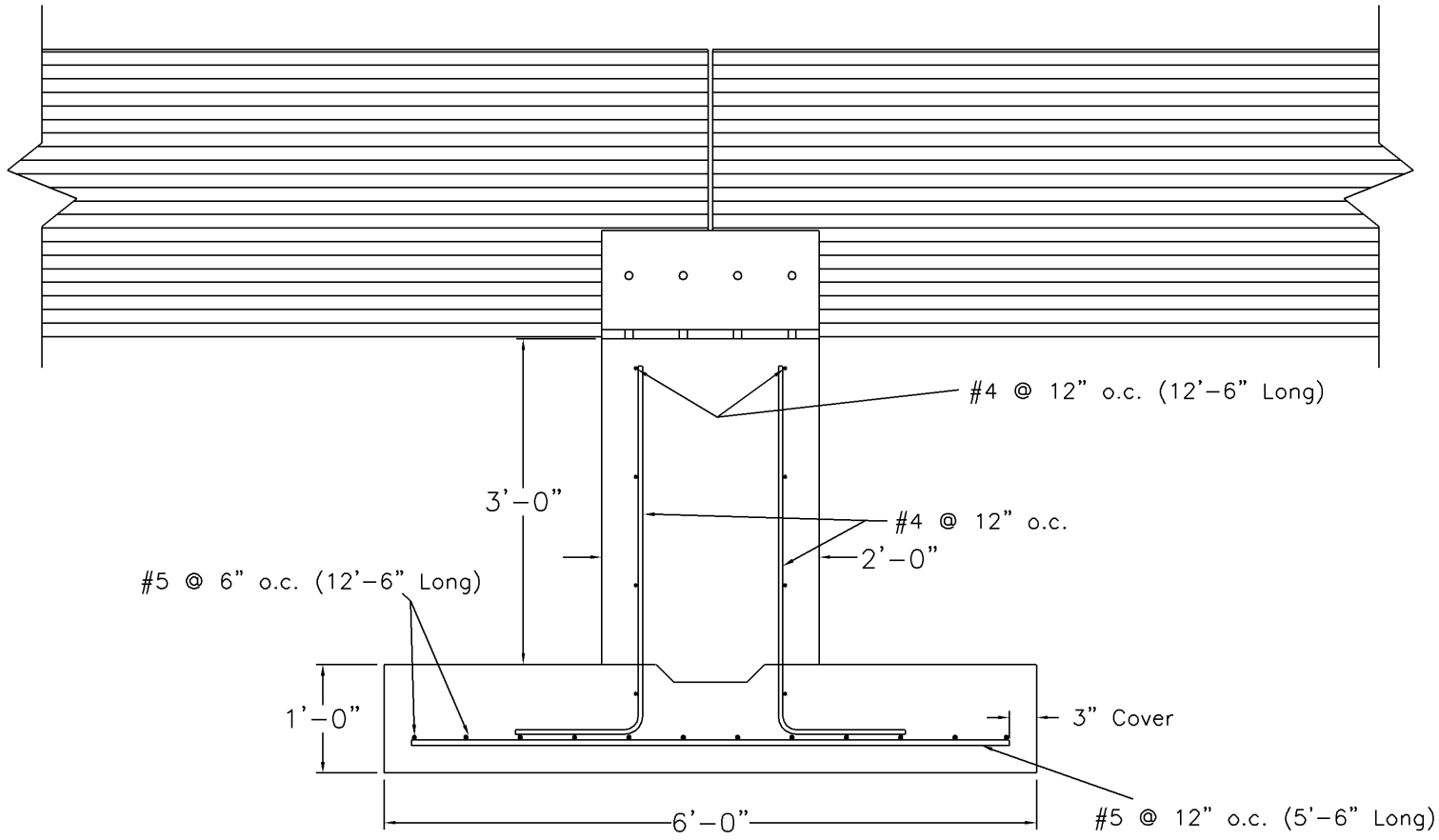
ELEVATION VIEW

Figure 2. Bridge Substructure Details - Plan and Elevation Views



ABUTMENT SUPPORTS

Figure 3. Bridge Substructure Details - Abutment Supports



PIER SUPPORTS

Figure 4. Bridge Substructure Details - Pier Supports

Figure 5. Bridge Substructure Construction

the concrete tarmac such that the surface of the bridge deck would be at an elevation approximately 51 mm below the grade of the concrete tarmac. This allowed for a wearing surface to be placed on the top of the bridge deck that would have a final grade at the same elevation as the concrete tarmac.

The inner two concrete bridge supports had a center-to-center spacing of 12.19 m whereas the outer two spacings were 12.12-m on center. The concrete bridge supports were constructed perpendicular to the roadway, providing a simple span between the concrete bridge supports, as shown in Figure 6. The top of the two exterior concrete bridge supports measured 457-mm wide by 3.96-m long by 914-mm high. The top of the two interior concrete bridge supports measured 610-mm wide by 3.96-m long by 914-mm high. The concrete bridge supports were attached to rectangular concrete spread footings measuring 305-mm thick by 1.83-m wide by 3.96-m long.

Three welded steel bearing assemblies were mounted to the top of each concrete bridge support to allow for the rigid attachment between the supports and bridge girders, as shown in Figure 6. The bearing assemblies were fabricated with 19-mm steel plate, as shown in Figures 1 through 4. Stainless steel threaded rods, measuring 19-mm diameter by 381-mm long, were embedded and epoxied into the top surface of the concrete bridge supports and used for the rigid attachment. Neoprene bearing pads, measuring 19-mm thick, were placed in the bearing assemblies to soften the contact interface between the assemblies and the girders. Originally, the bearing assemblies were fabricated to fit 273-mm wide girders. However, the bridge design was modified after the bearing assemblies were fabricated, including in a reduction in the girder width to 222-mm wide. Therefore, shims were used to adapt the bearing assemblies to fit 222-mm wide girders.

Figure 6. Bridge Substructure and Retaining Walls

4.1.3 Bridge Superstructure

Following the completion of the bridge substructure, the bridge superstructure was constructed. The superstructure consisted of nine glulam girders, twenty-four glulam diaphragms, and thirty transverse glulam deck panels. The bridge superstructure was constructed with three girders spanning between any two concrete bridge supports. For any two girders in a span, four glulam diaphragms were bolted between the girders to provide lateral stiffness to the bridge structure. Each glulam girder measured 222-mm wide by 768-mm deep by 12.17-m long, while the glulam diaphragms measured 130-mm wide by 629-mm deep by 997-mm long. The glulam panels were attached to the girders using standard aluminum deck brackets. Each glulam panel measured 130-mm thick by 1,216-mm wide by 3.96-m long. All glulam superstructure components were fabricated with Southern Yellow Pine and treated with pentachlorophenol in heavy oil to a minimum net retention of 9.61 kg/m³ as specified in American Wood-Preservers' Association (AWPA) Standard C14 (22). The girders were fabricated to meet Grade 24F-V3 while the deck panels, and diaphragms were fabricated from Combination No. 47 material.

One of the advantages of timber bridges is the ease of construction and the fact that a bridge can be erected in seasonal conditions that would not be conducive to poured concrete construction. These advantages became evident in this project as it took less than three days in sub-freezing temperatures with minimal equipment and a relatively small labor force to erect the bridge superstructure. The sequence of the superstructure construction is shown in Figures 7 through 9.

Figure 7. Bridge Superstructure Construction

Figure 8. Bridge Superstructure Construction

Figure 9. Bridge Superstructure Construction

5 TEST CONDITIONS

5.1 Test Facility

The testing facility is located at the Lincoln Air-Park on the northwest (NW) side of the Lincoln Municipal Airport and is approximately 8.0 km NW of the University of Nebraska-Lincoln.

5.2 Vehicle Tow and Guidance System

A reverse cable tow system with a 1:2 mechanical advantage was used to propel the test vehicle. The distance traveled and the speed of the tow vehicle were one-half that of the test vehicle. The test vehicle was released from the tow cable before impact with the barrier. A fifth wheel, built by Nucleus Corporation, was located on the tow vehicle and used in conjunction with a digital speedometer to increase the accuracy of the test vehicle impact speed.

A vehicle guidance system developed by Hinch ([23](#)) was used to steer the test vehicle. A guide-flag, attached to the left-front wheel and the guide cable, was sheared off before impact. The 9.5-mm diameter guide cable was tensioned to approximately 13.3 kN, and supported laterally and vertically every 30.48 m by hinged stanchions. The hinged stanchions stood upright while holding up the guide cable, but as the vehicle was towed down the line, the guide-flag struck and knocked each stanchion to the ground. For the pickup truck test, the vehicle guidance system was approximately 305-m long. For the single-unit truck tests, the vehicle guidance system was approximately 610-m long.

5.3 Test Vehicle

5.3.1 Wood System

Four full-scale vehicle crash tests were performed during the development of the wood bridge railing and approach guardrail transition system. Tests TRBR-1 and TRBR-2 were performed

on the bridge railing, while tests TRBR-3 and TRBR-4 were conducted on the approach guardrail transition.

For test TRBR-1, a 1986 Ford F-800 Series single-unit truck was used as the test vehicle. The test inertial and gross static weights were 8,000 kg. The test vehicle is shown in Figure 10, and vehicle dimensions are shown in Figure 11.

For test TRBR-2, a 1988 Ford F-250 ¾-ton pickup truck was used as the test vehicle. The test inertial and gross static weights were 1,993 kg. The test vehicle is shown in Figure 12, and vehicle dimensions are shown in Figure 13.

For test TRBR-3, a 1987 Ford F-250 ¾-ton pickup truck was used as the test vehicle. The test inertial and gross static weights were 2,029 kg. The test vehicle is shown in Figure 14, and vehicle dimensions are shown in Figure 15.

For test TRBR-4, a 1988 Ford F-700 Series single-unit truck was used as the test vehicle. The test inertial and gross static weights were 8,003 kg. The test vehicle is shown in Figure 16, and vehicle dimensions are shown in Figure 17.

5.3.2 Steel System

Four full-scale vehicle crash tests were performed during the development of the steel bridge railing and approach guardrail transition system. Tests STTR-1 and STTR-2 were performed on the bridge railing, while tests STTR-3 and STTR-4 were conducted on the approach guardrail transition.

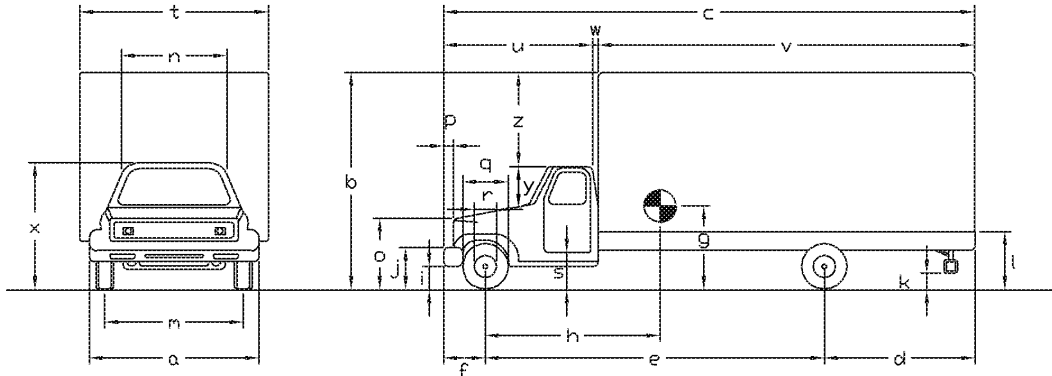
For test STTR-1, a 1990 Ford F-250 ¾-ton pickup truck was used as the test vehicle. The test inertial and gross static weights were 1,994 kg. The test vehicle is shown in Figure 18, and vehicle dimensions are shown in Figure 19.

For test STTR-2, a 1985 Ford F-800 Series single-unit truck was used as the test vehicle. The

test inertial and gross static weights were 8,067 kg. The test vehicle is shown in Figure 20, and

Figure 10. Test Vehicle, Test TRBR-1

Date: 3/11/97 Test Number: TRBR-1 Model: F-800
 Tire Sz FR: 9.00-20 Odometer: 1343246 Make: FORD
 Tire Sz RR: 9.00-20 V.I.N. #: 1FNDF8284GVA57624 Year: 1986



Vehicle Geometry (mm)

a> fr. bump. width 2362 j> fr. bump. top 813 s> bot. door height 864
 b> overall height 3759 k> rr. bump. bot. 572-597 t> overall width 2432
 c> overall length 8407 l> rr. frame top 1232-1264 u> cab length 2604
 d> rear overhang 3061 m> fr. track width 2032 v> box length 5652
 e> wheel base 4483 n> roof width 1537 w> gap width 152
 f> front overhang 902 o> hood height 1562 x> overall fr. height 2223
 g> C.G. height 1226 p> bump. extension 38 y> roof-hood dist. 527
 h> C.G. hor. dist. 2987 q> fr. tire width 1016 z> roof height dif. 1537
 i> fr. bump. bot. 508 r> fr. wheel width 572

wheel center height front 368
 wheel center height rear 505

Weights (kg)

	Curb	Test Inertial	Gross Static
W _{front axel}	<u>1946</u>	<u>2671</u>	<u>2671</u>
W _{rear axel}	<u>3338</u>	<u>5329</u>	<u>5329</u>
W _{TOTAL}	<u>5284</u>	<u>8000</u>	<u>8000</u>

Ballast _____

wheel well clearance (FR) 1181
 wheel well clearance (RR) 1118
 Engine Type V-8 gasoline
 Engine Size 429 cid
 Transmission Type:
 Automatic or (Manual)
 FWD or (RWD) or 4WD

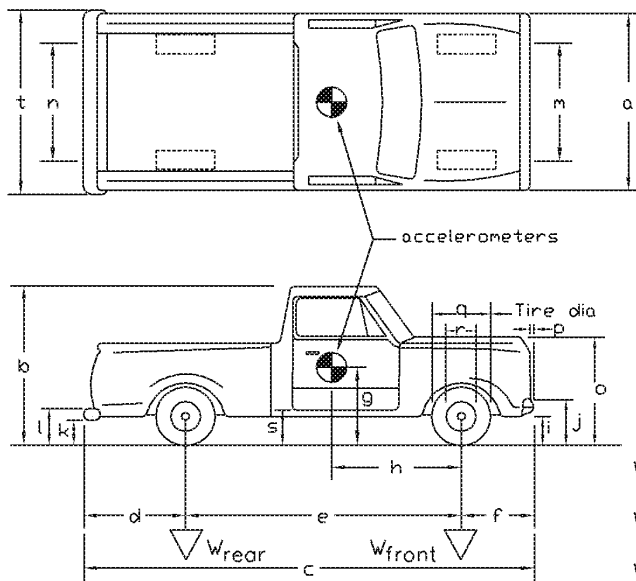
Note any damage prior to test: _____

Figure 11. Vehicle Dimensions, Test TRBR-1

Figure 12. Test Vehicle, Test TRBR-2

Date: 3/19/97 Test Number: TRBR-2 Model: F-250
 Make: FORD Vehicle I.D.#: 1FTHE25Y4JPA46516
 Tire Size: 235/85 R16 Year: 1988 Odometer: 81522

*(All Measurements Refer to Impacting Side)



Vehicle Geometry - mm

a 1930 b 1842
 c 5410 d 1270
 e 3378 f 762
 g 673 h 1521
 i 464 j 724
 k 559 l 737
 m 1664 n 1638
 o 1219 p 59
 q 787 r 445
 s 527 t 1937

Wheel Center Height Front 381
 Wheel Center Height Rear 387
 Wheel Well Clearance (FR) 864
 Wheel Well Clearance (RR) 946

Weights	Curb	Test Inertial	Gross Static
W_{front}	<u>1036</u>	<u>1096</u>	<u>1096</u>
W_{rear}	<u>786</u>	<u>897</u>	<u>897</u>
W_{total}	<u>1822</u>	<u>1993</u>	<u>1993</u>

Engine Type 6 cylinder

Engine Size 300 cid

Transmission Type:

(Automatic) or Manual

FWD or (RWD) or 4WD

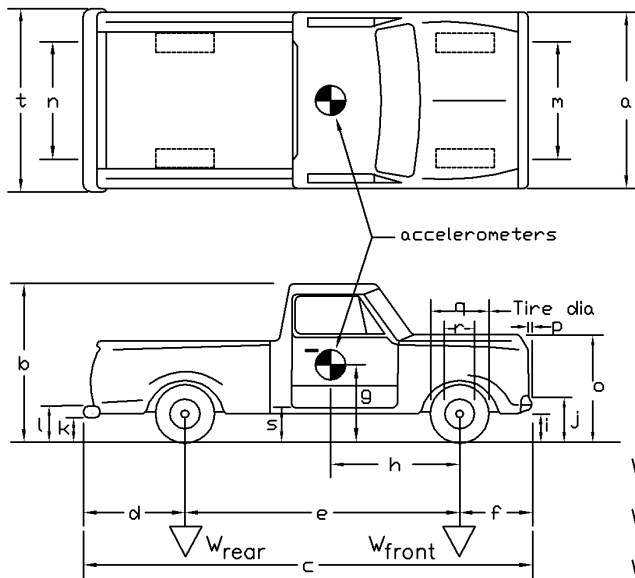
Note any damage prior to test: No driveshaft, bumper height off 1" across, twisted frame, cab repaired

Figure 13. Vehicle Dimensions, Test TRBR-2

Figure 14. Test Vehicle, Test TRBR-3

Date: 5/15/97 Test Number: TRBR-3 Model: F-250
 Make: Ford Vehicle I.D.#: 1FTHF25L5HKB03981
 Tire Size: 235/85 R16 Year: 1987 Odometer: 78278

*(All Measurements Refer to Impacting Side)



Vehicle Geometry - mm

a 1943 b 1905
 c 5410 d 1289
 e 3340 f 781
 g 713 h 1415
 i 489 j 743
 k 584 l 749
 m 1664 n 1638
 o 1232 p 70
 q 781 r 451
 s 527 t 1930

Wheel Center Height Front 375
 Wheel Center Height Rear 387
 Wheel Well Clearance (FR) 889
 Wheel Well Clearance (RR) 972

Weights - kg	Curb	Test Inertial	Gross Static
W_{front}	<u>1264</u>	<u>1179</u>	<u>1179</u>
W_{rear}	<u>1009</u>	<u>850</u>	<u>850</u>
W_{total}	<u>2273</u>	<u>2029</u>	<u>2029</u>

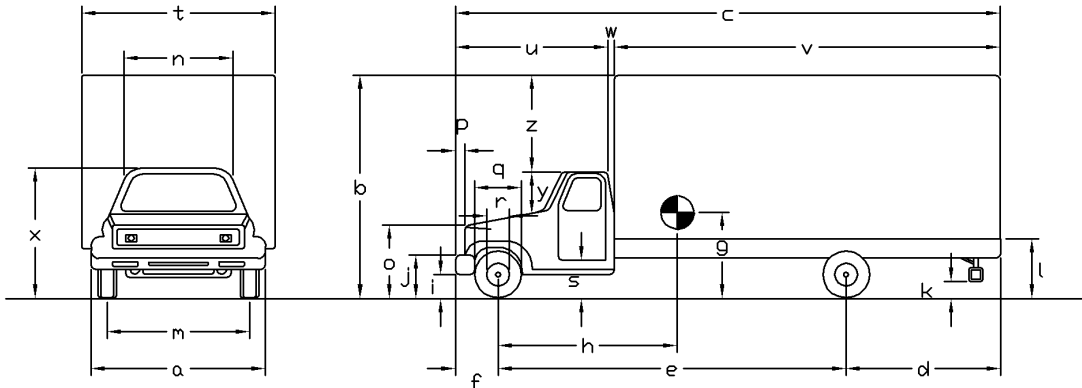
Engine Type V8
 Engine Size 460 cid
 Transmission Type:
 Automatic or (Manual)
 FWD or (RWD) or 4WD

Note any damage prior to test: centerline distance = 1321mm

Figure 15. Vehicle Dimensions, Test TRBR-3

Figure 16. Test Vehicle, Test TRBR-4

Date: 8/5/97 Test Number: TRBR-4 Model: F-700
 Tire Sz FR: 900 R20 Odometer: 109779 Make: FORD
 Tire Sz RR: 1000 R20 v.i.n. #: 1FDNF7077HVA51497 Year: 1987



Vehicle Geometry (mm)

a > fr. bump. width	<u>2400</u>	j > fr. bump. top	<u>845</u>	s > bot. door height	<u>940</u>
b > overall height	<u>3372</u>	k > rr. bump. bot.	<u>464</u>	t > overall width	<u>2413</u>
c > overall length	<u>7633</u>	l > rr. frame top	<u>1099</u>	u > cab length	<u>2724</u>
d > rear overhang	<u>2299</u>	m > fr. track width	<u>2007</u>	v > box length	<u>5093</u>
e > wheel base	<u>4458</u>	n > roof width	<u>1549</u>	w > gap width	<u>108</u>
f > front overhang	<u>1029</u>	o > hood height	<u>1581</u>	x > overall fr. height	<u>*****</u>
g > C.G. height	<u>1240</u>	p > bump. extension	<u>76</u>	y > roof-hood dist.	<u>502</u>
h > C.G. hor. dist.	<u>3049</u>	q > fr. tire width	<u>1003</u>	z > roof height dif.	<u>1099</u>
i > fr. bump. bot.	<u>533</u>	r > fr. wheel width	<u>572</u>	wheel center height front	<u>495</u>
				wheel center height rear	<u>514</u>

Weights (kg)

	Curb	Test Inertial	Gross Static	
W _{front axel}	<u>1943</u>	<u>2529</u>	<u>2529</u>	wheel well clearance (FR)
W _{rear axel}	<u>2614</u>	<u>5474</u>	<u>5474</u>	wheel well clearance (RR)
W _{TOTAL}	<u>4557</u>	<u>8003</u>	<u>8003</u>	Engine Type
				Engine Size
				Transmission Type:
				Automatic or <u>(Manual)</u>
				FWD or <u>(RWD)</u> or 4WD

Ballast Steel-1592 kg, Sand-1860 kg

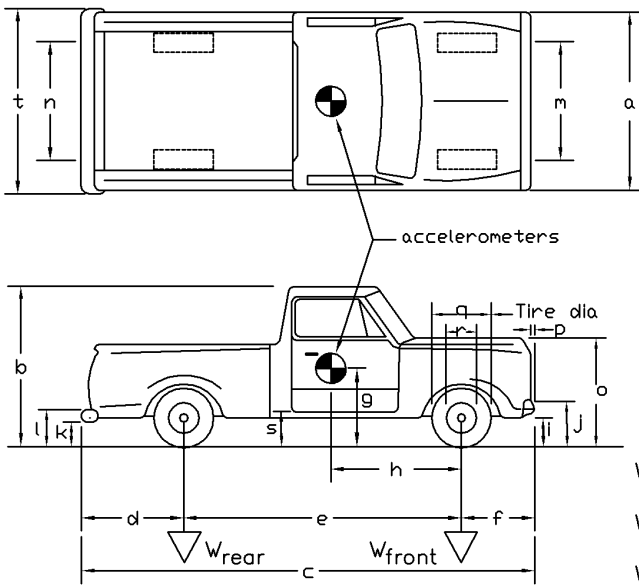
Note any damage prior to test: _____

Figure 17. Vehicle Dimensions, Test TRBR-4

Figure 18. Test Vehicle, Test STTR-1

Date: 2/17/98 Test Number: STTR-1 Model: F250
 Make: Ford Vehicle I.D.#: 1FTHF25L5HKB03981
 Tire Size: 235/85R16 Year: 1990 Odometer: 96,593

*(All Measurements Refer to Impacting Side)



Vehicle Geometry - mm

a 1918 b 1880
 c 5404 d 1270
 e 3378 f 756
 g 711 h 1485
 i 457 j 737
 k 584 l 756
 m 1645 n 1626
 o 1219 p 64
 q 762 r 445
 s 521 t 1930

Wheel Center Height Front 375
 Wheel Center Height Rear 375
 Wheel Well Clearance (FR) 876
 Wheel Well Clearance (RR) 953

Engine Type straight 6 cyl.

Engine Size 300 ci

Transmission Type:

Automatic or (Manual)

FWD or (RWD) or 4WD

Weights - kg	Curb	Test Inertial	Gross Static
W_{front}	<u>1111</u>	<u>1117</u>	<u>1117</u>
W_{rear}	<u>897</u>	<u>876</u>	<u>876</u>
W_{total}	<u>2008</u>	<u>1993</u>	<u>1993</u>

Note any damage prior to test: dent on front-left hood, rip on left door

Figure 19. Vehicle Dimensions, Test STTR-1

Figure 20. Test Vehicle, Test STTR-2

vehicle dimensions are shown in Figure 21.

For test STTR-3, a 1988 Ford F-250 $\frac{3}{4}$ -ton pickup truck was used as the test vehicle. The test inertial and gross static weights were 1,997 kg. The test vehicle is shown in Figure 22, and vehicle dimensions are shown in Figure 23.

For test STTR-4, a 1988 Chevrolet C60 Series single-unit truck was used as the test vehicle. The test inertial and gross static weights were 8,006 kg. The test vehicle is shown in Figure 24, and vehicle dimensions are shown in Figure 25.

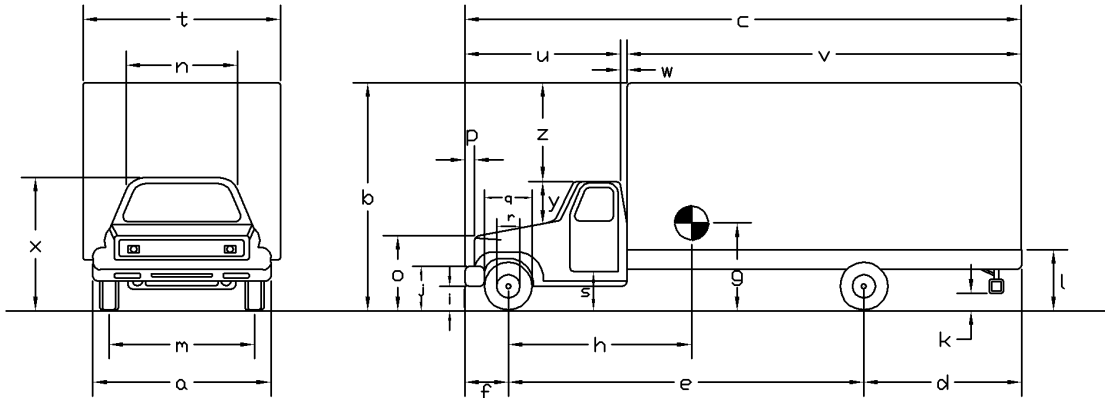
5.3.3 Center-of-Mass Determination, Vehicle Targets, and Alignment

The Suspension Method (24) was used to determine the vertical component of the center of gravity for the pickup truck test vehicles. This method is based on the principle that the center of gravity of any freely suspended body is in the vertical plane through the point of suspension. The vehicle was suspended successively in three positions, and the respective planes containing the center of gravity were established. The intersection of these planes pinpointed the location of the center of gravity. The Elevated Axle Method (25) was used to determine the vertical component of the center of gravity for the single-unit truck tests. This method converts measured wheel weights at different elevations to the location of the vertical component of the center of gravity. The longitudinal component of the center of gravity was determined using the measured axle weights. The locations of the final centers of gravity are shown in Figures 10 through 25. Vehicle ballast, consisting of steel plates and/or sand bags, was used to obtain the desired test weight.

Square, black and white-checkered targets were placed on the vehicle to aid in the analysis of the high-speed film, as shown in Figures 10, 12, 14, 16, 18, 20, 22, 24, and 26 through 33. Targets were placed on the center of gravity which were viewable on the both sides of the vehicle and on

the

Date: 4/17/98 Test Number: STTR-2 Model: F800
 Tire Sz FR: 10.00-20 Odometer: 126,169 Make: Ford
 Tire Sz RR: 10.00-20 V.I.N. #: 1FDPF8Z89FVA36985 Year: 1986



Vehicle Geometry (mm)

a> fr. bump. width	<u>2350</u>	j> fr. bump. top	<u>800</u>	s> bot. door height	<u>902</u>
b> overall height	<u>3632</u>	k> rr. bump. bot.	<u>425</u>	t> overall width	<u>2350</u>
c> overall length	<u>8280</u>	l> rr. frame top	<u>1181</u>	u> cab length	<u>2616</u>
d> rear overhang	<u>2635</u>	m> fr. track width	<u>2032</u>	v> trler/box length	<u>5632</u>
e> wheel base	<u>4794</u>	n> roof width	<u>1537</u>	w> gap width	<u>32</u>
f> front overhang	<u>851</u>	o> hood height	<u>1549</u>	x> overall fr. height	<u>2235</u>
g> C.G. height	<u>1260</u>	p> bump. extension	<u>32</u>	y> roof-hood dist.	<u>521</u>
h> C.G. hor. dist.	<u>3053</u>	q> fr. tire width	<u>584</u>	z> roof height dif.	<u>1295</u>
i> fr. bump. bot.	<u>495</u>	r> fr. wheel width	<u>1016</u>	wheel center height front	<u>495</u>

Weights (lbs)

	Curb	Test Inertial	Gross Static	
W _{front axel}	<u>2003</u>	<u>2937</u>	<u>2937</u>	wheel center height rear
W _{rear axel}	<u>3027</u>	<u>5130</u>	<u>5130</u>	<u>513</u>
W _{TOTAL}	<u>5030</u>	<u>8067</u>	<u>8067</u>	wheel well clearance (FR)
				<u>1168</u>
				wheel well clearance (RR)
				<u>1143</u>
				Engine Type
				<u>V8</u>
				Engine Size
				<u>429 ci</u>
				Transmission Type:
				Automatic or <u>(Manual)</u>
				FWD or <u>(RWD)</u> or 4WD

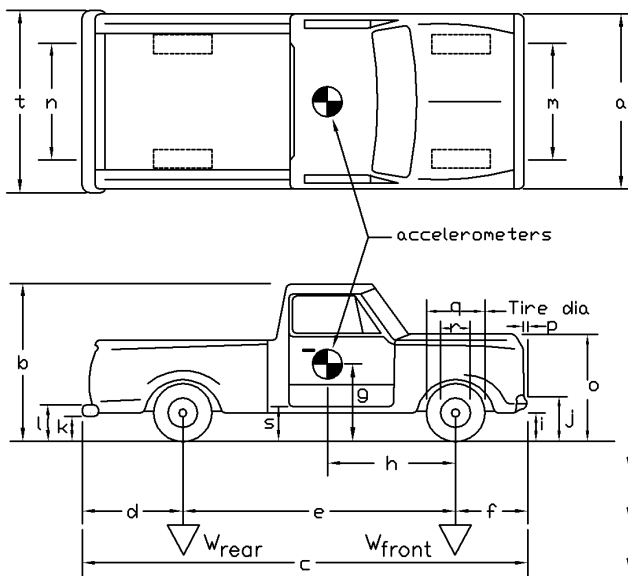
Note any damage prior to test: _____

Figure 21. Vehicle Dimensions, Test STTR-2

Figure 22. Test Vehicle, Test STTR-3

Date: 4/28/98 Test Number: STTR-3 Model: F250
 Make: Ford Vehicle I.D.#: 1FTHF25H2JPB14389
 Tire Size: LT235/85R16E Year: 1988 Odometer: 68,810

*(All Measurements Refer to Impacting Side)



Vehicle Geometry - mm

a 1943 b 1880
 c 5461 d 1295
 e 3378 f 756
 g 711 h 1452
 i 419 j 711
 k 572 l 762
 m 3378 n 3378
 o 1276 p 70
 q 775 r 445
 s 521 t 1930

Wheel Center Height Front 381
 Wheel Center Height Rear 389
 Wheel Well Clearance (FR) 870
 Wheel Well Clearance (RR) 978

Weights - kg	Curb	Test Inertial	Gross Static
W_{front}	<u>1178</u>	<u>1139</u>	<u>1139</u>
W_{rear}	<u>979</u>	<u>858</u>	<u>858</u>
W_{total}	<u>2157</u>	<u>1997</u>	<u>1997</u>

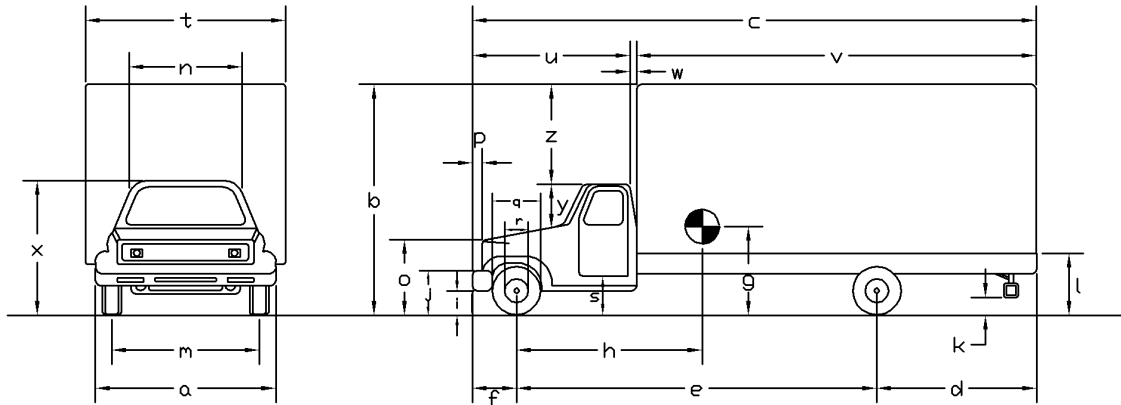
Engine Type V8
 Engine Size 5.8L
 Transmission Type:
 Automatic or (Manual)
 FWD or (RWD) or 4WD

Note any damage prior to test: minor windshield cracks

Figure 23. Vehicle Dimensions, Test STTR-3

Figure 24. Test Vehicle, Test STTR-4

Date: 8/27/98 Test Number: STTR-4 Model: 7000 Series
 Tire Sz FR: 9.00-20 Odometer: 85,893 Make: Chevrolet
 Tire Sz RR: 9.00-20 V.I.N. #: 1GB67D1B9JV104187 Year: 1988



Vehicle Geometry (mm)

a > fr. bump. width	<u>2140</u>	j > fr. bump. top	<u>813</u>	s > bot. door height	<u>851</u>
b > overall height	<u>3588</u>	k > rr. bump. bot.	<u>476</u>	t > overall width	<u>2435</u>
c > overall length	<u>7547</u>	l > rr. frame top	<u>1127</u>	u > cab length	<u>2464</u>
d > rear overhang	<u>1949</u>	m > fr. track width	<u>2000</u>	v > trlr./box length	<u>4988</u>
e > wheel base	<u>4807</u>	n > roof width	<u>1473</u>	w > gap width	<u>95</u>
f > front overhang	<u>800</u>	o > hood height	<u>1549</u>	x > overall fr. height	<u>2203</u>
g > C.G. height	<u>1257</u>	p > bump. extension	<u>89</u>	y > roof-hood dist.	<u>540</u>
h > C.G. hor. dist.	<u>3086</u>	q > fr. tire width	<u>991</u>	z > roof height dif.	<u>1384</u>
i > fr. bump. bot.	<u>495</u>	r > fr. wheel width	<u>581</u>	wheel center height front	<u>470</u>

Weights (lbs)

	Curb	Test Inertial	Gross Static	
W _{front axel}	<u>2147</u>	<u>2862</u>	<u>2862</u>	wheel center height rear
W _{rear axel}	<u>2526</u>	<u>5144</u>	<u>5144</u>	<u>483</u>
W _{TOTAL}	<u>4673</u>	<u>8006</u>	<u>8006</u>	wheel well clearance (FR)
				<u>1140</u>
				wheel well clearance (RR)
				<u>1019</u>
				Engine Type
				<u>V8</u>
				Engine Size
				<u>7.4L 454 ci</u>
				Transmission Type:
				Automatic or <u>(Manual)</u>
				FWD or <u>(RWD)</u> or 4WD

Note any damage prior to test: minor hood damage

Figure 25. Vehicle Dimensions, Test STTR-4

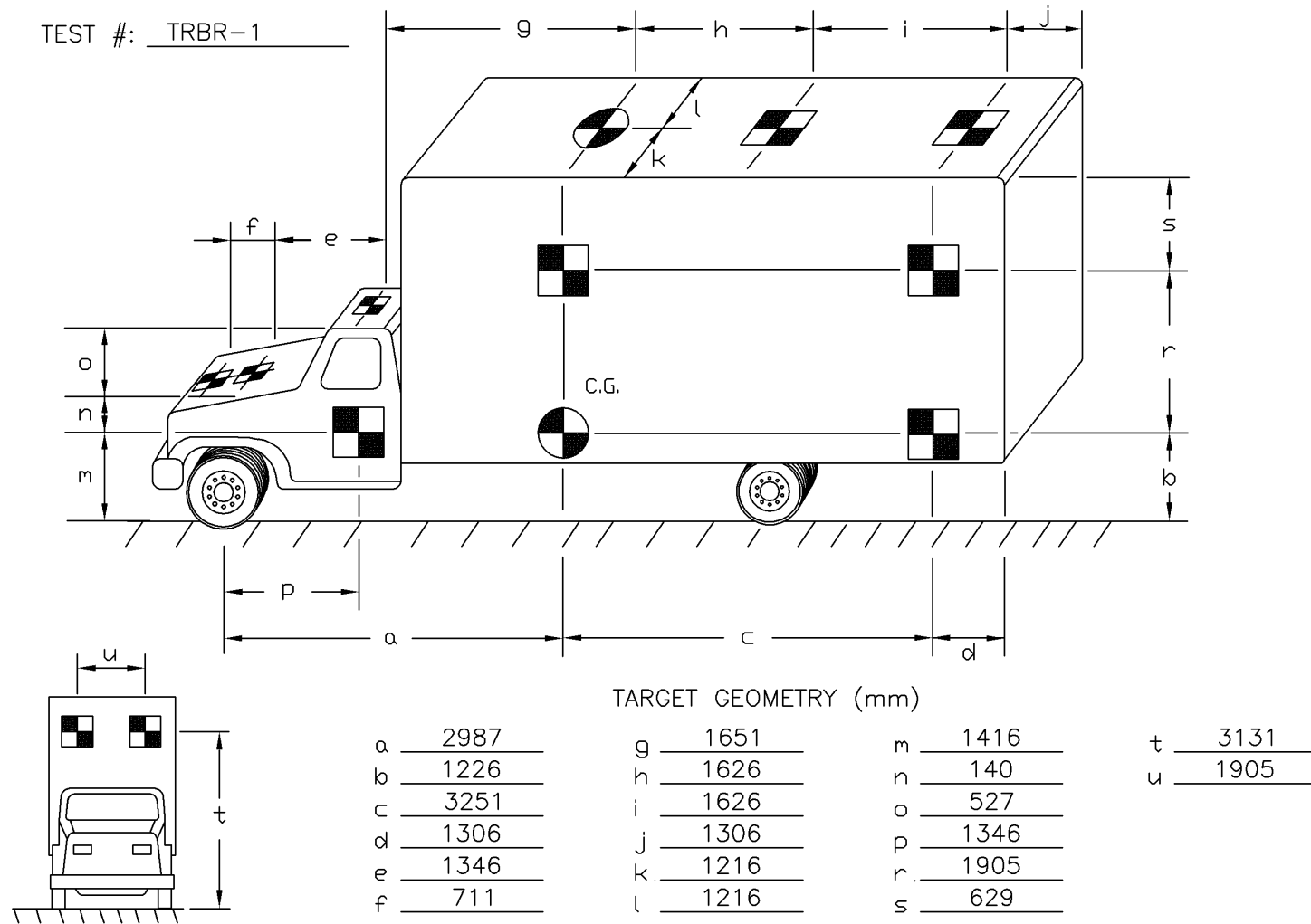
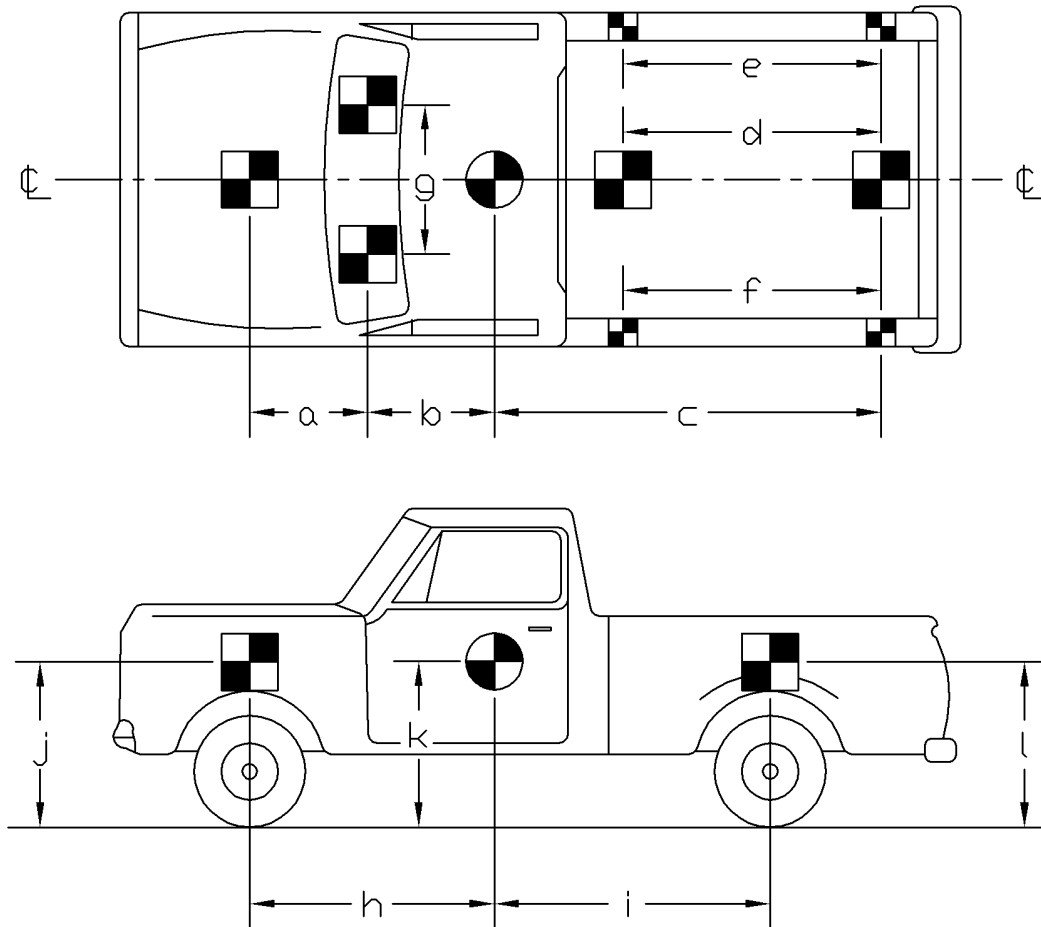


Figure 26. Vehicle Target Locations, Test TRBR-1

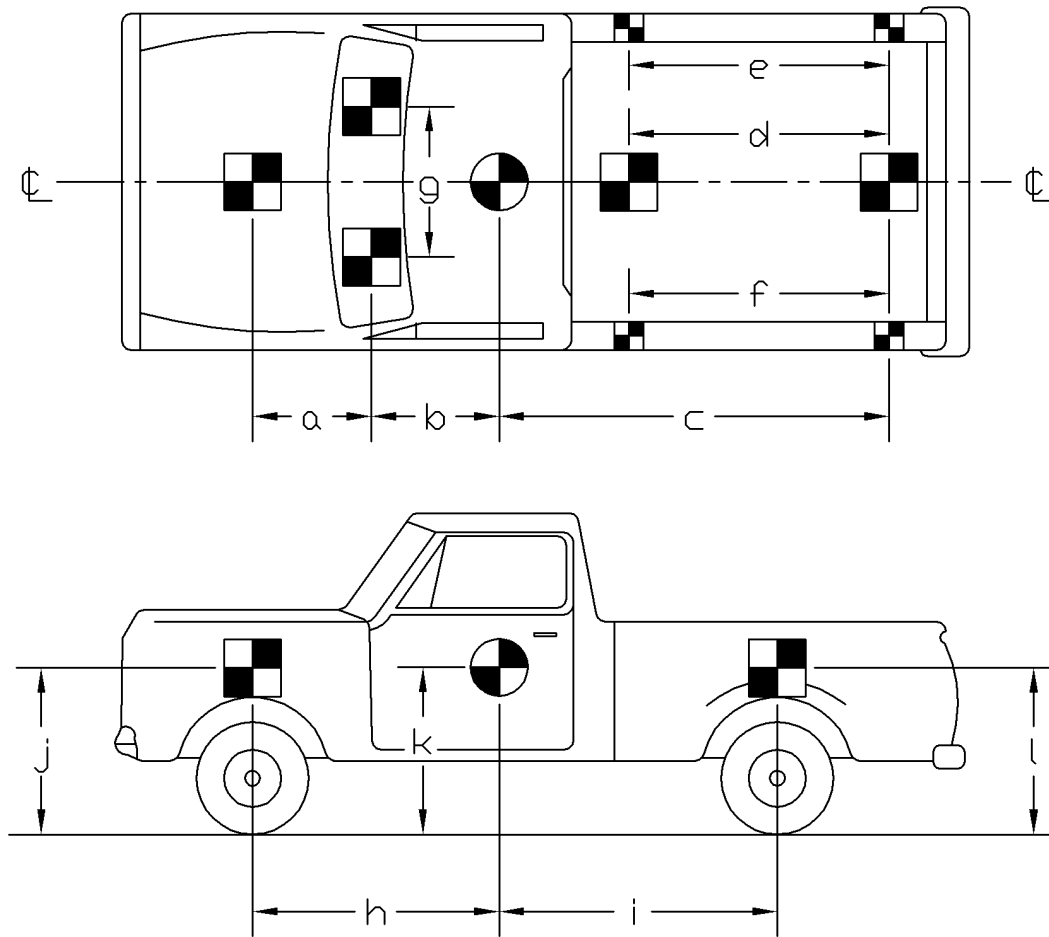


TEST #: TRBR-2

TARGET GEOMETRY (mm)

a	<u>1137</u>	b	<u>699</u>	c	<u>2692</u>	d	<u>1651</u>
e	<u>1949</u>	f	<u>1829</u>	g	<u>959</u>	h	<u>1521</u>
i	<u>1880</u>	j	<u>1073</u>	k	<u>669</u>	l	<u>1080</u>

Figure 27. Vehicle Target Locations, Test TRBR-2



TEST #: TRBR-3

TARGET GEOMETRY (mm)

a 876 b 546 c 2629 d 1403
 e 1695 f 1695 g 921 h 1422
 i 1918 j 876 k 711 l 1067

Figure 28. Vehicle Target Locations, Test TRBR-3

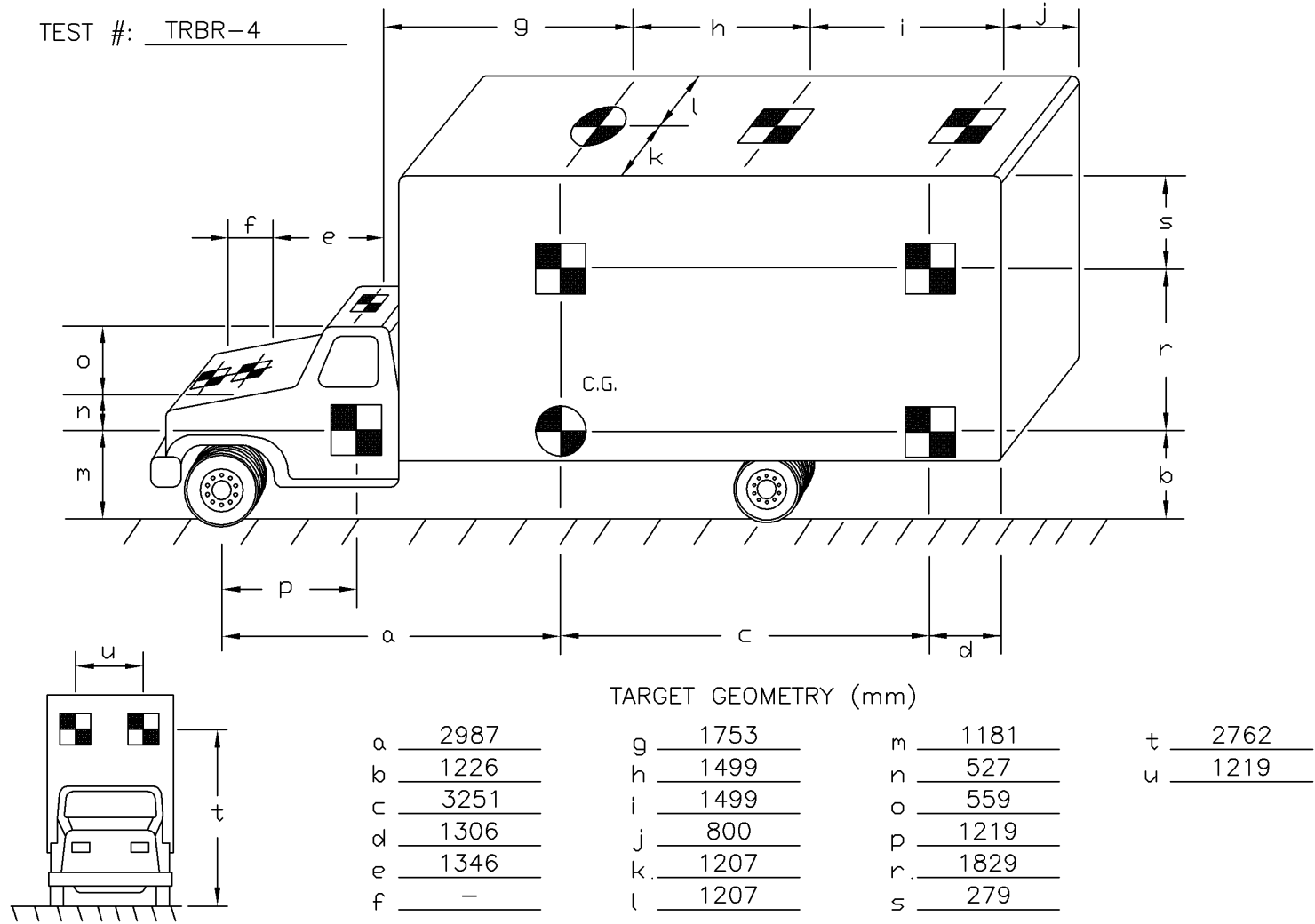
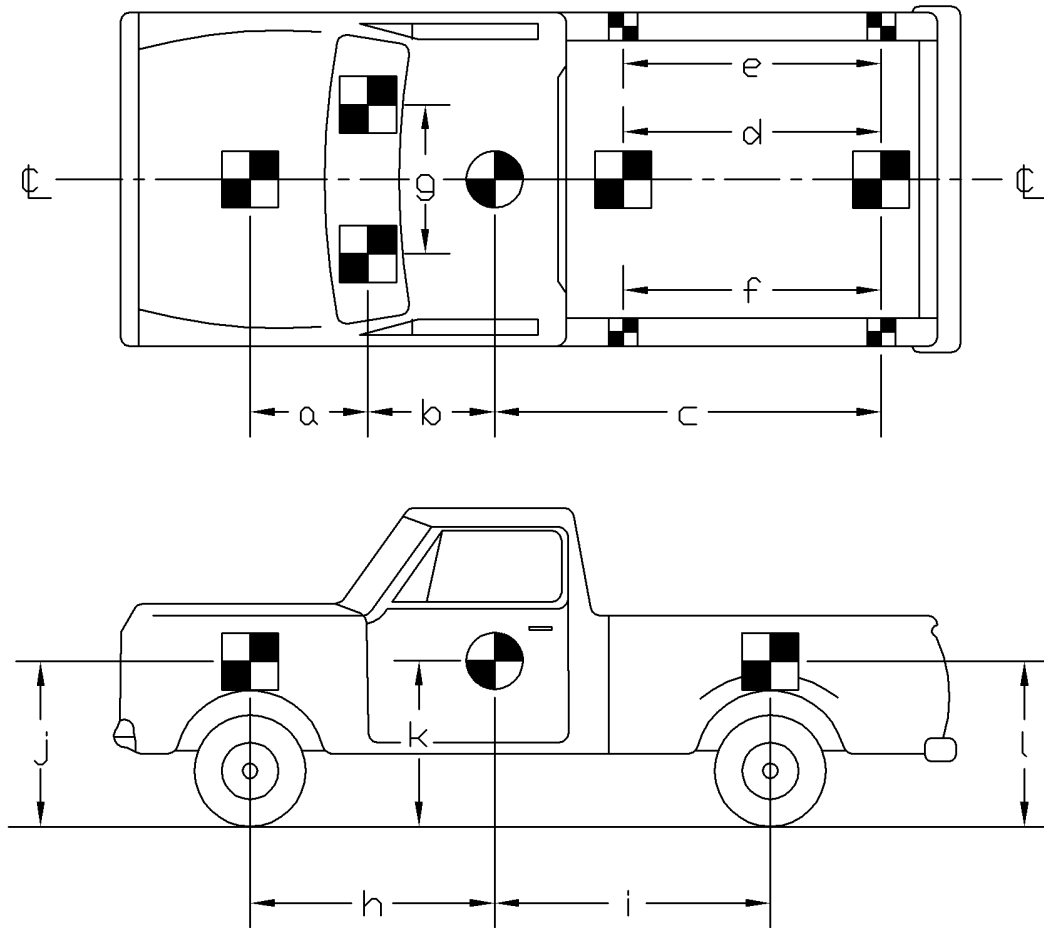


Figure 29. Vehicle Target Locations, Test TRBR-4



TEST #: STTR-1

TARGET GEOMETRY (mm)

a 991 b 533 c 2731 d 1753
 e 1946 f 1949 g 940 h 1486
 i 1899 j 1067 k 718 l 1124

Figure 30. Vehicle Target Locations, Test STTR-1

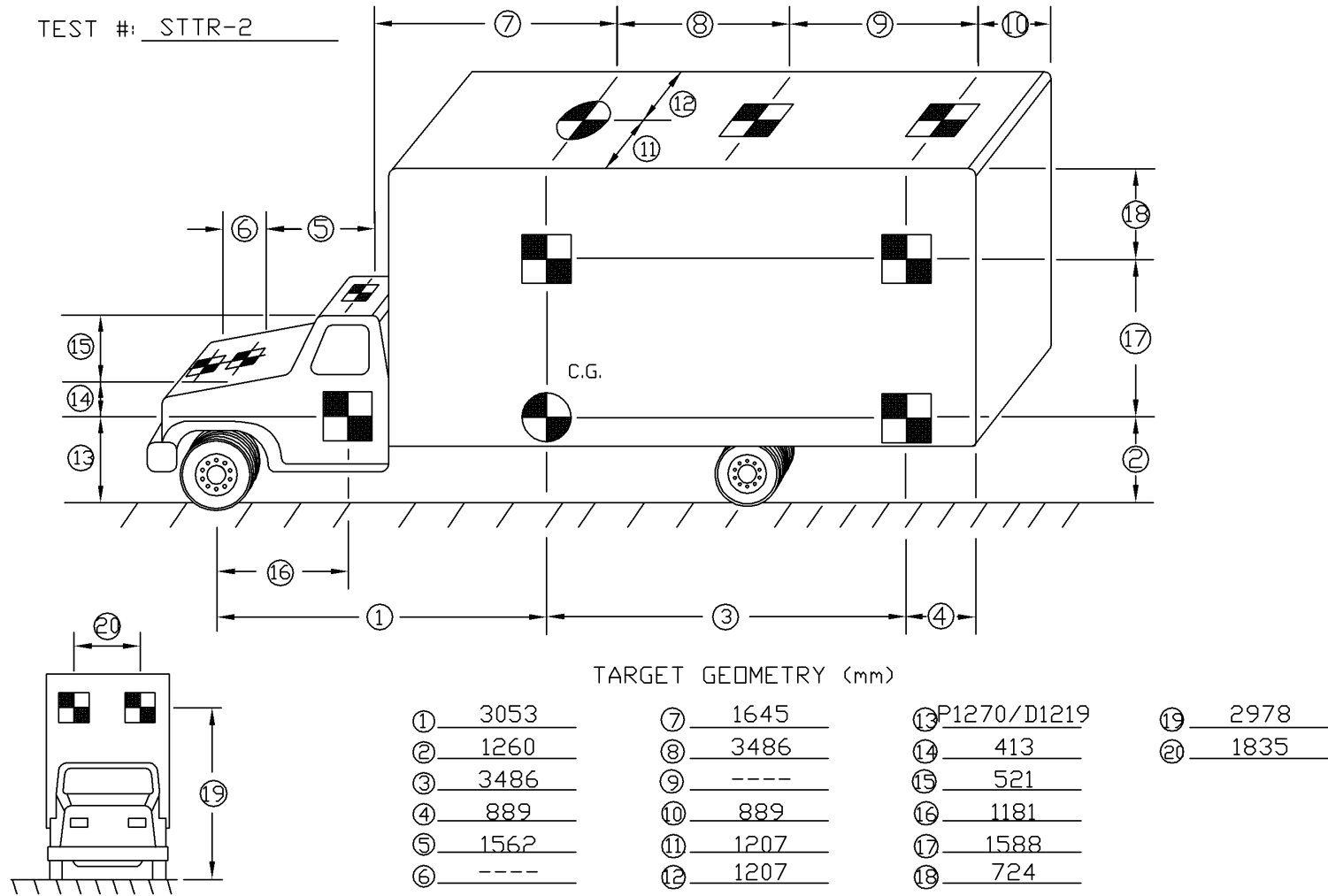
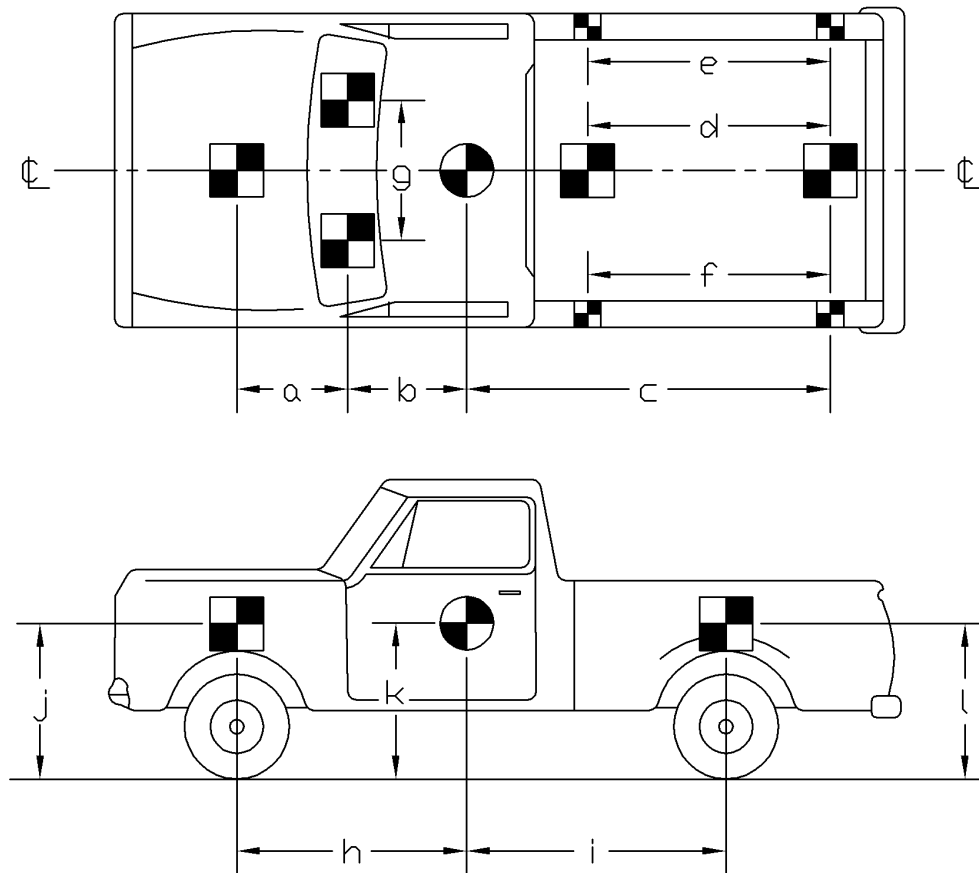


Figure 31. Vehicle Target Locations, Test STTR-2



TEST #: STTR-3

TARGET GEOMETRY (mm)

a 1270 b 610 c 2908 d 1854
 e 2172 f 2172 g 1067 h 1452
 i 1925 j 1003 k 711 l 1086

Figure 32. Vehicle Target Locations, Test STTR-3

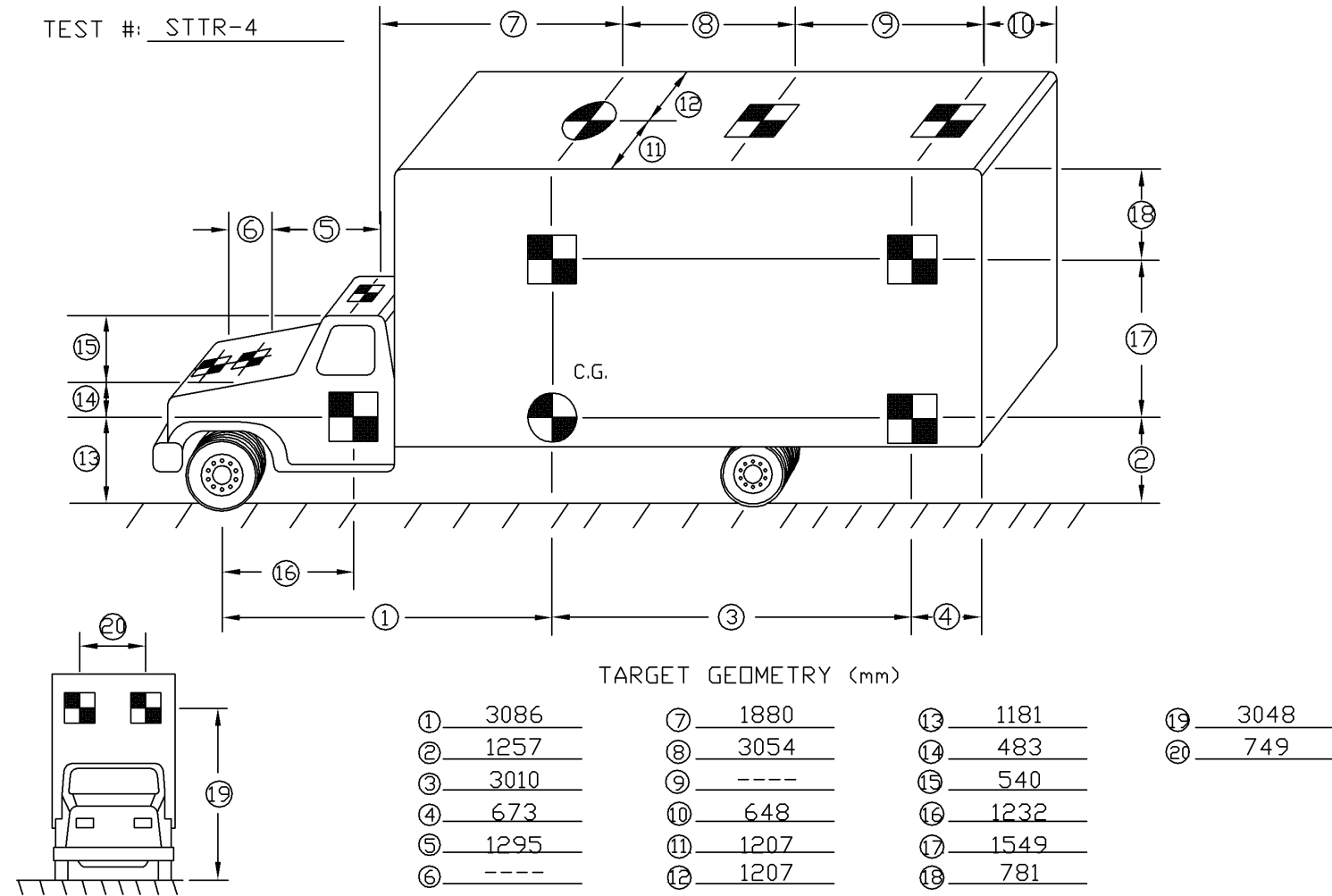


Figure 33. Vehicle Target Locations, Test STTR-4

top of the vehicle. The remaining targets were located for reference so that they could be viewed from the high-speed cameras for film analysis.

The front wheels of the test vehicles were aligned for camber, caster, and toe-in values of zero so that the vehicles would track properly along the guide cable. Two 5B flash bulbs were mounted on both the hood and roof of the vehicles to pinpoint the time of impact with the barrier on the high-speed film. The flash bulbs were fired by a pressure tape switch mounted on the front face of the bumper. A remote controlled brake system was installed in the test vehicles so the vehicles could be brought safely to a stop after the test.

5.4 Data Acquisition Systems

5.4.1 Accelerometers

One triaxial piezoresistive accelerometer system with a range of ± 200 G's was used to measure the acceleration in the longitudinal, lateral, and vertical directions at a sample rate of 10,000 Hz. The environmental shock and vibration sensor/recorder system, Model EDR-4M6, was developed by Instrumented Sensor Technology (IST) of Okemos, Michigan and includes three differential channels as well as three single-ended channels. The EDR-4 was configured with 6 Mb of RAM memory and a 1,500 Hz lowpass filter. Computer software, "DynaMax 1 (DM-1)" and "DADiSP" were used to digitize, analyze, and plot the accelerometer data.

A backup triaxial piezoresistive accelerometer system with a range of ± 200 G's was also used to measure the acceleration in the longitudinal, lateral, and vertical directions at a sample rate of 3,200 Hz. The environmental shock and vibration sensor/recorder system, Model EDR-3, was developed by Instrumented Sensor Technology (IST) of Okemos, Michigan. The EDR-3 was configured with 256 Kb of RAM memory and a 1,120 Hz lowpass filter. Computer software,

"DynaMax 1 (DM-1)" and "DADiSP" were used to digitize, analyze, and plot the accelerometer data.

5.4.2 Rate Transducer

A Humphrey 3-axis rate transducer with a range of 250 deg/sec in each of the three directions (pitch, roll, and yaw) was used to measure the angular velocity of the test vehicles. The rate transducer was rigidly attached to the vehicles near the center of gravity of the test vehicle. Rate transducer signals, excited by a 28 volt DC power source, were received through the three single-ended channels located externally on the EDR-4M6 and stored in the internal memory. The raw data measurements were then downloaded for analysis and plotting. Computer software, "DynaMax 1 (DM-1)" and "DADiSP" were used to digitize, analyze, and plot the rate transducer data.

5.4.3 High-Speed Photography

For tests TRBR-1 through TRBR-4 and tests STTR-1 through STTR-4, five high-speed 16-mm Red Lake Locam cameras, with operating speeds of approximately 500 frames/sec, were used to film the crash tests. A Locam was placed above the barrier to provide a field of view perpendicular to the ground. A Locam was placed downstream from the impact point and had a field of view parallel to the barrier. A Locam was placed on the traffic side of the barrier and had a field of view perpendicular to the barrier. A Locam was placed upstream and behind the barrier. Finally, a Locam was placed downstream and behind the barrier. A schematic of all five camera locations for each test is shown in Figures 34 through 41.

For tests TRBR-1, TRBR-2, STTR-1, and STTR-2, four white reference lines were painted on the bridge deck wearing surface on the traffic side of the bridge rail. The lines were incremented on approximately 2.4-m centers and provided a visible reference system for use in the analysis of

the overhead high-speed film. The film was analyzed using the Vanguard Motion Analyzer. Actual

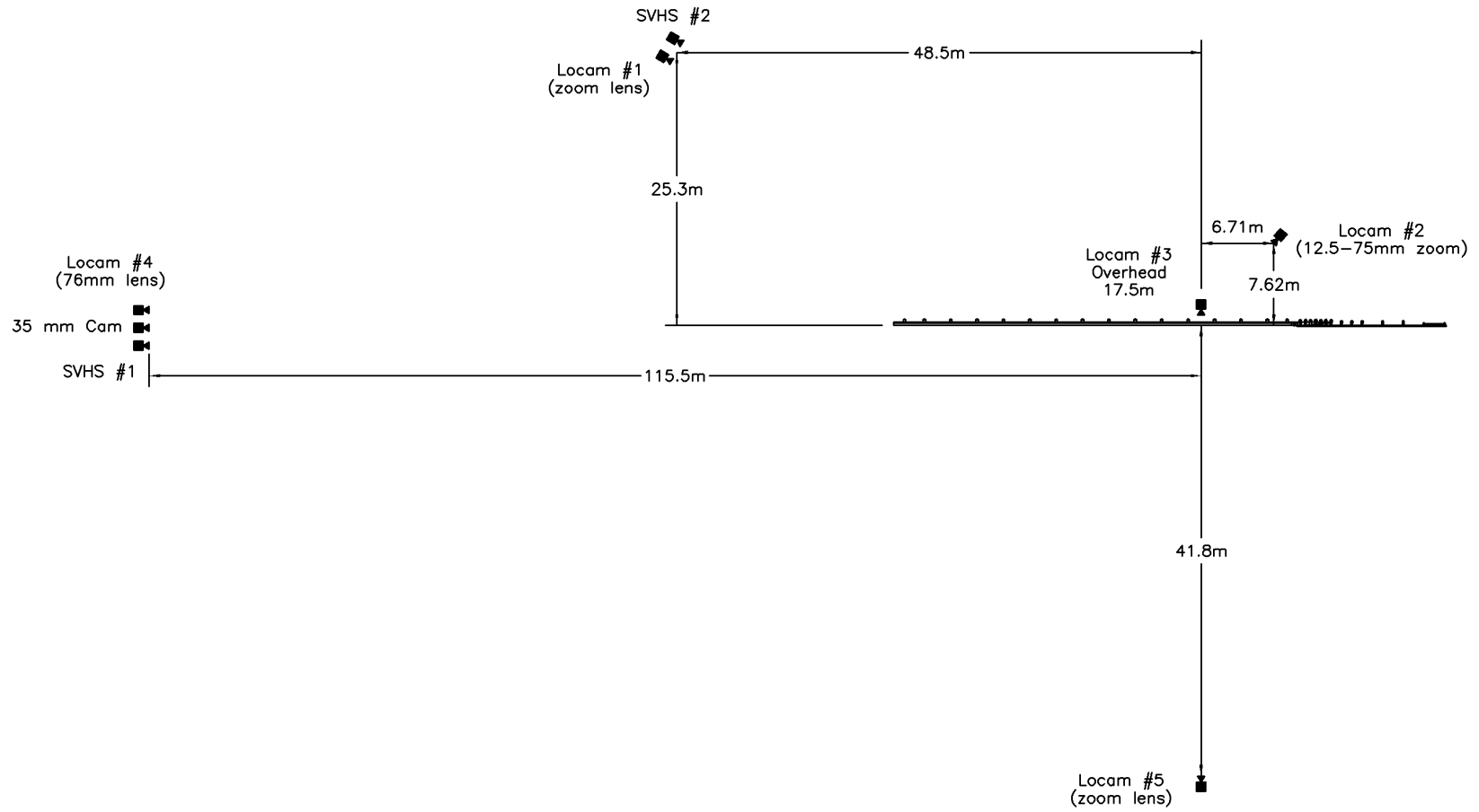


Figure 34. Location of High-Speed Cameras, Test TRBR-1

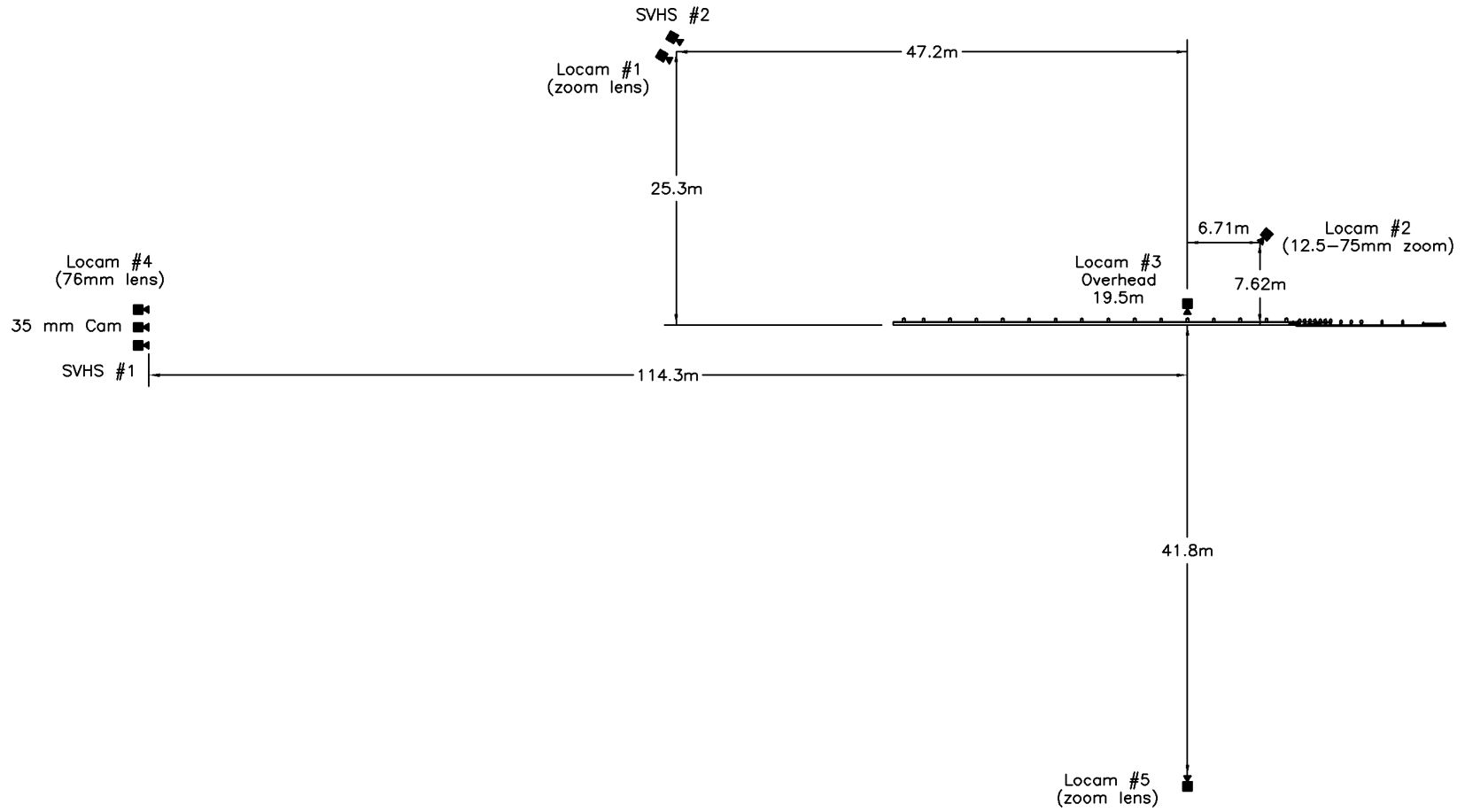


Figure 35. Location of High-Speed Cameras, Test TRBR-2

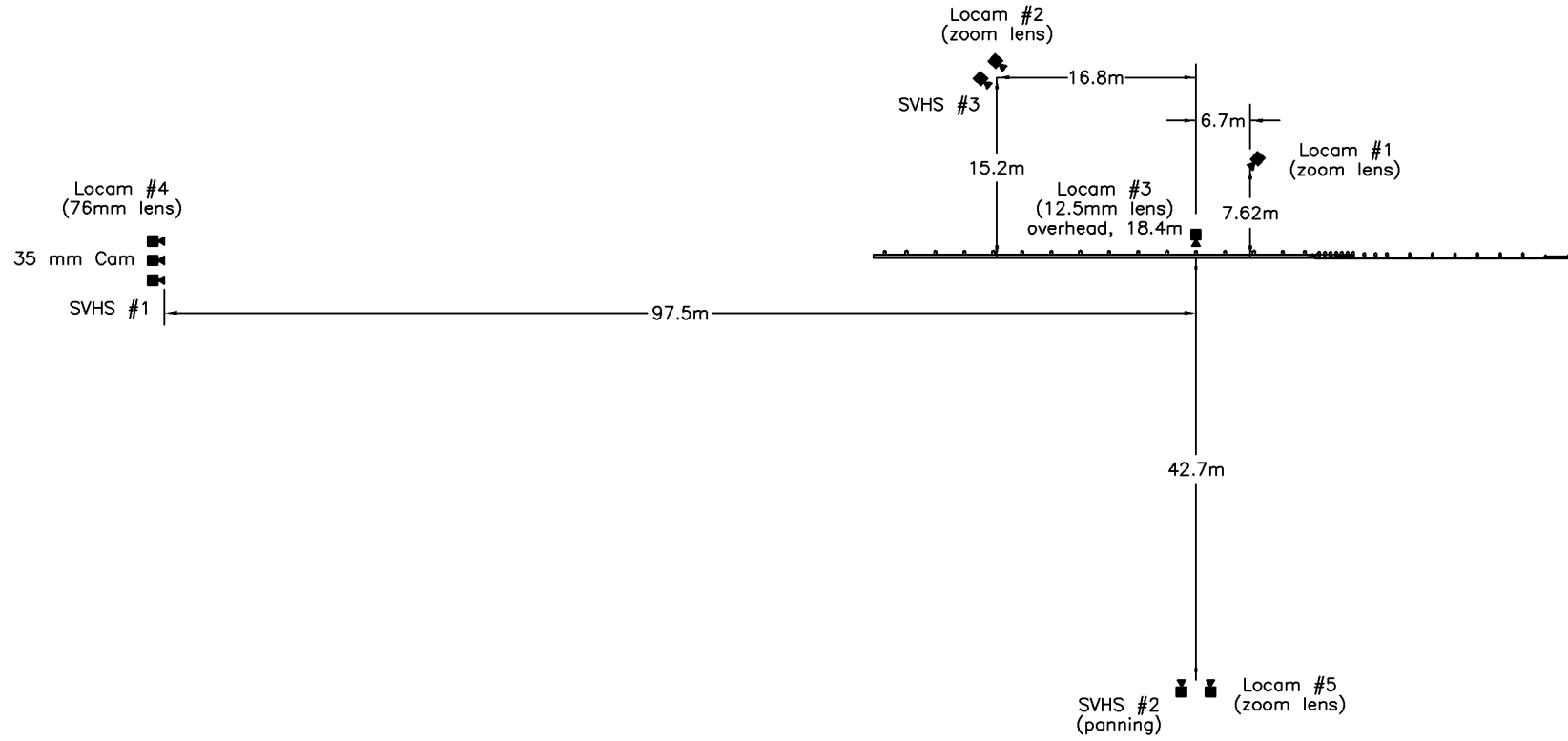


Figure 36. Location of High-Speed Cameras, Test TRBR-3

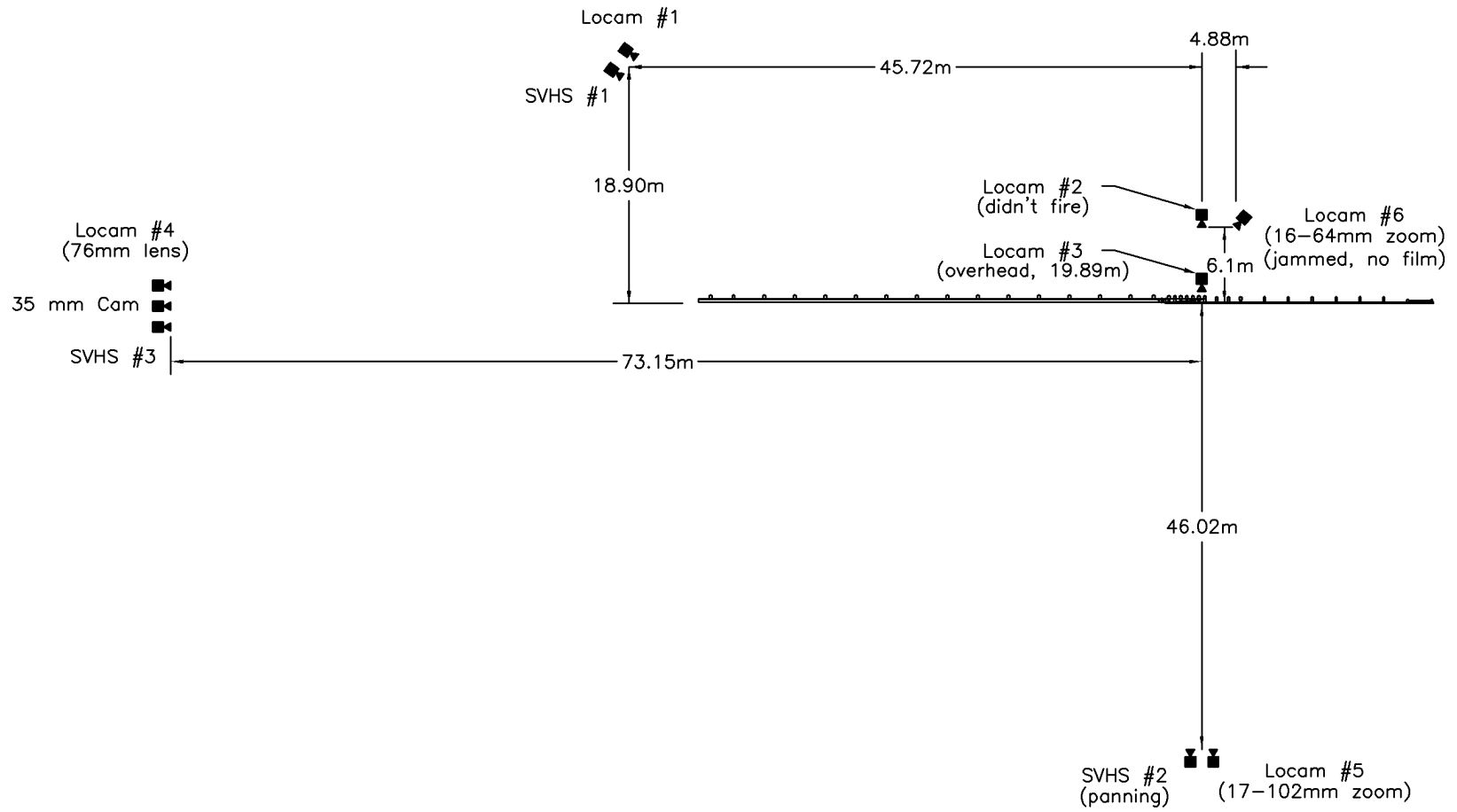


Figure 37. Location of High-Speed Cameras, Test TRBR-4

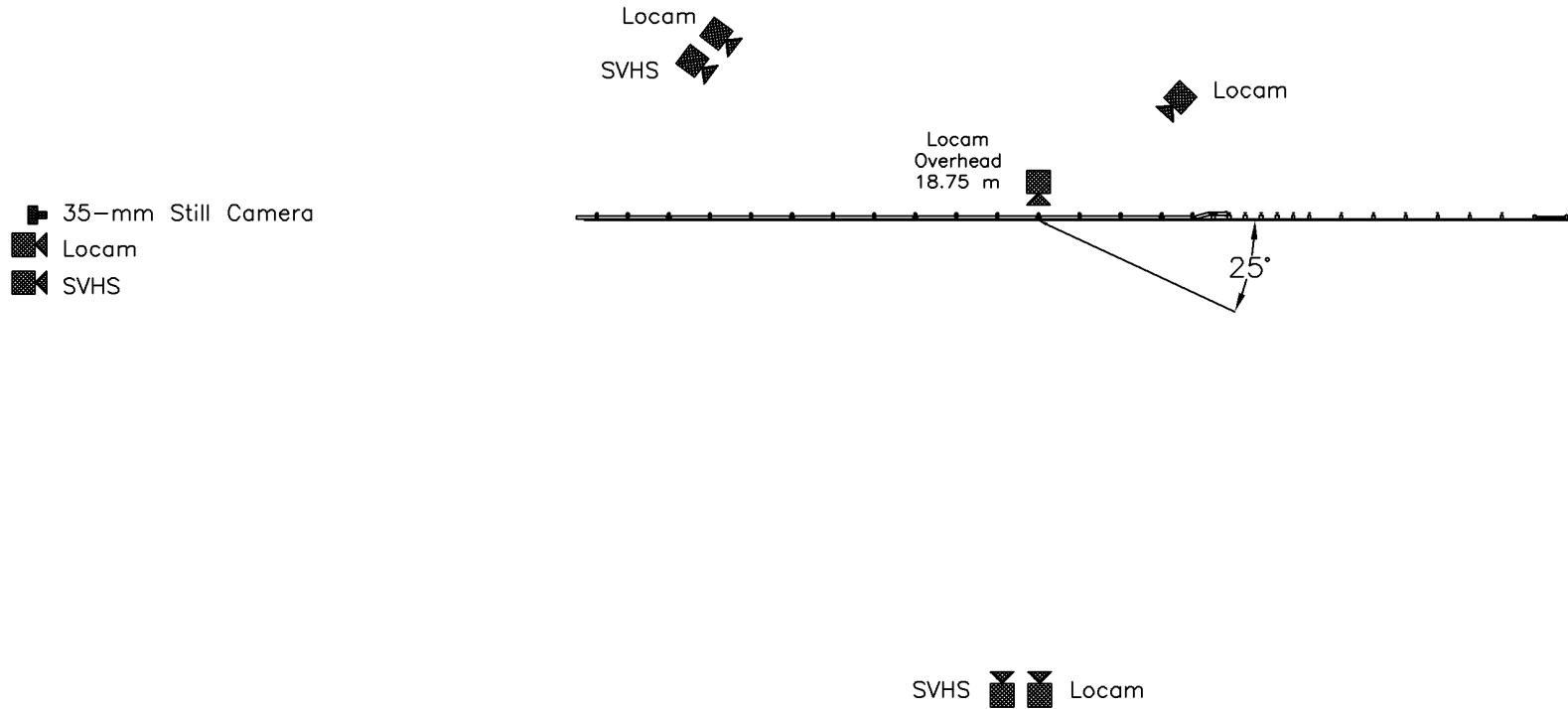


Figure 38. Location of High-Speed Cameras, Test STTR-1

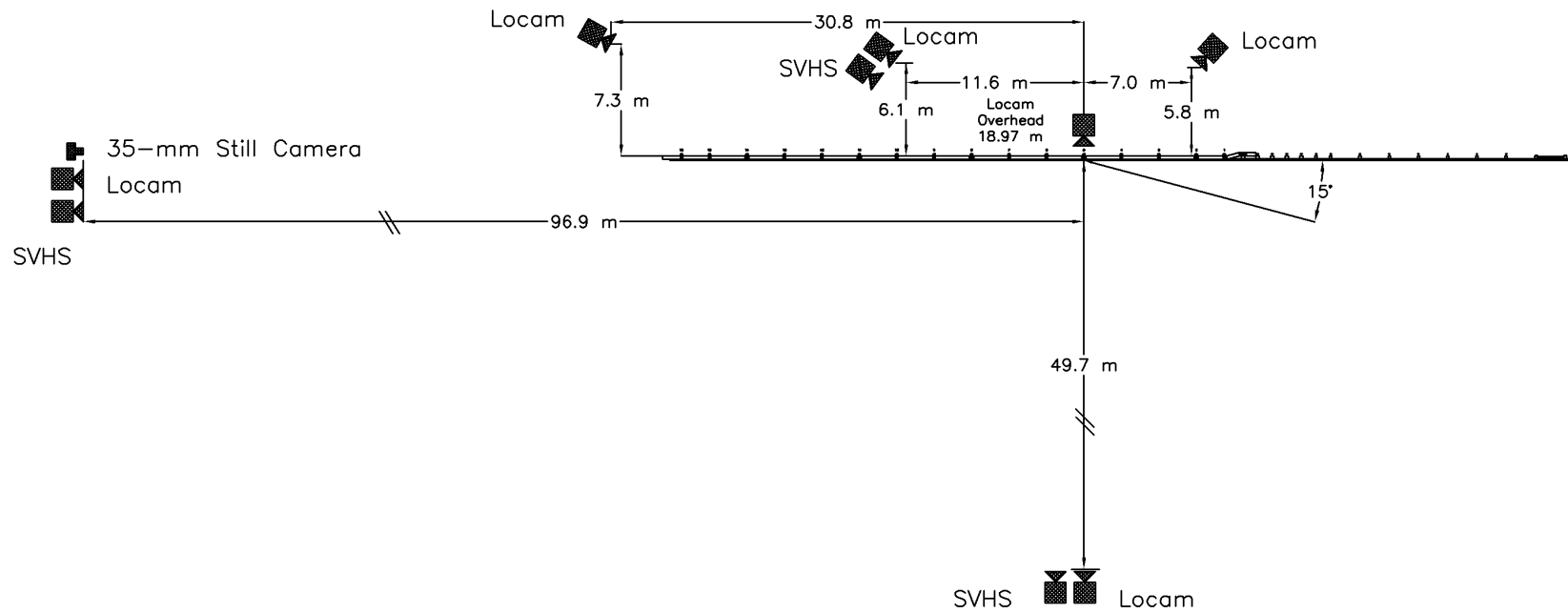


Figure 39. Location of High-Speed Cameras, Test STTR-2

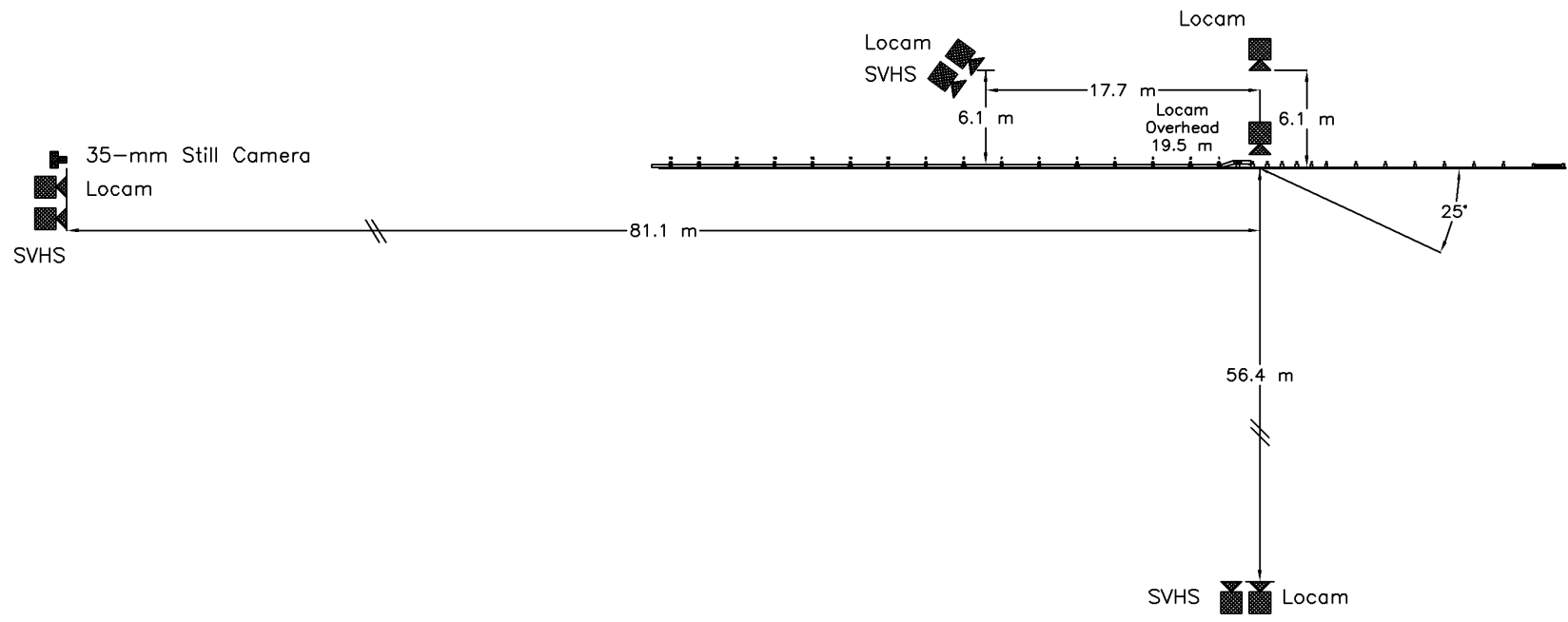


Figure 40. Location of High-Speed Cameras, Test STTR-3

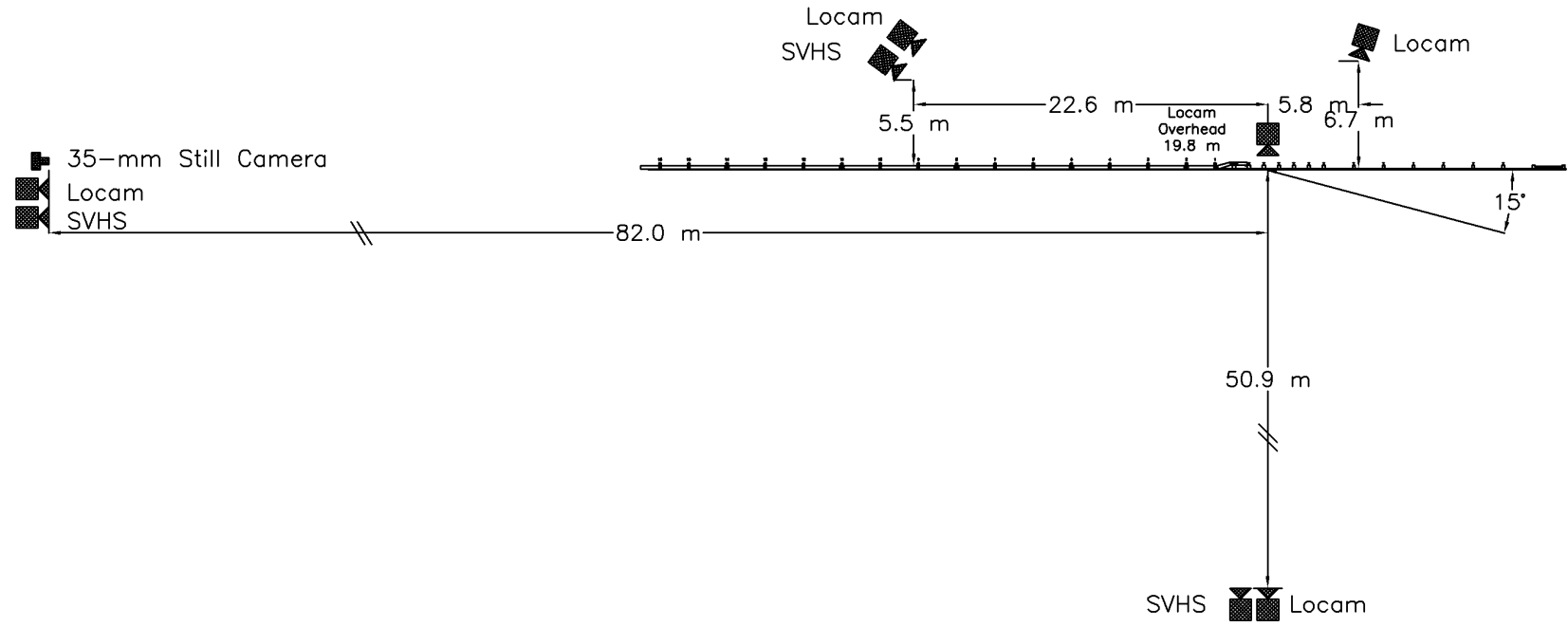


Figure 41. Location of High-Speed Cameras, Test STTR-4

camera speed and camera divergence factors were considered in the analysis of the high-speed film.

5.4.4 Pressure Tape Switches

For each test, five pressure-activated tape switches, equally spaced, were used to determine the speed of the vehicle before impact. Each tape switch fired a strobe light which sent an electronic timing signal to the data acquisition system as the left-front tire of the test vehicle passed over it. Test vehicle speeds were determined from electronic timing mark data recorded on "EGAA" software. Strobe lights and high-speed film analysis are used only as a backup in the event that vehicle speeds cannot be determined from the electronic data.

5.4.5 Bridge Railing Instrumentation

For tests TRBR-1, TRBR-2, STTR-1, and STTR-2, electronic sensors were placed on selected regions and components of the bridge railing systems. Two types of sensors, strain gauges and string potentiometers, were used for the crash tests and are described below.

5.4.5.1 Strain Gauges

For test TRBR-1, ten strain gauges were installed on several of the bridge railing components, consisting of six gauges located within the horizontal post bolts, three gauges located on the steel rail splice plates, and one gauge located on the upper glulam rail. The strain gauge positions are shown in Figure 42.

For test TRBR-2, ten strain gauges were installed on several of the bridge railing components, consisting of six gauges located within the horizontal post bolts and four gauges located on the steel rail splice plates. The strain gauge positions are shown in Figure 43.

For test STTR-1, twenty strain gauges were installed on several of the bridge railing components of bridge post nos. 6 and 7, consisting of four gauges located on the horizontal post

Figure 42. Strain Gauge and String Potentiometer Locations, Test TRBR-1

Figure 43. Strain Gauge and String Potentiometer Locations, Test TRBR-2

bolts, ten gauges located on the top deck mounting plates, two gauges located on the bottom deck mounting plates, and four gauges located on the front and back flanges of bridge posts. The typical strain gauge positions are shown in Figure 44. Actual strain gauge locations are shown in Appendix A.

For test STTR-2, twenty strain gauges were installed on several of the bridge railing components of bridge post nos. 5 through 7, consisting of six gauges located on the horizontal post bolts, seven gauges located on the top deck mounting plates, three gauges located on the bottom deck mounting plates, two gauges located on the front and back flanges of bridge posts, and two gauges located on the upper structural tube rail. The typical strain gauge positions are shown in Figure 45. Actual strain gauge locations are shown in Appendix B.

For test TRBR-1 and TRBR-2, two types of strain gauges were used. For the instrumentation of the horizontal bolts, BTM-6C bolt strain gauges were installed in the ends of strategically selected bolts. The nominal resistance of the gauges was 120 ± 0.5 ohms with a gauge factor equal to 2.1. The operating temperature limits of the gauge was -10 to +80 degrees Celsius. The strain limits of the gauges were 0.5% in bolt tension or compression ($5000 \mu\epsilon$). The bolt strain gauges are manufactured by the Tokyo Sokki Kenkyujo Co., Ltd., and marketed in the United States by Texas Measurements, Inc. The other components were instrumented with weldable strain gauges, consisting of gauge type LWK-06-W250B-350. The nominal resistance of the gauges was 350.0 ± 1.4 ohms with a gauge factor equal to 2.02. The operating temperature limits of the gauges was -195 to +260 degrees Celsius. The strain limits of the gauges were 0.5% in tension or compression ($5000 \mu\epsilon$). The strain gauges were manufactured by the Micro-Measurements Division of Measurements Group, Inc. of Raleigh, North Carolina. The installation procedure required that the metal surface

be clean and free

Figure 44. Strain Gauge Locations, Test STTR-1

Figure 45. Strain Gauge Locations, Test STTR-2

from debris and oxidation. Once the surface had been prepared, the gauges were spot welded to the test surface. For tests STTR-1 and STTR-2, only weldable strain gauges, as previously described, were used.

A Measurements Group Vishay Model 2310 signal conditioning amplifier was used to condition and amplify the low-level signals to high-level outputs for multichannel, simultaneous dynamic recording on "Test Point" software. After each signal was amplified, it was sent to a Keithly Metrabyte DAS-1802HC data acquisition board, and then stored permanently on the portable computer. The sample rate for all gauges was 10,000 samples per second (10,000 Hz), and the duration of sampling was 6 seconds.

5.4.5.2 String Potentiometers

For test TRBR-1, five string potentiometers (linear position transducers) were installed on the outside vertical edge of the outer glulam girders. The string potentiometer positions are shown in Figure 42.

For test TRBR-2, five string potentiometers (linear position transducers) were installed on the backside of the upper glulam rail and glulam posts. The string potentiometer positions are shown in Figure 43.

Two UniMeasure PA-50 and three UniMeasure PA-20 string potentiometers were used. The PA-50 potentiometers had a range of 1270 mm and the PA-20 potentiometers had a range of 508 mm. The PA-50 and PA-20 units were modified for dynamic testing and configured with a maximum cable retraction acceleration of 100 G's.

During the test, the output voltage signals from the string potentiometers were sent to a Keithly Metrabyte DAS-1802HC data acquisition board, acquired by the "Test Point" software, and

then stored permanently on the portable computer. The sample rate for the string potentiometers was 10,000 samples per second (10,000 Hz), and the duration of sampling was 6 seconds.

6 WOOD SYSTEM DEVELOPMENT

6.1 Background

Prior to this research, there have been no TL-4 bridge railing systems developed for use on transverse glulam timber deck bridges. However, in 1993, a TL-4 glulam timber rail with curb bridge railing system was developed for use on a longitudinal glulam timber deck bridge and successfully full-scale crash tested by MwRSF (4-8). The glulam timber rail with curb, which was referred to as the *GC-8000* bridge railing system, consisted of a single glulam timber upper rail mounted on a sawn lumber post. The post was connected by a single bolt to a sawn lumber curb that was supported by sawn lumber scupper blocks. The curb and scupper blocks were connected to the bridge deck with vertical bolts and timber connectors.

The *GC-8000* bridge railing system served as the basis for the design of the TL-4 wood bridge railing system for use on transverse glulam timber deck bridges. The *GC-8000* bridge railing system was modified so that it could be used with transverse deck panels rather than the previously used longitudinal deck panels. With the change in timber deck configurations, the researchers believed that an increase in bridge post spacing was required in order to accommodate the use of standard 1,219-mm wide transverse deck panels. Development of the TL-4 wood system also consisted of re-sizing the structural components previously used with the *GC-8000* bridge railing system to withstand the higher forces generated from the increased post spacing. Other improvements were made to the connection details based on the performance of the *GC-8000* bridge railing system.

6.2 Design Issues

Several design issues were addressed during the development of the new TL-4 wood bridge

railing system, including bridge length, girder size, deck thickness, post spacing, material selection, geometry considerations, and connection details.

Historically, crash tests of longitudinal barriers with single-unit trucks have revealed that adequate length of barrier must be provided downstream from initial impact. This minimum barrier length is necessary to: (1) evaluate vehicle stability during redirection but prior to the vehicle reaching the end of the barrier; and (2) study the vehicle interaction with the top of the bridge railing components. Therefore, the length of the bridge superstructure was chosen to be approximately 36.58-m long in order to provide the necessary bridge railing length approximately equal in magnitude.

Early in the project, significant discussions occurred between MwRSF researchers, FPL engineers, and industry leaders on the selection of the girder size and deck thickness. For a 12.19-m span length, the girder widths discussed, ranged between 222 and 273 mm, while the beam depth varied between 768 and 838 mm. Two deck sizes were also considered, a 130-mm versus a 171-mm thickness. From a more conservative approach, the glulam members would be selected using the larger dimensions mentioned previously, thus providing reserve structural capacity. However, from an economics approach, the glulam members would be chosen using the smaller dimensions. After much thought, it was mutually decided to use a 130-mm deck thickness supported by girders measuring 222-mm wide by 768-mm deep. Therefore, if the development of the bridge railing systems were successful using the smaller sizes, then significant economy would be provided for each timber bridge constructed which required a TL-4 bridge railing.

Standard 1,219-mm wide transverse glulam deck panels were used to form the timber bridge deck. Thus, it was necessary to determine a post spacing that would provide adequate load

distribution from the rails to the deck, allow for reasonable size rail elements, and provide a consistent connection detail for each panel location where a post would attach to the deck. A post spacing of 1,219 mm, or any multiple of 1,219 mm, would be required in order to prefabricate a standard deck panel with the ability to mount a standard bridge railing system to the panel. A post spacing of 1,219 mm was deemed too conservative and costly, therefore a 2,438-mm post spacing was used, as shown in Figure 46. However, using a 2,438-mm post spacing instead of the 1,905-mm post spacing used in the *GC-8000* bridge railing system resulted in a 28% increase in the rail bending moment and post shear force.

Two wood material alternatives, glulam timber and sawn lumber, were considered for use as the rail elements, posts, blockouts, and scupper blocks in the wood bridge railing system based on strength, cost, and availability. In general, wood's strength, lightweight characteristics versus steel and concrete, and energy-absorbing properties are desirable features for bridge rails. Also, timber provides a natural and aesthetically pleasing appearance especially suited to natural surroundings. Commercial sawn lumber is usually limited by the size of trees at harvesting, which limits both the diameter and length of the timbers. In the context of bridge rail design, this size limitation affects the availability and cost of the major rail members, as well as increases the number of splices on bridges with lengths greater than 6.10 m (26). Glulam timber, however, is virtually unlimited in depth, width, and length and can be manufactured in a wide range of shapes. Glulam provides higher design strengths than sawn lumber and provides better utilization of the available timber resource by permitting the manufacture of large wood structural elements from smaller lumber sizes. Also, glulam timber is manufactured to strict tolerances which ensures greater uniformity and ease of construction. Based on these advantages, glulam was selected over sawn

timber for all components of the new, wood bridge railing system, as shown in Figures 47 and 48 (26).

Following the 8000S crash test performed on the *GC-8000* bridge railing system, it was discovered that vehicle snagging had occurred when the vehicle's truck box extended over the top of the bridge rail and contacted several bridge posts and blockouts. The maximum measured contact distance between the truck box and posts was measured to be approximately 229 mm below the top of one of the posts. Therefore, a modified post-to-rail connection was selected to reduce the potential for vehicle snagging on the top of the posts and blockouts by placing the top surfaces of the posts and blockouts 76 mm below the top of the rail. Although visible contact marks were measured 229 mm below the top of one post, a 76-mm offset was chosen as a reasonable distance based on the fact that most vehicle contact marks were actually between 51 to 76 mm for a majority of the *GC-8000* posts and blockouts.

Other concerns which arose during the crash testing of the *GC-8000* bridge railing system were the splitting of the sawn lumber curb rails and scupper blocks along the vertical bolt line and the cracking of the upper glulam rail near the ends of the steel splice plates. The splitting of the curb rails and scupper blocks was addressed by using a stronger glulam material rather than sawn lumber. The potential for cracking of the upper rail near connection joints was reduced by eliminating the single, interior splice plate configuration, as used in the *GC-8000* railing system, and implementing a double, splice plate configuration attached to the each outer face, as shown in Figure 49.

Figure 46. Wood Bridge Railing System

Figure 47. Wood Bridge Railing System

Figure 48. Wood Bridge Railing System - Bridge Posts

Figure 49. Wood Bridge Railing System - Rail Splices

7 WOOD SYSTEM DESIGN DETAILS

7.1 Wood Bridge Railing

The bridge railing system consisted of five major components: (1) an upper rail; (2) spacer blocks; (3) posts; (4) a lower curb rail; and (5) scupper blocks. Photographs of the bridge railing system have been shown previously in Figures 46 through 49. The overall layout of the bridge railing system is shown in Figure 50. Design details of the bridge railings system are shown in Figures 51 through 54.

All five bridge components were glulam timber, fabricated from Southern Yellow Pine (SYP), and treated with pentachlorophenol in heavy oil to a minimum net retention of 9.61 kg/m³ as specified in AWWA Standard C14 (22). The upper rail and posts were fabricated from Combination No. 48 material (Douglas Fir (DF) - Combination No. 2 optional) while the lower curb rail, spacer blocks, and scupper blocks were fabricated from Combination No. 47 material (DF - Combination No. 1 optional).

The upper rail was 222-mm wide by 343-mm deep with a 838-mm top mounting height, as measured from the top of the asphalt wearing surface to the top of the upper rail. Two rail splices were required on the upper rail to attain the total rail length of approximately 36.58 m. Details for the upper rail-splices are shown in Figure 53. The upper rail was offset from the posts with spacer blocks measuring 79-mm thick by 222-mm wide by 267-mm deep. The upper rail and spacer blocks were attached to the posts with two 19-mm diameter by 635-mm long ASTM A307 galvanized dome head bolts at non-splice locations. At all upper rail-splice locations, four 19-mm diameter by 635-mm long ASTM A307 galvanized dome head bolts were used.

Sixteen posts, measuring 222-mm wide by 267-mm deep by 943-mm long, were used to

support the upper rail. Bridge posts were spaced 2,438 mm on centers along the length of the bridge railing, except at each end where the first two posts were spaced 1,829 mm on centers. Each post was bolted to the lower curb rail with one 32-mm diameter by 648-mm long, ASTM A307 galvanized dome head bolt. ASTM A36 steel plate washers, measuring 152-mm square by 6.3-mm thick, were used under both the bolt head and the nut. Two 127-mm long, ASTM A36 steel angles, measuring 102 mm by 102 mm by 9.5 mm, were used at each post location to prevent post rotation. Each steel angle attached to the back side of each scupper block with a 16-mm diameter by 152-mm long, ASTM A307 lag screw.

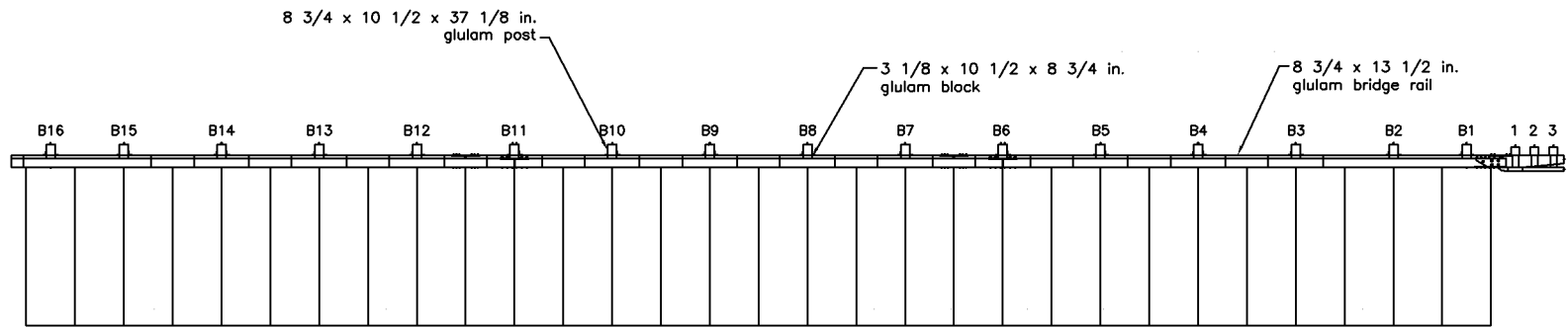
The lower curb rail measured 171-mm deep by 305-mm wide. The top of the curb rail was positioned 292 mm above the asphalt wearing surface. Two rail splices were required on the lower curb rail to attain the total rail length of approximately 37.19 m. Details for the lower curb rail-splices are shown in Figure 53.

The lower curb rail was supported by one scupper block at post nos. 3 through 14. The twelve scupper blocks measured 171-mm deep by 305-mm wide by 1,372-mm long. Six 19-mm diameter by 521-mm long, ASTM A307 galvanized dome head bolts were used to attach the lower curb rail and scupper blocks to the timber deck surface. Special scupper blocks were used between post nos. 1 and 2 as well as between post nos. 15 and 16 to provide increased deck attachment, load distribution, and structural capacity near the bridge rail ends, as shown in Figure 54. The connections between the curb rail and scupper blocks as well as between the scupper blocks and deck surface were also made using 102-mm diameter shear plate connectors.

The upper and lower glulam rails were anchored at the downstream end of the bridge railing system with a rigid assembly consisting of welded steel plates and structural steel tubes that were

bolted to both rails and anchored to the concrete tarmac. The anchor, as shown in Figures 46 and 47, was necessary to develop the tensile capacity of the rails at the downstream end of the bridge railing system.

Finally, the construction of the bridge railing system was similar to that of the superstructure in regards to the ease of construction with minimal equipment and manpower. The bridge railing construction was completed in three days with a three-person crew and equipment that consisted of a forklift and an assortment of electric, pneumatic, and hand tools. The bridge railing components were prefabricated offsite, with the exception of the field-drilled holes placed through the deck panels and the shear plate grooves made on the top surface of the deck panels. The sequence of the bridge railing construction was completed by first bolting the scupper blocks and curb rails to the deck. Subsequently, the posts were bolted to the curb rail. Finally, the upper rail and spacer blocks were attached to the posts.



81

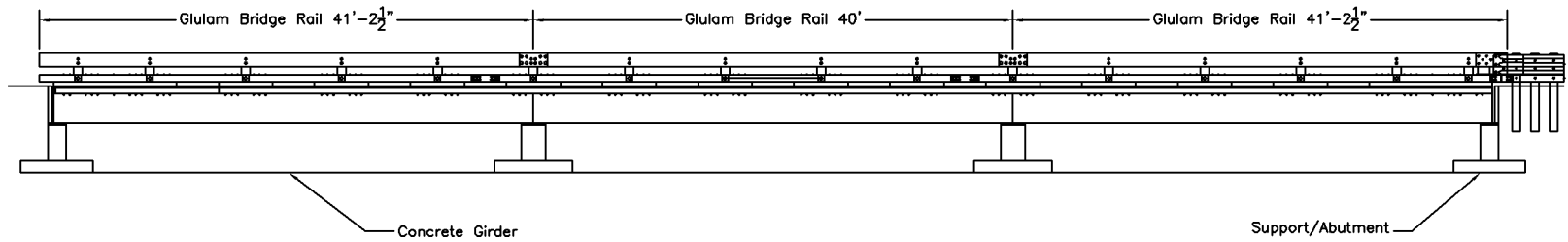
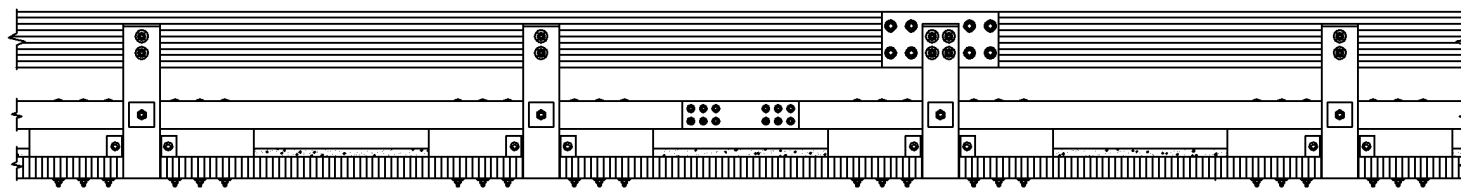
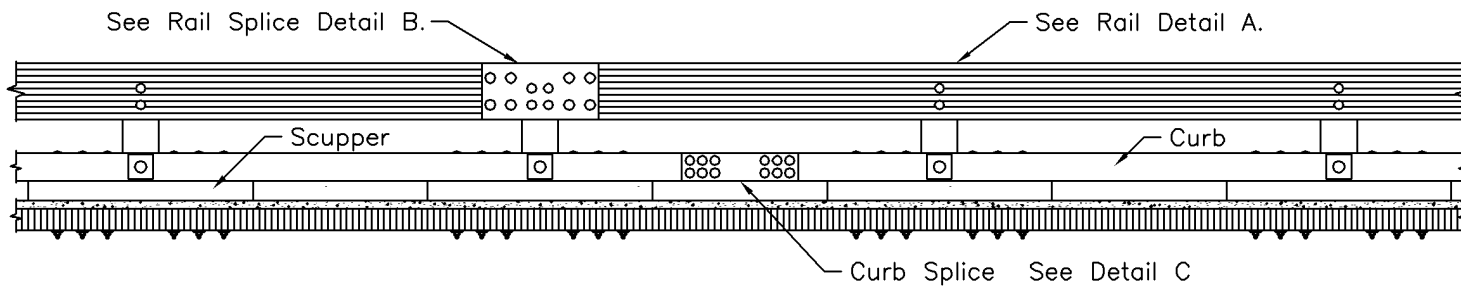
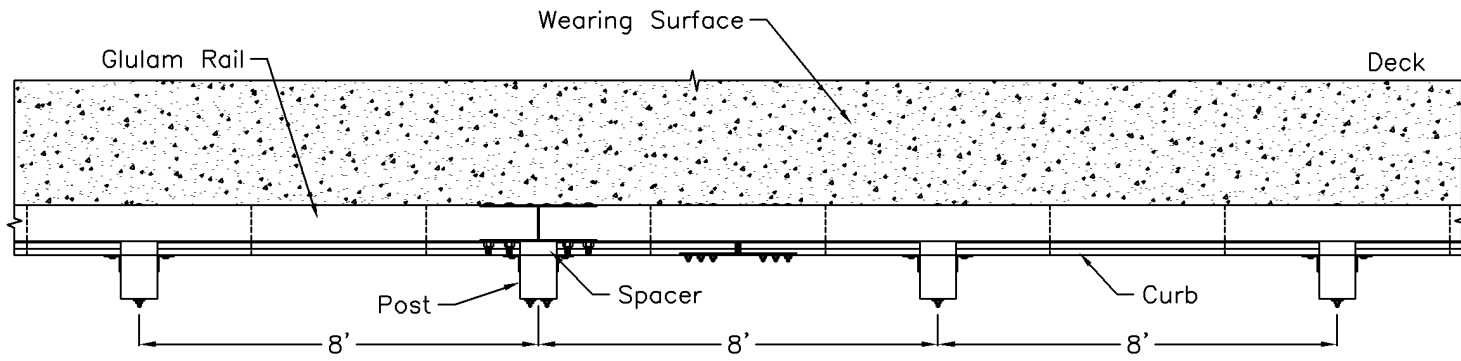


Figure 50. Overall Layout of Wood Bridge Railing System



82

Figure 51. General Configuration of Wood Bridge Railing System

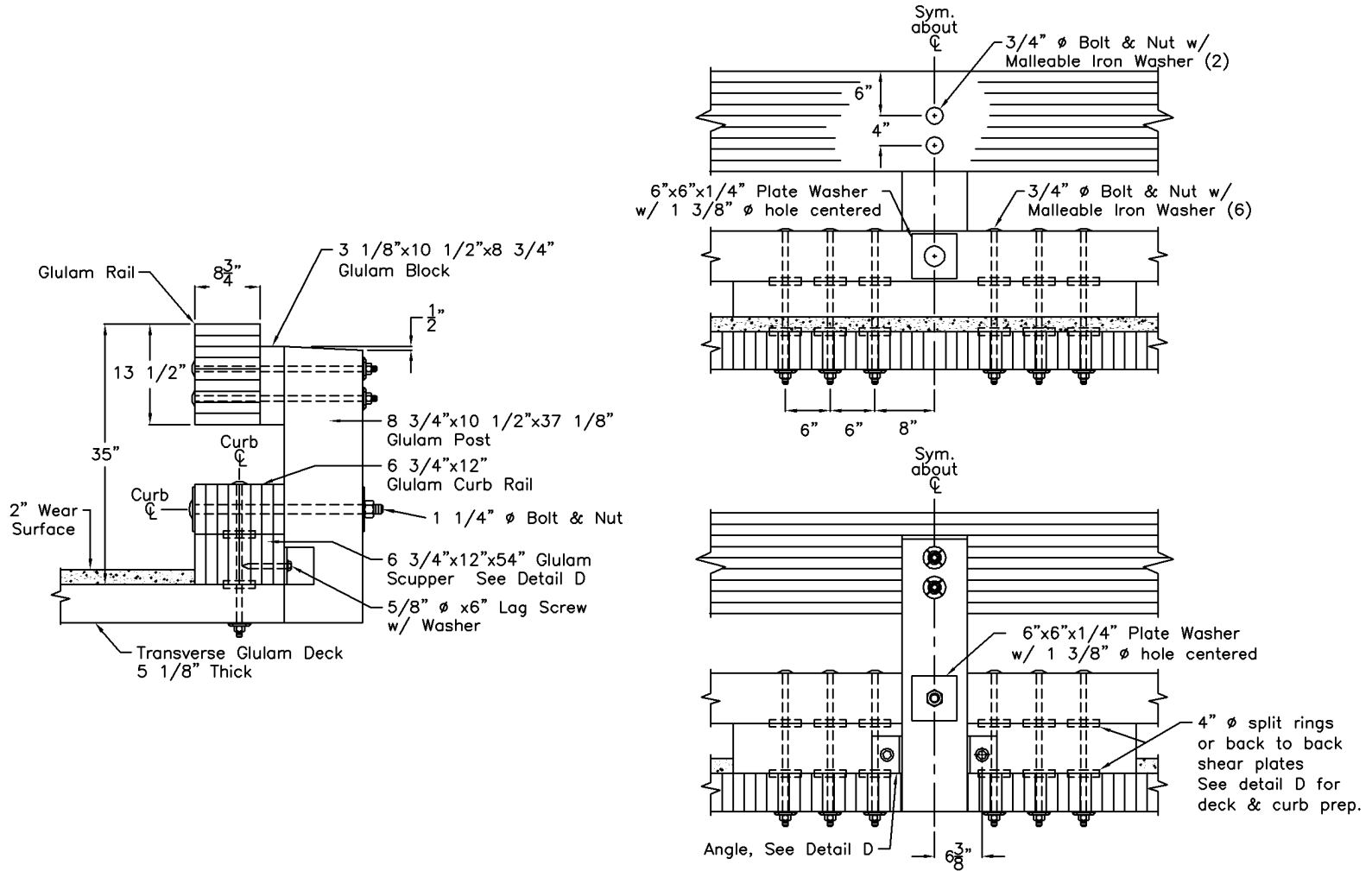
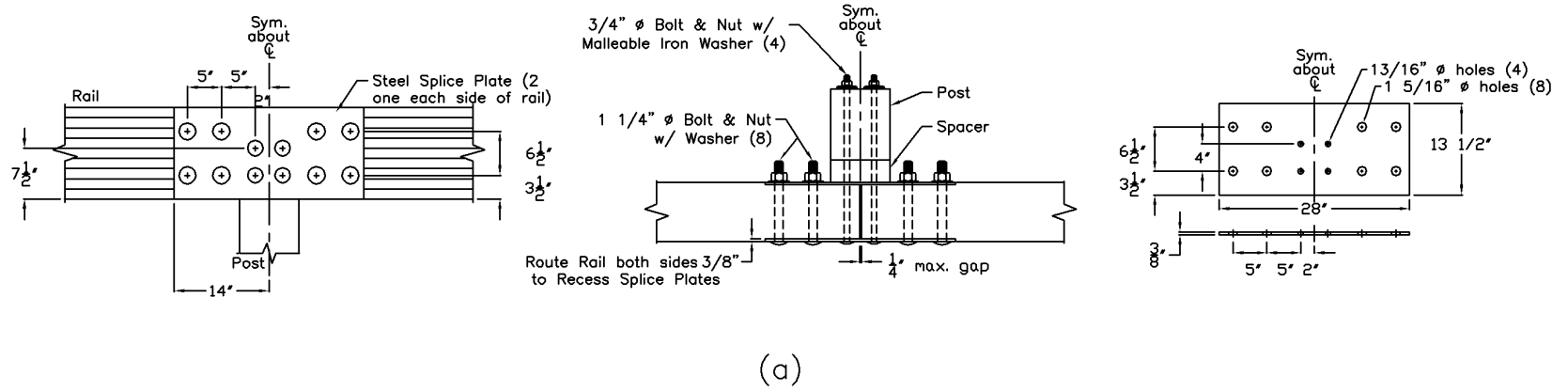
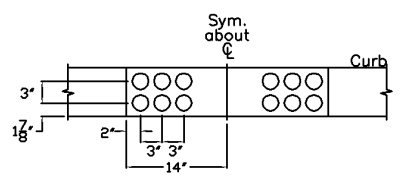
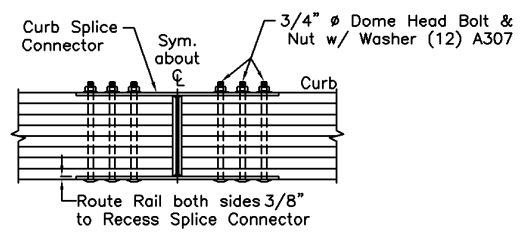


Figure 52. Bridge Railing Design Details - Wood System



(a)



(b)

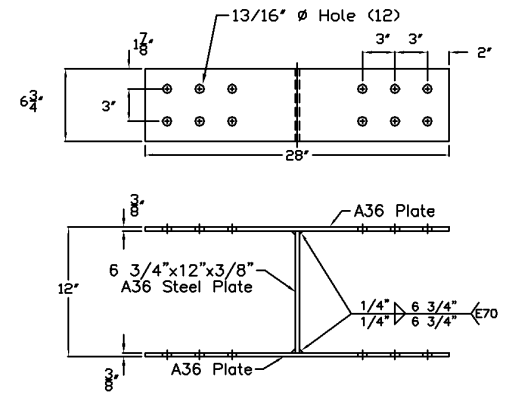
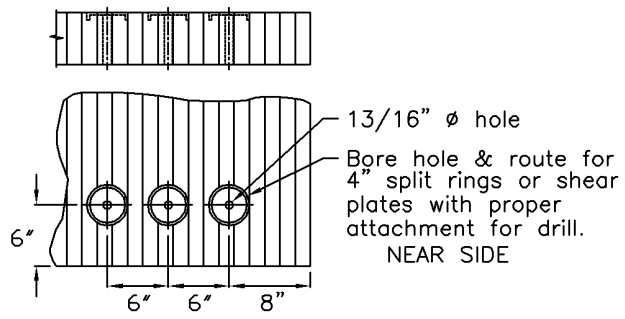
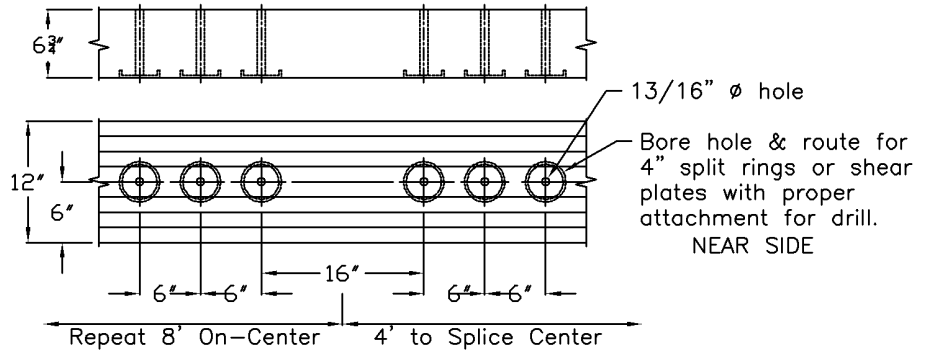


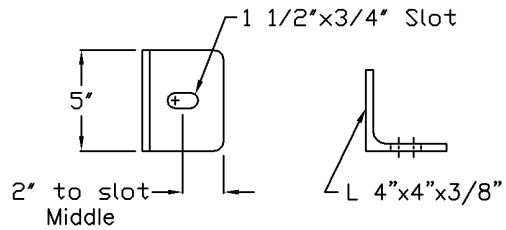
Figure 53. Rail Splice Design Details - Wood System (Note - (a) upper rail and (b) lower curb rail)



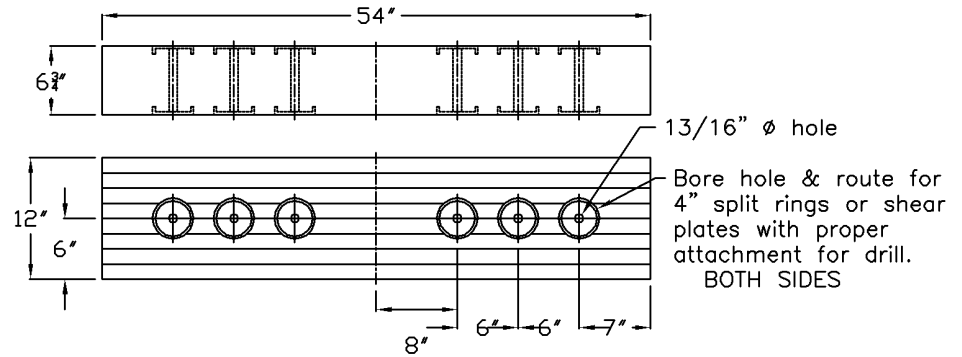
Deck Preparation



Curb Rail Preparation



Angle



Scupper Block

Figure 54. Miscellaneous Design Details

7.2 Approach Guardrail Transition

An approach guardrail transition system was attached to the upstream end of the bridge railing system and was used to connect the standard guardrail to the bridge rail. The approach guardrail transition system consisted of nine major components: (1) a thrie beam terminal connector; (2) a thrie beam rail section; (3) a W-beam to thrie beam transition section; (4) standard W-beam guardrail; (5) timber guardrail posts; (6) a curb transition rail; (7) a transition block; (8) a transition scupper block; and (9) a simulated end anchorage system. Photographs of the approach guardrail transition system are shown in Figures 55 through 58. The overall layout of the approach guardrail transition system is shown in Figure 59. Design details of the approach guardrail transition system are provided in Figures 60 through 65.

The transition block, curb transition rail, and transition scupper block were glulam timber, fabricated from SYP, and treated with pentachlorophenol in heavy oil to a minimum net retention of 9.61 kg/m^3 as specified in AWP Standard C14 (22). The transition block was fabricated from Combination No. 48 material (DF - Combination No. 2 optional) while the curb transition rail and transition scupper block were fabricated from Combination No. 47 material (DF - Combination No. 1 optional).

The approach guardrail transition system was constructed with two different railings, an upper steel thrie beam rail and a lower glulam timber curb rail. The thrie beam rail was 3,810-mm long and fabricated from 3.42-mm thick steel. A 2.66-mm thick W-beam to thrie beam transition section, measuring 1,905-mm long, was used to connect the thrie beam guardrail to 15,240 mm of standard 2.66-mm W-beam guardrail. The thrie beam and W-beam rails had a top mounting height of 804 mm and 702 mm, respectively, as measured from the roadway surface to the top of the rails.

Lap-splice connections between the steel rail sections were configured to reduce vehicle snagging at the splice during the crash tests.

A 2.66-mm thick thrie beam terminal connector was used to attach the thrie beam rail to the upper glulam rail of the bridge railing system. Subsequently, the thrie beam terminal connector bolted to a 13-mm thick steel rail transition plate that mounted to the traffic-side face of the glulam upper rail. A glulam curb transition block was developed and bolted to the bottom of the upper glulam rail. The curb transition block was required in order to increase the depth of the upper rail and provide a surface for rigidly attaching the lower one-third of the thrie beam terminal connector to the upper rail. The downstream end of block was beveled away from the traffic-side face to eliminate any potential for vehicle snag resulting from a “reverse hit” impact.

The glulam curb transition rail was positioned below the thrie beam with the top of the curb 292 mm above the roadway surface. The curb transition rail was 3,331-mm long and attached to the traffic-side face of the first seven transition posts adjacent to the upstream end of the bridge railing. The curb transition rail was 305-mm wide at the attachment to post no. 1 but tapered down to approximately 51 mm upstream of the point of attachment to post no. 7. Subsequently, the curb transition rail was bolted to the upstream end of the lower glulam curb rail of the bridge railing system using a curb transition splice plate. The curb transition splice plate was fabricated with three 9.5-mm thick steel plates welded to form an I-shape.

At both ends of the bridge railing system and between bridge post nos. 1 and 2, a glulam transition scupper block was used to support the lower glulam curb rail and attach the curb rail to the timber deck surface. The transition scupper block measured 171-mm deep by 305-mm wide by 3,124-mm long and was rigidly connected using twelve 19-mm diameter by 521-mm long, ASTM

A307 galvanized dome head bolts.

The system was constructed with eighteen guardrail posts, as shown in Figures 59 through 65. Post nos. 1 through 10 and 11 through 18 were fabricated from SYP, Grade No. 1D and No. 1 or better material, respectively, and treated with chromated copper arsenate (CCA). Post nos. 1 through 4 consisted of 203-mm wide by 203-mm deep by 1,981-mm long timber guardrail posts. Post nos. 5 through 10 consisted of 203-mm wide by 203-mm deep by 1,829-mm long timber guardrail posts. Post nos. 11 through 16 consisted of 152-mm wide by 203-mm deep by 1,829-mm long timber guardrail posts. Post nos. 17 and 18 consisted of 140-mm wide by 191-mm deep BCT timber posts and were placed in steel foundation tubes. Post No. 17 through 18 and the foundation tubes were part of an anchorage system used to develop the required tensile capacity of the guardrail.

For post nos. 1 through 16, treated timber blockouts were used to space the thrie beam and W-beam guardrails away from the traffic-side face of each guardrail post. The blockouts were fabricated from SYP, Grade No. 1 material and treated with CCA. For post nos. 1 through 7, a wood blockout, measuring 152-mm wide x 305-mm deep x 533-mm long, was used with thrie beam guardrail. At post no. 8, a wood blockout, measuring 152-mm wide x 203-mm deep x 572-mm long, was used with thrie beam guardrail without the lower curb transition rail. At post no. 9, a wood blockout, measuring 152-mm wide x 203-mm deep x 435-mm long, was used at the midspan of the W-beam to thrie beam transition section. For post nos. 10 through 16, a wood blockout, measuring 152-mm wide x 203-mm deep x 356-mm long, was used with W-beam guardrail.

The soil embedment depths of the posts were as follows: 1,152 mm for post nos. 1 through 4; 999 mm for post nos. 5 through 7; 993 mm for post no. 8; 1,063 mm for post no. 9; and 1,101 mm for post nos. 10 through 16, as shown in Figure 65. The timber posts were placed in a compacted

coarse, crushed limestone material that met Grading B of AASHTO M147-65 (1990) as found in NCHRP Report No. 350.

Figure 55. Approach Guardrail Transition - Front View

Figure 56. Approach Guardrail Transition - Back View

Figure 57. Approach Guardrail Transition - Parallel View

Figure 58. Connection to Wood Bridge Railing System

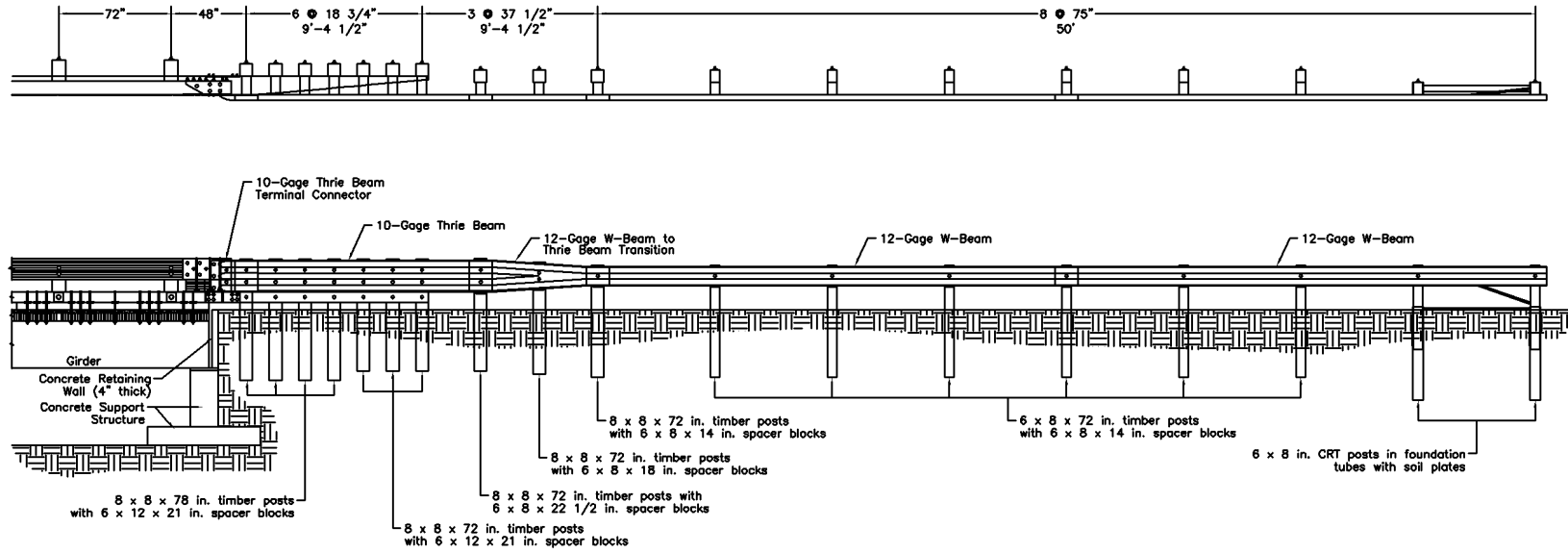


Figure 59. Overall Layout of Approach Guardrail Transition System - Wood System

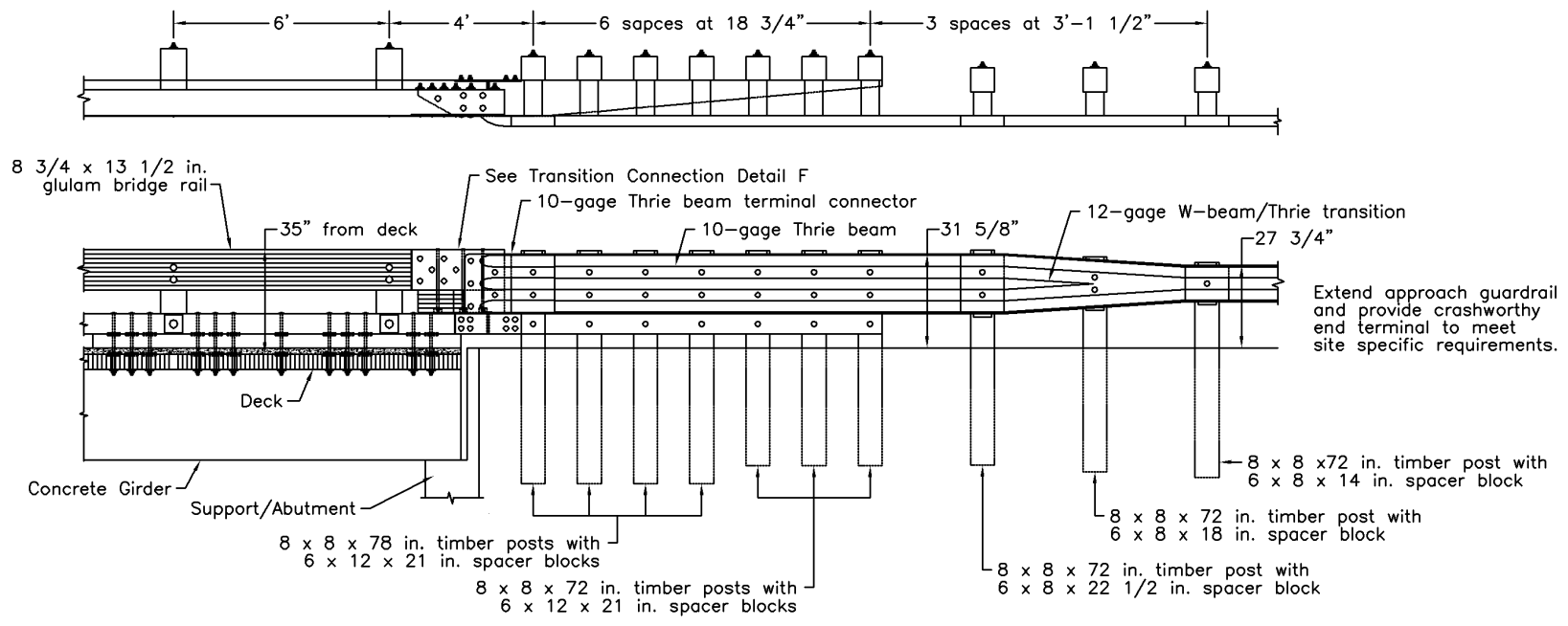


Figure 60. General Configuration of Approach Guardrail Transition System - Wood System

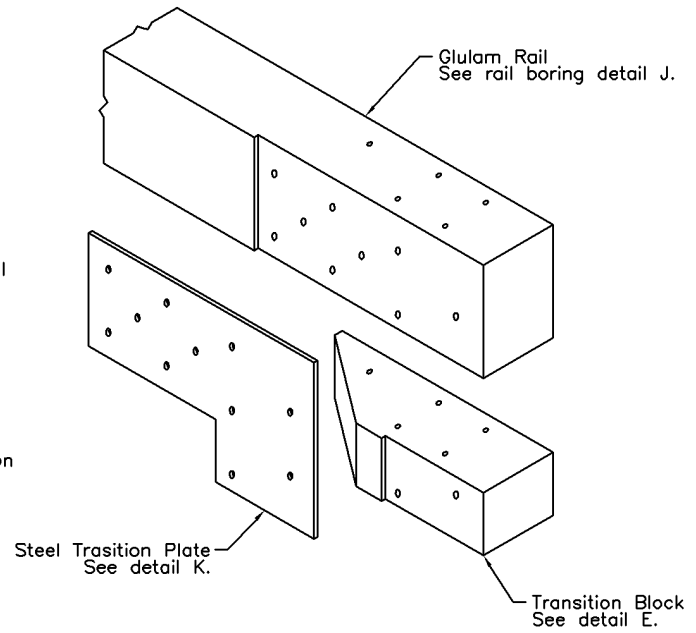
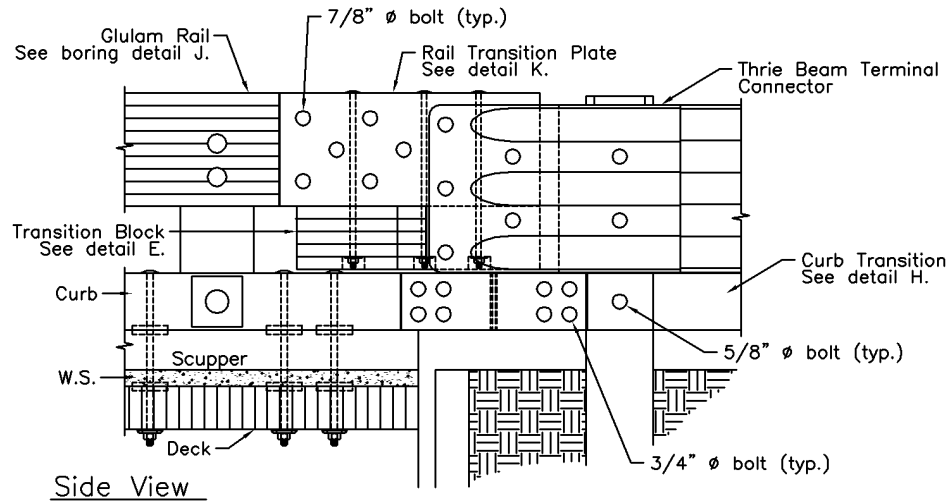
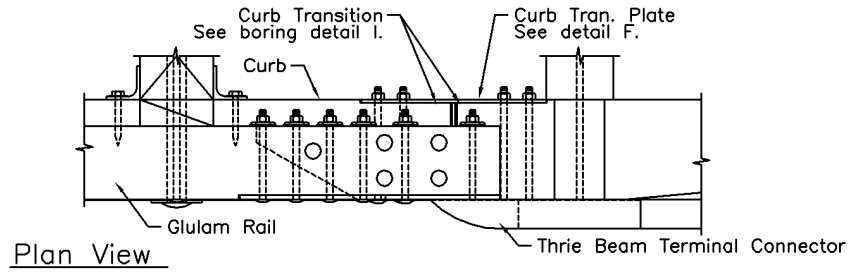
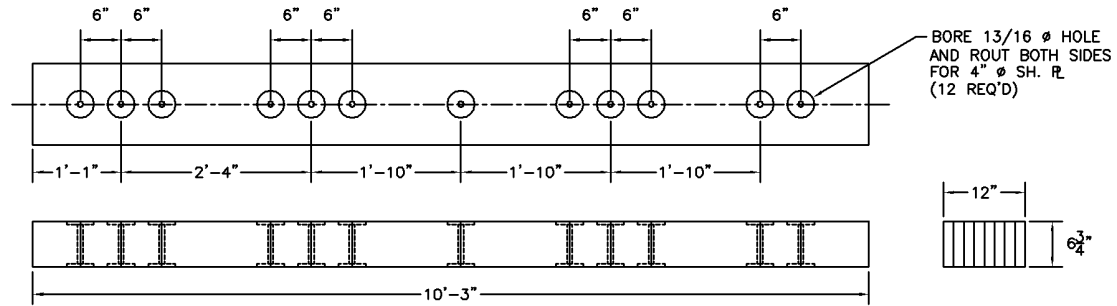
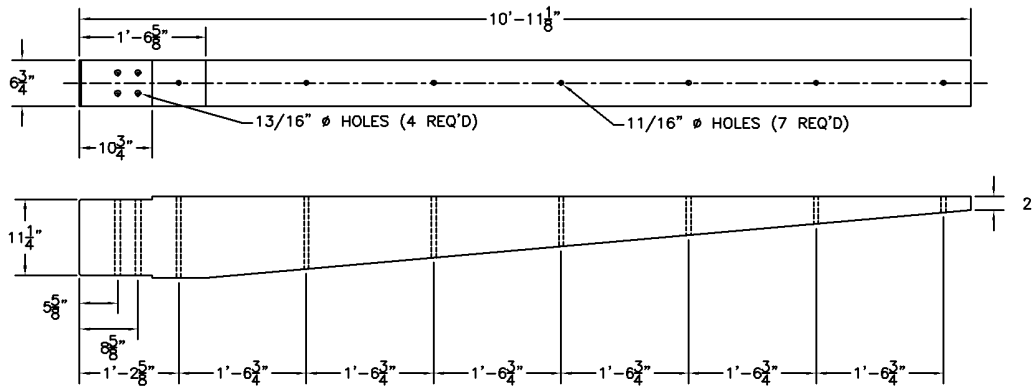


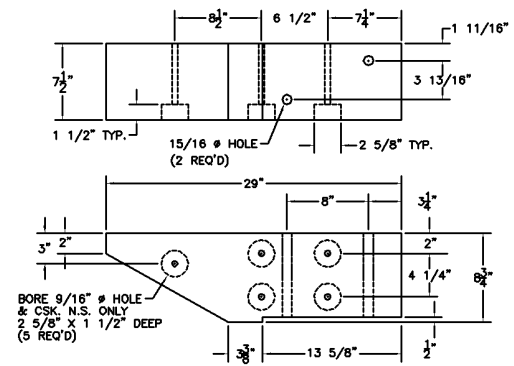
Figure 61. Transition Connection Details - Wood System



Transition Scupper Block

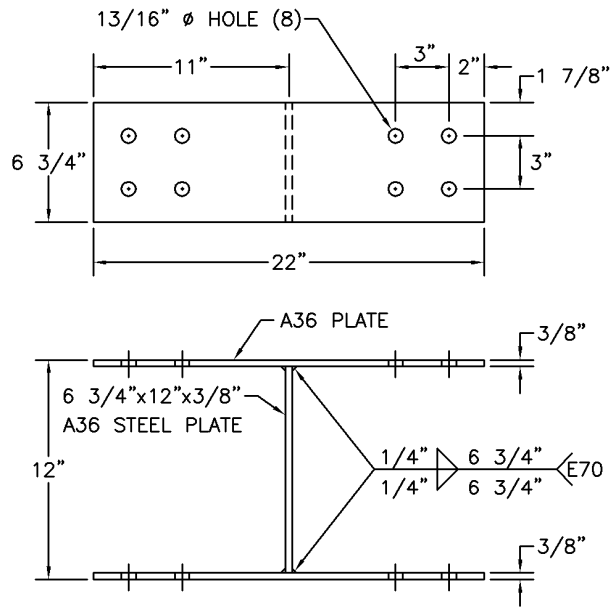


Curb Transition

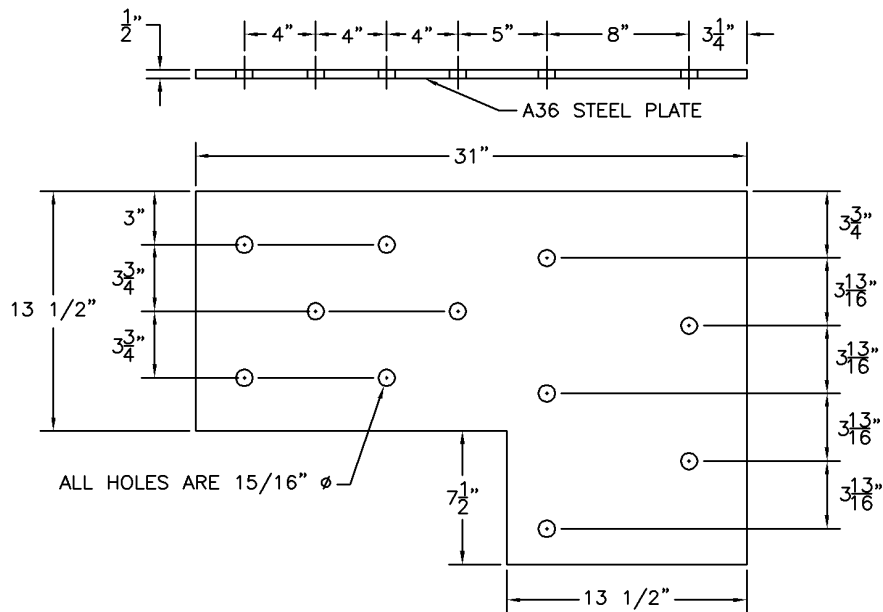


Curb Transition Block

Figure 62. Transition Scupper Block, Curb Transition, and Curb Transition Block - Wood System

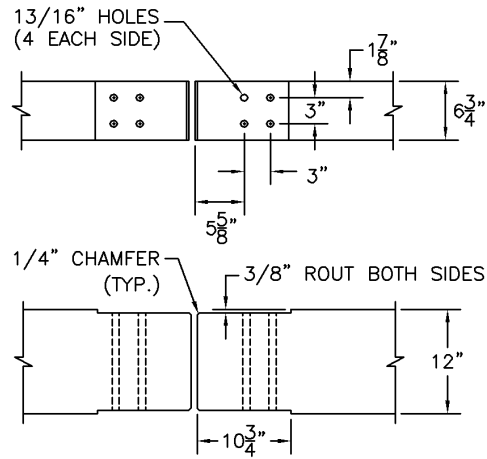


Curb Transition Splice Plate

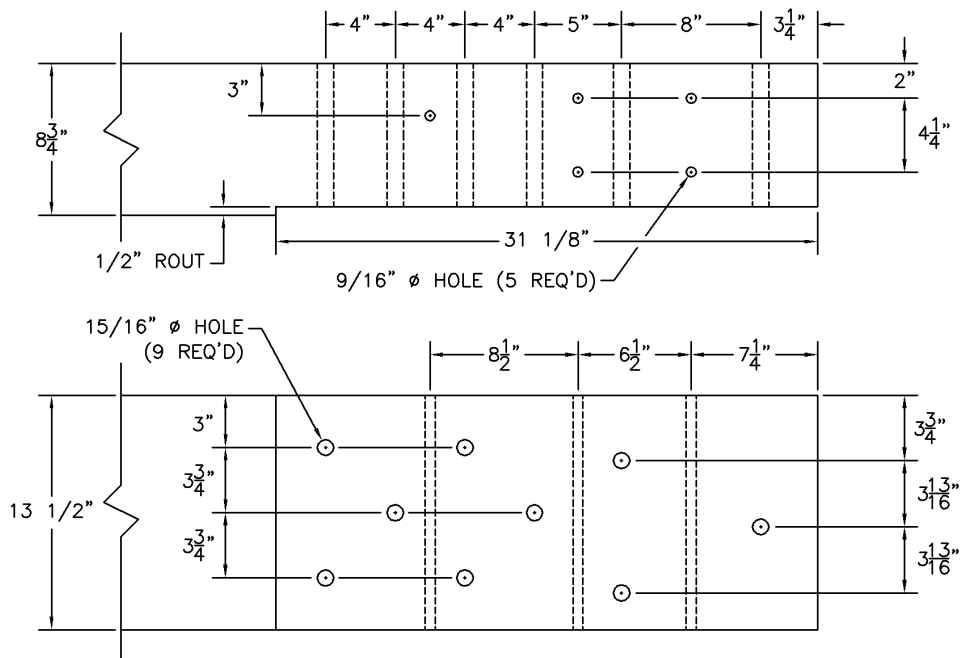


Rail Transition Plate

Figure 63. Curb Transition Splice Plate and Rail Transition Plate - Wood System



Curb Transition Boring



Rail Transition Boring

Figure 64. Curb Transition and Rail Transition Boring Details

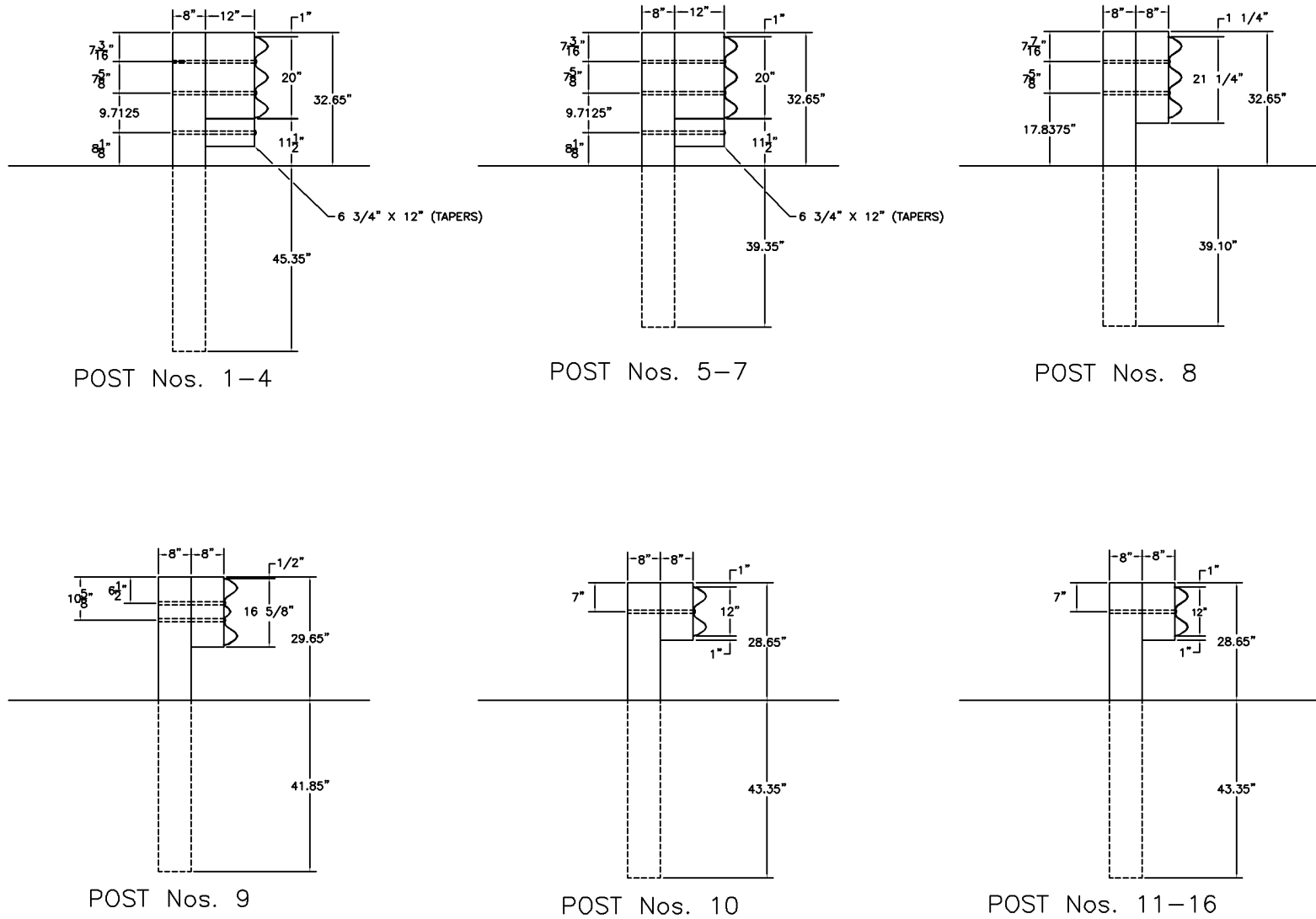


Figure 65. Transition Post Configurations (6 views of posts embedded in soil)

8 COMPUTER SIMULATION

8.1 Introduction

Computer simulation modeling with BARRIER VII (27) was performed to analyze and predict the dynamic performance of the timber bridge railing and approach guardrail transition systems prior to full-scale vehicle crash testing. The simulations were conducted modeling: (1) a 2000-kg pickup truck impacting at a speed of 100.0 km/hr and at an angle of 25 degrees; and (2) an 8,000-kg single-unit truck impacting at a speed of 80 km/hr and at an angle of 15 degrees. The BARRIER VII finite element models of the wood bridge railing and approach guardrail transition systems as well as the idealized finite element, 2-dimensional vehicle models for the pickup truck and single-unit truck are shown in Appendix C. Typical computer simulation input data files for each system and vehicle are shown in Appendix D. Computer simulation was also used to determine the critical impact point (CIP) for the wood bridge railing and approach guardrail transition systems.

8.2 BARRIER VII Results

8.2.1 Bridge Railing Results

The simulation results indicated that the wood bridge railing system described in Section No. 7 would satisfactorily redirect the 2,000-kg pickup truck and the 8,000-kg single unit truck. In addition, all structural hardware would remain functional during both of the vehicle impacts with the bridge railing system.

For the 2,000-kg pickup truck impact simulation, the CIP was determined to occur with an impact at the centerline of bridge post no. 5. The maximum dynamic and permanent set deflections of the timber bridge rail, as measured from the roadway surface to the center of the rail, were 138 mm and 47 mm, respectively. The maximum 0.010-sec average lateral and longitudinal

decelerations were 13.4 and 10.8 g's, respectively. The peak 0.050-sec average impact force perpendicular to the bridge railing was 291.4 kN. The pickup truck became parallel to the bridge railing at 0.179 sec with a velocity of 77.6 km/hr. At 0.250 sec after impact, the pickup truck exited the bridge railing with a velocity of 74.6 km/hr and at an angle of 9.0 degrees.

For the 8,000-kg single-unit truck impact simulation, the CIP was determined to occur with an impact between bridge post nos. 4 and 5 or 1,219-mm upstream from the centerline of bridge post no. 5. The maximum dynamic and permanent set deflections of the timber bridge rail, as measured from the roadway surface to the center of the rail, were 113 mm and 13 mm, respectively. The maximum 0.010-sec average lateral and longitudinal decelerations were 3.6 and 2.2 g's, respectively. The peak 0.050-sec average impact force perpendicular to the bridge railing was 305.3 kN. The truck became parallel to the bridge railing at 0.324 sec with a velocity of 71.3 km/hr. At 0.590 sec after impact, the truck exited the bridge railing with a velocity of 69.2 km/hr and at an angle of 10.6 degrees.

8.2.2 Approach Guardrail Transition Results

The simulation results indicated that the approach guardrail transition system would satisfactorily redirect the 2,000-kg pickup truck and the 8,000-kg single unit truck. In addition, all structural hardware would remain functional during both of the vehicle impacts with the approach guardrail transition system.

For the 2,000-kg pickup truck impact simulation, the CIP was determined to occur with an impact between transition post nos. 2 and 3 or 238-mm upstream of transition post no. 3. The maximum dynamic and permanent set deflections of the thrie beam rail, as measured from the roadway surface to the center of the rail, were 216 mm and 47 mm, respectively. The maximum

0.010-sec average lateral and longitudinal decelerations were 12.8 and 11.1 g's, respectively. The peak 0.050-sec average impact force perpendicular to the bridge railing was 263.1 kN. The pickup truck became parallel to the bridge railing at 0.190 sec with a velocity of 75.4 km/hr. At 0.280 sec after impact, the pickup truck exited the bridge railing with a velocity of 73.0 km/hr and at an angle of 8.4 degrees.

For the 8,000-kg single-unit truck impact simulation, the CIP was determined to occur with an impact between transition post nos. 5 and 6 or 238-mm upstream from post no. 6. The maximum dynamic and permanent set deflections of the three beam rail, as measured from the roadway surface to the center of the rail, were 208 mm and 50 mm, respectively. The maximum 0.010-sec average lateral and longitudinal decelerations were 3.6 and 2.5 g's, respectively. The peak 0.050-sec average impact force perpendicular to the bridge railing was 302.2 kN. The truck became parallel to the bridge railing at 0.323 sec with a velocity of 69.9 km/hr. At 0.590 sec after impact, the truck exited the bridge railing with a velocity of 68.0 km/hr and at an angle of 12.5 degrees.

9 CRASH TEST NO. 1 (WOOD SYSTEM - BRIDGE RAILING)

9.1 Test TRBR-1

The 8,000-kg single-unit truck impacted the bridge railing at a speed of 74.8 km/hr and at an angle of 16.0 degrees. A summary of the test results and the sequential photographs are shown in Figure 66. Additional sequential photographs are shown in Figures 67 and 68. Documentary photographs of the crash test are shown in Figures 69 through 71.

9.2 Test Description

Initial impact occurred at the midspan between bridge post nos. 4 and 5, or approximately 8,903 mm downstream from the upstream end of the bridge rail, as shown in Figure 72. After the initial impact with the bridge rail, the right-front corner of the bumper and quarter panel crushed inward. At 0.137 sec, the leading corner of the box began to overlap the top of the rail. At 0.160 sec, the front of the truck reached post no. 6, and it reached post no. 7 at 0.274 sec. The right-rear tire came into contact with the rail at 0.284 sec. At 0.313 sec, the maximum dynamic lateral rail deflection of 84 mm was measured at post no. 5. At 0.362 sec, the truck box began rolling clockwise toward the rail while the truck cab rolled away from the rail. At 0.394 sec, the left-rear tires lost contact with the ground. At 0.410 sec, the front of the truck was at post no. 8. At 0.426 sec, the right-front tire began to fold under the frame. At 0.525 sec after impact, the longitudinal centerline of the truck box was approximately parallel to the bridge rail with a velocity of 58.7 km/hr. At 0.546 sec, the front of the truck reached post no. 9. At 0.592 sec, the right-front corner of the truck box leaned over the rail and snagged the top of post no. 8. The truck box achieved a maximum clockwise roll angle of approximately 28 degrees at 0.710 sec. At 0.829 sec, 1.054 sec, and 1.230 sec, the right-front corner of the box passed over the top of post nos. 9, 10, and 11, respectively. At approximately

1.522 sec, the truck box rolled away from the rail. Subsequently, the vehicle exited the bridge railing at a speed of approximately 47.3 km/hr and an angle of 0 degrees. The vehicle's trajectory is shown in Figure 66. The vehicle's front-end came to rest approximately 36.9-m downstream from the impact point on the bridge railing, as shown in Figure 73.

9.3 Bridge Rail Damage

The moderate bridge railing damage is shown in Figures 74 and 75. Significant gouging and scrapes occurred to the glulam rail from the midspan between post nos. 4 and 5 to post no. 6, as shown in Figure 74. Minor gouges and scrapes were found on top of the upper rail and occurred when the truck box leaned on the rail, as shown in Figures 74 and 75. The curb rail received gouges between post nos. 4 and 5, as shown in Figure 74.

Bridge post nos. 8 and 9 were damaged near the top of each post due to contact between the truck box and timber posts. Vehicle contact on post no. 8 was measured approximately 102 mm below the top of the post, and approximately 25 mm below the top of post no. 9. No visual damage was evident to the spacer blocks, scupper blocks, or shear plates. Also, no visual damage or displacement relative to the girders was evident on the deck panels. Zero displacement between the girders and deck panels was measured at all potentiometer locations.

Three steel plate washers, located on the back face of the curb rail at post nos. 4 through 6, were deformed due to high axial tension transmitted to the bolts. Several steel dome head bolts were also damaged at the top rail splice located at post no. 6. Also, the curb rail steel splice H-plate between post nos. 5 and 6 was slightly deformed.

The maximum lateral permanent set deflections for midspan rail and post locations, as determined from field measurements in the impact region, were approximately 10 mm and 8 mm,

respectively. The maximum dynamic lateral deflections for midspan rail and post locations, as determined from high-speed film analysis, were 69 mm and 84 mm, respectively. The effective coefficient of friction was determined to be approximately 0.65.

9.4 Vehicle Damage

Exterior vehicle damage was moderate, as shown in Figures 76 through 78. Vehicle damage occurred to several body locations, such as right-side door and quarter panels, front bumper, right-side wheels and rims, front axle, truck box and support frame, and the side-mounted foot step. The right corner of the front bumper and the right-side door and quarter panels were crushed inward as shown in Figure 76. The lower right-front corner of the truck box was deformed inward, as shown in Figure 76. The front axle, with attached tires and steel rims, was removed from the truck and came to rest under the truck frame, as shown in Figures 76 and 77. The right-rear steel rim was also deformed, as shown in Figure 77. The truck box was shifted to the right of the longitudinal centerline of the truck cab and support frame. U-bolts, used to attach the box to the frame, were also deformed due to the box shift, as shown in Figure 78.

9.5 Occupant Risk Values

The longitudinal and lateral occupant impact velocities were determined to be 2.15 m/sec and 2.78 m/sec, respectively. The maximum 0.010-sec average occupant ridedown decelerations in the longitudinal and lateral directions were 3.27 g's and 5.00 g's, respectively. It is noted that the occupant impact velocities and occupant ridedown decelerations were within the suggested limits provided in NCHRP Report No. 350. The results of the occupant risk, determined from accelerometer data, are summarized in Figure 66. Results are shown graphically in Appendix E.

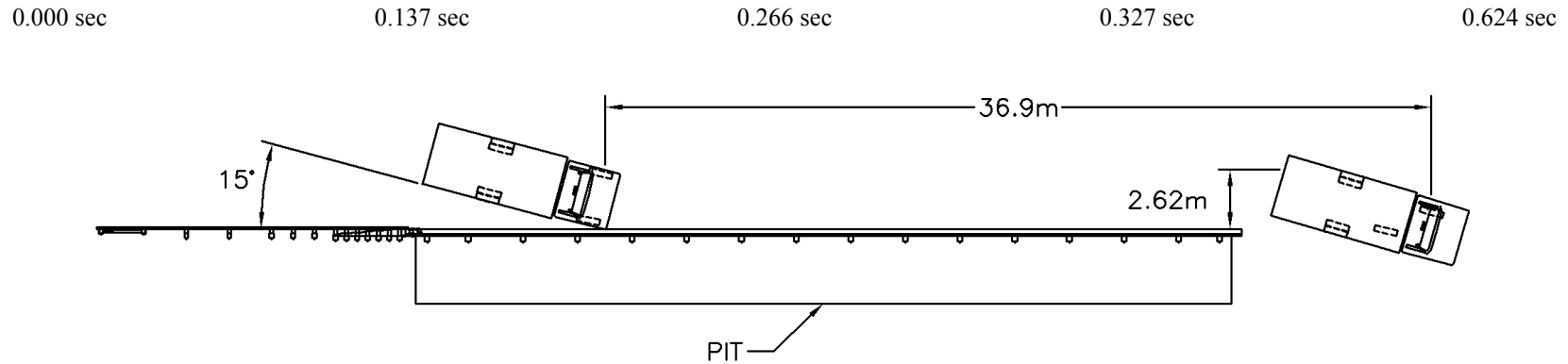
9.6 Discussion

The analysis of the test results for test TRBR-1 showed that the barrier adequately contained and redirected the vehicle with controlled lateral displacement of the barrier. Minor deformations to the occupant compartment were evident but not considered excessive enough to cause serious injuries to the occupants. The vehicle remained upright both during and after the collision. Vehicle roll, pitch, and yaw angular displacements were noted, but they were deemed acceptable. After collision, the vehicle's trajectory did not intrude into adjacent traffic lanes. In addition, the vehicle's exit angle was less than 60 percent of the impact angle. Therefore, test TRBR-1 conducted on the wood bridge rail system was determined to be acceptable according to the NCHRP Report No. 350 performance criteria.

Prior to performing the pickup truck test, the first two top rails and first curb rail located on the upstream end of the bridge were replaced. In addition, post nos. 8 and 9, as well as all visibly damaged bolts and steel hardware near the impact region were replaced.

9.7 Barrier Instrumentation Results

For test TRBR-1, strain gauges and string potentiometers were located on selected components of the wood bridge railing system. The results of the strain gauge and string potentiometer analyses are summarized in Table 3. Results of the strain gauge and string potentiometer are also shown graphically in Appendices F and G, respectively.



- Test Number TRBR-1
- Date 3/11/97
- Appurtenance Wood Bridge Rail with Curb Rail System for Transverse Decks
- Total Length 37.19 m
- Wood Upper Rail
 - Material Southern Yellow Pine, Combination No. 48
 - Dimensions 222 mm x 343 mm x 36.58 m
 - Top Mounting Height 838 mm
- Upper Rail Wood Post Nos. 1-16
 - Material Southern Yellow Pine, Combination No. 48
 - Dimensions 222 mm x 267 mm x 943 mm
- Upper Rail Wood Spacer Blocks Nos. 1-16
 - Material Southern Yellow Pine, Combination No. 47
 - Dimensions 79 mm x 222 mm x 267 mm
- Wood Lower Curb Rail
 - Material Southern Yellow Pine, Combination No. 47
 - Dimensions 171 mm x 305 mm x 36.58 mm
 - Top Mounting Height 292 mm
- Lower Curb Rail Wood Scupper Blocks Nos. 3-14
 - Material Southern Yellow Pine, Combination No. 47
 - Dimensions 171 mm x 305 mm x 1,372 mm
- Vehicle Model 1986 Ford F-800 Series Single-Unit Truck
 - Curb 5,284 kg
 - Test Inertial 8,000 kg
 - Gross Static 8,000 kg
- Vehicle Speed
 - Impact 74.8 km/hr
 - Exit 47.3 km/hr
- Vehicle Angle
 - Impact 16.0 deg
 - Exit 0 deg
- Vehicle Snagging None
- Vehicle Stability Satisfactory
- Effective Coefficient of Friction (μ) 0.65
- Occupant Ridedown Deceleration (10 msec avg.)
 - Longitudinal (not required) 3.27 < 20 G's
 - Lateral (not required) 5.00
- Occupant Impact Velocity
 - Longitudinal (not required) 2.15 < 12 m/s
 - Lateral (not required) 2.78
- Vehicle Damage Moderate
 - TAD²⁸ 1-RFQ-4
 - SAE²⁹ 01-RFEW3
- Vehicle Stopping Distance 36.9 m downstream
2.6 m lateral
- Bridge Rail Damage Moderate
- Maximum Deflections
 - Permanent Set 10 mm
 - Dynamic 84 mm

Figure 66. Summary of Test Results and Sequential Photographs, Test TRBR-1

0.000 sec

0.426 sec

0.090 sec

0.525 sec

0.146 sec

0.635 sec

0.325 sec

1.171 sec

0.362 sec

1.522 sec

0.394 sec

2.566 sec

Figure 67. Additional Sequential Photographs, Test TRBR-1

0.000 sec

0.294 sec

0.058 sec

0.492 sec

0.190 sec

0.520 sec

0.240 sec

0.592 sec

Figure 68. Additional Sequential Photographs, Test TRBR-1

Figure 69. Documentary Photographs, Test TRBR-1

Figure 70. Documentary Photographs, Test TRBR-1

Figure 71. Documentary Photographs, Test TRBR-1

Figure 72. Impact Locations, Test TRBR-1

Figure 73. Final Vehicle Position, Test TRBR-1

Figure 74. Barrier Damage, Test TRBR-1

Figure 75. Typical Top of Post and Rail Damage, Test TRBR-1

Figure 76. Vehicle Damage, Test TRBR-1

Figure 77. Front and Rear Wheel Assembly Damage, Test TRBR-1

Figure 78. Damage to Truck Box Attachment Hardware, Test TRBR-1

Table 3. Strain Gauge and String Potentiometer Results, Test TRBR-1

Hardware Type	Gauge No.	Gauge Location	Maximum μ Strain ¹ (mm/mm)	Maximum Load ² (kN)	Maximum Stress ^{3,4} (MPa)	Comments
Strain Gauge	1	Post Bolt No. 3	486	62.02	99.2	Bolt attaching curb rail to post
	2	Post Bolt No. 4	806	102.65	164.2	Bolt attaching curb rail to post
	3	Post Bolt No. 5	1,043	126.98	203.1	Bolt attaching curb rail to post
	4	Post Bolt No. 6	1,036	125.99	201.5	Bolt attaching curb rail to post
	5	Post Bolt No. 7	806	128.12	204.9	Bolt attaching curb rail to post
	6	Post Bolt No. 8	551	68.74	110.0	Bolt attaching curb rail to post
	7	Top Rail Plate No. 1	NA	NA	NA	Traffic-side face at post no. 6
	8	Top Rail Plate No. 1	657	NA	136.0	Back-side face at post no. 6
	9	Curb Rail Plate No. 1	212	NA	43.9	Back-side face at midspan between post nos. 5 and 6
	10	Wood Rail	NA	NA	NA	Back-side face at midspan between post nos. 5 and 6
String Potentiometer	Gauge No.	Gauge Location	Relative Maximum Deck to Girder Displacement (mm)		Comments	
	1	String Pot No. 1	0.094		Midspan girder no. 1 (outer girder)	
	2	String Pot No. 2	0.538		¾-point girder no. 1 (outer girder)	
	3	String Pot No. 3	0.224		⅞-point girder no. 1 (outer girder)	
	4	String Pot No. 4	1.049		Joint between girder no. 1 and 2 (outer girder)	
	5	String Pot No. 5	0.300		¼-point girder no. 2 (outer girder)	

¹ - All strain values are shown as the absolute value only.

² - All load values calculated using calibration factor obtained from individual load test data.

³ - For bolts, elastic stress values are shown as the absolute value only and calculated by dividing the load by the tensile stress area equal to 625.16 mm² (0.969 in²). Minimum yield stress for the bolts is 248 MPa (36 ksi).

⁴ - For plates, elastic stress values are shown as the absolute value only and calculated by multiplying the strain by the modulus of elasticity equal to 207,000 MPa (30,000 ksi). Minimum yield stress for the plates is 248 MPa (36 ksi).

NA - Not available or not applicable.

10 CRASH TEST NO. 2 (WOOD SYSTEM - BRIDGE RAILING)

10.1 Test TRBR-2

The 1,993-kg pickup truck impacted the bridge railing at a speed of 99.2 km/hr and at an angle of 27.4 degrees. A summary of the test results and the sequential photographs are shown in Figure 79. Additional sequential photographs are shown in Figures 80 and 81. Documentary photographs of the crash test are shown in Figures 82 through 84.

10.2 Test Description

Initial impact occurred at the centerline of bridge post no. 5 or approximately 10,122 mm downstream from the upstream end of the bridge rail, as shown in Figure 85. After the initial impact with the bridge rail, the right-front tire was deformed, allowing the steel rim to gouge into the traffic-side face of both the curb and upper glulam rails. Subsequently, the right-front corner of the bumper and quarter panel crushed inward. At 0.122 sec, the maximum dynamic lateral deflection of 203 mm was measured at post no. 5. At 0.187 sec, the front of the truck was at post no. 7. The left-front tire lost contact with the ground at 0.191 sec. At 0.238 sec after impact, the vehicle became parallel to the bridge rail with a velocity of 66.0 km/hr when the right-rear tire contacted the rail. At 0.299 sec, the right-front tire lost contact with the ground, and the front of the truck was at post no. 8. At 0.323 sec, the entire pickup truck was airborne. The vehicle exited the bridge railing at a speed of approximately 62.3 km/hr and an angle of 2.1 degrees at 0.437 sec. At 0.514 sec, the left-front tire re-contacted the deck surface. At 0.667 sec, the vehicle achieved a maximum clockwise roll angle of approximately 33.7 degrees toward the rail. The vehicle's post-impact trajectory is shown in Figure 79. The vehicle's front-end came to rest approximately 47.5-m downstream from post no. 5, as shown in Figure 86. The rebound distance, as measured from the traffic-side face of the bridge

rail to the right side of the vehicle, was approximately 2.92 m.

10.3 Bridge Rail Damage

The moderate bridge railing damage is shown in Figures 87 and 88. Significant gouging and scrapes occurred to the upper glulam rail between post nos. 5 and 6, as shown in Figure 87. The curb rail was gouged slightly downstream of post no. 5, as shown in Figure 87.

Three steel plate washers, located on the back face of the curb rail at post nos. 5 through 7, were deformed due to high axial tension transmitted to the bolts, as shown in Figure 88. The steel splice plate located on the traffic-side face of the upper glulam rail at post no. 6 was deformed due to the vehicle snagging on the upstream edge of the plate. Also, the curb rail steel splice H-plate between post nos. 5 and 6 was slightly deformed.

The maximum lateral permanent set deflections for midspan rail and post locations, as determined from field measurements in the impact region, were approximately 22 mm and 29 mm, respectively. The maximum dynamic lateral deflections for midspan rail and post locations, as determined from high-speed film analysis, were 126 mm and 203 mm, respectively. The effective coefficient of friction was determined to be approximately 0.48.

10.4 Vehicle Damage

Exterior vehicle damage was moderate, as shown in Figures 89 through 91. Vehicle damage occurred to several body locations, such as right-side door and quarter panels, front bumper, right-side wheels and rims, windshield, and interior floorboard. The right corner of the front bumper and quarter panels were crushed inward due to contact with the upper glulam rail, as shown in Figure 89. The right-front wheel assembly was pushed back toward the firewall, as shown in Figure 89. The right-front tire was deflated and partially removed from the steel rim, and the right-front steel rim

was deformed, as shown in Figures 89 and 90. The right-rear wheel assembly and axle were pushed back, and the steel rim and tire were deformed and deflated, respectively, as shown in Figure 90. The front windshield was cracked on the passenger side. Maximum occupant compartment deformations to the floorboard were 127-mm lateral displacement near the firewall region, 102-mm longitudinal displacement near the right-side floorboard, and 91-mm vertical displacement under the seat along the centerline of the hump. Interior vehicle deformations to the floorboard, as shown in Figure 91, were judged insufficient to cause serious injury to the vehicle occupants. No deformation occurred to the interior front dashboard.

10.5 Occupant Risk Values

The longitudinal and lateral occupant impact velocities were determined to be 7.39 m/sec and 7.50 m/sec, respectively. The maximum 0.010-sec average occupant ridedown decelerations in the longitudinal and lateral directions were 7.09 g's and 8.95 g's, respectively. It is noted that the occupant impact velocities and occupant ridedown decelerations were within the suggested limits provided in NCHRP Report No. 350. The results of the occupant risk, determined from accelerometer data, are summarized in Figure 79 and are shown graphically in Appendix H. The results from the rate transducer are shown graphically in Appendix I.

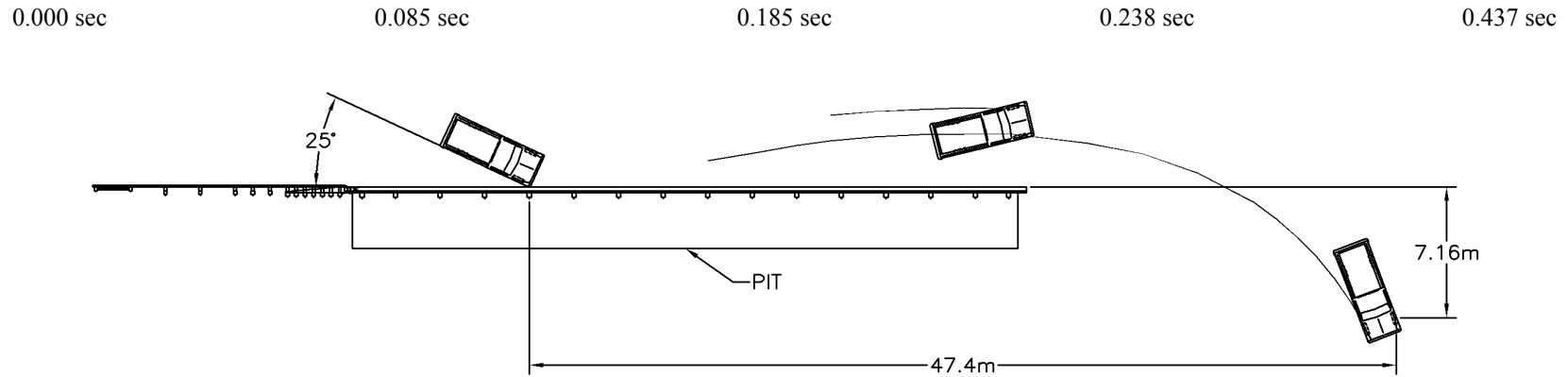
10.6 Discussion

The analysis of the test results for test TRBR-2 showed that the barrier adequately contained and redirected the vehicle with controlled lateral displacement of the barrier. Minor deformations to the occupant compartment were evident but not considered excessive enough to cause serious injuries to the occupants. The vehicle remained upright both during and after the collision. Vehicle roll, pitch, and yaw angular displacements were noted, but they were deemed acceptable. After

collision, the vehicle's trajectory did not intrude into adjacent traffic lanes. In addition, the vehicle's exit angle was less than 60 percent of the impact angle. Therefore, test TRBR-2 conducted on the wood bridge rail system was determined to be acceptable according to the NCHRP Report No. 350 performance criteria.

10.7 Barrier Instrumentation Results

For test TRBR-2, strain gauges and string potentiometers were located on selected components of the wood bridge railing system. However, no strain gauge or string potentiometer instrumentation data was acquired due to technical difficulties encountered in the data acquisition system, as a central data wire became dislodged.



- Test Number TRBR-2
- Date 3/19/97
- Appurtenance Wood Bridge Rail with Curb Rail System for Transverse Decks
- Total Length 37.19 m
- Wood Upper Rail
 - Material Southern Yellow Pine, Combination No. 48
 - Dimensions 222 mm x 343 mm x 36.58 m
 - Top Mounting Height 838 mm
- Upper Rail Wood Post Nos. 1 - 16
 - Material Southern Yellow Pine, Combination No. 48
 - Dimensions 222 mm x 267 mm x 943 mm
- Upper Rail Wood Spacer Block Nos. 1 - 16
 - Material Southern Yellow Pine, Combination No. 47
 - Dimensions 79 mm x 222 mm x 267 mm
- Wood Lower Curb Rail
 - Material Southern Yellow Pine, Combination No. 47
 - Dimensions 171 mm x 305 mm x 36.58 m
 - Top Mounting Height 292 mm
- Lower Curb Rail Wood Scupper Block Nos. 3 - 14
 - Material Southern Yellow Pine, Combination No. 47
 - Dimensions 171 mm x 305 mm x 1,372 mm
- Vehicle Model 1988 Ford F-250 ¾-Ton Pickup Truck
 - Curb ... 1,822 kg
 - Test Inertial 1,993 kg
 - Gross Static 1,993 kg
- Vehicle Speed
 - Impact 99.2 km/hr
 - Exit 62.3 km/hr
- Vehicle Angle
 - Impact 27.4 deg
 - Exit 2.1 deg
- Vehicle Snagging None
- Vehicle Stability Satisfactory
- Effective Coefficient of Friction (μ) 0.48
- Occupant Ridedown Deceleration (10 msec avg.)
 - Longitudinal 7.09 < 20 G's
 - Lateral (not required) 8.95
- Occupant Impact Velocity
 - Longitudinal 7.39 < 12 m/s
 - Lateral (not required) 7.50
- Vehicle Damage Moderate
 - TAD²⁸ 1-RFQ-6
 - SAE²⁹ 01-RYAW5
- Vehicle Stopping Distance 47.4 m downstream
7.2 m lateral behind
- Bridge Rail Damage Moderate
- Maximum Deflections
 - Permanent Set 29 mm
 - Dynamic 203 mm

Figure 79. Summary of Test Results and Sequential Photographs, Test TRBR-2

0.000 sec

0.344 sec

0.082 sec

0.551 sec

0.179 sec

0.667 sec

0.217 sec

0.853 sec

0.323 sec

2.842 sec

Figure 80. Additional Sequential Photographs, Test TRBR-2

0.000 sec

0.000 sec

0.070 sec

0.062 sec

0.092 sec

0.088 sec

0.190 sec

0.191 sec

0.321 sec

0.345 sec

Figure 81. Additional Sequential Photographs, Test TRBR-2

Figure 82. Documentary Photographs, Test TRBR-2

Figure 83. Documentary Photographs, Test TRBR-2

Figure 84. Documentary Photographs, Test TRBR-2

Figure 85. Impact Locations, Test TRBR-2

Figure 86. Final Vehicle Position, Test TRBR-2

Figure 87. Barrier Damage, Test TRBR-2

Figure 88. Steel Plate Deformations at Post No. 6, Test TRBR-2

Figure 89. Vehicle Damage, Test TRBR-2

Figure 90. Front and Rear Wheel Assembly Damage, Test TRBR-2

Figure 91. Occupant Compartment Deformations, Test TRBR-2

11 CRASH TEST NO. 3 (WOOD SYSTEM - APPROACH GUARDRAIL TRANSITION)

11.1 Test TRBR-3

The 2,029-kg pickup truck impacted the approach guardrail transition at a speed of 104.9 km/hr and at an angle of 26.4 degrees. A summary of the test results and the sequential photographs are shown in Figure 92. Additional sequential photographs are shown in Figures 93 and 94. Documentary photographs of the crash test are shown in Figures 95 through 96.

11.2 Test Description

Initial impact occurred at the midspan between transition post nos. 3 and 4 or 1,432 mm upstream from the upstream end of the glulam bridge rail, as shown in Figures 97. After the initial impact with the approach guardrail transition, the right-front quarter panel and bumper were crushed inward. Subsequently, at 0.022 sec after impact, the right-front corner of the vehicle was at transition post no. 2 and with the engine hood extending over the rail. At 0.040 sec, the right-front corner of the vehicle was at transition post no. 1. The right-front corner of the vehicle was positioned at the midpoint between transition post no. 1 and bridge post no. 1 at 0.061 sec. At 0.067 sec, the right-front quarter panel contacted the upstream end of the upper glulam rail, resulting in moderate quarter panel deformations. The pickup truck's right-front corner was near bridge post no. 1 at 0.089 sec with the engine hood positioned laterally behind the back of the bridge post. In addition, deformations were evident in the right-side door as a gap appeared at the top. The maximum dynamic lateral deflection of 163 mm was measured at transition post no. 1 at 0.089 sec. The maximum vehicle extension over the bridge rail occurred at 0.091 sec. At 0.120 sec, the vehicle's right-front corner was approximately at the midpoint between bridge post nos. 1 and 2 and with bridge post no. 1 visibly rotated backward. At 0.150 sec, the left-front tire became airborne, while

at 0.156 sec, the pickup truck's right corner was positioned at bridge post no. 2. At 0.158 sec, contact was made between the three beam rail and the right corner of the rear bumper, resulting in the vehicle's right-rear corner lifting up above the guardrail. At 0.212 sec, significant twisting about the vehicle's roll axis was observed between the pickup truck cab and box, resulting in the cab rotated clockwise (CW) toward the rail and the box rotated counter-clockwise (CCW) away from the rail. At 0.222 sec, the left-rear tire became airborne. At 0.243 sec after impact, the vehicle became parallel to the bridge rail with a velocity of 73.0 km/hr when the right-front corner of the vehicle reached bridge post no. 3. At 0.250 sec, the pickup truck's right-rear corner of the bumper extended over the guardrail and snagged on the top of wood blockout for transition post no. 1. Subsequently, the right-front tire became airborne at 0.258 sec after impact. At 0.306 sec, the deformed right-rear bumper was positioned on the top surface of the glulam rail, gouging into the wood material as it moved longitudinally along the rail. The vehicle became completely airborne at 0.322 sec after impact. At 0.365 sec, the pickup truck's front end was separating away from the bridge rail. At 0.391 sec, the right-rear bumper was positioned approximately at bridge post no. 2. At 0.494 sec, the right-front tire was in contact with the ground. The vehicle exited the bridge railing at a speed of approximately 71.1 km/hr and an angle of 11.9 degrees at 0.553 sec. At 0.684 sec, the vehicle achieved a maximum clockwise roll angle of approximately 17.3 degrees toward the rail. The vehicle's post-impact trajectory is shown in Figure 92. The vehicle's front-end came to rest approximately 73.2-m downstream from the midspan location between transition post nos. 3 and 4, as shown in Figure 98. The rebound distance was approximately 7.16 m, as measured laterally from the traffic-side face of the barrier to the right side of the vehicle and longitudinally downstream from impact at a point of 30.48 m plus the length of the vehicle.

11.3 Bridge Rail and Approach Guardrail Transition Damage

The minor damage to the approach guardrail transition and bridge railing is shown in Figures 99 through 101. Damage consisted mostly of deformed thrie beam, displaced guardrail posts, and scrapes, black marks, and gouging on the various rails, posts, and blocks. As shown in Figures 99 and 100, gouging occurred on the middle and lower corrugations of the thrie beam rail near transition post no. 3. Black marks, scrapes, and gouging were visible on the thrie beam from the impact location through the thrie beam terminal connector. No visual contact marks or scrapes were found on the face of the timber curb rail below the thrie beam, except for the region where the deformed thrie contacted the curb corner. Minor contact marks were found on the curb transition splice plate. The spacer blocks for transition post nos. 1 and 2 were also contacted and gouged. Following a visual inspection after the crash test, no damage was observed in the guardrail posts. In addition, the maximum ground line soil deformations, occurring at transition post no. 1, were measured to be 19 mm and 22 mm on the front and back sides of the guardrail posts, respectively.

Gouging was observed on the upper surface of the top glulam bridge rail from the upstream end to 51 mm downstream of bridge post no. 2. Black contact marks and gouging were also observed on the upper rail's front face over the same length. On the upper rail's steel transition plate, contact marks and gouging were found on the front face. The right-side rear axle hub also contacted this plate as a bolt head from the hub was embedded in the front face. For the lower curb rail, contact marks and gouging were observed on the front surface from the curb transition splice plate to 686 mm downstream of bridge post no. 1. Minor gouging was also found on the curb transition block. Two steel plate washers, located on the back face of the curb rail at post nos. 1 and 2, were deformed due to high axial tension transmitted to the bolts.

The maximum lateral permanent set deflections for midspan rail and post locations, as determined from field measurements in the impact region, were approximately 33 mm and 35 mm, respectively. The maximum dynamic lateral deflections for bridge post and transition post locations, as determined from high-speed film analysis, were 149 mm and 163 mm, respectively. The effective coefficient of friction was determined to be approximately 0.45.

11.4 Vehicle Damage

Exterior vehicle damage was moderate, as shown in Figures 102 through 104. Vehicle damage occurred to several body locations, such as right-side door and quarter panels, front and rear bumpers, right-side wheels and rims, steel frame and suspension, windshield, and interior floorboard. The right corner of the rear bumper was deformed upward and twisted, and the right-rear quarter panel was deformed near the bottom, as shown in Figure 102. The right-rear steel rim was also deformed and with wood fibers embedded between the steel rim and tire. In addition, a bolt head was sheared off the axle assembly and embedded in the steel transition plate. The exterior of the right-rear cab wall between the door and the box was deformed. As shown in Figure 102, the right-side door was also deformed, as it was pushed outward near the top, crushed inward near the lower region, and compressed longitudinally. Minor cracking was observed in the right and left edges of the front windshield. The right-front quarter panel was crushed inward, and the engine hood was released. The front frame and engine compartment was shifted laterally approximately 203 mm away from the longitudinal centerline of the vehicle. The right-front wheel assembly and suspension components were fractured off and positioned under the left-front side of the truck cab, as shown in Figure 103. The right-front tire was cut and deflated. Maximum occupant compartment deformations to the floorboard were 140-mm lateral displacement near the forward region of the

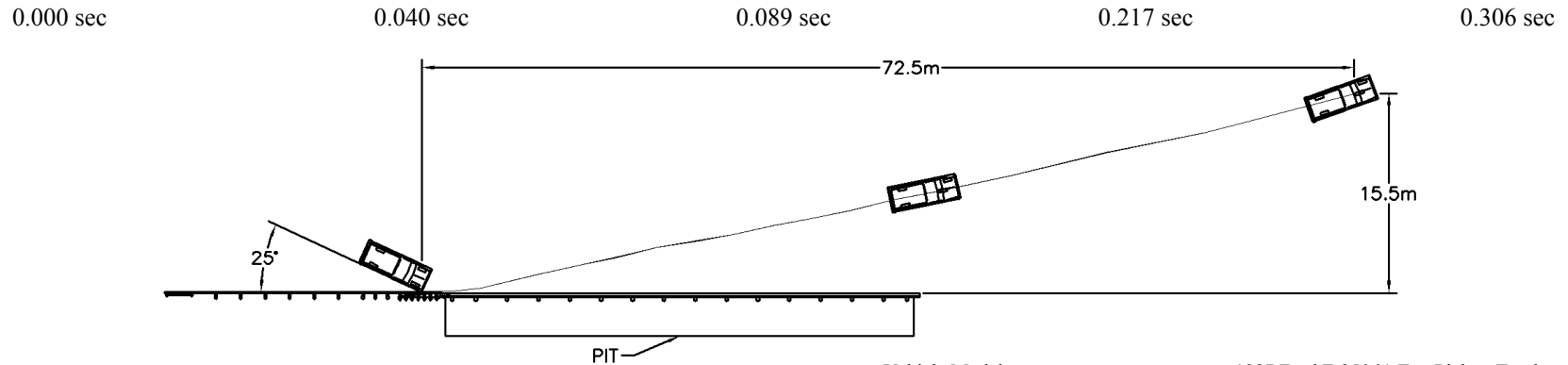
right-side door, 76-mm longitudinal displacement near the right-side floorboard, and 95-mm vertical displacement under the seat along the centerline of the hump. Interior vehicle deformations to the floorboard, as shown in Figure 104, were judged insufficient to cause serious injury to the vehicle occupants. No deformation occurred to the interior front dashboard.

11.5 Occupant Risk Values

The longitudinal and lateral occupant impact velocities were determined to be 6.54 m/sec and 7.44 m/sec, respectively. The maximum 0.010-sec average occupant ridedown decelerations in the longitudinal and lateral directions were 7.12 g's and 10.24 g's, respectively. It is noted that the occupant impact velocities and occupant ridedown decelerations were within the suggested limits provided in NCHRP Report No. 350. The results of the occupant risk, determined from accelerometer data, are summarized in Figure 92 and are shown graphically in Appendix J. The results from the rate transducer are shown graphically in Appendix K.

11.6 Discussion

The analysis of the test results for test TRBR-3 showed that the barrier adequately contained and redirected the vehicle with controlled lateral displacement of the barrier. Minor deformations to the occupant compartment were evident but not considered excessive enough to cause serious injuries to the occupants. The vehicle remained upright both during and after the collision. Vehicle roll, pitch, and yaw angular displacements were noted, but they were deemed acceptable. After collision, the vehicle's trajectory intruded only slightly into adjacent traffic lanes. In addition, the vehicle's exit angle was less than 60 percent of the impact angle. Therefore, test TRBR-3 conducted on the approach guardrail transition attached to the wood bridge rail system was determined to be acceptable according to the NCHRP Report No. 350 performance criteria.



- Test Number TRBR-3
- Date 5/15/97
- Appurtenance Approach Guardrail Transition attached to a Wood Bridge Rail with Curb Rail System for Transverse Decks
- Total Length 20.96 m
- Steel Thrie Beam Rail
 - Thickness 3.42 mm
 - Top Mounting Height 804 mm
- Steel W-Beam Rail
 - Thickness 2.66 mm
 - Top Mounting Height 702 mm
- Wood Posts (Post Nos. 1 - 10)
 - Material Southern Yellow Pine, Grade No. 1D (CCA)
 - Post Nos. 1 -4 203 mm x 203 mm x 1,981 mm
 - Post Nos. 5 - 10 203 mm x 203 mm x 1,829 mm
- Wood Posts (Post Nos. 11 - 18)
 - Material Southern Yellow Pine, Grade No. 1 or Better (CCA)
 - Post Nos. 11 -16 152 mm x 203 mm x 1,829 mm
 - Post Nos. 17 - 18 (BCT) ... 140 mm x 191 mm x 1,080 mm
- Wood Spacer Blocks (Post Nos. 1 - 16)
 - Material Southern Yellow Pine, Grade No. 1 (CCA)
 - Post Nos. 1 - 7 152 mm x 305 mm x 533 mm
 - Post No. 8 152 mm x 203 mm x 572 mm
 - Post No. 9 152 mm x 203 mm x 435 mm
 - Post Nos. 10 - 16 152 mm x 203 mm x 356 mm

- Vehicle Model 1987 Ford F-250 ¾-Ton Pickup Truck
 - Curb 2,273 kg
 - Test Inertial 2,029 kg
 - Gross Static 2,029 kg
- Vehicle Speed
 - Impact 104.9 km/hr
 - Exit 71.1 km/hr
- Vehicle Angle
 - Impact 26.4 deg
 - Exit 11.9 deg
- Vehicle Snagging None
- Vehicle Stability Satisfactory
- Effective Coefficient of Friction (μ) 0.45
- Occupant Ridedown Deceleration (10 msec avg.)
 - Longitudinal 7.12 < 20 G's
 - Lateral (not required) 10.24
- Occupant Impact Velocity
 - Longitudinal 6.54 < 12 m/s
 - Lateral (not required) 7.44
- Vehicle Damage Moderate
 - TAD²⁸ 1-RFQ-5
 - SAE²⁹ 01-RDAW6
- Vehicle Stopping Distance 72.5 m downstream
 - 15.5 m lateral
- Barrier Damage Minor
- Maximum Deflections
 - Permanent Set 35 mm
 - Dynamic 163 mm

Figure 92. Summary of Test Results and Sequential Photographs, Test TRBR-3

0.000 sec

0.243 sec

0.028 sec

0.365 sec

0.091 sec

0.494 sec

0.150 sec

0.821 sec

Figure 93. Additional Sequential Photographs, Test TRBR-3

0.000 sec

0.000 sec

0.067 sec

0.052 sec

0.158 sec

0.120 sec

0.212 sec

0.174 sec

0.250 sec

0.250 sec

Figure 94. Additional Sequential Photographs, Test TRBR-3

Figure 95. Documentary Photographs, Test TRBR-3

Figure 96. Documentary Photographs, Test TRBR-3

Figure 97. Impact Locations, Test TRBR-3

Figure 98. Final Vehicle Position, Test TRBR-3

Figure 99. Barrier Damage, Test TRBR-3

Figure 100. Thrie Beam Rail Damage, Test TRBR-3

Figure 101. Permanent Set Deflections, Test TRBR-3

Figure 102. Vehicle Damage, Test TRBR-3

Figure 103. Front Wheel Assembly Damage, Test TRBR-3

Figure 104. Occupant Compartment Deformations, Test TRBR-3

12 CRASH TEST NO. 4 (WOOD SYSTEM - APPROACH GUARDRAIL TRANSITION)

12.1 Test TRBR-4

The 8,003-kg single-unit truck impacted the approach guardrail transition at a speed of 82.5 km/hr and at an angle of 13.7 degrees. A summary of the test results and the sequential photographs are shown in Figure 105. Additional sequential photographs are shown in Figures 106 and 107. Documentary photographs of the crash test are shown in Figures 108 and 109.

12.2 Test Description

Initial impact occurred at the midspan between transition post nos. 6 and 7 or 2,861 mm upstream from the upstream end of the glulam bridge rail, as shown in Figure 110. After the initial impact with the approach guardrail transition, the right-front quarter panel and bumper were crushed inward. Subsequently, at 0.056 sec after impact, the right-front corner of the vehicle was at transition post no. 3 and with the quarter panel extending over the rail laterally to the back side of the wood blockout. At 0.102 sec, the right-front corner of the vehicle was at transition post no. 1 and with the quarter panel positioned above the midpoint of the post. At this same time, twisting of the truck cab toward the rail was observed as the right-front corner of the front bumper crushed inward. At 0.110 sec, the vehicle's left-front tire turned toward the barrier system. At 0.154 sec, the right-front corner of the vehicle was at bridge post no. 1 while extending over the top. At this same time, the right-front corner of the truck box was positioned near transition post no. 4 and with no apparent snagging. At 0.188 sec, the truck cab became level with the horizontal plane, and it was observed that material was fractured off from the right-front quarter panel. Subsequently, at 0.220 sec, the vehicle's right-front corner reached its maximum lateral extent over the bridge rail, slightly beyond the back side of the posts. The right-front corner of the truck was at bridge post no.2 at 0.232 sec

after impact. At 0.266 sec, the vehicle's right-front corner was near bridge post no. 1 and with the truck box twisting CW with respect to the truck cab. At 0.288 sec, the left-front tire turned away from the bridge rail to a position nearly perpendicular to the direction of travel. The maximum dynamic lateral deflection of 124 mm was measured at transition post no. 3 at 0.290 sec. At 0.337 sec, the right-rear tires contact the barrier, as a dust blow became visible in the vicinity due to the tire's air release. Subsequently, at 0.340 sec, the vehicle's front end was nearly positioned at bridge post no. 3 and with the truck box starting to lean into the bridge rail. The left-rear tires became airborne at 0.424 sec after impact. At 0.480 sec, the right-front corner of the box has dropped behind and below the backside of the upper bridge rail. At 0.508 sec, the vehicle's truck box was nearly parallel to the bridge rail as the box was leaning on the rail surface. At this time, the vehicle's velocity was 67.8 km/hr. At 0.620 sec, the left-rear tires reached a maximum height above the ground and with the truck box visibly sliding off the steel frame rails. Later, at 0.677 sec, the right-rear underside of the truck box was positioned on top of the glulam bridge rail and with the front cab pitching forward due to the uplift at the truck's rear end. At 0.700 sec, the rear end of the truck box was sliding over the bridge rail as the left-rear tires remained airborne. At 0.832 sec, the entire truck box was traveling over the bridge rail, and the truck cab appeared to be stable on the traffic-side face of the bridge railing. Subsequently, the truck cab began to redirect away from the bridge rail at 0.903 sec. At 1.200 sec, the truck cab was pulled back toward the bridge rail as the truck box proceeded to move over the rail. Following this event, the truck cab eventually came to rest on the back side of the bridge, completely separated from the truck frame. The vehicle exited the bridge railing at a speed of approximately 25.3 km/hr and an angle of less than 1 degree at 2.818 sec. The vehicle's post-impact trajectory is shown in Figure 105. The vehicle's front-end came to rest approximately

39.0-m downstream from the midspan location between transition post nos. 6 and 7, as shown in Figure 111. The rebound distance was approximately 0.76 m, as measured laterally from the traffic-side face of the barrier to the right side of the vehicle and longitudinally downstream from impact at a point of 30.48 m plus the length of the vehicle.

During the impact event, a failure occurred in the connection hardware between the truck box and steel frame, causing the box to release from the frame and travel over the bridge railing. From an analysis of the high-speed photography, it was evident that this occurred after the truck had reached the bridge railing region and was not a result from any specific contact with components of the approach guardrail transition. Since a single-unit truck had been successfully performed on the bridge railing system (test no. TRBR-1) and with no vehicle snagging occurring in the transition region, the researchers determined that a retest was not required. Further investigation revealed that this truck box release resulted from an inadequate number and size of steel connection hardware.

12.3 Bridge Rail and Approach Guardrail Transition Damage

The minor damage to the approach guardrail transition and bridge railing is shown in Figures 112 and 113. Damage consisted mostly of deformed thrie beam, displaced guardrail posts, and scrapes, black marks, and gouging on the various rails, posts, and blocks. As shown in Figure 112, gouging occurred on upper, middle, and lower corrugations of the thrie beam rail between transition post nos. 3 through 6. Black marks and scrapes were visible on the thrie beam from the midspan between transition post nos. 5 and 6 through the thrie beam terminal connector. No contact marks, gouging, or damage was observed on the transition posts nor attached blockouts. The maximum ground line soil deformations were measured to be 14 mm on the front side of transition post no. 3 and 13 mm on the back side of the transition post no. 4, respectively. Gouging was observed on the

upper and front surfaces of the top glulam bridge rail as well as to the top surfaces of bridge post nos. 3 through 13.

The maximum lateral permanent set deflections for midspan rail and post locations, as determined from field measurements in the impact region, were approximately 49 mm and 52 mm, respectively. The maximum dynamic lateral deflection for transition post locations, as determined from high-speed film analysis, was 124 mm. The effective coefficient of friction was determined to be approximately 0.64.

12.4 Vehicle Damage

Exterior vehicle damage was extensive, as shown in Figures 114 and 115. However, it should be noted that significant portion of this damage occurred as a result of the truck box becoming detached from the steel truck frame. Vehicle damage occurred to several body locations, such as truck cab's right side, front quarter panel, front bumper, right-side wheels, rear steel frame, rear box and attachment hardware, and front and rear axles and suspension. As shown in Figures 114 and 115, the rear truck box came off the steel frame during the impact sequence. This failure occurred for several reasons. First, the right-side frame rail extension failed due to poor welding, as shown in Figure 115. Second, fabrication and welding of the rear bumper failed due to poor workmanship. Finally, all four sets of the 12.7-mm diameter threaded rods attaching the truck box to the frame failed. This was likely due to an inadequate number and size of connectors. It is noted that the truck and box were assembled by experienced personnel at a regional truck sales and repair business which followed industry guidelines for reattaching a box to a frame. The right-rear axle released from the leaf-spring due to fracture of the attachment hardware. The inner right-rear tire was deflated. The outer right-rear tire was punctured and deflated and with deformations to the steel rim.

Interior occupant compartment deformations to the right-side floorboard near the door were found but barely visible. Those deformations were judged insufficient to cause serious injury to the vehicle occupants. The right corner of the front bumper, quarter panel, and side step were crushed inward and deformed. The right-front wheel assembly and axle were released and pushed under the center of the truck behind the cab.

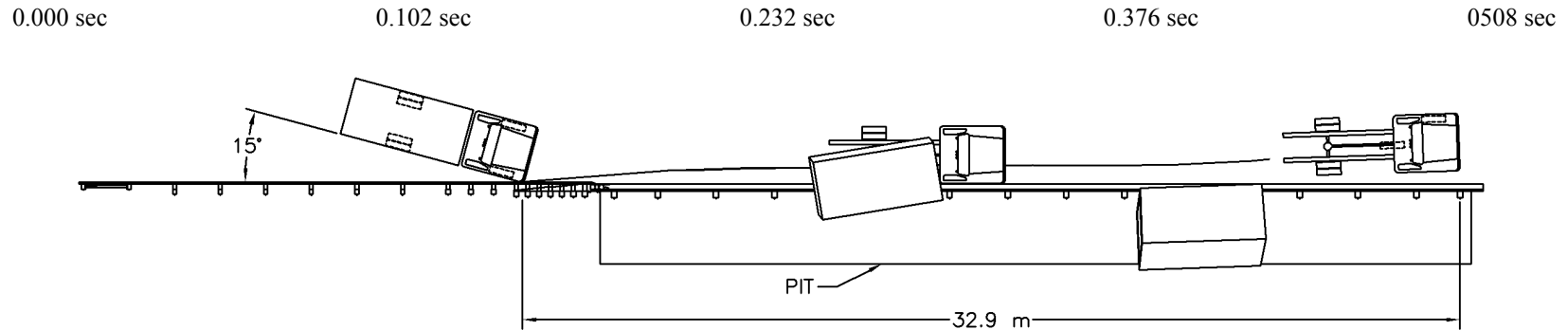
12.5 Occupant Risk Values

The longitudinal and lateral occupant impact velocities were determined to be 2.77 m/sec and 2.61 m/sec, respectively. The maximum 0.010-sec average occupant ridedown decelerations in the longitudinal and lateral directions were 4.91 g's and 4.36 g's, respectively. It is noted that the occupant impact velocities and occupant ridedown decelerations were within the suggested limits provided in NCHRP Report No. 350. The results of the occupant risk, determined from accelerometer data, are summarized in Figure 105 and are shown graphically in Appendix L. The results from the rate transducer are shown graphically in Appendix M.

12.6 Discussion

The analysis of the test results for test TRBR-4 showed that the barrier adequately contained and redirected the vehicle with controlled lateral displacement of the barrier. Minor deformations to the occupant compartment were evident but not considered excessive enough to cause serious injuries to the occupants. The vehicle remained upright both during and after the collision. Although the truck box detached from the frame and fell over the bridge rail, the researchers determined that this failure was due to inadequacies in its attachment rather than concerns with barrier design. Therefore, it was decided to not rerun the crash test. Vehicle roll, pitch, and yaw angular displacements were noted, but they were deemed acceptable. After collision, the vehicle's trajectory

intruded only slightly into adjacent traffic lanes. In addition, the vehicle's exit angle was less than 60 percent of the impact angle. Therefore, test TRBR-4 conducted on the approach guardrail transition attached to the wood bridge rail system was determined to be acceptable according to the NCHRP Report No. 350 performance criteria.



- Test Number TRBR-4
- Date 8/5/97
- Appurtenance Approach Guardrail Transition attached to a Wood Bridge Rail with Curb Rail System for Transverse Decks
- Total Length 20.96 m
- Steel Thrie Beam Rail
 - Thickness 3.42 mm
 - Top Mounting Height 804 mm
- Steel W-Beam Rail
 - Thickness 2.66 mm
 - Top Mounting Height 702 mm
- Wood Posts (Post Nos. 1 - 10)
 - Material Southern Yellow Pine, Grade No. 1D (CCA)
 - Post Nos. 1 -4 203 mm x 203 mm x 1,981 mm
 - Post Nos. 5 - 10 203 mm x 203 mm x 1,829 mm
- Wood Posts (Post Nos. 11 - 18)
 - Material Southern Yellow Pine, Grade No. 1 or Better (CCA)
 - Post Nos. 11 -16 152 mm x 203 mm x 1,829 mm
 - Post Nos. 17 - 18 (BCT) ... 140 mm x 191 mm x 1,080 mm
- Wood Spacer Blocks (Post Nos. 1 - 16)
 - Material Southern Yellow Pine, Grade No. 1 (CCA)
 - Post Nos. 1 - 7 152 mm x 305 mm x 533 mm
 - Post No. 8 152 mm x 203 mm x 572 mm
 - Post No. 9 152 mm x 203 mm x 435 mm
 - Post Nos. 10 - 16 152 mm x 203 mm x 356 mm

- Vehicle Model 1987 Ford F-700 Series Single-Unit Truck
 - Curb 4,557 kg
 - Test Inertial 8,003 kg
 - Gross Static 8,003 kg
- Vehicle Speed
 - Impact 82.5 km/hr
 - Exit 25.3 km/hr
- Vehicle Angle
 - Impact 13.7 deg
 - Exit < 1 deg
- Vehicle Snagging None
- Vehicle Stability Satisfactory
- Effective Coefficient of Friction (μ) 0.64
- Occupant Ridedown Deceleration (10 msec avg.)
 - Longitudinal (not required) 4.91 < 20 G's
 - Lateral (not required) 4.36
- Occupant Impact Velocity
 - Longitudinal (not required) 2.77 < 12 m/s
 - Lateral (not required) 2.61
- Vehicle Damage Extensive
 - TAD²⁸ 1-RFQ-4
 - SAE²⁹ 01-RFEW3
- Vehicle Stopping Distance 32.9 m downstream
 - 1.6 m lateral
- Barrier Damage Minor
- Maximum Deflections
 - Permanent Set 49 mm
 - Dynamic 124 mm

Figure 105. Summary of Test Results and Sequential Photographs, Test TRBR-4

0.000 sec

0.903 sec

0.100 sec

1.299 sec

0.220 sec

1.769 sec

0.360 sec

1.933 sec

0.490 sec

2.478 sec

0.700 sec

2.818 sec

Figure 106. Additional Sequential Photographs, Test TRBR-4

0.000 sec

0.378 sec

0.102 sec

0.480 sec

0.188 sec

0.677 sec

0.337 sec

0.832 sec

Figure 107. Additional Sequential Photographs, Test TRBR-4

Figure 108. Documentary Photographs, Test TRBR-4

Figure 109. Documentary Photographs, Test TRBR-4

Figure 110. Impact Locations, Test TRBR-4

Figure 111. Final Vehicle Position, Test TRBR-4

Figure 112. Barrier Damage, Test TRBR-4

Figure 113. Permanent Set Deflections, Test TRBR-4

Figure 114. Vehicle Damage, Test TRBR-4

Figure 115. Vehicle Damage, Test TRBR-4

13 SUMMARY AND CONCLUSIONS - WOOD SYSTEM

A wood bridge railing system and an attached approach guardrail transition system were successfully developed and crash tested for use on transverse glulam timber deck bridges. Four full-scale vehicle crash tests - two on the bridge railing and two on the approach guardrail transition - were performed and determined to have acceptable safety performance according to TL-4 of NCHRP Report No. 350 (1). A summary of the safety performance evaluations for all four crash tests are provided in Table 4.

As previously mentioned, prior to the development of this wood bridge railing system, no other TL-4 railing systems had been developed for use on transverse glulam timber deck bridges. However, this research program clearly demonstrates that crashworthy wood railing systems are feasible for use on these types of bridges. The development of the wood bridge railing and transition system addressed the concerns for aesthetics, economy, material availability, ease of construction, and reasonable margin of structural adequacy. In addition, the wood bridge railing and transition system was relatively easy to install and should have reasonable construction labor costs. This wood railing system should also be adaptable to: (1) other transverse glulam timber deck bridges with thicknesses equal to or greater than 130 mm and with little or no modification; (2) longitudinal glulam timber deck bridges where sufficient deck strength is provided to resist the lateral impact forces; and (3) bridges supporting reinforced concrete decks that are capable of meeting the same lateral impact load requirements.

No significant damage to the test bridge was evident from the vehicle impact tests. For the wood bridge railing system, damage consisted primarily of rail gouging and scraping. All glulam timber railings remained intact and serviceable after the tests and replacement of the railing was not

considered necessary. For the approach guardrail transition system, damage consisted primarily of deformed thrie beam rail, displaced guardrail posts, and gouging and scraping of the glulam rail and thrie beam blockouts. All glulam timber railings remained intact and serviceable after the tests, while the steel thrie beam required replacement in the vicinity of the impact after each crash test.

Therefore, the successful completion of this phase of the research project resulted in a TL-4 wood bridge railing and approach guardrail transition system having acceptable safety performance and meeting current crash test safety standards.

Table 4. NCHRP Report No. 350 TL-4 Evaluation Results - Wood System (Bridge Railing and Transition)

176

Evaluation Factors	Evaluation Criteria	Test No.			
		TRBR-1	TRBR-2	TRBR-3	TRBR-4
Structural Adequacy	A. Test article should contain and redirect the vehicle; the vehicle should not penetrate, underride, or override the installation although controlled lateral deflection of the test article is acceptable.	S	S	S	S
Occupant Risk	D. Detached elements, fragments or other debris from the test article should not penetrate or show potential for penetrating the occupant compartment, or present an undue hazard to other traffic, pedestrians, or personnel in a work zone. Deformations of, or intrusions into, the occupant compartment that could cause serious injuries should not be permitted.	S	S	S	S
	F. The vehicle should remain upright during and after collision although moderate roll, pitching, and yawing are acceptable.	NR	S	S	NR
	G. It is preferable, although not essential, that the vehicle remain upright during and after collision.	S	NR	NR	S
	H. Longitudinal and lateral occupant impact velocities should fall below the preferred value of 9 m/s, or at least below the maximum allowable value of 12 m/s.	NR	NR	NR	NR
	I. Longitudinal and lateral occupant ridedown accelerations should fall below the preferred value of 15 g's, or at least below the maximum allowable value of 20 g's.	NR	NR	NR	NR
Vehicle Trajectory	K. After collision it is preferable that the vehicle's trajectory not intrude into adjacent traffic lanes.	S	S	M	S
	L. The occupant impact velocity in the longitudinal direction should not exceed 12 m/s and the occupant ridedown acceleration in the longitudinal direction should not exceed 20 g's.	NR	S	S	NR
	M. The exit angle from the test article preferably should be less than 60 percent of test impact angle, measured at time of vehicle loss of contact with test devise.	S	S	S	S

S - Satisfactory
M - Marginal
U - Unsatisfactory
NR - Not Required

14 STEEL SYSTEM DEVELOPMENT

14.1 Background

As stated previously in Section 6, there have been no TL-4 bridge railing systems developed for use on transverse glulam timber deck bridges prior to this research effort. However, in 1992, a PL-2 steel thrie beam and channel bridge railing system was developed for use on a longitudinal glulam timber deck bridge and successfully full-scale crash tested by MwRSF (4-8, 30). The steel thrie beam and channel rail, which was referred to as the *TBC-8000* bridge railing system, consisted of a single, 3.42-mm thick thrie beam rail mounted to steel wide-flange posts spaced 1,905 mm on center. The lower end of each post was bolted to a steel plate that was connected to the bridge deck with high-strength bars. In addition, a steel channel rail was attached to the top surface of the steel wide-flange spacer blocks.

The *TBC-8000* bridge railing system served as the basis for the design of the TL-4 steel bridge railing system for use on transverse glulam timber deck bridges. The *TBC-8000* bridge railing system was modified so that it could be used with transverse deck panels rather than the previously used longitudinal deck panels. With the change in timber deck configurations, the researchers believed that an increase in bridge post spacing was required in order to accommodate the use of standard 1,219-mm wide transverse deck panels. Development of the TL-4 steel system also consisted of re-sizing the structural components previously used with the *TBC-8000* bridge railing system to withstand the higher forces generated from the increased post spacing. Other improvements were made to the connection details based on the performance of the *TBC-8000* bridge railing system.

14.2 Design Issues

Several design issues were addressed during the development of the new TL-4 steel bridge railing system, including bridge length, girder size, deck thickness, post spacing, material selection, geometry considerations, and connection details.

Historically, crash tests of longitudinal barriers with single-unit trucks have revealed that adequate length of barrier must be provided downstream from initial impact. This minimum barrier length is necessary to: (1) evaluate vehicle stability during redirection but prior to the vehicle reaching the end of the barrier; and (2) study the vehicle interaction with the top of the bridge railing components. Therefore, the length of the bridge superstructure was chosen to be approximately 36.58-m long in order to provide the necessary bridge railing length approximately equal in magnitude.

Early in the project, significant discussions occurred between MwRSF researchers, FPL engineers, and industry leaders on the selection of the girder size and deck thickness. For a 12.19-m span length, the girder widths discussed, ranged between 222 and 273 mm, while the beam depth varied between 768 and 838 mm. Two deck sizes were also considered, a 130-mm versus a 171-mm thickness. From a more conservative approach, the glulam members would be selected using the larger dimensions mentioned previously, thus providing reserve structural capacity. However, from an economics approach, the glulam members would be chosen using the smaller dimensions. After much thought, it was mutually decided to use a 130-mm deck thickness supported by girders measuring 222-mm wide by 768-mm deep. Therefore, if the development of the bridge railing systems were successful using the smaller sizes, then significant economy would be provided for each timber bridge constructed which required a TL-4 bridge railing.

Standard 1,219-mm wide transverse glulam deck panels were used to form the timber bridge deck. Thus, it was necessary to determine a post spacing that would provide adequate load distribution from the rails to the deck, allow for reasonable size rail elements, and provide a consistent connection detail for each panel location where a post would attach to the deck. A post spacing of 1,219 mm, or any multiple of 1,219 mm, would be required in order to prefabricate a standard deck panel with the ability to mount a standard bridge railing system to the panel. A post spacing of 1,219 mm was deemed too conservative and costly, therefore a 2,438-mm post spacing was used, as shown in Figure 116. However, using a 2,438-mm post spacing, instead of the 1,905-mm post spacing used in the *TBC-8000* bridge railing system, resulted in a 28% increase in rail bending moment and post shear force.

The steel railing system was configured similarly to the PL-2 steel thrie beam and channel bridge railing system (*TBC-8000*) that was developed for longitudinal deck bridges. However, for this steel system, a structural tube member was used for the upper rail instead of using a channel section in order to account for the increased post spacing from 1,905 to 2,438 mm. This change was made to provide greater load distribution and increased resistance to lateral buckling of the upper rail member. In addition, the post-to-deck attachment hardware was changed from that used previously in the *TBC-8000* design. For the *TBC-8000* system, a single, vertical deck mounting plate was used to attach the post to the deck edge. However, for the new steel system, this concept was abandoned due to inadequate surface on the deck's outer edge. Therefore, two horizontal deck mounting plates were used to attach the post to the deck, one placed on both the top and bottom surfaces of the thin glulam panels and held in place using vertical bolts.

This new bridge railing was designed such that all of the system components were fabricated

from steel materials, including rail elements, spacer blocks, posts, deck mounting plates, and miscellaneous structural attachment hardware, as shown in Figures 117 and 118. The selection of an all-steel bridge railing system allowed for a more economical TL-4 railing alternative for use with transverse timber deck bridges.

Figure 116. Steel Bridge Railing System

Figure 117. Steel Bridge Railing System

Figure 118. Steel Bridge Railing System - Bridge Posts

15 STEEL SYSTEM DESIGN DETAILS

15.1 Steel Bridge Railing

The bridge railing system consisted of five major components: (1) wide-flange bridge posts; (2) rail blockouts; (3) a thrie beam rail; (4) an upper structural tube rail; and (5) deck-mounting plates. Photographs of the bridge railing system have been shown previously in Figures 116 through 118 of Section 14. The overall layout of the bridge railing system is shown in Figure 119. Design details of the bridge railing system are shown in Figures 120 through 127.

Sixteen galvanized ASTM A36 W152x22.3 structural wide-flange steel posts, measuring 961-mm long, were used to support the steel railing, as shown in Figures 118, 121, and 126. The bridge posts were spaced 2,438 mm on center. The lower end of each post was bolted to two ASTM A36 steel plates that were connected to the top and bottom surfaces of the bridge deck with vertical bolts, as shown in Figure 125. The top and bottom plate assemblies were attached to each post with four ASTM A325 hex head bolts, sized 25-mm diameter x 229-mm long for the top two plate bolts and 19-mm diameter x 76-mm long for the bottom two plate bolts. The plate assemblies were attached to the deck with twelve ASTM A307 22-mm diameter x 203-mm long bolts with 102-mm diameter shear plates located between both the upper and lower deck mounting plates on the glulam deck, as shown in Figure 125. The bolt location and spacing are shown in Figure 125.

As shown in Figures 119 and 120, the steel rail consisted of 3.42-mm thick thrie beam mounted 804 mm above the timber deck surface, as measured from the ground to the top of the rail. The thrie beam rail was offset 152 mm away from the posts with galvanized, ASTM A36 W152x22.3 structural wide-flange steel spacer blocks measuring 487-mm long, as shown in Figures 121, 126, and 127.

The structural tube rail consisted of galvanized, ASTM A500 Grade B TS 203-mm x 76-mm x 5-mm steel sections attached to the top of the steel spacer blocks, as shown in Figures 121 and 122. The distance from the bridge deck to the top of the tube rail was 914 mm. Design details of the tube railing sections are shown in Figure 123. The tube rail sections were attached to the spacer blocks with ASTM A36 structural steel angles measuring 89 mm x 89 mm x 8 mm, as shown in Figure 124. Each tube rail section was connected to one another at the ends using a fabricated steel splice tube which was welded together with four ASTM A36 steel plates, as shown in Figure 124. The layout of the tube rail sections is shown in Figure 119.

The steel thrie beam rail was anchored at the downstream end of the bridge railing system with a rigid assembly consisting of welded steel plates and structural steel tubes that were bolted to the thrie beam rail and anchored to the concrete tarmac located at the MwRSF's outdoor test site, as shown in Figures ? and ?. The downstream anchor assembly was necessary to develop the tensile capacity of the rail at the downstream end of the bridge railing system.

A 51-mm thick, concrete wearing surface was placed on top of the transverse glulam deck panels. This deck surface treatment was added in order to represent actual field conditions where an asphalt surface would likely be overlaid on the bridge for resistance to both wear and moisture. For the overlay, a 20.7 MPa concrete mix was used with Type III Portland cement, 9.5-mm minus aggregate, and fiber mesh additive.

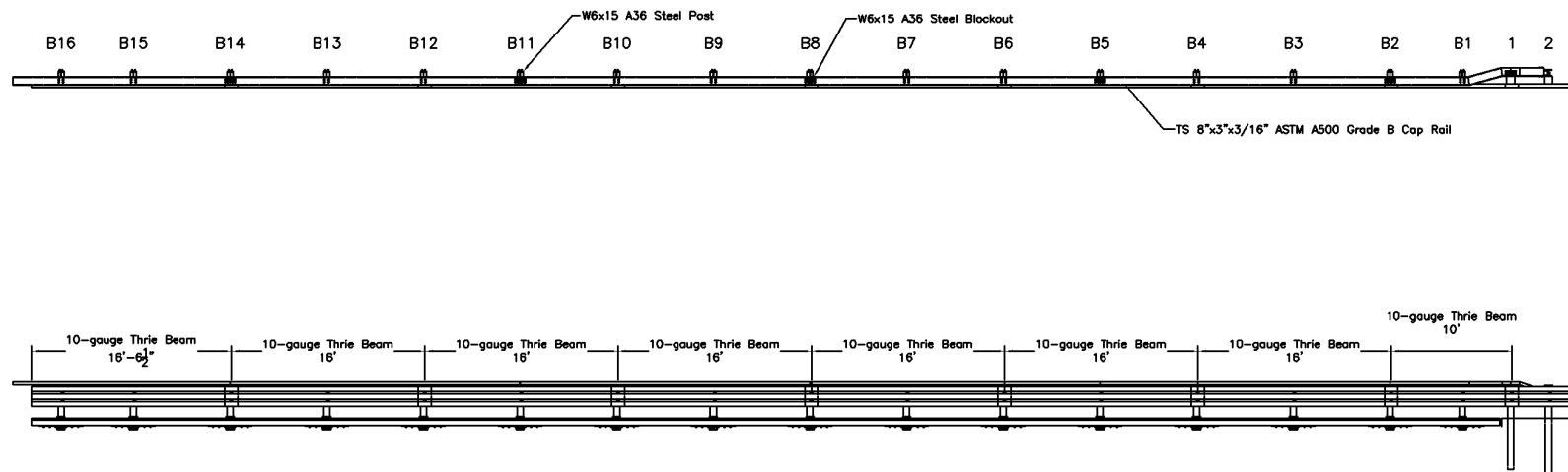


Figure 119. Overall Layout of Steel Bridge Railing System

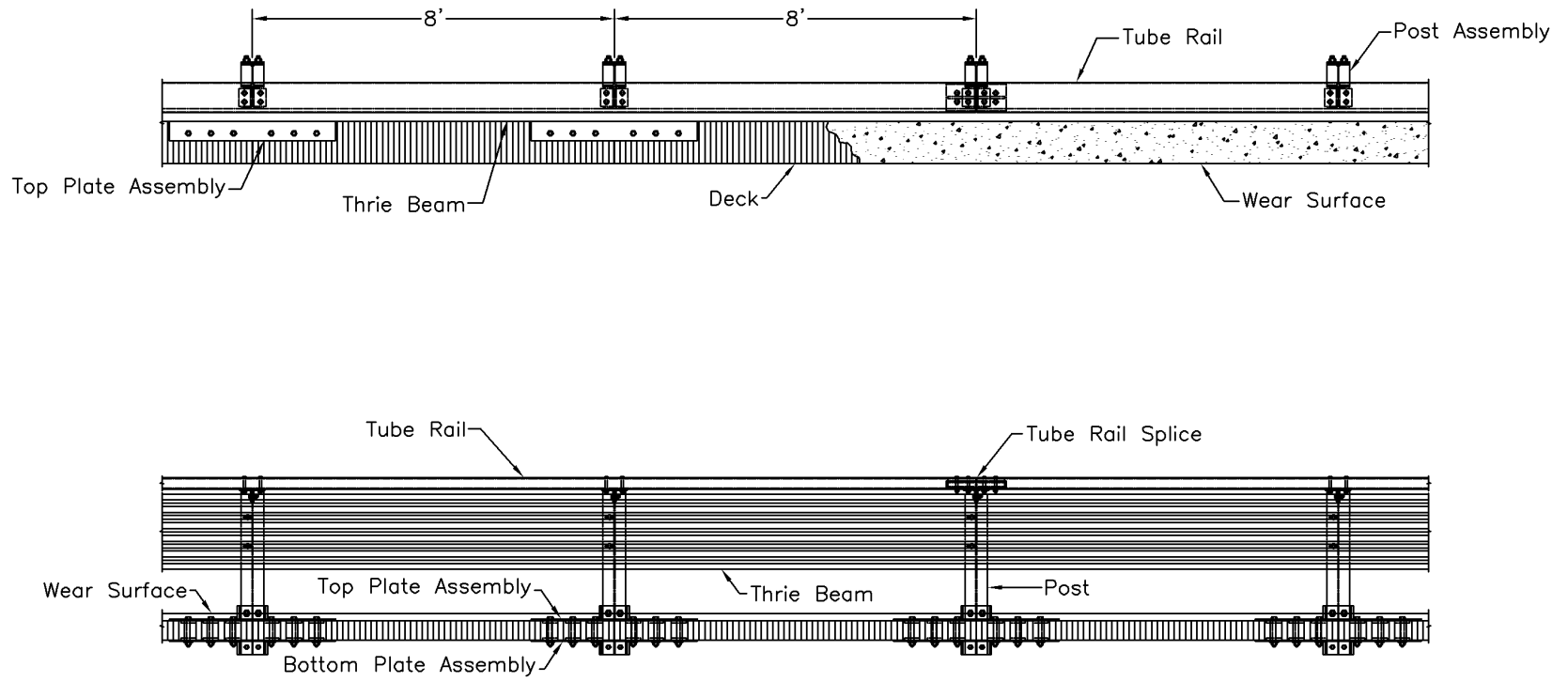


Figure 120. General Configuration of Steel Bridge Railing System

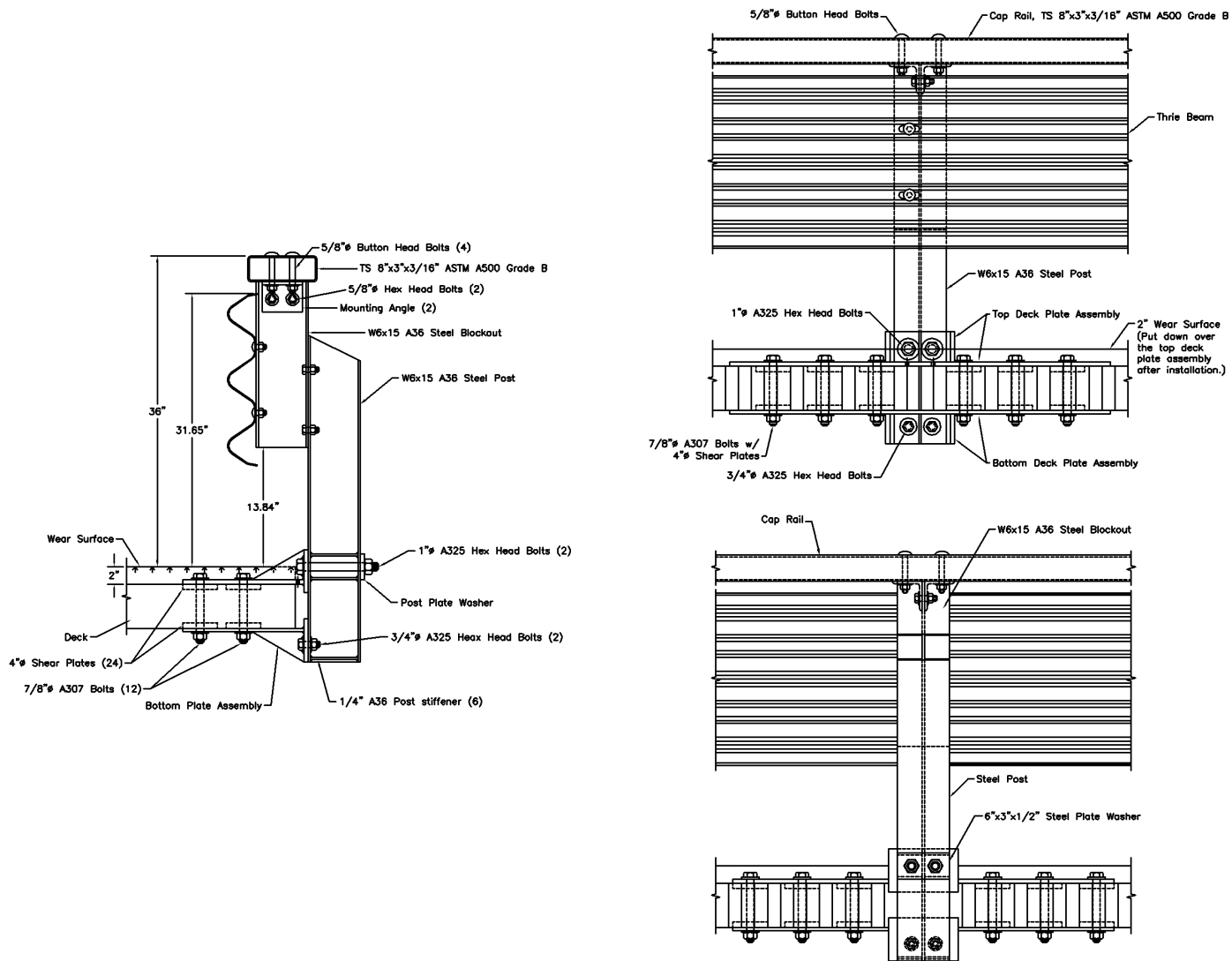
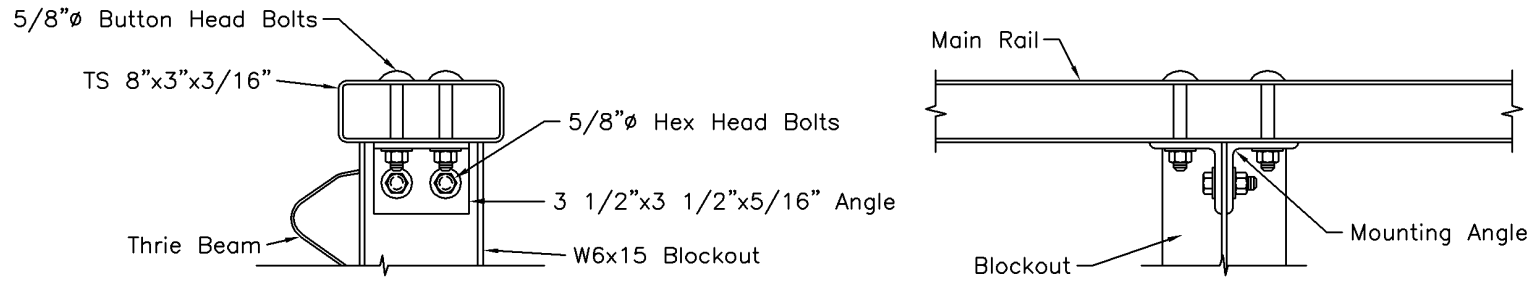
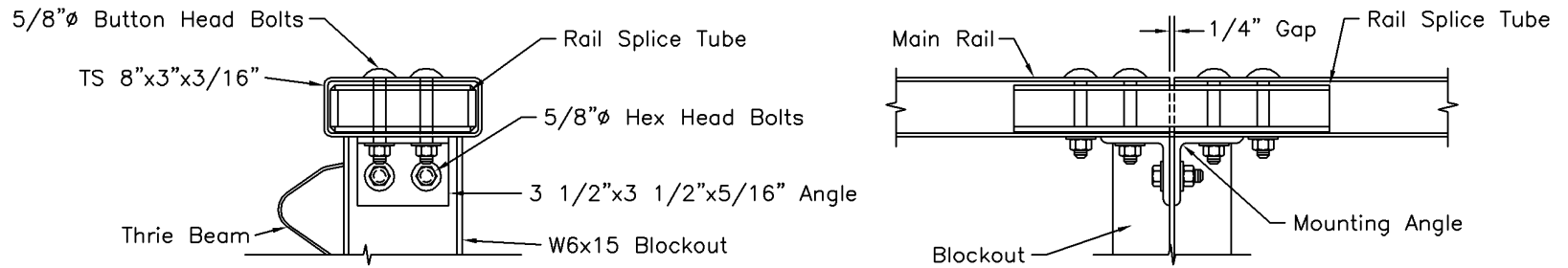


Figure 121. Bridge Railing Design Details - Steel System

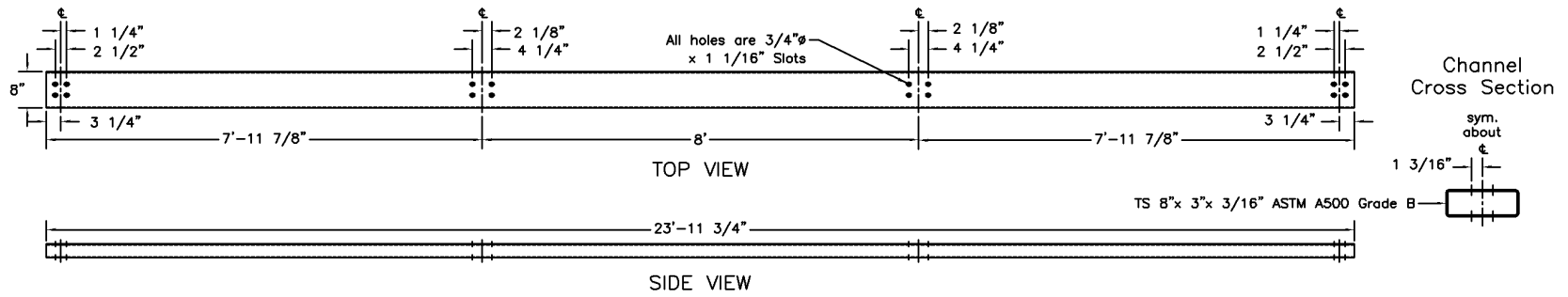


Tube Rail Connection



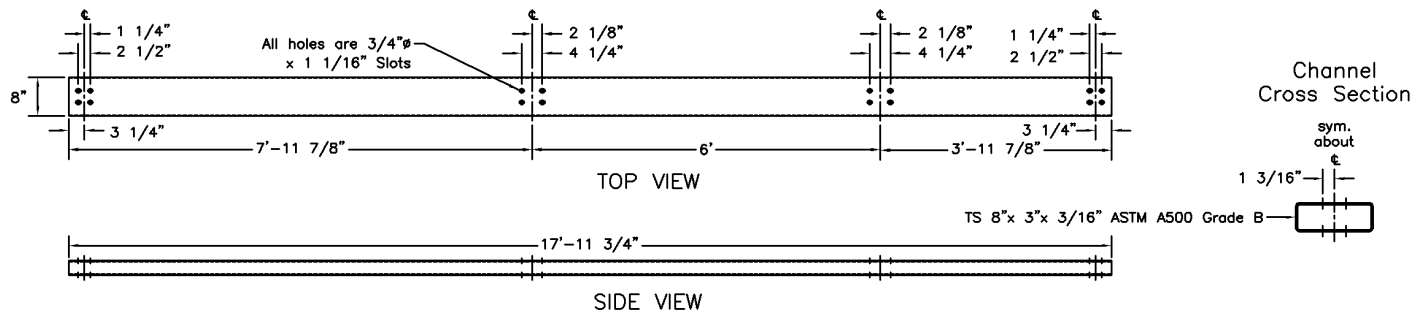
Tube Rail Splice

Figure 122. Tube Rail Connection and Tube Rail Splice Design Details



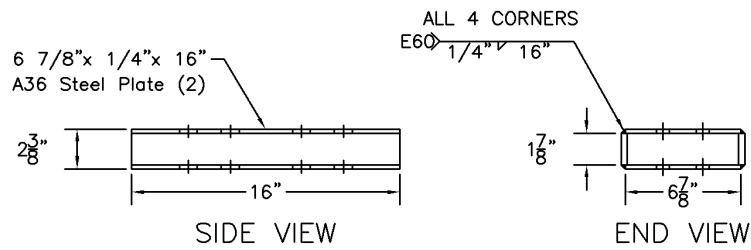
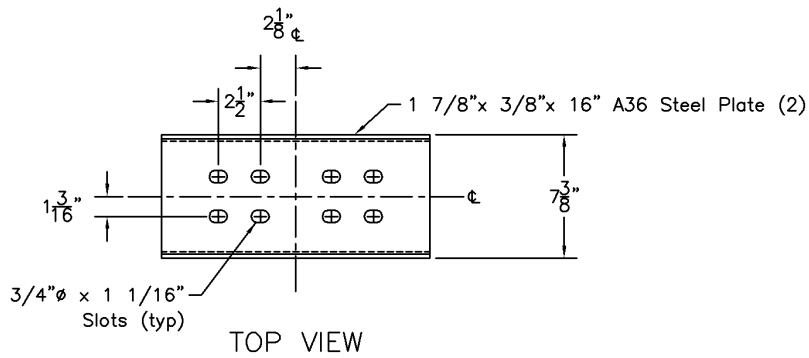
Upper Tube Rail, Type 1

190

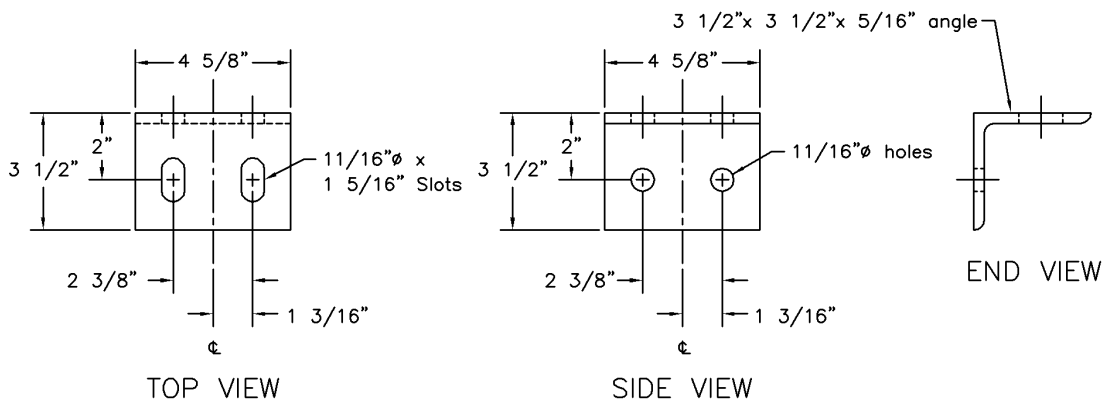


Upper Tube Rail, Type 2

Figure 123. Upper Tube Rails

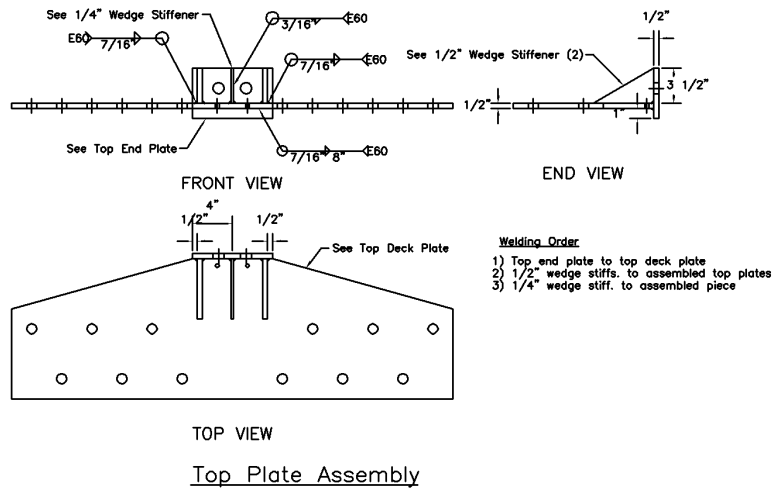


Rail Splice Tube

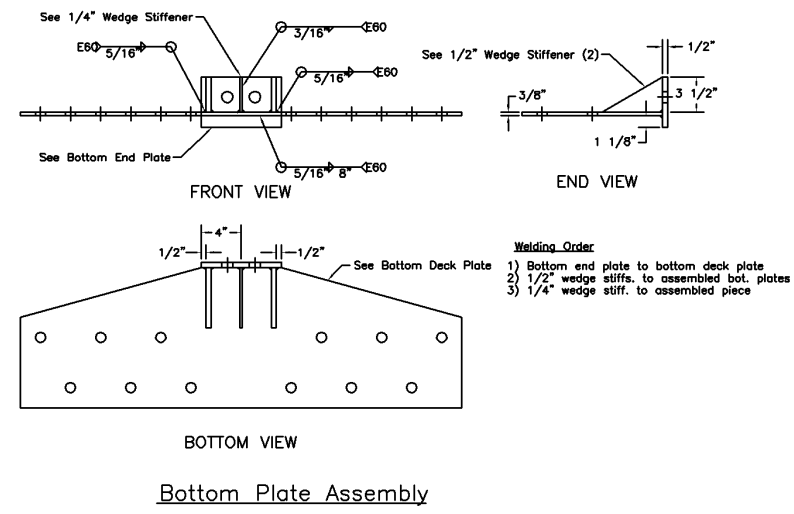
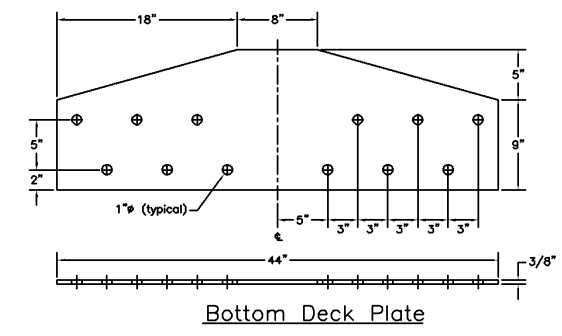
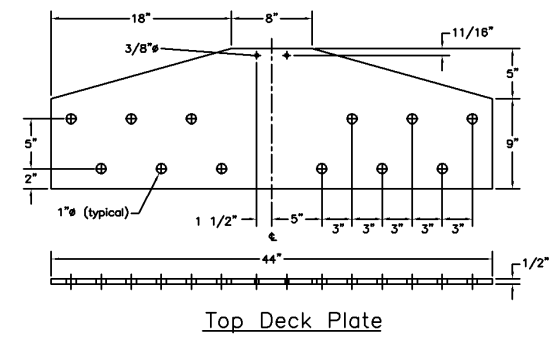


Mounting Angle

Figure 124. Rail Splice Tube and Mounting Angle Details



- Welding Order**
- 1) Top end plate to top deck plate
 - 2) 1/2" wedge stiff. to assembled top plates
 - 3) 1/4" wedge stiff. to assembled piece



- Welding Order**
- 1) Bottom end plate to bottom deck plate
 - 2) 1/2" wedge stiff. to assembled bot. plates
 - 3) 1/4" wedge stiff. to assembled piece

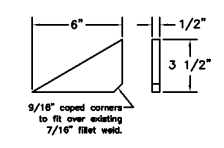
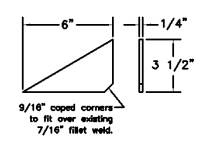
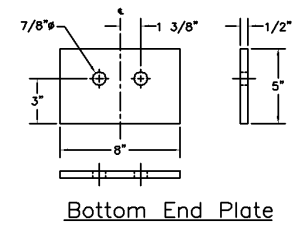
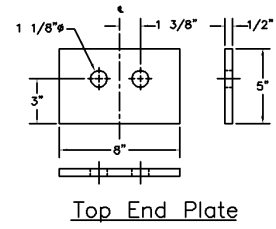


Figure 125. Top and Bottom Plate Assemblies

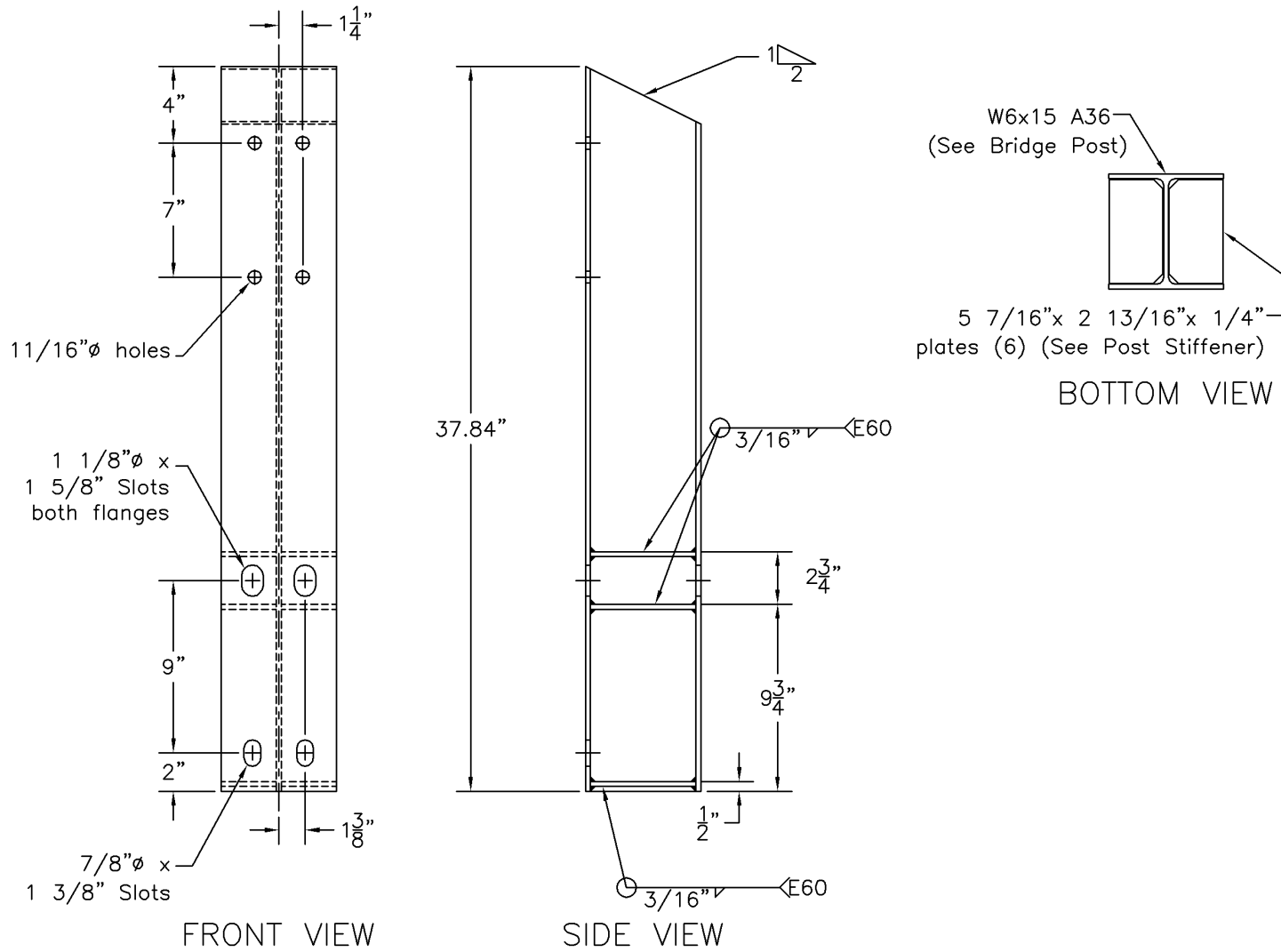


Figure 126. Bridge Post Assembly Details

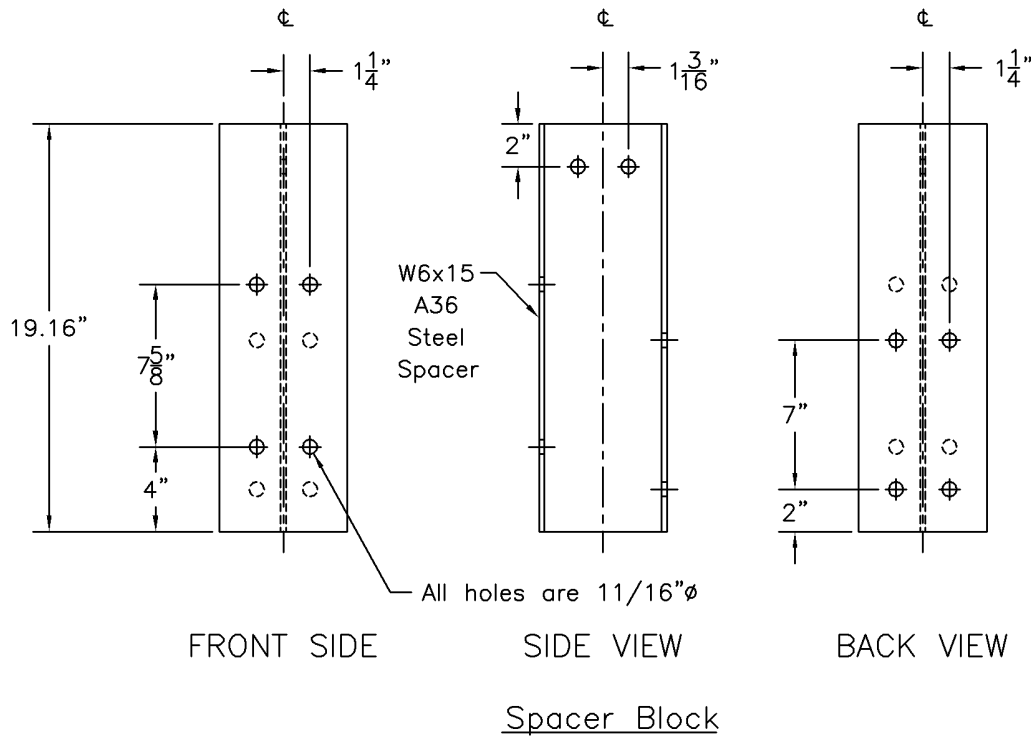
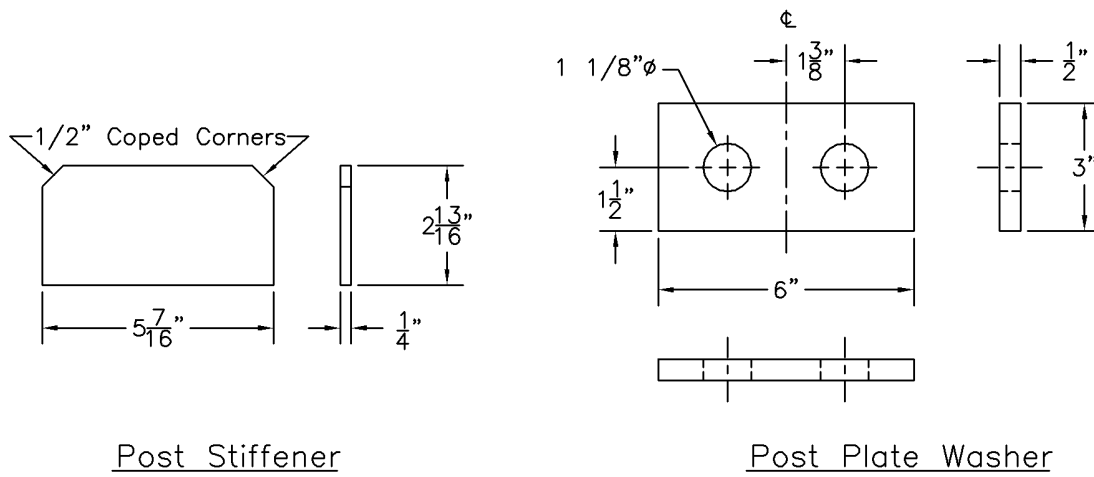


Figure 127. Post Stiffener, Post Plate Washer, and Spacer Block Details

15.2 Approach Guardrail Transition

An approach guardrail transition system was attached to the upstream end of the bridge railing system and was used to connect the standard guardrail to the bridge rail. The approach guardrail transition system consisted of nine major components: (1) a thrie beam rail section; (2) a W-beam to thrie beam transition section; (3) standard W-beam guardrail; (5) steel guardrail posts; (6) timber blockouts; (7) two transition tube rails and tube rail terminator; and (8) a simulated end anchorage system. Photographs of the approach guardrail transition system are shown in Figures 128 through 131. The overall layout of the approach guardrail transition system is shown in Figure 132. Design details of the approach guardrail transition system are provided in Figures 133 through 138.

The thrie beam rail was fabricated from 3.42-mm thick steel and measured 3,810-mm long. A 2.66-mm thick W-beam to thrie beam transition section, measuring 1,905-mm long, was used to connect the thrie beam guardrail to 15,240 mm of standard 2.66-mm thick W-beam guardrail. The thrie beam and W-beam rails had a top mounting height of 804 mm and 706 mm, respectively, as measured from the roadway surface to the top of the rails. Lap-splice connections between the steel rail sections were configured to reduce vehicle snagging at the splice during the crash tests.

Transition tube rail no. 1 consisted of three pieces of galvanized, ASTM A500 Grade B TS 203-mm x 76-mm x 5-mm steel sections welded together as shown in Figure 134. Transition tube rail no. 1 was attached to the top of the steel spacer blocks at bridge post nos. 1 and 2 and transition post no. 1, as shown in Figure 134. Transition tube rail no. 2 consisted of two pieces of galvanized, ASTM A500 Grade B TS 203-mm x 76-mm x 5-mm steel sections welded together as shown in Figure 134. Transition tube rail no. 2 was attached to the steel spacer block at transition post no.

1 and the tube rail terminator, as shown in Figure 134. Design details of the transition tube rail sections and tube rail terminator are shown in Figures 134 through 136. The two transition tube rail sections were spliced together with an ASTM A36 structural steel splice tube, as shown in Figures 134 and 135. The layout of the two transition tube rails, the transition splice tube, and the tube rail terminator is shown in Figure 134.

The system was constructed with fifteen guardrail posts, as shown in Figures 132 and 137 through 138. Post nos. 1 through 5 consisted of galvanized, ASTM A36 steel W152x22.3 sections measuring 2,134-mm long. Post nos. 6 and 7 were W152x13.4 steel sections measuring 1,981-mm long. Post nos. 8 through 13 were also W152x13.4 sections but measuring 1,829-mm long. Post nos. 14 and 15 were timber posts measuring 140-mm wide x 190-mm deep x 1,080-mm long and were placed in steel foundation tubes. The timber posts and foundation tubes were part of an anchorage system used to develop the required tensile capacity of the guardrail at the upstream end of the system.

For post nos. 1 through 15, treated timber blockouts were used to space the thrie beam and W-beam guardrails away from the traffic-side face of each guardrail post. The blockouts were fabricated from SYP, Grade No. 1 material and treated with CCA. For post nos. 1 through 5, a wood blockout, measuring 203-mm wide x 203-mm deep x 483-mm long, was used with thrie beam guardrail. At post no. 6, a wood blockout, measuring 152-mm wide x 203-mm deep x 483-mm long, was used at the midspan of the W-beam to thrie beam transition section. For post nos. 7 through 13, a wood blockout, measuring 152-mm wide x 203-mm deep x 368-mm long, was used with W-beam guardrail.

The soil embedment depths for post nos. 1, 2 through 5, 6, 7, and 8 through 13 were 1,295

mm, 1,372 mm, 1,191 mm, 1,247 mm, and 1,095 mm, respectively, as shown in Figures 137 and 138. The steel posts were placed in a compacted coarse, crushed limestone material that met Grading B of AASHTO M147-65 (1990) as found in NCHRP Report No. 350.

Figure 128. Approach Guardrail Transition - Front View

Figure 129. Approach Guardrail Transition - Back View

Figure 130. Approach Guardrail Transition - Parallel View

Figure 131. Connection to Steel Bridge Railing System

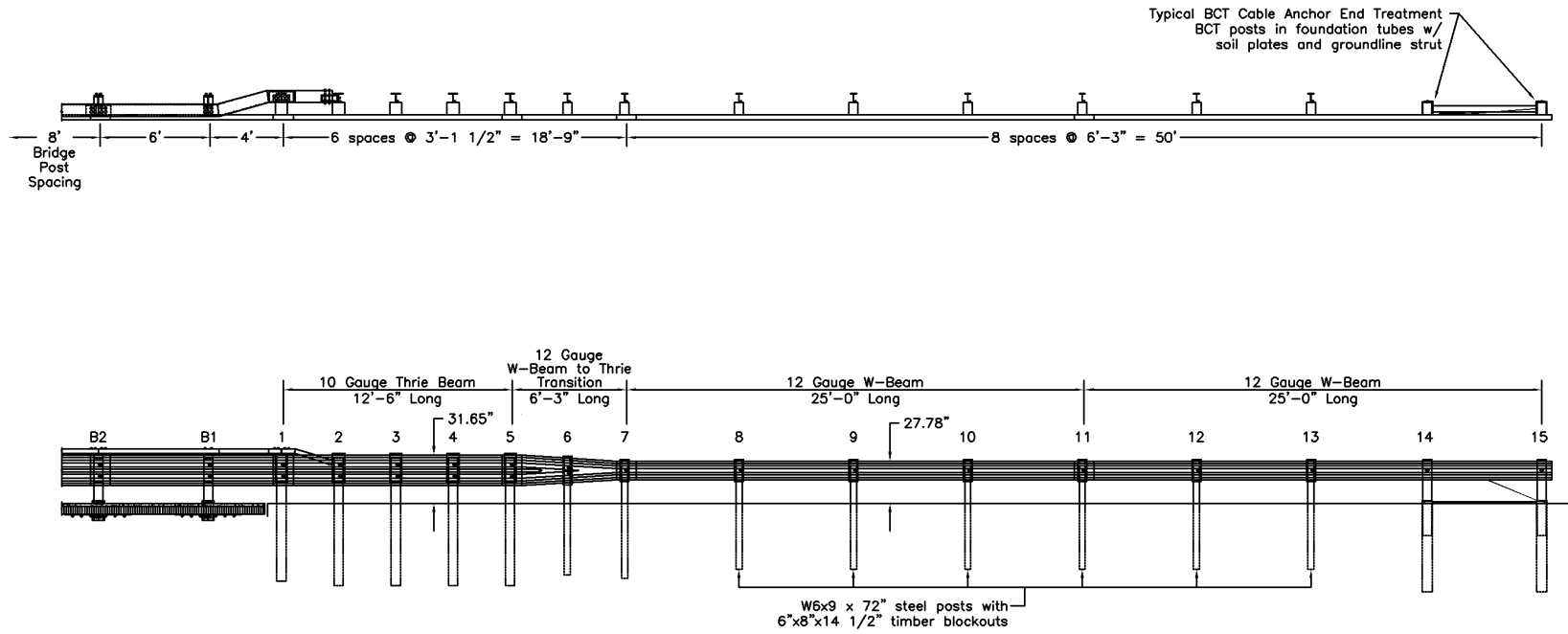


Figure 132. Overall Layout of Approach Guardrail Transition System - Steel System

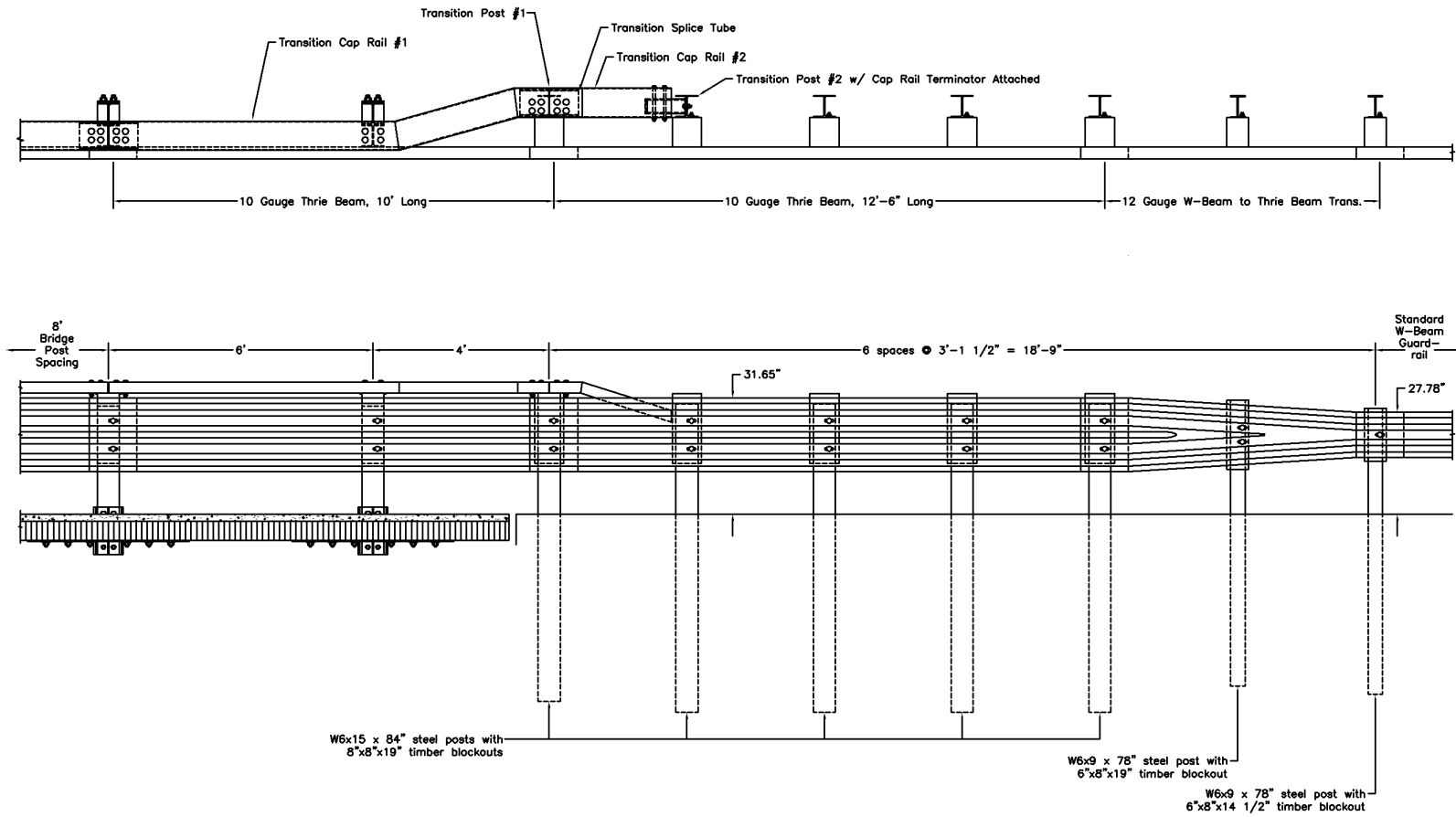
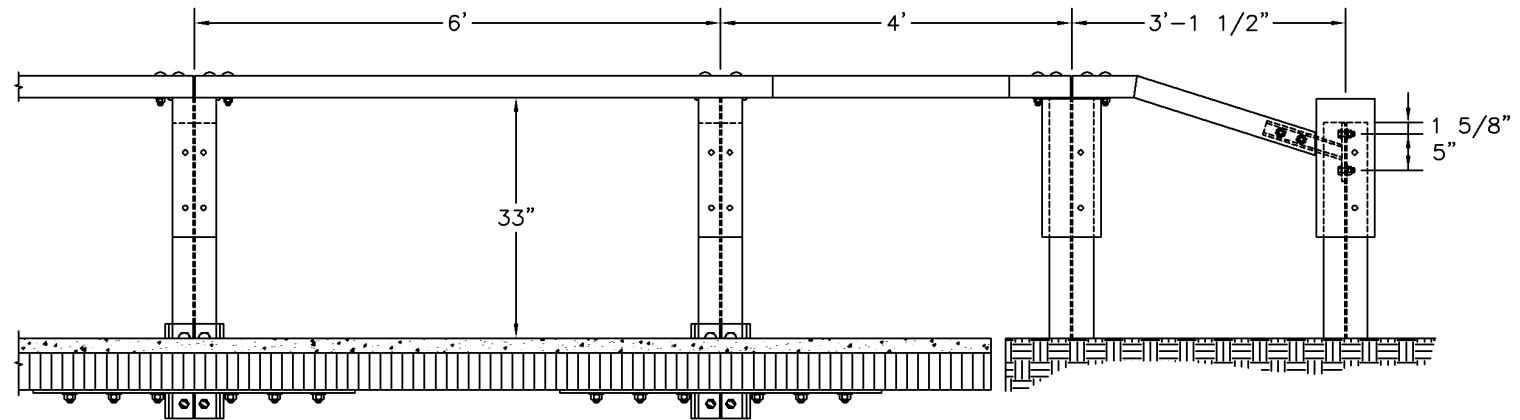
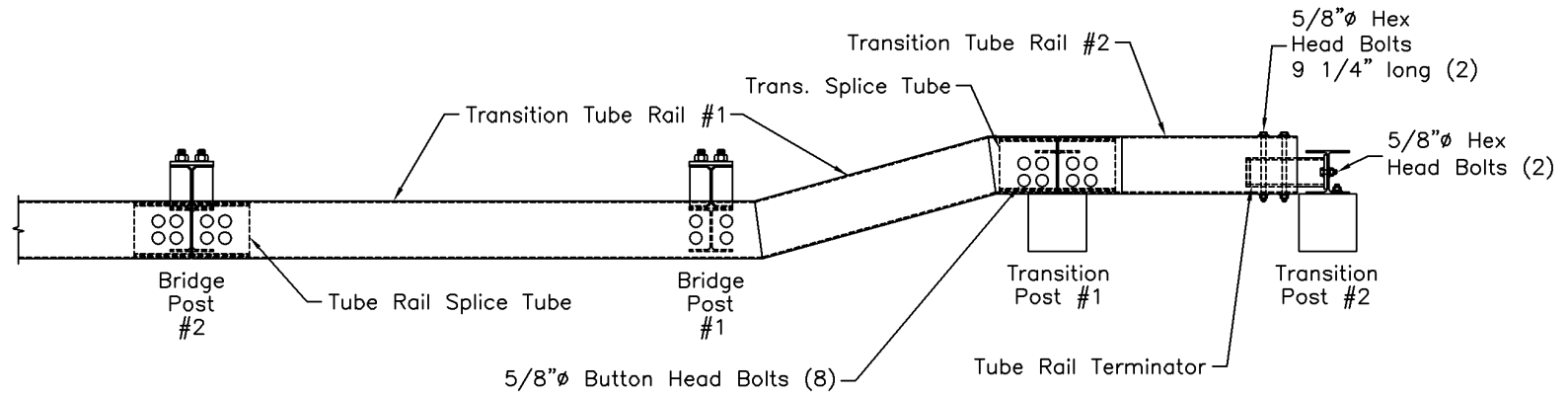
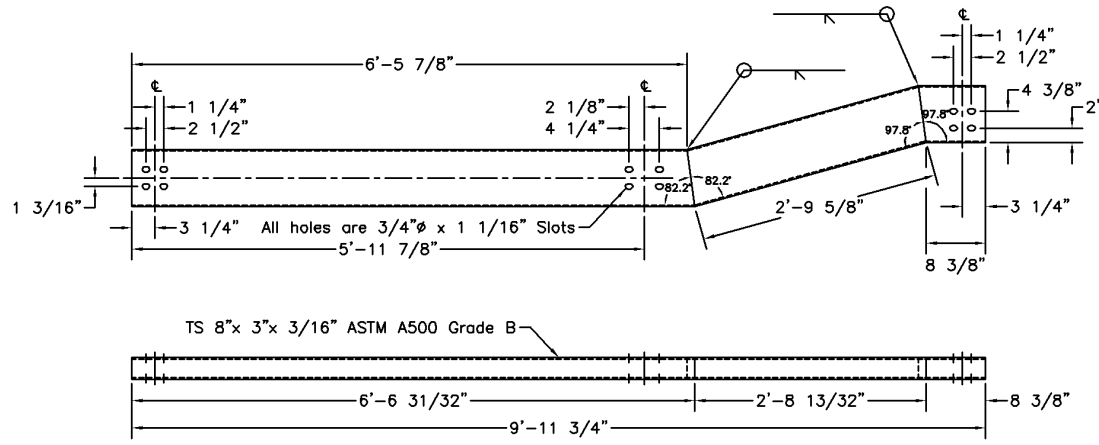


Figure 133. General Configuration of Approach Guardrail Transition System - Steel System

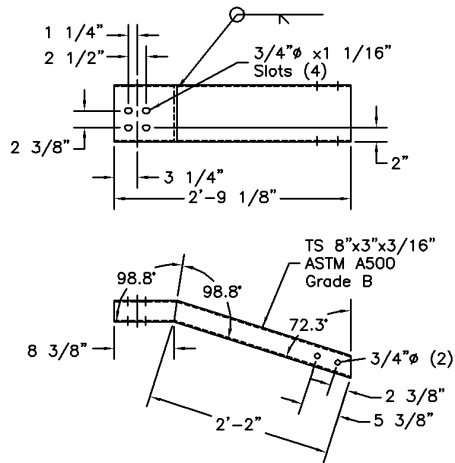


NOTE: Thrie Beam rail omitted for detail clarity.

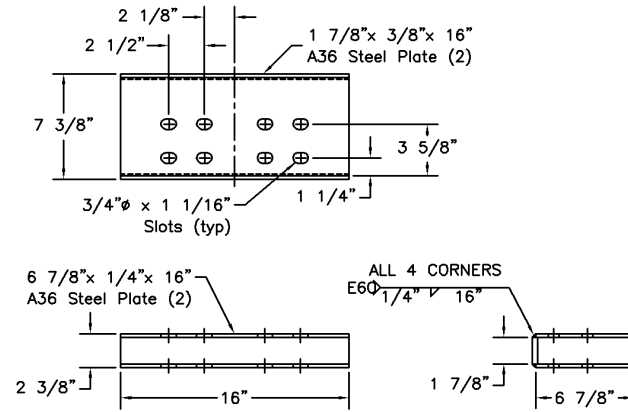
Figure 134. Tube Rail Transition Details - Steel System



Tube Transition Rail #1



Tube Transition Rail #2



Transition Splice Tube

Figure 135. Tube Transition Rails and Transition Splice Tube Details - Steel System

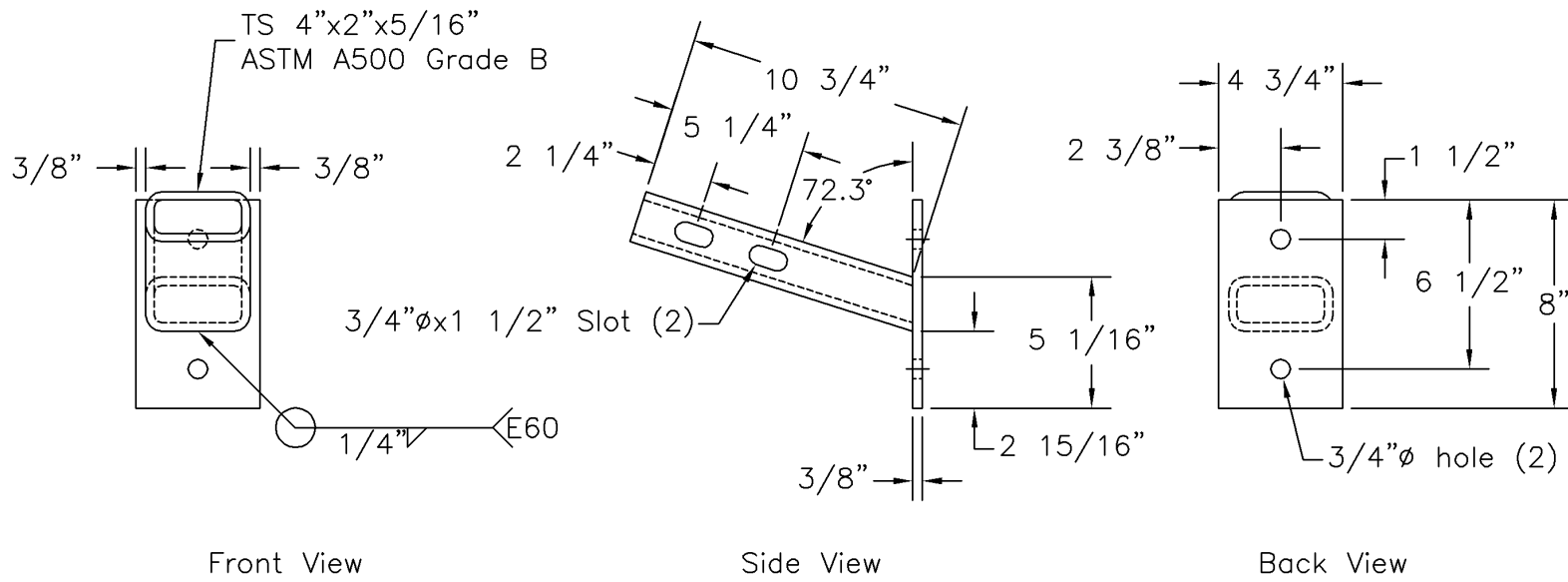


Figure 136. Tube Rail Terminator Details - Steel System

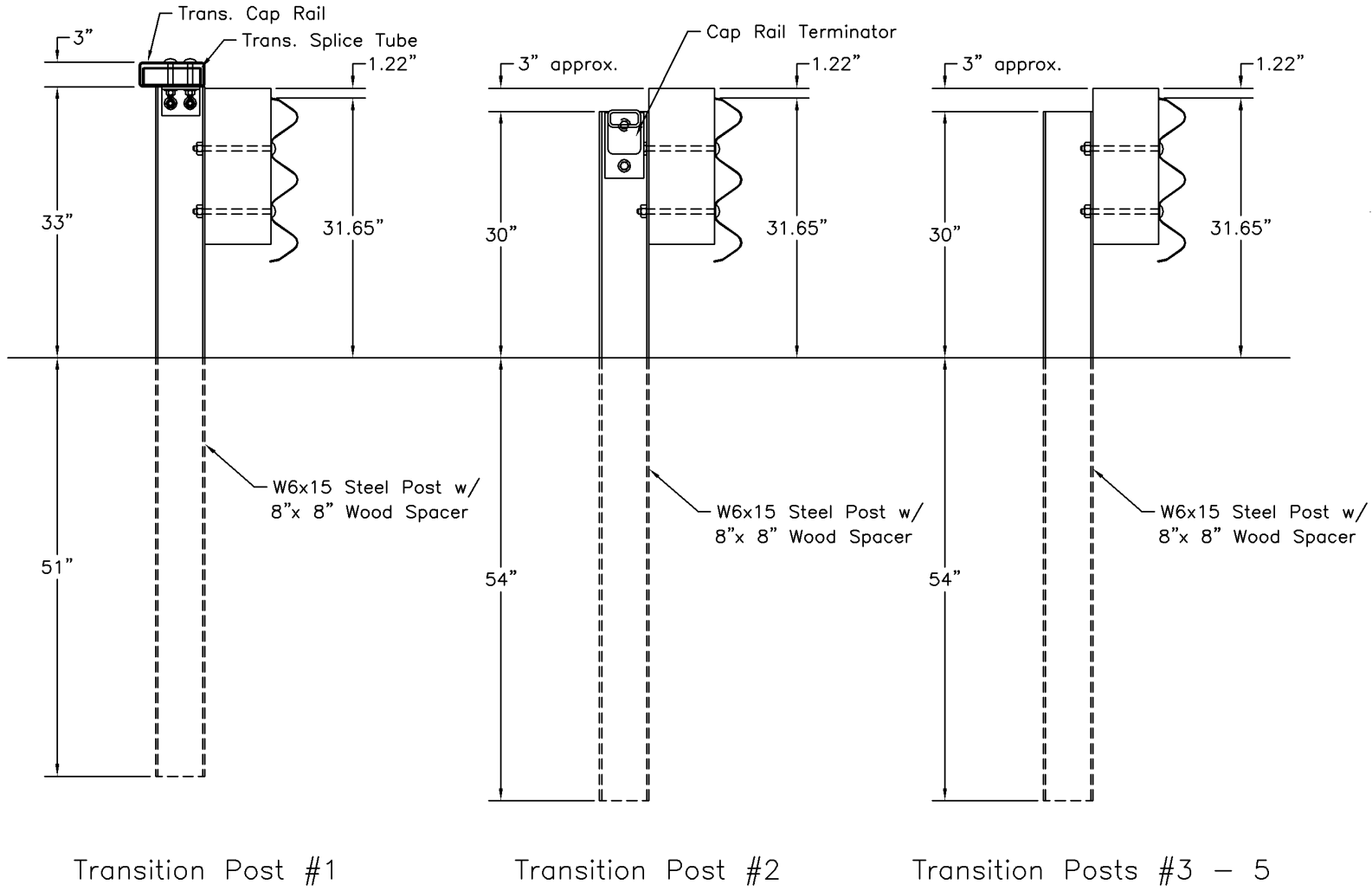


Figure 137. Transition Post Nos. 1 through 5 Configurations

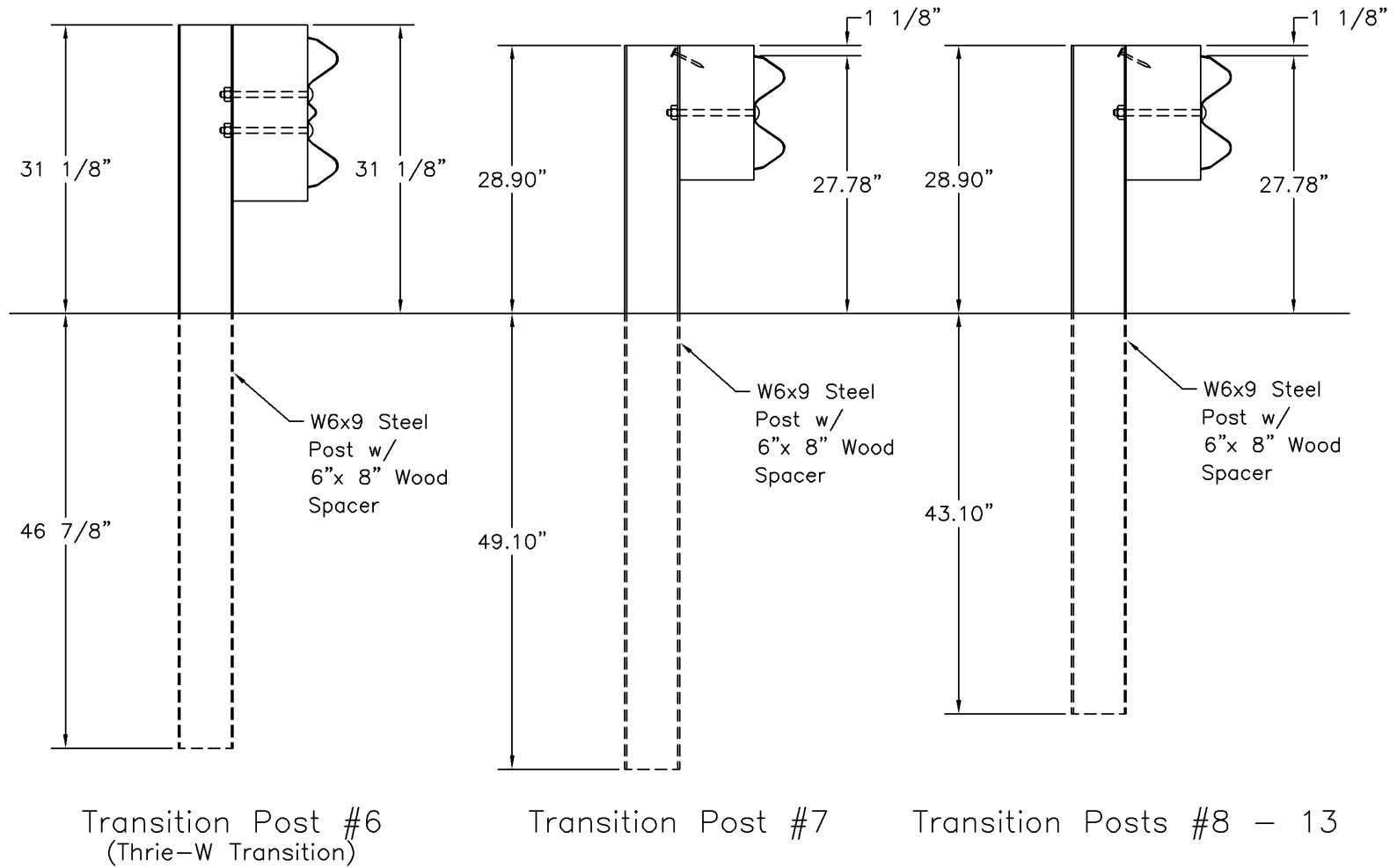


Figure 138. Transition Post Nos. 6 through 13 Configurations

16 COMPUTER SIMULATION

16.1 Introduction

Computer simulation modeling with BARRIER VII (27) was performed to analyze and predict the dynamic performance of the steel bridge railing and approach guardrail transition systems prior to full-scale vehicle crash testing. The simulations were conducted modeling: (1) a 2000-kg pickup truck impacting at a speed of 100.0 km/hr and at an angle of 25 degrees; and (2) an 8,000-kg single-unit truck impacting at a speed of 80 km/hr and at an angle of 15 degrees. The BARRIER VII finite element models of the bridge railing and approach guardrail transition systems are shown in Appendix N. Typical computer simulation input data files for each system and vehicle are shown in Appendix O. Computer simulation was also used to determine the CIP for the steel bridge railing and approach guardrail transition systems.

16.2 BARRIER VII Results

16.2.1 Bridge Railing Results

The simulation results indicated that the steel bridge railing system described in Section No. 15 would satisfactorily redirect the 2,000-kg pickup truck and the 8,000-kg single unit truck. In addition, all structural hardware would remain functional during both of the vehicle impacts with the bridge railing system.

For the 2,000-kg pickup truck impact simulation, the CIP was determined to occur with an impact between bridge post nos. 5 and 6 or 305-mm downstream from the centerline of post no. 5. The maximum dynamic and permanent set deflections of the steel thrie beam rail, as measured from the roadway surface to the center of the thrie beam rail, were 275 mm and 188 mm, respectively. The maximum dynamic and permanent set deflections of the steel tube rail, as measured from the

roadway surface to the center of the tube rail, were 287 mm and 189 mm, respectively. The maximum 0.010-sec average lateral and longitudinal decelerations were 11.8 and 13.7 g's, respectively. The peak 0.050-sec average impact force perpendicular to the bridge railing was 276.1 kN. The pickup truck became parallel to the bridge railing at 0.210 sec with a velocity of 71.2 km/hr. At 0.302 sec after impact, the pickup truck exited the bridge railing with a velocity of 68.0 km/hr and at an angle of 7.4 degrees.

For the 8,000-kg single-unit truck impact simulation, the CIP was determined to occur with an impact at the centerline of bridge post no. 6. The maximum dynamic and permanent set deflections of the three beam rail, as measured from the roadway surface to the center of the rail, were 335 mm and 183 mm, respectively. The maximum dynamic and permanent set deflections of the tube rail, as measured from the roadway surface to the center of the tube rail, were 359 mm and 292 mm, respectively. The maximum 0.010-sec average lateral and longitudinal decelerations were 3.0 and 2.5 g's, respectively. The peak 0.050-sec average impact force perpendicular to the bridge railing was 245.0 kN. The truck became parallel to the bridge railing at 0.327 sec with a velocity of 68.1 km/hr. At 0.682 sec after impact, the truck exited the bridge railing with a velocity of 63.5 km/hr and at an angle of 16.7 degrees.

16.2.2 Approach Guardrail Transition Results

The simulation results indicated that the approach guardrail transition system would satisfactorily redirect the 2,000-kg pickup truck and the 8,000-kg single unit truck. In addition, all structural hardware would remain functional during both of the vehicle impacts with the approach guardrail transition system.

For the 2,000-kg pickup truck impact simulation, the CIP was determined to occur with an

impact at the midspan between transition post no. 2 and 3 or 476-mm upstream of post no. 2. The maximum dynamic and permanent set deflections of the thrie beam rail, as measured from the roadway surface to the center of the thrie beam rail, were 261 mm and 167 mm, respectively. The maximum dynamic and permanent set deflections of the tube rail, as measured from the roadway surface to the center of the tube rail, were 111 mm and 47 mm, respectively. The maximum 0.010-sec average lateral and longitudinal decelerations were 12.0 and 13.2 g's, respectively. The peak 0.050-sec average impact force perpendicular to the bridge railing was 245.1 kN. The pickup truck became parallel to the bridge railing at 0.201 sec with a velocity of 69.2 km/hr. At 0.314 sec after impact, the pickup truck exited the bridge railing with a velocity of 67.2 km/hr and at an angle of 11.0 degrees.

For the 8,000-kg single-unit truck impact simulation, the CIP was determined to occur with an impact between transition post nos. 3 and 4 or 238-mm upstream from transition post no. 3. The maximum dynamic and permanent set deflections of the thrie beam rail, as measured from the roadway surface to the center of the thrie beam rail, were 235 mm and 113 mm, respectively. The maximum dynamic and permanent set deflections of the tube rail, as measured from the roadway surface to the center of the tube, were 141 mm and 37 mm, respectively. The maximum 0.010-sec average lateral and longitudinal decelerations were 3.0 and 2.3 g's, respectively. The peak 0.050-sec average impact force perpendicular to the bridge railing was 230.9 kN. The truck became parallel to the bridge railing at 0.360 sec with a velocity of 69.4 km/hr. At 0.628 sec after impact, the truck exited the bridge railing with a velocity of 64.8 km/hr and at an angle of 8.1 degrees.

17 CRASH TEST NO. 1 (STEEL SYSTEM - BRIDGE RAILING)

17.1 Test STTR-1

The 1,994-kg pickup truck impacted the bridge railing at a speed of 93.7 km/hr and at an angle of 25.5 degrees. A summary of the test results and the sequential photographs are shown in Figure 139. Additional sequential photographs are shown in Figures 140 and 141. Documentary photographs of the crash test are shown in Figures 142 and 143.

17.2 Test Description

Initial impact occurred between bridge post nos. 5 and 6, or approximately 10,427 mm downstream from the upstream end of the bridge rail, as shown in Figure 144. At 0.033 sec after initial impact with the bridge rail, the truck was located at the midspan between post nos. 5 and 6. At this same time, the right-front corner of the truck's hood protruded over the rail as the right-front corner of the truck crushed inward. At 0.069 sec, the right-front corner was at post no. 6. At 0.110 sec, the front bumper shifted to the left as the hood continued to protrude over the top of the system. At 0.131 sec, the severely damaged right-front corner was at the midspan between post nos. 6 and 7 as the truck began to redirect. At this same time, the right-side door was deformed as the cab and box twisted toward one another. At 0.158 sec, the truck cab rolled into the rail while the left-front tire became airborne. At 0.176 sec, the right-front corner was at post no. 7. At 0.207 sec, the left-rear and right-rear tires became airborne. At 0.223 sec, the right-rear corner of the truck contacted the rail as the right-front corner of the truck was at the midspan between post nos. 7 and 8. At 0.249 sec after impact, the truck became parallel to the bridge rail with a velocity of 65.8 km/hr. At 0.282 sec, the right-front corner of the truck, while out of contact with the rail, was at post no. 8. At 0.307 sec, the truck yawed away from the rail. At this same time, the truck rolled into the rail with both

left tires still airborne. At 0.320 sec, the truck returned to a non-pitched state but still airborne with only the right-side tires in contact with the ground. At 0.359 sec after impact, the truck exited the bridge rail at an angle of less than 1 degree and a speed of 62.3 km/hr. At 0.431 sec, the right-front corner of the truck was at post no. 9 but not in contact with the rail as the truck moved laterally away from the rail. At 0.512 sec, the right-front tire was deformed and rotated 90 degrees into the engine compartment. At this same time, the truck pitched forward while still at the same roll angle. At 0.650 sec, the truck returned to an unrolled state. At 0.774 sec, the left-front tire contacted the ground while the truck traveled downstream and laterally away from the rail. At this same time, the rear-end remained pitched upwards as the roll ceased. At 0.975 sec, the truck rolled away from the bridge rail. At 1.251 sec, the truck returned to a non-pitched and non-rolled state. The vehicle's trajectory is shown in Figure 139. The vehicle's rear-end came to rest approximately 52.0 m downstream from the impact point and 5.9 m laterally away from the traffic-side face of the bridge railing, as shown in Figure 145.

17.3 Bridge Rail Damage

Damage to the bridge rail was moderate, as shown in Figures 146 through 149. Bridge railing damage consisted mostly of deformed thrie beam and tube rail sections, contact marks on a bridge rail section, deformed steel posts, and damaged spacer blocks. The physical damage to the thrie beam rail revealed that approximately 4.9 m of rail was damaged between post nos. 5 and 7. The thrie beam rail damage consisted of significant gouging of the lower corrugation, flattening of the middle and lower corrugations, and scrape marks along all corrugations. Spalling of the galvanized coating on the back side of the thrie beam rail between post nos. 5 and 6 indicated that there was intense vehicle contact with the thrie beam rail. The top of the thrie beam rail buckled at

post no. 5. The length of vehicle contact along the top of the tube rail was approximately 7.3 m. Physical evidence revealed that lateral buckling of the tube rail occurred between post nos. 5 and 6.

Four steel posts, post nos. 4 through 7, were permanently deformed during the test, as shown in Figures 148 and 149. The blockouts at post nos. 5 through 7 were also deformed. The bolt connecting the bottom of the thrie beam rail to the steel blockout sheared off at post no. 6. At post nos. 5 through 7, the concrete deck cracked near the bolts through the top plate assembly and post. No significant post or guardrail damage occurred upstream of post no. 4 nor downstream of post no. 8.

The maximum lateral permanent set deflections for midspan rail and post locations, as determined from field measurements in the impact region, were approximately 117 mm and 78 mm, respectively. The maximum dynamic lateral deflections for midspan rail and post locations, as determined from high-speed film analysis, were 137 mm and 111 mm, respectively. The effective coefficient of friction was determined to be approximately 0.47.

17.4 Vehicle Damage

Exterior vehicle damage was moderate, as shown in Figures 150 through 152. Vehicle damage occurred to several body locations, such as right-side door and quarter panel, front bumper, right-side wheels and rims, front axle, right-side of the pickup box, windshield, and interior floorboard. The right corner of the frontal bumper and the right-side door and quarter panel were crushed inward due to contact with the thrie beam rail, as shown in Figures 150 and 151. The right-front wheel assembly was pushed back toward the firewall, as shown in Figure 151. The right-rear steel rim was deformed with a 102-mm long indentation found on the rim's perimeter. Four of the

nuts were removed from the studs on this same wheel. The front bumper buckled 305-mm off center toward the right side. The hood shifted toward the left side. The front windshield was cracked on the right side. Maximum occupant compartment deformations to the floorboard were 83-mm lateral displacement near the center region of the right-side door, 38-mm longitudinal displacement near the firewall region, and 108-mm vertical displacement near the center of the floorboard's center hump. Interior vehicle deformations to the floorboard, as shown in Figure 152, were judged insufficient to cause serious injury to the vehicle occupants. No deformations occurred to the interior front dashboard nor the roof.

17.5 Occupant Risk Values

The longitudinal and lateral occupant impact velocities were determined to be 6.59 m/sec and 7.88 m/sec, respectively. The maximum 0.010-sec average occupant ridedown decelerations in the longitudinal and lateral directions were 8.89 g's and 20.58 g's, respectively. It is noted that the occupant impact velocities and occupant ridedown decelerations were within the suggested limits provided in NCHRP Report No. 350. The results of the occupant risk, determined from accelerometer data, are summarized in Figure 139. Results are shown graphically in Appendix P. The results from the rate transducer are shown graphically in Appendix Q.

17.6 Discussion

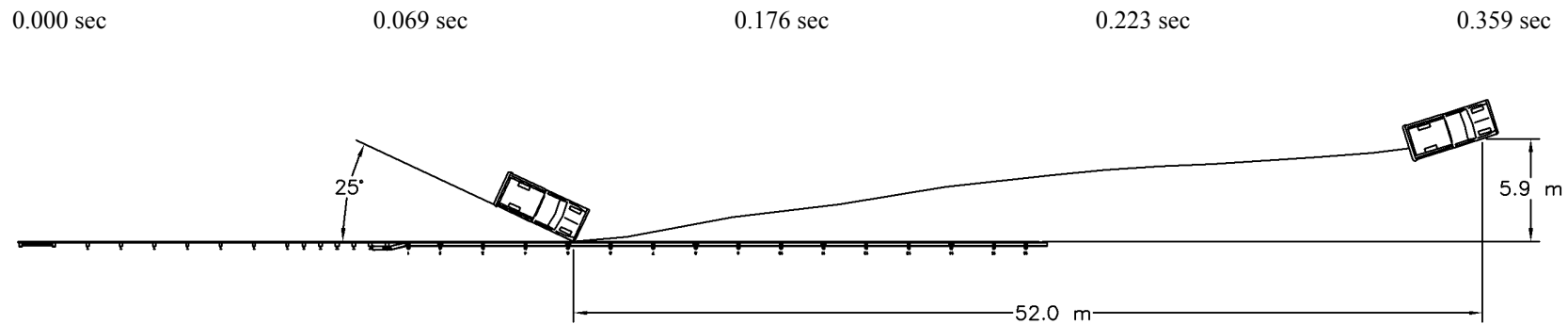
The analysis of the test results for test STTR-1 showed that the bridge railing adequately contained and redirected the vehicle with controlled lateral displacements of the bridge rail. There were no detached elements nor fragments which showed potential for penetrating the occupant compartment or presented undue hazard to other traffic. Minor deformations to the occupant compartment were evident but not considered excessive enough to cause serious injuries to the

occupants. The test vehicle did not penetrate or ride over the bridge rail and remained upright during and after the collision. Vehicle roll, pitch, and yaw angular displacements were noted, but they were deemed acceptable because they did not adversely influence occupant risk safety criteria nor cause rollover. After collision, the vehicle's trajectory revealed minimum intrusion into adjacent traffic lanes. In addition, the vehicle's exit angle was less than 60 percent of the impact angle. Therefore, test STTR-1 conducted on the steel bridge rail system was determined to be acceptable according to the NCHRP Report No. 350 performance criteria.

Prior to performing the single-unit truck test, two sections of thrie beam located between bridge post nos. 4 and 8 were replaced. The top tube rail section was also replaced between post nos. 5 and 8. In addition, post nos. 4 through 7 along with the blockouts at post nos. 5 through 7 were replaced. The top and bottom plate assemblies at post no. 6 were also replaced prior to the single-unit truck test.

17.7 Barrier Instrumentation Results

For test STTR-1, strain gauges were located on selected components of the steel bridge railing system. The results of the strain gauge analysis are summarized in Table 5 and shown graphically in Appendix R.



- Test Number STTR-1
- Date 2/17/98
- Appurtenance Steel Bridge Rail with Tube Rail System for Transverse Decks
- Total Length 37.19 m
- Steel Thrie Beam Rail
 - Type AASHTO M180
 - Thickness 3.42 mm
 - Top Mounting Height 804 mm
- Steel Structural Tube Rail
 - Type TS 203x76x4.76 - ASTM A500 Grade B
 - Top Mounting Height 914 mm
- Steel Post Nos. 1-16
 - Material ASTM A36
 - Dimensions W152x22.3 by 961-mm long
- Steel Spacer Block Nos. 1 - 16
 - Material ASTM A36
 - Dimensions W152x22.3 by 487-mm long
- Vehicle Model 1990 Ford F-250 3/4-Ton Pickup Truck
 - Curb 2,008 kg
 - Test Inertial 1,994 kg
 - Gross Static 1,994 kg
- Vehicle Speed
 - Impact 93.7 km/hr
 - Exit 62.3 km/hr
- Vehicle Angle
 - Impact 25.5 deg
 - Exit 1.5 deg
- Vehicle Snagging None
- Vehicle Stability Satisfactory
- Effective Coefficient of Friction (μ) 0.47
- Occupant Ridedown Deceleration (10 msec avg.)
 - Longitudinal 8.89 < 20 G's
 - Lateral (not required) 20.58
- Occupant Impact Velocity
 - Longitudinal 6.59 < 12 m/s
 - Lateral (not required) 7.88
- Vehicle Damage Moderate
 - TAD²⁸ 1-RFQ-6
 - SAE²⁹ 01-RYAW4
- Vehicle Stopping Distance 52.0 m downstream
5.9 m lateral
- Bridge Rail Damage Moderate
- Maximum Deflections
 - Permanent Set 117 mm
 - Dynamic 137 mm

Figure 139. Summary of Test Results and Sequential Photographs, Test STTR-1

0.000 sec

0.307 sec

0.069 sec

0.512 sec

0.110 sec

0.774 sec

0.158 sec

0.975 sec

0.207 sec

1.251 sec

Figure 140. Additional Sequential Photographs, Test STTR-1

0.000 sec

0.320 sec

0.069 sec

0.472 sec

0.154 sec

0.650 sec

0.216 sec

Figure 141. Additional Sequential Photographs, Test STTR-1

Figure 142. Documentary Photographs, Test STTR-1

Figure 143. Documentary Photographs, Test STTR-1

Figure 144. Impact Locations, Test STTR-1

Figure 145. Final Vehicle Position, Test STTR-1

Figure 146. Barrier Damage, Test STTR-1

Figure 147. Post No. 6 Deformations, Test STTR-1

Figure 148. Permanent Set Deformations, Test STTR-1

Figure 149. Typical Post and Blockout Deformations, Test STTR-1

Figure 150. Vehicle Damage, Test STTR-1

Figure 151. Vehicle Damage, Test STTR-1

Figure 152. Occupant Compartment Deformations, Test STTR-1

Table 5. Strain Gauge Results, Test STTR-1

Hardware Type	Gauge No.	Gauge Location	Maximum μ Strain ¹ (mm/mm)	Bolt Stress at Gauge ² (MPa)	Maximum Bolt Load ³ (kN)	Maximum Bolt Stress ⁴ (MPa)	Maximum Plate Stress ⁵ (MPa)	Comments
Strain Gauge	1B	Post Bolt No. 6	1,877	388.2	196.69	503.1	NA	Upstream side of bolt
	2	Post Bolt No. 6	2,534	524.1	265.55	679.2 (yield)	NA	Downstream side of bolt
	6	Top Plate No. 6	128	NA	NA	NA	26.5	Downstream - perpendicular to rail
	7	Top Plate No. 6	66	NA	NA	NA	13.6	Downstream - parallel to rail
	8	Bottom Plate No. 6	1,128	NA	NA	NA	233.3	Middle - perpendicular to rail
	9	Flange Post No. 6	1,580	NA	NA	NA	yield condition	Traffic-side face
	10	Flange Post No. 6	1,196	NA	NA	NA	247.4	Back-side face
	11	Post Bolt No. 7	1,644	340.0	172.28	440.6	NA	Upstream side of bolt
	12	Post Bolt No. 7	1,366	282.5	143.12	366.1	NA	Downstream side of bolt
	15	Top Plate No. 7	1,063	NA	NA	NA	219.9	Middle - perpendicular to rail
	18	Bottom Plate No. 7	936	NA	NA	NA	193.6	Middle - perpendicular to rail
	19	Flange Post No. 7	1,115	NA	NA	NA	230.5	Traffic-side face
20	Flange Post No. 7	1,012	NA	NA	NA	209.3	Back-side face	

¹ - All strain values are shown as the absolute value only.

² - For ASTM A325 steel bolts, elastic stress values are shown as absolute value only and calculated by multiplying the strain by the modulus of elasticity equal to 207,000 MPa (30,000 ksi). Minimum yield stress for the bolts is 634 MPa (92 ksi).

³ - For maximum bolt load, bolt stress is multiplied by the gross area of a 25-mm (1-in.) diameter bolt or 506.71 mm² (0.7854 in²).

⁴ - For ASTM A325 steel bolts, elastic stress values are shown as the absolute value only and calculated by dividing the maximum bolt load by the tensile stress area equal to 390.97 mm² (0.606 in²) in the threaded region. Minimum yield stress for the bolts is 634 MPa (92 ksi).

⁵ - For ASTM A36 steel plates, elastic stress values are shown as the absolute value only and calculated by multiplying the strain by the modulus of elasticity equal to 207,000 MPa (30,000 ksi). Minimum yield stress for the plates is 248 MPa (36 ksi).

NA - Not available or not applicable.

18 CRASH TEST NO. 2 (STEEL SYSTEM - BRIDGE RAILING)

18.1 Test STTR-2

The 8,067-kg single-unit truck impacted the bridge railing at a speed of 76.4 km/hr and at an angle of 14.6 degrees. A summary of the test results and the sequential photographs are shown in Figure 153. Additional sequential photographs are shown in Figures 154 and 155. Due to technical difficulties, documentary photographs of the crash test were unavailable.

18.2 Test Description

Initial impact occurred at the centerline of bridge post no. 5 or approximately 10,122 mm downstream from the upstream end of the bridge rail, as shown in Figure 156. At 0.047 sec, after initial impact, the front of the truck was at the midspan between post nos. 5 and 6. At 0.055 sec, the front bumper crushed inward toward the engine compartment. At 0.101 sec, the right-front corner of the truck was at post no. 6 as ripples appeared in the thrie beam rail. At this same time, the right-front fender extended over the top tube rail that was displaced. At 0.129 sec, the truck's cab rolled toward the rail while the box remained unaffected, and the right-front tire was deflated. At 0.136 sec, the right-front tire moved backward out of its normal position. At 0.156 sec, the front of the truck was at the midspan between post nos. 6 and 7, and the leading corner of the truck's box contacted the top tube rail at the midpoint between post nos. 5 and 6. At 0.168 sec, the right-front fender was extremely deformed and continued to extend over the top tube rail. At 0.205 sec, the front of the truck was at post no. 7. At 0.238 sec, the rear of the truck box contacted the rail as the box started to roll counter-clockwise (CCW) into the rail. At this same time, the front-right fender raised up off the tube rail. At 0.255 sec, the front of the truck was at the midspan between post no. 7 and 8 with the right-front corner protruding over the top tube rail. At this same time, the box

rolled into the rail independent of the cab. At 0.310 sec, the front of the truck was at post no. 8, and the rear of box remained in contact with the rail. At this same time, the truck hood jarred open, and the right-rear tire contacted the thrie beam rail slightly upstream of post no. 6, which deformed due to the impact. At 0.379 sec after impact, the truck became parallel to the rail with a velocity of 68.4 km/hr, but with the box shifted over the rail. At 0.402 sec, the left-front tire was laid over on its side, and the left-rear tires were off of the ground. At 0.479 sec, the back to the truck box landed on top of the rail. At 0.527 sec, the box rolled toward the rail. At 0.570 sec, the entire length of the truck box was in contact with the top of the rail. At this same time, the top of the truck box was leaning behind the rail. At 0.852 sec, the box was leaning over the rail at an approximate angle of 45 degrees. At 1.337 sec, the truck's box began to roll clockwise (CW) but still remained over the backside of the bridge rail. At 1.584 sec, the front of the truck cleared the downstream end of the bridge rail. At 1.782 sec after impact, the truck exited the downstream end of the bridge rail with a speed of 63.6 km/hr. At 2.515 sec, the truck's box returned to approximately an unrolled state. The vehicle's post-impact trajectory is shown in Figure 153. The vehicle's rear-end came to rest 16.9-m downstream from impact and 0.5-m laterally away from the traffic-side face of the bridge rail, as shown in Figure 157.

18.3 Bridge Rail Damage

Damage to the bridge rail was moderate, as shown in Figures 158 through 160. Bridge railing damage consisted mostly of deformed thrie beam and tube rail sections, contact marks on a bridge rail section, deformed steel posts, and damaged spacer blocks. The physical damage to the thrie beam was found between bridge post nos. 5 and 7. The thrie beam rail damage consisted of significant gouging of the middle corrugation and flattening of the lower corrugation. Contact marks

were also found along all corrugations on the thrie beam and tube rail from post no. 5 to the downstream end of the bridge rail. Spalling of the galvanized coating on the back side of the thrie beam rail between post nos. 5 and 7 indicated that there was intense vehicle contact with the thrie beam rail. Lateral buckling of the tube rail occurred at post no. 5.

Three steel posts, post nos. 5 through 7, were permanently deformed during the test, as shown in Figures 159 and 160. The blockouts at post nos. 5 and 6 were also deformed. At post nos. 5 and 6, the concrete deck cracked around the deck-to-post connection. No significant post or guardrail damage occurred upstream of post no. 5 nor to the downstream end anchor.

The maximum lateral permanent set deflections for midspan rail and post locations, as determined from field measurements in the impact region, were approximately 137 mm and 68 mm, respectively. The effective coefficient of friction was determined to be approximately 0.29.

18.4 Vehicle Damage

Exterior vehicle damage was moderate, as shown in Figures 161 through 163. Vehicle damage occurred to several body locations, such as right-side door, quarter panel, and side step, front bumper, front axle, right-side wheels and rims, left-side front wheel and rim, drive shaft, steel frame and suspension, and interior floorboard. The right corner of the front bumper and the right-side door, quarter panel, and side step were crushed inward, as shown in Figure 161. The front axle was disengaged and wedged under the truck, as shown in Figure 161. The right-front tire was cut and deflated, and the right-front steel rim was deformed, as shown in Figures 161 and 162. The right-rear steel rim was deformed, and the tire was deflated, as shown in Figure 161. The left-front tire was removed from the rim, and the steel rim was also deformed. The drive shaft disengaged at the middle between the rear end and the transmission, as shown in Figure 162. The left side of the

frame bent toward the right side from the rear axle to the rear end of the truck. The front of the box shifted 660 mm to the right. The welds between the box frame and left-side box cross member failed from the front of the box to the rear axle, as shown in Figure 162. Two U-bolts on the front-right side failed. The hood also jarred open, as shown in Figure 161. Interior occupant compartment deformations to the right-side floorboard near the door, as shown in Figure 163, were judged insufficient to cause serious injury to the vehicle occupants. No deformations occurred to the interior front dashboard, the roof, nor the truck box.

18.5 Occupant Risk Values

The longitudinal and lateral occupant impact velocities were determined to be 1.95 m/sec and 2.49 m/sec, respectively. The maximum 0.010-sec average occupant ridedown decelerations in the longitudinal and lateral directions were 7.95 g's and 4.64 g's, respectively. It is noted that the occupant impact velocities and occupant ridedown decelerations were within the suggested limits provided in NCHRP Report No. 350. The results of the occupant risk, determined from accelerometer data, are summarized in Figure 153 and are shown graphically in Appendix S. The results from the rate transducer are shown graphically in Appendix T.

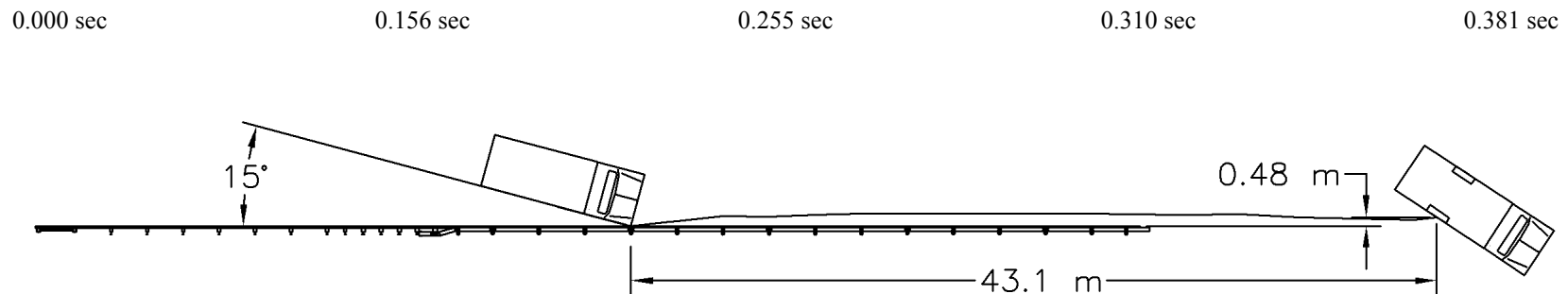
18.6 Discussion

The analysis of the test results for test STTR-2 showed that the bridge railing adequately contained and redirected the vehicle with controlled lateral displacements of the bridge rail. There were no detached elements nor fragments which showed potential for penetrating the occupant compartment or presented undue hazard to other traffic. Minor deformations to the occupant compartment were evident but not considered excessive enough to cause serious injuries to the occupants. The test vehicle did not penetrate or ride over the bridge rail and remained upright

during and after the collision. Vehicle roll, pitch, and yaw angular displacements were noted, but they were deemed acceptable because they did not adversely influence occupant risk safety criteria nor cause rollover. After collision, the vehicle's trajectory revealed minimum intrusion into adjacent traffic lanes. In addition, the vehicle's exit angle was less than 60 percent of the impact angle. Therefore, test STTR-2 conducted on the steel bridge rail system was determined to be acceptable according to the NCHRP Report No. 350 performance criteria.

18.7 Barrier Instrumentation Results

For test STTR-2, strain gauges were located on selected components of the steel bridge railing system. The results of the strain gauge analysis are summarized in Tables 6 and 7 and shown graphically in Appendix U.



● Test Number	STTR-2	● Vehicle Speed	
● Date	4/17/98	Impact	76.4 km/hr
● Appurtenance	Steel Bridge Rail with Tube Rail System for Transverse Decks	Exit	63.6 km/hr
● Total Length	37.19 m	● Vehicle Angle	
● Steel Thrie Beam Rail		Impact	14.6 deg
Type	AASHTO M180	Exit	< 1 deg
Thickness	3.42 mm	● Vehicle Snagging	None
Top Mounting Height	804 mm	● Vehicle Stability	Satisfactory
● Steel Structural Tube Rail		● Effective Coefficient of Friction (μ)	0.29
Type	TS 203x76x4.76 - ASTM A500 Grade B	● Occupant Ridedown Deceleration (10 msec avg.)	
Top Mounting Height	914 mm	Longitudinal (not required)	7.95 < 20 G's
● Steel Post Nos. 1 - 16		Lateral (not required)	4.64
Material	ASTM A36	● Occupant Impact Velocity	
Dimensions	W152x22.3 by 961-mm	Longitudinal (not required)	1.95 < 12 m/s
● Steel Spacer Block Nos. 1 - 16		Lateral (not required)	2.49
Material	ASTM A36	● Vehicle Damage	Moderate
Dimensions	W152x22.3 by 487-mm long	TAD ²⁸	1-RFQ-5
● Vehicle Model	1985 Ford F-800 Series Single-Unit Truck	SAE ²⁹	01-RFEW8
Curb	5,030 kg	● Vehicle Stopping Distance	16.9 m downstream
Test Inertial	8,067 kg	0.5 m lateral	
Gross Static	8,067 kg	● Bridge Rail Damage	Moderate
		● Maximum Deflections	
		Permanent Set	137 mm
		Dynamic	NA

Figure 153. Summary of Test Results and Sequential Photographs, Test STTR-2

0.000 sec

0.000 sec

0.129 sec

0.153 sec

0.238 sec

0.242 sec

0.376 sec

0.402 sec

1.337 sec

0.570 sec

2.515 sec

0.778 sec

Figure 154. Additional Sequential Photographs, Test STTR-2

0.000 sec

0.000 sec

0.107 sec

0.136 sec

0.166 sec

0.242 sec

0.309 sec

0.402 sec

0.479 sec

0.612 sec

Figure 155. Additional Sequential Photographs, Test STTR-2

Figure 156. Impact Locations, Test STTR-2

Figure 157. Final Vehicle Position, Test STTR-2

Figure 158. Barrier Damage, Test STTR-2

Figure 159. Post No. 6 Deformations, Test STTR-2

Figure 160. Permanent Set Deformations, Test STTR-2

Figure 161. Vehicle Damage, Test STTR-2

Figure 162. Truck Box and Frame Damage, Test STTR-2

Figure 163. Occupant Compartment Deformations, Test STTR-2

Table 6. Strain Gauge Results, Test STTR-2

Hardware Type	Gauge No.	Gauge Location	Maximum μ Strain ¹ (mm/mm)	Bolt Stress at Gauge ² (MPa)	Maximum Bolt Load ³ (kN)	Maximum Bolt Stress ⁴ (MPa)	Maximum Plate/Tube Stress ⁵ (MPa)	Comments
Strain Gauge	1	Post Bolt No. 5	1,718	355.5	180.05	460.5	NA	Upstream side of bolt
	2	Post Bolt No. 5	2,196	454.2	230.13	588.6	NA	Downstream side of bolt
	3	Top Plate No. 5	946	NA	NA	NA	195.7	Middle - perpendicular to rail
	4	Bottom Plate No. 5	1,280	NA	NA	NA	264.7 (possible yield)	Middle - perpendicular to rail
	5	Post Bolt No. 6	1,856	383.9	194.54	497.58	NA	Upstream side of bolt
	6*	Post Bolt No. 6	2,602	538.2	272.71	yield condition	NA	Downstream side of bolt
	7	Flange Post No. 6	1,433	NA	NA	NA	yield condition	Traffic-side
	8	Flange Post No. 6	798	NA	NA	NA	165.0	Back-side
	9	Top Plate No. 6	1,328	NA	NA	NA	274.7 (possible yield)	Middle - perpendicular to rail
	10	Bottom Plate No. 6	2,458	NA	NA	NA	yield condition	Middle - perpendicular to rail

248

¹ - All strain values are shown as the absolute value only.

² - For ASTM A325 steel bolts, elastic stress values are shown as absolute value only and calculated by multiplying the strain by the modulus of elasticity equal to 207,000 MPa (30,000 ksi). Minimum yield stress for the bolts is 634 MPa (92 ksi).

³ - For maximum bolt load, bolt stress is multiplied by the gross area of a 25-mm (1-in.) diameter bolt or 506.71 mm² (0.7854 in²).

⁴ - For ASTM A325 steel bolts, elastic stress values are shown as the absolute value only and calculated by dividing the maximum bolt load by the tensile stress area equal to 390.97 mm² (0.606 in²) in the threaded region. Minimum yield stress for the bolts is 634 MPa (92 ksi).

⁵ - For ASTM A36 steel plates, elastic stress values are shown as the absolute value only and calculated by multiplying the strain by the modulus of elasticity equal to 207,000 MPa (30,000 ksi). Minimum yield stress for the plates is 248 MPa (36 ksi). For ASTM A500 Grade B steel tubes, elastic stress values are shown as absolute value only and calculated by multiplying the strain by the modulus of elasticity equal to 207,000 MPa (30,000 ksi). Minimum yield stress for the plates is 317 MPa (46 ksi).

NA - Not available or not applicable.

* - Strain gauge reading reached full-scale of preset range. Thus, higher reading than what was observed may have occurred.

Table 7. Strain Gauge Results, Test STTR-2 (continued)

Hardware Type	Gauge No.	Gauge Location	Maximum μ Strain ¹ (mm/mm)	Bolt Stress at Gauge ² (MPa)	Maximum Bolt Load ³ (kN)	Maximum Bolt Stress ⁴ (MPa)	Maximum Plate/Tube Stress ⁵ (MPa)	Comments
Strain Gauge	11	Top Plate No. 6	176	NA	NA	NA	36.3	Upstream - perpendicular to rail
	12	Top Plate No. 6	141	NA	NA	NA	29.2	Downstream - perpendicular to rail
	13	Top Plate No. 6	504	NA	NA	NA	104.3	Middle upstream - perpendicular to rail
	14	Top Plate No. 6	584	NA	NA	NA	120.8	Middle downstream - perpendicular to rail
	15	Post Bolt No. 7	896	185.3	93.90	240.2	NA	Upstream side of bolt
	16	Post Bolt No. 7	910	188.2	95.36	243.9	NA	Downstream side of bolt
	17	Top Plate No. 7	1,240	NA	NA	NA	256.4 (possible yield)	Middle - perpendicular to rail
	18	Bottom Plate No. 7	933	NA	NA	NA	193.0	Middle - perpendicular to rail
	19	Steel Tube Rail	874	NA	NA	NA	180.8	Back-side face at midspan between post nos. 6 and 7
	20	Steel Tube Rail	668	NA	NA	NA	138.1	Bottom-side face at midspan between post nos. 6 and 7

¹ - All strain values are shown as the absolute value only.

² - For ASTM A325 steel bolts, elastic stress values are shown as absolute value only and calculated by multiplying the strain by the modulus of elasticity equal to 207,000 MPa (30,000 ksi). Minimum yield stress for the bolts is 634 MPa (92 ksi).

³ - For maximum bolt load, bolt stress is multiplied by the gross area of a 25-mm (1-in.) diameter bolt or 506.71 mm² (0.7854 in²).

⁴ - For ASTM A325 steel bolts, elastic stress values are shown as the absolute value only and calculated by dividing the maximum bolt load by the tensile stress area equal to 390.97 mm² (0.606 in²) in the threaded region. Minimum yield stress for the bolts is 634 MPa (92 ksi).

⁵ - For ASTM A36 steel plates, elastic stress values are shown as the absolute value only and calculated by multiplying the strain by the modulus of elasticity equal to 207,000 MPa (30,000 ksi). Minimum yield stress for the plates is 248 MPa (36 ksi). For ASTM A500 Grade B steel tubes, elastic stress values are shown as absolute value only and calculated by multiplying the strain by the modulus of elasticity equal to 207,000 MPa (30,000 ksi). Minimum yield stress for the plates is 317 MPa (46 ksi).

NA - Not available or not applicable.

19 CRASH TEST NO. 3 (STEEL SYSTEM - APPROACH GUARDRAIL TRANSITION)

19.1 Test STTR-3

The 1,997-kg pickup truck impacted the approach guardrail transition at a speed of 101.0 km/hr and at an angle of 25.6 degrees. A summary of the test results and the sequential photographs are shown in Figure 165. Additional sequential photographs are shown in Figures 166 and 167. Documentary photographs of the crash test are shown in Figures 168 through 169.

19.2 Test Description

Initial impact occurred at the midspan between transition post nos. 2 and 3 or 1,670 mm upstream from the upstream end of the steel bridge rail, as shown in Figures 170. At 0.046 sec after impact, the right-front corner of the truck was at transition post no. 1 as the bumper and right-front fender crushed inward and caught the blockout at transition post no. 1. At this same time, the hood extended over the system to the back of the transition posts. At 0.070 sec, the right-front corner of the truck was at the midspan between transition post no. 1 and bridge post no. 1 and positioned on top of the rail. At this same time, the hood released from the right-side hinge and rotated slightly toward the left side, the grill disengaged from the front of the truck, and the right-side door and fender crushed inward. At 0.085 sec, part of the right-front fender caught between the top tube rail's straight and angled pieces and subsequently tore. At 0.104 sec, the right-front corner of the truck was at bridge post no. 1. At this same time, bridge post no. 1 was deflected backward, and the hood appeared warped. At 0.119 sec, the left-front corner of the vehicle rose up as the front bumper and left-front tire shifted sideways away from the rail. At this same time, the passenger-side door deformed at the top. At 0.126 sec, the front edge of the truck box came into contact with the rail as the truck began to redirect. At this same time, the left-front tire was pushed outward from the truck.

At 0.148 sec, the cab and box junction was at transition post no. 1. At 0.158 sec, the right side of the truck was riding along the top tube rail at bridge post no. 2. At this same time, the right-rear tire contacted the rail near transition post no. 2. At 0.164 sec, the left-front tire was airborne. At 0.195 sec, the right side of the rear bumper contacted the thrie beam rail near the initial impact point. At 0.207 sec after impact, the truck became parallel to the bridge rail with a velocity of 75.7 km/hr and rolled CCW into the rail. At 0.213 sec, the rear end of the truck slid up and over the thrie beam at transition post no. 2, and the deformed rear bumper snagged on the blockout. At this same time, the right-front corner of the truck lost contact with the rail. At 0.236 sec, the left-rear tire became airborne. At 0.291 sec, the left-front and left-rear tires were positioned nearly horizontal in the air as most of the weight of the truck was placed upon the right-front tire. At 0.303 sec, the rear bumper was at bridge post no. 1, and the front of the truck was completely out of contact with the rail. At 0.377 sec, the rear bumper was at bridge post no. 2. At 0.399 sec after impact, the truck exited the bridge rail at an angle of 4.9 degrees and a speed of 73.5 km/hr. At 0.577 sec, the left-side tires were airborne as the truck continued to move away from the rail. At 0.687 sec, the left-front tire was back on the ground. At 0.953 sec, all the truck tires were back on the ground as the truck began to redirect back toward the rail. At 1.270 sec, the truck became parallel to the rail again but not in contact with the rail. At 2.649 sec, the truck crossed the face plane of the rail but beyond the end of the system. The vehicle's post-impact trajectory is shown in Figure 165. The vehicle's rear-end came to rest 56.7 m downstream from impact and 4.0 m laterally behind the bridge rail, as shown in Figure 171.

19.3 Bridge Rail and Approach Guardrail Terminal Damage

Damage to the approach guardrail transition and bridge railing was moderate, as shown in

Figures 172 through 174. The damage consisted mostly of deformed thrie beam, contact marks on a thrie beam section and a top tube rail section, displaced guardrail posts, and damaged spacer blocks. The physical damage to the thrie beam rail was found between transition post no. 3 through bridge post no. 2, as shown in Figure 172. The thrie beam damage consisted of moderate deformation and flattening of the impacted section of rail between transition post no. 3 and bridge post no. 1. Contact marks were found on the guardrail from the midspan between transition post nos. 2 and 3 through 610-mm upstream of bridge post no. 2. Contact marks were also found on the top and front faces of the top tube rail from 203-mm upstream of bridge post no. 1 through 381-mm upstream of bridge post no. 2.

No contact marks or damage was observed on the transition posts, but movement of the posts was evident by the 32-mm, 25-mm, 6-mm, and 3-mm soil gaps at the front faces of transition post nos. 1, 2, 3, and 4, respectively. The blockouts at transition post nos. 1 and 2 were contacted and damaged slightly, as shown in Figure 173. Bridge post no. 1 was permanently deformed during the test, as shown in Figure 173. The concrete deck cracked around the deck-to-post connection at bridge post no. 1. No significant guardrail damage occurred upstream of transition post no. 3 nor downstream of bridge post no. 3.

The maximum lateral permanent set deflections of the thrie beam for midspan rail and post locations were approximately 67 mm at 610-mm upstream from the centerline of bridge post no. 1 and 64 mm at bridge post no. 1, respectively, as determined from field measurements in the impact region. The maximum lateral permanent set deflections of the tube rail for midspan rail and post locations were approximately 70 mm at 610-mm upstream from the centerline of bridge post no. 1 and 75 mm at transition post no. 1, respectively, as determined from field measurements in the

impact region. The maximum lateral permanent set post deflection was approximately 67 mm at transition post no. 1, as measured in the field. The maximum dynamic lateral deflections of the thrie beam for midspan rail and post locations were 87 mm at 476 mm upstream from the centerline of transition post no. 1 and 88 mm at transition post no. 1, respectively, as determined from high-speed film analysis. The maximum dynamic lateral deflections of the tube for midspan rail and post locations were 119 mm at 610-mm upstream from the centerline of bridge post no. 1 and 143 mm at transition post no. 1, respectively, as determined from high-speed film analysis. The maximum lateral dynamic post deflection was approximately 91 mm at transition post no. 2, as determined from high-speed film analysis. The effective coefficient of friction was determined to be approximately 0.35.

19.4 Vehicle Damage

Exterior vehicle damage was moderate, as shown in Figures 175 through 177. Vehicle damage occurred to several body locations, such as right-side door and quarter panel, front bumper, right-side wheels and rims, truck box and tailgate, steel frame and suspension, and windshield. The right corner of the front bumper and the right-side door and quarter panel were crushed inward, as shown in Figures 175 and 176. The front bumper buckled 152 mm from the frame's right side toward the center of the pickup. Both doors jarred open slightly. The right-front wheel assembly was pushed back toward the firewall, as shown in Figure 176. The right-front steel rim was deformed, and the tire was deflated, as shown in Figure 176. Contact marks were found along the right side, including the door, the side of the pickup box, and the rear bumper. The pickup box shifted 25 mm to the left, as shown in Figure 175. The tailgate disengaged from the box, but the cables remained intact to the box and the tailgate. The engine also shifted slightly toward the left.

The suspension remained intact, but the lower support beam on the frame deformed approximately 90 degrees toward the rear. The front windshield was cracked on the right side, as shown in Figure 176. Interior occupant compartment deformations to the right-side floorboard near the door and the front dashboard, as shown in Figure 177, were judged insufficient to cause serious injury to the vehicle occupants.

19.5 Occupant Risk Values

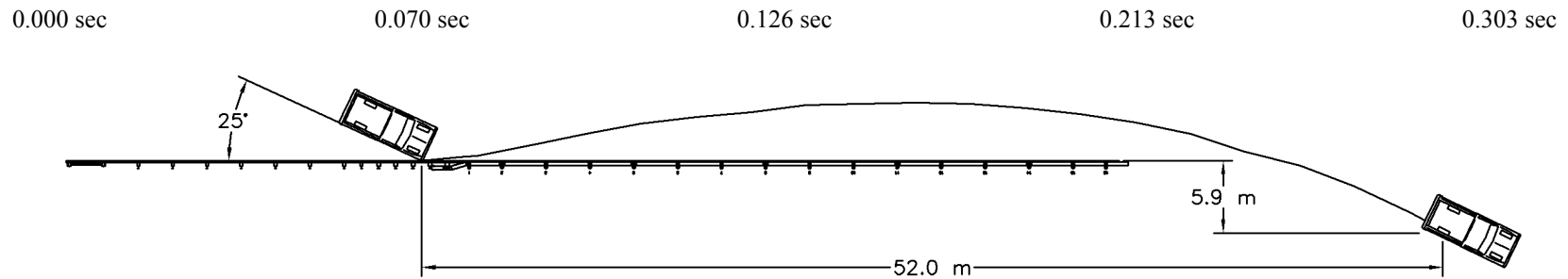
The longitudinal and lateral occupant impact velocities were determined to be 5.78 m/sec and 8.76 m/sec, respectively. The maximum 0.010-sec average occupant ridedown decelerations in the longitudinal and lateral directions were 5.97 g's and 11.08 g's, respectively. It is noted that the occupant impact velocities and occupant ridedown decelerations were within the suggested limits provided in NCHRP Report No. 350. The results of the occupant risk, determined from accelerometer data, are summarized in Figure 165 and are shown graphically in Appendix V. The results from the rate transducer are shown graphically in Appendix W.

19.6 Discussion

The analysis of the test results for test STTR-3 showed that the approach guardrail transition attached to a steel bridge rail adequately contained and redirected the vehicle with controlled lateral displacements of the guardrail transition. There were no detached elements nor fragments which showed potential for penetrating the occupant compartment or presented undue hazard to other traffic. Minor deformations to the occupant compartment were evident but not considered excessive enough to cause serious injuries to the occupants. The test vehicle did not penetrate or ride over the approach guardrail transition and remained upright during and after the collision. Vehicle roll, pitch, and yaw angular displacements were noted, but they were deemed acceptable because they did not

adversely influence occupant risk safety criteria nor cause rollover. After collision, the vehicle's trajectory revealed minimum intrusion into adjacent traffic lanes. In addition, the vehicle's exit angle was less than 60 percent of the impact angle. Therefore, test STTR-3 conducted on the approach guardrail transition attached to a steel bridge rail system was determined to be acceptable according to the NCHRP Report No. 350 performance criteria.

Prior to performing the single-unit truck test, two sections of thrie beam located between transition post no. 4 and bridge post no. 2 were replaced. The top tube rail was removed, inspected, and then reinstalled with new hardware. Bridge post no. 1 and the wooden blockouts at transition post nos. 1 and 2 were replaced. Transition post nos. 1 through 5 were re-aligned by removing a 914-mm wide x 914-mm long x 610-mm deep section of soil in this area. The soil was replaced with new optimum moisture soil in lifts and then tamped with a pneumatic hand tamper.



- Test Number STTR-3
- Date 4/28/1998
- Appurtenance Approach Guardrail Transition attached to a Steel Bridge Rail with Tube Rail System for Transverse Decks
- Total Length 20.96 m
- Steel Thrie Beam Rail
 - Thickness 3.42 mm
 - Top Mounting Height 804 mm
- Steel W-Beam Rail
 - Thickness 2.66 mm
 - Top Mounting Height 706 mm
- Steel Posts (Post Nos. 1 - 13)
 - Material ASTM A36
 - Post Nos. 1 - 5 W152x22.3 by 2,134-mm long
 - Post Nos. 6 - 7 W152x13.4 by 1,981-mm long
 - Post Nos. 8 - 13 W152x13.4 by 1,829-mm long
- Wood BCT Posts (Post Nos. 14 - 15)
 - Material Southern Yellow Pine, Grade No. 1 or Better (CCA)
 - Dimensions 140 mm x 191 mm x 1,080 mm
- Wood Spacer Blocks (Post Nos. 1 - 13)
 - Material Southern Yellow Pine, Grade No. 1 (CCA)
 - Post Nos. 1 - 5 203 mm x 203 mm x 483 mm
 - Post No. 6 152 mm x 203 mm x 483 mm
 - Post Nos. 7 - 13 152 mm x 203 mm x 368 mm

- Vehicle Model 1988 Ford F-250 ¾-Ton Pickup Truck
 - Curb 2,157 kg
 - Test Inertial 1,997 kg
 - Gross Static 1,997 kg
- Vehicle Speed
 - Impact 101.0 km/hr
 - Exit 73.5 km/hr
- Vehicle Angle
 - Impact 25.6 deg
 - Exit 4.9 deg
- Vehicle Snagging None
- Vehicle Stability Satisfactory
- Effective Coefficient of Friction (μ) 0.35
- Occupant Ridedown Deceleration (10 msec avg.)
 - Longitudinal 5.97 < 20 G's
 - Lateral (not required) 11.08
- Occupant Impact Velocity
 - Longitudinal 5.78 < 12 m/s
 - Lateral (not required) 8.76
- Vehicle Damage Moderate
 - TAD²⁸ 1-RFQ-5
 - SAE²⁹ 01-RYAW5
- Vehicle Stopping Distance 56.7 m downstream
 - 4.0 m laterally behind
- Barrier Damage Moderate
- Maximum Deflections
 - Permanent Set 75 mm
 - Dynamic 143 mm

Figure 165. Summary of Test Results and Sequential Photographs, Test STTR-3

0.000 sec

0.000 sec

0.119 sec

0.076 sec

0.186 sec

0.104 sec

0.236 sec

0.128 sec

0.577 sec

0.160 sec

0.953 sec

0.226 sec

Figure 166. Additional Sequential Photographs, Test STTR-3

0.000 sec

0.000 sec

0.041 sec

0.108 sec

0.085 sec

0.132 sec

0.148 sec

0.188 sec

0.195 sec

0.232 sec

Figure 167. Additional Sequential Photographs, Test STTR-3

Figure 168. Documentary Photographs, Test STTR-3

Figure 169. Documentary Photographs, Test STTR-3

Figure 170. Impact Locations, Test STTR-3

Figure 171. Final Vehicle Position, Test STTR-3

Figure 172. Barrier Damage, Test STTR-3

Figure 173. Barrier Damage, Test STTR-3

Figure 174. Permanent Set Deformations, Test STTR-3

Figure 175. Vehicle Damage, Test STTR-3

Figure 176. Vehicle Damage, Test STTR-3

Figure 177. Occupant Compartment Deformations, Test STTR-3

20 CRASH TEST NO. 4 (STEEL SYSTEM - APPROACH GUARDRAIL TRANSITION)

20.1 Test STTR-4

The 8,006-kg single-unit truck impacted the approach guardrail transition at a speed of 81.8 km/hr and at an angle of 15.2 degrees. A summary of the test results and the sequential photographs are shown in Figure 178. Additional sequential photographs are shown in Figures 179 and 180. Documentary photographs of the crash test are shown in Figures 181 through 183.

20.2 Test Description

Initial impact occurred between transition post nos. 3 and 4 or 2,384 mm upstream from the upstream end of the steel bridge rail, as shown in Figure 184. At 0.032 sec, the right-front corner of the truck was at transition post no. 3. At 0.080 sec, the deformed right-front corner of the truck was at transition post no. 2, and the front of the right-front fender snagged the blockout at transition post no. 2. At this same time, the front nose of the truck rolled into the rail. At 0.085 sec, the rear of the right-front fender snagged the blockout at transition post no. 3. At 0.114 sec, the right-front corner of the box was in contact with the rail at the midspan between transition post nos. 3 and 4. At this same time, the right-front corner of the truck was at transition post no. 1, and the nose of the truck began to roll into the rail. At 0.161 sec, the right-front corner of the truck was at bridge post no. 1. At 0.209 sec, the right-front corner of the box was at transition post no. 1. At this same time, the crushed right-front fender slid along the top tube rail. At 0.243 sec, the right-front corner of the truck was at bridge post no. 2 as the rear end of the truck was yawing and rolling toward the rail. At 0.261 sec, the rear corner of the box passed the vertical plane of the rail face. At 0.293 sec, the right-front corner of the box landed on top of the tube rail as the box continued to roll into the rail. At 0.312 sec, the left-rear tires were airborne. At 0.333 sec, the truck became parallel to the bridge

rail with a velocity of 69.1 km/hr. At this same time, the box rolled into the rail. At 0.395 sec, the box was rolling extensively into the rail as the truck was redirecting. At 0.420 sec, the right edge of the box was riding along the top tube rail. At this same time, the truck cab was out of contact with the rail, and the left-front tire began to rise off the ground. At 0.438 sec, the left-front tire was airborne. At 0.530 sec, the back edge of the box cleared bridge post no. 1. At 0.606 sec, the front edge of the box was no longer in contact with the rail, but the back corner of the box remained in contact with the rail. At 0.820 sec, the truck exited the bridge rail at an angle of 7.8 degrees and a speed of 65.2 km/hr. At 1.174 sec, the left-front tire contacted the ground, and shortly thereafter the left-rear tire contacted the ground. The vehicle's post-impact trajectory is shown in Figure 178. The vehicle's rear-end came to rest downstream from impact and laterally behind end of the system, as shown in Figure 185.

20.3 Bridge Rail and Approach Guardrail Transition Damage

Damage to the approach guardrail transition attached to a steel bridge rail was minimal, as shown in Figures 186 through 188. The damage consisted mostly of deformed thrie beam, contact marks on a thrie beam section, a tube rail section, and blockouts, and displaced guardrail posts. The physical damage to the thrie beam rail was found between transition post no. 4 and bridge post no. 2, as shown in Figure 186, indicated that there was intense vehicle contact with the thrie beam rail. The thrie beam damage consisted of significant gouging and flattening of the middle corrugation from the midspan of transition post nos. 3 and 4 through the splice at transition post no. 1 and gouging of the lower corrugation 305-mm upstream of transition post no. 3. Spalling of the galvanized coating on the back side of the thrie beam rail was observed between transition post no. 3 and bridge post no. 2, as shown in Figure 187. Contact marks were found on the guardrail from

594-mm upstream of transition post no. 3 through bridge post no. 2. Contact marks were also found on the top and front faces of the tube rail from 279-mm upstream of transition post no. 1 through bridge post no. 3, as shown in Figures 186 and 188.

Light contact marks were found on transition post no. 1. No contact marks or damage was observed on any other transition posts, but movement of the posts was evident by the 6-mm, 3-mm, and 6-mm soil gaps at the back face of transition post nos. 2 and 3 and at the front face of transition post nos. 4, respectively. The blockout at transition post no. 2 was contacted and damaged slightly, as shown in Figure 187. The concrete deck cracked from the upstream end through bridge post no. 2. No significant guardrail damage occurred upstream of transition post no. 4 nor downstream of bridge post no. 3.

The maximum lateral permanent set deflections of the thrie beam for midspan rail and post locations were approximately 14 mm at 476-mm upstream from the centerline of transition post no. 2 and 16 mm at transition post no. 3, respectively, as determined from field measurements in the impact region. The maximum lateral permanent set deflections of the tube rail for midspan rail and post locations were approximately 38 mm at 610-mm upstream from the centerline of bridge post no. 1 and 32 mm at transition post no. 1, respectively, as determined from field measurements in the impact region. The maximum lateral permanent set post deflection was approximately 30 mm at transition post nos. 1 and 2, as measured in the field. The maximum lateral dynamic deflections of the thrie beam for midspan rail and post locations were 83 mm at 476-mm upstream from the centerline of transition post no. 2 and 79 mm at transition post no. 3, respectively, as determined from high-speed film analysis. The maximum lateral dynamic deflections of the tube rail for midspan rail and post locations were 61 mm at 610-mm upstream from the centerline of bridge post

no. 1 and 93 mm at transition post no. 2, respectively, as determined from high-speed film analysis. The maximum lateral dynamic post deflection was 92 mm at transition post no. 2, as determined from high-speed film analysis. The effective coefficient of friction was determined to be approximately 0.46.

20.4 Vehicle Damage

Exterior vehicle damage was minor, as shown in Figures 189 through 190. Vehicle damage occurred to several body locations, such as the right-side quarter panel, front bumper, right-rear rim, and truck box. The right-side quarter panel and right corner of the front bumper were crushed inward, as shown in Figures 189 and 190. The right-rear steel rim was deformed extensively, as shown in Figure 190. A small gouge on the right side of the truck box was located slightly in front of the right-rear tire. The front axle was bent and shifted toward the rear of the cab, as shown in Figure 189. The right-front shock and brake line disengaged. The hood jarred open. Minor dents were evident on the right-side gas tank. There was no intrusion nor deformation of the occupant compartment. No other damage to the vehicle was observed.

20.5 Occupant Risk Values

The longitudinal and lateral occupant impact velocities were determined to be 1.60 m/sec and 4.33 m/sec, respectively. The maximum 0.010-sec average occupant ridedown decelerations in the longitudinal and lateral directions were 8.51 g's and 8.12 g's, respectively. It is noted that the occupant impact velocities and occupant ridedown decelerations were within the suggested limits provided in NCHRP Report No. 350. The results of the occupant risk, determined from accelerometer data, are summarized in Figure 178 and are shown graphically in Appendix X. The results from the rate transducer are shown graphically in Appendix Y.

20.6 Discussion

The analysis of the test results for test STTR-4 showed that the approach guardrail transition attached to a steel bridge rail adequately contained and redirected the vehicle with controlled lateral displacements of the guardrail transition. There were no detached elements nor fragments which showed potential for penetrating the occupant compartment or presented undue hazard to other traffic. Deformations of, or intrusion into, the occupant compartment that could have caused serious injury did not occur. The test vehicle did not penetrate or ride over the approach guardrail transition and remained upright during and after the collision. Vehicle roll, pitch, and yaw angular displacements were noted, but they were deemed acceptable because they did not adversely influence occupant risk safety criteria nor cause rollover. After collision, the vehicle's trajectory revealed minimum intrusion into adjacent traffic lanes. In addition, the vehicle's exit angle was less than 60 percent of the impact angle. Therefore, test STTR-4 conducted on the approach guardrail transition attached to a steel bridge rail system was determined to be acceptable according to the NCHRP Report No. 350 performance criteria.

0.000 sec

0.080 sec

0.161 sec

0.243 sec

0333 sec

● Test Number	STTR-4	● Vehicle Model	1988 Chevrolet C60 Single-Unit Truck
● Date	8/27/98	Curb	4,672 kg
● Appurtenance	Approach Guardrail Transition attached to a Steel Bridge Rail with Tube Rail System for Transverse Decks	Test Inertial	8,006 kg
● Total Length	20.96 m	Gross Static	8,006 kg
● Steel Thrie Beam Rail		● Vehicle Speed	
Thickness	3.42 mm	Impact	81.8 km/hr
Top Mounting Height	804 mm	Exit	65.2 km/hr
● Steel W-Beam Rail		● Vehicle Angle	
Thickness	2.66 mm	Impact	15.2 deg
Top Mounting Height	706 mm	Exit	7.8 deg
● Steel Posts (Post Nos. 1 - 13)		● Vehicle Snagging	None
Material	ASTM A36	● Vehicle Stability	Satisfactory
Post Nos. 1 - 5	W152x22.3 by 2,134-mm long	● Effective Coefficient of Friction (μ)	0.46
Post Nos. 6 - 7	W152x13.4 by 1,981-mm long	● Occupant Ridedown Deceleration (10 msec avg.)	
Post Nos. 8 - 13	W152x13.4 by 1,829-mm long	Longitudinal (not required)	8.51 < 20 G's
● Wood BCT Posts (Post Nos. 14 - 15)		Lateral (not required)	8.12
Material	Southern Yellow Pine, Grade No. 1 or Better (CCA)	● Occupant Impact Velocity	
Dimensions	140 mm x 191 mm x 1,080 mm	Longitudinal (not required)	1.60 < 12 m/s
● Wood Spacer Blocks (Post Nos. 1 - 13)		Lateral (not required)	4.33
Material	Southern Yellow Pine, Grade No. 1 (CCA)	● Vehicle Damage	Minor
Post Nos. 1 - 5	203 mm x 203 mm x 483 mm	TAD ²⁸	1-RFQ-4
Post No. 6	152 mm x 203 mm x 483 mm	SAE ²⁹	01-RYEW7
Post Nos. 7 - 13	152 mm x 203 mm x 368 mm	● Vehicle Stopping Distance	downstream and laterally behind
		● Barrier Damage	Minor
		● Maximum Deflections	
		Permanent Set	38 mm
		Dynamic	93 mm

Figure 178. Summary of Test Results and Sequential Photographs, Test STTR-4

0.000 sec

0.000 sec

0.140 sec

0.136 sec

0.312 sec

0.206 sec

0.606 sec

0.293 sec

0.820 sec

0.403 sec

Figure 179. Additional Sequential Photographs, Test STTR-4

0.000 sec

0.000 sec

0.084 sec

0.106 sec

0.172 sec

0.368 sec

0.250 sec

0.640 sec

0.366 sec

1.152 sec

Figure 180. Additional Sequential Photographs, Test STTR-4

Figure 181. Documentary Photographs, Test STTR-4

Figure 182. Documentary Photographs, Test STTR-4

Figure 183. Documentary Photographs, Test STTR-4

Figure 184. Impact Locations, Test STTR-4

Figure 185. Final Vehicle Position, Test STTR-4

Figure 186. Barrier Damage, Test STTR-4

Figure 187. Barrier Damage, Test STTR-4

Figure 188. Permanent Set Deformations, Test STTR-4

Figure 189. Vehicle Damage, Test STTR-4

Figure 190. Vehicle Damage, Test STTR-4

21 SUMMARY AND CONCLUSIONS - STEEL SYSTEM

A steel bridge railing system and an attached approach guardrail transition system were successfully developed and crash tested for use on transverse glulam timber deck bridges. Four full-scale vehicle crash tests - two on the bridge railing and two on the approach guardrail transition - were performed and determined to have acceptable safety performance according to TL-4 of NCHRP Report No. 350 (1). A summary of the safety performance evaluations for all four crash tests are provided in Table 8.

As previously mentioned, prior to the development of this steel bridge railing system, no other TL-4 railing systems had been developed for use on transverse glulam timber deck bridges except for the wood bridge railing system developed within the scope of this study. However, this research program clearly demonstrates that crashworthy steel railing systems are feasible for use on these types of bridges. The development of the steel bridge railing and transition system addressed the concerns for aesthetics, economy, material availability, ease of construction, and reasonable margin of structural adequacy. In addition, the steel bridge railing and transition system was relatively easy to install and should have reasonable construction labor costs. This steel railing system should also be adaptable to: (1) other transverse glulam timber deck bridges with thicknesses equal to or greater than 130 mm and with little or no modification; (2) longitudinal glulam timber deck bridges where sufficient deck strength is provided to resist the lateral impact forces; and (3) bridges supporting reinforced concrete decks that are capable of meeting the same lateral impact load requirements.

No significant damage to the test bridge was evident from the vehicle impact tests. For the bridge railing system, damage consisted primarily of permanent deformation of the three beam rail,

tube rail, wide flange posts, and rail spacers. Although all of the steel members remained intact and serviceable after the tests, steel members with visual permanent set deformations required replacement in the vicinity of the impact after each crash test. For the approach guardrail transition system, damaged consisted primarily of deformed thrie beam rail and bridge posts and displaced guardrail posts. Although all of the steel members remained intact and serviceable after the tests, steel members with visual permanent set deformations required replacement in the vicinity of the impact after each crash test.

Therefore, the successful completion of this phase of the research project resulted in a TL-4 steel bridge railing and approach guardrail transition system having acceptable safety performance and meeting current crash test safety standards.

Table 8. NCHRP Report No. 350 TL-4 Evaluation Results - Steel System (Bridge Railing and Transition)

Evaluation Factors	Evaluation Criteria	Test No.			
		STTR-1	STTR-2	STTR-3	STTR-4
Structural Adequacy	A. Test article should contain and redirect the vehicle; the vehicle should not penetrate, underride, or override the installation although controlled lateral deflection of the test article is acceptable.	S	S	S	S
Occupant Risk	D. Detached elements, fragments or other debris from the test article should not penetrate or show potential for penetrating the occupant compartment, or present an undue hazard to other traffic, pedestrians, or personnel in a work zone. Deformations of, or intrusions into, the occupant compartment that could cause serious injuries should not be permitted.	S	S	S	S
	F. The vehicle should remain upright during and after collision although moderate roll, pitching, and yawing are acceptable.	S	NR	S	NR
	G. It is preferable, although not essential, that the vehicle remain upright during and after collision.	NR	S	NR	S
	H. Longitudinal and lateral occupant impact velocities should fall below the preferred value of 9 m/s, or at least below the maximum allowable value of 12 m/s.	NR	NR	NR	NR
	I. Longitudinal and lateral occupant ridedown accelerations should fall below the preferred value of 15 g's, or at least below the maximum allowable value of 20 g's.	NR	NR	NR	NR
Vehicle Trajectory	K. After collision it is preferable that the vehicle's trajectory not intrude into adjacent traffic lanes.	M	S	M	S
	L. The occupant impact velocity in the longitudinal direction should not exceed 12 m/s and the occupant ridedown acceleration in the longitudinal direction should not exceed 20 g's.	S	NR	S	NR
	M. The exit angle from the test article preferably should be less than 60 percent of test impact angle, measured at time of vehicle loss of contact with test device.	S	S	S	S

S - Satisfactory
M - Marginal
U - Unsatisfactory
NR - Not Required

22 RECOMMENDATIONS - STEEL SYSTEM

As stated previously, the steel bridge railing system for use with transverse timber deck bridges was instrumented with sensors located on key components in an attempt to measure the actual forces imparted into the bridge deck. Following the analysis of the crash test and instrumentation results, it was determined that the bridge railing and transition systems performed well as designed, and that no design changes were necessary. Finally, it is recommended that the Federal Highway Administration approve the TL-4 steel bridge railing and approach guardrail transition systems for use on Federal-aid highways.

When analyzing the test results, the loads imparted into key structural hardware were less than expected. For the two 25-mm diameter ASTM A325 bolts which connected the post to the top mounting plate, the combined design load for both bolts was about 540 kN. However, the maximum combined bolt force was measured to be only about 470 kN. With this reduced loading into the plate assembly, the measured strain values near the outer regions of the top mounting plate were found to be about 10 to 12 percent of the values near the central region. Therefore, the researchers determined that the 22-mm diameter ASTM A307 bolts which connected the top and bottom mounting plates to the deck should be reduced from 12 to 10.

23 REFERENCES

1. Ross, H.E., Sicking, D.L., Zimmer, R.A. and Michie, J.D., *Recommended Procedures for the Safety Performance Evaluation of Highway Features*, National Cooperative Highway Research Program (NCHRP) Report No. 350, Transportation Research Board, Washington, D.C., 1993.
2. *Guide Specifications for Bridge Railings*, American Association of State Highway and Transportation Officials, Washington, D.C., 1989.
3. Faller, R.K., Ritter, M.A., Holloway, J.C., Pfeifer, B.G., and B.T. Rosson, *Performance Level 1 Bridge Railings for Timber Decks*, Transportation Research Record No. 1419, Transportation Research Board, National Research Council, Washington D.C., 1993.
4. Ritter, M.A., Lee, P.D.H., Faller, R.K., Rosson, B.T., and S.R. Duwaldi, *Plans for Crash Tested Bridge Railings for Longitudinal Wood Decks*, General Technical Report No. FPL-GTR-87, United States Department of Agriculture, Forest Service, Forest Products Laboratory, Madison, Wisconsin, September 1995.
5. Ritter, M.A. and R.K. Faller, *Crashworthy Bridge Railings for Longitudinal Wood Decks*, Paper presented by Ritter at the 1994 Pacific Timber Engineering Conference, Gold Coast, Australia, July 11-15, 1994.
6. Ritter, M.A., Faller, R.K., and Duwaldi, S.R., *Crash-Tested Bridge Railings for Timber Bridges*, Presented by Ritter at the Fourth International Bridge Engineering Conference, Volume 2, Conference Proceedings 7, San Francisco, California, August 28-30, 1995, Transportation Research Board, Washington, D.C., August 1995.
7. Faller, R.K., Rosson, B.T., Ritter, M.A., Lee, P.D.H., and Duwadi, S.R., *Railing Systems for Longitudinal Timber Deck Bridges*, Presented at the National Conference on Wood Transportation Structures, Madison, Wisconsin, October 23-25, 1996, General Technical Report No. FPL-GTR-94, United States Department of Agriculture - Forest Service - Forest Products Laboratory and Federal Highway Administration, October 1996.
8. Rosson, B.T., Faller, R.K., and M.A. Ritter, *Performance Level 2 and Test Level 4 Bridge Railings for Timber Decks*, Transportation Research Record No. 1500, Transportation Research Board, National Research Council, Washington D.C., 1995.
9. Faller, R.K., Rosson, B.T., Ritter, M.A., and Sicking, D.L., *Design and Evaluation of Two Low-Volume Bridge Railings*, Presented at the Sixth International Conference on Low-Volume Roads, Volume 2, Conference Proceedings 6, University of Minnesota, Minneapolis, Minnesota, June 25-29, 1995, Transportation Research Board, Washington, D.C., June 1995.

10. Ritter, M.A., Faller, R.K., Sicking, D.L., and Bunnell, S., *Development of Low-Volume Curb-Type Bridge Railings for Timber Bridge Decks*, Draft Report Submitted to the United States Department of Agriculture-Forest Service-Forest Products Laboratory, Transportation Report No. TRP-03-31-93, Midwest Roadside Safety Facility, University of Nebraska-Lincoln, December 1993.
11. Faller, R.K., Soyland, K., Rosson, B.T., Stutzman, T.M., *TL-1 Curb-Type Bridge Railing for Longitudinal Glulam Timber Decks Located on Low-Volume Roads*, Draft Report Submitted to the United States Department of Agriculture-Forest Service-Forest Products Laboratory, Transportation Research Report No. TRP-03-54-96, Performed by the Midwest Roadside Safety Facility, Civil Engineering Department, University of Nebraska-Lincoln, April 1996.
12. Faller, R.K., Rosson, B.T., and Fowler, M.D., *Top-Mounted W-Beam Bridge Railing for Longitudinal Glulam Timber Decks Located on Low-Volume Roads*, Draft Report Submitted to the United States Department of Agriculture-Forest Service-Forest Products Laboratory, Transportation Report No. TRP-03-61-96, Midwest Roadside Safety Facility, University of Nebraska-Lincoln, September 1996.
13. Faller, R.K., and Rosson, B.T., *Development of a Flexible Bridge Railing for Longitudinal Timber Decks*, Draft Report Submitted to the United States Department of Agriculture-Forest Service-Forest Products Laboratory, Transportation Report No. TRP-03-62-96, Midwest Roadside Safety Facility, University of Nebraska-Lincoln, June 1997.
14. Hancock, K.L., Hansen, A.G. and J.B. Mayer, *Aesthetic Bridge Rails, Transitions, and Terminals for Park Roads and Parkways*, Report No. FHWA-RD-90-052, Submitted to the Office of Safety and Traffic Operations R&D, Federal Highway Administration, Performed by the Scientex Corporation, May 1990.
15. Raju, P.R., GangaRao, H.V.S., Mak, K.K. and D.C. Alberson, *Timber Bridge Rail Testing and Evaluation: Timber Bridge Rail, Posts, and Deck on Steel Stringers*, Final Report, Volume 1, Constructed Facilities Center, West Virginia University, Morgantown, WV, October 1993.
16. Raju, P.R., GangaRao, H.V.S., Mak, K.K. and D.C. Alberson, *Timber Bridge Rail and Transition Rail Testing and Evaluation: Glulam Bridge Rail and Deck on Glulam Stringers*, Final Report, Volume 2, Constructed Facilities Center, West Virginia University, Morgantown, WV, October 1993.
17. Raju, P.R., GangaRao, H.V.S., Mak, K.K. and D.C. Alberson, *Timber Bridge Rail and Transition Rail Testing and Evaluation: W-Beam Steel Rail, Timber Posts and Glulam Deck on Steel Stringers*, Final Report, Volume 3, Constructed Facilities Center, West Virginia University, Morgantown, WV, October 1993.
18. Raju, P.R., GangaRao, H.V.S., Duwaldi, S.R. and H.K. Thippeswamy, *Development and*

- Testing of Timber Bridge and Transition Rails for Transverse Glued-Laminated Bridge Decks*, Transportation Research Record No. 1460, Transportation Research Board, National Research Council, Washington D.C., 1994.
19. Buth, C.E., Campise, W.L., Griffin, III, L.I., Love, M.L., and Sicking, D.L., *Performance Limits of Longitudinal Barrier Systems - Volume I - Summary Report*, Report No. FHWA/RD-86/153, Submitted to the Office of Safety and Traffic Operations, Federal Highway Administration, Performed by Texas Transportation Institute, May 1986.
 20. Ivey, D.L., Robertson, R., and Buth, C.E., *Test and Evaluation of W-Beam and Thrie-Beam Guardrails*, Report No. FHWA/RD-82/071, Submitted to the Office of Research, Federal Highway Administration, Performed by Texas Transportation Institute, March 1986.
 21. Ross, H.E., Jr., Perera, H.S., Sicking, D.L., and Bligh, R.P., *Roadside Safety Design for Small Vehicles*, National Cooperative Highway Research Program (NCHRP) Report No. 318, Transportation Research Board, Washington, D.C., May 1989.
 22. *American Wood-Preservers' Association Book of Standards*, American Wood-Preservers' Association, Woodstock, Md., 1991.
 23. Hinch, J., Yang, T-L, and Owings, R., *Guidance Systems for Vehicle Testing*, ENSCO, Inc., Springfield, VA, 1986.
 24. *Center of Gravity Test Code - SAE J874 March 1981*, SAE Handbook Vol. 4, Society of Automotive Engineers, Inc., Warrendale, Pennsylvania, 1986.
 25. Taborck, J.J., "Mechanics of Vehicles - 7", *Machine Design Journal*, May 30, 1957.
 26. Ritter, M.A., *Timber Bridges - Design, Construction, Inspection, and Maintenance*, United States Department of Agriculture, Forest Service, EM 7700-8, June 1990.
 27. Powell, G.H., *BARRIER VII: A Computer Program For Evaluation of Automobile Barrier Systems*, Prepared for: Federal Highway Administration, Report No. FHWA RD-73-51, April 1973.
 28. *Vehicle Damage Scale for Traffic Investigators*, Second Edition, Technical Bulletin No. 1, Traffic Accident Data (TAD) Project, National Safety Council, Chicago, Illinois, 1971.
 29. *Collision Deformation Classification - Recommended Practice J224 March 1980*, Handbook Volume 4, Society of Automotive Engineers (SAE), Warrendale, Pennsylvania, 1985.
 30. Polivka, K.A., Faller, R.K., Ritter, M.A., and Rosson, B.T., *Development of the TBC-8000 Bridge Railing*, Draft Report to the U.S. Department of Agriculture, Forest Service, Forest

Products Laboratory, Report No. TRP-03-30-93, Midwest Roadside Safety Facility, Civil Engineering Department, University of Nebraska-Lincoln, September 5, 2000.

24 APPENDICES

APPENDIX A

Strain Gauge Locations – Test STTR-1

Figure A-1. Strain Gauge Nos. 1 through 7 Locations, Test STTR-1

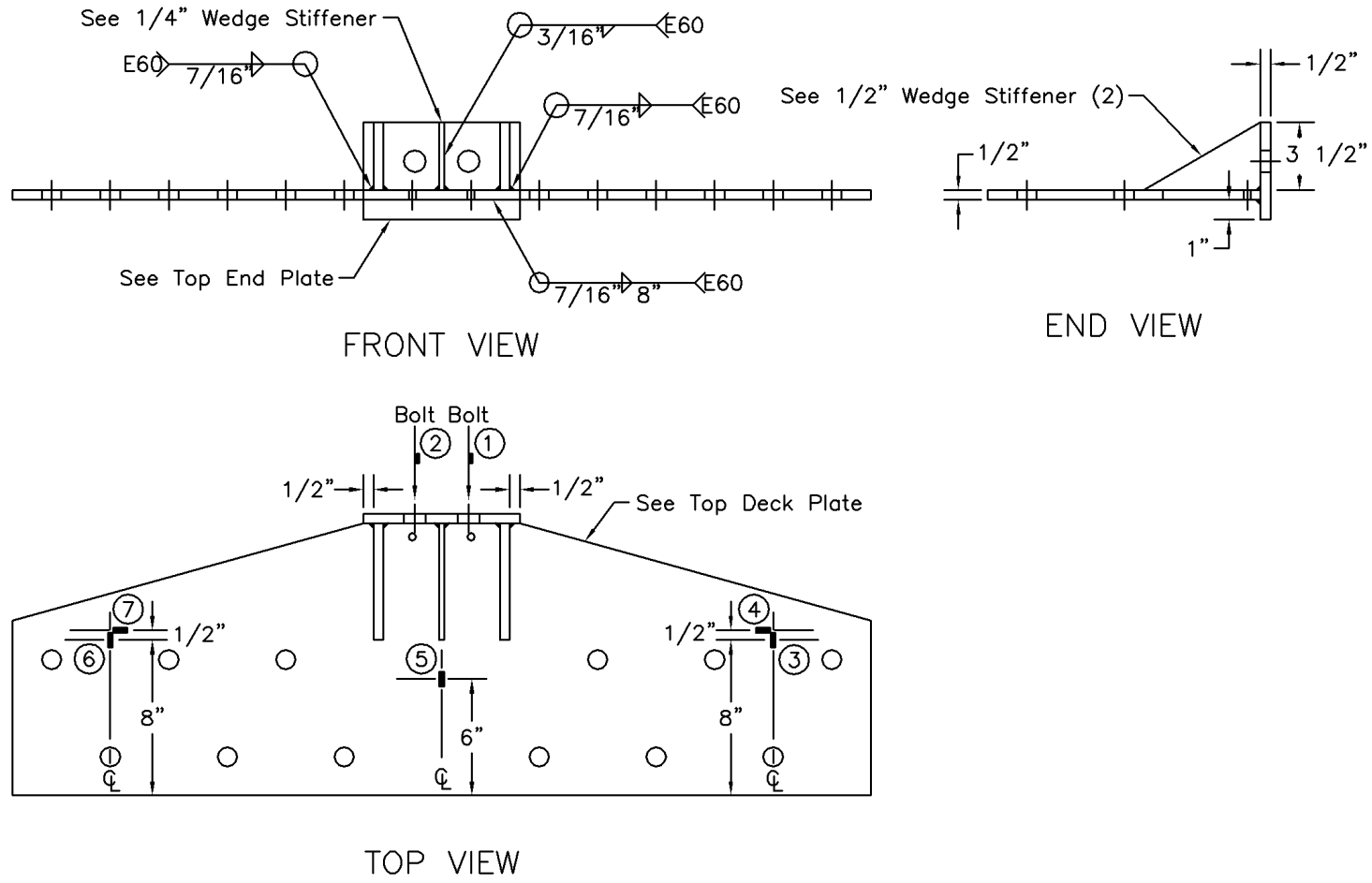
Figure A-2. Strain Gauge No. 8 Location, Test STTR-1

Figure A-3. Strain Gauge Nos. 9 and 10 Locations, Test STTR-1

Figure A-4. Strain Gauge Nos. 11 through 17 Locations, Test STTR-1

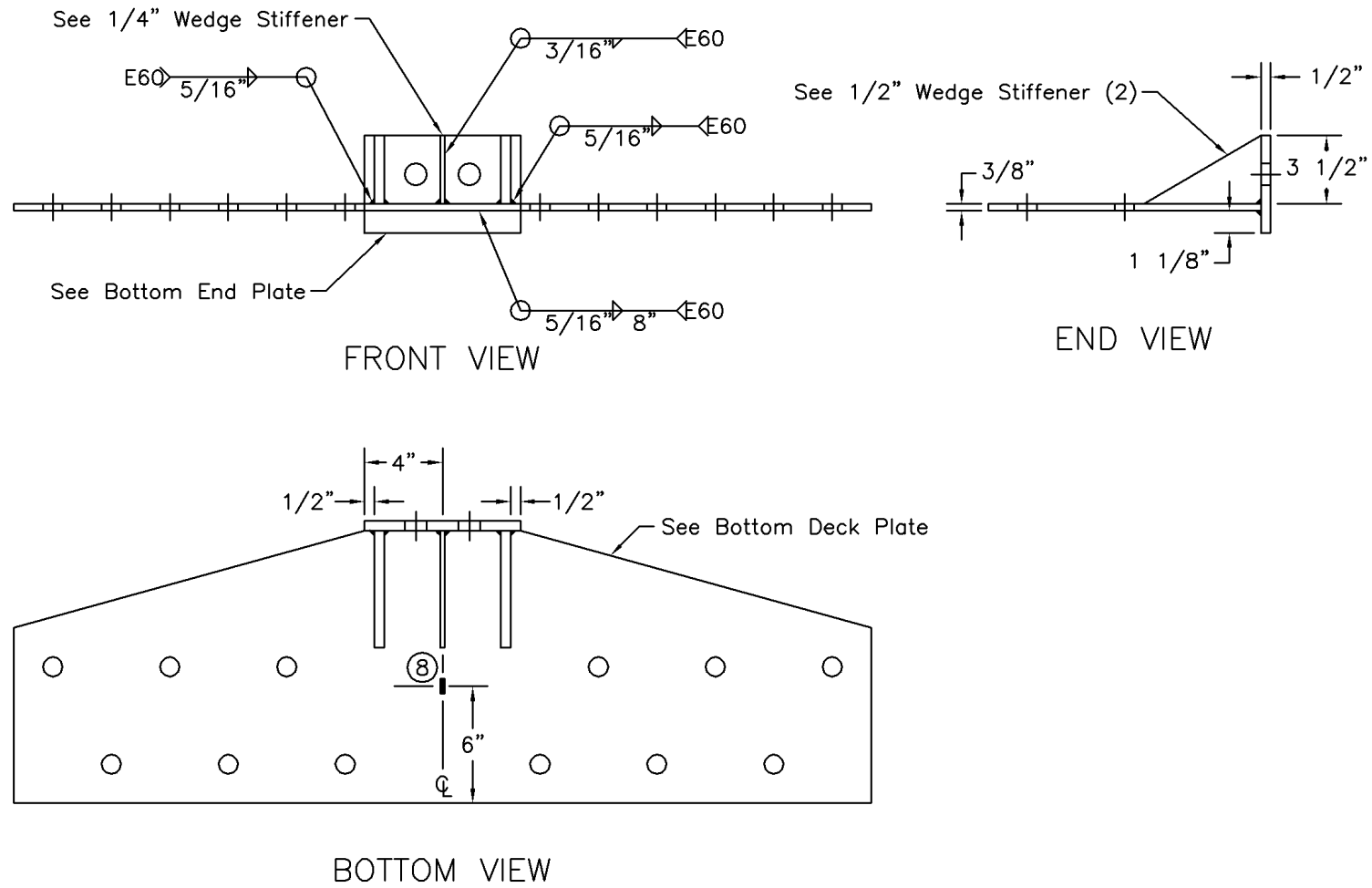
Figure A-5. Strain Gauge No. 18 Location, Test STTR-1

Figure A-6. Strain Gauge Nos. 19 and 20 Locations, Test STTR-1



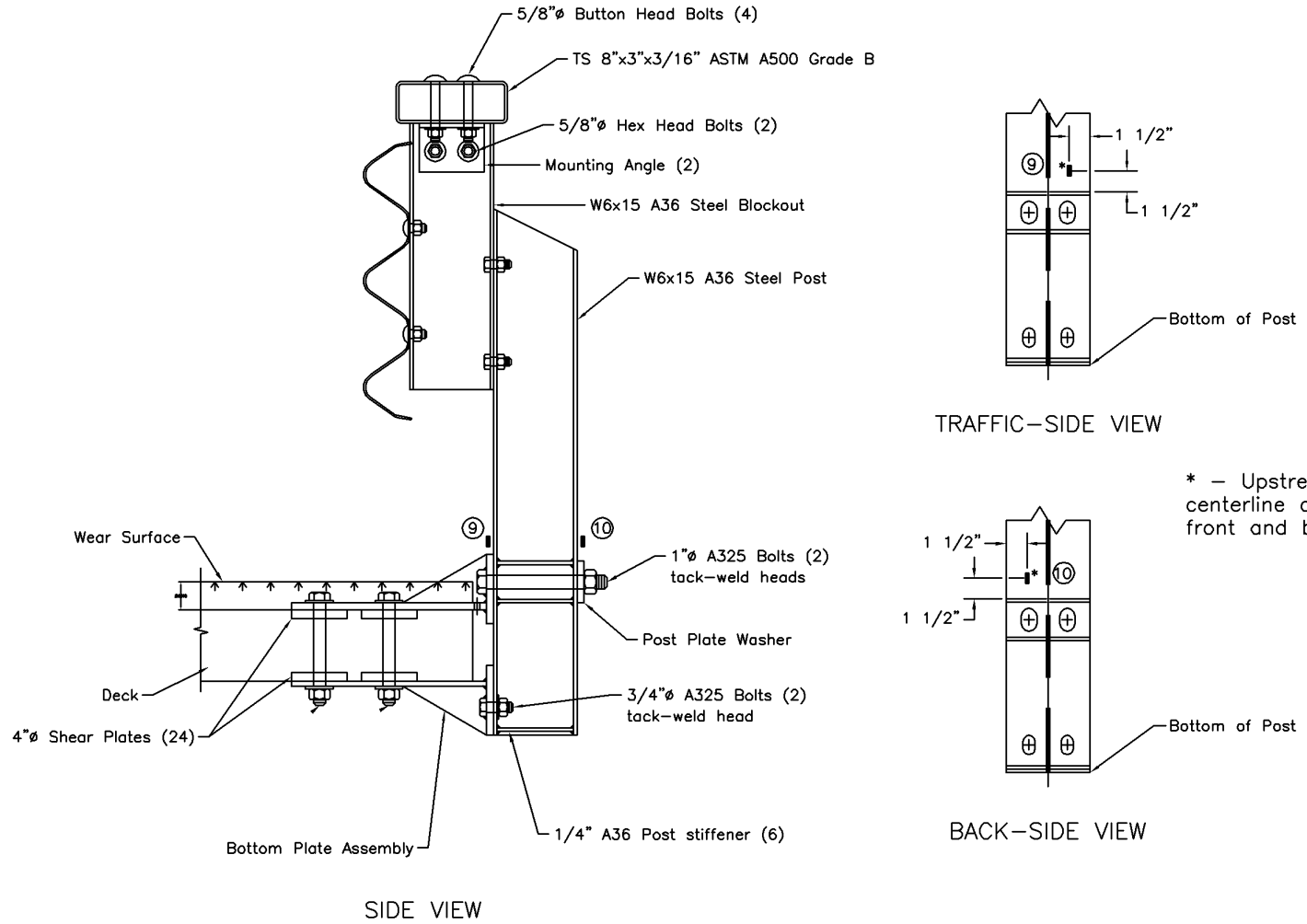
Post No. 6 Top Plate Assembly

Figure A-1. Strain Gauge Nos. 1 through 7 Locations, Test STTR-1



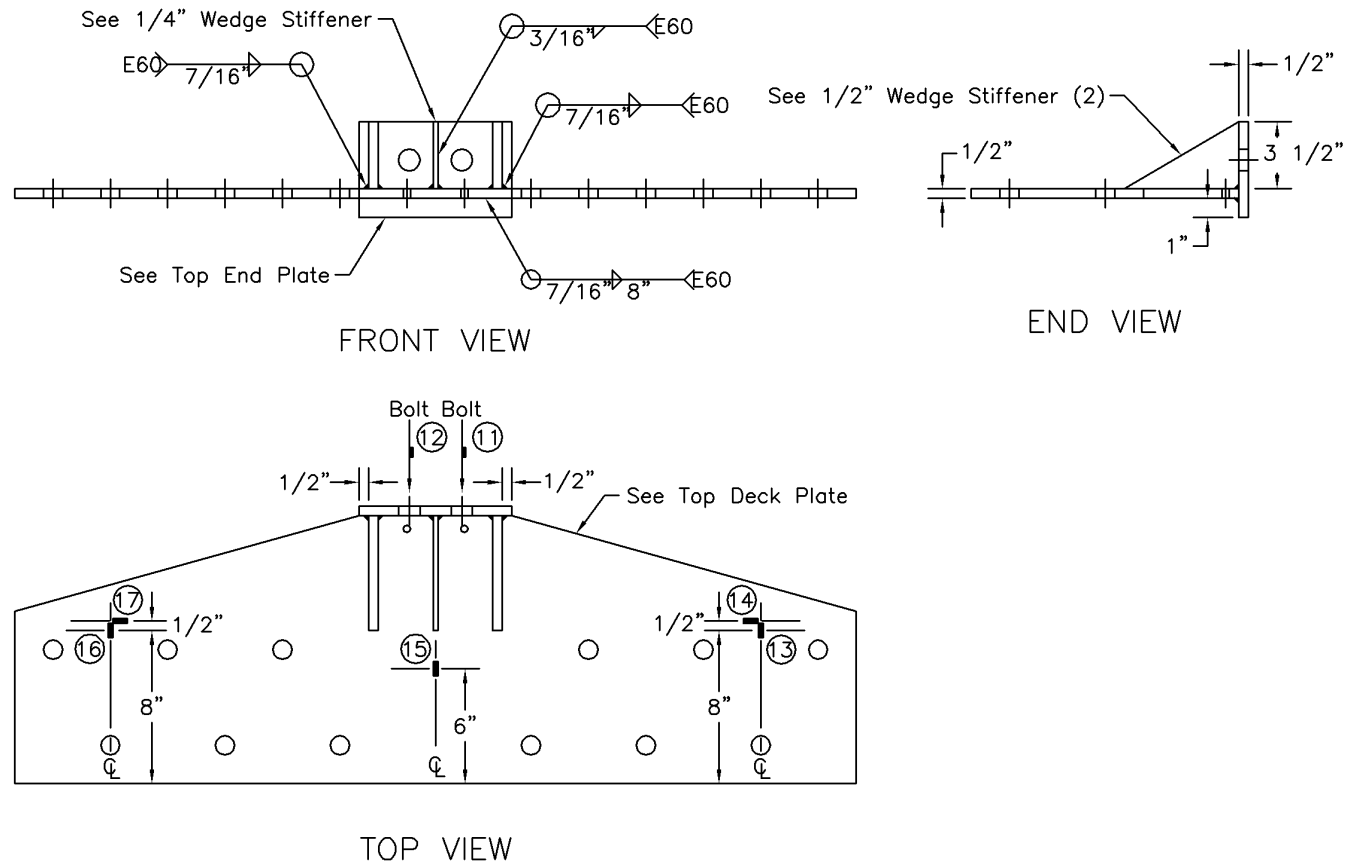
Post No. 6 Bottom Plate Assembly

Figure A-2. Strain Gauge No. 8 Location, Test STTR-1



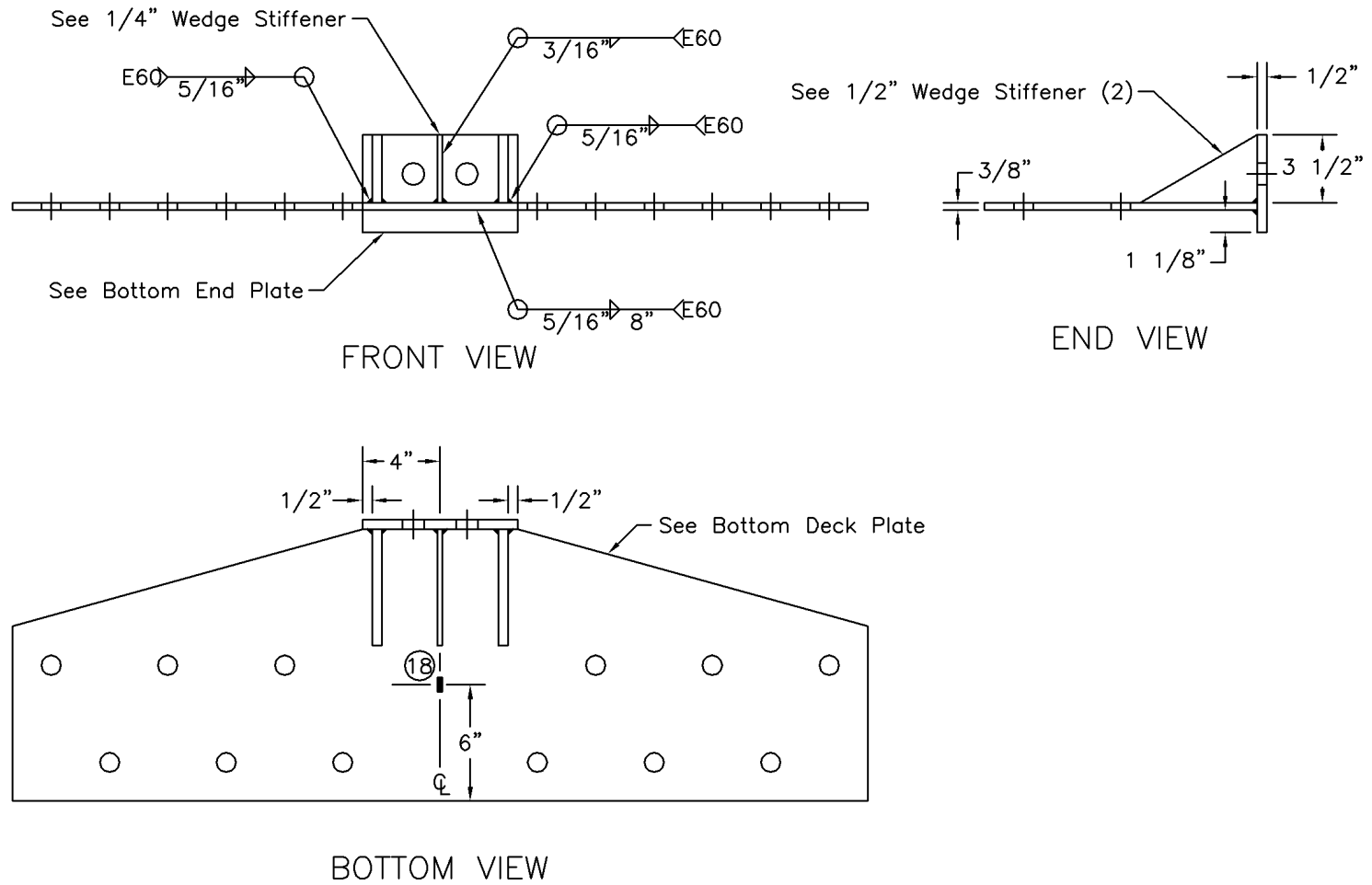
Post No. 6

Figure A-3. Strain Gauge Nos. 9 and 10 Locations, Test STTR-1



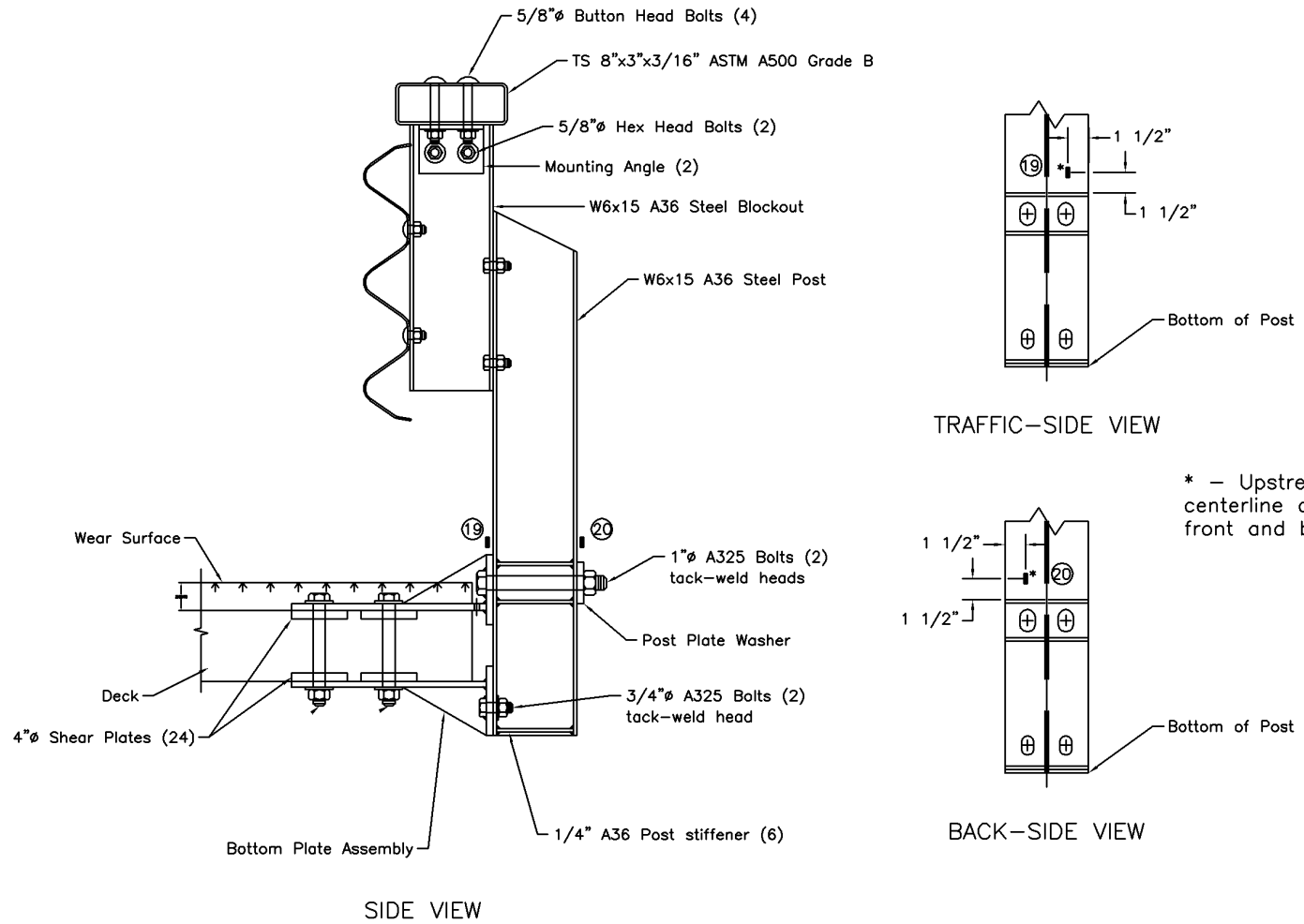
Post No. 7 Top Plate Assembly

Figure A-4. Strain Gauge Nos. 11 through 17 Locations, Test STTR-1



Post No. 7 Bottom Plate Assembly

Figure A-5. Strain Gauge No. 18 Location, Test STTR-1



Post No. 7

Figure A-6. Strain Gauge Nos. 19 and 20 Locations, Test STTR-1

APPENDIX B

Strain Gauge Locations – Test STTR-2

Figure B-1. Strain Gauge Nos. 1 through 3 Locations, Test STTR-2

Figure B-2. Strain Gauge No. 4 Location, Test STTR-2

Figure B-3. Strain Gauge Nos. 5, 6, 9, and 11 through 14 Locations, Test STTR-2

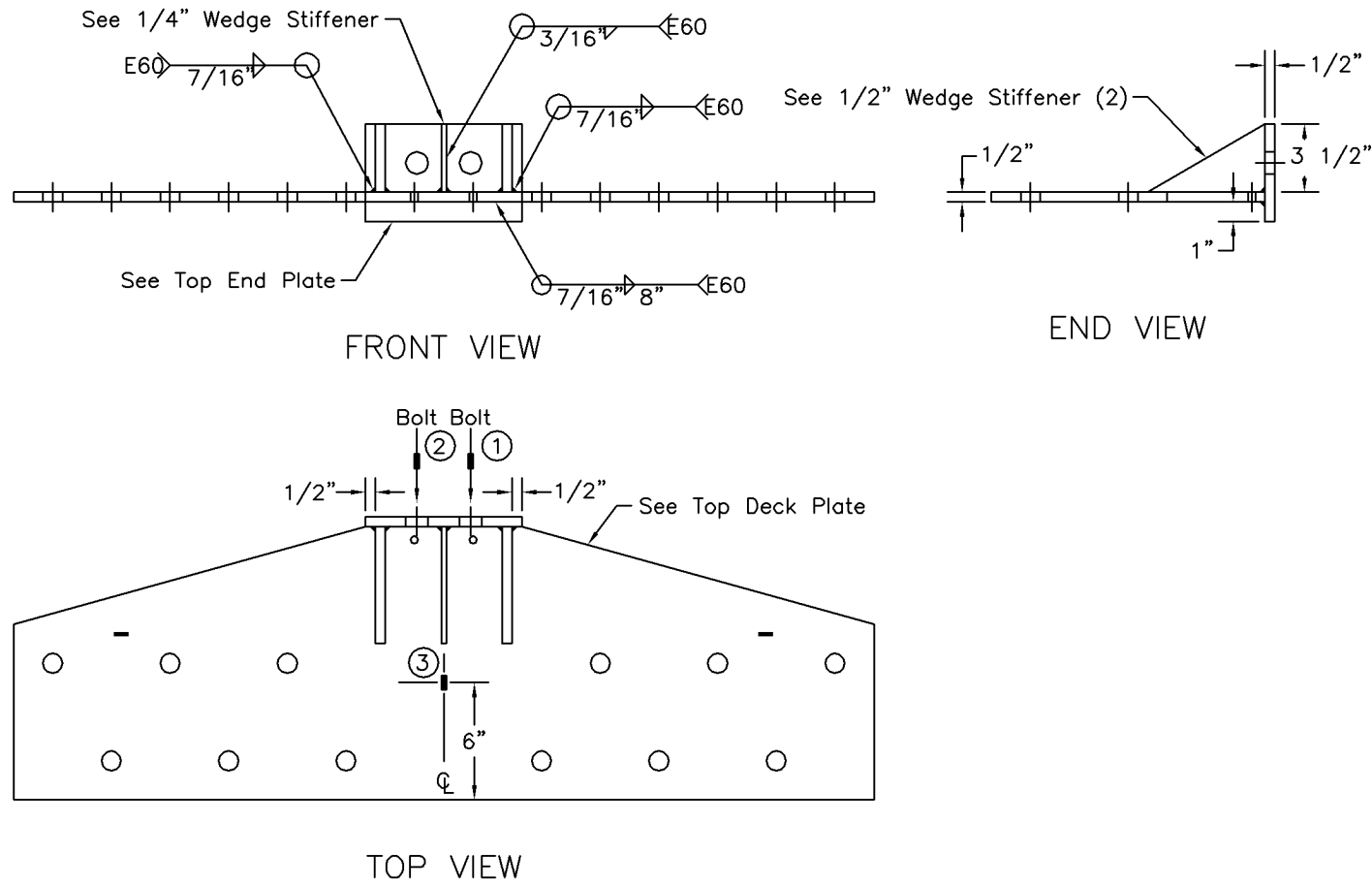
Figure B-4. Strain Gauge Nos. 7 and 8 Locations, Test STTR-2

Figure B-5. Strain Gauge No. 10 Location, Test STTR-2

Figure B-6. Strain Gauge Nos. 15 through 17 Locations, Test STTR-2

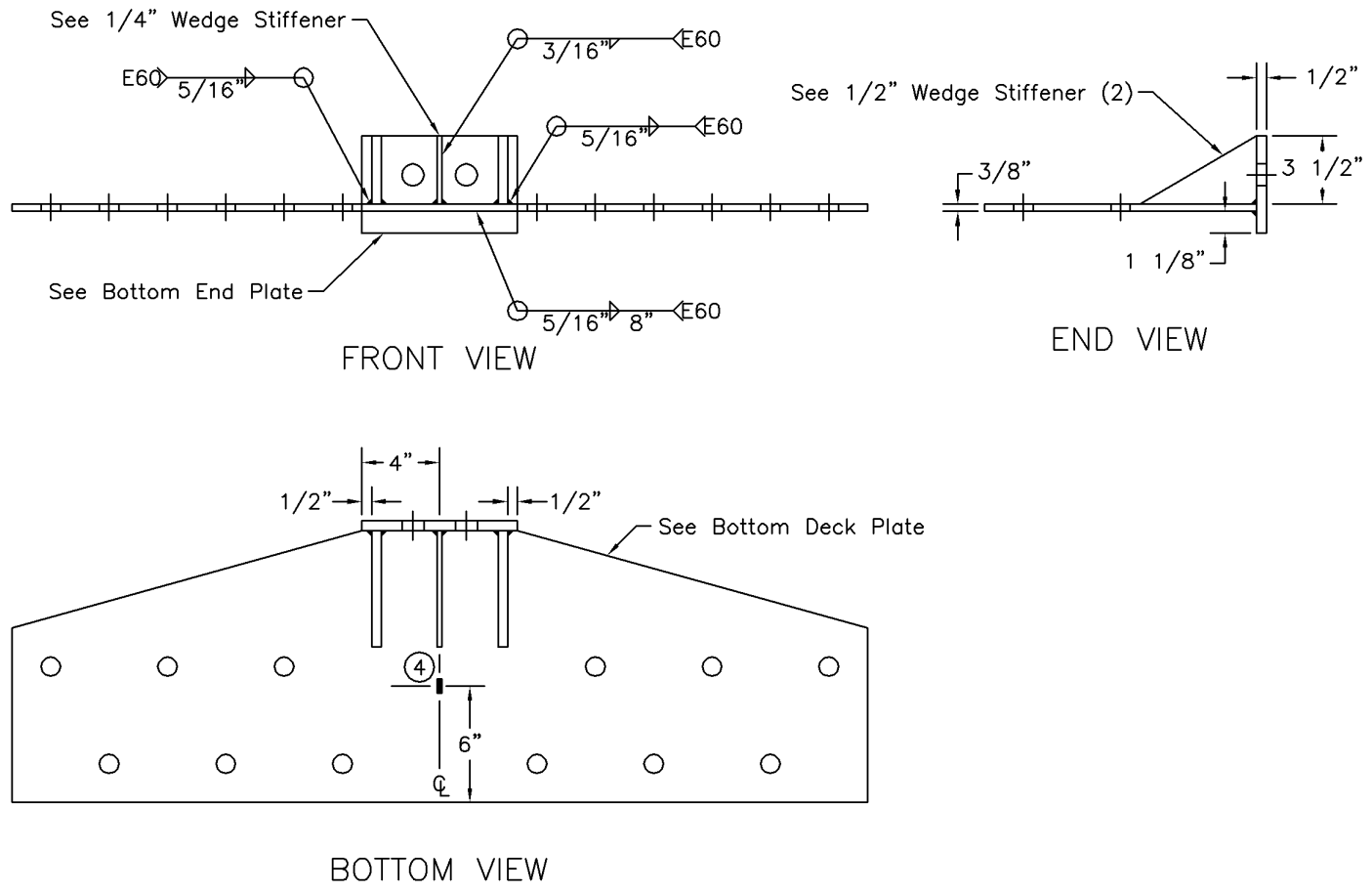
Figure B-7. Strain Gauge No. 18 Location, Test STTR-2

Figure B-8. Strain Gauge Nos. 19 and 20 Locations, Test STTR-2



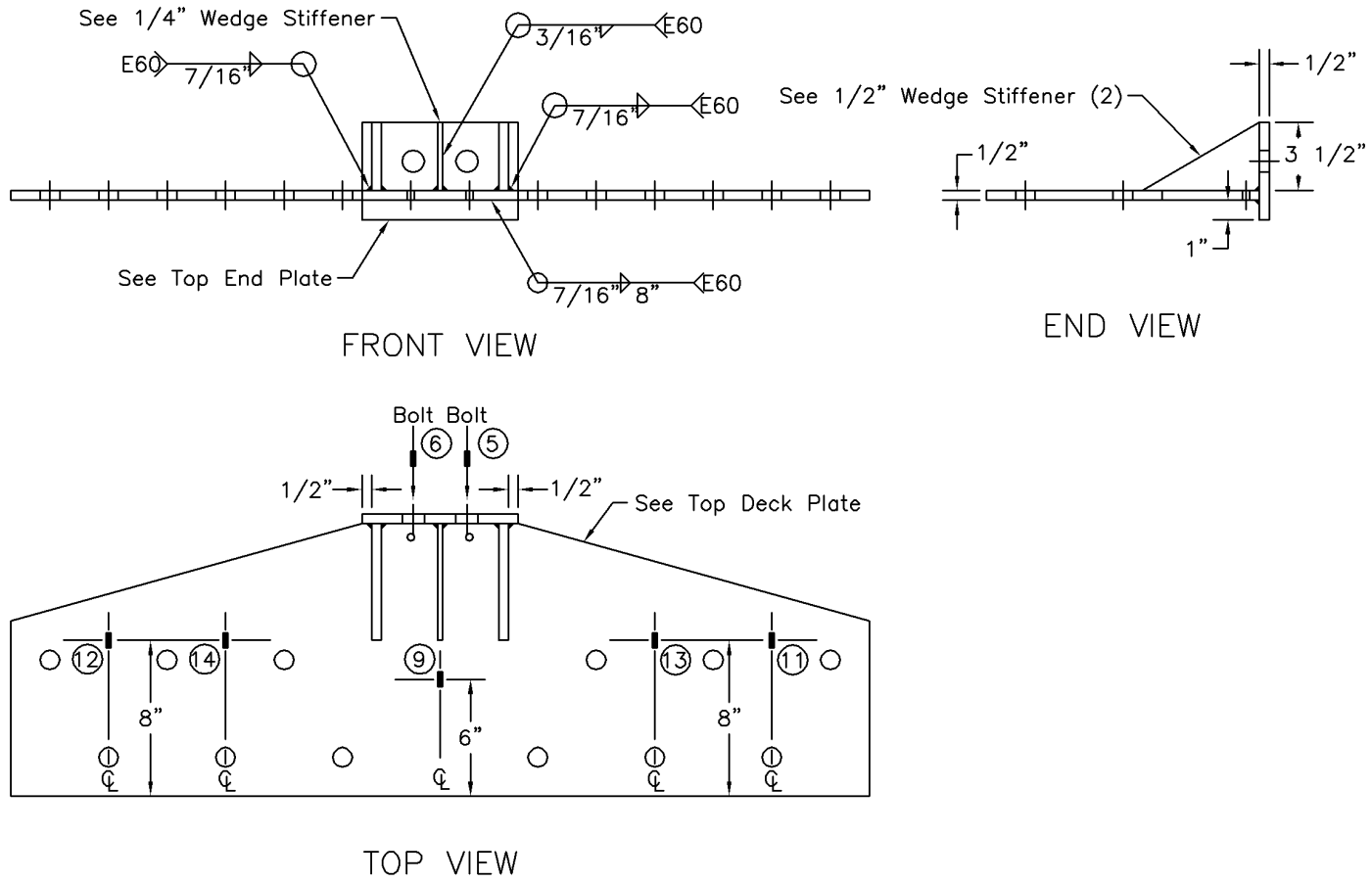
Post No. 5 Top Plate Assembly

Figure B-1. Strain Gauge Nos. 1 through 3 Locations, Test STTR-2



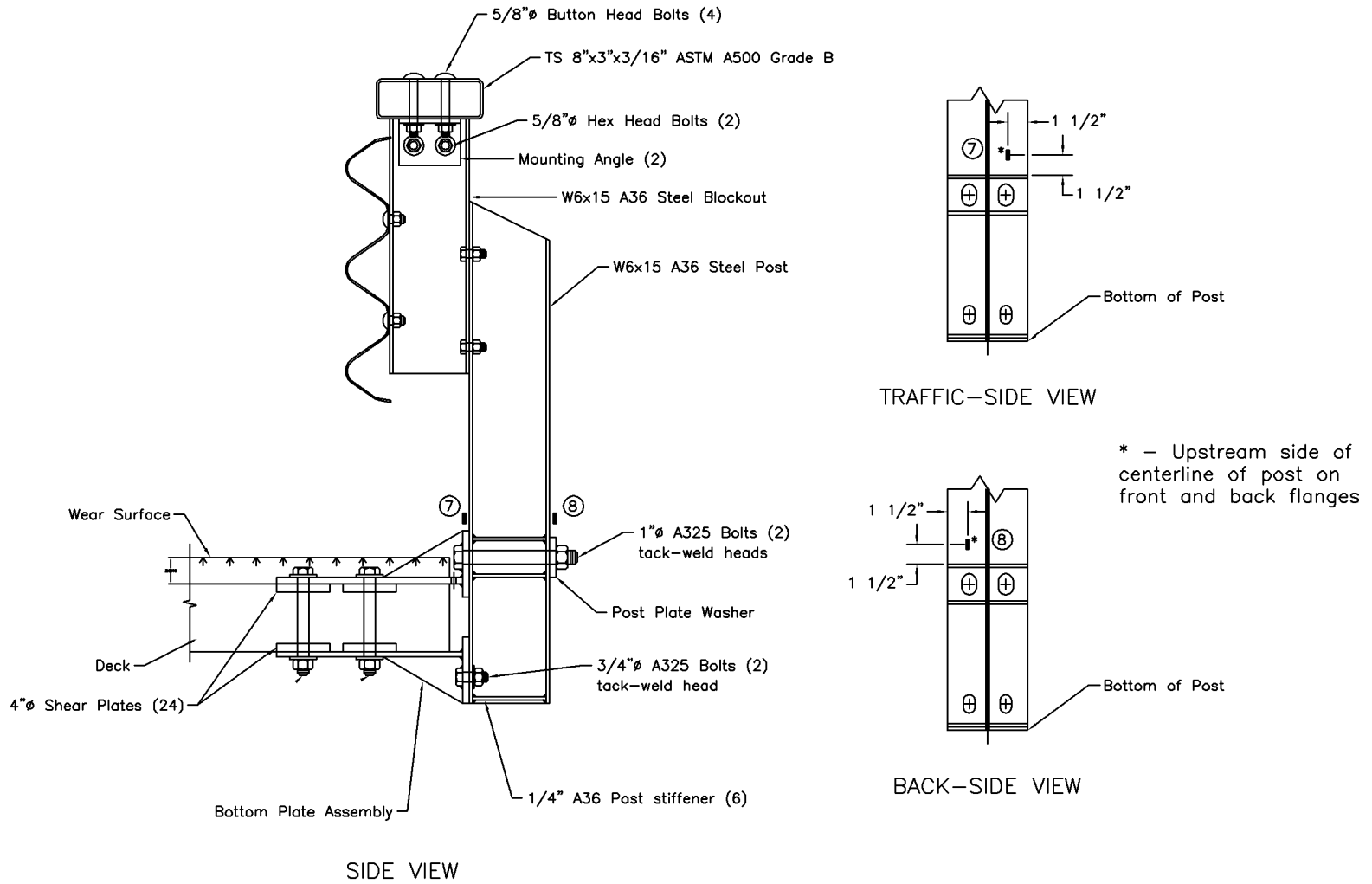
Post No. 5 Bottom Plate Assembly

Figure B-2. Strain Gauge No. 4 Location, Test STTR-2



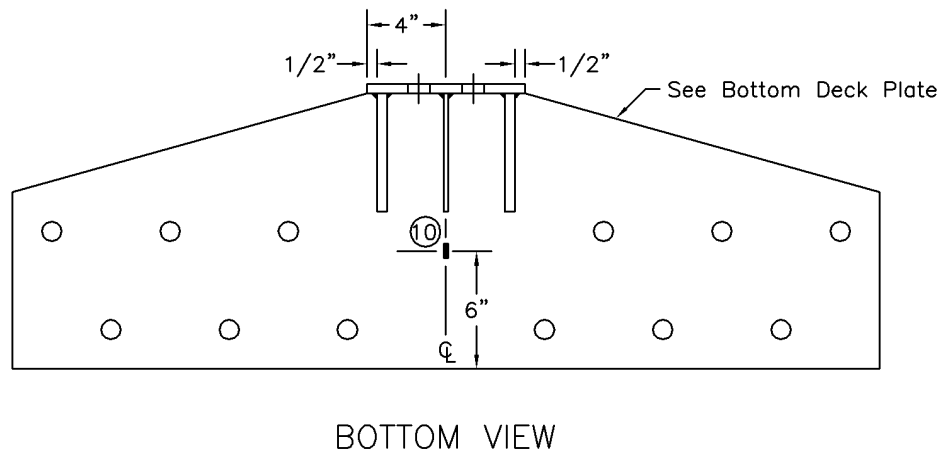
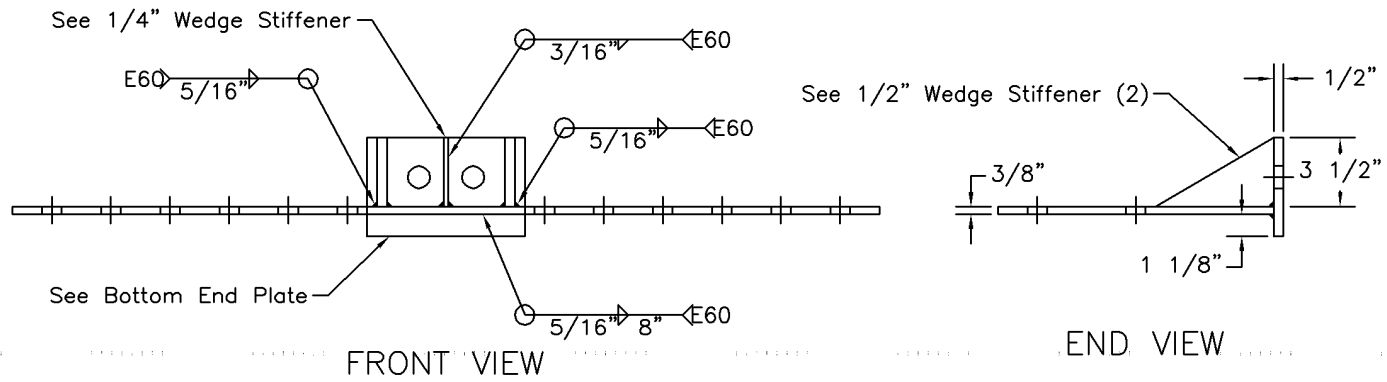
Post No. 6 Top Plate Assembly

Figure B-3. Strain Gauge Nos. 5, 6, 9, and 11 through 14 Locations, Test STTR-2



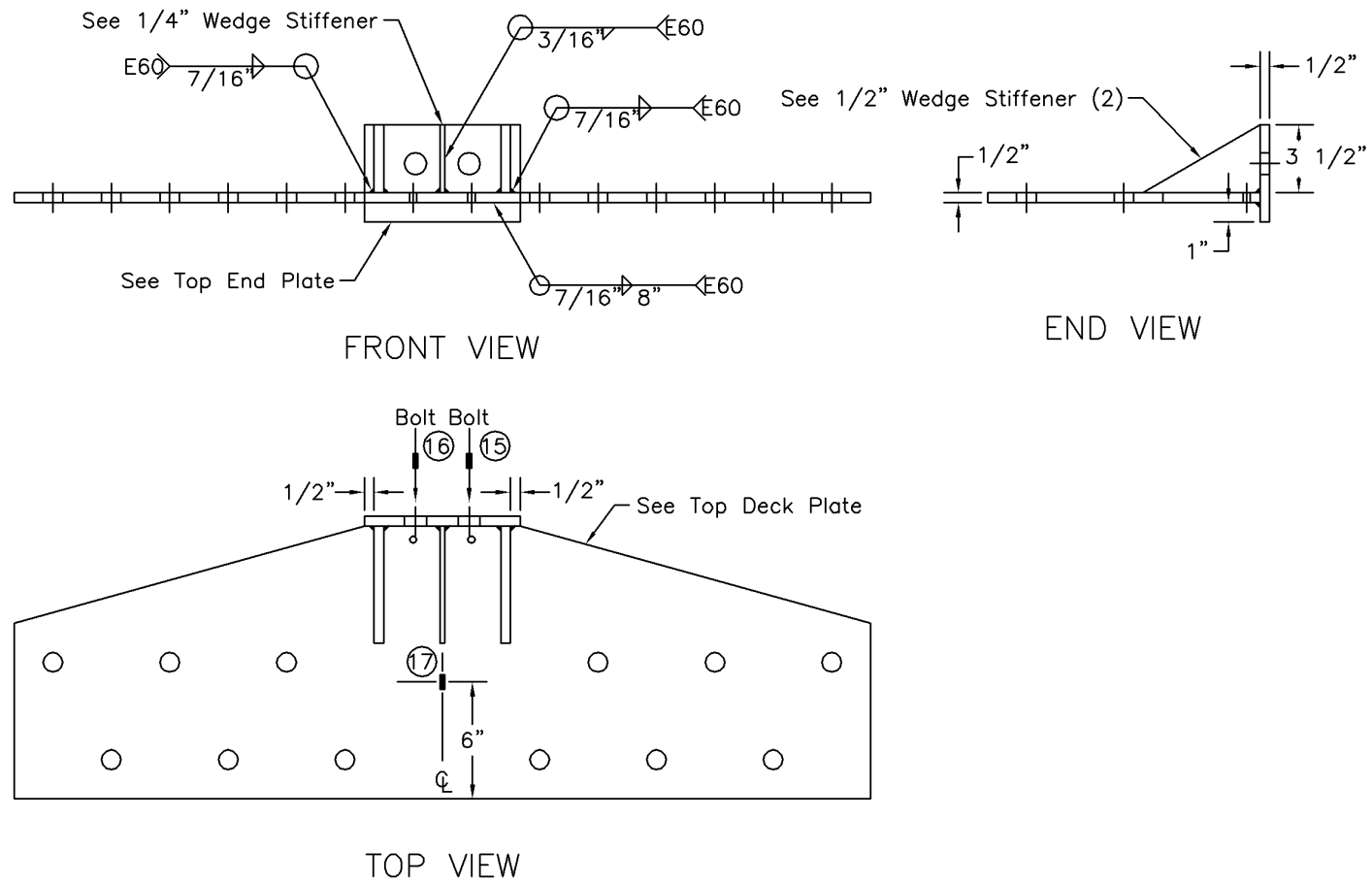
Post No. 6

Figure B-4. Strain Gauge Nos. 7 and 8 Locations, Test STTR-2



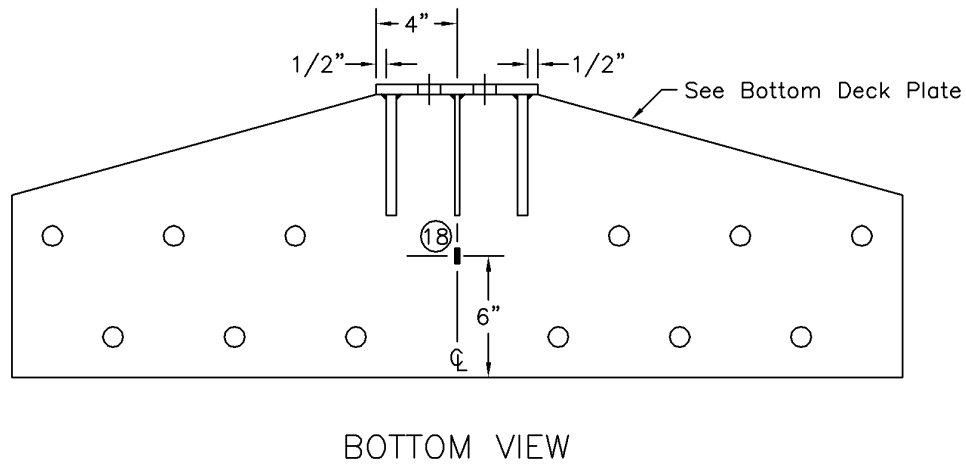
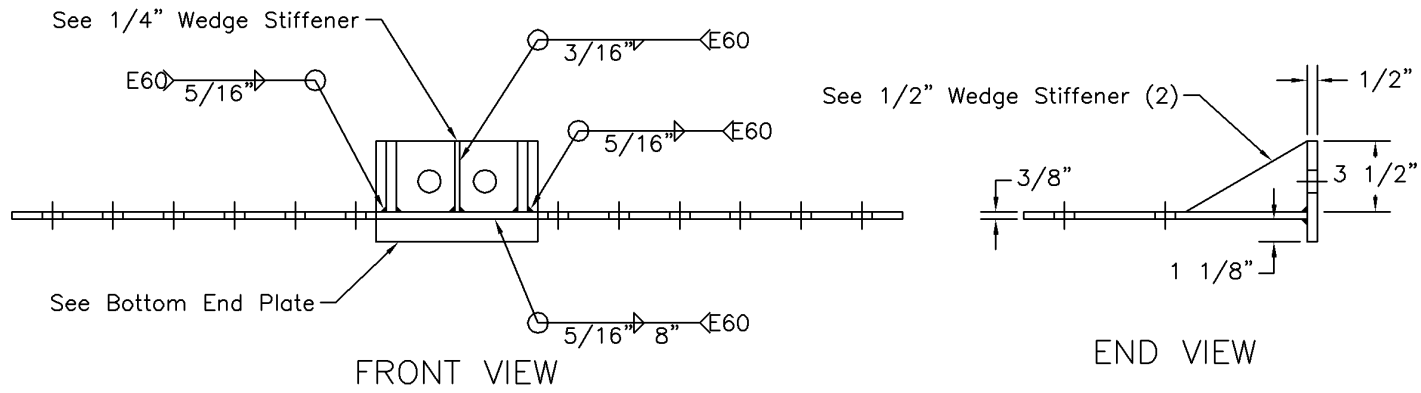
Post No. 6 Bottom Plate Assembly

Figure B-5. Strain Gauge No. 10 Location, Test STTR-2



Post No. 7 Top Plate Assembly

Figure B-6. Strain Gauge Nos. 15 through 17 Locations, Test STTR-2



Post No. 7 Bottom Plate Assembly

Figure B-7. Strain Gauge No. 18 Location, Test STTR-2

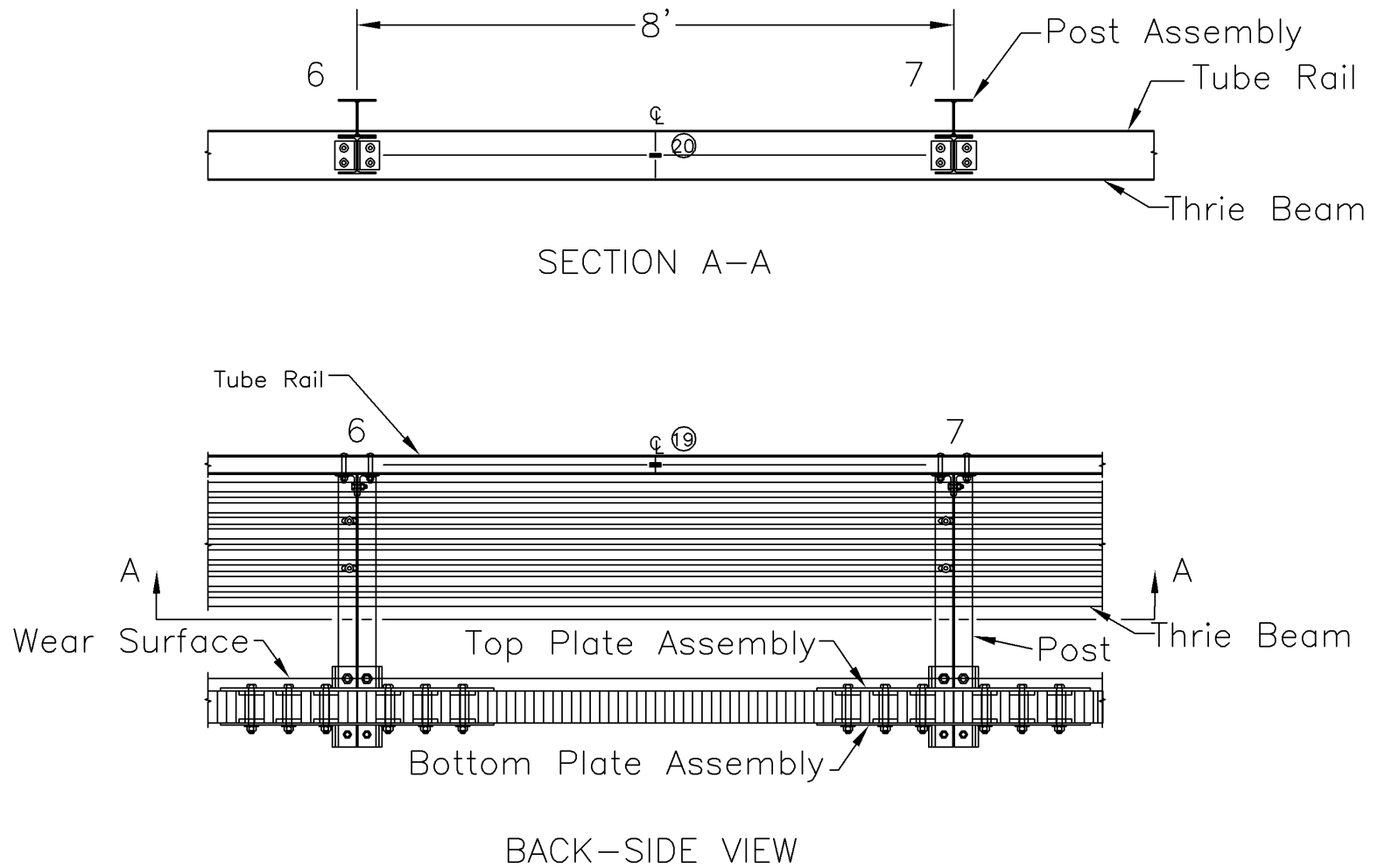


Figure B-8. Strain Gauge Nos. 19 and 20 Locations, Test STTR-2

APPENDIX C

BARRIER VII Computer Models - Wood System

Figure C-1. Model of the Wood Bridge Railing System

Figure C-2. Model of the Approach Guardrail System attached to the Wood Bridge Railing

Figure C-3. Idealized Finite Element, 2 Dimensional Vehicle Model for the 2,000-kg Pickup Truck

Figure C-4. Idealized Finite Element, 2 Dimensional Vehicle Model for the 8,000-kg Straight Truck

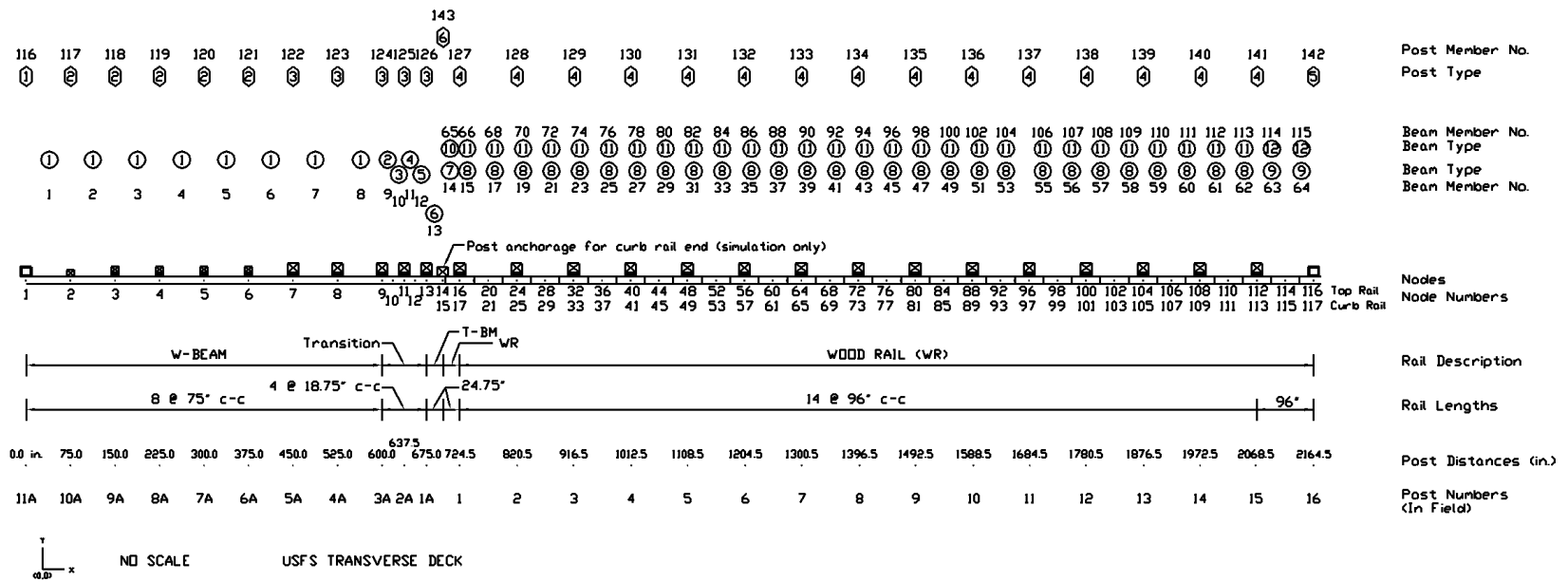


Figure C-1. Model of the Wood Bridge Railing System

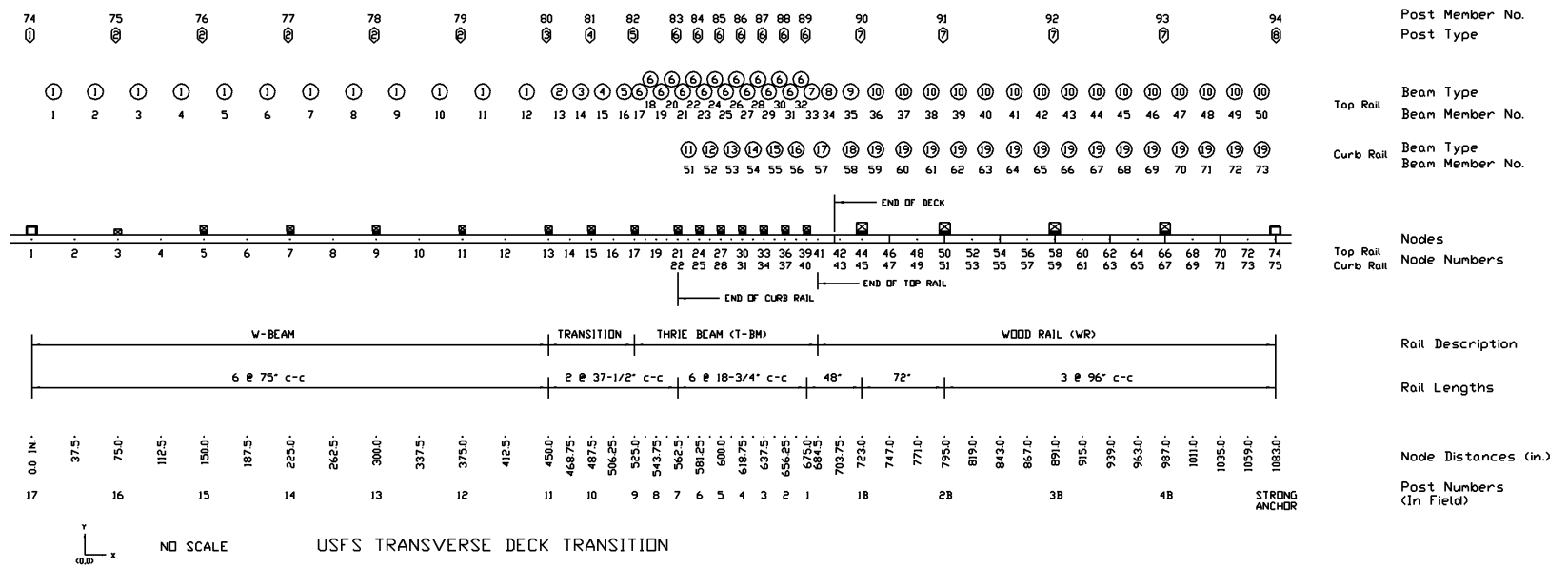


Figure C-2. Model of the Approach Guardrail System attached to the Wood Bridge Railing

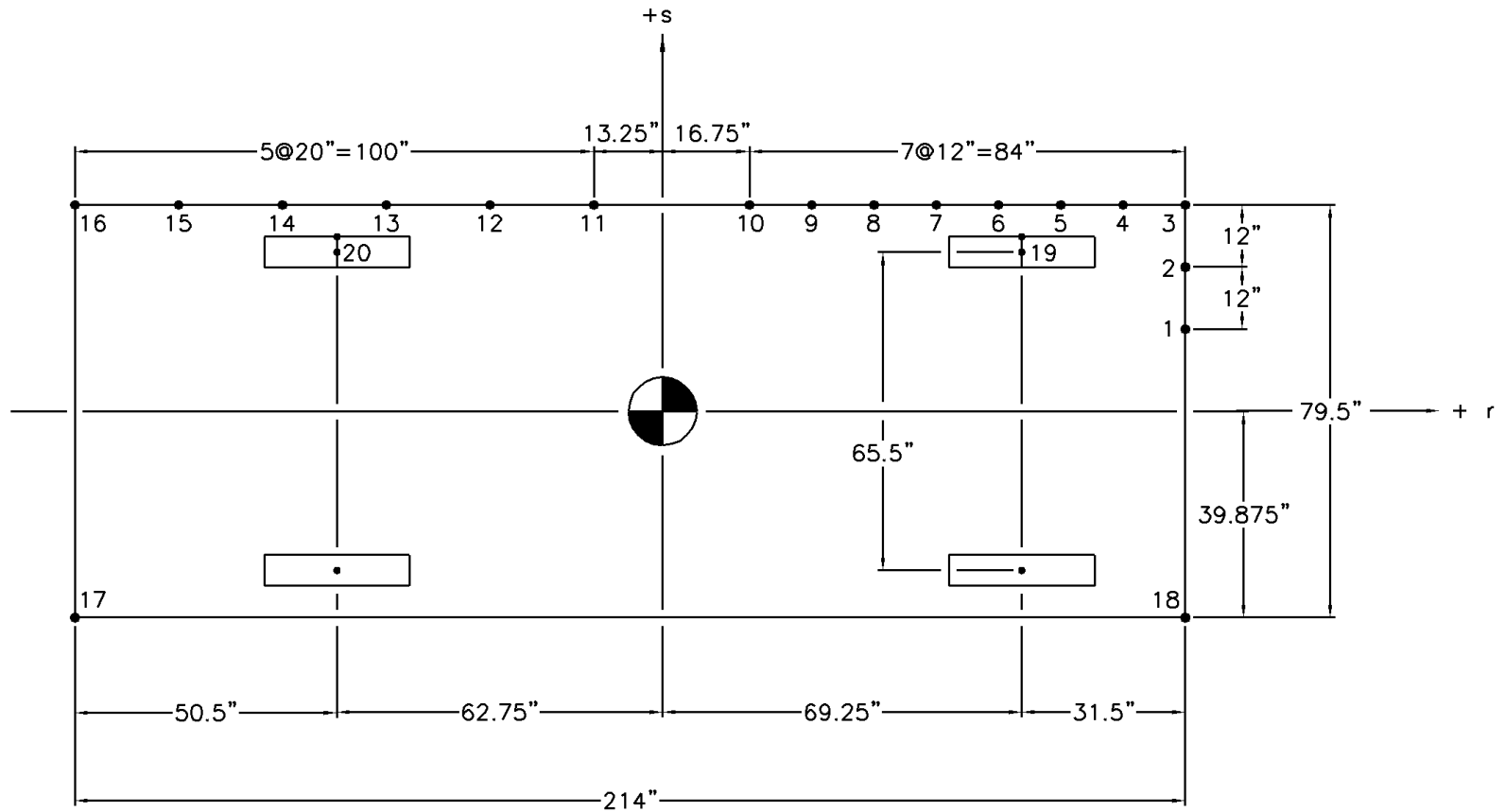


Figure C-3. Idealized Finite Element, 2 Dimensional Vehicle Model for the 2,000-kg Pickup Truck

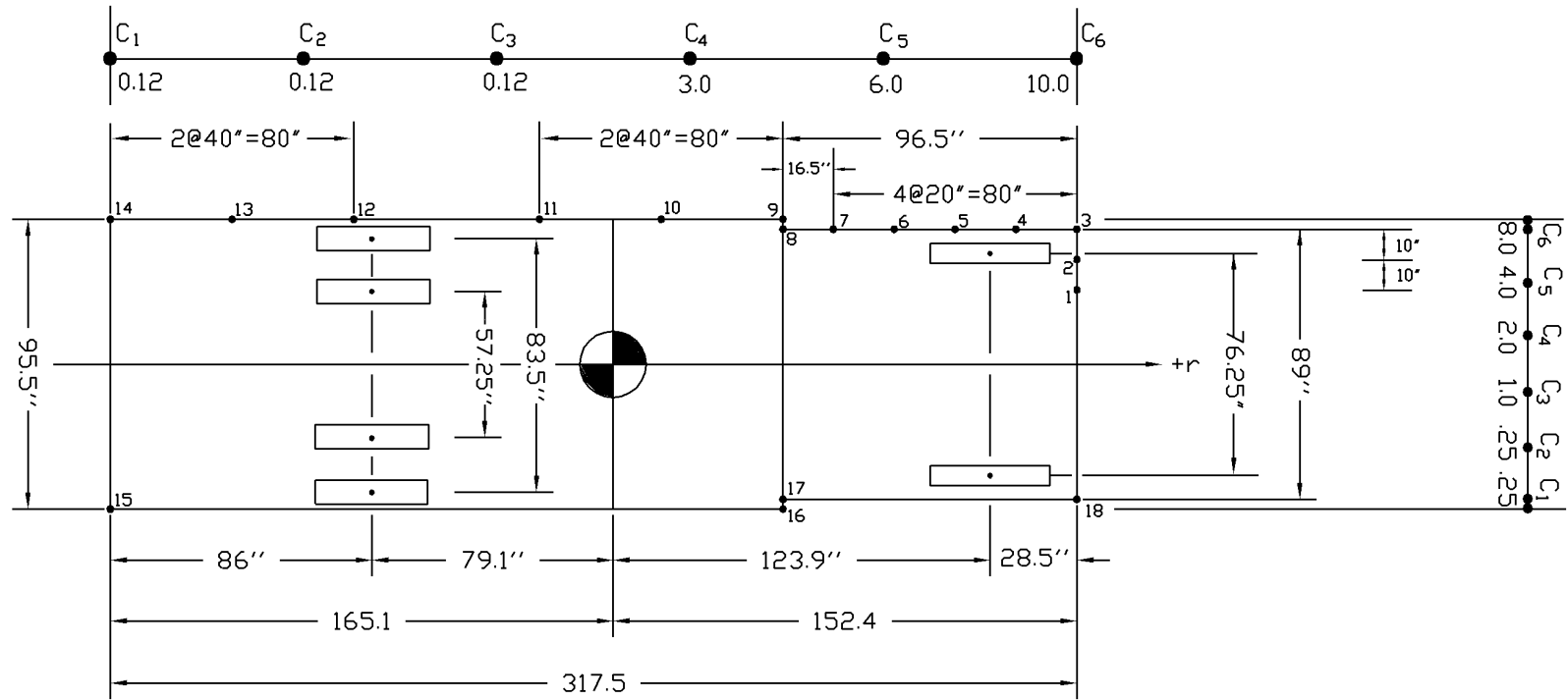


Figure C-4. Idealized Finite Element, 2 Dimensional Vehicle Model for the 8,000-kg Straight Truck

APPENDIX D

Typical BARRIER VII Input Data Files - Wood System

Note that the example BARRIER VII input data files included in Appendix D corresponds with the critical impact point for tests TRBR-1, TRBR-2, TRBR-3, and TRBR-4, respectively.

NCHRP TL-4 CURB BRIDGE RAILING (8000kg,15deg,80km/hr,8.75x13.5,6.75x12,8.75x10.5) - Run

No. 7										
117	11	6	2	143	20	2	0			
	0.0010	0.0010			0.80	200	0	1.0	1	
1	5	5	5	5	5	1				
1		0.0		0.0						
9		600.0		0.0						
13		675.0		0.0						
14		699.75		0.0						
15		699.75		0.0						
16		724.5		0.0						
17		724.5		0.0						
96		1684.5		0.0						
97		1684.5		0.0						
116		2164.5		0.0						
117		2164.5		0.0						
1	9	7	1		0.0					
9	13	3	1		0.0					
16	96	39	2		0.0					
17	97	39	2		0.0					
96	116	9	2		0.0					
97	117	9	2		0.0					
1	65		0.3							
116	114	112	110	108	106	104	102	100	98	
96	94	92	90	88	86	84	82	80	78	
76	74	72	70	68	66	64	62	60	58	
56	54	52	50	48	46	44	42	40	38	
36	34	32	30	28	26	24	22	20	18	
16	14	13	12	11	10	9	8	7	6	
5	4	3	2	1						
2	52		0.3							
117	115	113	111	109	107	105	103	101	99	
97	95	93	91	89	87	85	83	81	79	
77	75	73	71	69	67	65	63	61	59	
57	55	53	51	49	47	45	43	41	39	
37	35	33	31	29	27	25	23	21	19	
17	15									
100	12									
1		2.31		1.99	75.00	30000.0		6.92	99.5	68.5 0.10
2		2.48		2.13	18.75	30000.0		7.41	106.5	73.5 0.10
3		2.83		2.41	18.75	30000.0		8.38	120.5	83.5 0.10
4		3.17		2.68	18.75	30000.0		9.35	134.0	93.5 0.10
5		3.52		2.96	18.75	30000.0		10.32	148.0	103.5 0.10
6		3.76		3.10	24.75	30000.0		10.81	155.0	110.0 0.10
7		753.7		118.1	24.75	1400.0		41.0	67.9	1098.4 0.10
8		753.7		118.1	24.00	1400.0		41.0	67.9	1098.4 0.10
9		753.7		118.1	48.00	1400.0		41.0	67.9	1098.4 0.10
10		972.0		81.0	24.75	1500.0		28.1	46.6	1032.8 0.10
11		972.0		81.0	24.00	1500.0		28.1	46.6	1032.8 0.10
12		972.0		81.0	48.00	1500.0		28.1	46.6	1032.8 0.10
300	6									
1		21.0		0.0	6338.0	13943.0		94.7	6820.0	1540.0 0.10
	310.0		70.0		1.0	1.0				
2		21.0		0.0	15.0	11.0		50.0	315.0	231.0 0.10
	18.8		13.8		20.0	20.0				
3		21.0		0.0	15.0	15.0		77.0	315.0	315.0 0.10
	18.8		18.8		20.0	20.0				
4		18.0		0.25	9.01	13.05		106.3	683.4	820.1 0.10
	52.8		52.8		5.8	4.8				
5		18.0		0.25	6338.0	13943.0		94.7	6820.0	1540.0 0.10
	310.0		70.0		1.0	1.0				
6		8.25		0.0	6338.0	13943.0		94.7	6820.0	1540.0 0.10
	310.0		70.0		1.0	1.0				
1	1	2	8	1	101	0.0		0.0	0.0	
9	9	10	0	0	102	0.0		0.0	0.0	

10	10	11	0	0	103	0.0	0.0	0.0		
11	11	12	0	0	104	0.0	0.0	0.0		
12	12	13	0	0	105	0.0	0.0	0.0		
13	13	14	0	0	106	0.0	0.0	0.0		
14	14	16	0	0	107	0.0	0.0	0.0		
15	16	18	54	2	108	0.0	0.0	0.0		
55	96	98	64	2	109	0.0	0.0	0.0		
65	15	17	0	0	110	0.0	0.0	0.0		
66	17	19	105	2	111	0.0	0.0	0.0		
106	97	99	115	2	112	0.0	0.0	0.0		
116	1	0	0	0	301	0.0	0.0	0.0	0.0	0.0
117	2	0	121	1	302	0.0	0.0	0.0	0.0	0.0
122	7	0	124	1	303	0.0	0.0	0.0	0.0	0.0
125	11	0	126	2	303	0.0	0.0	0.0	0.0	0.0
127	16	17	137	8	304	0.0	0.0	0.0	0.0	0.0
138	100	101	141	4	304	0.0	0.0	0.0	0.0	0.0
142	116	117	0	0	305	0.0	0.0	0.0	0.0	0.0
143	15	0	0	0	306	0.0	0.0	0.0	0.0	0.0
17637.0	561483.4	20	7	6	0	1				
1	0.082	0.21	1.5	18.0						
2	0.063	0.19	2.0	12.0						
3	0.045	0.17	3.0	4.0						
4	0.800	0.95	2.5	2.5						
5	0.900	1.05	3.5	2.0						
6	0.35	0.25	10.0	3.0						
7	2.5	3.5	4.5	3.0						
1	152.4	24.5	1	10.0	1	0	0	0		
2	152.4	34.5	1	10.0	1	0	0	0		
3	152.4	44.5	1	15.0	1	0	0	0		
4	132.4	44.5	1	20.0	1	0	0	0		
5	112.4	44.5	2	20.0	1	0	0	0		
6	92.4	44.5	2	20.0	1	0	0	0		
7	72.4	44.5	2	18.25	1	0	0	0		
8	55.9	44.5	2	11.5	1	0	0	0		
9	55.9	47.75	3	23.25	0	0	0	0		
10	15.9	47.75	4	40.0	0	0	0	0		
11	-24.1	47.75	5	40.0	0	0	0	0		
12	-85.1	47.75	5	40.0	0	0	0	0		
13	-125.1	47.75	5	40.0	0	0	0	0		
14	-165.1	47.75	5	20.0	0	0	0	0		
15	-165.1	-47.75	5	1.0	0	0	0	0		
16	55.9	-47.75	3	1.0	0	0	0	0		
17	55.9	-44.5	2	1.0	0	0	0	0		
18	152.4	-44.5	1	1.0	0	0	0	0		
19	-79.1	45.75	7	1.0	1	0	0	0		
20	123.9	42.12	6	1.0	1	0	0	0		
1	123.9	38.12	0.0	2214.						
2	123.9	-38.12	0.0	2214.						
3	-79.1	41.75	0.0	2755.						
4	-79.1	-41.75	0.0	2755.						
5	-79.1	28.62	0.0	2755.						
6	-79.1	-28.62	0.0	2755.						
1	0.0	0.0								
3	1060.5	0.0	15.0	49.7	0.0	0.0	10.0			

10	10	11	0	0	103	0.0	0.0	0.0		
11	11	12	0	0	104	0.0	0.0	0.0		
12	12	13	0	0	105	0.0	0.0	0.0		
13	13	14	0	0	106	0.0	0.0	0.0		
14	14	16	0	0	107	0.0	0.0	0.0		
15	16	18	54	2	108	0.0	0.0	0.0		
55	96	98	64	2	109	0.0	0.0	0.0		
65	15	17	0	0	110	0.0	0.0	0.0		
66	17	19	105	2	111	0.0	0.0	0.0		
106	97	99	115	2	112	0.0	0.0	0.0		
116	1	0	0	0	301	0.0	0.0	0.0	0.0	0.0
117	2	0	121	1	302	0.0	0.0	0.0	0.0	0.0
122	7	0	124	1	303	0.0	0.0	0.0	0.0	0.0
125	11	0	126	2	303	0.0	0.0	0.0	0.0	0.0
127	16	17	137	8	304	0.0	0.0	0.0	0.0	0.0
138	100	101	141	4	304	0.0	0.0	0.0	0.0	0.0
142	116	117	0	0	305	0.0	0.0	0.0	0.0	0.0
143	15	0	0	0	306	0.0	0.0	0.0	0.0	0.0
4410.0	40000.0	20	6	4	0	1				
1	0.055	0.12	6.00	17.0						
2	0.057	0.15	7.00	18.0						
3	0.062	0.18	10.00	12.0						
4	0.110	0.35	12.00	6.0						
5	0.35	0.45	6.00	5.0						
6	1.45	1.50	15.00	1.0						
1	100.75	15.875	1	12.0	1	0	0	0		
2	100.75	27.875	1	12.0	1	0	0	0		
3	100.75	39.875	2	12.0	1	0	0	0		
4	88.75	39.875	2	12.0	1	0	0	0		
5	76.75	39.875	2	12.0	1	0	0	0		
6	64.75	39.875	2	12.0	1	0	0	0		
7	52.75	39.875	2	12.0	1	0	0	0		
8	40.75	39.875	2	12.0	1	0	0	0		
9	28.75	39.875	2	12.0	1	0	0	0		
10	16.75	39.875	2	12.0	1	0	0	0		
11	-13.25	39.875	3	12.0	1	0	0	0		
12	-33.25	39.875	3	12.0	1	0	0	0		
13	-53.25	39.875	3	12.0	1	0	0	0		
14	-73.25	39.875	3	12.0	1	0	0	0		
15	-93.25	39.875	3	12.0	1	0	0	0		
16	-113.25	39.875	4	12.0	1	0	0	0		
17	-113.25	-39.875	4	12.0	0	0	0	0		
18	100.75	-39.875	1	12.0	0	0	0	0		
19	69.25	37.75	5	1.0	1	0	0	0		
20	-62.75	37.75	6	1.0	1	0	0	0		
1	69.25	37.75	0.0	608.						
2	69.25	-37.75	0.0	608.						
3	-62.75	37.75	0.0	492.						
4	-62.75	-37.75	0.0	492.						
1	0.0	0.0								
3	1012.5	0.0	25.0	62.14	0.0	0.0	5.0			

4	27.6	27.6	20.1	20.1						
4	21.0	0.0	1.67	1.67	93.9	444.2	444.2	0.10		
5	27.6	27.6	20.1	20.1						
5	21.0	0.0	1.67	1.67	93.9	413.6	413.6	0.10		
6	27.6	27.6	20.1	20.1						
6	21.0	8.13	1.67	1.67	93.9	413.6	413.6	0.10		
7	27.6	27.6	20.1	20.1						
7	18.0	0.25	9.01	13.05	106.3	683.4	820.1	0.10		
8	52.8	52.8	5.8	4.8						
8	18.0	0.25	6338.0	13943.0	94.7	6820.0	1540.0	0.10		
	310.0	70.0	1.0	1.0						
1	1	2	12	1	101	0.0	0.0	0.0		
13	13	14	0	0	102	0.0	0.0	0.0		
14	14	15	0	0	103	0.0	0.0	0.0		
15	15	16	0	0	104	0.0	0.0	0.0		
16	16	17	0	0	105	0.0	0.0	0.0		
17	17	18	20	1	106	0.0	0.0	0.0		
21	21	23	0	0	106	0.0	0.0	0.0		
22	23	24	0	0	106	0.0	0.0	0.0		
23	24	26	0	0	106	0.0	0.0	0.0		
24	26	27	0	0	106	0.0	0.0	0.0		
25	27	29	0	0	106	0.0	0.0	0.0		
26	29	30	0	0	106	0.0	0.0	0.0		
27	30	32	0	0	106	0.0	0.0	0.0		
28	32	33	0	0	106	0.0	0.0	0.0		
29	33	35	0	0	106	0.0	0.0	0.0		
30	35	36	0	0	106	0.0	0.0	0.0		
31	36	38	0	0	106	0.0	0.0	0.0		
32	38	39	0	0	106	0.0	0.0	0.0		
33	39	41	0	0	107	0.0	0.0	0.0		
34	41	42	0	0	108	0.0	0.0	0.0		
35	42	44	0	0	109	0.0	0.0	0.0		
36	44	46	50	2	110	0.0	0.0	0.0		
51	22	25	0	0	111	0.0	0.0	0.0		
52	25	28	0	0	112	0.0	0.0	0.0		
53	28	31	0	0	113	0.0	0.0	0.0		
54	31	34	0	0	114	0.0	0.0	0.0		
55	34	37	0	0	115	0.0	0.0	0.0		
56	37	40	0	0	116	0.0	0.0	0.0		
57	40	43	0	0	117	0.0	0.0	0.0		
58	43	45	0	0	118	0.0	0.0	0.0		
59	45	47	73	2	119	0.0	0.0	0.0		
74	1	0	0	0	301	0.0	0.0	0.0	0.0	0.0
75	3	0	79	2	302	0.0	0.0	0.0	0.0	0.0
80	13	0	0	0	303	0.0	0.0	0.0	0.0	0.0
81	15	0	0	0	304	0.0	0.0	0.0	0.0	0.0
82	17	0	0	0	305	0.0	0.0	0.0	0.0	0.0
83	21	22	89	3	306	0.0	0.0	0.0	0.0	0.0
90	44	45	0	0	307	0.0	0.0	0.0	0.0	0.0
91	50	51	93	8	307	0.0	0.0	0.0	0.0	0.0
94	74	75	0	0	308	0.0	0.0	0.0	0.0	0.0
	4410.0	40000.0	20	6	4	0	1			
1	0.055	0.12	6.00	17.0						
2	0.057	0.15	7.00	18.0						
3	0.062	0.18	10.00	12.0						
4	0.110	0.35	12.00	6.0						
5	0.35	0.45	6.00	5.0						
6	1.45	1.50	15.00	1.0						
1	100.75	15.875	1	12.0	1	0	0	0		
2	100.75	27.875	1	12.0	1	0	0	0		
3	100.75	39.875	2	12.0	1	0	0	0		
4	88.75	39.875	2	12.0	1	0	0	0		
5	76.75	39.875	2	12.0	1	0	0	0		
6	64.75	39.875	2	12.0	1	0	0	0		
7	52.75	39.875	2	12.0	1	0	0	0		

8	40.75	39.875	2	12.0	1	0	0	0
9	28.75	39.875	2	12.0	1	0	0	0
10	16.75	39.875	2	12.0	1	0	0	0
11	-13.25	39.875	3	12.0	1	0	0	0
12	-33.25	39.875	3	12.0	1	0	0	0
13	-53.25	39.875	3	12.0	1	0	0	0
14	-73.25	39.875	3	12.0	1	0	0	0
15	-93.25	39.875	3	12.0	1	0	0	0
16	-113.25	39.875	4	12.0	1	0	0	0
17	-113.25	-39.875	4	12.0	0	0	0	0
18	100.75	-39.875	1	12.0	0	0	0	0
19	69.25	37.75	5	1.0	1	0	0	0
20	-62.75	37.75	6	1.0	1	0	0	0
1	69.25	37.75		0.0	608.			
2	69.25	-37.75		0.0	608.			
3	-62.75	37.75		0.0	492.			
4	-62.75	-37.75		0.0	492.			
1	0.0	0.0						
3	628.13	0.0	25.0	62.14		0.0	0.0	5.0

4	27.6	27.6	20.1	20.1						
4	21.0	0.0	1.67	1.67	93.9	444.2	444.2	0.10		
5	27.6	27.6	20.1	20.1						
5	21.0	0.0	1.67	1.67	93.9	413.6	413.6	0.10		
6	27.6	27.6	20.1	20.1						
6	21.0	8.13	1.67	1.67	93.9	413.6	413.6	0.10		
7	27.6	27.6	20.1	20.1						
7	18.0	0.25	9.01	13.05	106.3	683.4	820.1	0.10		
8	52.8	52.8	5.8	4.8						
8	18.0	0.25	6338.0	13943.0	94.7	6820.0	1540.0	0.10		
	310.0	70.0	1.0	1.0						
1	1	2	12	1	101	0.0	0.0	0.0		
13	13	14	0	0	102	0.0	0.0	0.0		
14	14	15	0	0	103	0.0	0.0	0.0		
15	15	16	0	0	104	0.0	0.0	0.0		
16	16	17	0	0	105	0.0	0.0	0.0		
17	17	18	20	1	106	0.0	0.0	0.0		
21	21	23	0	0	106	0.0	0.0	0.0		
22	23	24	0	0	106	0.0	0.0	0.0		
23	24	26	0	0	106	0.0	0.0	0.0		
24	26	27	0	0	106	0.0	0.0	0.0		
25	27	29	0	0	106	0.0	0.0	0.0		
26	29	30	0	0	106	0.0	0.0	0.0		
27	30	32	0	0	106	0.0	0.0	0.0		
28	32	33	0	0	106	0.0	0.0	0.0		
29	33	35	0	0	106	0.0	0.0	0.0		
30	35	36	0	0	106	0.0	0.0	0.0		
31	36	38	0	0	106	0.0	0.0	0.0		
32	38	39	0	0	106	0.0	0.0	0.0		
33	39	41	0	0	107	0.0	0.0	0.0		
34	41	42	0	0	108	0.0	0.0	0.0		
35	42	44	0	0	109	0.0	0.0	0.0		
36	44	46	50	2	110	0.0	0.0	0.0		
51	22	25	0	0	111	0.0	0.0	0.0		
52	25	28	0	0	112	0.0	0.0	0.0		
53	28	31	0	0	113	0.0	0.0	0.0		
54	31	34	0	0	114	0.0	0.0	0.0		
55	34	37	0	0	115	0.0	0.0	0.0		
56	37	40	0	0	116	0.0	0.0	0.0		
57	40	43	0	0	117	0.0	0.0	0.0		
58	43	45	0	0	118	0.0	0.0	0.0		
59	45	47	73	2	119	0.0	0.0	0.0		
74	1	0	0	0	301	0.0	0.0	0.0	0.0	0.0
75	3	0	79	2	302	0.0	0.0	0.0	0.0	0.0
80	13	0	0	0	303	0.0	0.0	0.0	0.0	0.0
81	15	0	0	0	304	0.0	0.0	0.0	0.0	0.0
82	17	0	0	0	305	0.0	0.0	0.0	0.0	0.0
83	21	22	89	3	306	0.0	0.0	0.0	0.0	0.0
90	44	45	0	0	307	0.0	0.0	0.0	0.0	0.0
91	50	51	93	8	307	0.0	0.0	0.0	0.0	0.0
94	74	75	0	0	308	0.0	0.0	0.0	0.0	0.0
17637.0	561483.4	20	7	6	0	1				
1	0.082	0.21		1.5	18.0					
2	0.063	0.19		2.0	12.0					
3	0.045	0.17		3.0	4.0					
4	0.800	0.95		2.5	2.5					
5	0.900	1.05		3.5	2.0					
6	0.35	0.25		10.0	3.0					
7	2.5	3.5		4.5	3.0					
1	152.4	24.5	1	10.0	1	0	0	0		
2	152.4	34.5	1	10.0	1	0	0	0		
3	152.4	44.5	1	15.0	1	0	0	0		
4	132.4	44.5	1	20.0	1	0	0	0		
5	112.4	44.5	2	20.0	1	0	0	0		
6	92.4	44.5	2	20.0	1	0	0	0		

7	72.4	44.5	2	18.25	1	0	0	0
8	55.9	44.5	2	11.5	1	0	0	0
9	55.9	47.75	3	23.25	0	0	0	0
10	15.9	47.75	4	40.0	0	0	0	0
11	-24.1	47.75	5	40.0	0	0	0	0
12	-85.1	47.75	5	40.0	0	0	0	0
13	-125.1	47.75	5	40.0	0	0	0	0
14	-165.1	47.75	5	20.0	0	0	0	0
15	-165.1	-47.75	5	1.0	0	0	0	0
16	55.9	-47.75	3	1.0	0	0	0	0
17	55.9	-44.5	2	1.0	0	0	0	0
18	152.4	-44.5	1	1.0	0	0	0	0
19	-79.1	45.75	7	1.0	1	0	0	0
20	123.9	42.12	6	1.0	1	0	0	0
1	123.9	38.12		0.0	2214.			
2	123.9	-38.12		0.0	2214.			
3	-79.1	41.75		0.0	2755.			
4	-79.1	-41.75		0.0	2755.			
5	-79.1	28.62		0.0	2755.			
6	-79.1	-28.62		0.0	2755.			
1	0.0	0.0						
3	571.875	0.0	15.0	49.7		0.0	0.0	10.0

APPENDIX E

Accelerometer Data Analysis - Test TRBR-1

Figure E-1. Graph of Longitudinal Deceleration, Test TRBR-1

Figure E-2. Graph of Longitudinal Occupant Impact Velocity, Test TRBR-1

Figure E-3. Graph of Longitudinal Occupant Displacement, Test TRBR-1

Figure E-4. Graph of Lateral Deceleration, Test TRBR-1

Figure E-5. Graph of Lateral Occupant Impact Velocity, Test TRBR-1

Figure E-6. Graph of Lateral Occupant Displacement, Test TRBR-1

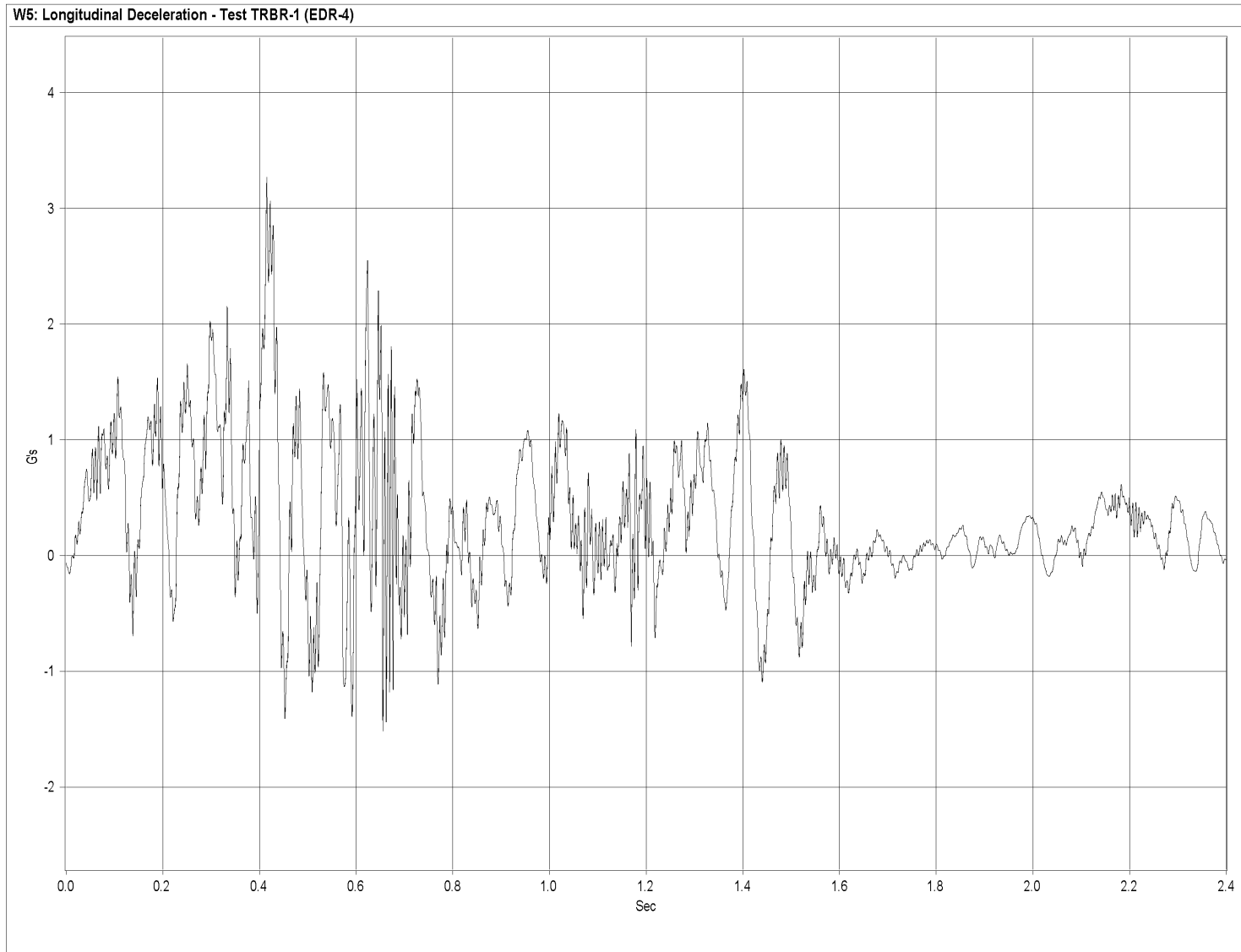


Figure E-1. Graph of Longitudinal Deceleration, Test TRBR-1

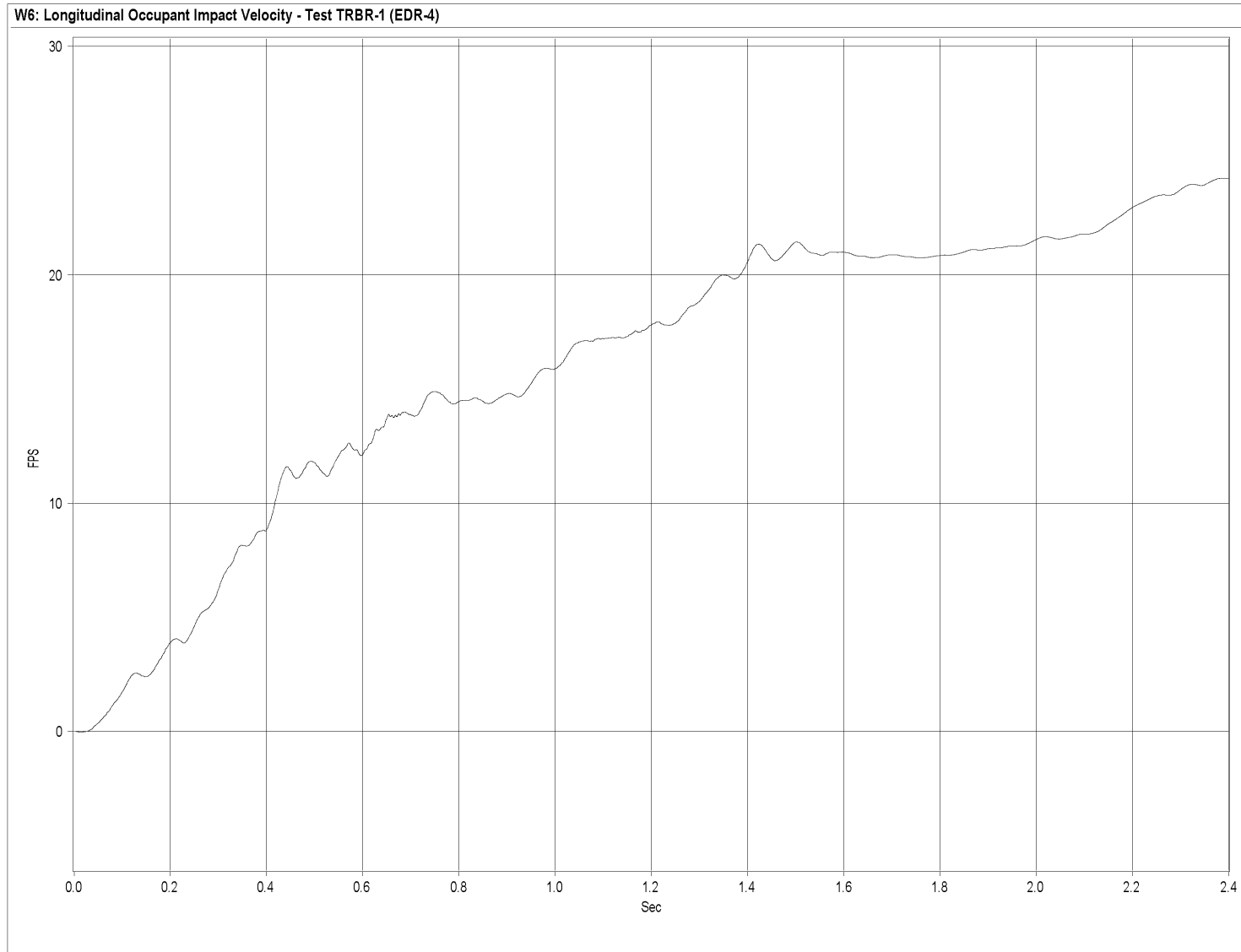


Figure E-2. Graph of Longitudinal Occupant Impact Velocity, Test TRBR-1

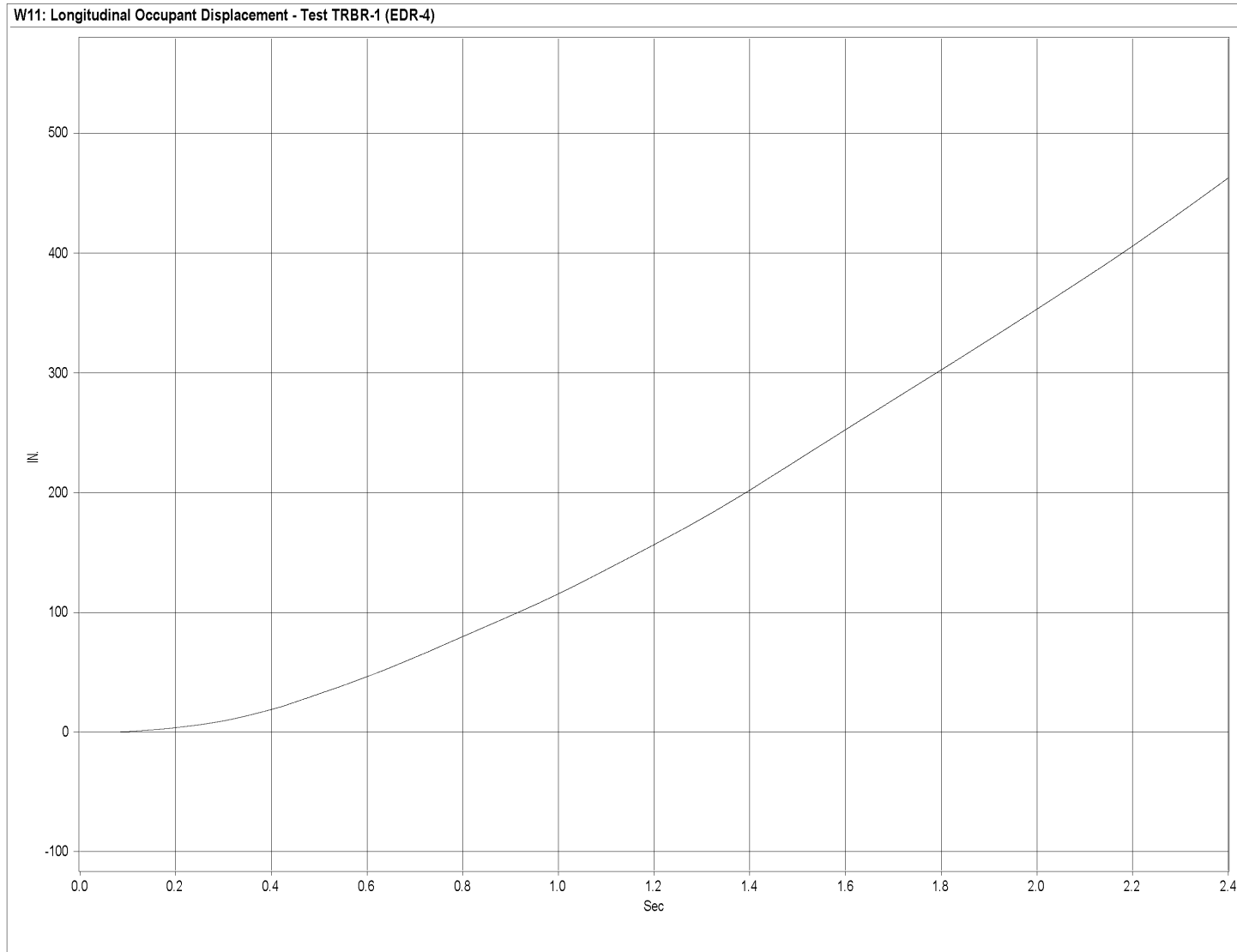


Figure E-3. Graph of Longitudinal Occupant Displacement, Test TRBR-1

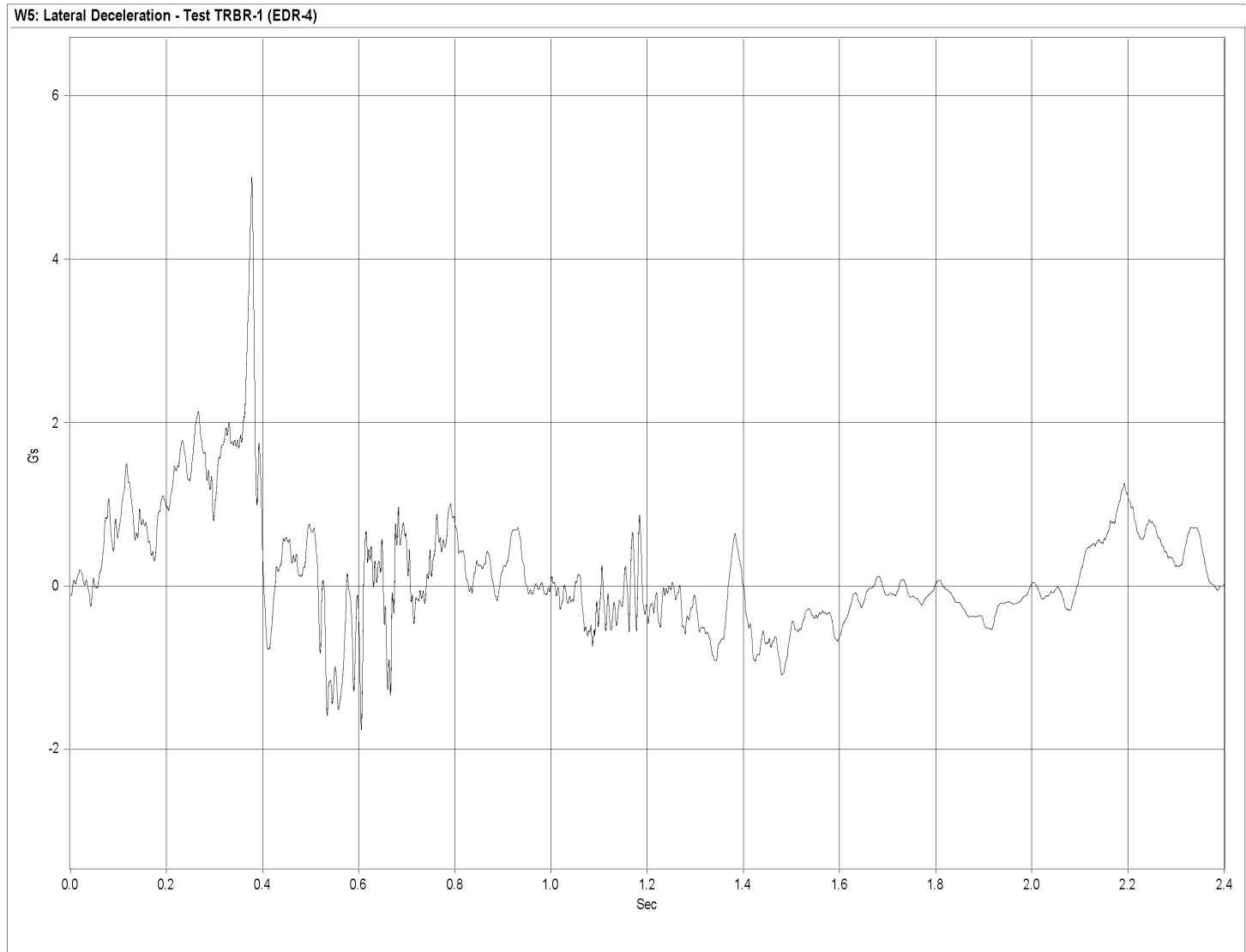


Figure E-4. Graph of Lateral Deceleration, Test TRBR-1

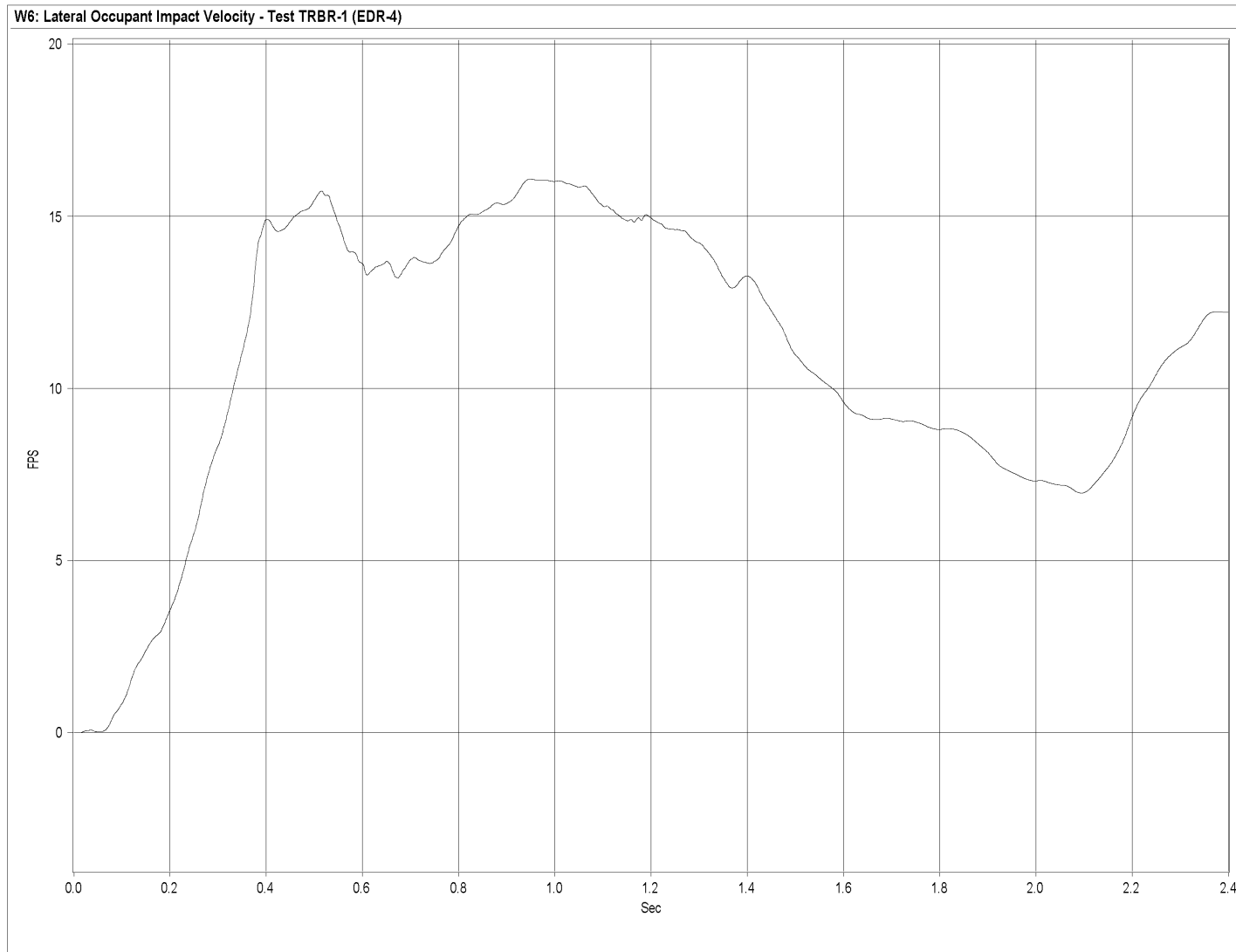


Figure E-5. Graph of Lateral Occupant Impact Velocity, Test TRBR-1

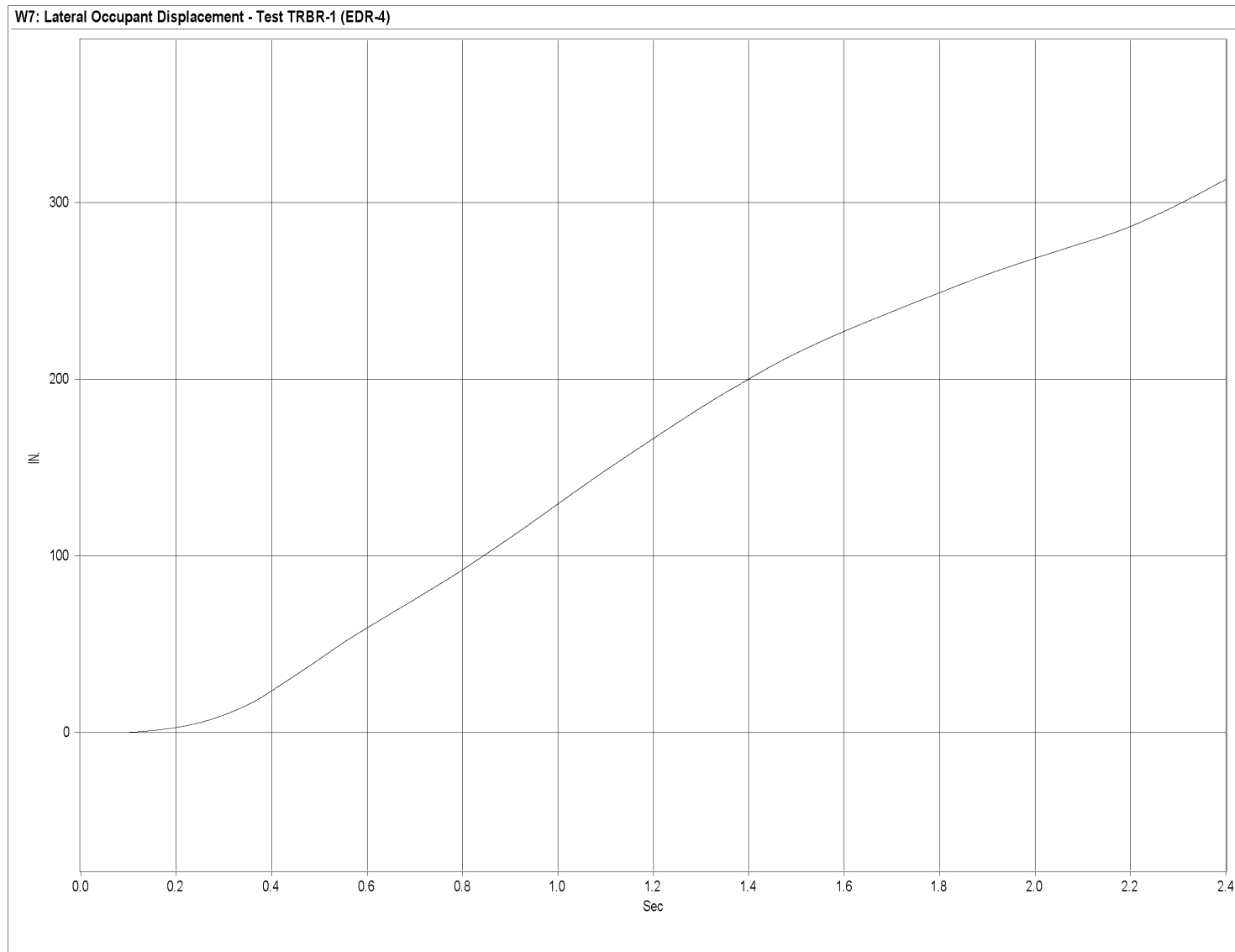


Figure E-6. Graph of Lateral Occupant Displacement, Test TRBR-1

APPENDIX F

Strain Gauge Data Analysis - Test TRBR-1

Figure F-1. Graph of Post No. 3 Bolt Load, Test TRBR-1

Figure F-2. Graph of Post No. 4 Bolt Load, Test TRBR-1

Figure F-3. Graph of Post No. 5 Bolt Load, Test TRBR-1

Figure F-4. Graph of Post No. 6 Bolt Load, Test TRBR-1

Figure F-5. Graph of Post No. 7 Bolt Load, Test TRBR-1

Figure F-6. Graph of Post No. 8 Bolt Load, Test TRBR-1

Figure F-7. Graph of Traffic-Side Top Splice Plate at Post No. 6 Stress, Test TRBR-1

Figure F-8. Graph of Back-Side Top Splice Plate at Post No. 6 Stress, Test TRBR-1

Figure F-9. Graph of Back-Side Curb Rail Splice Plate at Midspan Between Post Nos. 5 and 6
Stress, Test TRBR-1

Figure F-10. Graph of Back-Side Wood Rail at Midspan Between Post Nos. 5 and 6
Stress, Test TRBR-1

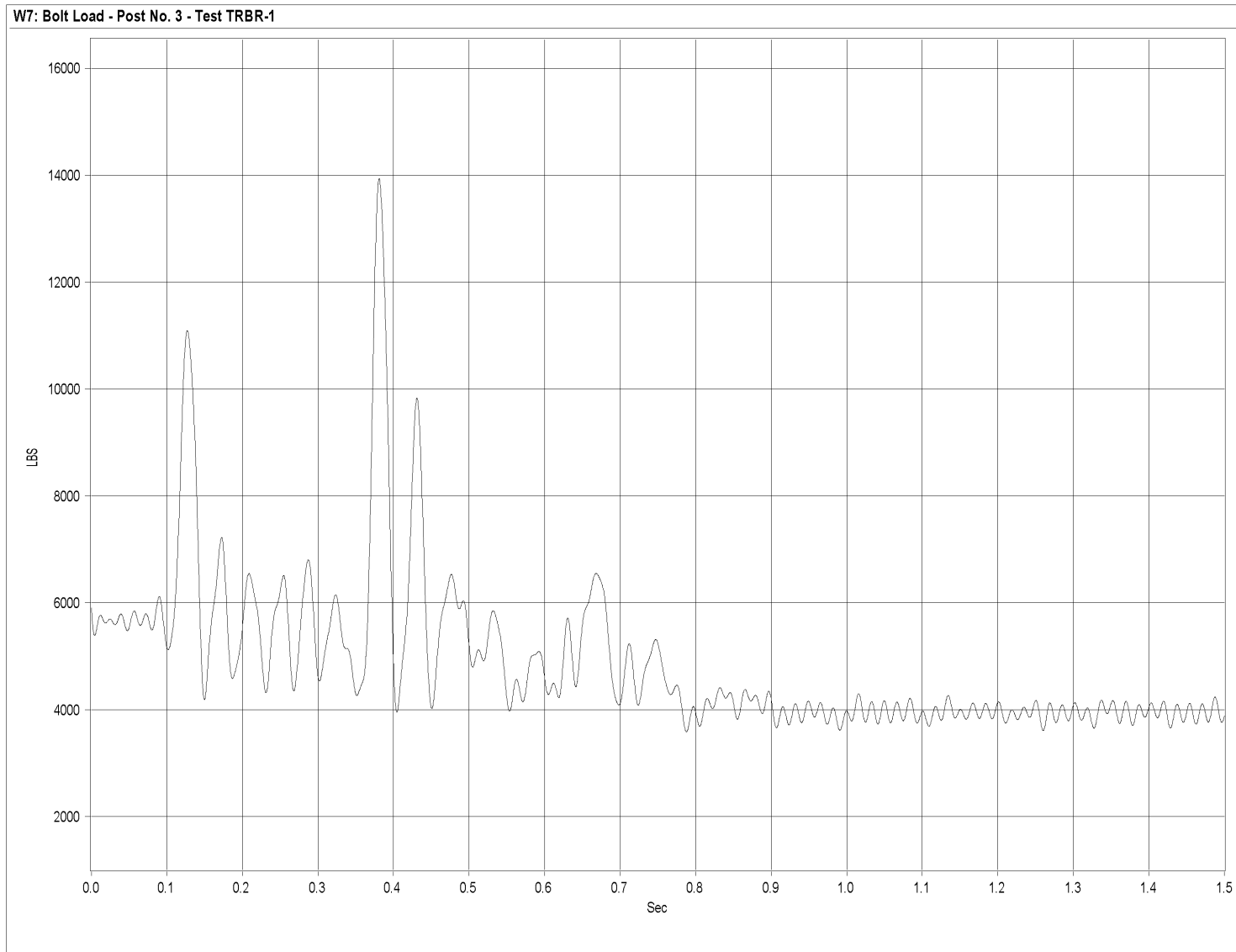


Figure F-1. Graph of Post No. 3 Bolt Load, Test TRBR-1

338

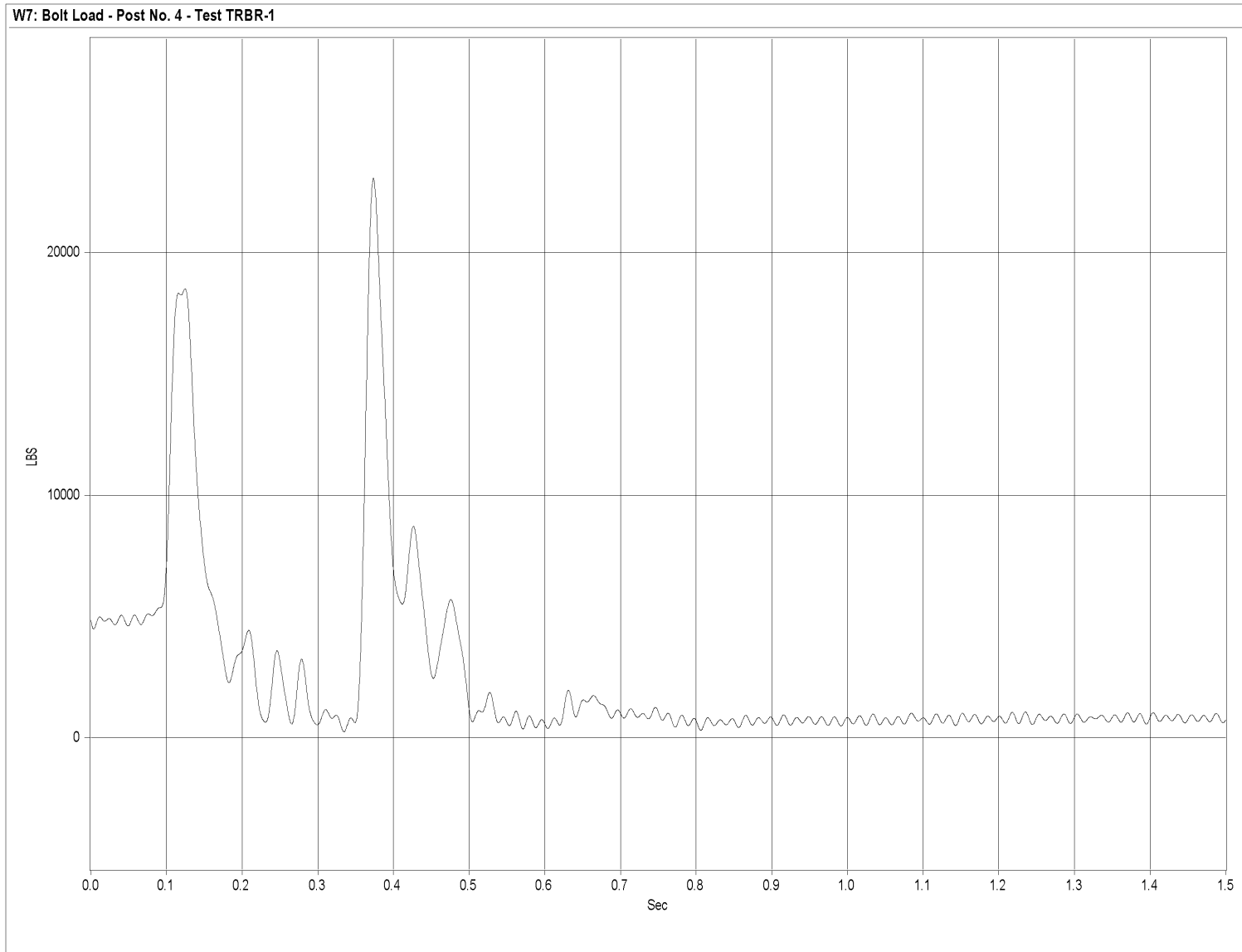


Figure F-2. Graph of Post No. 4 Bolt Load, Test TRBR-1

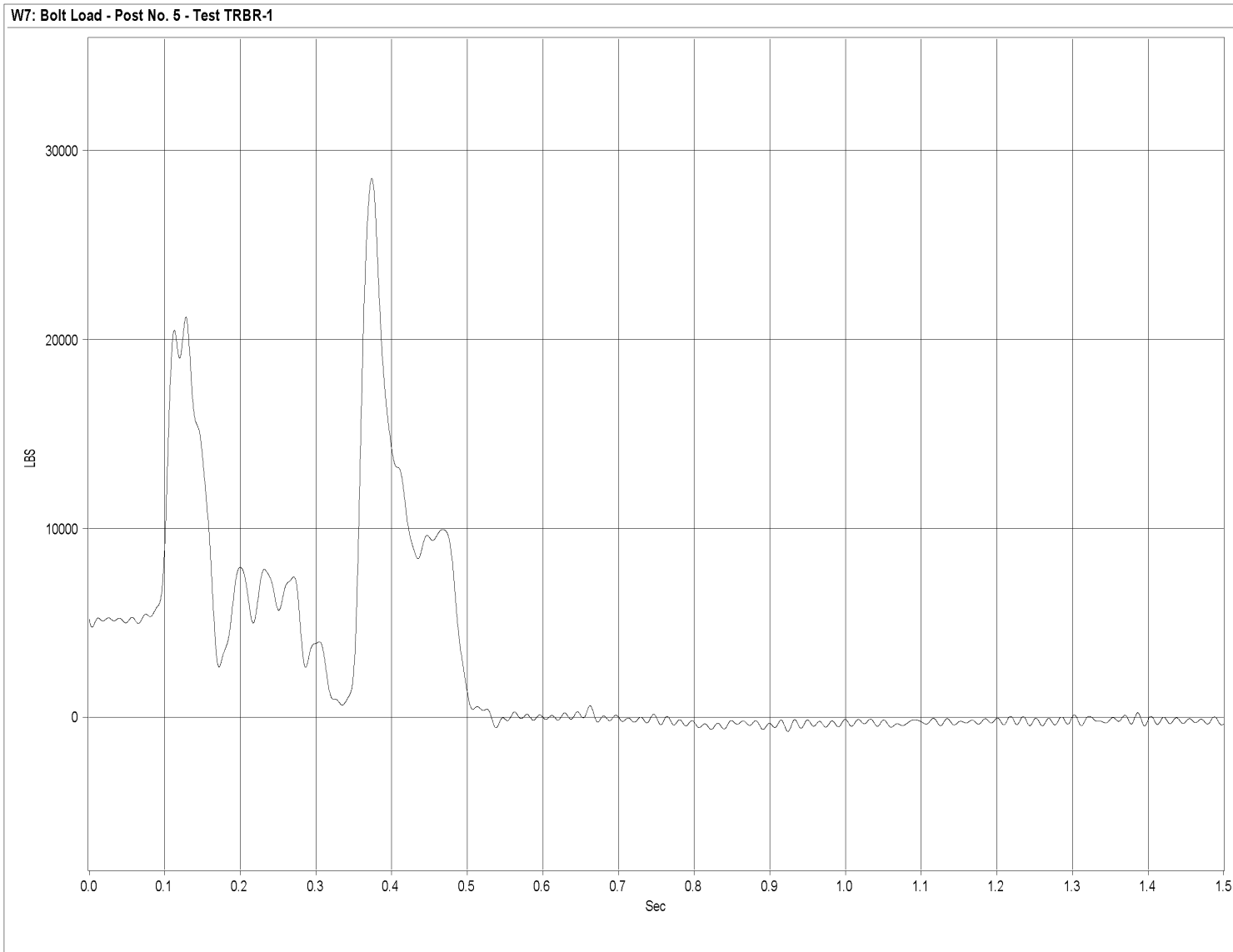


Figure F-3. Graph of Post No. 5 Bolt Load, Test TRBR-1

340

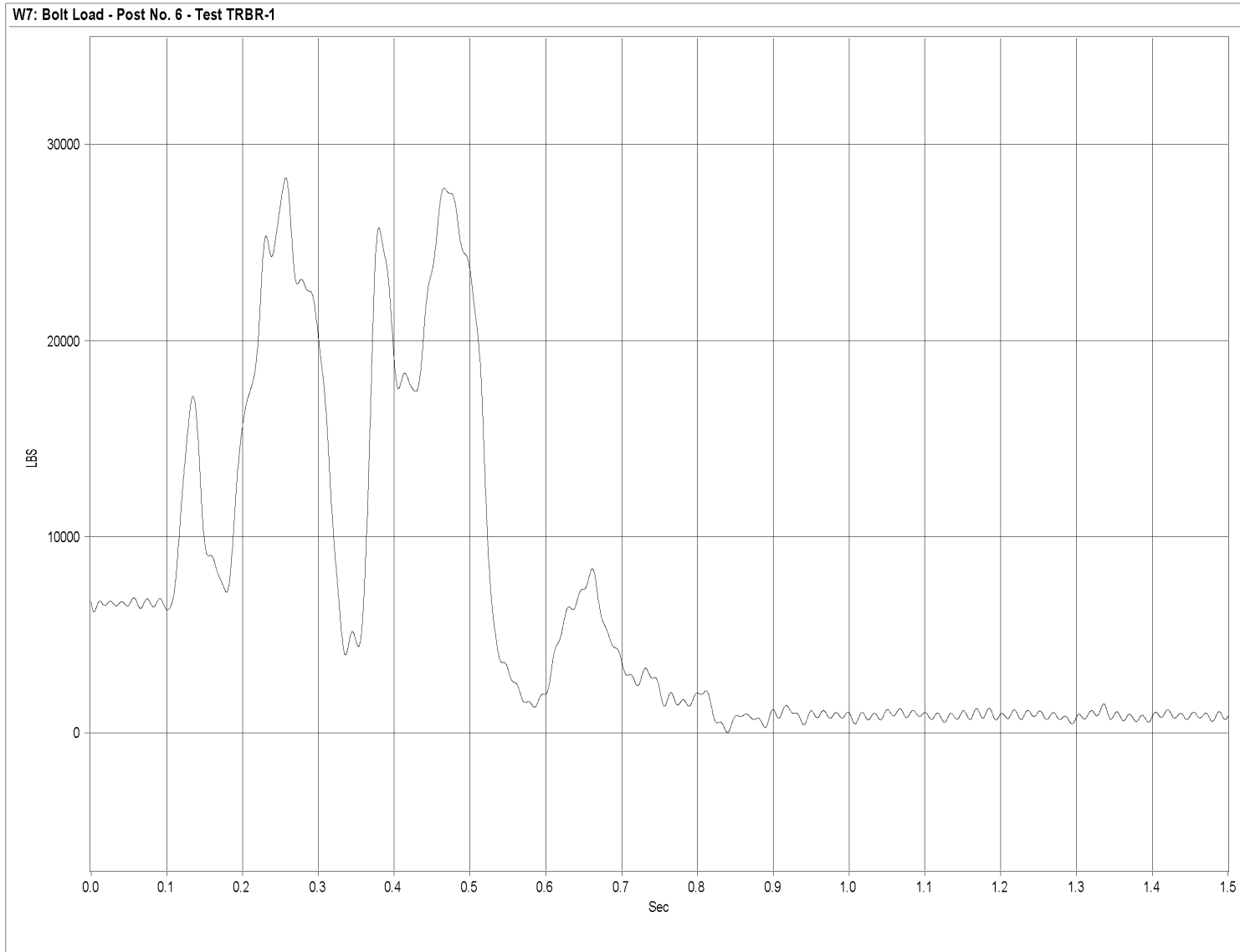


Figure F-4. Graph of Post No. 6 Bolt Load, Test TRBR-1

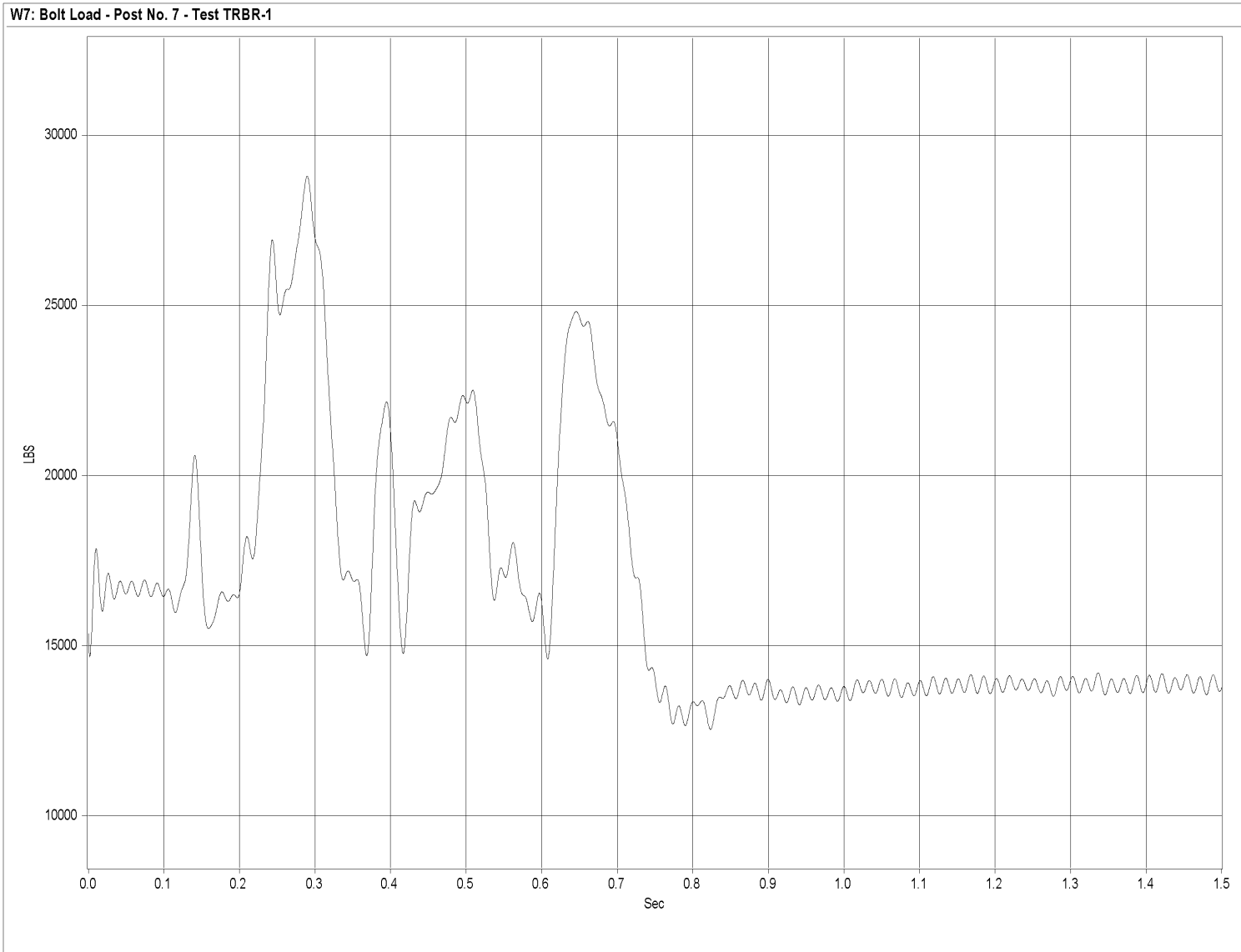


Figure F-5. Graph of Post No. 7 Bolt Load, Test TRBR-1

342

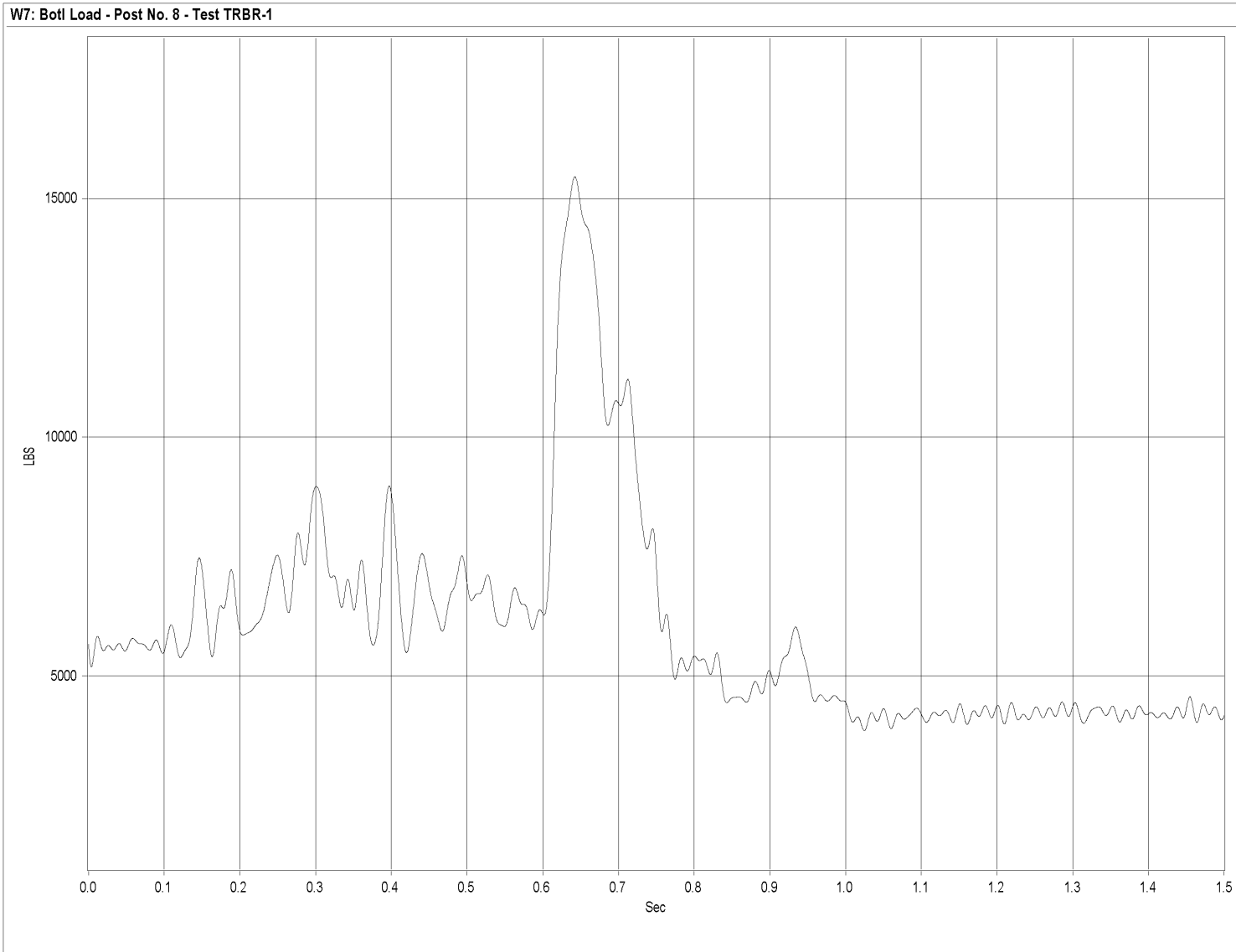


Figure F-6. Graph of Post No. 8 Bolt Load, Test TRBR-1

343

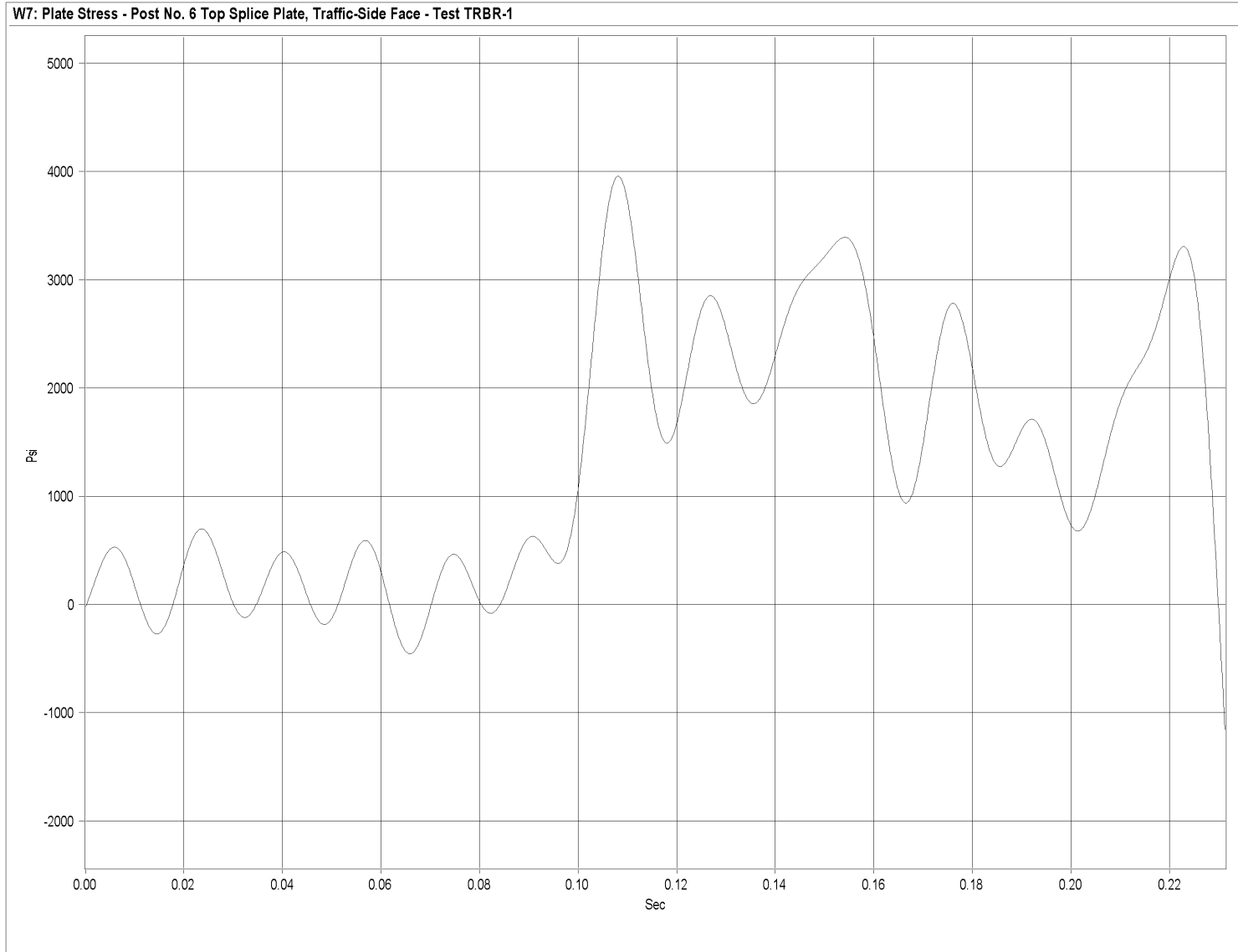


Figure F-7. Graph of Traffic-Side Top Splice Plate at Post No. 6 Stress, Test TRBR-1

344

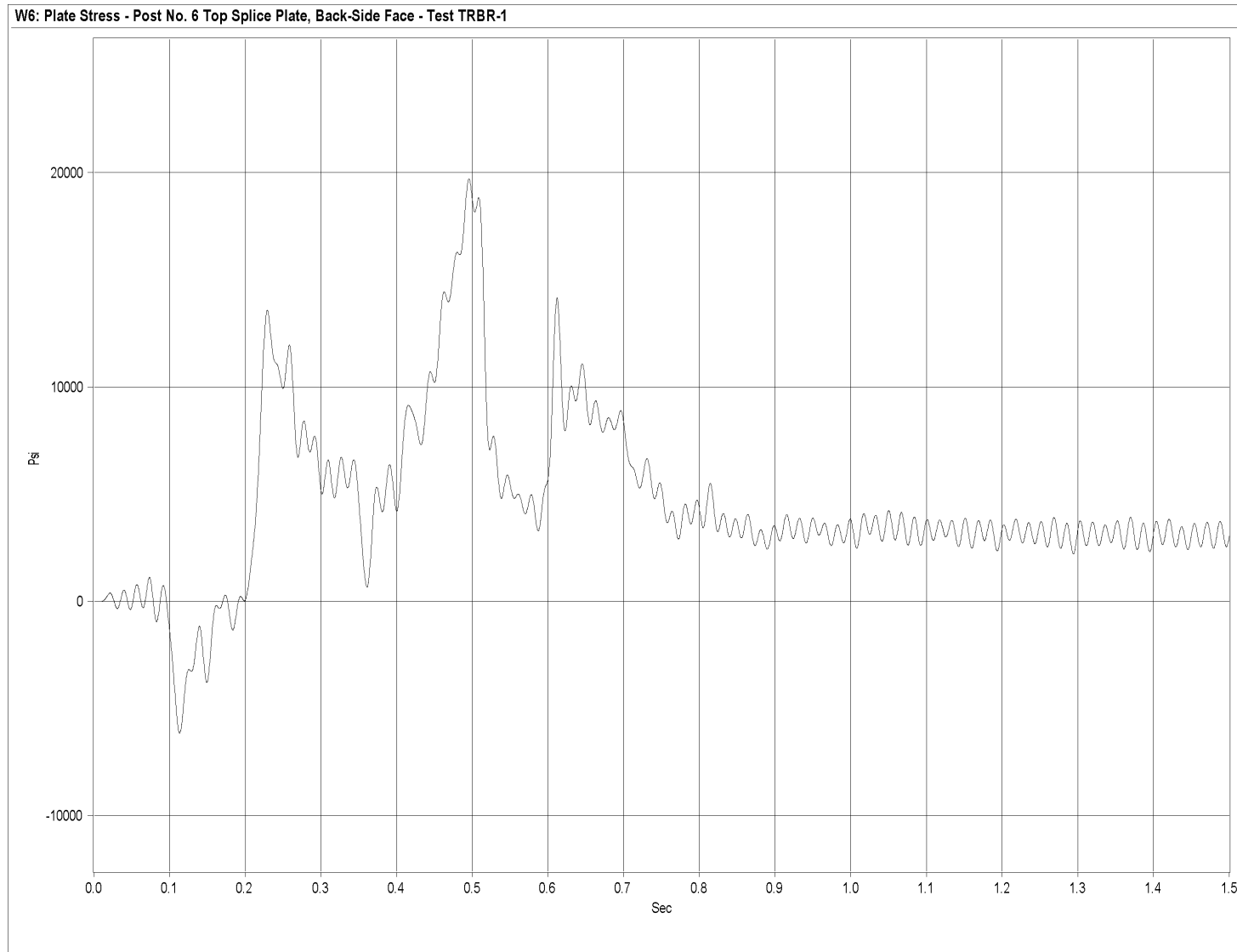


Figure F-8. Graph of Back-Side Top Splice Plate at Post No. 6 Stress, Test TRBR-1

345

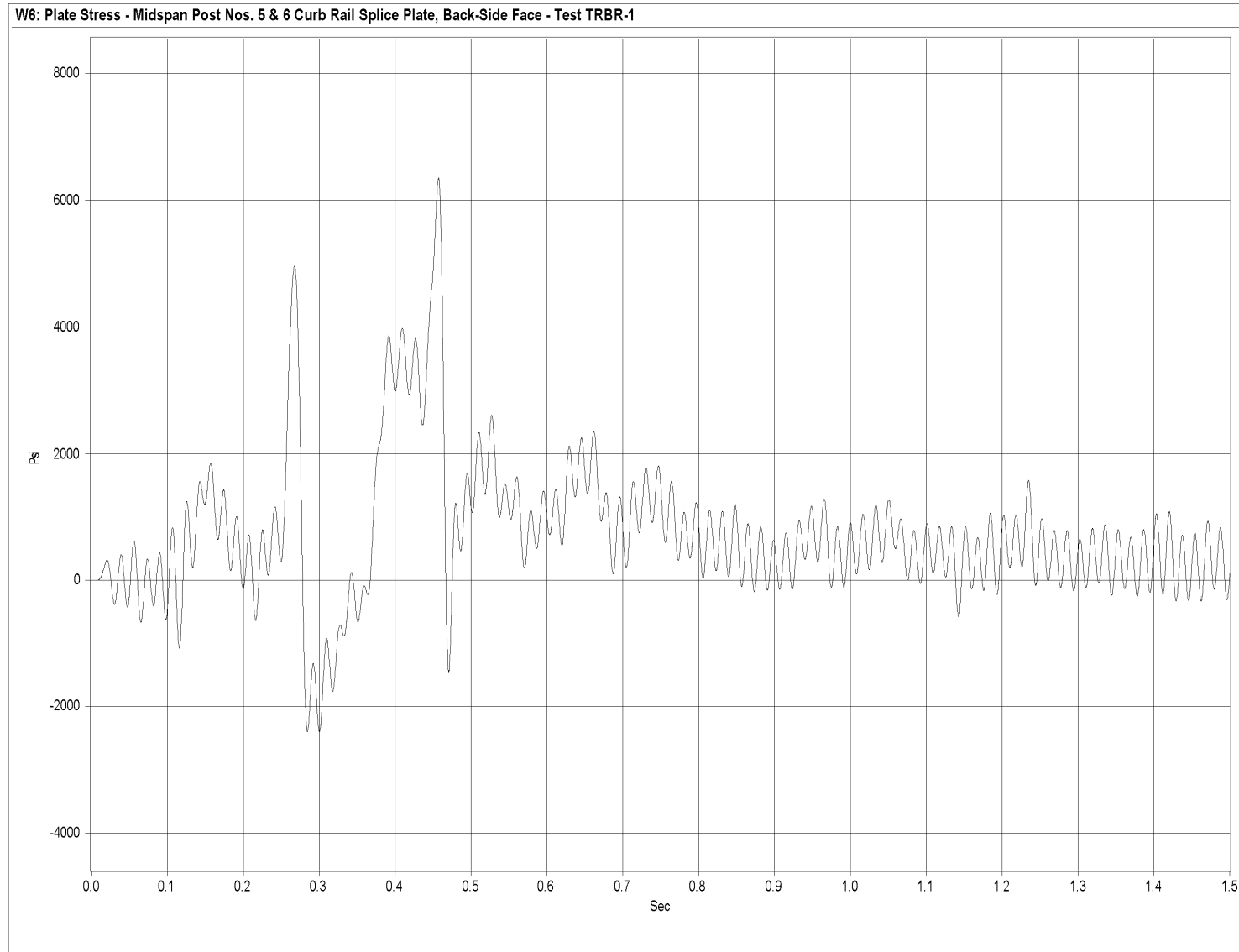


Figure F-9. Graph of Back-Side Curb Rail Splice Plate at Midspan Between Post Nos. 5 and 6 Stress, Test TRBR-1

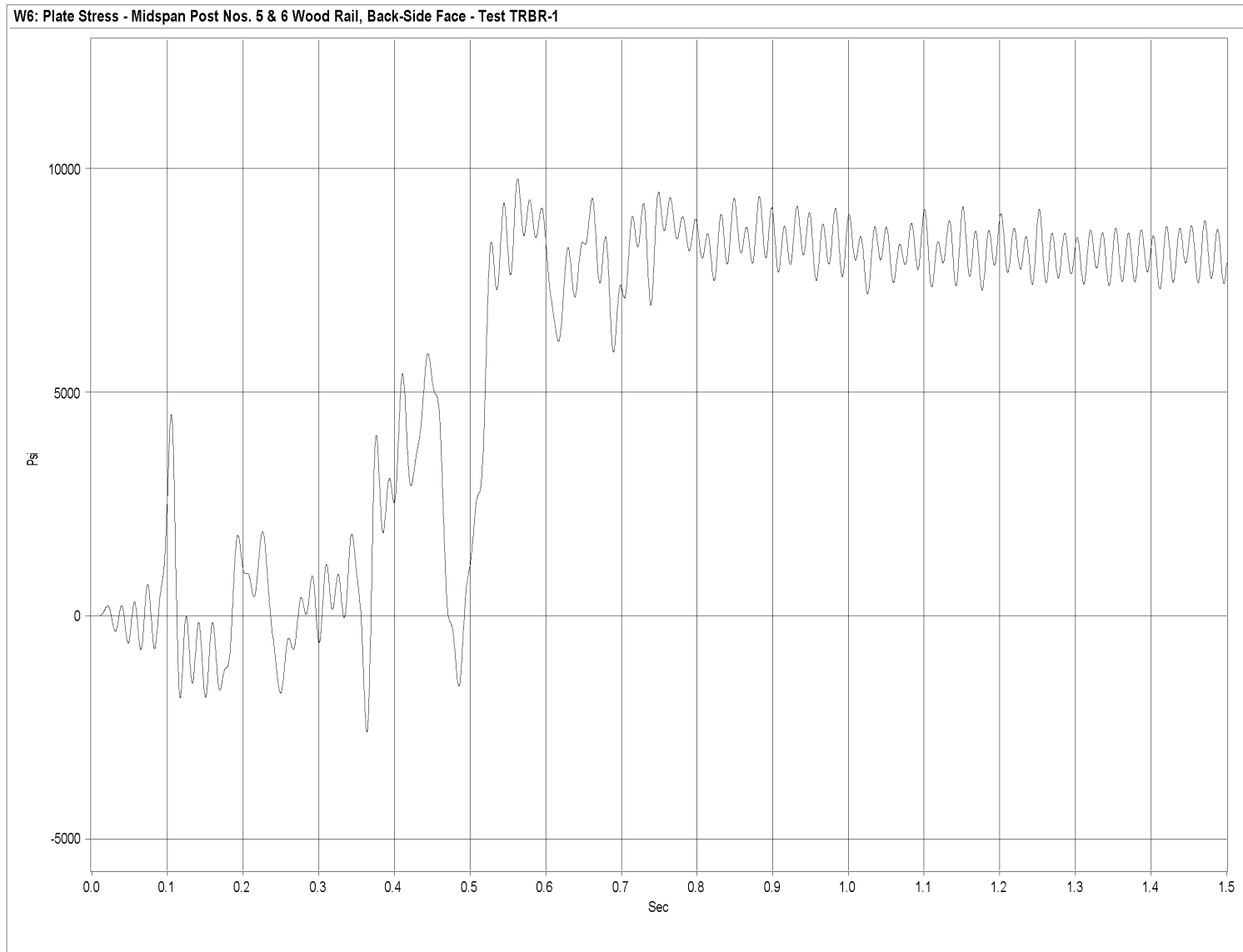


Figure F-10. Graph of Back-Side Wood Rail at Midspan Between Post Nos. 5 and 6 Stress, Test TRBR-1

APPENDIX G

String Potentiometer Data Analysis - Test TRBR-1

Figure G-1. Graph of Deflection at Midspan of Timber Rail No. 1, Test TRBR-1

Figure G-2. Graph of Deflection at $\frac{3}{4}$ -point of Timber Rail No. 1, Test TRBR-1

Figure G-3. Graph of Deflection at $\frac{7}{8}$ -point of Timber Rail No. 1, Test TRBR-1

Figure G-4. Graph of Deflection at Point Between Timber Rail Nos. 1 and 2, Test TRBR-1

Figure G-5. Graph of Deflection at $\frac{1}{4}$ -point of Timber Rail No. 2, Test TRBR-1

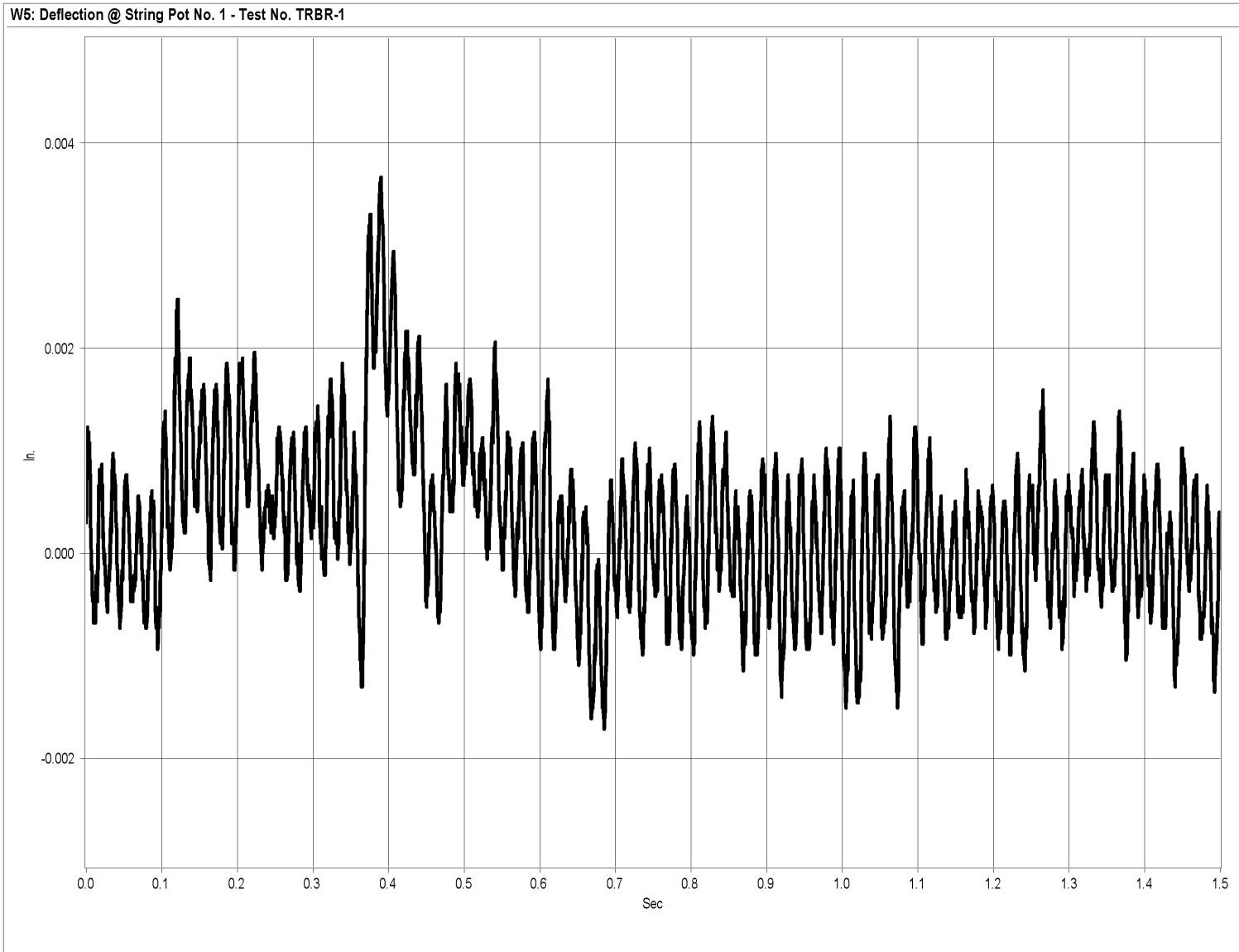


Figure G-1. Graph of Deflection at Midspan of Timber Rail No. 1, Test TRBR-1

349

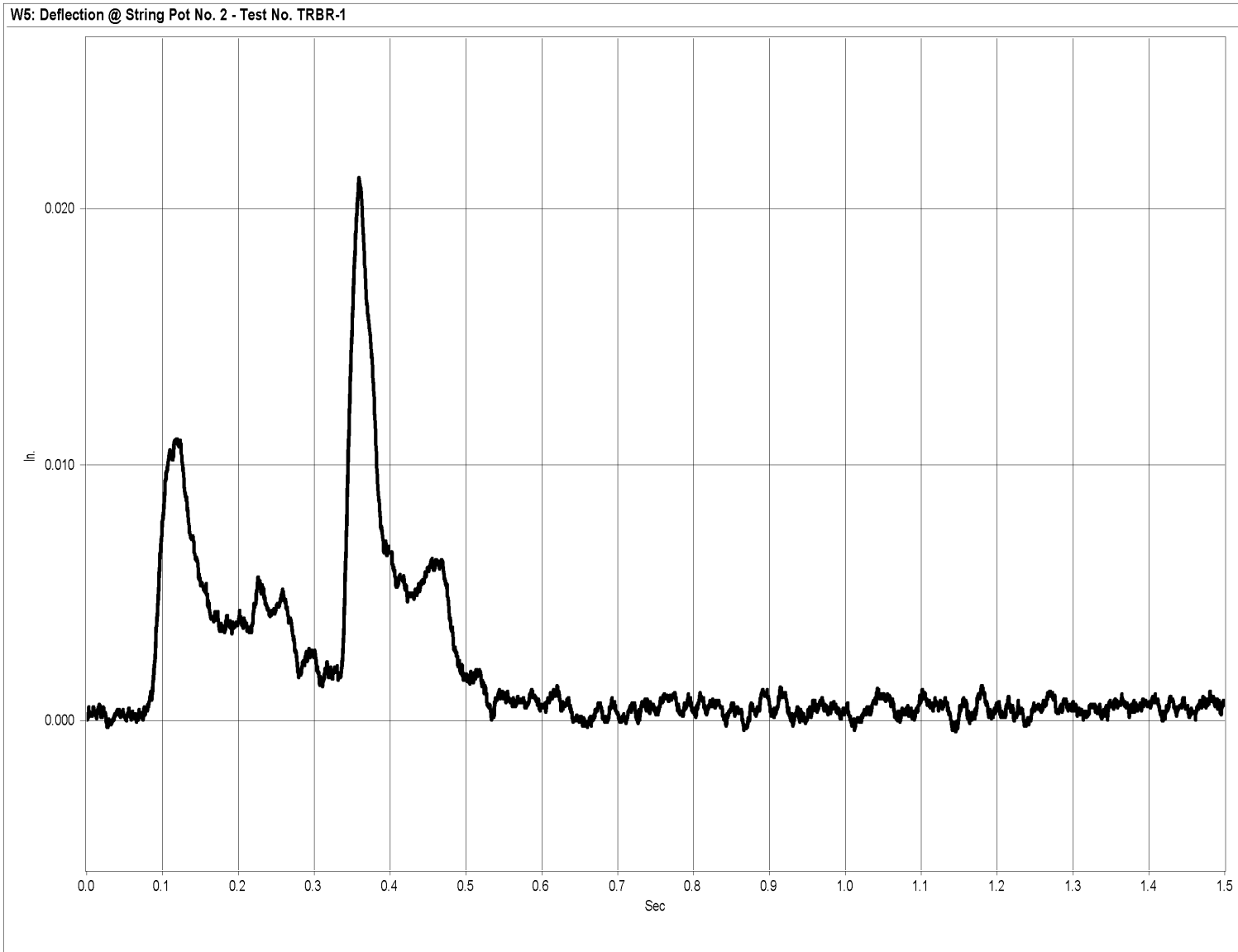


Figure G-2. Graph of Deflection at $\frac{3}{4}$ -point of Timber Rail No. 1, Test TRBR-1

350

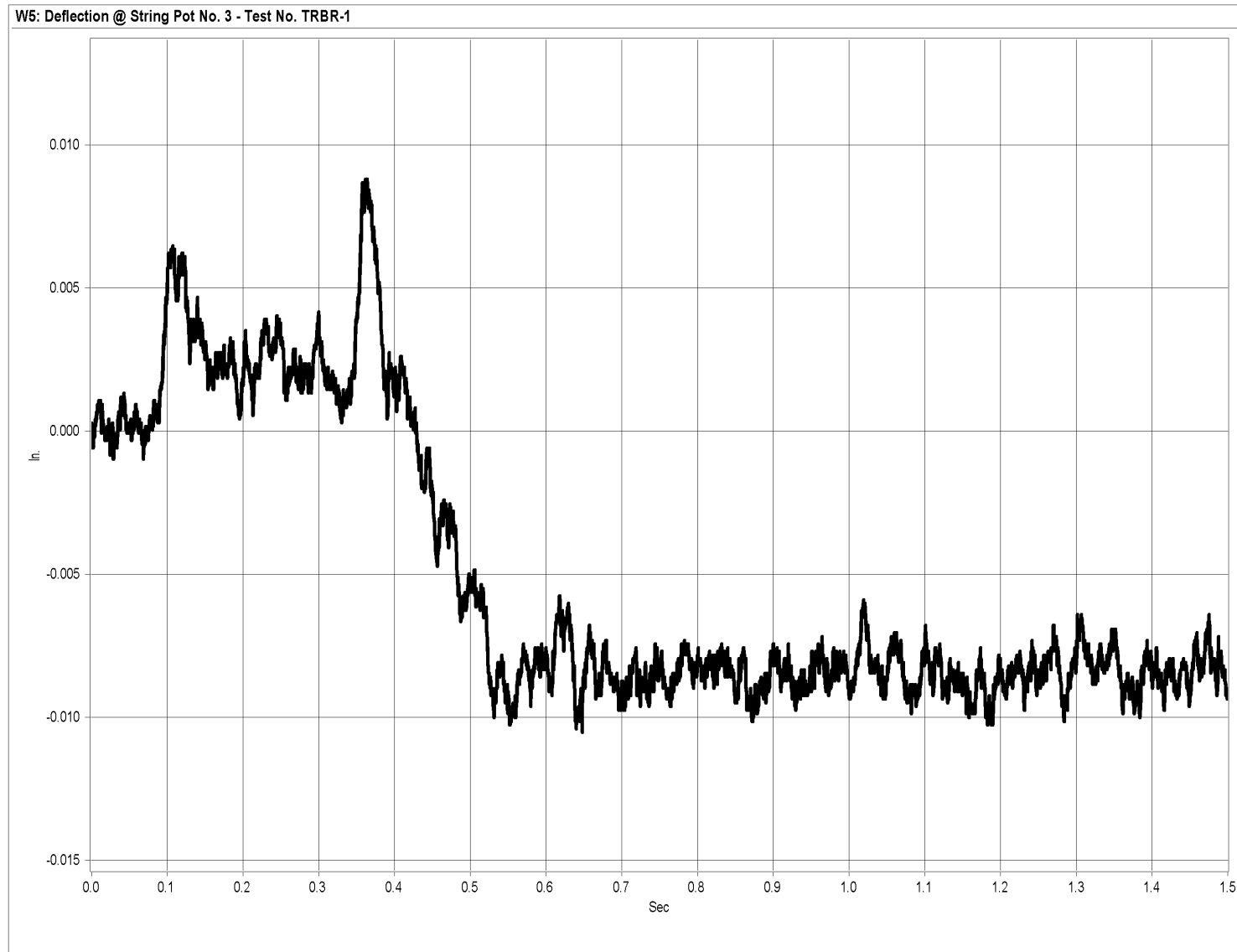


Figure G-3. Graph of Deflection at $\frac{7}{8}$ -point of Timber Rail No. 1, Test TRBR-1

351

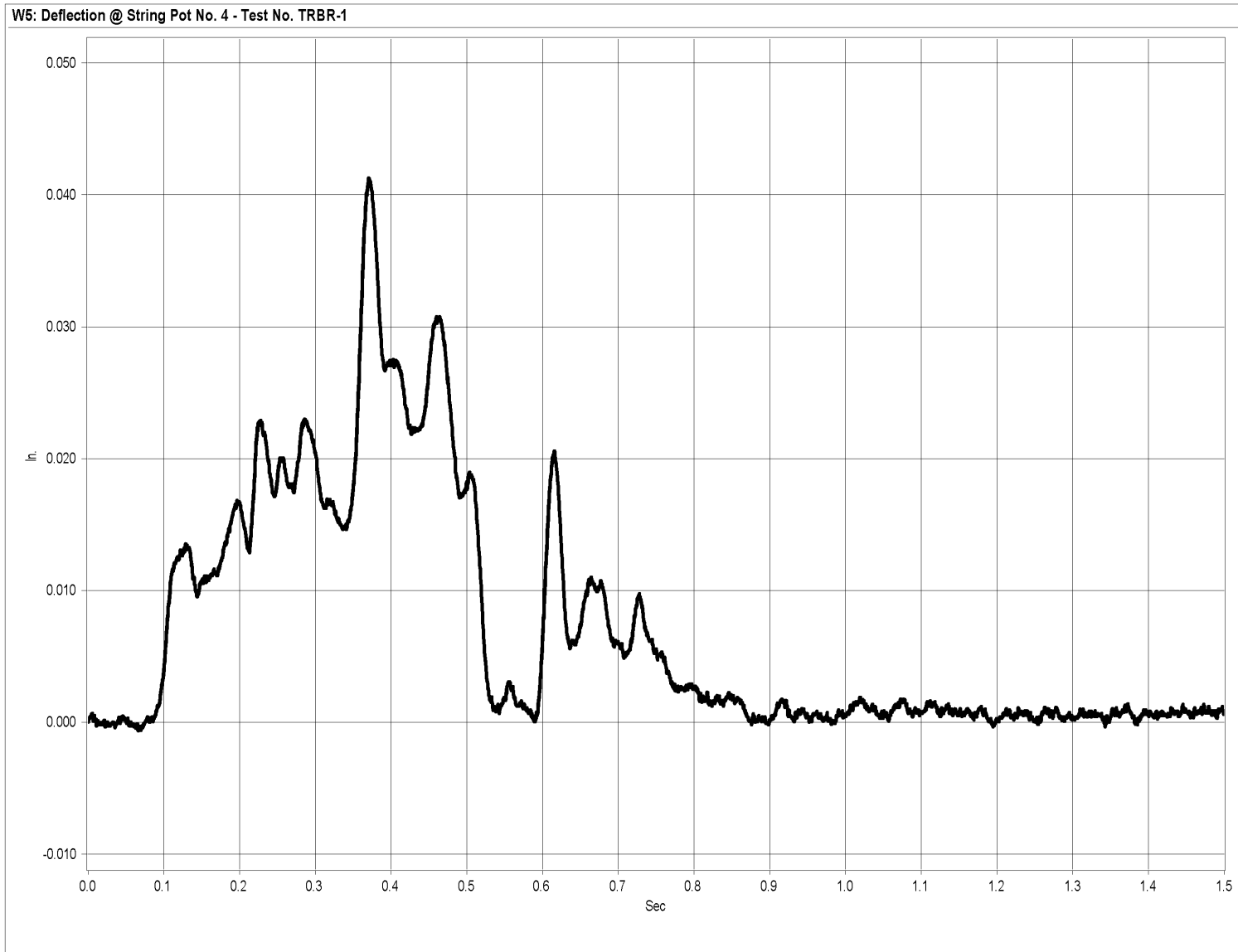


Figure G-4. Graph of Deflection at Point Between Timber Rail Nos. 1 and 2, Test TRBR-1

352

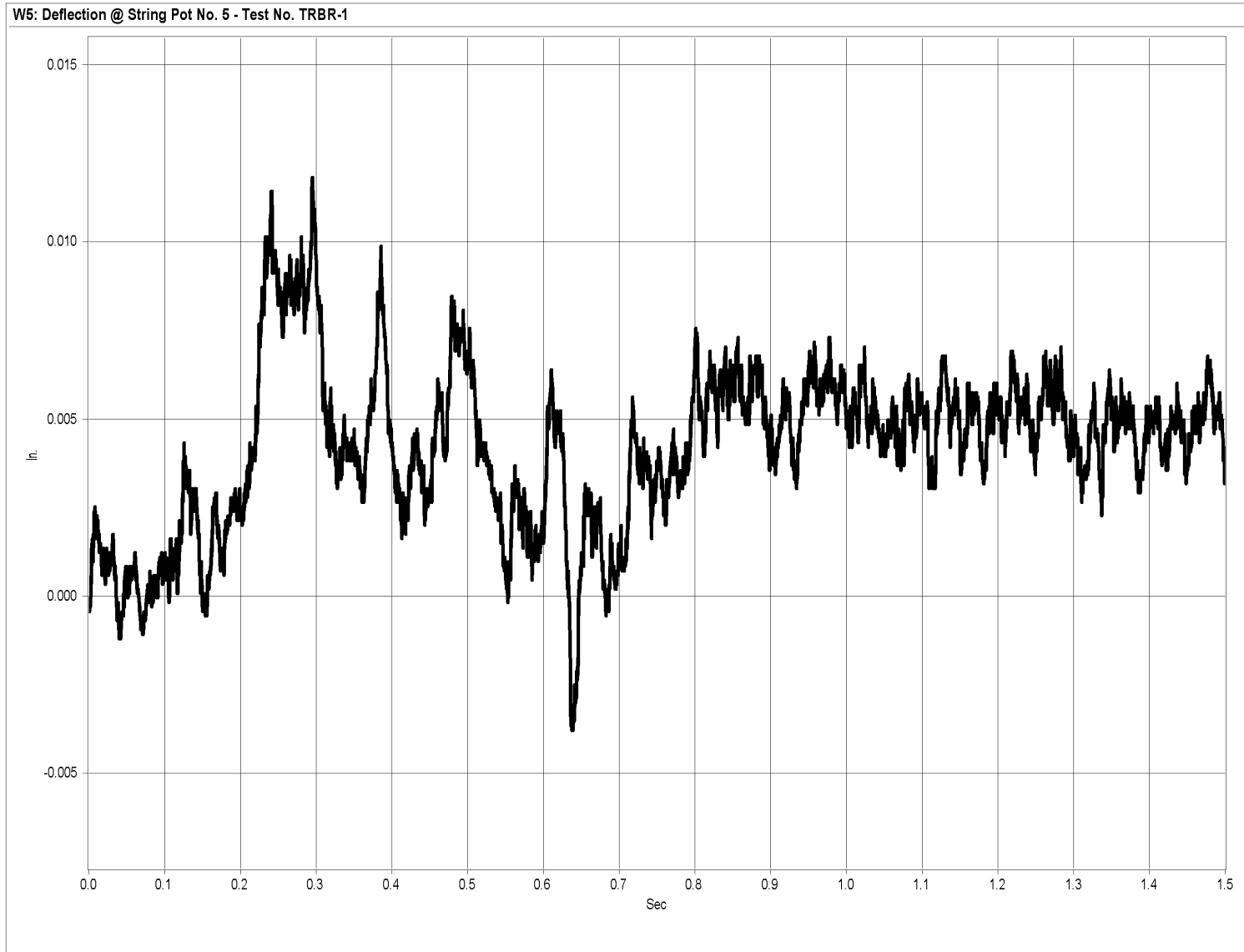


Figure G-5. Graph of Deflection at 1/4-point of Timber Rail No. 2, Test TRBR-1

APPENDIX H

Accelerometer Data Analysis - Test TRBR-2

Figure H-1. Graph of Longitudinal Deceleration, Test TRBR-2

Figure H-2. Graph of Longitudinal Occupant Impact Velocity, Test TRBR-2

Figure H-3. Graph of Longitudinal Occupant Displacement, Test TRBR-2

Figure H-4. Graph of Lateral Deceleration, Test TRBR-2

Figure H-5. Graph of Lateral Occupant Impact Velocity, Test TRBR-2

Figure H-6. Graph of Lateral Occupant Displacement, Test TRBR-2

354

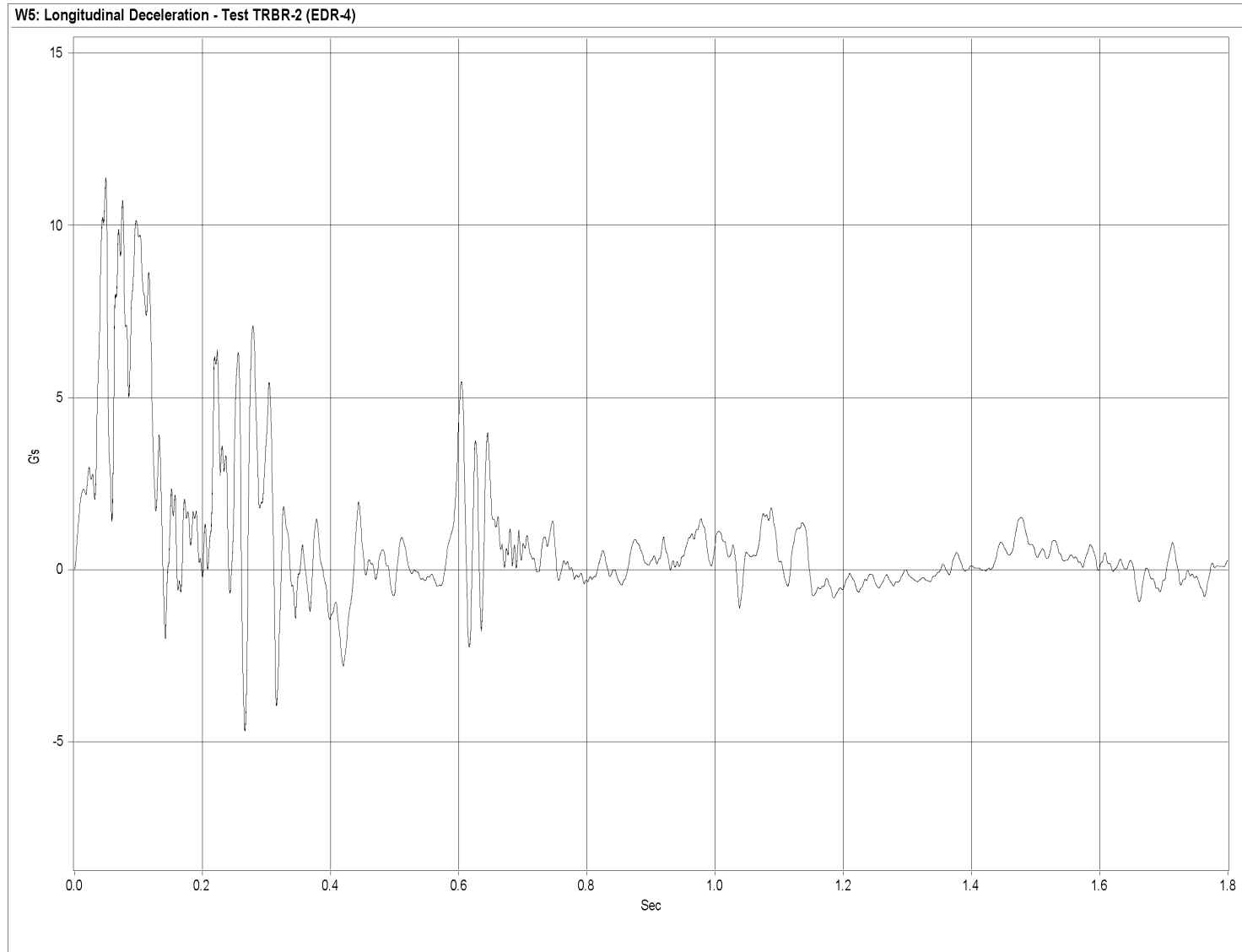


Figure H-1. Graph of Longitudinal Deceleration, Test TRBR-2

355

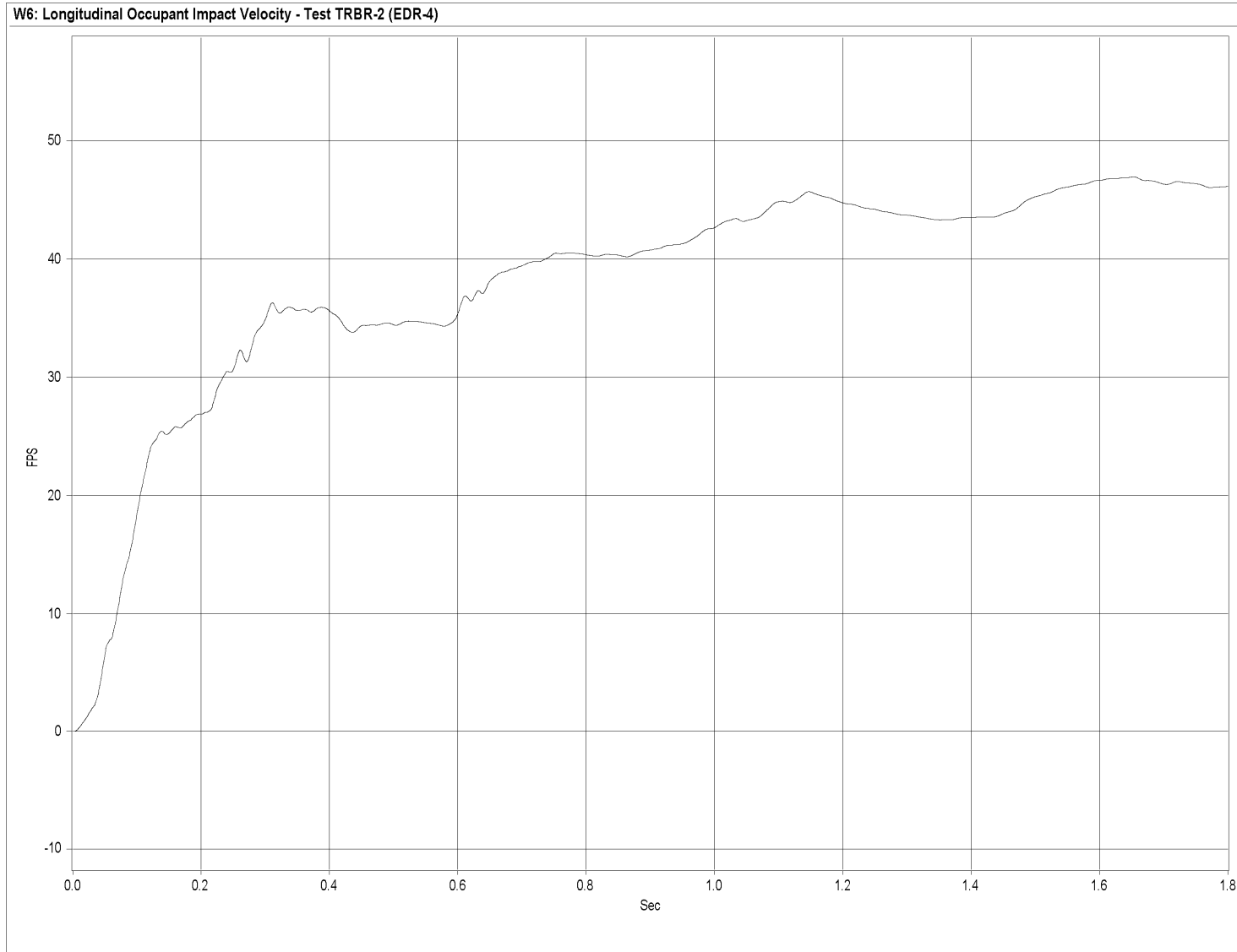


Figure H-2. Graph of Longitudinal Occupant Impact Velocity, Test TRBR-2

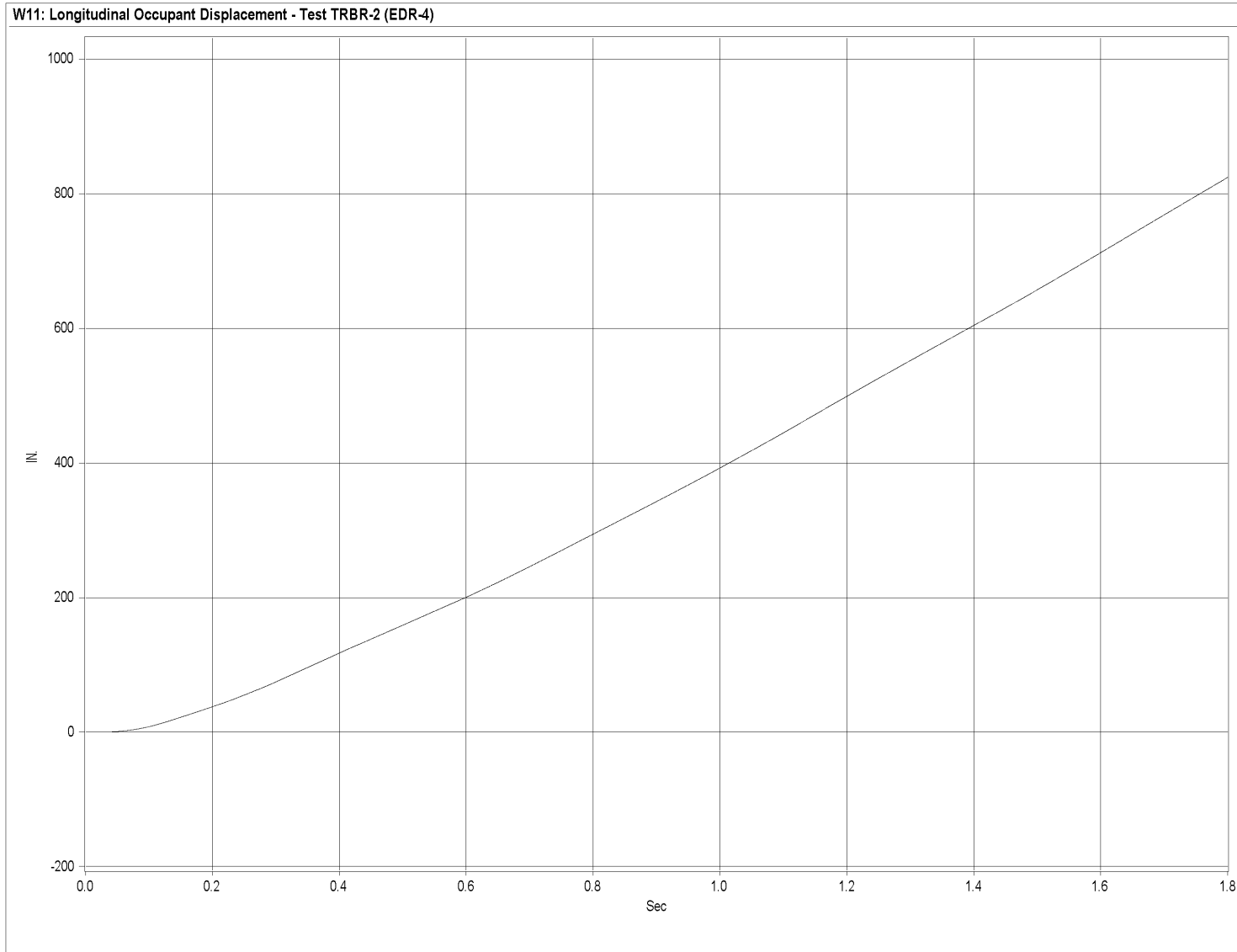


Figure H-3. Graph of Longitudinal Occupant Displacement, Test TRBR-2

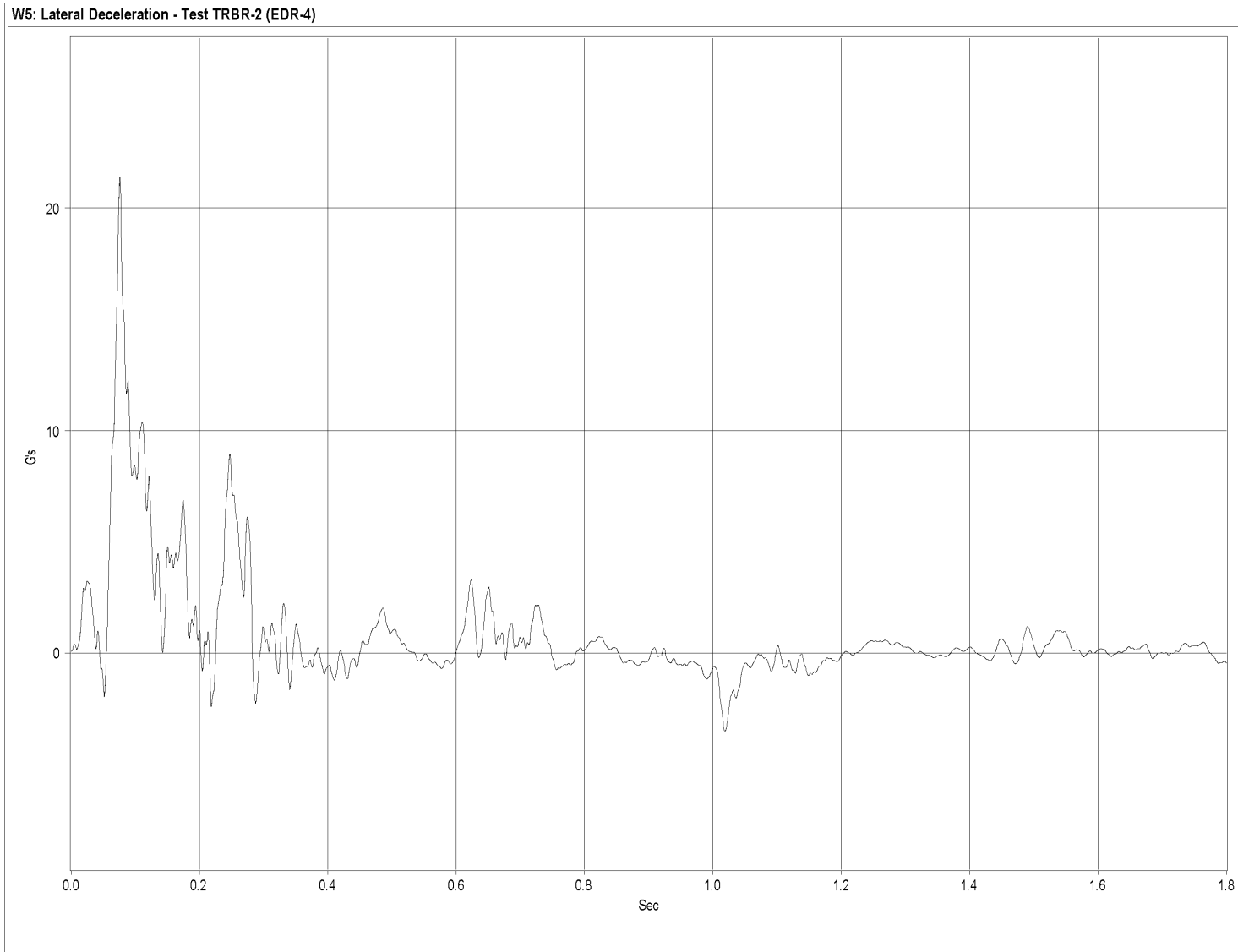


Figure H-4. Graph of Lateral Deceleration, Test TRBR-2

358

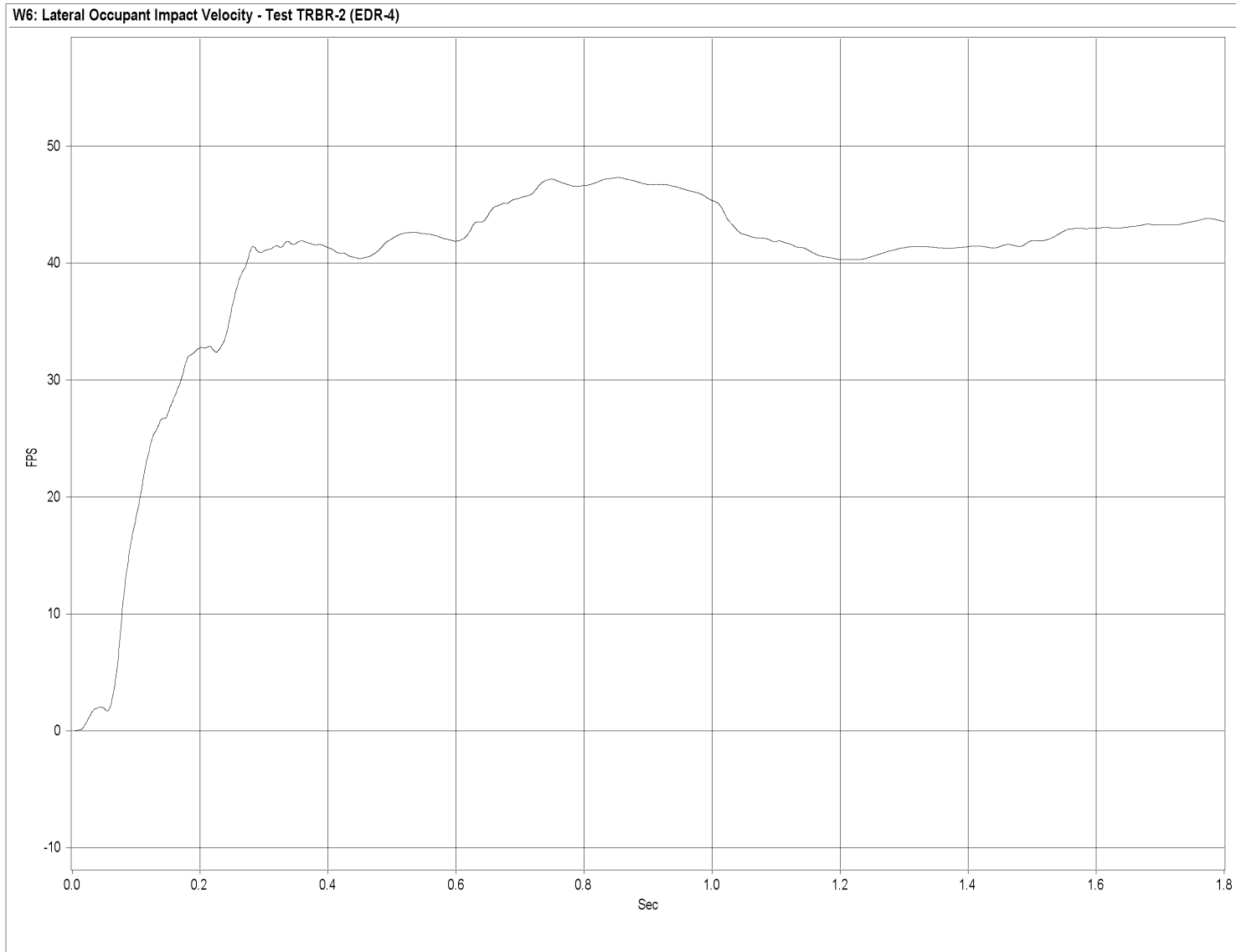


Figure H-5. Graph of Lateral Occupant Impact Velocity, Test TRBR-2

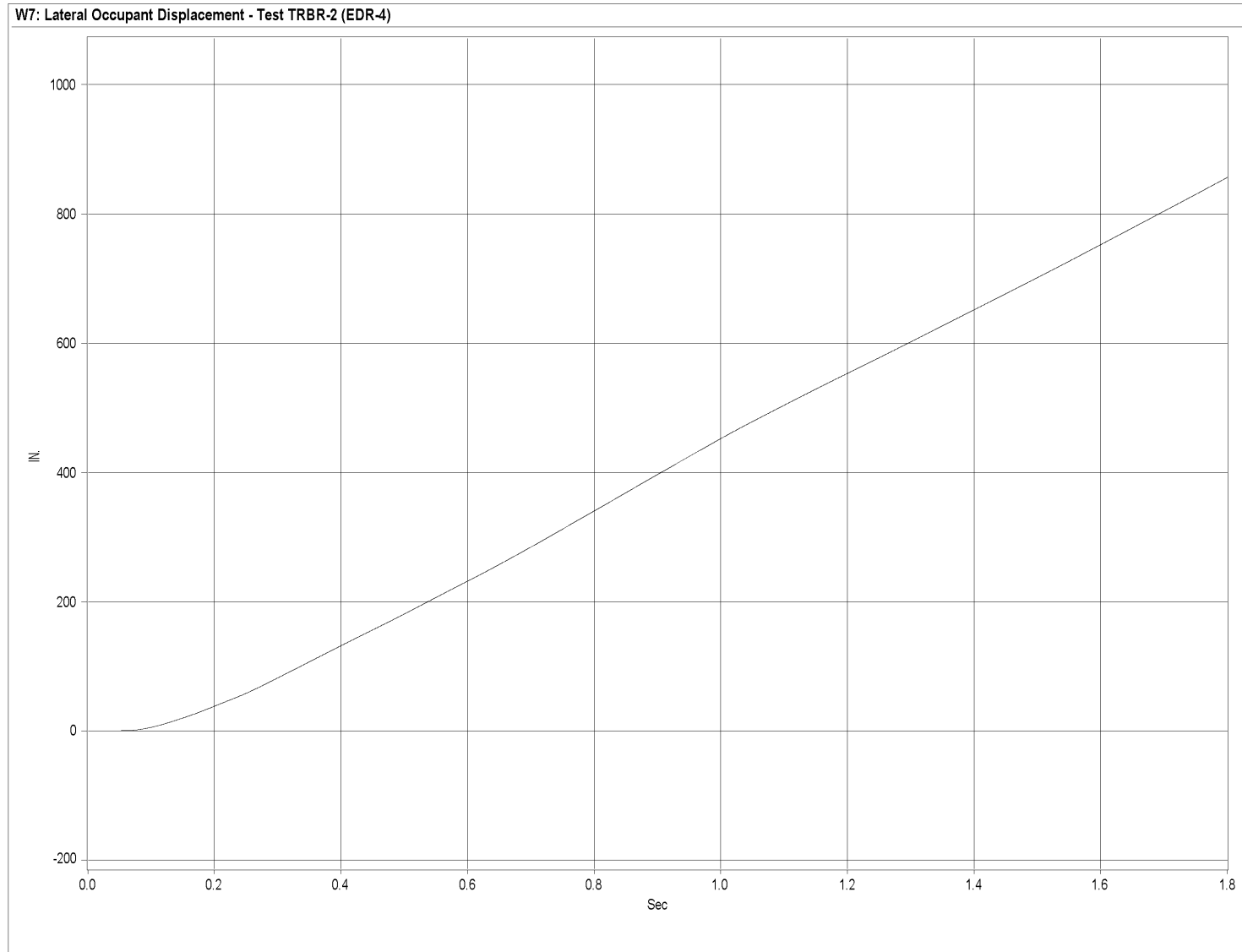


Figure H-6. Graph of Lateral Occupant Displacement, Test TRBR-2

APPENDIX I

Rate Transducer Data Analysis - Test TRBR-2

Figure I-1. Graph of Roll, Pitch, and Yaw Angular Displacements, Test TRBR-2

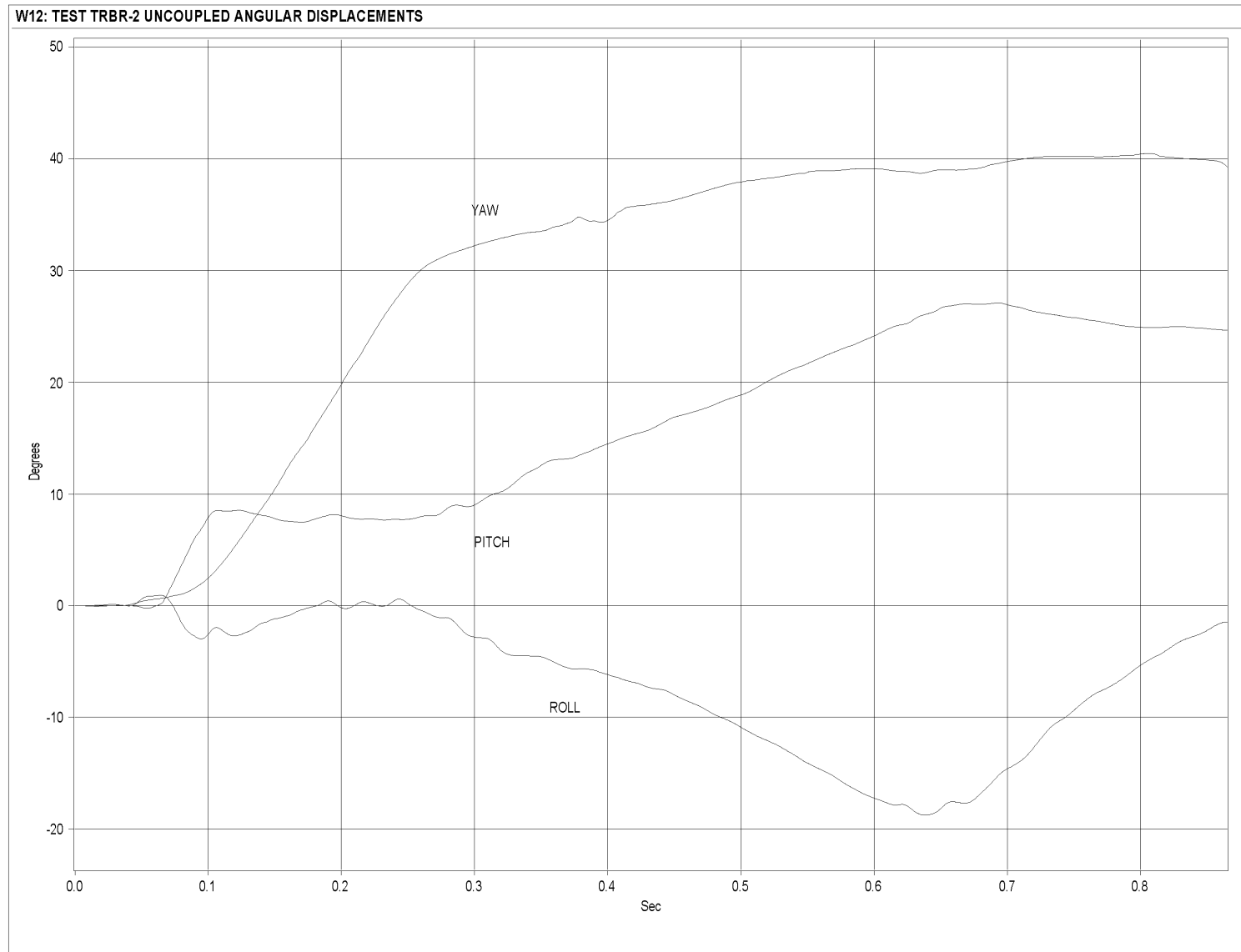


Figure I-1. Graph of Roll, Pitch, and Yaw Angular Displacements, Test TRBR-2

APPENDIX J

Accelerometer Data Analysis - Test TRBR-3

Figure J-1. Graph of Longitudinal Deceleration, Test TRBR-3

Figure J-2. Graph of Longitudinal Occupant Impact Velocity, Test TRBR-3

Figure J-3. Graph of Longitudinal Occupant Displacement, Test TRBR-3

Figure J-4. Graph of Lateral Deceleration, Test TRBR-3

Figure J-5. Graph of Lateral Occupant Impact Velocity, Test TRBR-3

Figure J-6. Graph of Lateral Occupant Displacement, Test TRBR-3

363

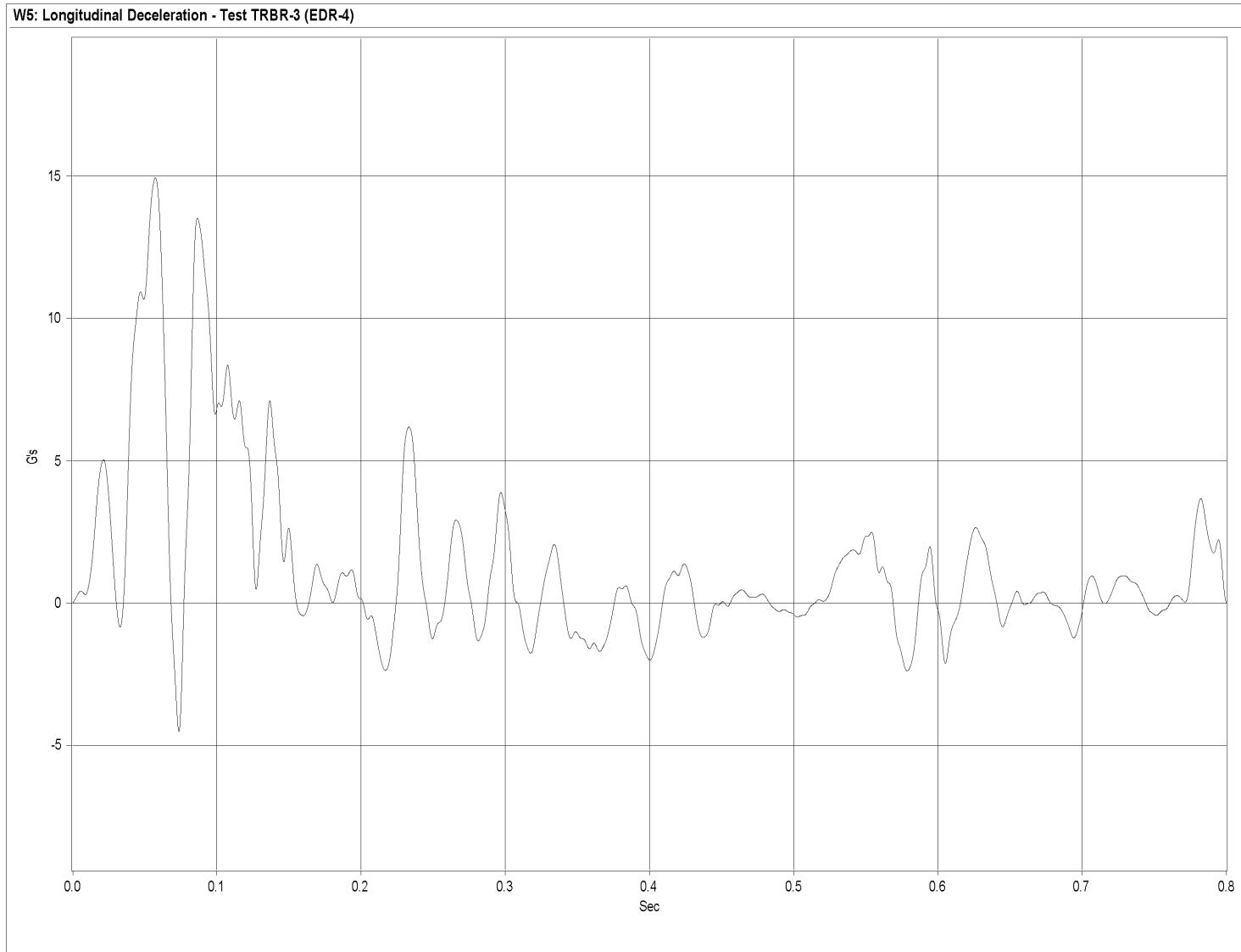


Figure J-1. Graph of Longitudinal Deceleration, Test TRBR-3

364

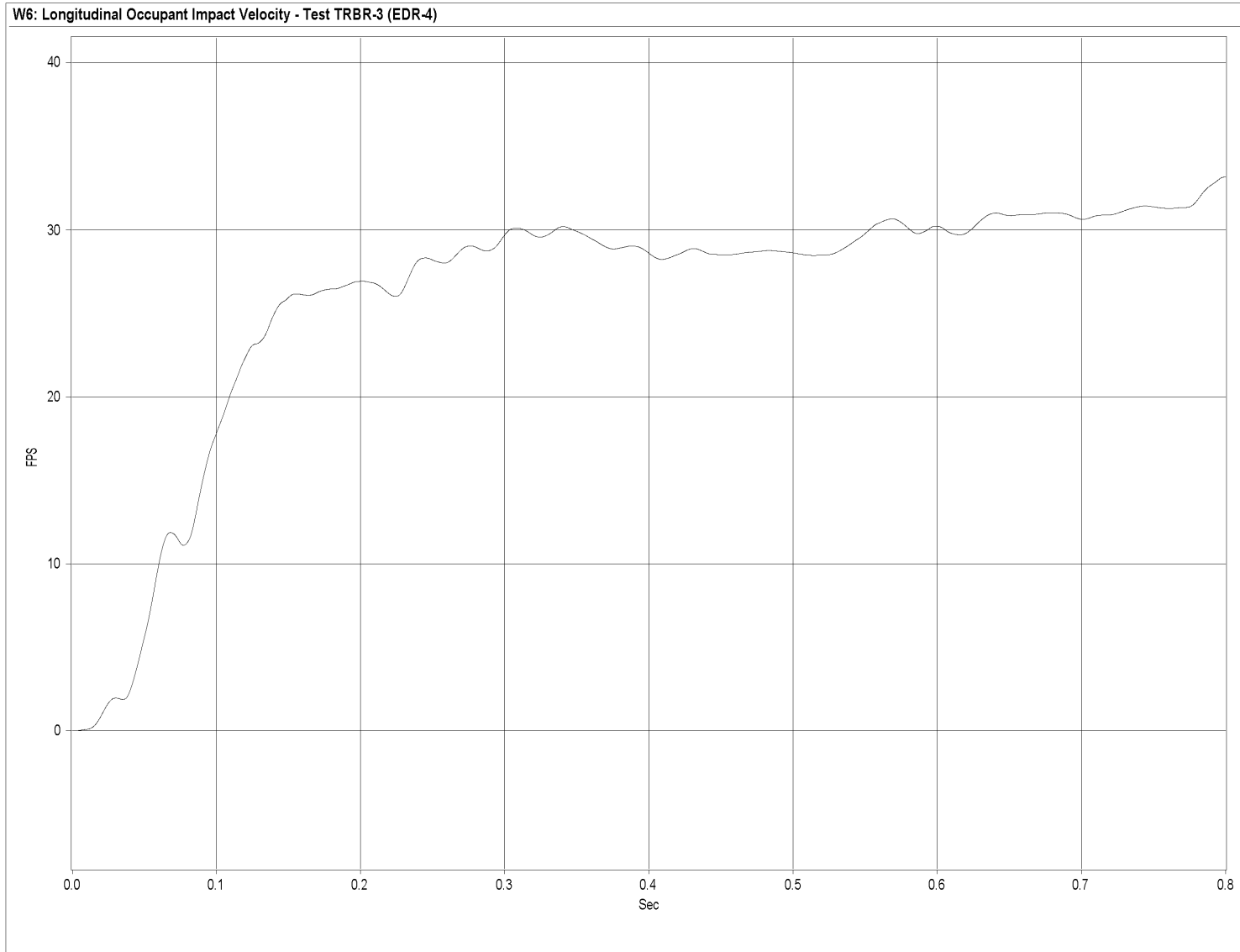


Figure J-2. Graph of Longitudinal Occupant Impact Velocity, Test TRBR-3

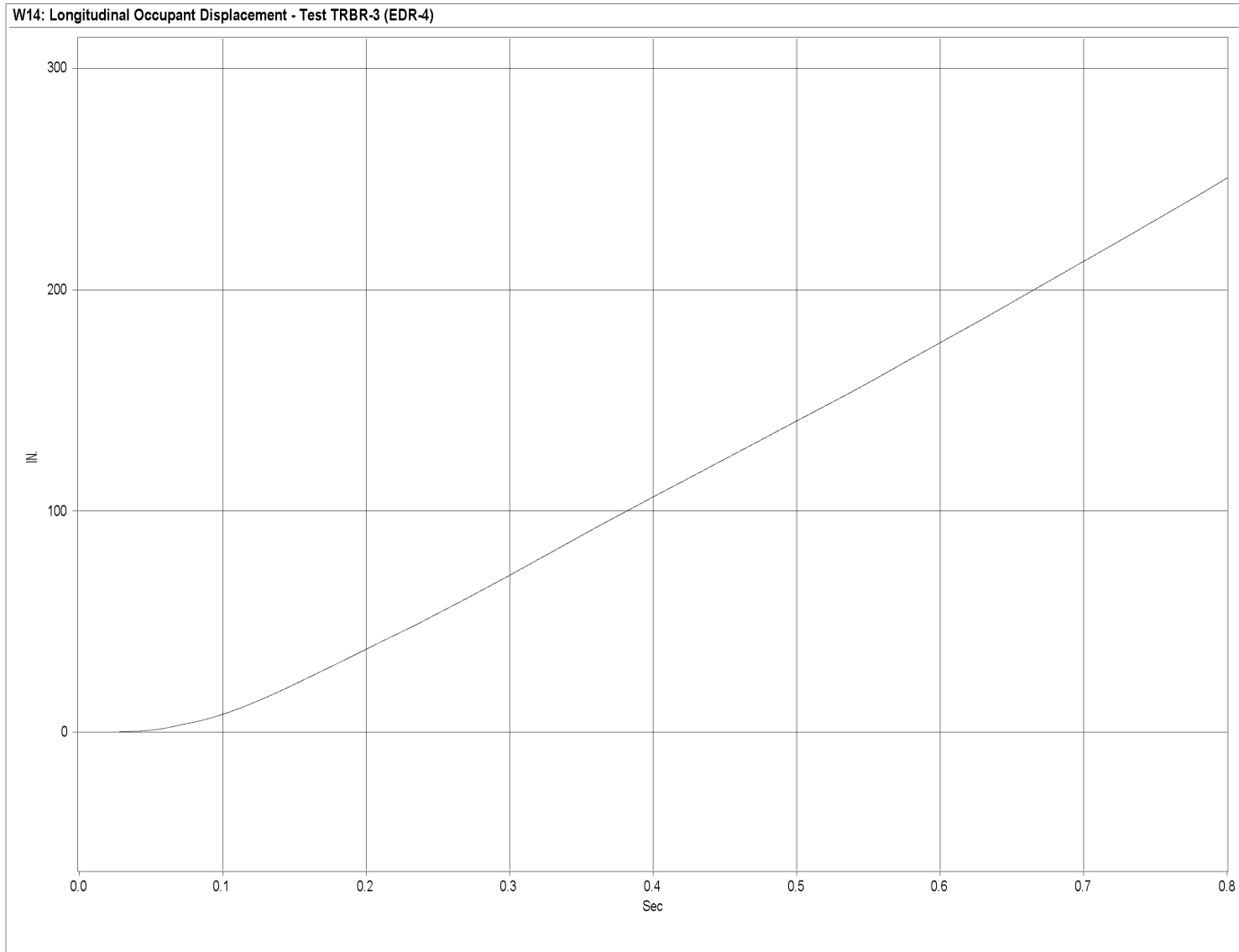


Figure J-3. Graph of Longitudinal Occupant Displacement, Test TRBR-3

366

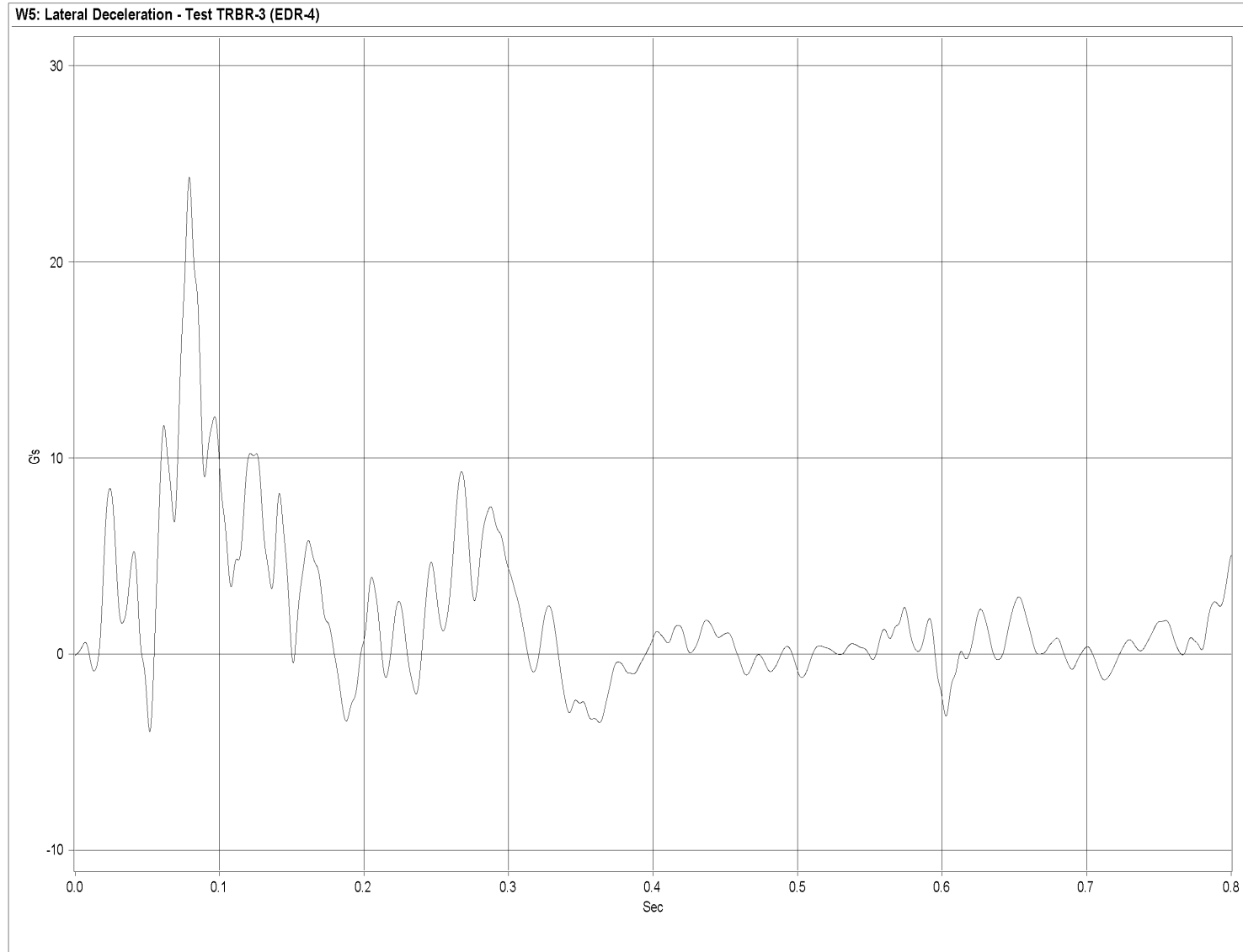


Figure J-4. Graph of Lateral Deceleration, Test TRBR-3

367

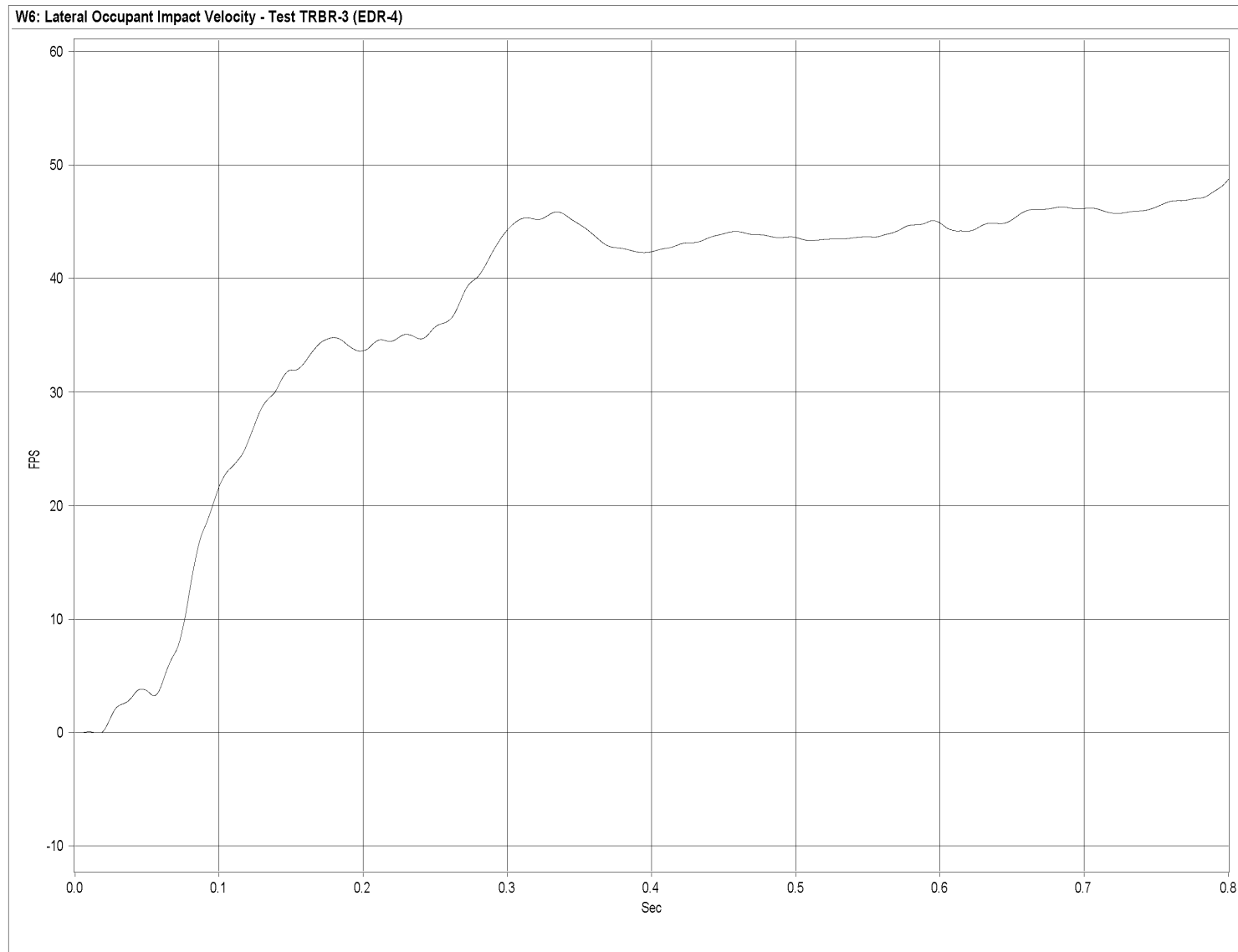


Figure J-5. Graph of Lateral Occupant Impact Velocity, Test TRBR-3

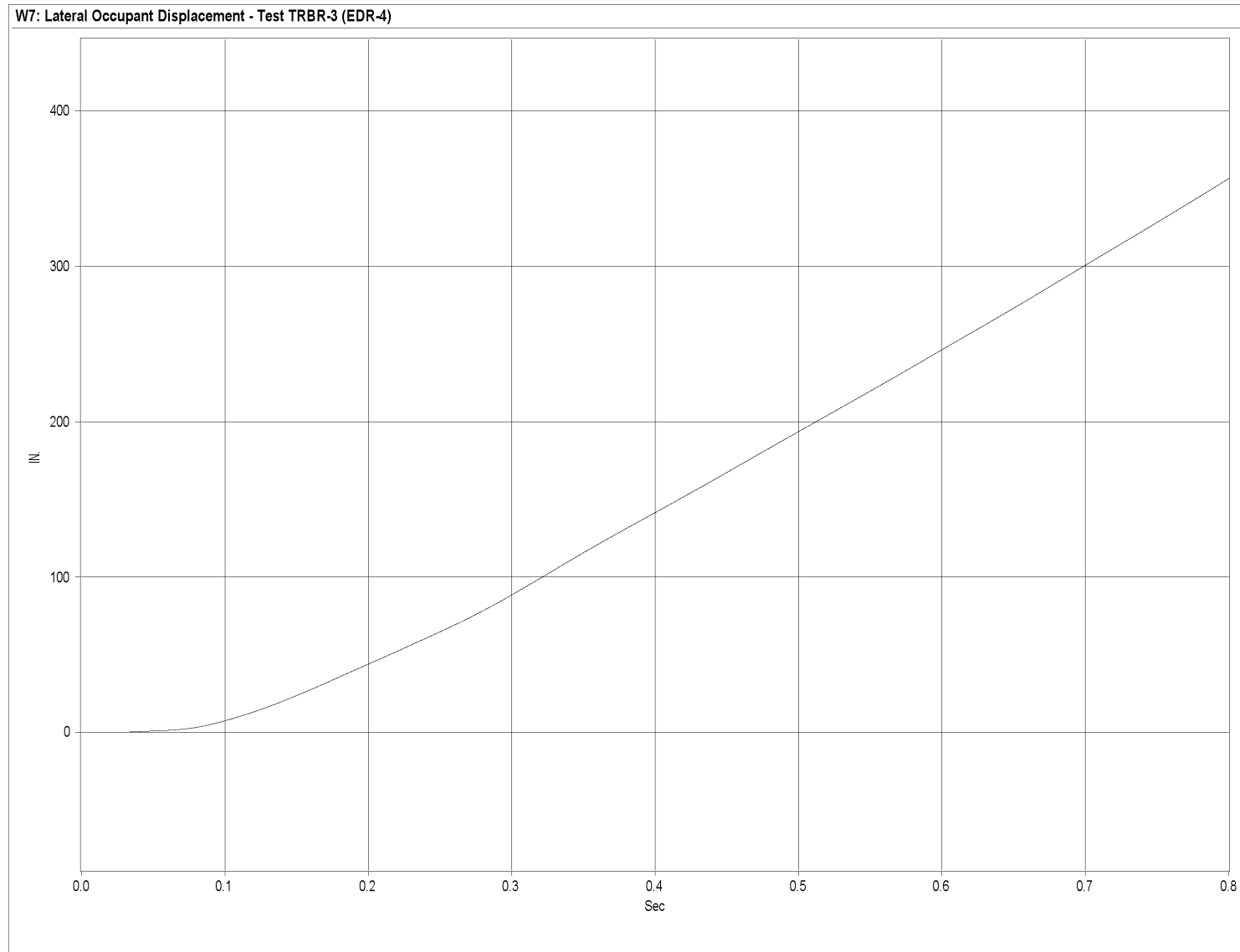


Figure J-6. Graph of Lateral Occupant Displacement, Test TRBR-3

APPENDIX K

Rate Transducer Data Analysis - Test TRBR-3

Figure K-1. Graph of Roll, Pitch, and Yaw Angular Displacements, Test TRBR-3

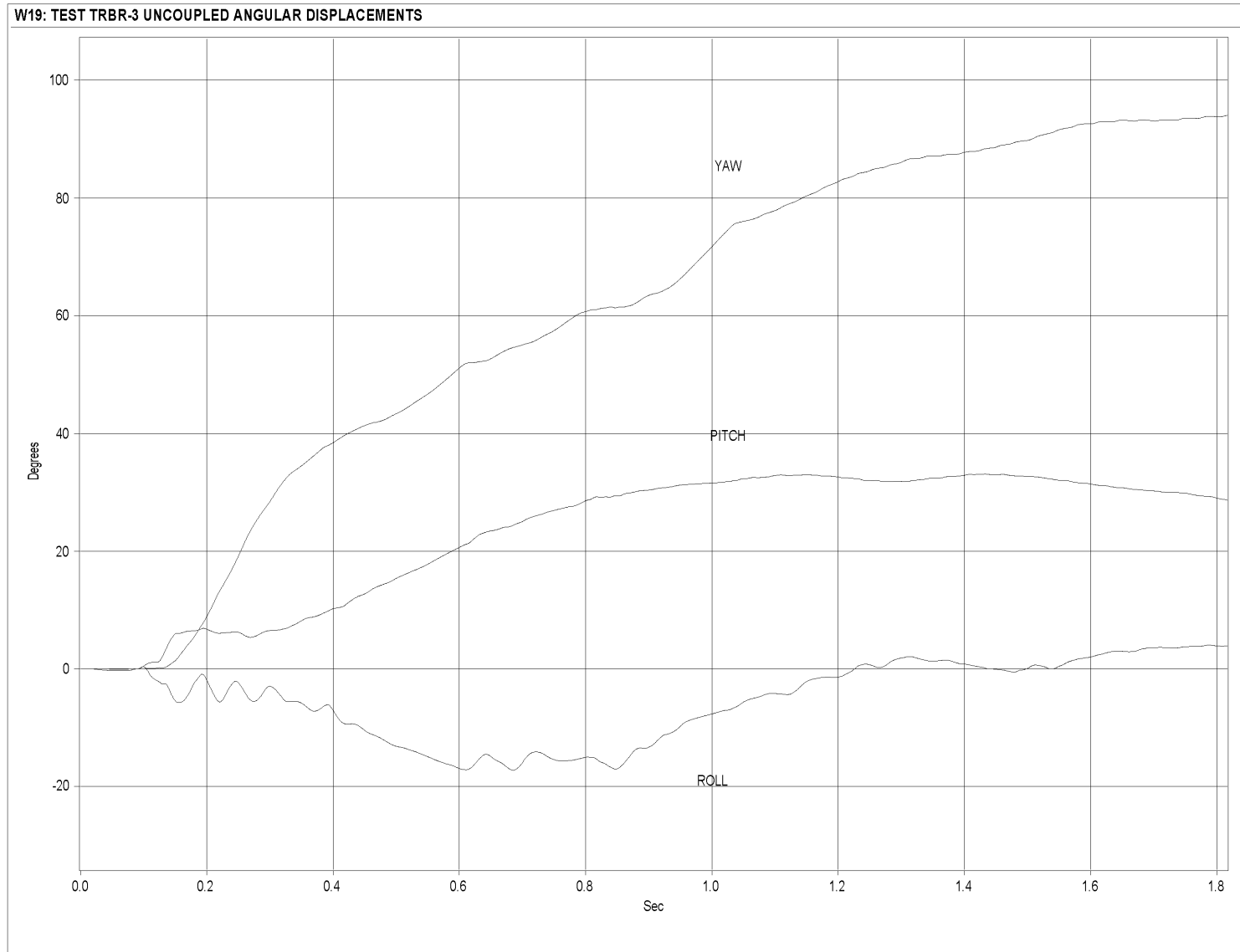


Figure K-1. Graph of Roll, Pitch, and Yaw Angular Displacements, Test TRBR-3

APPENDIX L

Accelerometer Data Analysis - Test TRBR-4

Figure L-1. Graph of Longitudinal Deceleration, Test TRBR-4

Figure L-2. Graph of Longitudinal Occupant Impact Velocity, Test TRBR-4

Figure L-3. Graph of Longitudinal Occupant Displacement, Test TRBR-4

Figure L-4. Graph of Lateral Deceleration, Test TRBR-4

Figure L-5. Graph of Lateral Occupant Impact Velocity, Test TRBR-4

Figure L-6. Graph of Lateral Occupant Displacement, Test TRBR-4

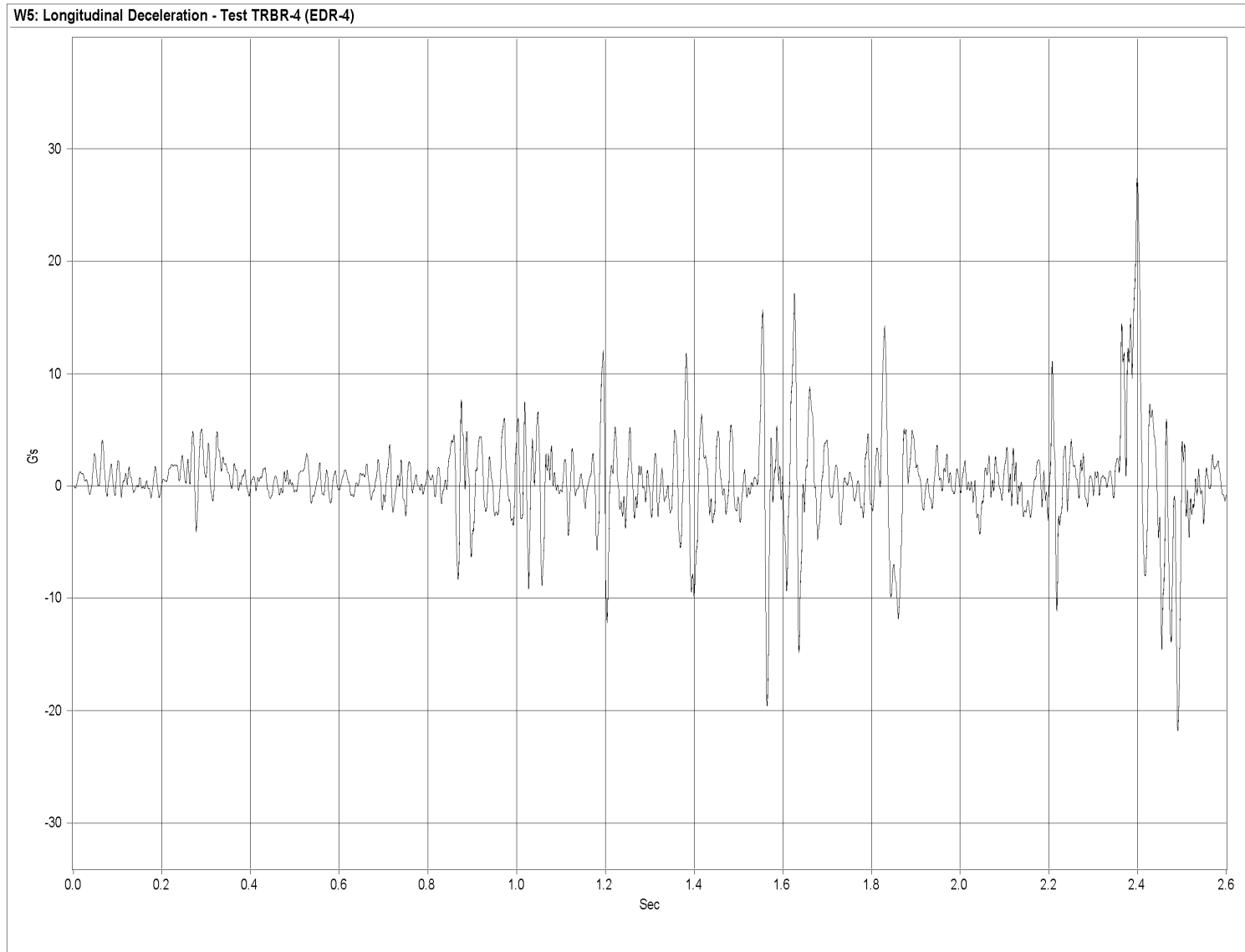


Figure L-1. Graph of Longitudinal Deceleration, Test TRBR-4

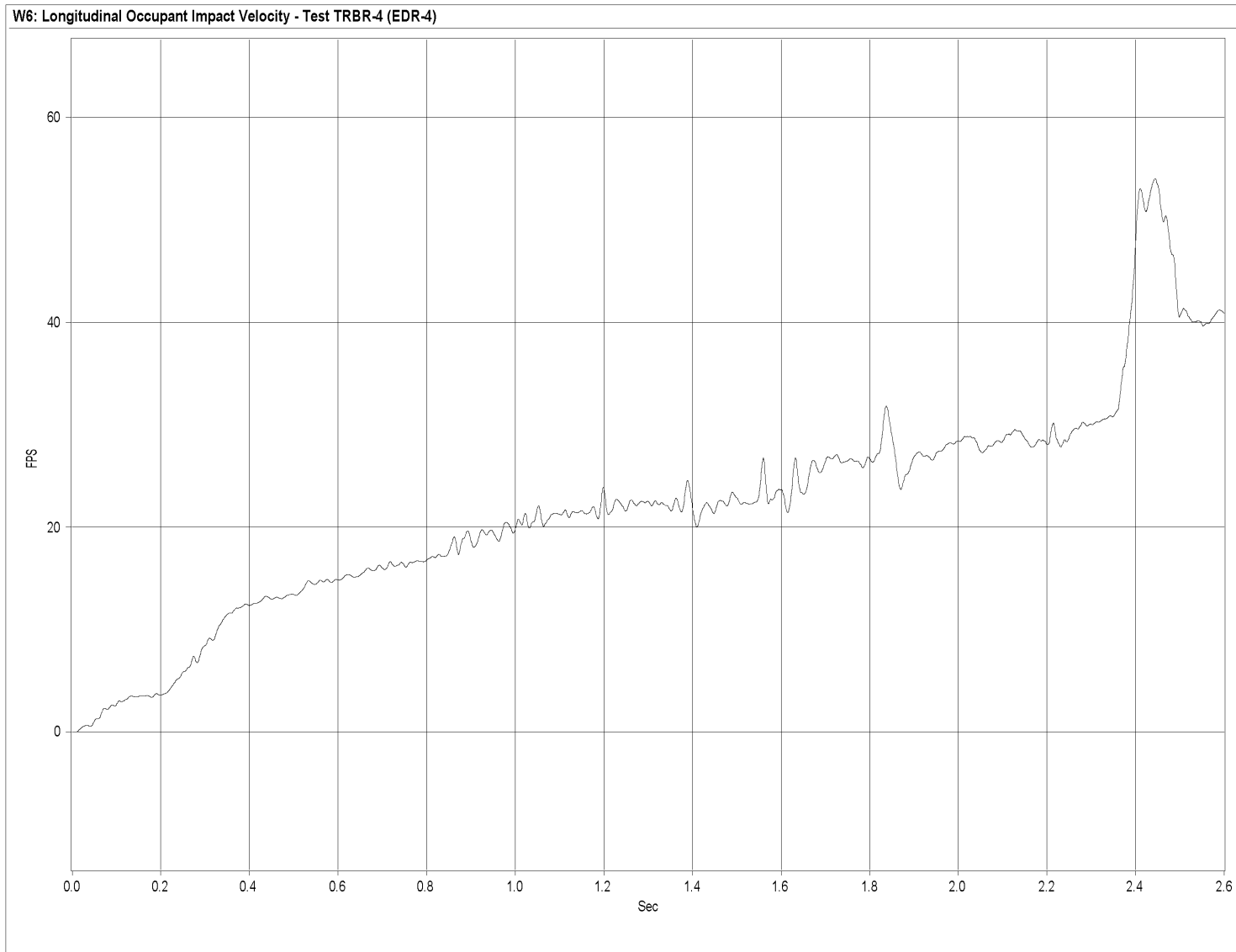


Figure L-2. Graph of Longitudinal Occupant Impact Velocity, Test TRBR-4

374

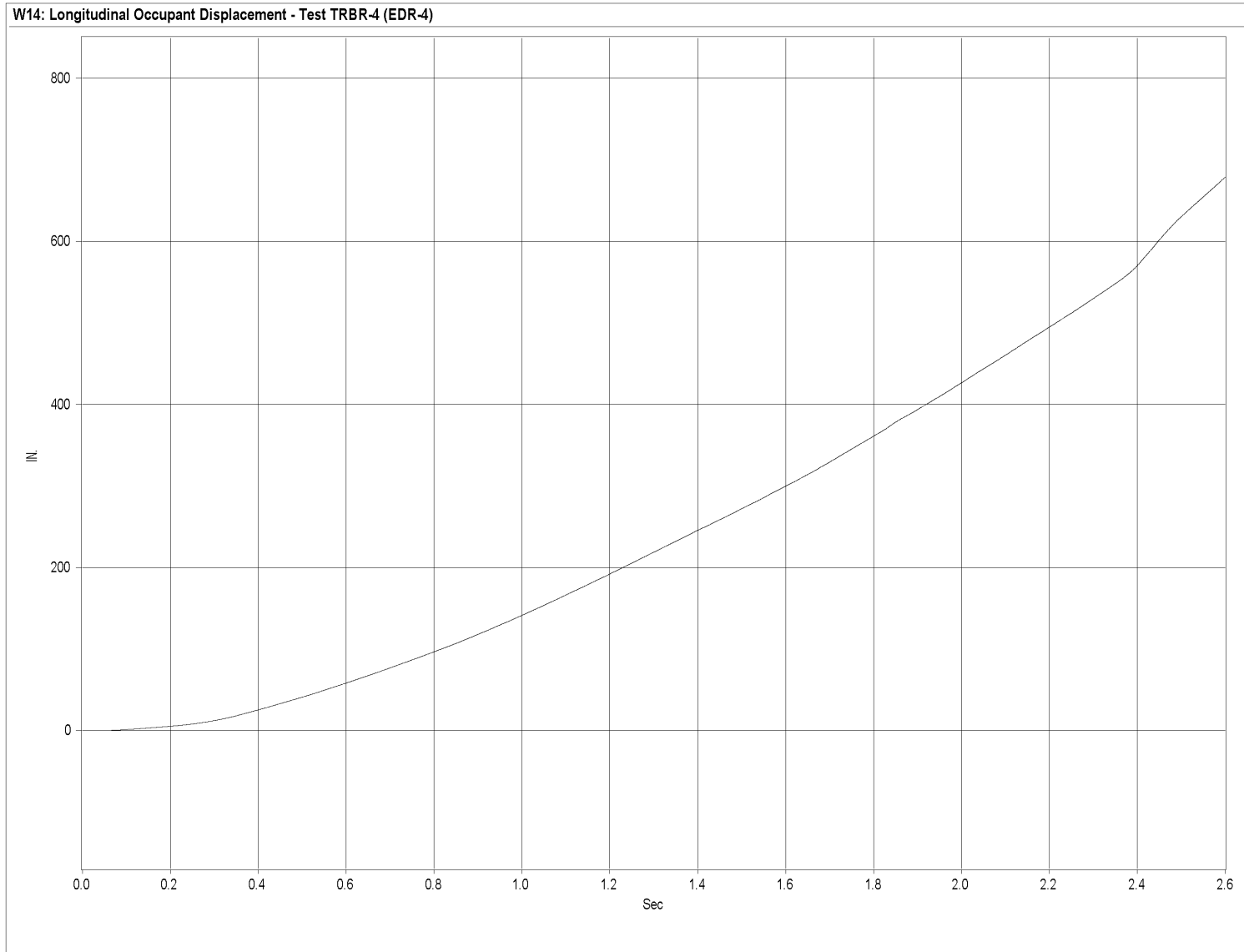


Figure L-3. Graph of Longitudinal Occupant Displacement, Test TRBR-4

375

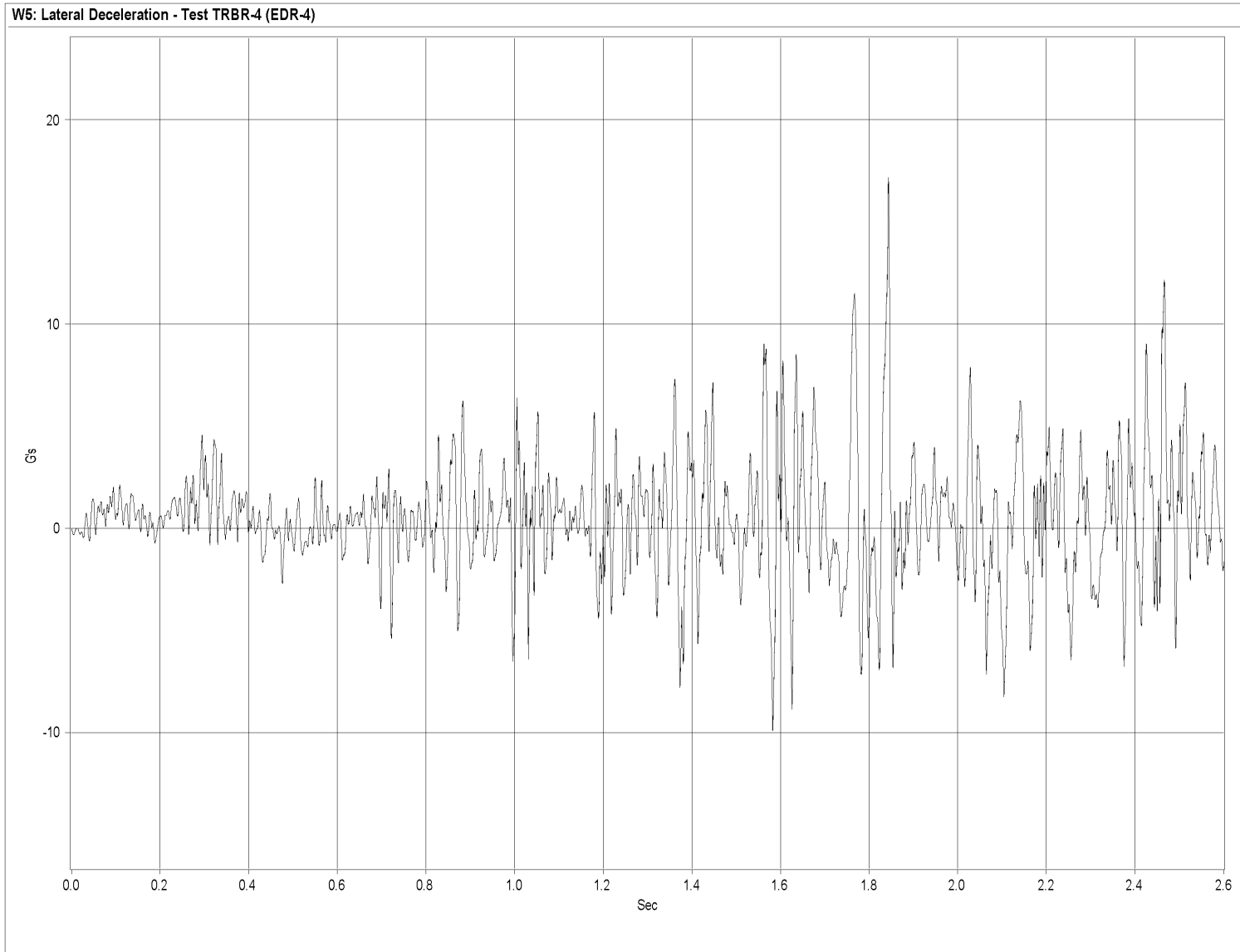


Figure L-4. Graph of Lateral Deceleration, Test TRBR-4

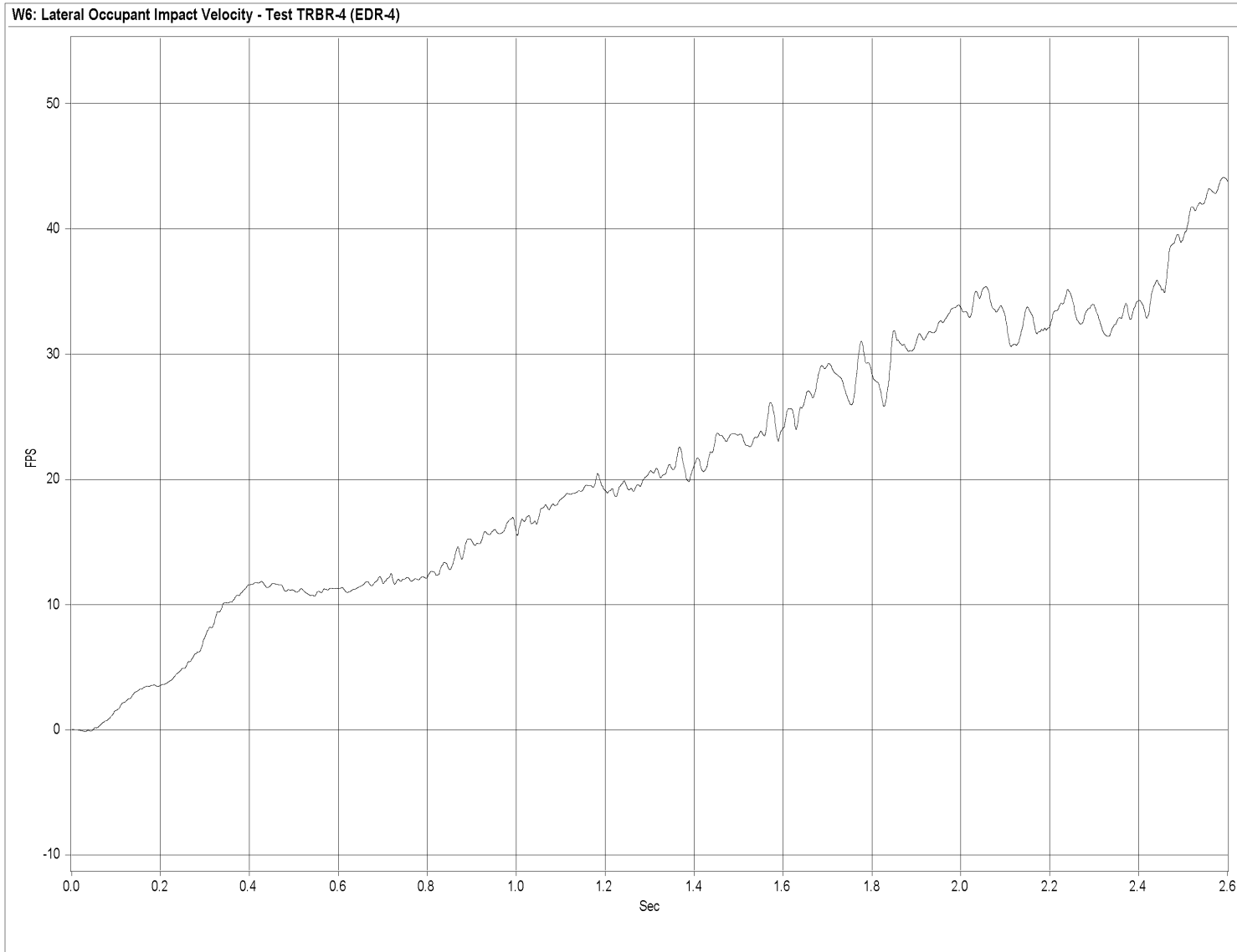


Figure L-5. Graph of Lateral Occupant Impact Velocity, Test TRBR-4

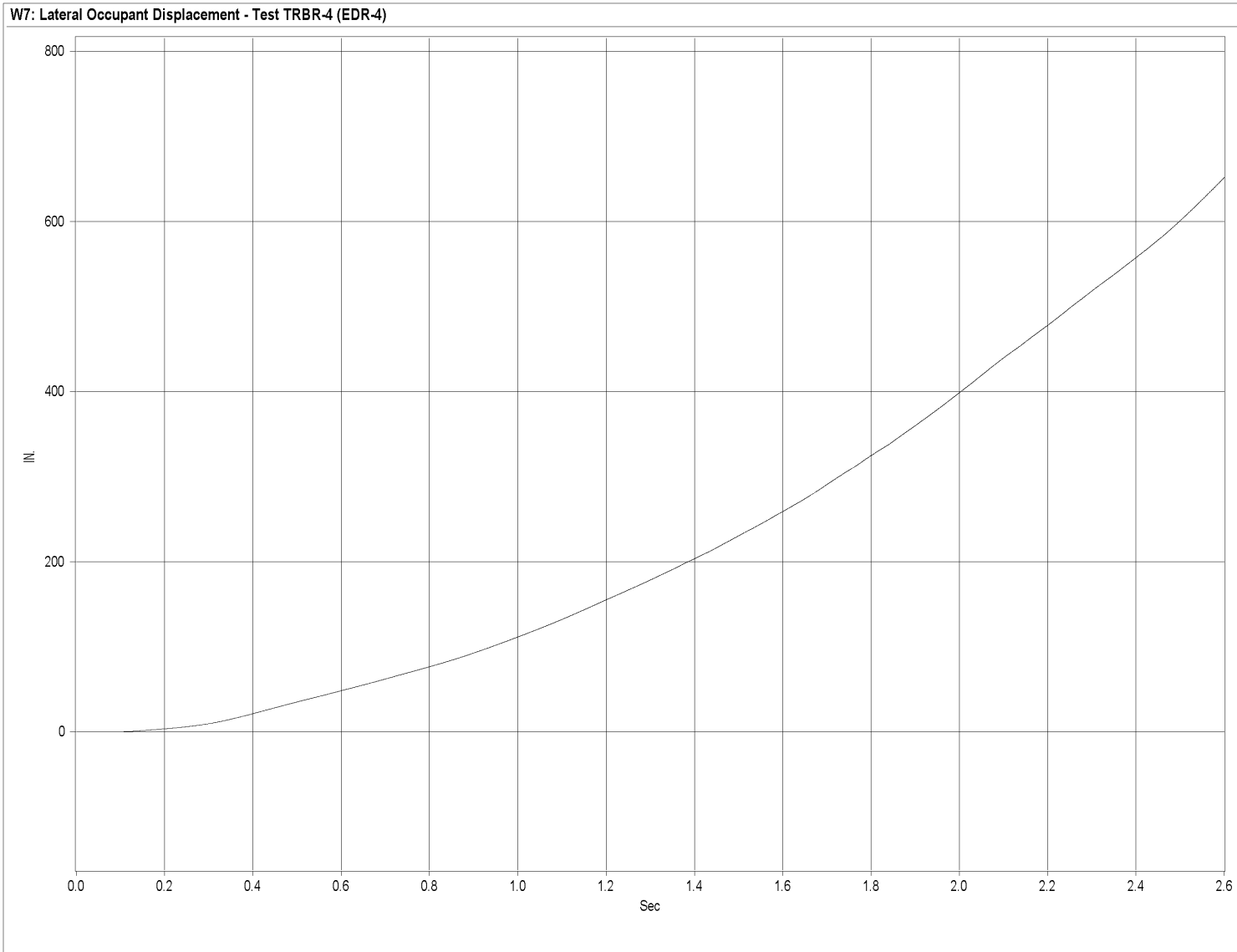


Figure L-6. Graph of Lateral Occupant Displacement, Test TRBR-4

APPENDIX M

Rate Transducer Data Analysis - Test TRBR-4

Figure M-1. Graph of Roll, Pitch, and Yaw Angular Displacements, Test TRBR-4

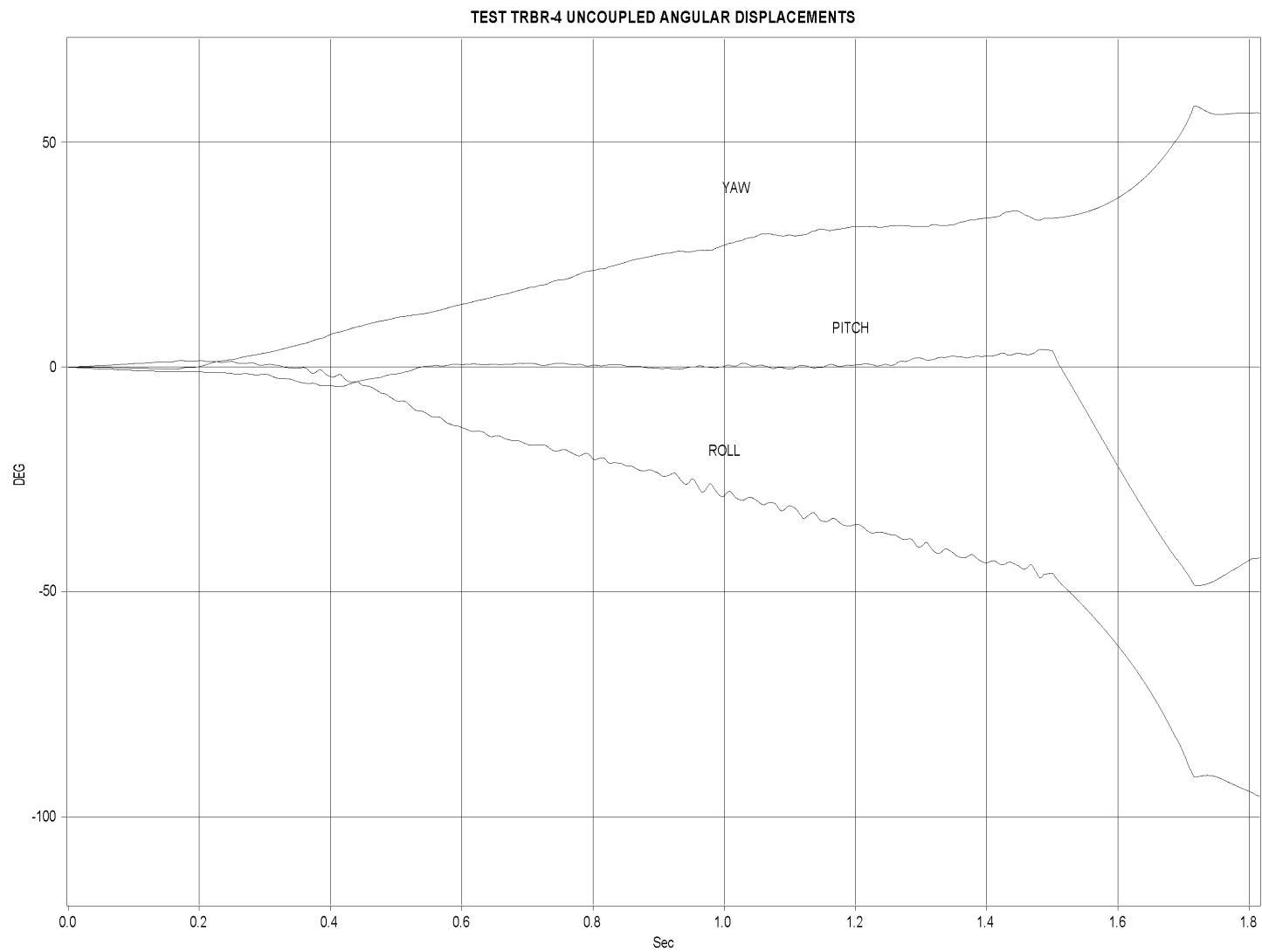


Figure M-1. Graph of Roll, Pitch, and Yaw Angular Displacements, Test TRBR-4

APPENDIX N

BARRIER VII Computer Models - Steel System

Figure N-1. Model of the Steel Bridge Railing System

Figure N-2. Model of the Approach Guardrail System attached to the Steel Bridge Railing

APPENDIX O

Typical BARRIER VII Input Data Files - Steel System

Note that the example BARRIER VII input data files included in Appendix O corresponds with the critical impact point for tests STTR-1, STTR-2, STTR-3, and STTR-4, respectively.

USFS TL-4 STEEL BRIDGE RAIL (TRANSVERSE DECK PROJECT) - RUN21I - NODE 47/48 (10-GA. THRIE BEAM AND TUBE RAIL 8x3x3/16)

118	18	12	2	134	24	2	0													
	0.0001		0.0001		2.00	1000	0		1.0	1										
1	5	5	5	5	5	1														
1		0.0		0.0																
2		0.0		0.0																
3		48.00		0.0																
4		48.00		0.0																
7		120.00		0.0																
8		120.00		0.0																
31		408.00		0.0																
32		408.00		0.0																
64		600.00		0.0																
63		600.00		0.0																
95		984.00		0.0																
96		984.00		0.0																
111		1368.00		0.0																
112		1368.00		0.0																
115		1440.00		0.0																
116		1440.00		0.0																
117		1488.00		0.0																
118		1488.00		0.0																
3	7	1	2		0.0															
4	8	1	2		0.0															
7	31	11	2		0.0															
8	32	11	2		0.0															
31	63	15	2		0.0															
32	64	15	2		0.0															
63	95	15	2		0.0															
64	96	15	2		0.0															
95	111	7	2		0.0															
96	112	7	2		0.0															
111	115	1	2		0.0															
112	116	1	2		0.0															
1	59		0.35																	
117	115	113	111	109	107	105	103	101	99											
97	95	93	91	89	87	85	83	81	79											
77	75	73	71	69	67	65	63	61	59											
57	55	53	51	49	47	45	43	41	39											
37	35	33	31	29	27	25	23	21	19											
17	15	13	11	9	7	5	3	1												
2	59		0.35																	
118	116	114	112	110	108	106	104	102	100											
98	96	94	92	90	88	86	84	82	80											
78	76	74	72	70	68	66	64	62	60											
58	56	54	52	50	48	46	44	42	40											
38	36	34	32	30	28	26	24	22	20											
18	16	14	12	10	8	6	4	2												
100	10																			
1		4.82		4.00	48.00	30000.0		13.95	200.0	140.0	0.10									
2		4.82		4.00	36.00	30000.0		13.95	200.0	140.0	0.10									
3		4.82		4.00	24.00	30000.0		13.95	200.0	140.0	0.10									
4		4.82		4.00	12.00	30000.0		13.95	200.0	140.0	0.10									
5		4.82		4.00	48.00	30000.0		13.95	200.0	140.0	0.10									
6		29.6		3.89	48.00	30000.0		13.25	5.0	436.54	0.10									
7		29.6		3.89	36.00	30000.0		13.25	5.0	436.54	0.10									
8		29.6		3.89	24.00	30000.0		13.25	5.0	436.54	0.10									
9		29.6		3.89	12.00	30000.0		13.25	5.0	436.54	0.10									
10		29.6		3.89	48.00	30000.0		13.25	5.0	436.54	0.10									
300	2																			
1		21.65		32.25	1000.0	1000.0		250.0	10000.0	10000.0	0.10									
	200.0		200.0		2.0	2.0														
2		21.65		32.25	33.95	10.00		40.0	256.5	583.2	0.10									
	50.0		50.0		5.0	9.0														

1	1	3			101	0.0	0.0	0.0		
2	3	5	3	2	102	0.0	0.0	0.0		
4	7	9	15	2	103	0.0	0.0	0.0		
16	31	33	31	2	104	0.0	0.0	0.0		
32	63	65	47	2	103	0.0	0.0	0.0		
48	95	97	55	2	105	0.0	0.0	0.0		
56	111	113	57	2	102	0.0	0.0	0.0		
58	115	117			101	0.0	0.0	0.0		
59	2	4			106	0.0	0.0	0.0		
60	4	6	61	2	107	0.0	0.0	0.0		
62	8	10	73	2	108	0.0	0.0	0.0		
74	32	34	89	2	109	0.0	0.0	0.0		
90	64	66	105	2	108	0.0	0.0	0.0		
106	96	98	113	2	110	0.0	0.0	0.0		
114	112	114	115	2	107	0.0	0.0	0.0		
116	116	118			106	0.0	0.0	0.0		
117	1	2			301	0.0	0.0	0.0	0.0	0.0
118	3	4	119	4	302	0.0	0.0	0.0	0.0	0.0
120	15	16	122	8	302	0.0	0.0	0.0	0.0	0.0
123	47	48	124	16	302	0.0	0.0	0.0	0.0	0.0
125	71	72	128	8	302	0.0	0.0	0.0	0.0	0.0
129	99	100	132	4	302	0.0	0.0	0.0	0.0	0.0
133	115	116			302	0.0	0.0	0.0	0.0	0.0
134	117	118			301	0.0	0.0	0.0	0.0	0.0
180	50.0	561483.4	20	7	6	0	1			
1	0.082	0.21			1.5		18.0			
2	0.063	0.19			2.0		12.0			
3	0.045	0.17			3.0		4.0			
4	0.800	0.95			2.5		2.5			
5	0.900	1.05			3.5		2.0			
6	0.35	0.25			10.0		3.0			
7	2.5	3.5			4.5		3.0			
1	152.4	24.5	1		10.0	1	1	0	0	
2	152.4	34.5	1		10.0	1	1	0	0	
3	152.4	44.5	1		15.0	1	1	0	0	
4	132.4	44.5	1		20.0	1	1	0	0	
5	112.4	44.5	2		20.0	1	1	0	0	
6	92.4	44.5	2		20.0	1	1	0	0	
7	72.4	44.5	2		18.25	1	1	0	0	
8	55.9	44.5	2		11.5	1	1	0	0	
9	55.9	47.75	3		23.25	0	0	0	0	
10	15.9	47.75	4		40.0	0	0	0	0	
11	-24.1	47.75	5		40.0	0	0	0	0	
12	-85.1	47.75	5		40.0	0	0	0	0	
13	-125.1	47.75	5		40.0	0	0	0	0	
14	-165.1	47.75	5		20.0	0	0	0	0	
15	-165.1	-47.75	5		1.0	0	0	0	0	
16	55.9	-47.75	3		1.0	0	0	0	0	
17	55.9	-44.5	2		1.0	0	0	0	0	
18	152.4	-44.5	1		1.0	0	0	0	0	
19	-79.1	45.75	7		1.0	1	1	0	0	
20	123.9	42.12	6		1.0	1	1	0	0	
1	123.9	38.12		0.0	2214.					
2	123.9	-38.12		0.0	2214.					
3	-79.1	41.75		0.0	1157.					
4	-79.1	-41.75		0.0	1157.					
5	-79.1	28.62		0.0	1157.					
6	-79.1	-28.62		0.0	1157.					
1	0.0	0.0								
3	504.00	0.0		15.0	49.71		0.0	0.0		1.0

USFS TL-4 STEEL TRANSITION (TRANSVERSE DECK PROJECT) - NTRUN11NEW - NODE 33 (10-GA. THRIE
 BEAM AND TUBE RAIL 8x3x3/16)

80	29	27	2	99	29	2	0		
	0.0001		0.0001		0.60	600	0	1.0	1
1	5	5	5	5	5	1			
1		0.0		0.0					
3		75.0		0.0					
5		150.0		0.0					
7		225.0		0.0					
9		300.0		0.0					
11		375.0		0.0					
13		450.0		0.0					
15		525.0		0.0					
19		600.0		0.0					
21		637.50		0.0					
23		675.0		0.0					
27		712.50		0.0					
31		750.0		0.0					
35		787.50		0.0					
36		787.50		0.0					
43		825.0		0.0					
44		825.0		0.0					
51		873.0		0.0					
52		873.0		0.0					
59		945.0		0.0					
60		945.0		0.0					
67		1041.0		0.0					
68		1041.0		0.0					
71		1137.0		0.0					
72		1137.0		0.0					
75		1233.0		0.0					
76		1233.0		0.0					
79		1329.0		0.0					
80		1329.0		0.0					
1	3	1	1		0.0				
3	5	1	1		0.0				
5	7	1	1		0.0				
7	9	1	1		0.0				
9	11	1	1		0.0				
11	13	1	1		0.0				
13	15	1	1		0.0				
15	19	3	1		0.0				
19	21	1	1		0.0				
21	23	1	1		0.0				
23	27	3	1		0.0				
27	31	3	1		0.0				
31	35	3	1		0.0				
35	43	3	2		0.0				
43	51	3	2		0.0				
51	59	3	2		0.0				
59	67	3	2		0.0				
67	71	1	2		0.0				
71	75	1	2		0.0				
75	79	1	2		0.0				
36	44	3	2		0.0				
44	52	3	2		0.0				
52	60	3	2		0.0				
60	68	3	2		0.0				
68	72	1	2		0.0				
72	76	1	2		0.0				
76	80	1	2		0.0				
1	57		0.35						
79	77	75	73	71	69	67	65	63	61
59	57	55	53	51	49	47	45	43	41
39	37	35	34	33	32	31	30	29	28

27	26	25	24	23	22	21	20	19	18										
17	16	15	14	13	12	11	10	9	8										
7	6	5	4	3	2	1													
2	23		0.35																
80	78	76	74	72	70	68	66	64	62										
60	58	56	54	52	50	48	46	44	42										
40	38	36																	
100	16																		
1		2.30		1.99		37.50		30000.0		6.92		99.5		68.5	0.10				
2		2.30		1.99		18.75		30000.0		6.92		99.5		68.5	0.10				
3		2.475		2.125		18.75		30000.0		7.405		106.25		73.75	0.10				
4		2.84		2.40		18.75		30000.0		8.375		120.0		84.0	0.10				
5		3.205		2.68		18.75		30000.0		9.35		134.0		94.0	0.10				
6		3.575		2.96		18.75		30000.0		10.325		148.0		104.25	0.10				
7		4.82		4.00		9.375		30000.0		13.95		200.0		140.0	0.10				
8		4.82		4.00		12.00		30000.0		13.95		200.0		140.0	0.10				
9		4.82		4.00		18.00		30000.0		13.95		200.0		140.0	0.10				
10		4.82		4.00		24.00		30000.0		13.95		200.0		140.0	0.10				
11		4.82		4.00		48.00		30000.0		13.95		200.0		140.0	0.10				
12		29.6		3.89		9.375		30000.0		13.25		5.0		436.54	0.10				
13		29.6		3.89		12.00		30000.0		13.25		5.0		436.54	0.10				
14		29.6		3.89		18.00		30000.0		13.25		5.0		436.54	0.10				
15		29.6		3.89		24.00		30000.0		13.25		5.0		436.54	0.10				
16		29.6		3.89		48.00		30000.0		13.25		5.0		436.54	0.10				
300	11																		
1		21.65		0.0		1000.0		1000.0		250.0		10000.0		10000.0	0.10	Strong			
Post Anchor		200.0		200.0		2.0		2.0											
2		21.65		0.0		4.00		4.00		54.0		92.88		270.62	0.10	W6x9 by			
6' Long		6.0		15.0		16.0		16.0											
3		21.65		0.0		4.00		4.00		58.5		92.88		270.62	0.10	W6x9 by			
6.5' Long		6.0		15.0		16.0		16.0											
4		21.65		0.0		4.00		4.00		58.5		92.88		270.62	0.10	W6x9 by			
6.5' Long		6.0		15.0		16.0		16.0											
5		21.65		0.0		8.0		8.0		105.0		256.5		539.52	0.10	W6x15			
by 7' Long		15.0		30.0		16.0		16.0											
6		21.65		0.0		8.0		8.0		105.0		256.5		539.52	0.10	W6x15			
by 7' Long		15.0		30.0		16.0		16.0											
7		21.65		0.0		8.0		8.0		105.0		256.5		539.52	0.10	W6x15			
by 7' Long		15.0		30.0		16.0		16.0											
8		21.65		26.00		8.0		8.0		105.0		256.5		539.52	0.10	W6x15			
by 7' Long		15.0		30.0		16.0		16.0											
9		21.65		33.00		8.0		8.0		105.0		256.5		539.52	0.10	W6x15			
by 7' Long		15.0		30.0		16.0		16.0											
10		21.65		33.00		33.95		10.00		40.0		256.5		583.2	0.10	W6x15			
Bridge Post		50.0		50.0		5.0		9.0											
11		21.65		33.00		1000.0		1000.0		250.0		10000.0		10000.0	0.10	Strong			
Post Anchor		200.0		200.0		2.0		2.0											
1	1	2	14	1	101		0.0		0.0		0.0								
15	15	16	18	1	102		0.0		0.0		0.0								
19	19	20		1	103		0.0		0.0		0.0								
20	20	21		1	104		0.0		0.0		0.0								
21	21	22		1	105		0.0		0.0		0.0								
22	22	23		1	106		0.0		0.0		0.0								
23	23	24	34	1	107		0.0		0.0		0.0								

35	35	37	38	2	107	0.0	0.0	0.0		
39	43	45	42	2	108	0.0	0.0	0.0		
43	51	53	46	2	109	0.0	0.0	0.0		
47	59	61	50	2	110	0.0	0.0	0.0		
51	67	69	56	2	111	0.0	0.0	0.0		
57	36	38	60	2	112	0.0	0.0	0.0		
61	44	46	64	2	113	0.0	0.0	0.0		
65	52	54	68	2	114	0.0	0.0	0.0		
69	60	62	72	2	115	0.0	0.0	0.0		
73	68	70	78	2	116	0.0	0.0	0.0		
79	1		80	2	301	0.0	0.0	0.0	0.0	0.0
81	3		86	2	302	0.0	0.0	0.0	0.0	0.0
87	19				303	0.0	0.0	0.0	0.0	0.0
88	21				304	0.0	0.0	0.0	0.0	0.0
89	23				305	0.0	0.0	0.0	0.0	0.0
90	27				306	0.0	0.0	0.0	0.0	0.0
91	31				307	0.0	0.0	0.0	0.0	0.0
92	35	36			308	0.0	0.0	0.0	0.0	0.0
93	43	44			309	0.0	0.0	0.0	0.0	0.0
94	51	52	96	8	310	0.0	0.0	0.0	0.0	0.0
97	71	72	98	4	310	0.0	0.0	0.0	0.0	0.0
99	79	80			311	0.0	0.0	0.0	0.0	0.0
4400.0	40000.0	20		6	4	0	1			
1	0.055	0.12			6.00		17.0			
2	0.057	0.15			7.00		18.0			
3	0.062	0.18			10.00		12.0			
4	0.110	0.35			12.00		6.0			
5	0.35	0.45			6.00		5.0			
6	1.45	1.50			15.00		1.0			
1	100.75	15.875		1	12.0	1	0	0	0	
2	100.75	27.875		1	12.0	1	0	0	0	
3	100.75	39.875		2	12.0	1	0	0	0	
4	88.75	39.875		2	12.0	1	0	0	0	
5	76.75	39.875		2	12.0	1	0	0	0	
6	64.75	39.875		2	12.0	1	0	0	0	
7	52.75	39.875		2	12.0	1	0	0	0	
8	40.75	39.875		2	12.0	1	0	0	0	
9	28.75	39.875		2	12.0	1	0	0	0	
10	16.75	39.875		2	12.0	1	0	0	0	
11	-13.25	39.875		3	12.0	1	0	0	0	
12	-33.25	39.875		3	12.0	1	0	0	0	
13	-53.25	39.875		3	12.0	1	0	0	0	
14	-73.25	39.875		3	12.0	1	0	0	0	
15	-93.25	39.875		3	12.0	1	0	0	0	
16	-113.25	39.875		4	12.0	1	0	0	0	
17	-113.25	-39.875		4	12.0	0	0	0	0	
18	100.75	-39.875		1	12.0	0	0	0	0	
19	69.25	37.75		5	1.0	1	0	0	0	
20	-62.75	37.75		6	1.0	1	0	0	0	
1	69.25	32.75			0.0	608.				
2	69.25	-32.75			0.0	608.				
3	-62.75	32.75			0.0	492.				
4	-62.75	-32.75			0.0	492.				
1	0.0	0.0								
3	768.75	0.0			25.0	62.14	0.0	0.0	1.0	

USFS TL-4 STEEL TRANSITION (TRANSVERSE DECK PROJECT) - 8STRUN8NEW - NODE 30 (10-GA. THRIE
 BEAM AND TUBE RAIL 8x3x3/16)

80	29	27	2	99	29	2	0		
	0.0001		0.0001		2.00	900	0	1.0	1
1	5	5	5	5	5	1			
1		0.0		0.0					
3		75.0		0.0					
5		150.0		0.0					
7		225.0		0.0					
9		300.0		0.0					
11		375.0		0.0					
13		450.0		0.0					
15		525.0		0.0					
19		600.0		0.0					
21		637.50		0.0					
23		675.0		0.0					
27		712.50		0.0					
31		750.0		0.0					
35		787.50		0.0					
36		787.50		0.0					
43		825.0		0.0					
44		825.0		0.0					
51		873.0		0.0					
52		873.0		0.0					
59		945.0		0.0					
60		945.0		0.0					
67		1041.0		0.0					
68		1041.0		0.0					
71		1137.0		0.0					
72		1137.0		0.0					
75		1233.0		0.0					
76		1233.0		0.0					
79		1329.0		0.0					
80		1329.0		0.0					
1	3	1	1		0.0				
3	5	1	1		0.0				
5	7	1	1		0.0				
7	9	1	1		0.0				
9	11	1	1		0.0				
11	13	1	1		0.0				
13	15	1	1		0.0				
15	19	3	1		0.0				
19	21	1	1		0.0				
21	23	1	1		0.0				
23	27	3	1		0.0				
27	31	3	1		0.0				
31	35	3	1		0.0				
35	43	3	2		0.0				
43	51	3	2		0.0				
51	59	3	2		0.0				
59	67	3	2		0.0				
67	71	1	2		0.0				
71	75	1	2		0.0				
75	79	1	2		0.0				
36	44	3	2		0.0				
44	52	3	2		0.0				
52	60	3	2		0.0				
60	68	3	2		0.0				
68	72	1	2		0.0				
72	76	1	2		0.0				
76	80	1	2		0.0				
1	57		0.35						
79	77	75	73	71	69	67	65	63	61
59	57	55	53	51	49	47	45	43	41
39	37	35	34	33	32	31	30	29	28

27	26	25	24	23	22	21	20	19	18										
17	16	15	14	13	12	11	10	9	8										
7	6	5	4	3	2	1													
2	23		0.35																
80	78	76	74	72	70	68	66	64	62										
60	58	56	54	52	50	48	46	44	42										
40	38	36																	
100	16																		
1		2.30		1.99		37.50	30000.0		6.92		99.5		68.5	0.10					
2		2.30		1.99		18.75	30000.0		6.92		99.5		68.5	0.10					
3		2.475		2.125		18.75	30000.0		7.405		106.25		73.75	0.10					
4		2.84		2.40		18.75	30000.0		8.375		120.0		84.0	0.10					
5		3.205		2.68		18.75	30000.0		9.35		134.0		94.0	0.10					
6		3.575		2.96		18.75	30000.0		10.325		148.0		104.25	0.10					
7		4.82		4.00		9.375	30000.0		13.95		200.0		140.0	0.10					
8		4.82		4.00		12.00	30000.0		13.95		200.0		140.0	0.10					
9		4.82		4.00		18.00	30000.0		13.95		200.0		140.0	0.10					
10		4.82		4.00		24.00	30000.0		13.95		200.0		140.0	0.10					
11		4.82		4.00		48.00	30000.0		13.95		200.0		140.0	0.10					
12		29.6		3.89		9.375	30000.0		13.25		5.0		436.54	0.10					
13		29.6		3.89		12.00	30000.0		13.25		5.0		436.54	0.10					
14		29.6		3.89		18.00	30000.0		13.25		5.0		436.54	0.10					
15		29.6		3.89		24.00	30000.0		13.25		5.0		436.54	0.10					
16		29.6		3.89		48.00	30000.0		13.25		5.0		436.54	0.10					
300	11																		
1		21.65		0.0		1000.0	1000.0		250.0		10000.0		10000.0	0.10	Strong				
Post Anchor		200.0		200.0		2.0	2.0												
2		21.65		0.0		4.00	4.00		54.0		92.88		270.62	0.10	W6x9 by				
6' Long		6.0		15.0		16.0	16.0												
3		21.65		0.0		4.00	4.00		58.5		92.88		270.62	0.10	W6x9 by				
6.5' Long		6.0		15.0		16.0	16.0												
4		21.65		0.0		4.00	4.00		58.5		92.88		270.62	0.10	W6x9 by				
6.5' Long		6.0		15.0		16.0	16.0												
5		21.65		0.0		8.0	8.0		105.0		256.5		539.52	0.10	W6x15				
by 7' Long		15.0		30.0		16.0	16.0												
6		21.65		0.0		8.0	8.0		105.0		256.5		539.52	0.10	W6x15				
by 7' Long		15.0		30.0		16.0	16.0												
7		21.65		0.0		8.0	8.0		105.0		256.5		539.52	0.10	W6x15				
by 7' Long		15.0		30.0		16.0	16.0												
8		21.65		26.00		8.0	8.0		105.0		256.5		539.52	0.10	W6x15				
by 7' Long		15.0		30.0		16.0	16.0												
9		21.65		33.00		8.0	8.0		105.0		256.5		539.52	0.10	W6x15				
by 7' Long		15.0		30.0		16.0	16.0												
10		21.65		33.00		33.95	10.00		40.0		256.5		583.2	0.10	W6x15				
Bridge Post		50.0		50.0		5.0	9.0												
11		21.65		33.00		1000.0	1000.0		250.0		10000.0		10000.0	0.10	Strong				
Post Anchor		200.0		200.0		2.0	2.0												
1	1	2	14	1	101	0.0	0.0	0.0											
15	15	16	18	1	102	0.0	0.0	0.0											
19	19	20		1	103	0.0	0.0	0.0											
20	20	21		1	104	0.0	0.0	0.0											
21	21	22		1	105	0.0	0.0	0.0											
22	22	23		1	106	0.0	0.0	0.0											
23	23	24	34	1	107	0.0	0.0	0.0											

35	35	37	38	2	107	0.0	0.0	0.0		
39	43	45	42	2	108	0.0	0.0	0.0		
43	51	53	46	2	109	0.0	0.0	0.0		
47	59	61	50	2	110	0.0	0.0	0.0		
51	67	69	56	2	111	0.0	0.0	0.0		
57	36	38	60	2	112	0.0	0.0	0.0		
61	44	46	64	2	113	0.0	0.0	0.0		
65	52	54	68	2	114	0.0	0.0	0.0		
69	60	62	72	2	115	0.0	0.0	0.0		
73	68	70	78	2	116	0.0	0.0	0.0		
79	1		80	2	301	0.0	0.0	0.0	0.0	0.0
81	3		86	2	302	0.0	0.0	0.0	0.0	0.0
87	19				303	0.0	0.0	0.0	0.0	0.0
88	21				304	0.0	0.0	0.0	0.0	0.0
89	23				305	0.0	0.0	0.0	0.0	0.0
90	27				306	0.0	0.0	0.0	0.0	0.0
91	31				307	0.0	0.0	0.0	0.0	0.0
92	35	36			308	0.0	0.0	0.0	0.0	0.0
93	43	44			309	0.0	0.0	0.0	0.0	0.0
94	51	52	96	8	310	0.0	0.0	0.0	0.0	0.0
97	71	72	98	4	310	0.0	0.0	0.0	0.0	0.0
99	79	80			311	0.0	0.0	0.0	0.0	0.0
180	50.0	561.4	83.4	20	7	6	0	1		
1	0.082		0.21			1.5		18.0		
2	0.063		0.19			2.0		12.0		
3	0.045		0.17			3.0		4.0		
4	0.800		0.95			2.5		2.5		
5	0.900		1.05			3.5		2.0		
6	0.35		0.25			10.0		3.0		
7	2.5		3.5			4.5		3.0		
1	152.4		24.5	1		10.0	1	0	0	0
2	152.4		34.5	1		10.0	1	0	0	0
3	152.4		44.5	1		15.0	1	0	0	0
4	132.4		44.5	1		20.0	1	0	0	0
5	112.4		44.5	2		20.0	1	0	0	0
6	92.4		44.5	2		20.0	1	0	0	0
7	72.4		44.5	2		18.25	1	0	0	0
8	55.9		44.5	2		11.5	1	0	0	0
9	55.9		47.75	3		23.25	0	0	0	0
10	15.9		47.75	4		40.0	0	0	0	0
11	-24.1		47.75	5		40.0	0	0	0	0
12	-85.1		47.75	5		40.0	0	0	0	0
13	-125.1		47.75	5		40.0	0	0	0	0
14	-165.1		47.75	5		20.0	0	0	0	0
15	-165.1		-47.75	5		1.0	0	0	0	0
16	55.9		-47.75	3		1.0	0	0	0	0
17	55.9		-44.5	2		1.0	0	0	0	0
18	152.4		-44.5	1		1.0	0	0	0	0
19	-79.1		45.75	7		1.0	1	0	0	0
20	123.9		42.12	6		1.0	1	0	0	0
1	123.9		38.12			0.0		2214.		
2	123.9		-38.12			0.0		2214.		
3	-79.1		41.75			0.0		1157.		
4	-79.1		-41.75			0.0		1157.		
5	-79.1		28.62			0.0		1157.		
6	-79.1		-28.62			0.0		1157.		
1	0.0		0.0							
3	740.625		0.0			15.0	49.71	0.0	0.0	10.0

APPENDIX P

Accelerometer Data Analysis - Test STTR-1

Figure P-1. Graph of Longitudinal Deceleration, Test STTR-1

Figure P-2. Graph of Longitudinal Occupant Impact Velocity, Test STTR-1

Figure P-3. Graph of Longitudinal Occupant Displacement, Test STTR-1

Figure P-4. Graph of Lateral Deceleration, Test STTR-1

Figure P-5. Graph of Lateral Occupant Impact Velocity, Test STTR-1

Figure P-6. Graph of Lateral Occupant Displacement, Test STTR-1

395

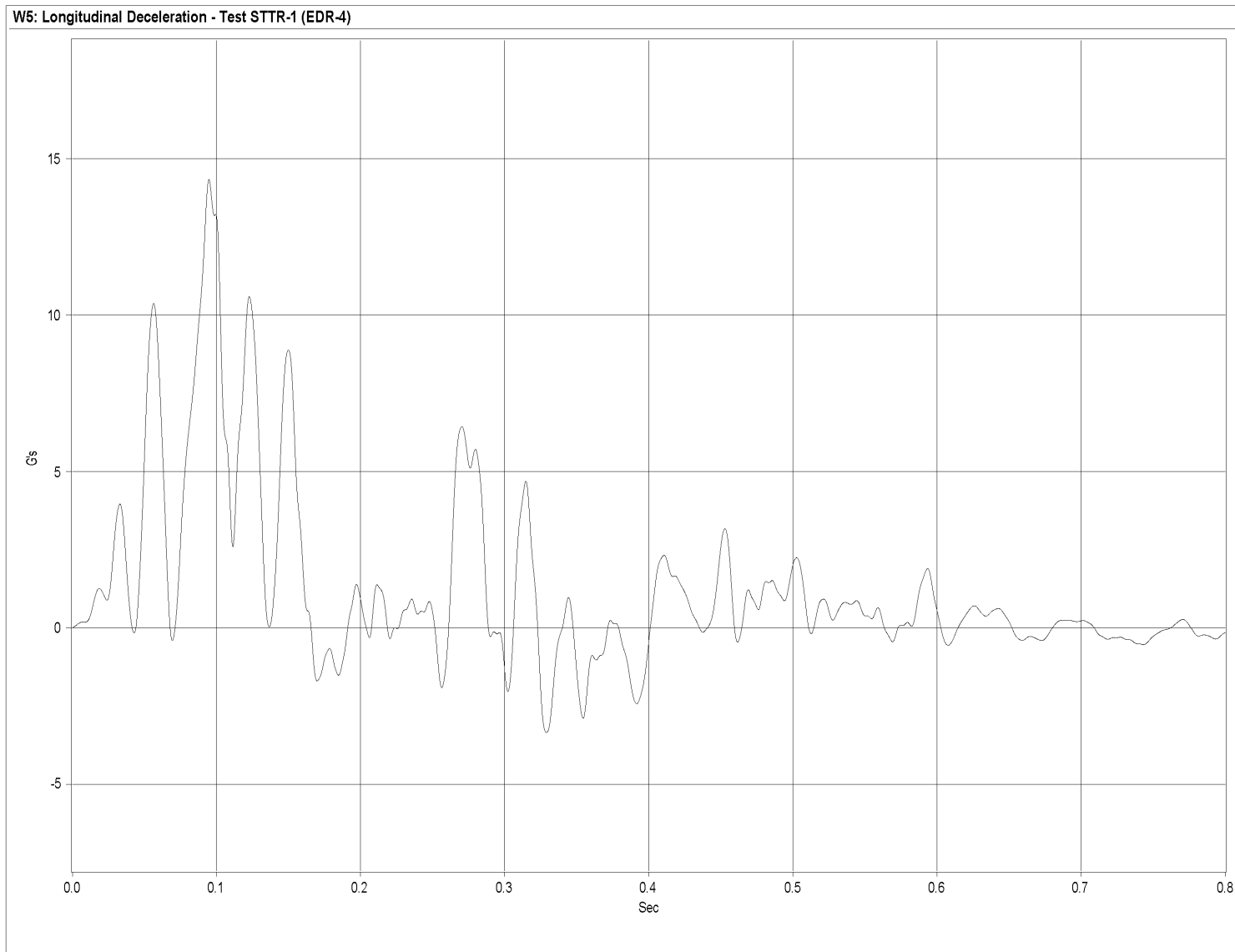


Figure P-1. Graph of Longitudinal Deceleration, Test STTR-1

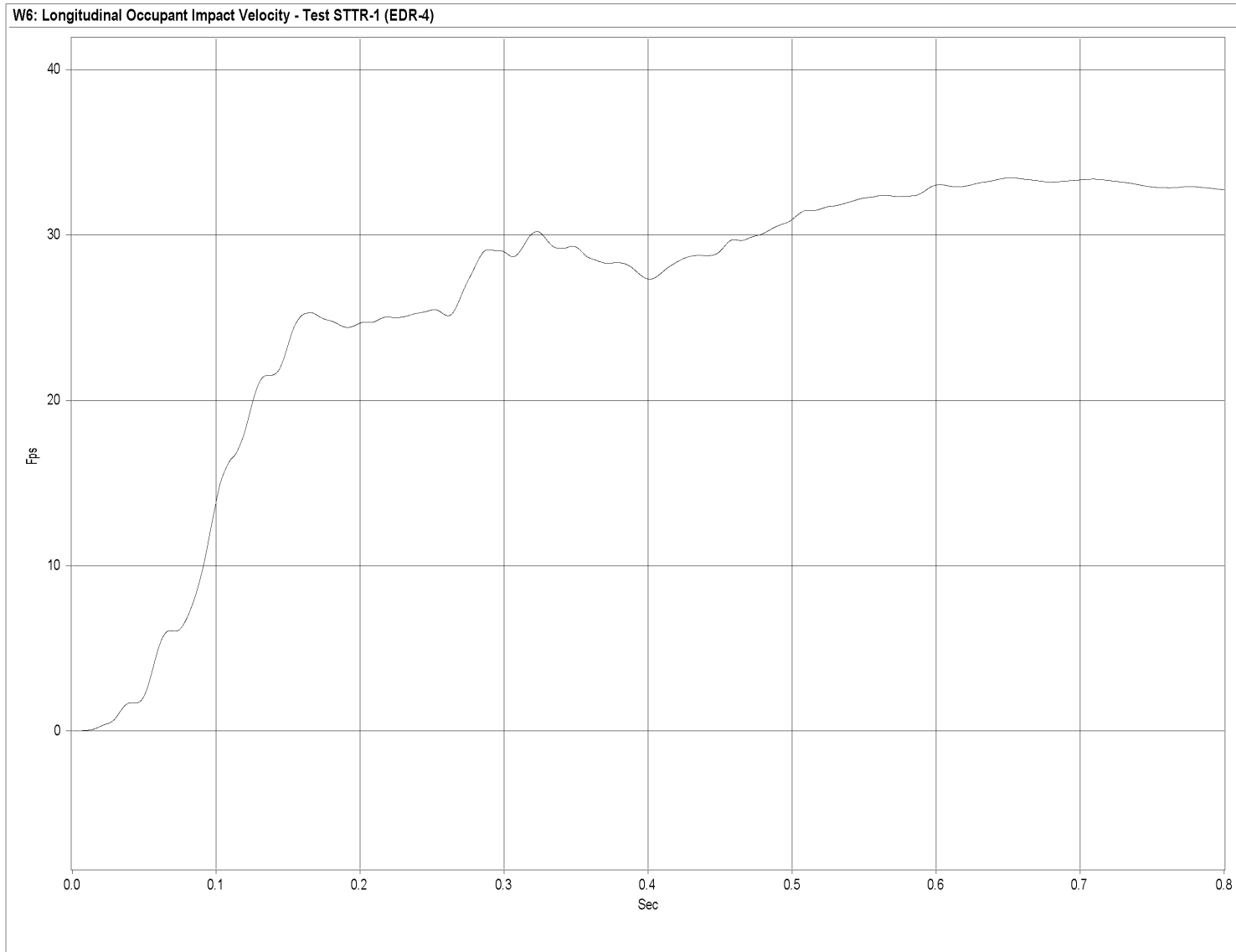


Figure P-2. Graph of Longitudinal Occupant Impact Velocity, Test STTR-1

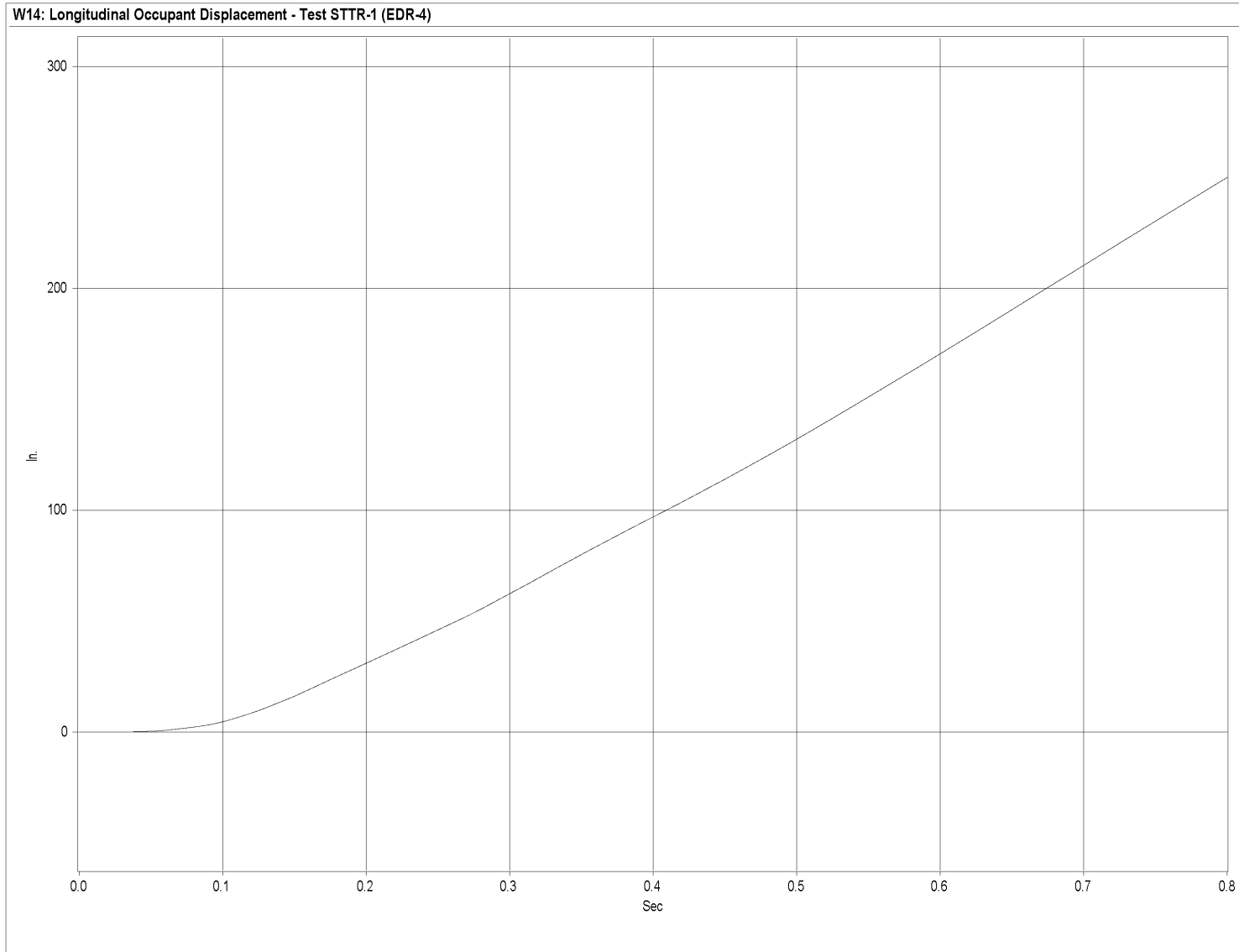


Figure P-3. Graph of Longitudinal Occupant Displacement, Test STTR-1

398

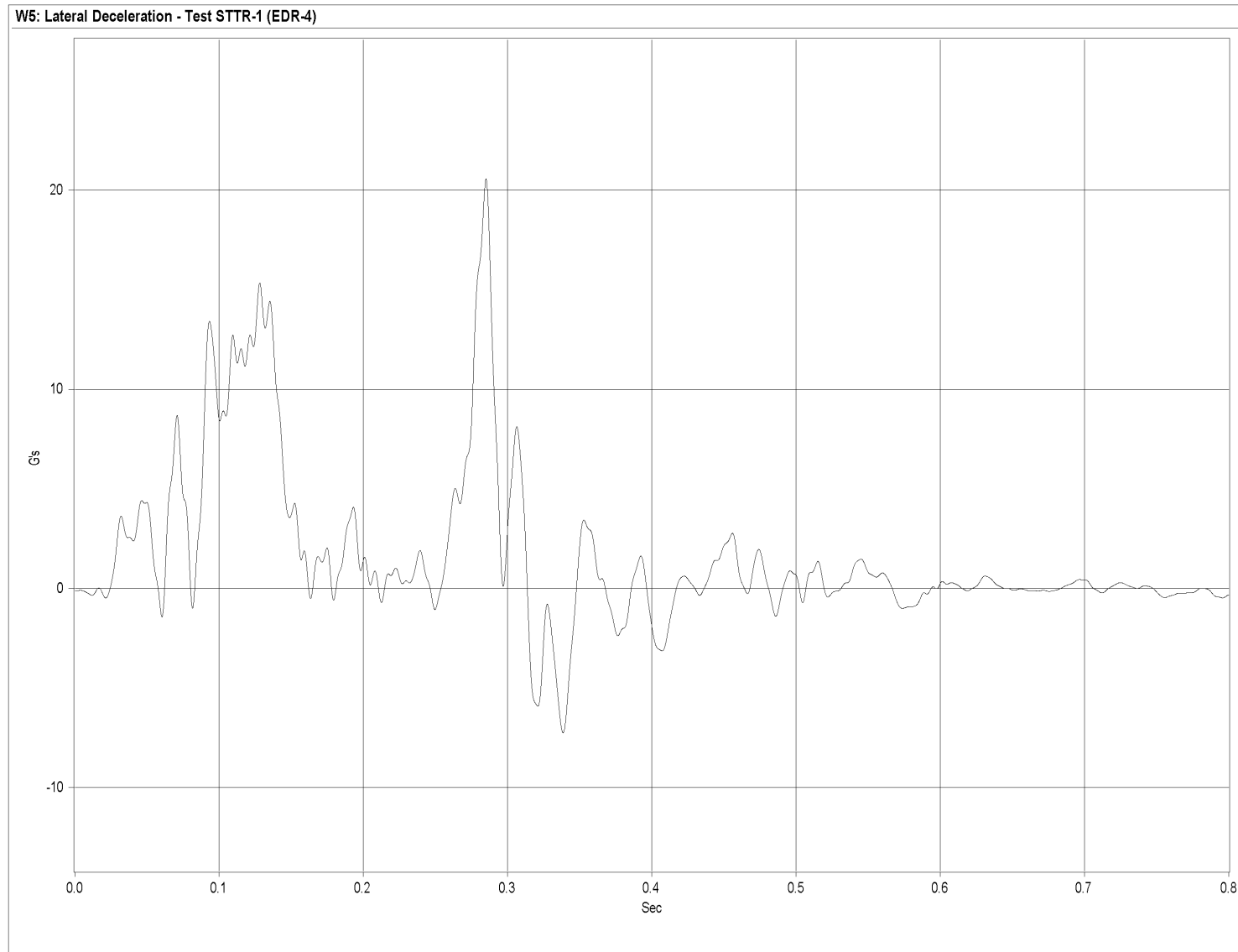


Figure P-4. Graph of Lateral Deceleration, Test STTR-1

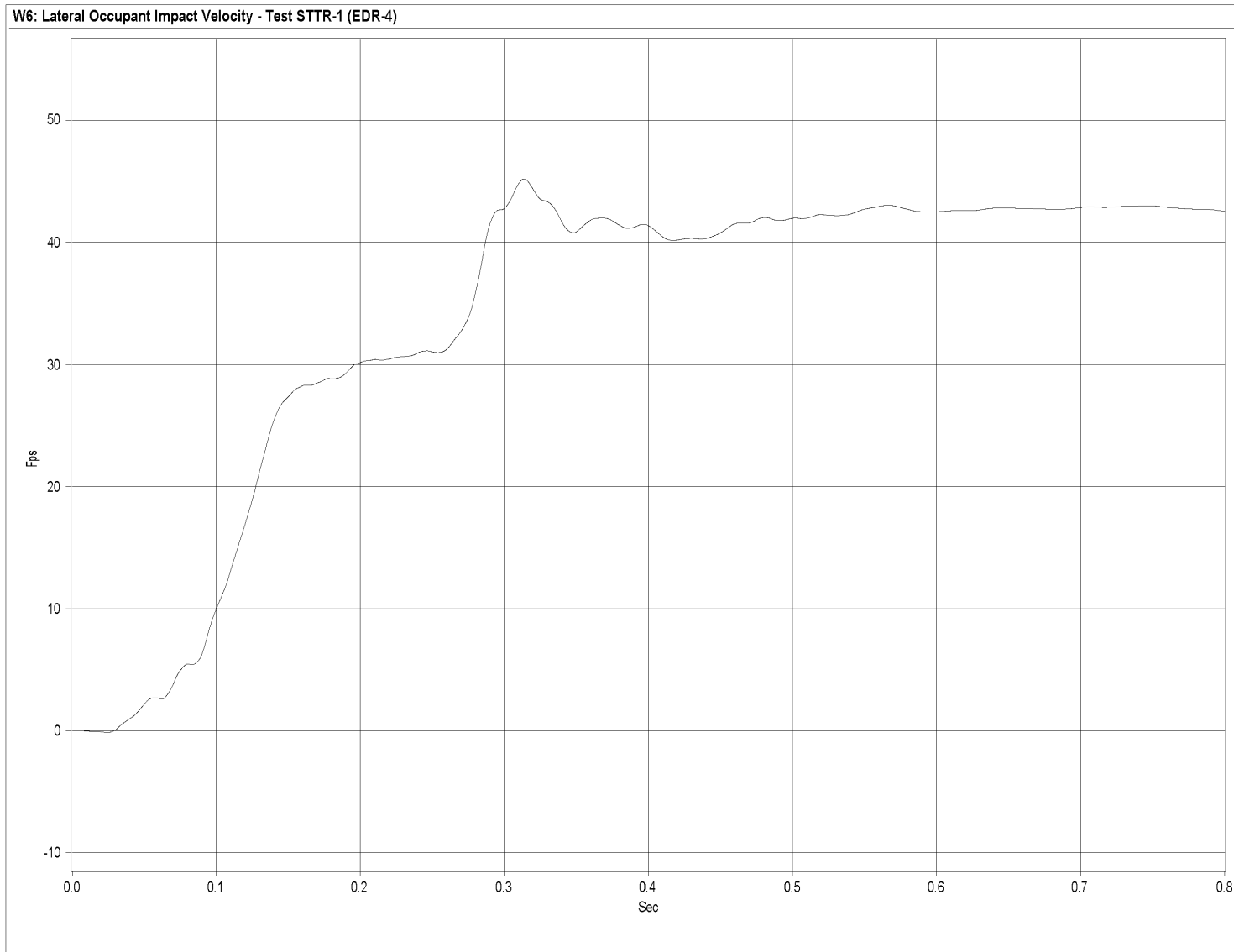


Figure P-5. Graph of Lateral Occupant Impact Velocity, Test STTR-1

400

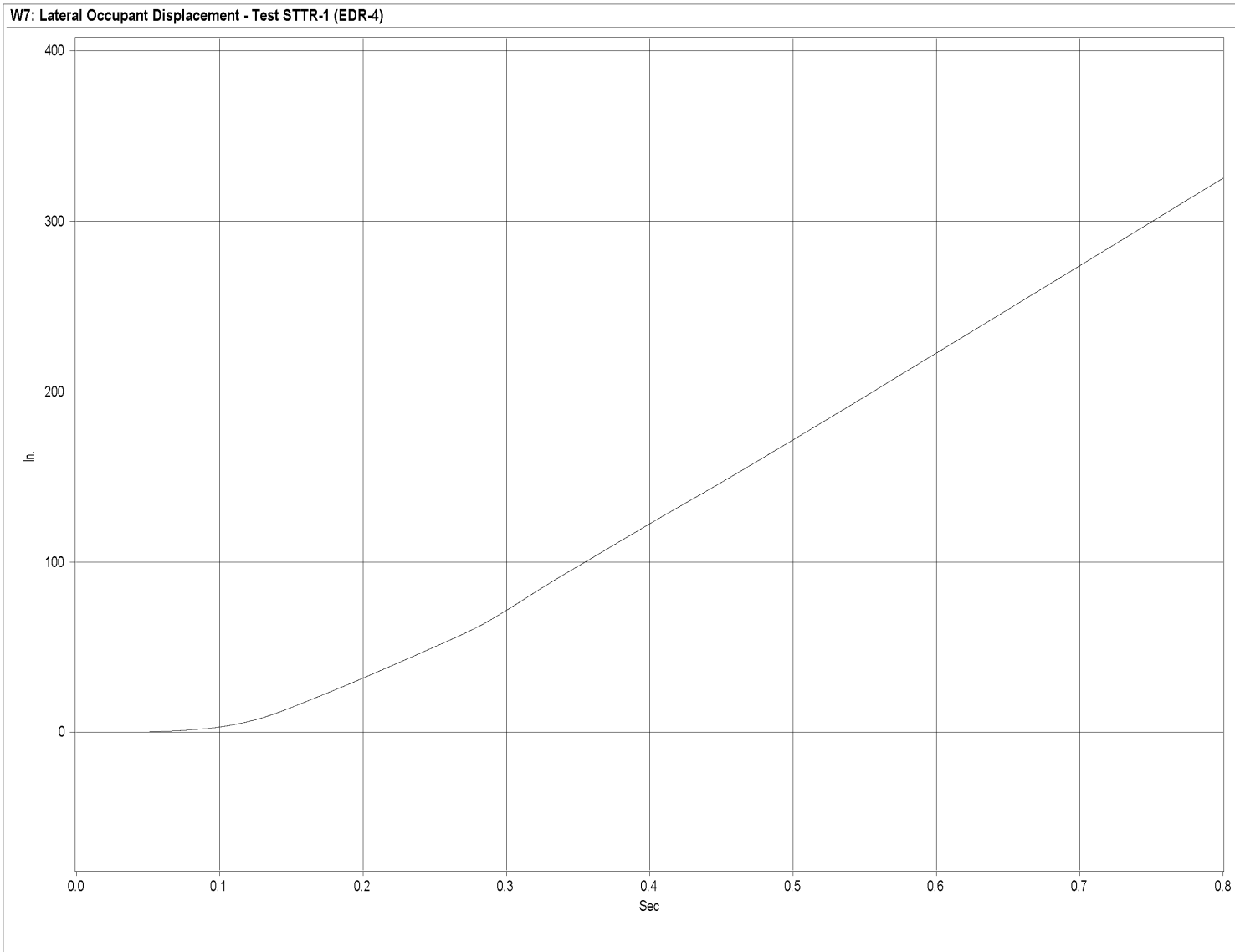


Figure P-6. Graph of Lateral Occupant Displacement, Test STTR-1

APPENDIX Q

Rate Transducer Data Analysis - Test STTR-1

Figure Q-1. Graph of Roll, Pitch, and Yaw Angular Displacements, Test STTR-1

402

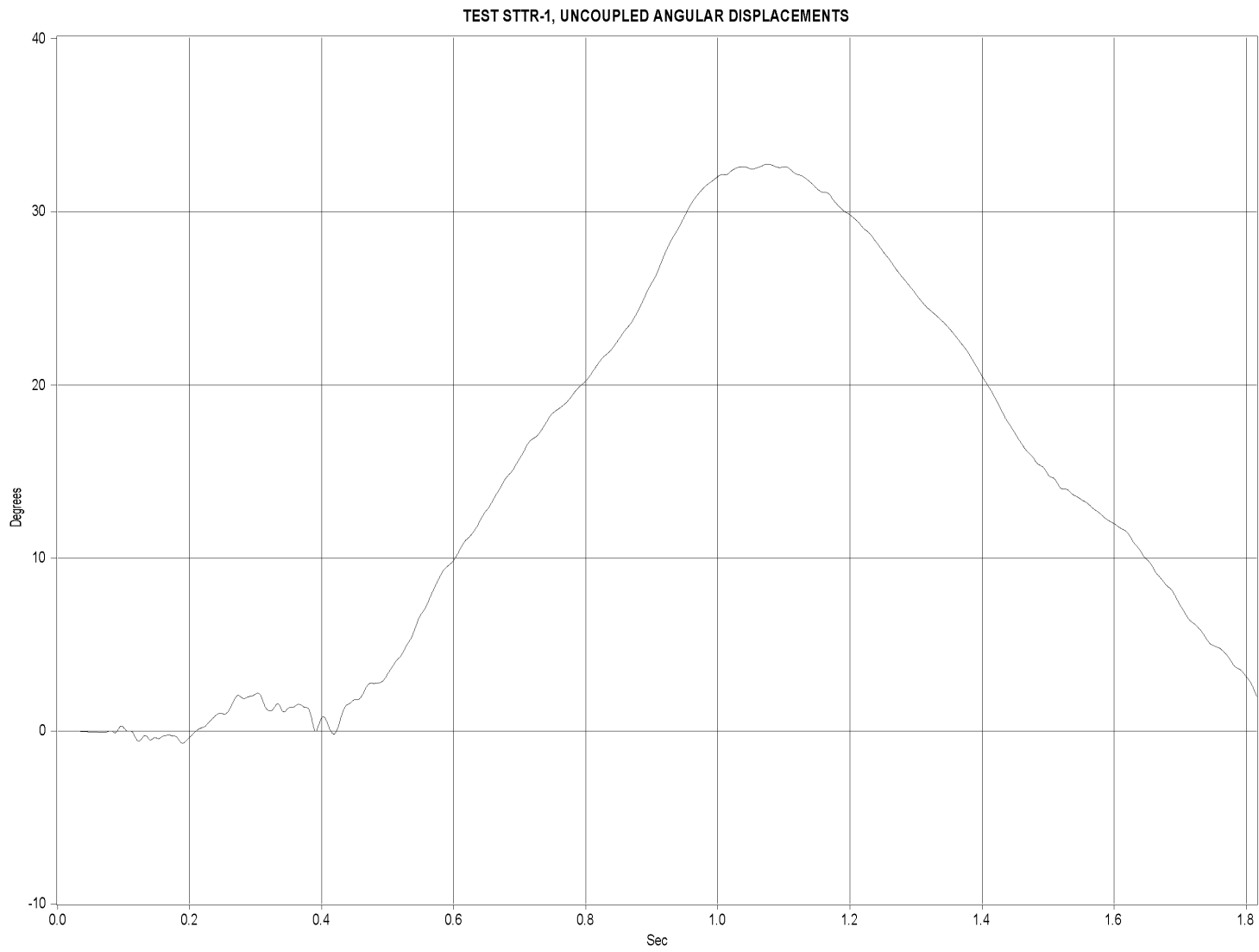


Figure Q-1. Graph of Roll, Pitch, and Yaw Angular Displacements, Test STTR-1

APPENDIX R

Strain Gauge Data Analysis - Test STTR-1

Figure R-1. Graph of Post No. 6 Upstream-Side Bolt Strain, Test STTR-1

Figure R-2. Graph of Post No. 6 Upstream-Side Bolt Stress, Test STTR-1

Figure R-3. Graph of Post No. 6 Downstream-Side Bolt Strain, Test STTR-1

Figure R-4. Graph of Post No. 6 Downstream-Side Bolt Stress, Test STTR-1

Figure R-5. Graph of Top Plate Post No. 6 - Downstream and Perpendicular to Rail - Strain,
Test STTR-1

Figure R-6. Graph of Top Plate Post No. 6 - Downstream and Perpendicular to Rail - Stress,
Test STTR-1

Figure R-7. Graph of Top Plate Post No. 6 - Downstream and Parallel to Rail - Strain, Test STTR-1

Figure R-8. Graph of Top Plate Post No. 6 - Downstream and Parallel to Rail - Stress, Test STTR-1

Figure R-9. Graph of Bottom Plate Post No. 6 - Middle and Perpendicular to Rail - Strain,
Test STTR-1

Figure R-10. Graph of Bottom Plate Post No. 6 - Middle and Perpendicular to Rail - Stress,
Test STTR-1

Figure R-11. Graph of Traffic-Side Flange Post No. 6 Strain, Test STTR-1

Figure R-12. Graph of Back-Side Flange Post No. 6 Strain, Test STTR-1

Figure R-13. Graph of Back-Side Flange Post No. 6 Stress, Test STTR-1

Figure R-14. Graph of Post No. 7 Upstream-Side Bolt Strain, Test STTR-1

Figure R-15. Graph of Post No. 7 Upstream-Side Bolt Stress, Test STTR-1

Figure R-16. Graph of Post No. 7 Downstream-Side Bolt Strain, Test STTR-1

Figure R-17. Graph of Post No. 7 Downstream-Side Bolt Stress, Test STTR-1

Figure R-18. Graph of Top Plate Post No. 7 - Middle and Perpendicular to Rail - Strain,

Test STTR-1

Figure R-19. Graph of Top Plate Post No. 7 - Middle and Perpendicular to Rail - Stress, Test STTR-1

Figure R-20. Graph of Bottom Plate Post No. 7 - Middle and Perpendicular to Rail - Strain, Test STTR-1

Figure R-21. Graph of Bottom Plate Post No. 7 - Middle and Perpendicular to Rail - Stress, Test STTR-1

Figure R-22. Graph of Traffic-Side Flange Post No. 7 Strain, Test STTR-1

Figure R-23. Graph of Traffic-Side Flange Post No. 7 Stress, Test STTR-1

Figure R-24. Graph of Back-Side Flange Post No. 7 Strain, Test STTR-1

Figure R-25. Graph of Back-Side Flange Post No. 7 Stress, Test STTR-1

405

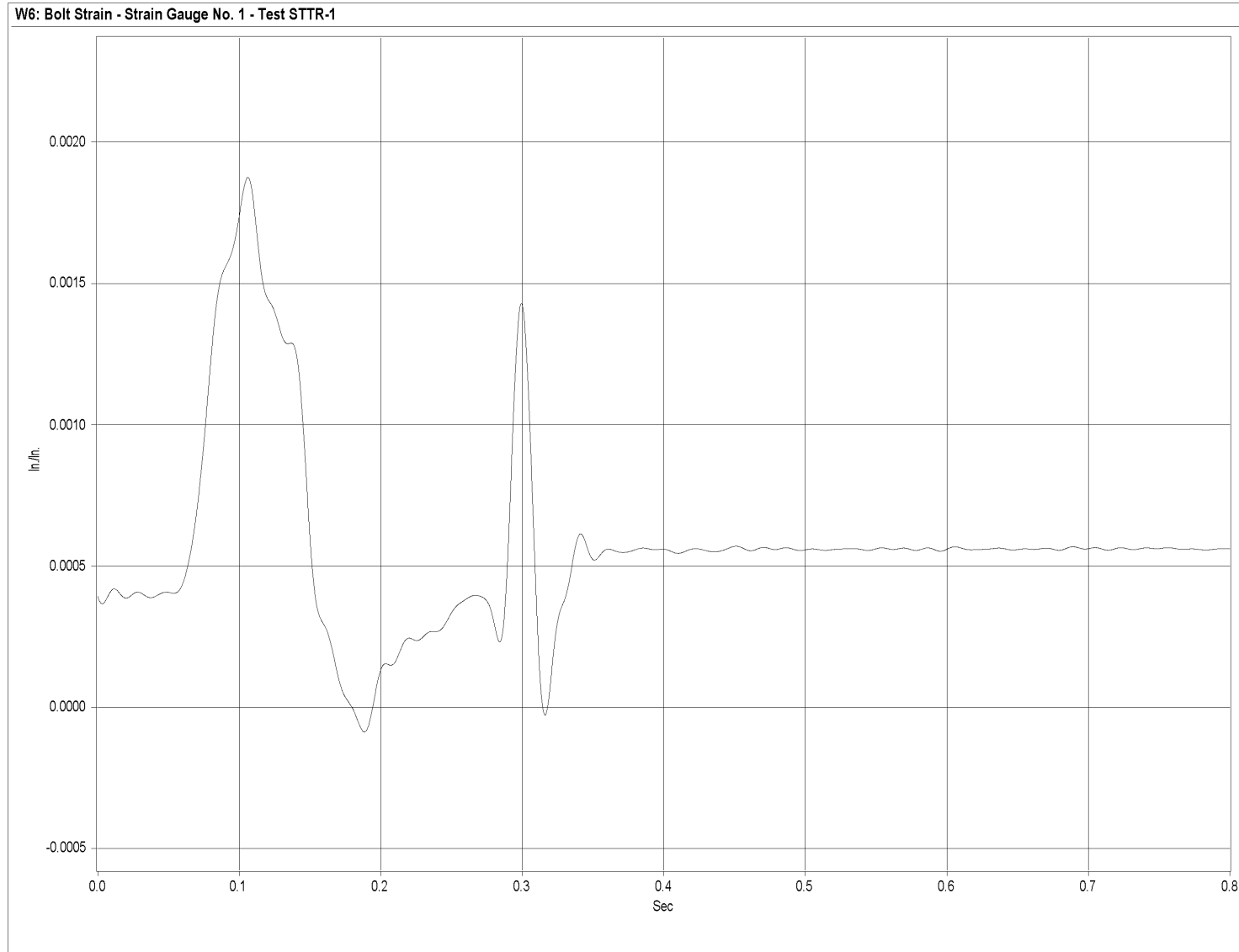


Figure R-1. Graph of Post No. 6 Upstream-Side Bolt Strain, Test STTR-1

406

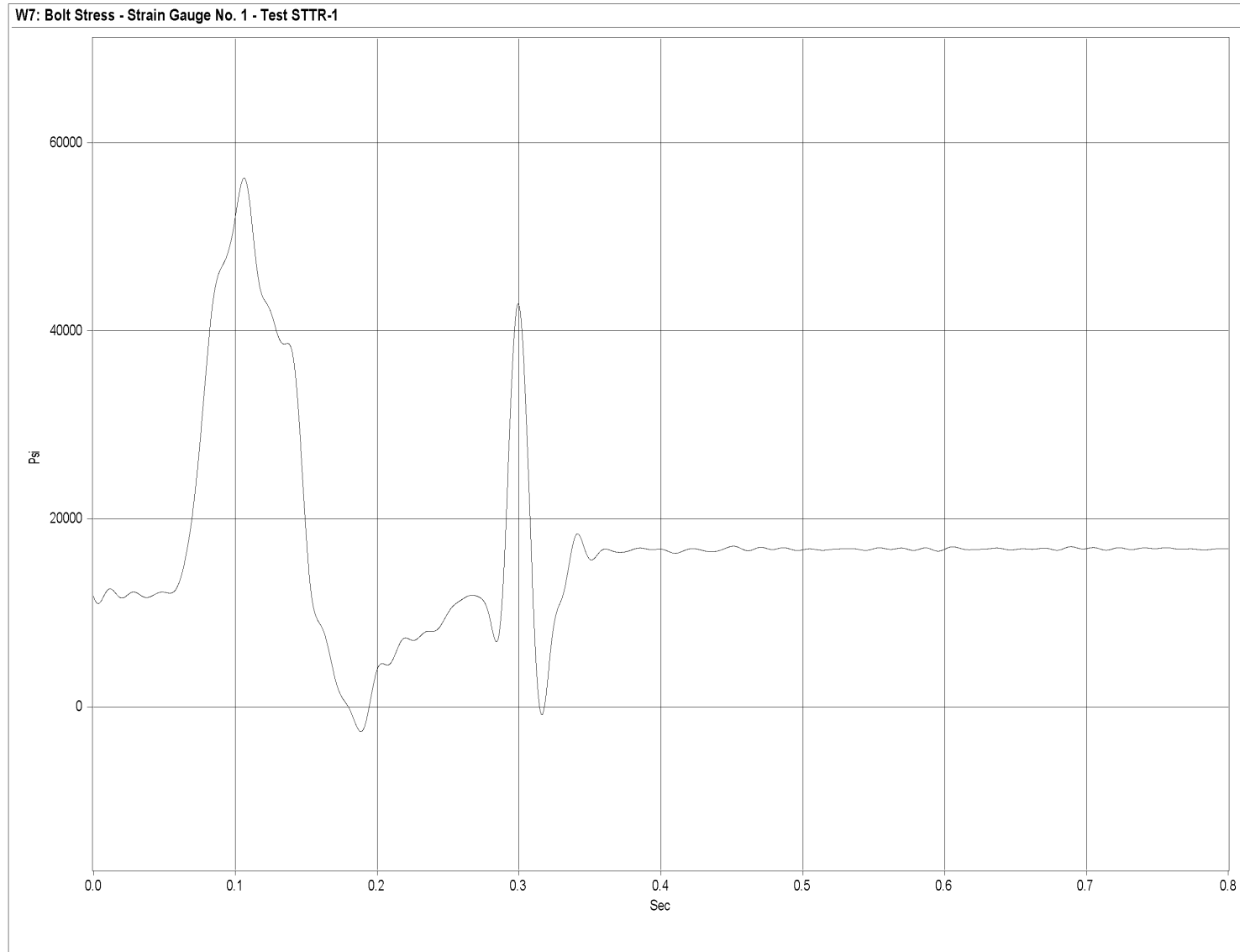


Figure R-2. Graph of Post No. 6 Upstream-Side Bolt Stress, Test STTR-1

407

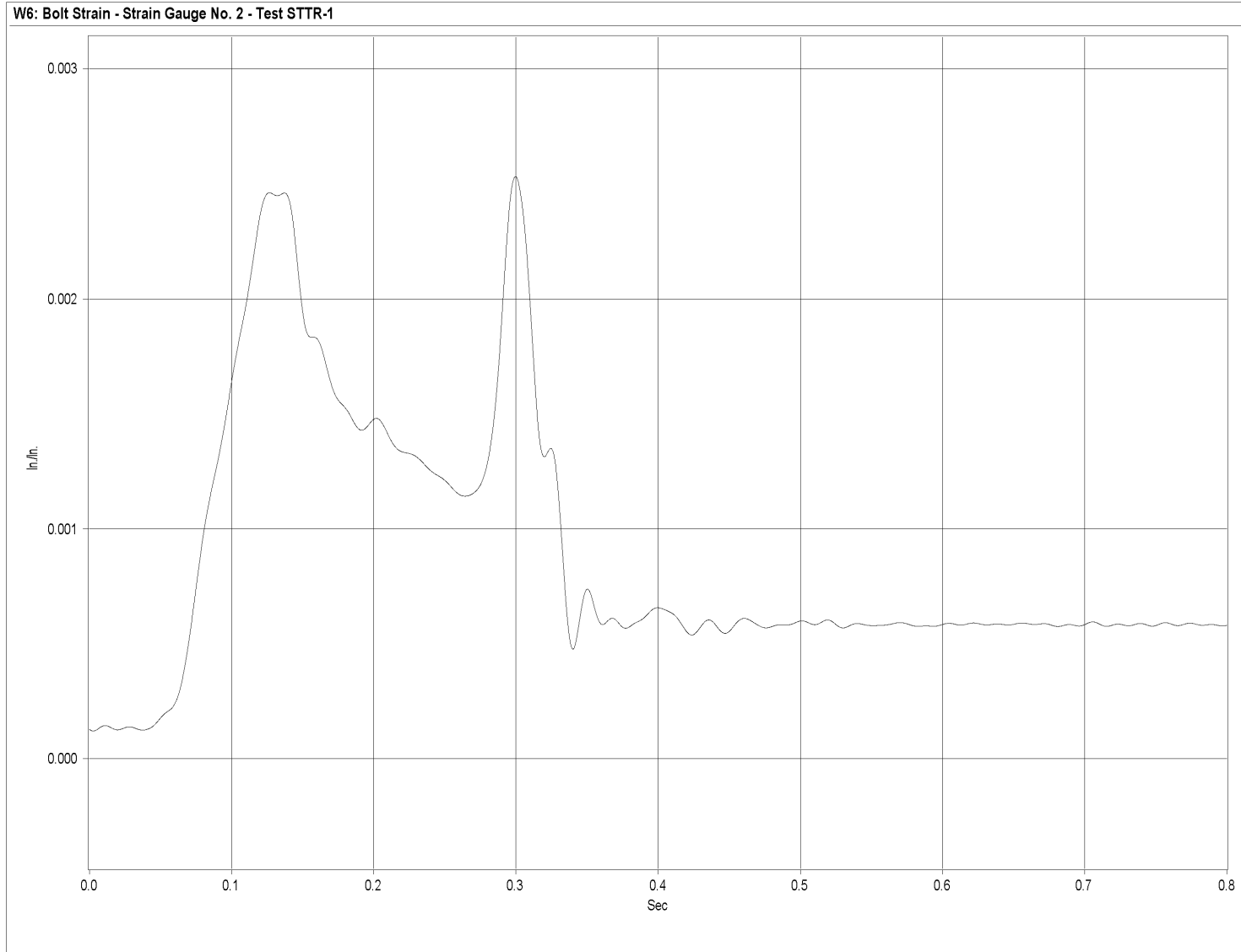


Figure R-3. Graph of Post No. 6 Downstream-Side Bolt Strain, Test STTR-1

408

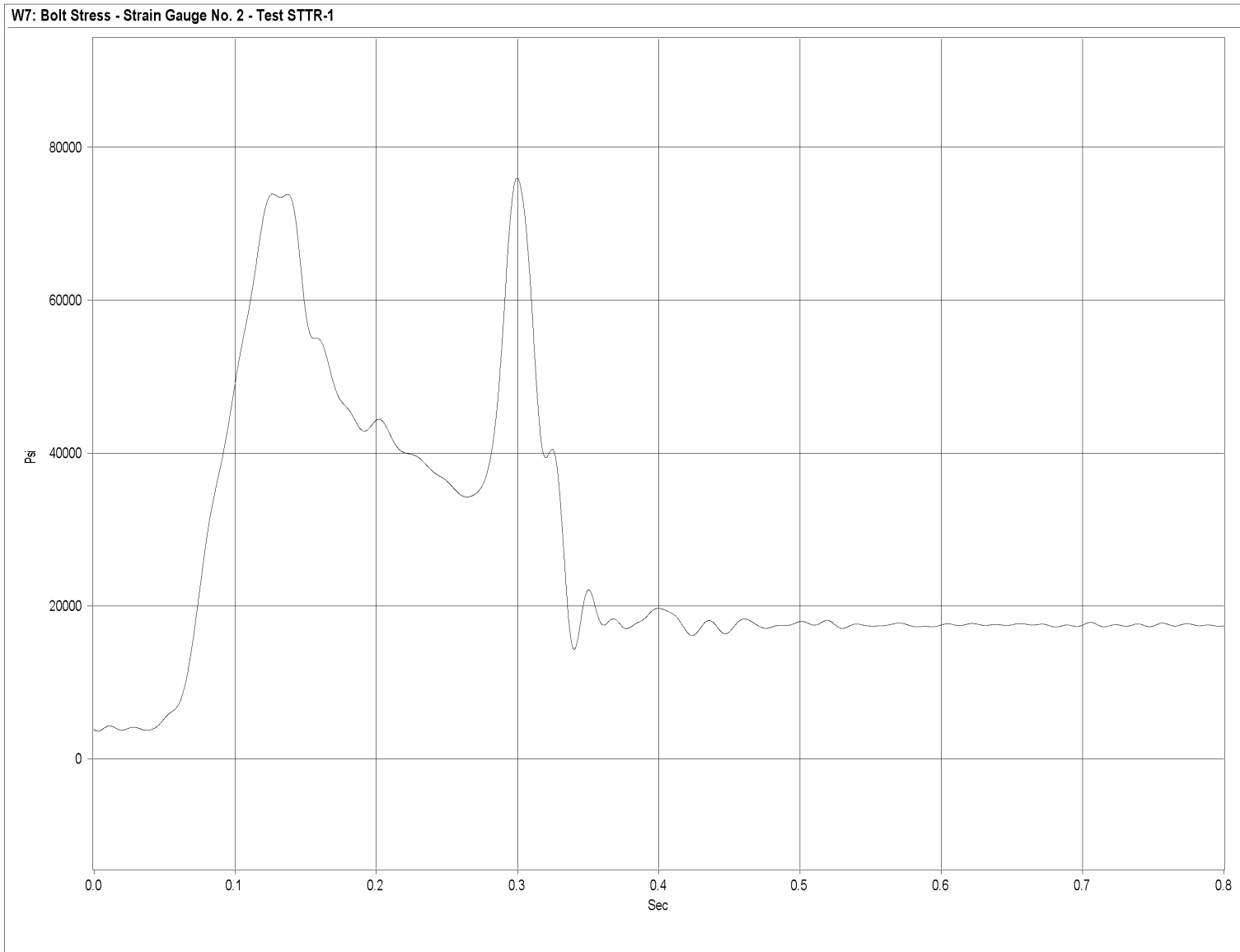


Figure R-4. Graph of Post No. 6 Downstream-Side Bolt Stress, Test STTR-1

409

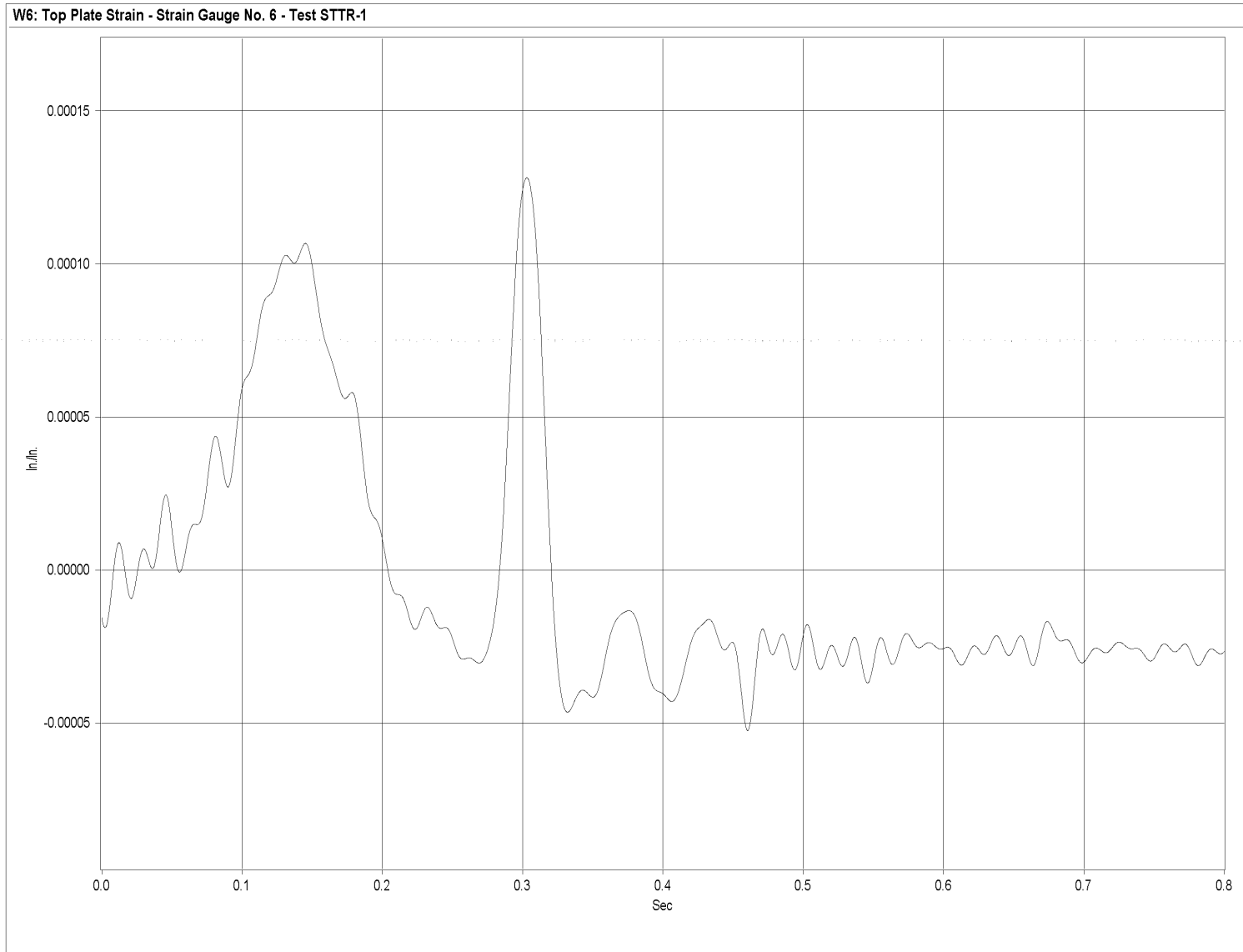


Figure R-5. Graph of Top Plate Post No. 6 - Downstream and Perpendicular to Rail - Strain, Test STTR-1

410

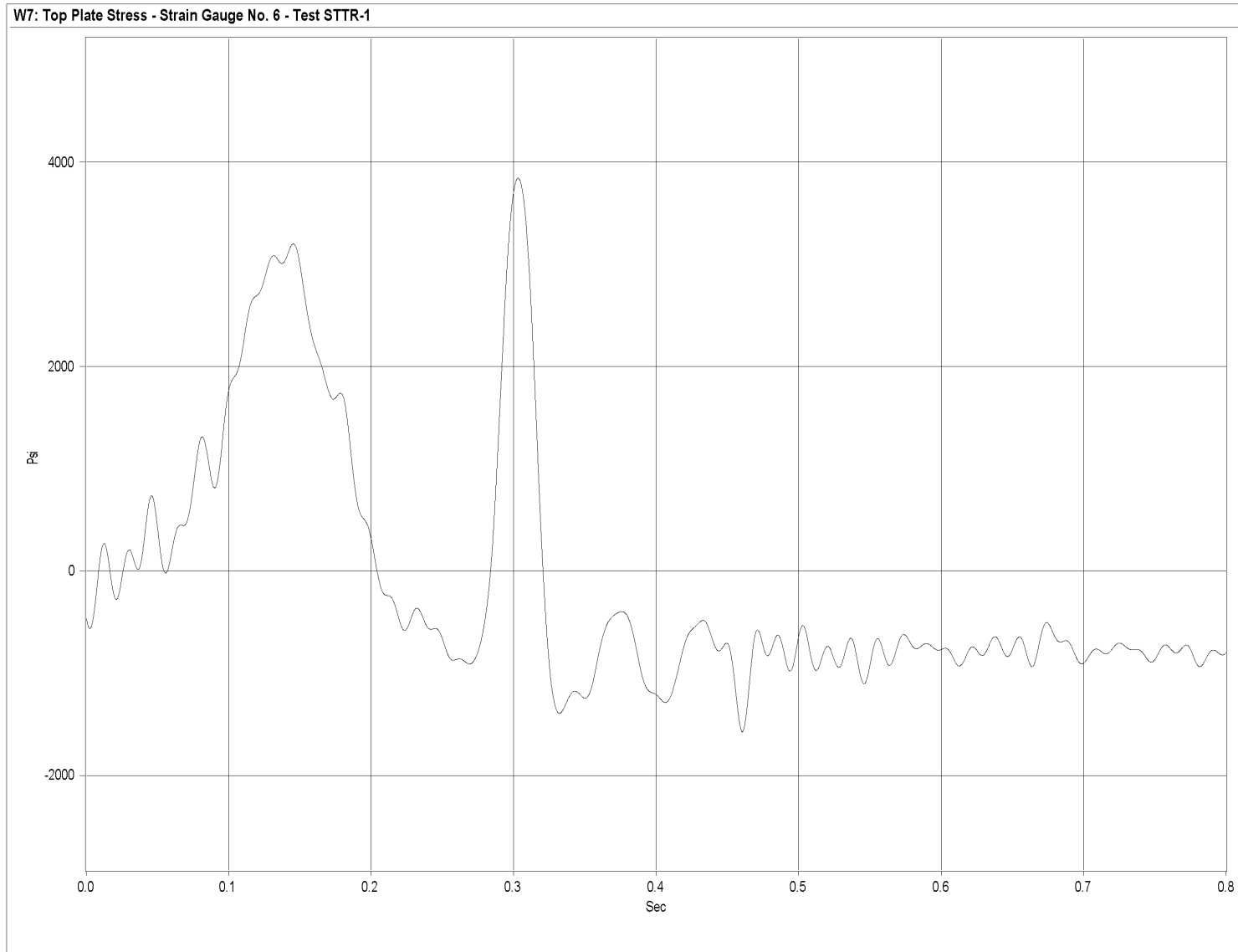


Figure R-6. Graph of Top Plate Post No. 6 - Downstream and Perpendicular to Rail - Stress, Test STTR-1

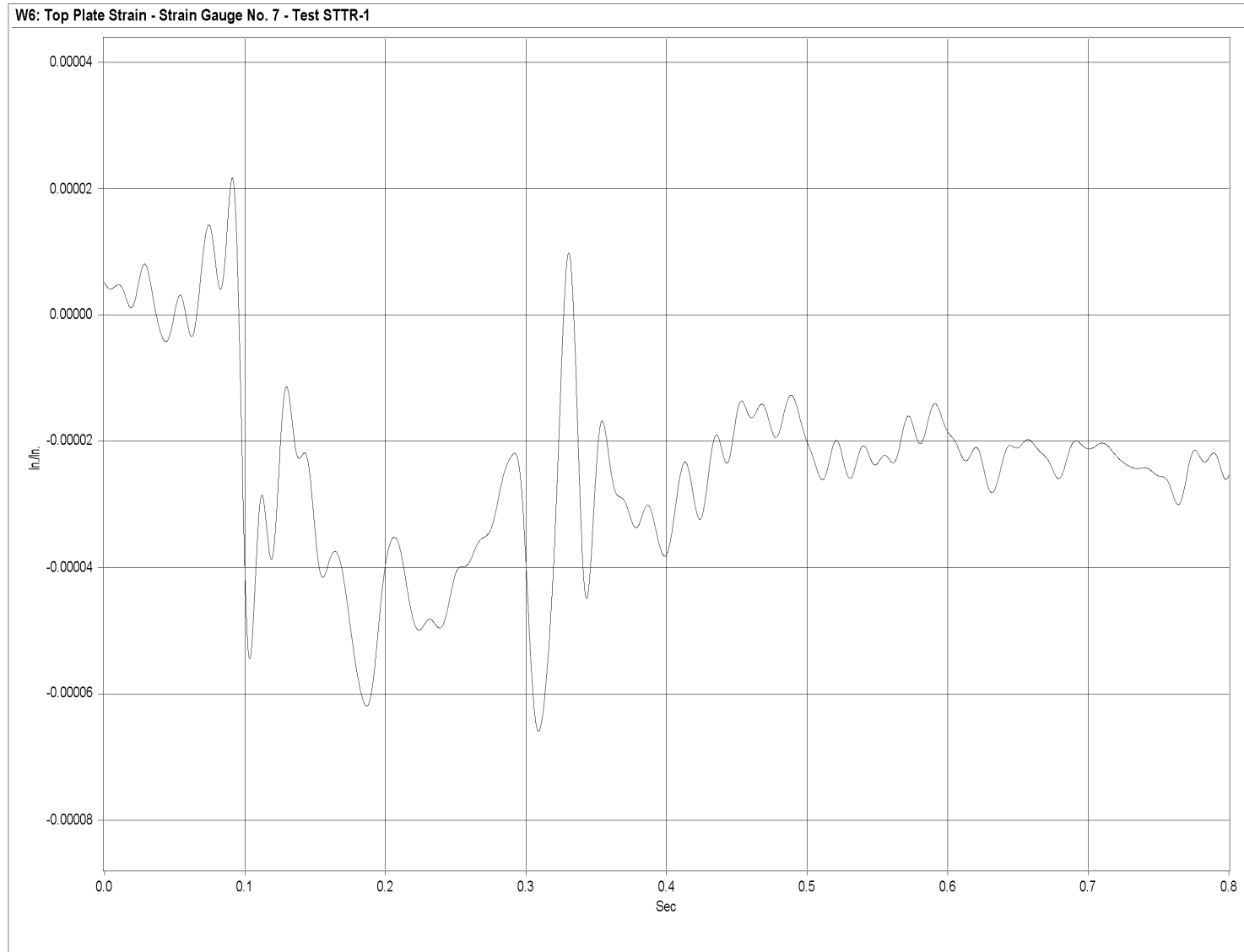


Figure R-7. Graph of Top Plate Post No. 6 - Downstream and Parallel to Rail - Strain, Test STTR-1

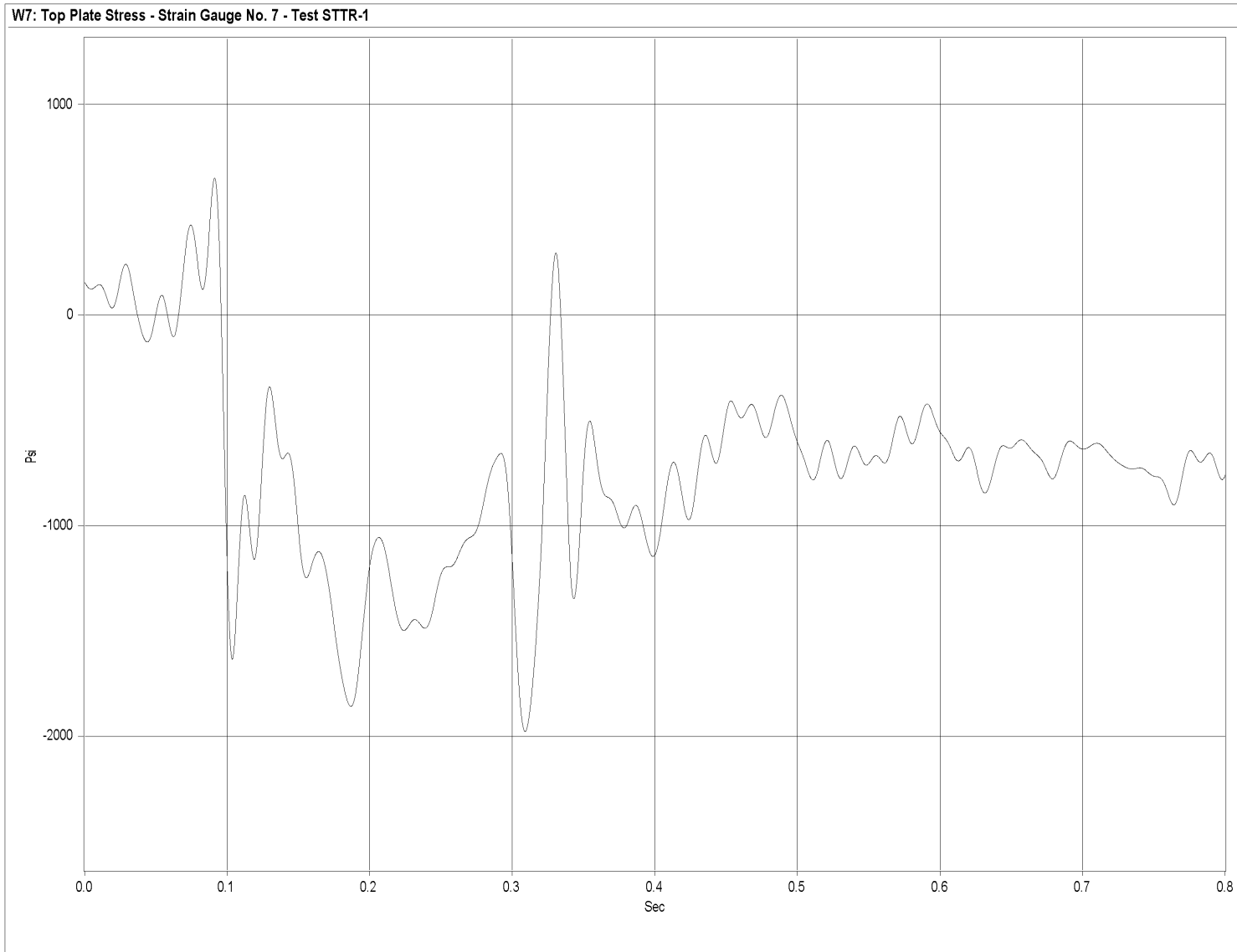


Figure R-8. Graph of Top Plate Post No. 6 - Downstream and Parallel to Rail - Stress, Test STTR-1

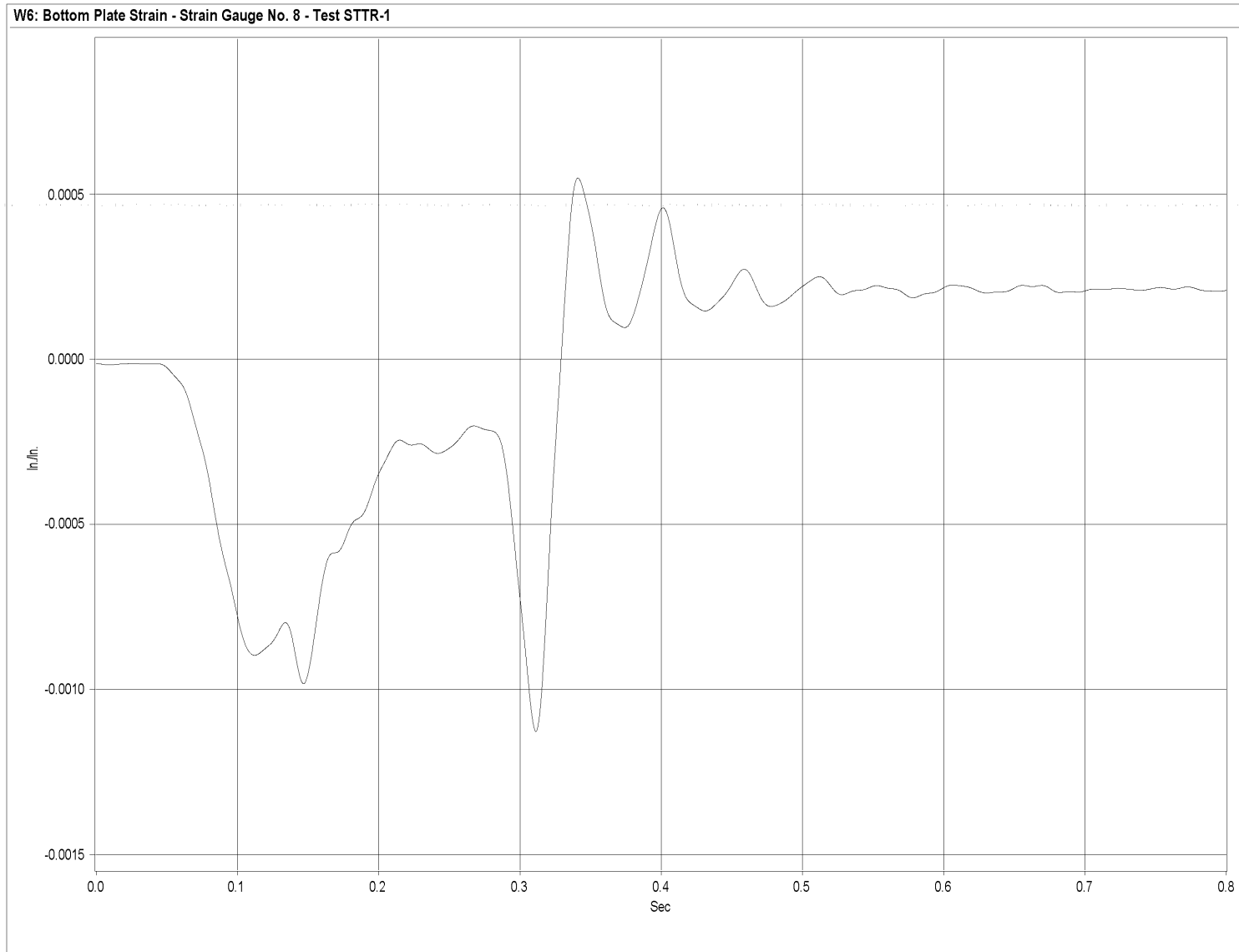


Figure R-9. Graph of Bottom Plate Post No. 6 - Middle and Perpendicular to Rail - Strain, Test STTR-1

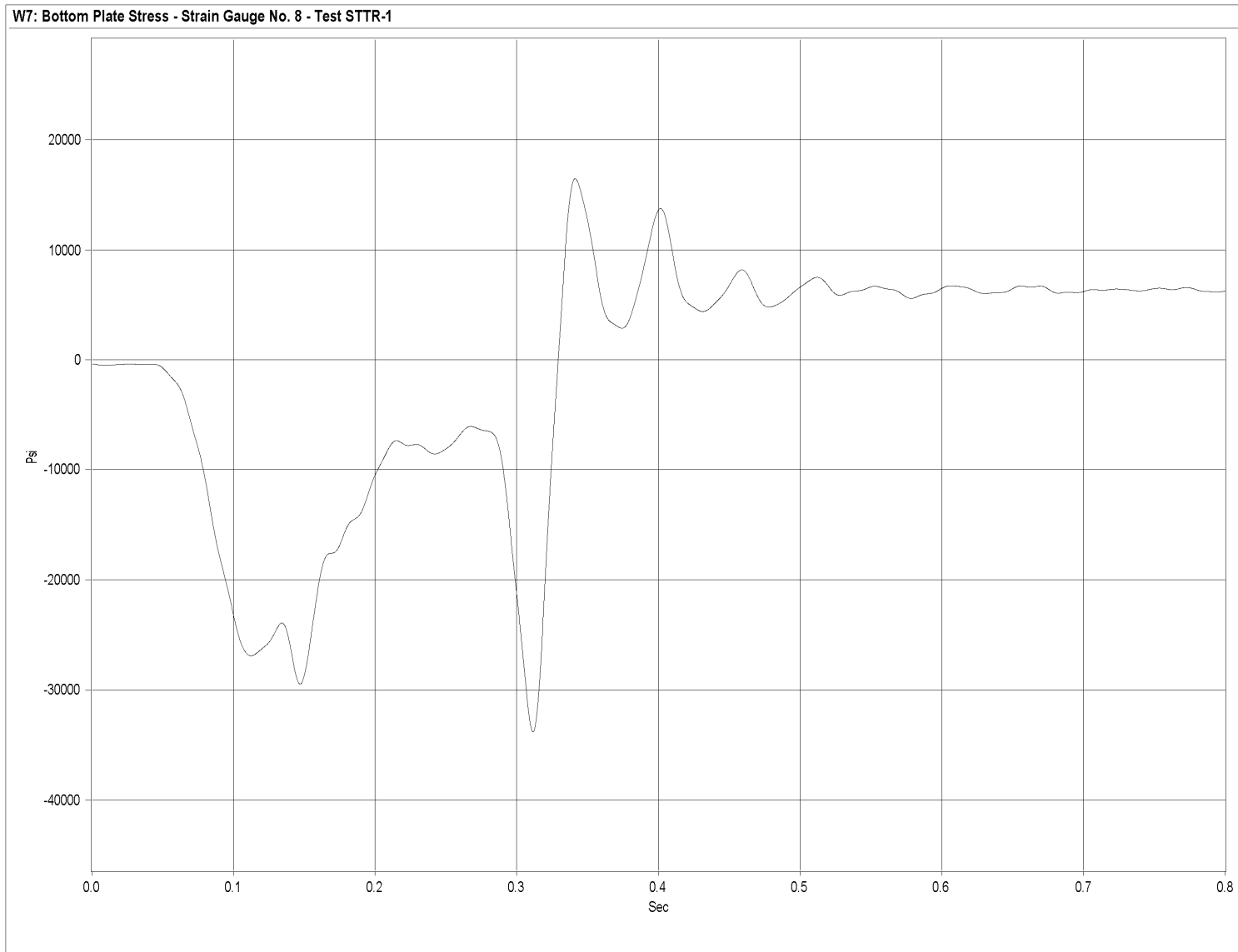


Figure R-10. Graph of Bottom Plate Post No. 6 - Middle and Perpendicular to Rail - Stress, Test STTR-1

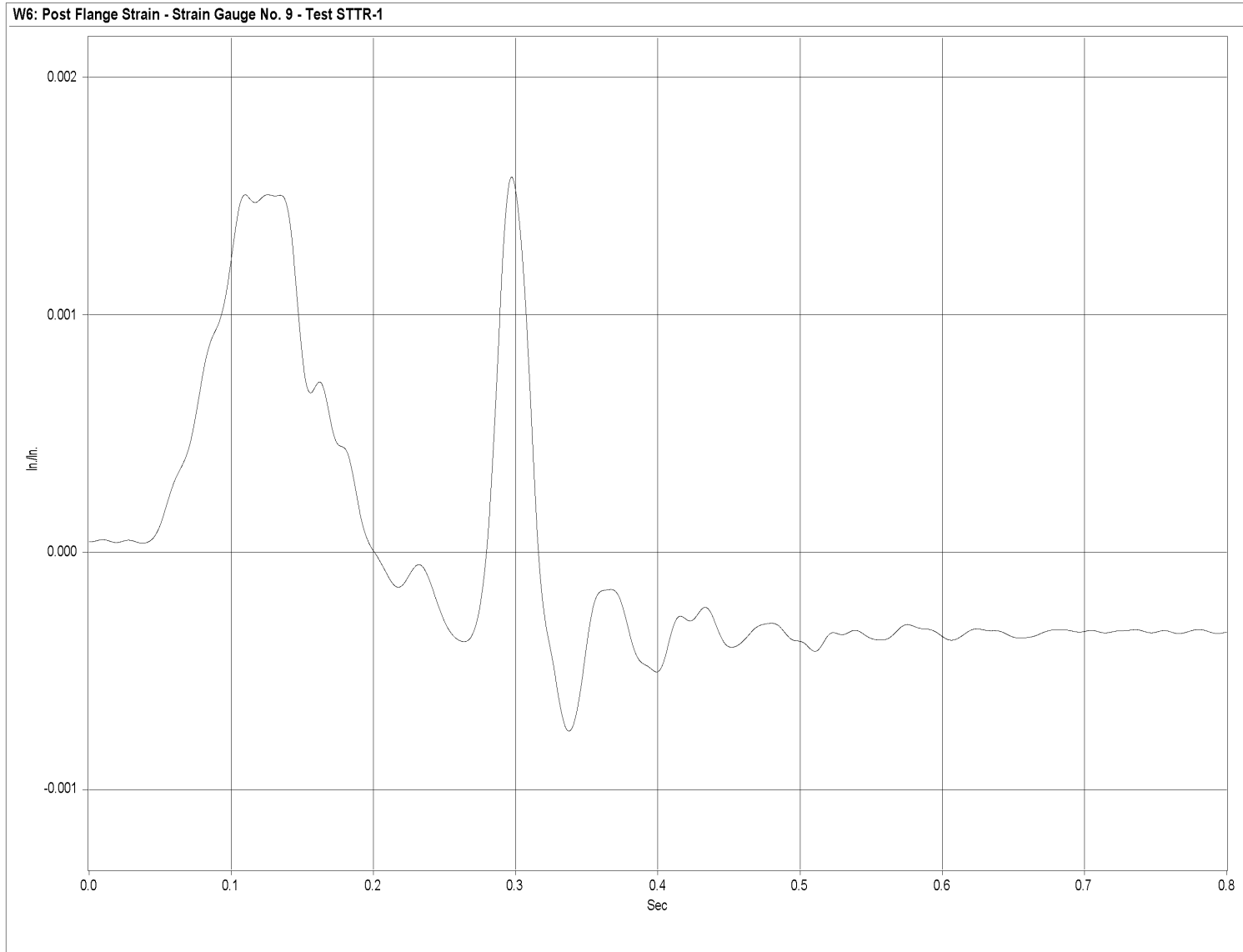


Figure R-11. Graph of Traffic-Side Flange Post No. 6 Strain, Test STTR-1

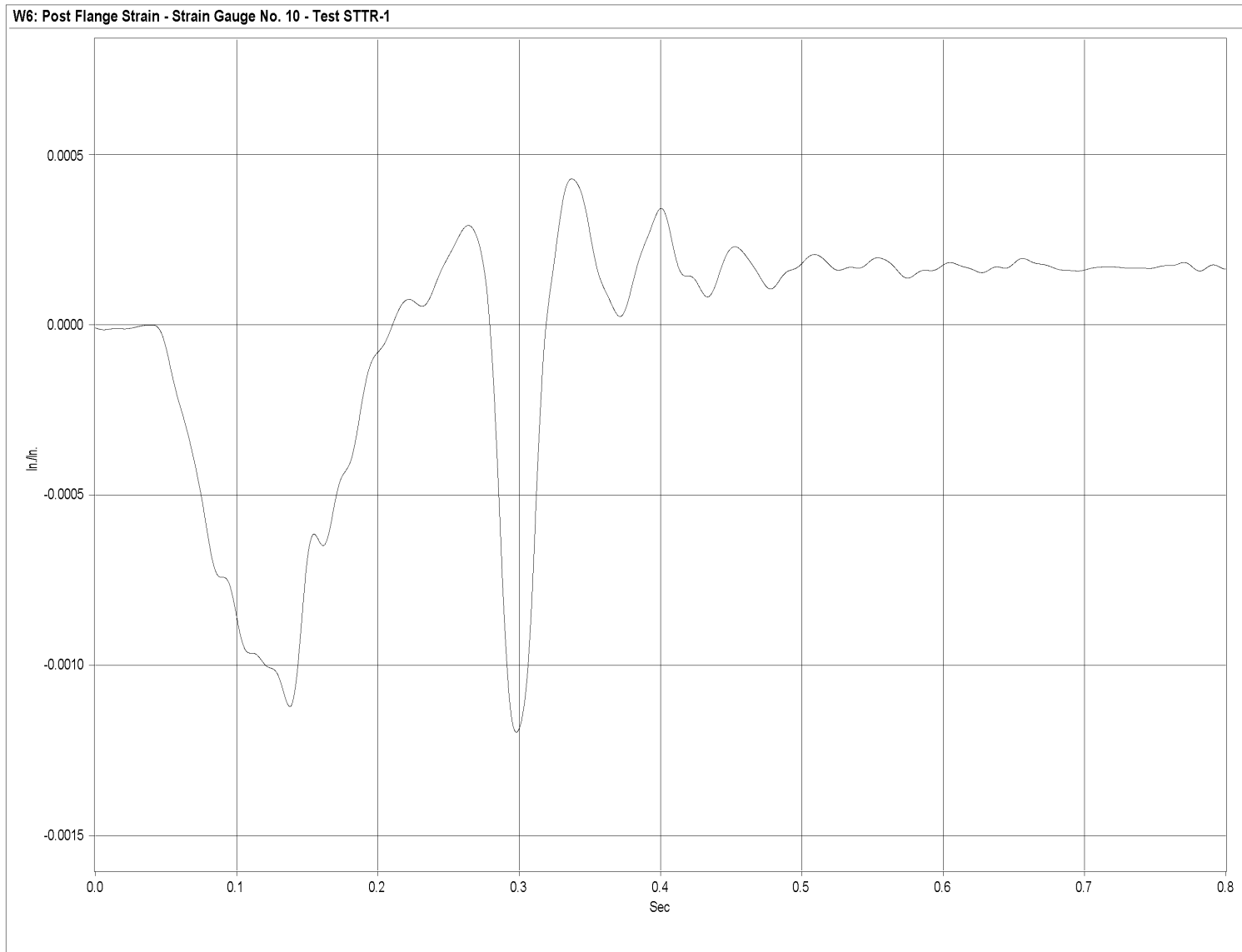


Figure R-12. Graph of Back-Side Flange Post No. 6 Strain, Test STTR-1

417

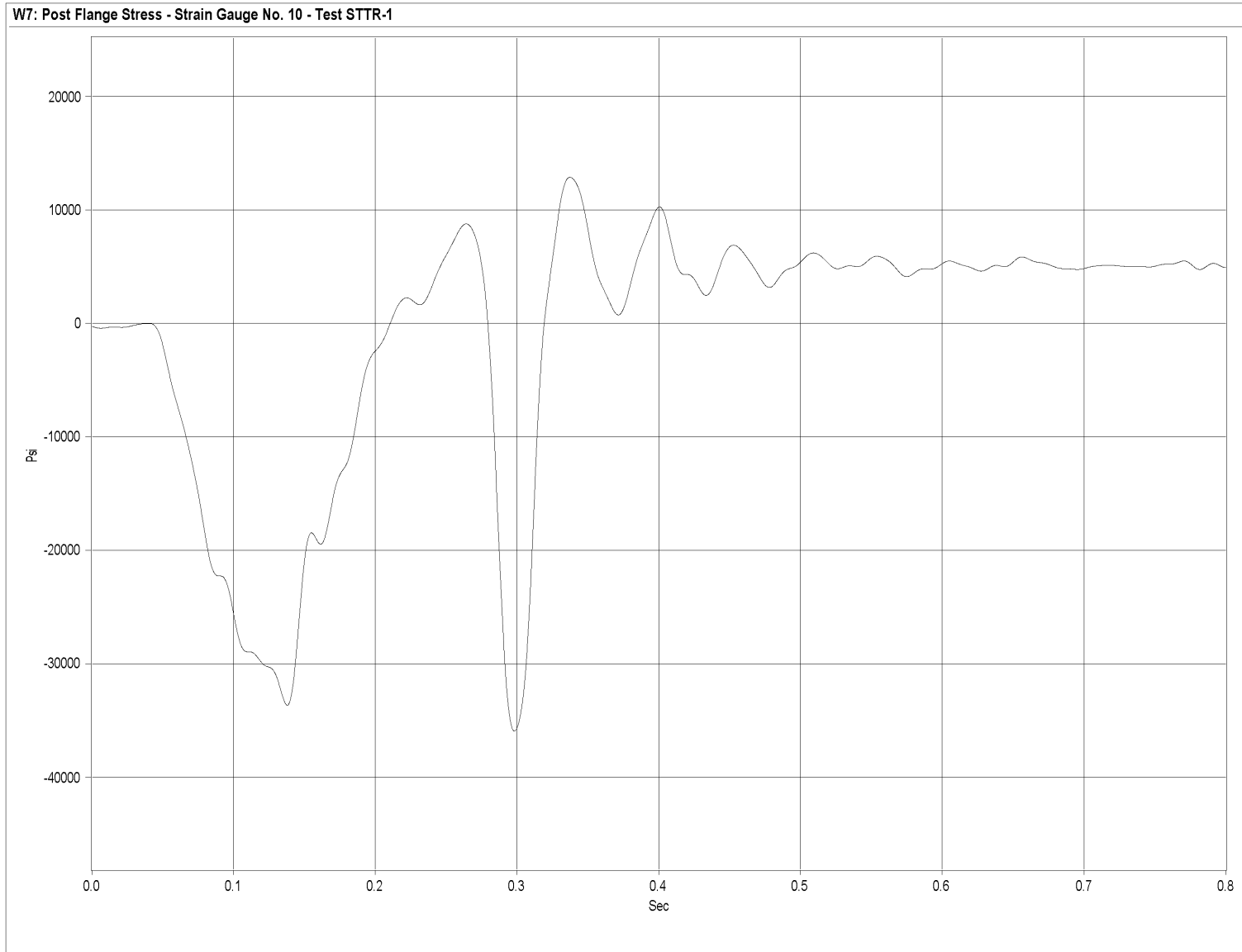


Figure R-13. Graph of Back-Side Flange Post No. 6 Stress, Test STTR-1

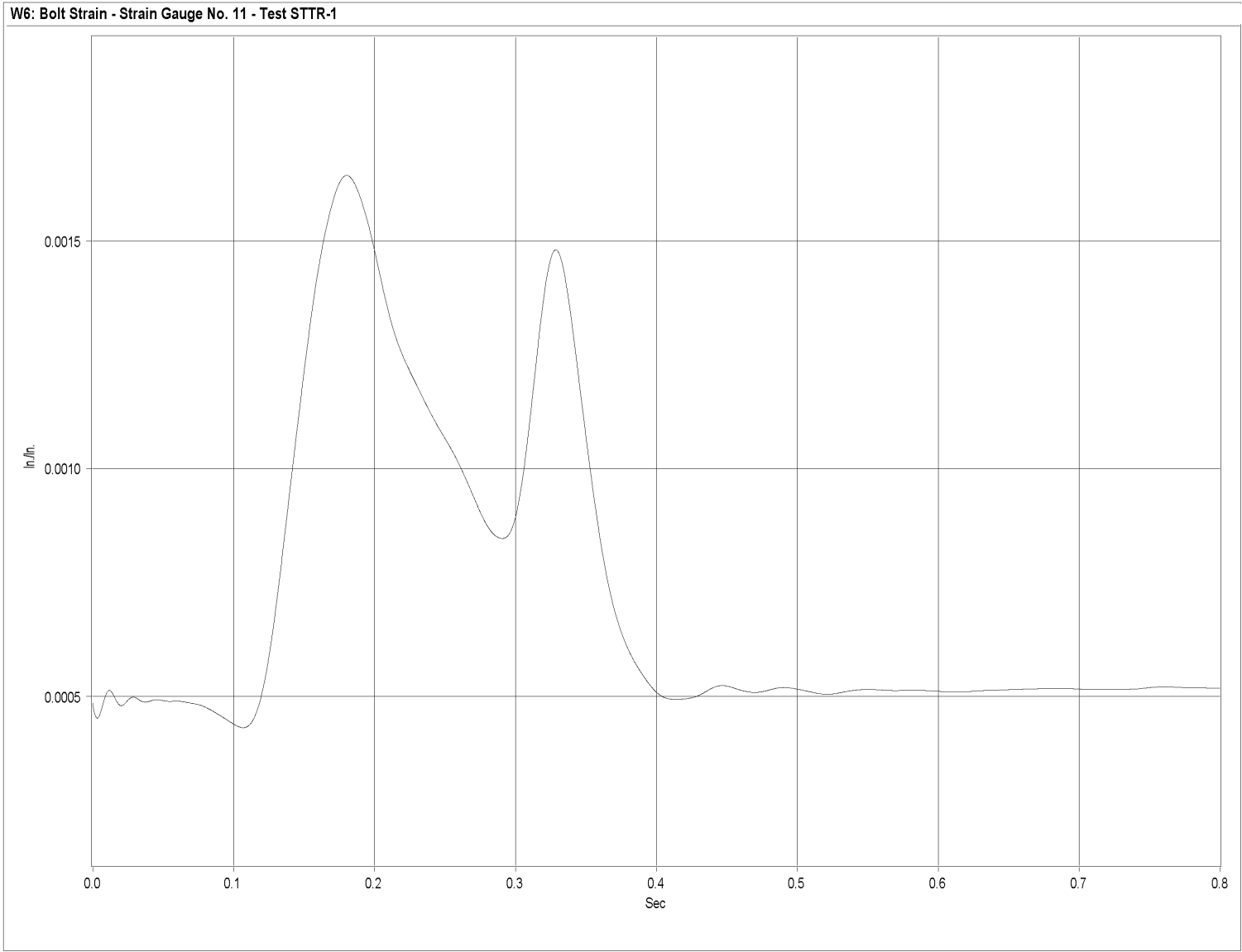


Figure R-14. Graph of Post No. 7 Upstream-Side Bolt Strain, Test STTR-1

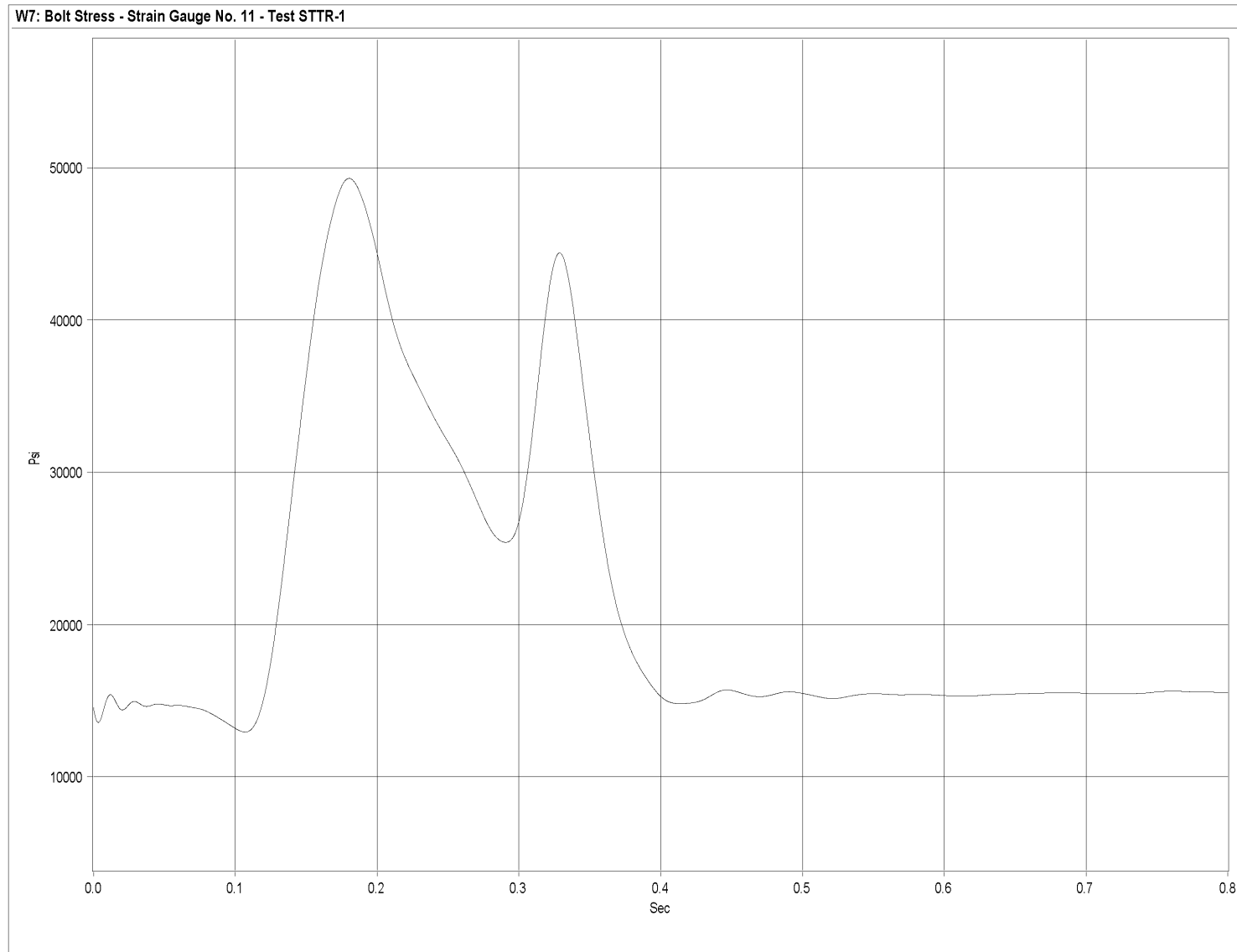


Figure R-15. Graph of Post No. 7 Upstream-Side Bolt Stress, Test STTR-1

420

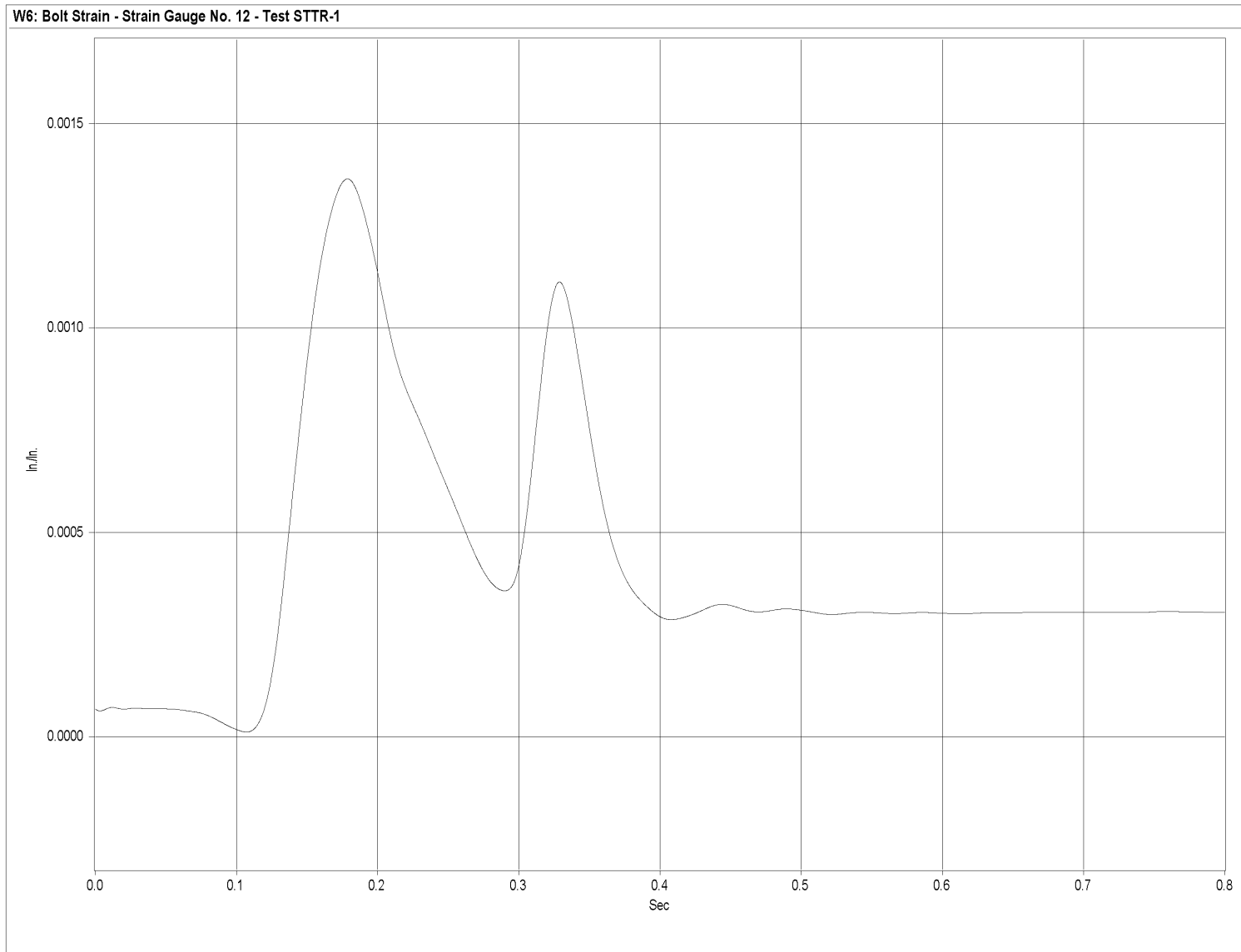


Figure R-16. Graph of Post No. 7 Downstream-Side Bolt Strain, Test STTR-1

421

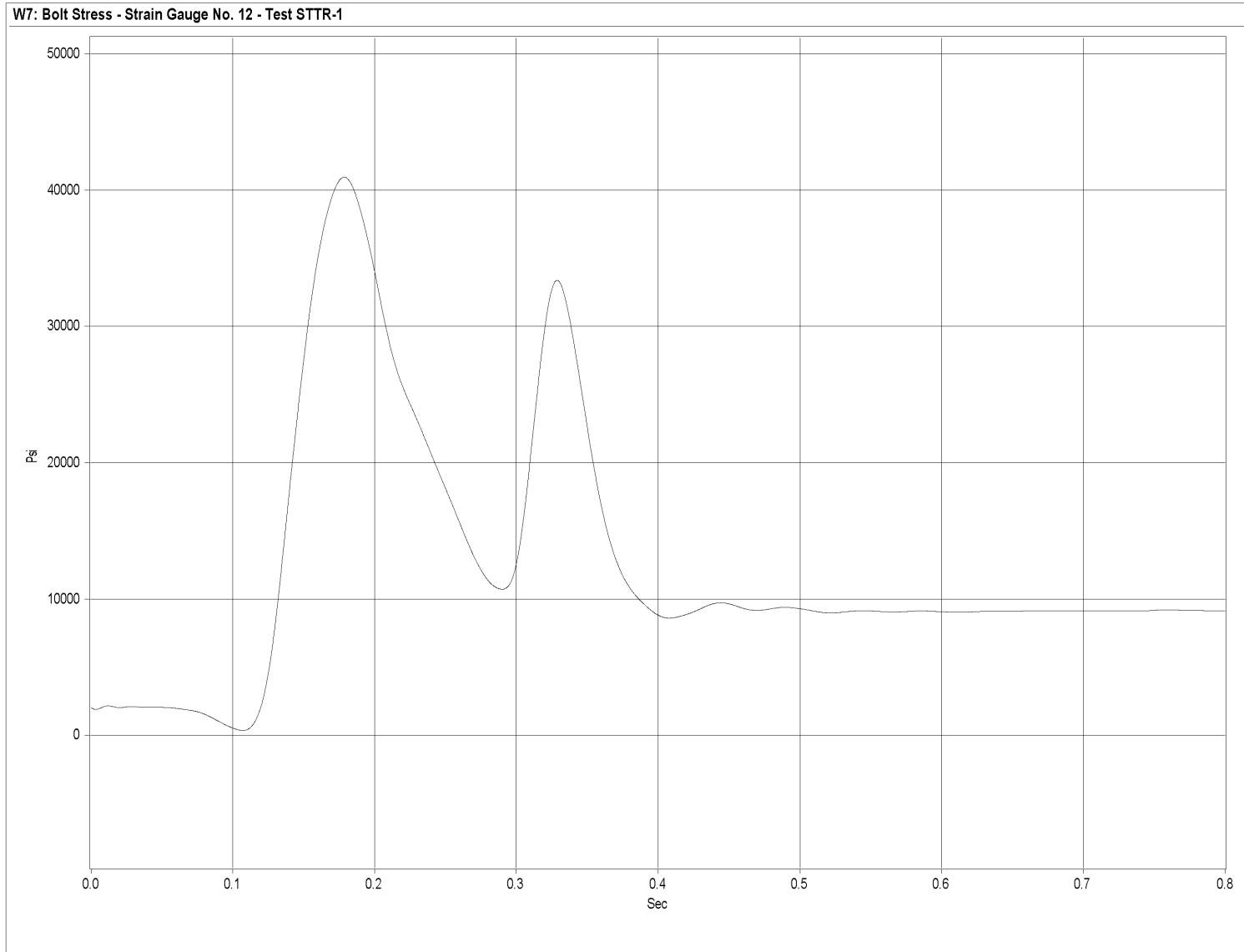


Figure R-17. Graph of Post No. 7 Downstream-Side Bolt Stress, Test STTR-1

422

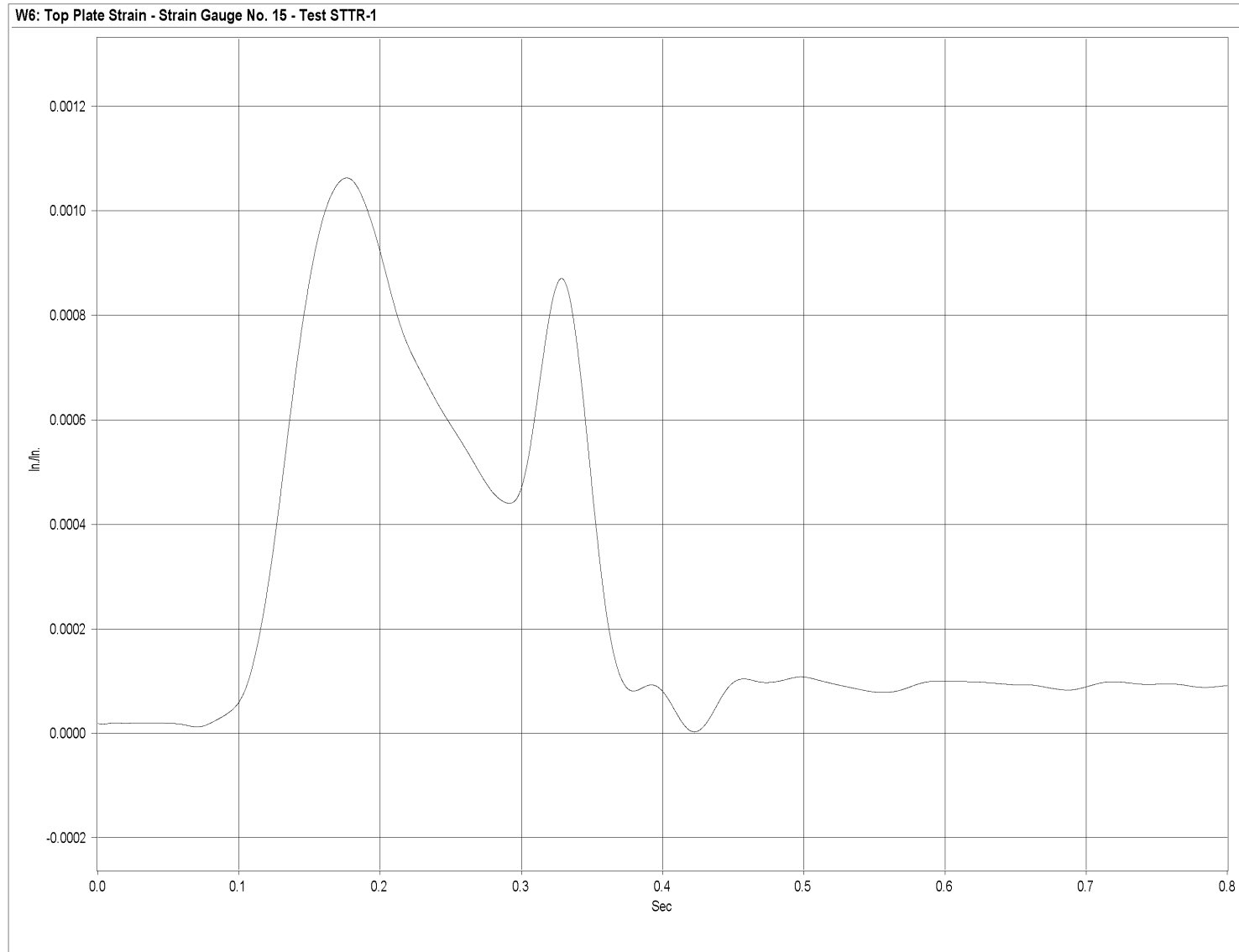


Figure R-18. Graph of Top Plate Post No. 7 - Middle and Perpendicular to Rail - Strain, Test STTR-1

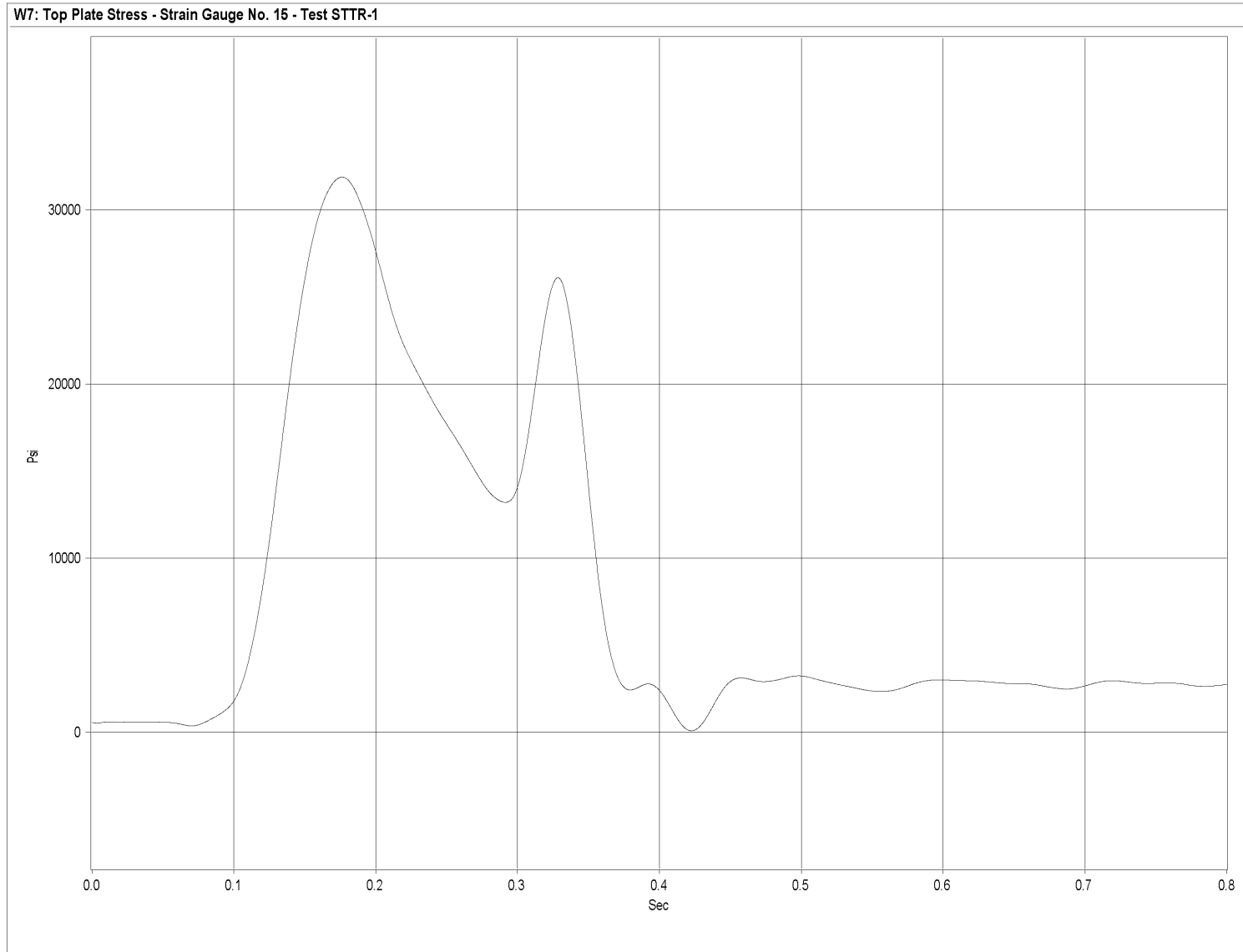


Figure R-19. Graph of Top Plate Post No. 7 - Middle and Perpendicular to Rail - Stress, Test STTR-1

424

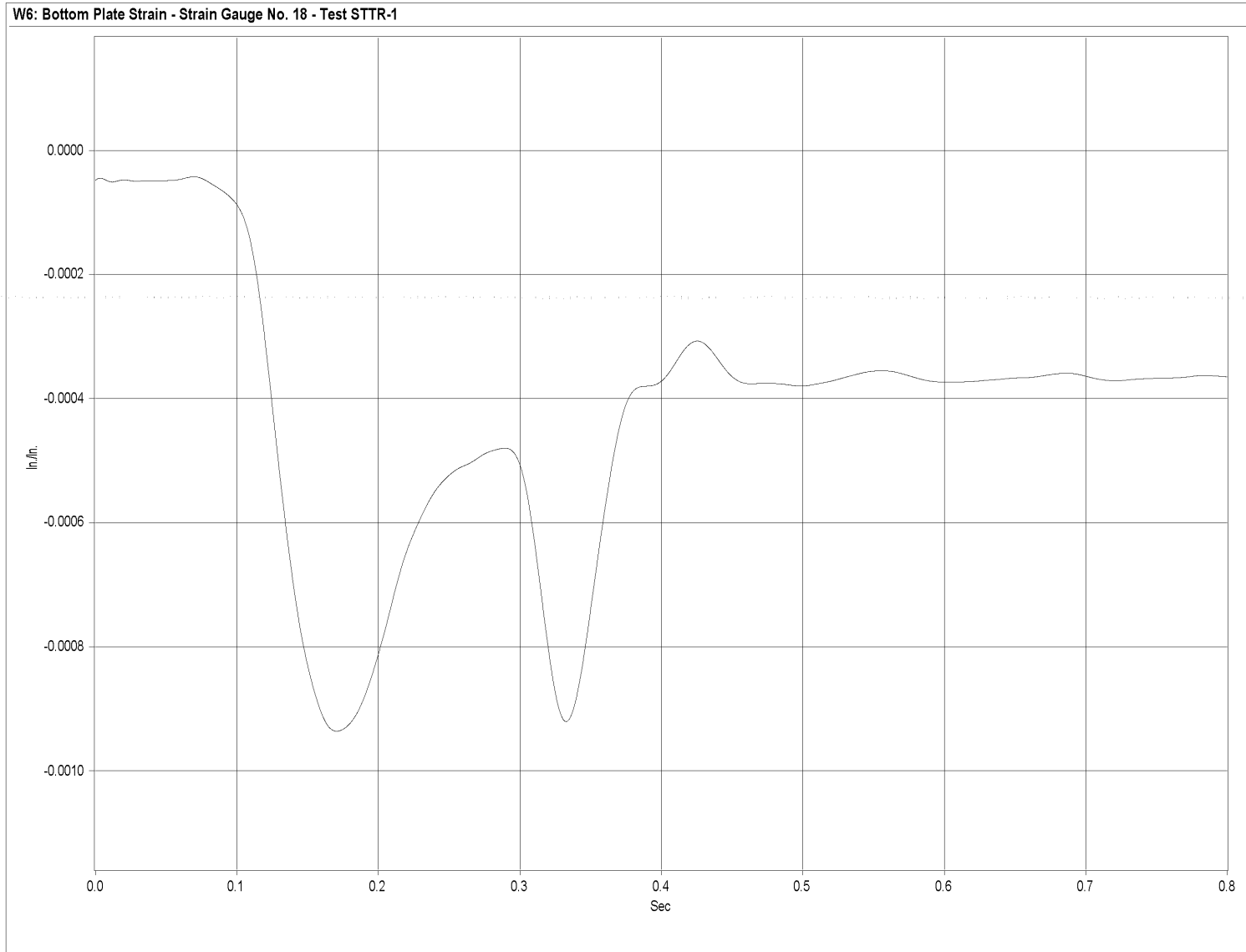


Figure R-20. Graph of Bottom Plate Post No. 7 - Middle and Perpendicular to Rail - Strain, Test STTR-1

425

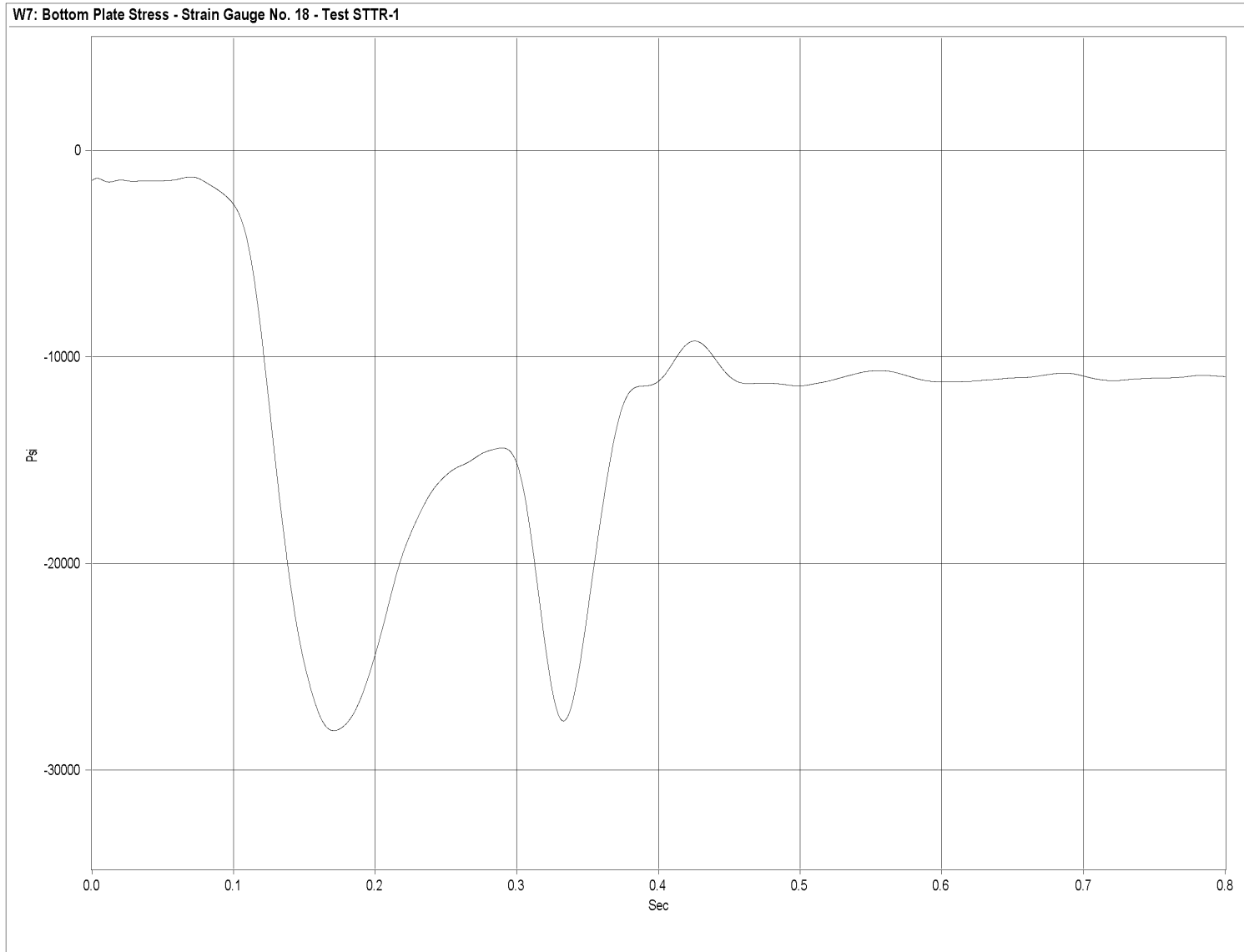


Figure R-21. Graph of Bottom Plate Post No. 7 - Middle and Perpendicular to Rail - Stress, Test STTR-1

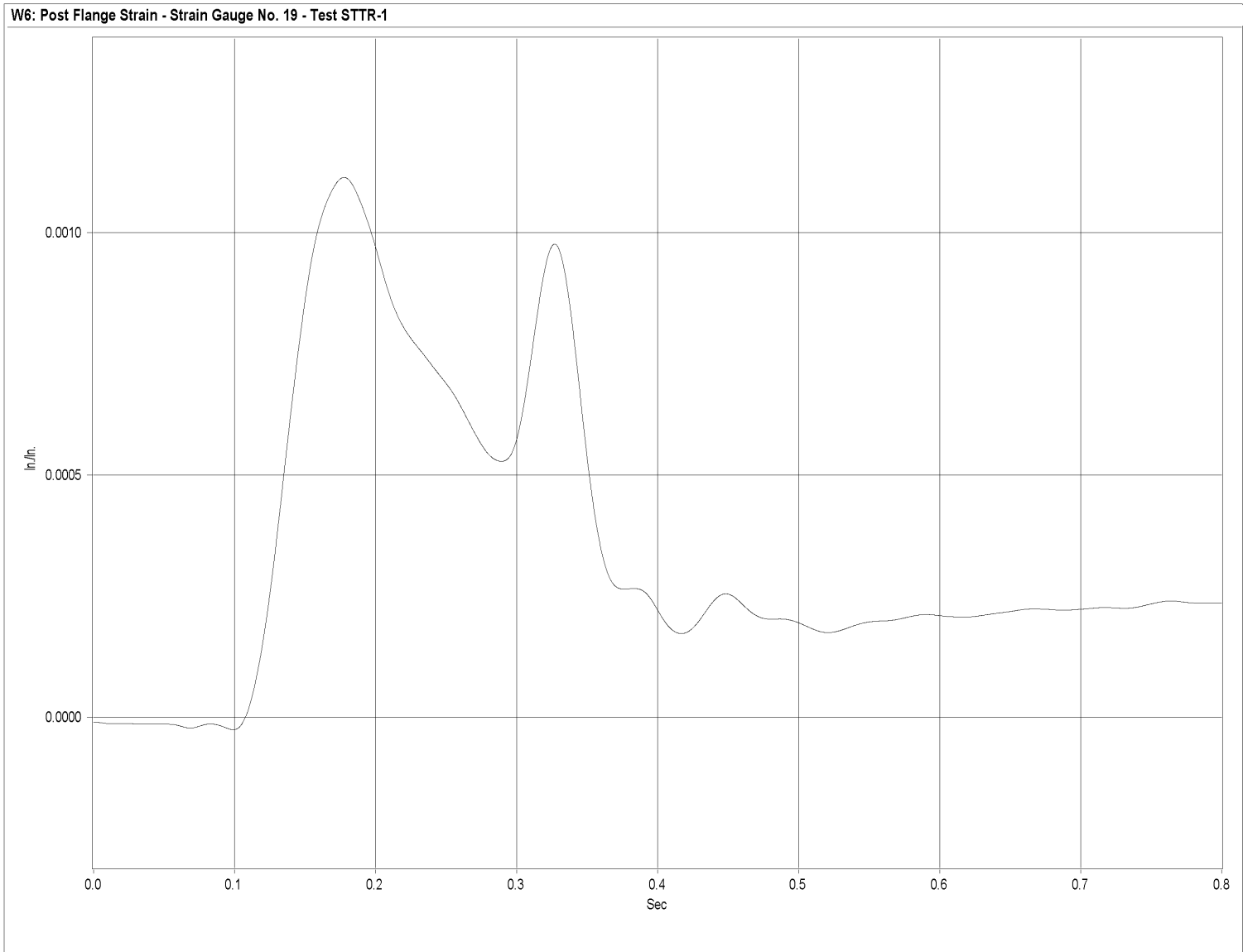


Figure R-22. Graph of Traffic-Side Flange Post No. 7 Strain, Test STTR-1

427

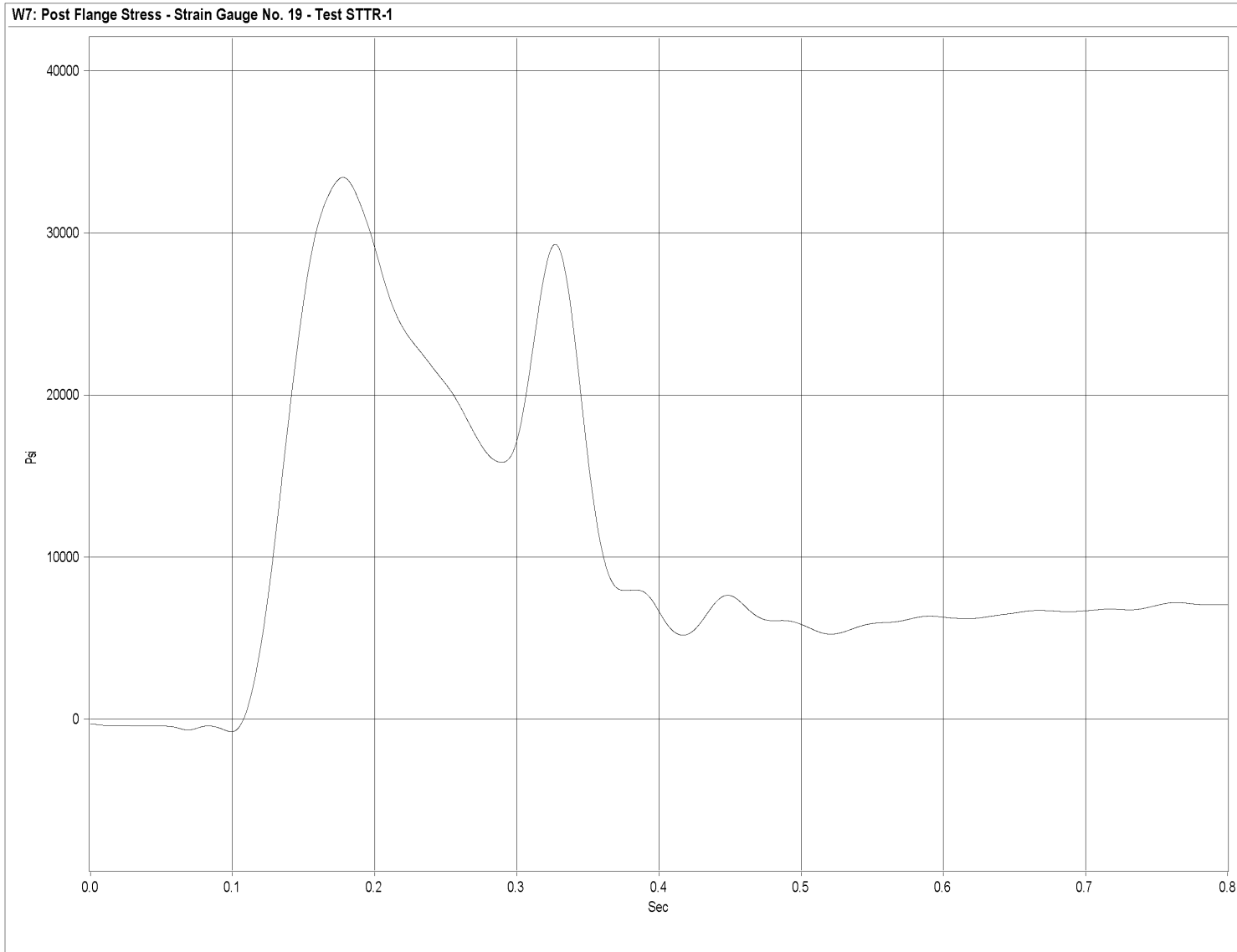


Figure R-23. Graph of Traffic-Side Flange Post No. 7 Stress, Test STTR-1

428

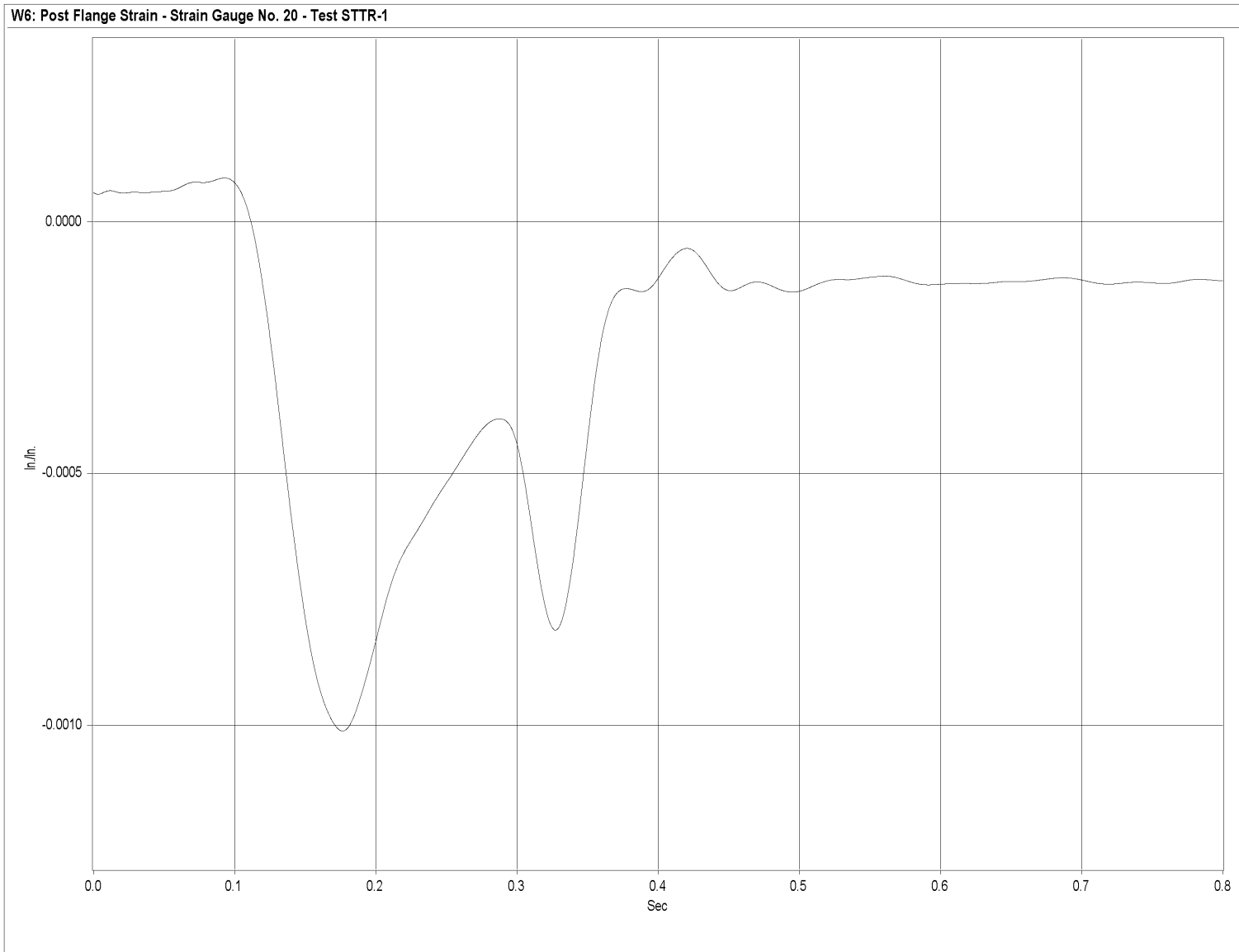


Figure R-24. Graph of Back-Side Flange Post No. 7 Strain, Test STTR-1

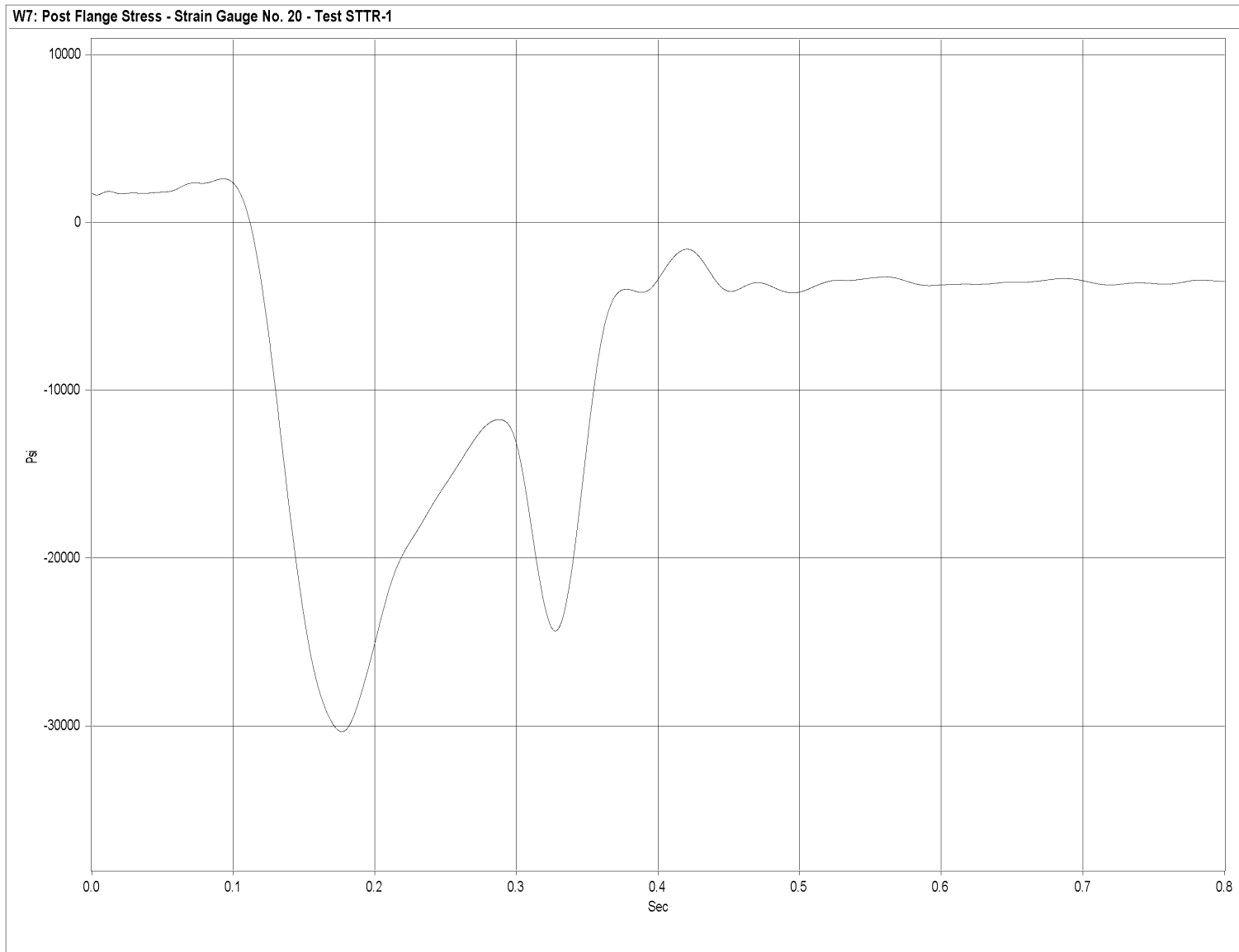


Figure R-25. Graph of Back-Side Flange Post No. 7 Stress, Test STTR-1

APPENDIX S

Accelerometer Data Analysis - Test STTR-2

Figure S-1. Graph of Longitudinal Deceleration, Test STTR-2

Figure S-2. Graph of Longitudinal Occupant Impact Velocity, Test STTR-2

Figure S-3. Graph of Longitudinal Occupant Displacement, Test STTR-2

Figure S-4. Graph of Lateral Deceleration, Test STTR-2

Figure S-5. Graph of Lateral Occupant Impact Velocity, Test STTR-2

Figure S-6. Graph of Lateral Occupant Displacement, Test STTR-2

431

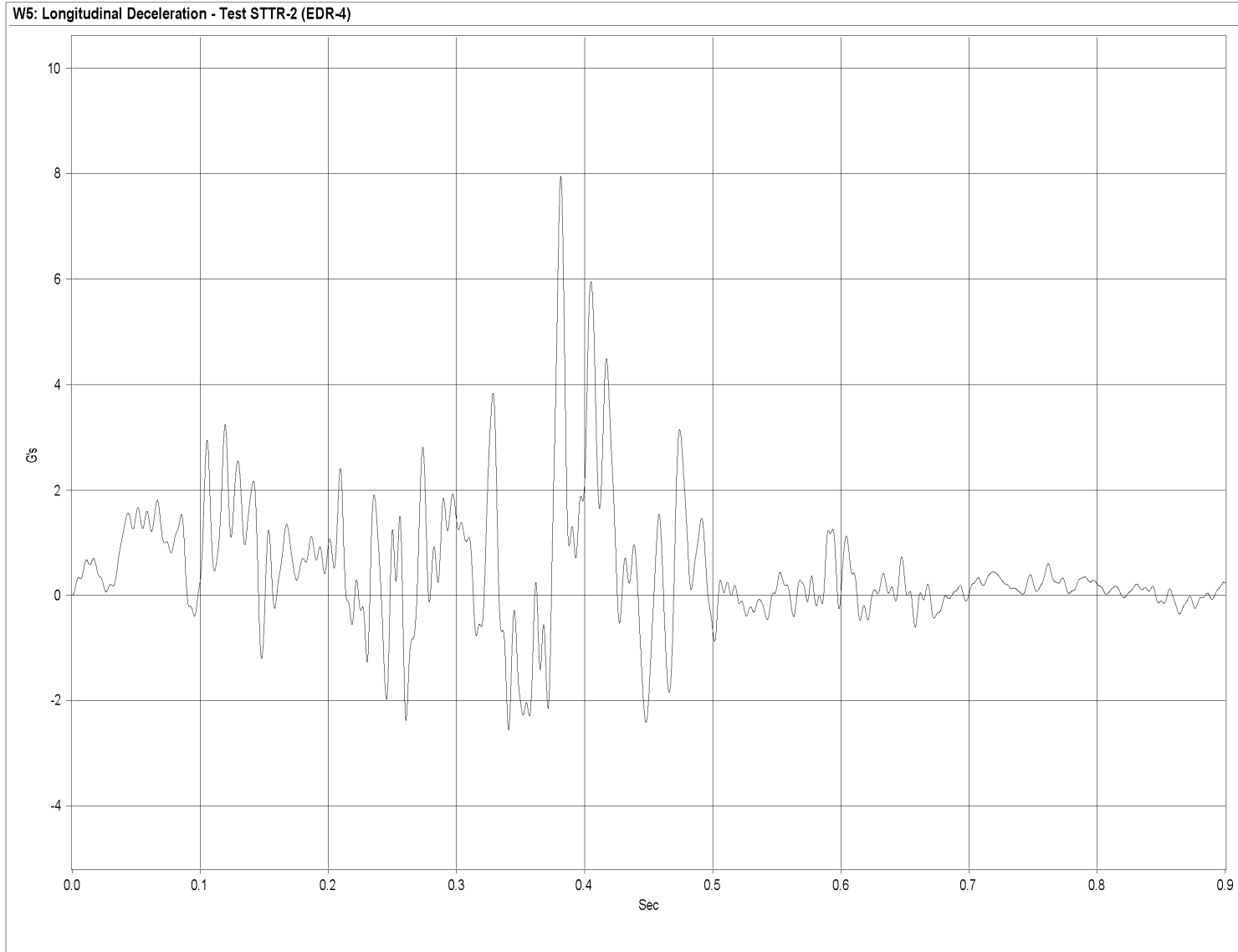


Figure S-1. Graph of Longitudinal Deceleration, Test STTR-2

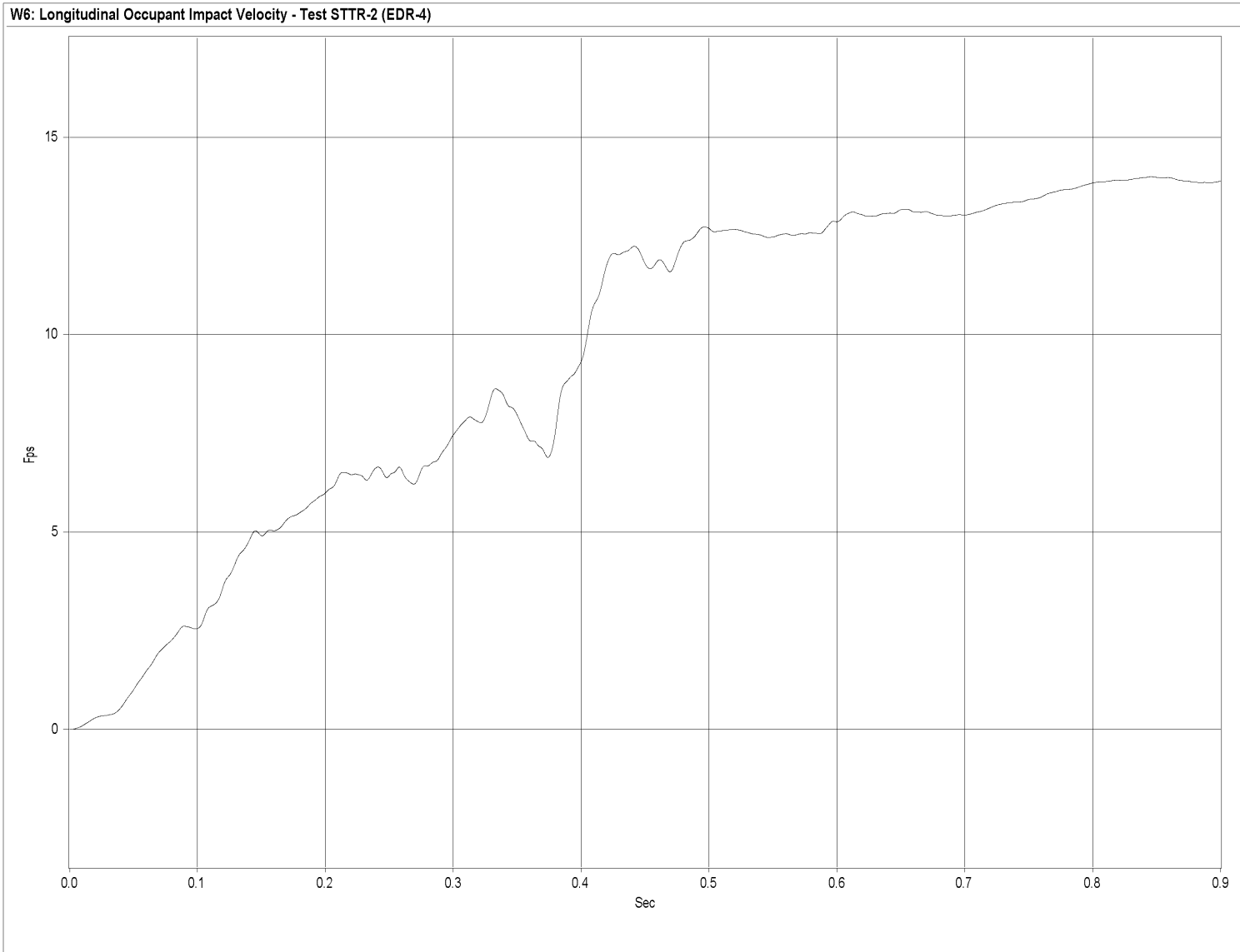


Figure S-2. Graph of Longitudinal Occupant Impact Velocity, Test STTR-2

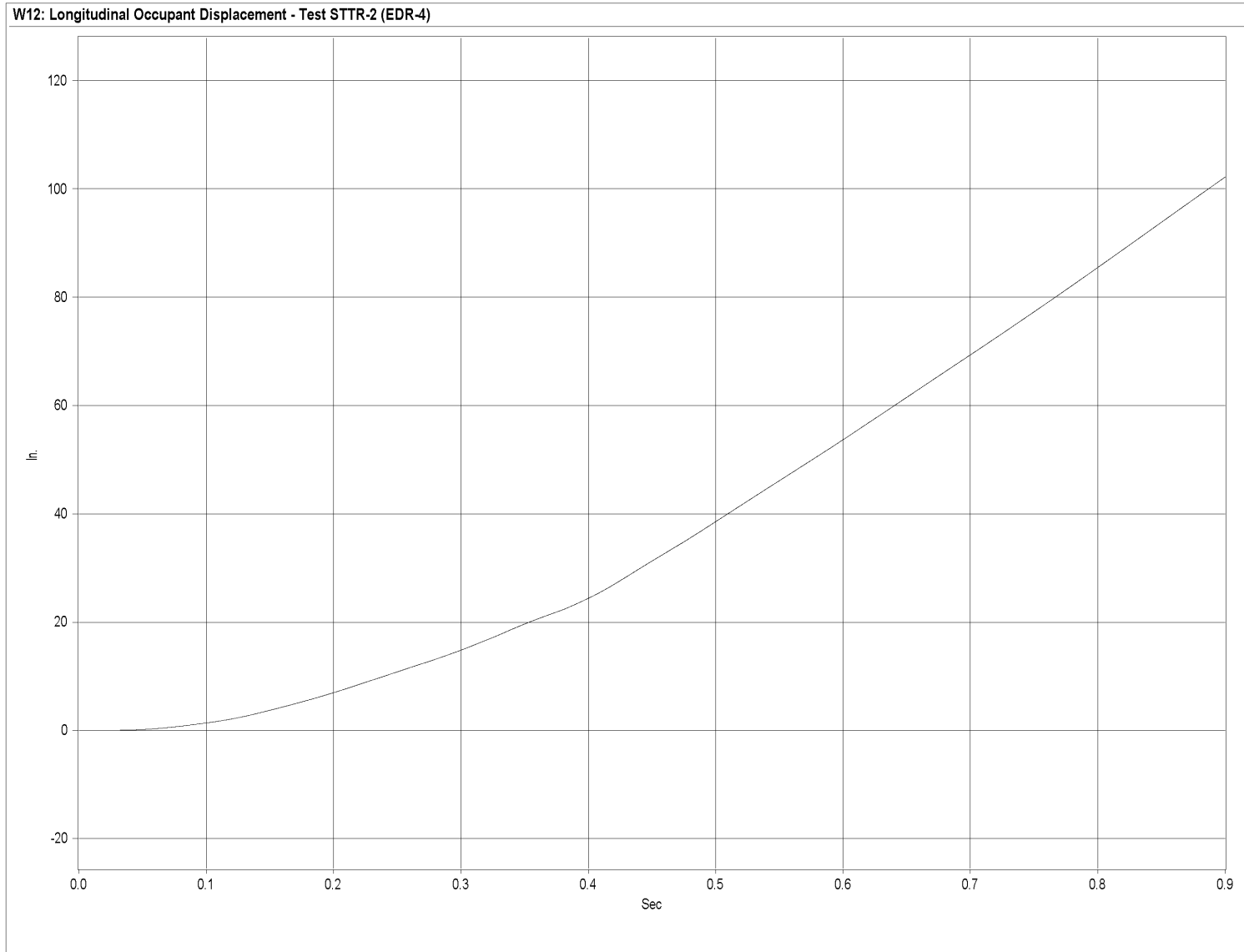


Figure S-3. Graph of Longitudinal Occupant Displacement, Test STTR-2

434

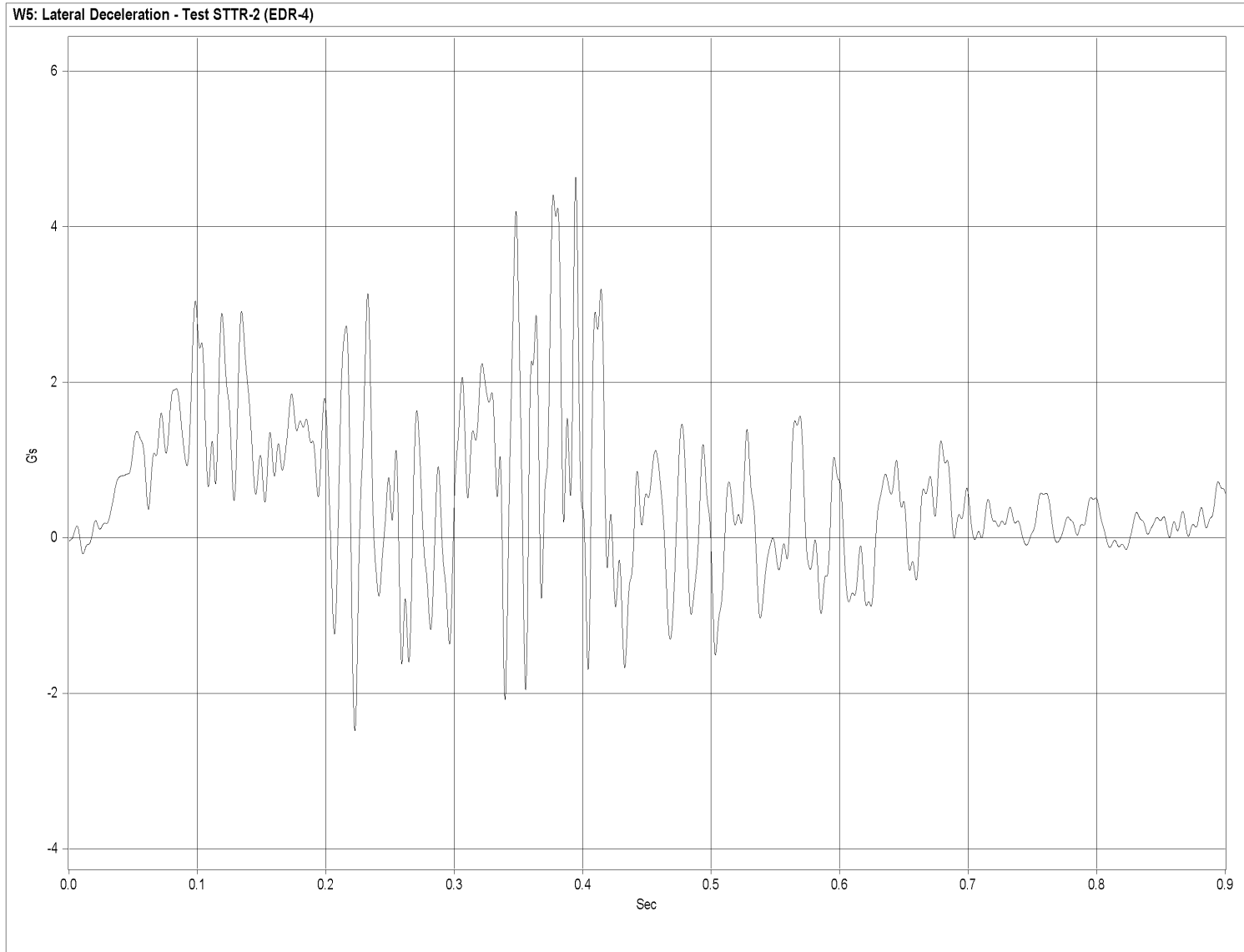


Figure S-4. Graph of Lateral Deceleration, Test STTR-2

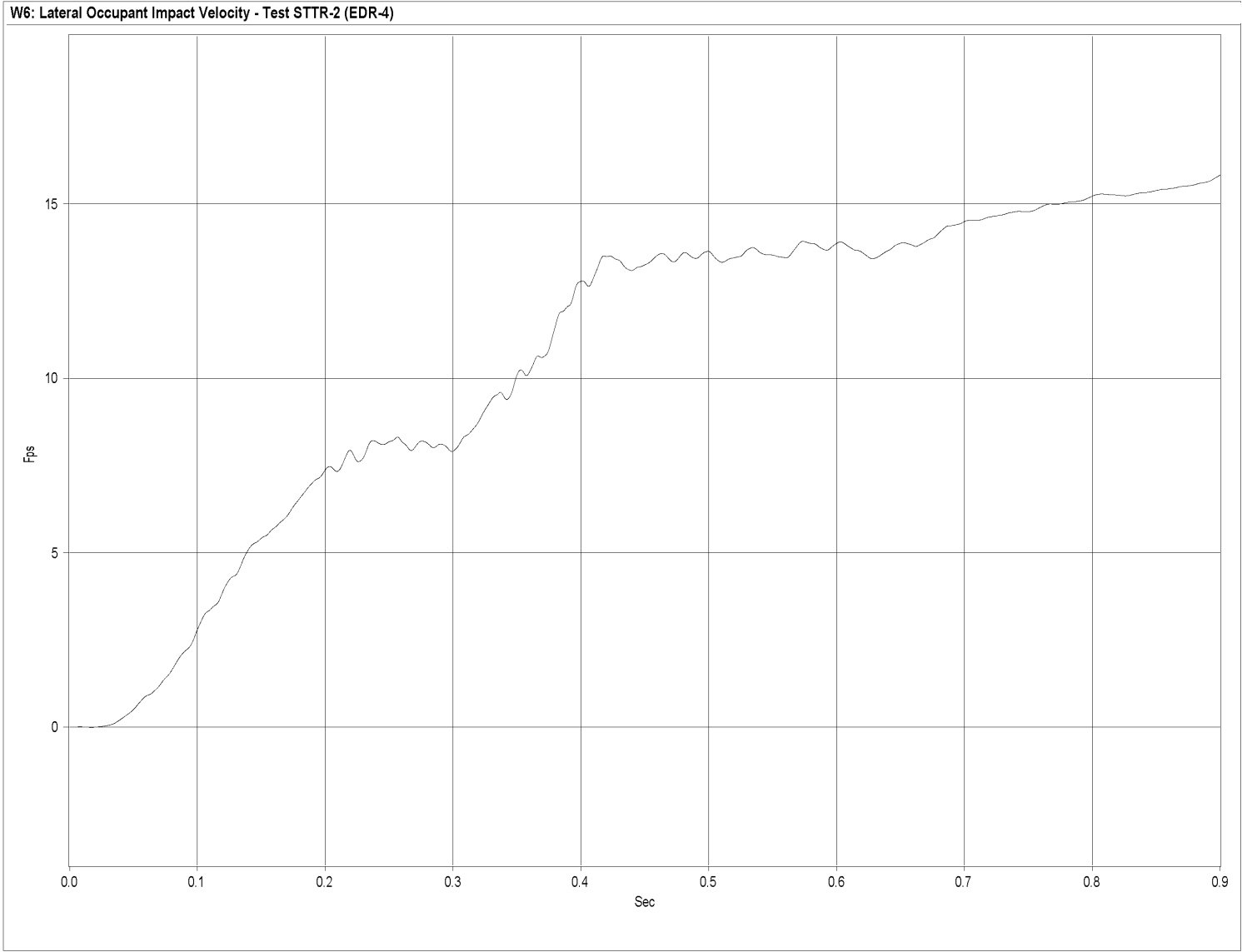


Figure S-5. Graph of Lateral Occupant Impact Velocity, Test STTR-2

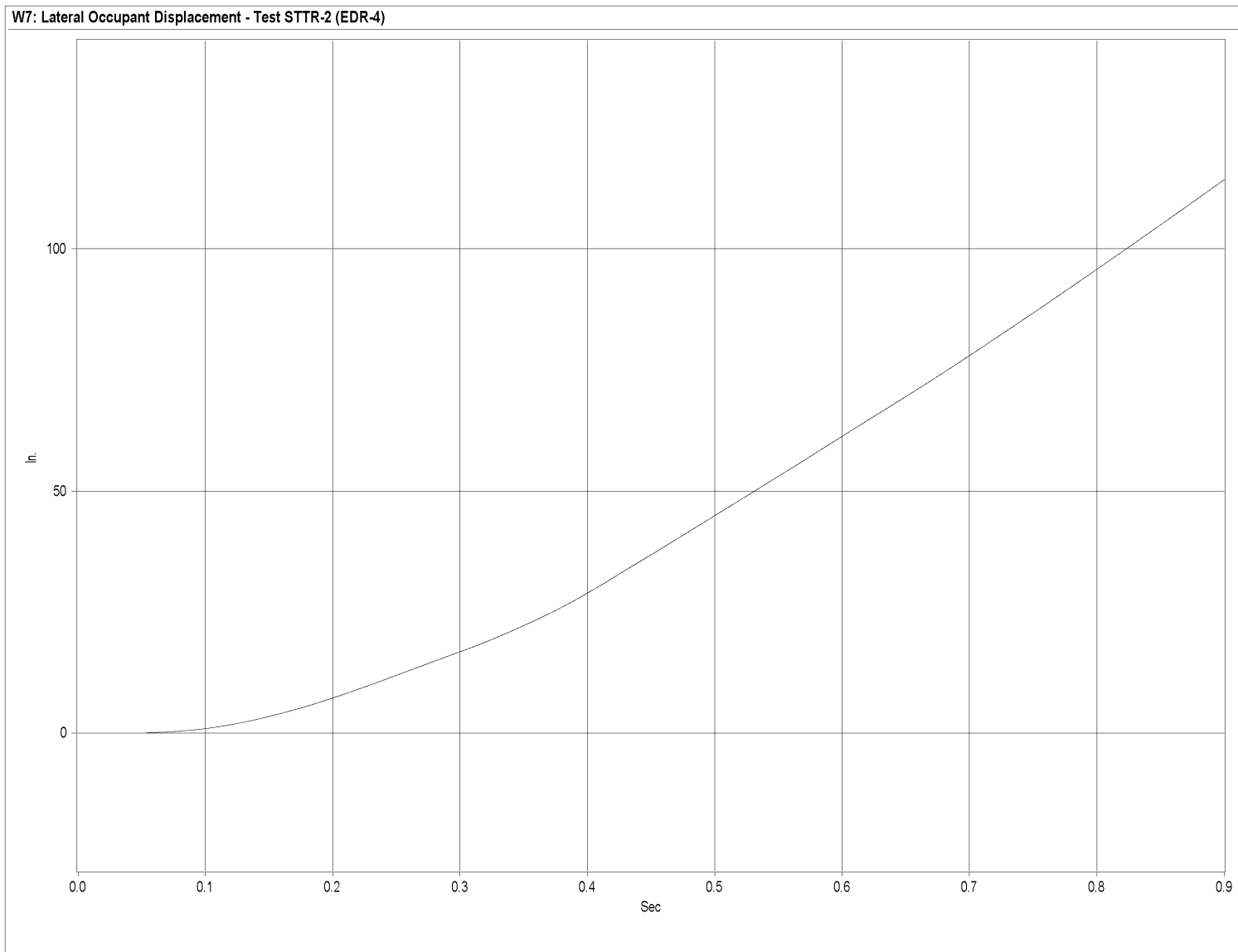


Figure S-6. Graph of Lateral Occupant Displacement, Test STTR-2

APPENDIX T

Rate Transducer Data Analysis - Test STTR-2

Figure T-1. Graph of Roll, Pitch, and Yaw Angular Displacements, Test STTR-2

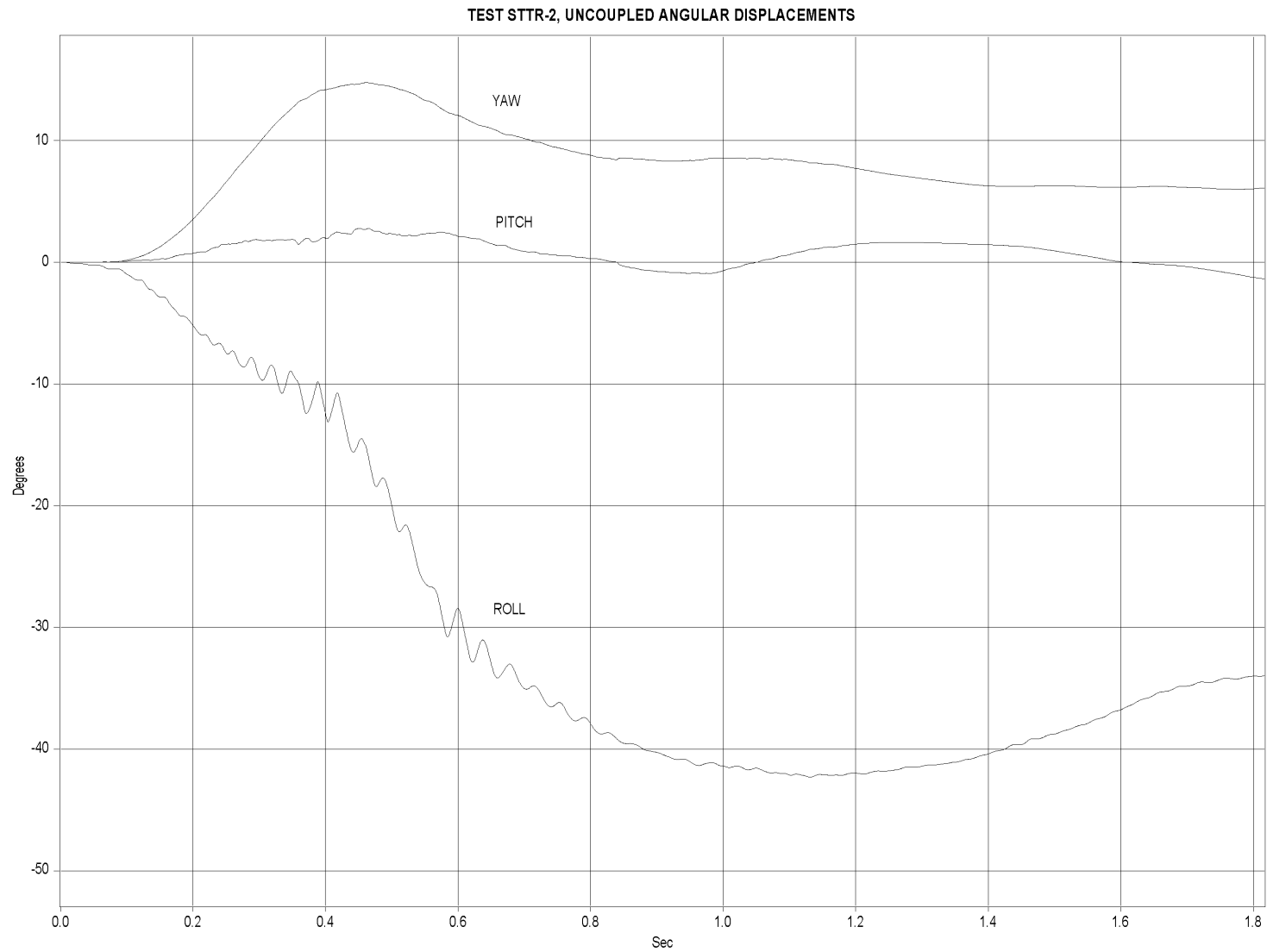


Figure T-1. Graph of Roll, Pitch, and Yaw Angular Displacements, Test STTR-2

APPENDIX U

Strain Gauge Data Analysis - Test STTR-2

Figure U-1. Graph of Post No. 5 Upstream-Side Bolt Strain, Test STTR-2

Figure U-2. Graph of Post No. 5 Upstream-Side Bolt Stress, Test STTR-2

Figure U-3. Graph of Post No. 5 Downstream-Side Bolt Strain, Test STTR-2

Figure U-4. Graph of Post No. 5 Downstream-Side Bolt Stress, Test STTR-2

Figure U-5. Graph of Top Plate Post No. 5 - Middle and Perpendicular to Rail - Strain, Test STTR-2

Figure U-6. Graph of Top Plate Post No. 5 - Middle and Perpendicular to Rail - Stress, Test STTR-2

Figure U-7. Graph of Bottom Plate Post No. 5 - Middle and Perpendicular to Rail - Strain,
Test STTR-2

Figure U-8. Graph of Bottom Plate Post No. 5 - Middle and Perpendicular to Rail - Stress,
Test STTR-2

Figure U-9. Graph of Post No. 6 Upstream-Side Bolt Strain, Test STTR-2

Figure U-10. Graph of Post No. 6 Upstream-Side Bolt Stress, Test STTR-2

Figure U-11. Graph of Post No. 6 Downstream-Side Bolt Strain, Test STTR-2

Figure U-12. Graph of Post No. 6 Downstream-Side Bolt Stress, Test STTR-2

Figure U-13. Graph of Traffic-Side Flange Post No. 6 Strain, Test STTR-2

Figure U-14. Graph of Back-Side Flange Post No. 6 Strain, Test STTR-2

Figure U-15. Graph of Back-Side Flange Post No. 6 Stress, Test STTR-2

Figure U-16. Graph of Top Plate Post No. 6 - Middle and Perpendicular to Rail - Strain,
Test STTR-2

Figure U-17. Graph of Top Plate Post No. 6 - Middle and Perpendicular to Rail - Stress,
Test STTR-2

Figure U-18. Graph of Bottom Plate Post No. 6 - Middle and Perpendicular to Rail - Strain,

Test STTR-2

Figure U-19. Graph of Top Plate Post No. 6 - Upstream and Perpendicular to Rail - Strain, Test STTR-2

Figure U-20. Graph of Top Plate Post No. 6 - Upstream and Perpendicular to Rail - Stress, Test STTR-2

Figure U-21. Graph of Top Plate Post No. 6 - Downstream and Perpendicular to Rail - Strain, Test STTR-2

Figure U-22. Graph of Top Plate Post No. 6 - Downstream and Perpendicular to Rail - Stress, Test STTR-2

Figure U-23. Graph of Top Plate Post No. 6 - Middle Upstream and Perpendicular to Rail - Strain, Test STTR-2

Figure U-24. Graph of Top Plate Post No. 6 - Middle Upstream and Perpendicular to Rail - Stress, Test STTR-2

Figure U-25. Graph of Top Plate Post No. 6 - Middle Downstream and Perpendicular to Rail - Strain, Test STTR-2

Figure U-26. Graph of Top Plate Post No. 6 - Middle Downstream and Perpendicular to Rail - Stress, Test STTR-2

Figure U-27. Graph of Post No. 7 Upstream-Side Bolt Strain, Test STTR-2

Figure U-28. Graph of Post No. 7 Upstream-Side Bolt Stress, Test STTR-2

Figure U-29. Graph of Post No. 7 Downstream-Side Bolt Strain, Test STTR-2

Figure U-30. Graph of Post No. 7 Downstream-Side Bolt Stress, Test STTR-2

Figure U-31. Graph of Top Plate Post No. 7 - Middle and Perpendicular to Rail - Strain, Test STTR-2

Figure U-32. Graph of Top Plate Post No. 7 - Middle and Perpendicular to Rail - Stress, Test STTR-2

Figure U-33. Graph of Bottom Plate Post No. 7 - Middle and Perpendicular to Rail - Strain, Test STTR-2

Figure U-34. Graph of Bottom Plate Post No. 7 - Middle and Perpendicular to Rail - Stress,

Test STTR-2

Figure U-35. Graph of Back-Side Steel Tube Rail at Midspan Between Post Nos. 6 and 7 Strain, Test STTR-2

Figure U-36. Graph of Back-Side Steel Tube Rail at Midspan Between Post Nos. 6 and 7 Stress, Test STTR-2

Figure U-37. Graph of Bottom-Side Steel Tube Rail at Midspan Between Post Nos. 6 and 7 Strain, Test STTR-2

Figure U-38. Graph of Bottom-Side Steel Tube Rail at Midspan Between Post Nos. 6 and 7 Stress, Test STTR-2

442

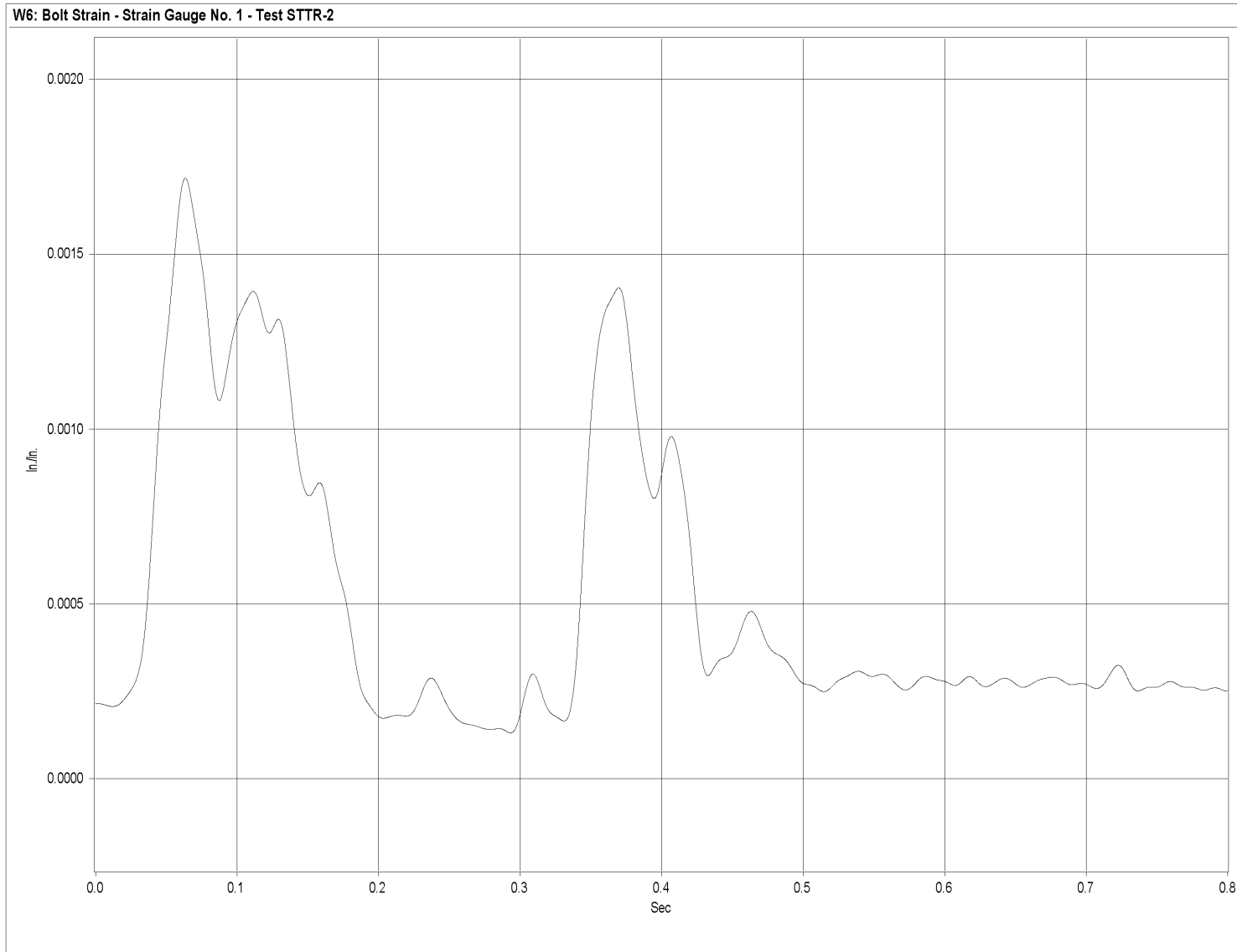


Figure U-1. Graph of Post No. 5 Upstream-Side Bolt Strain, Test STTR-2

443

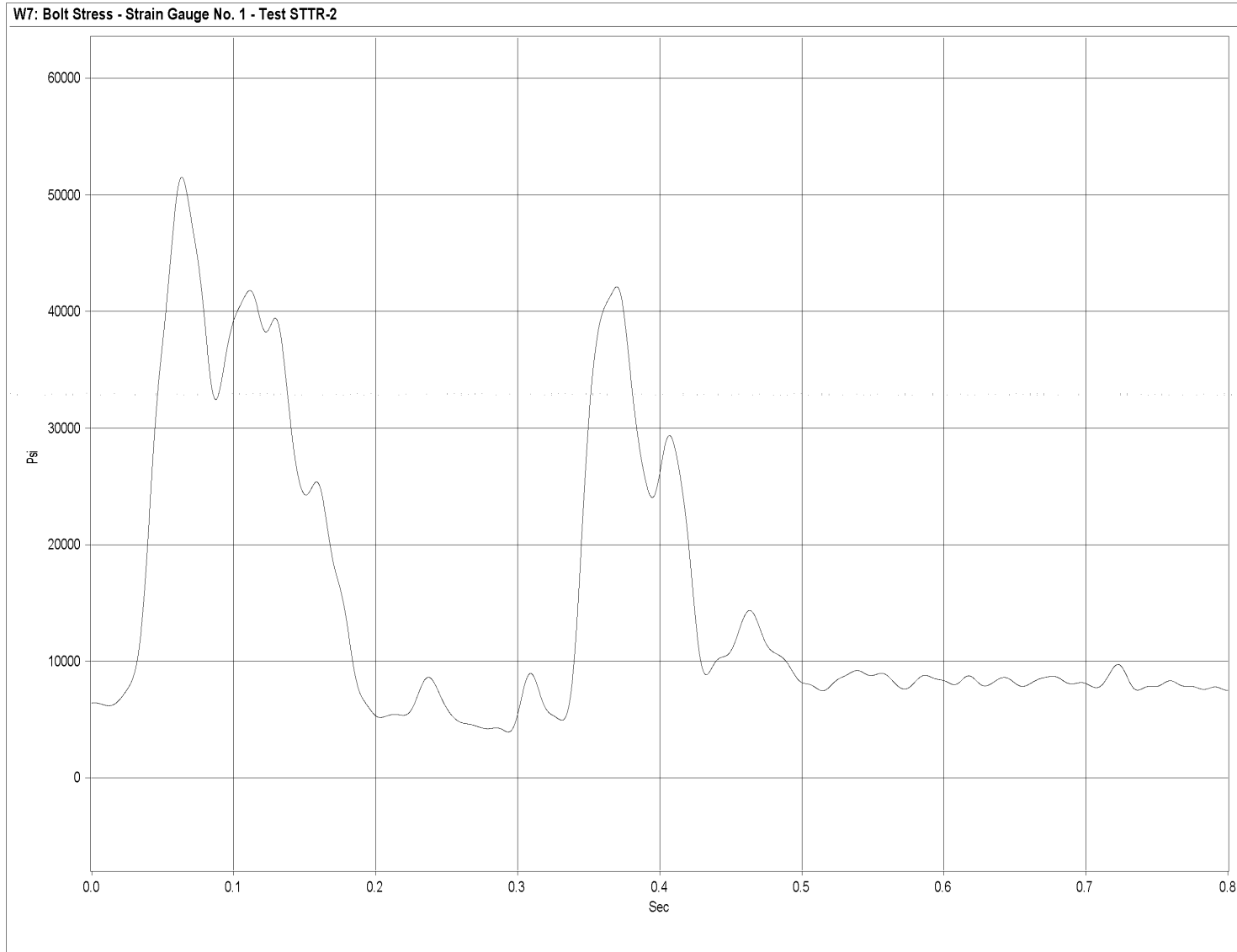


Figure U-2. Graph of Post No. 5 Upstream-Side Bolt Stress, Test STTR-2

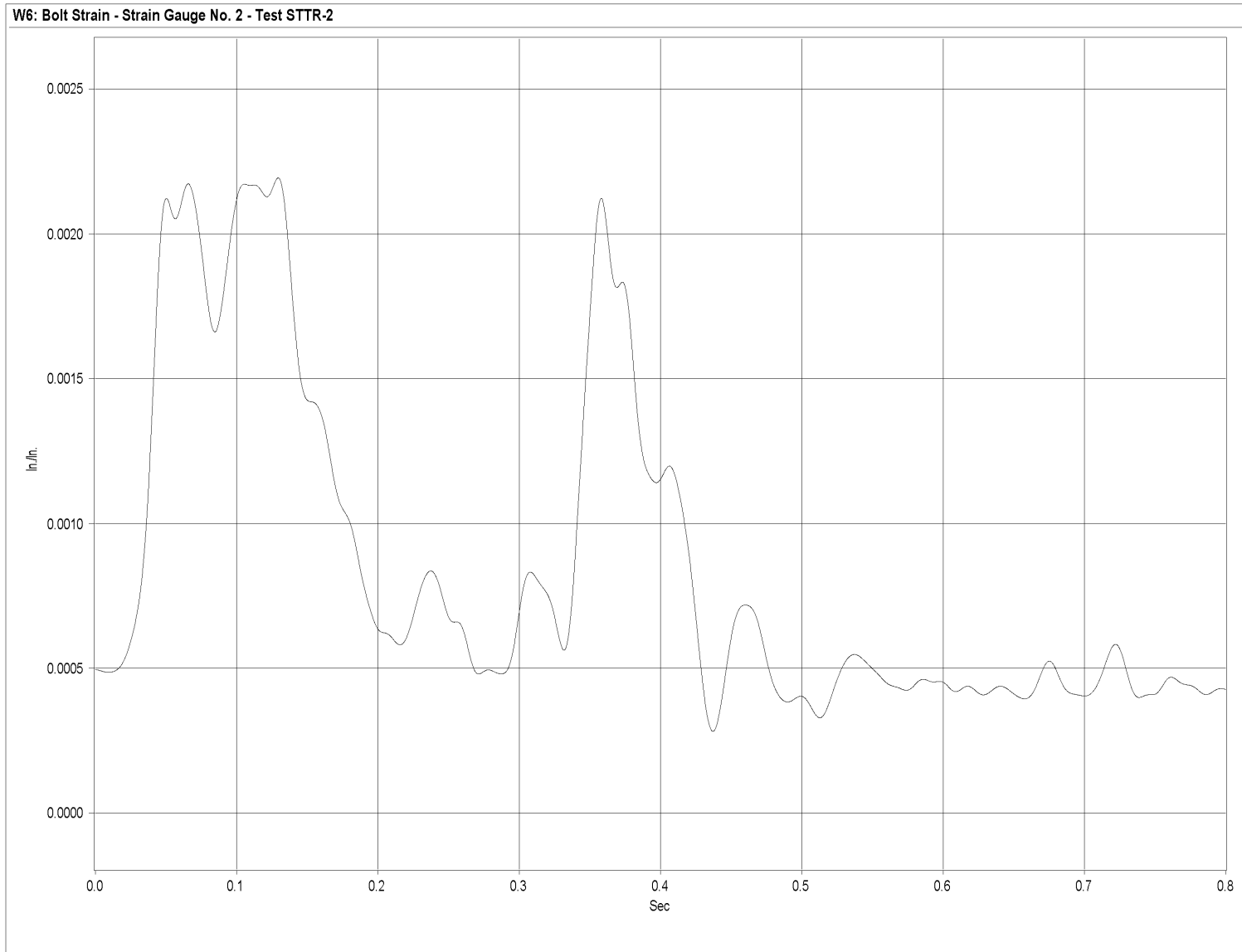


Figure U-3. Graph of Post No. 5 Downstream-Side Bolt Strain, Test STTR-2

445

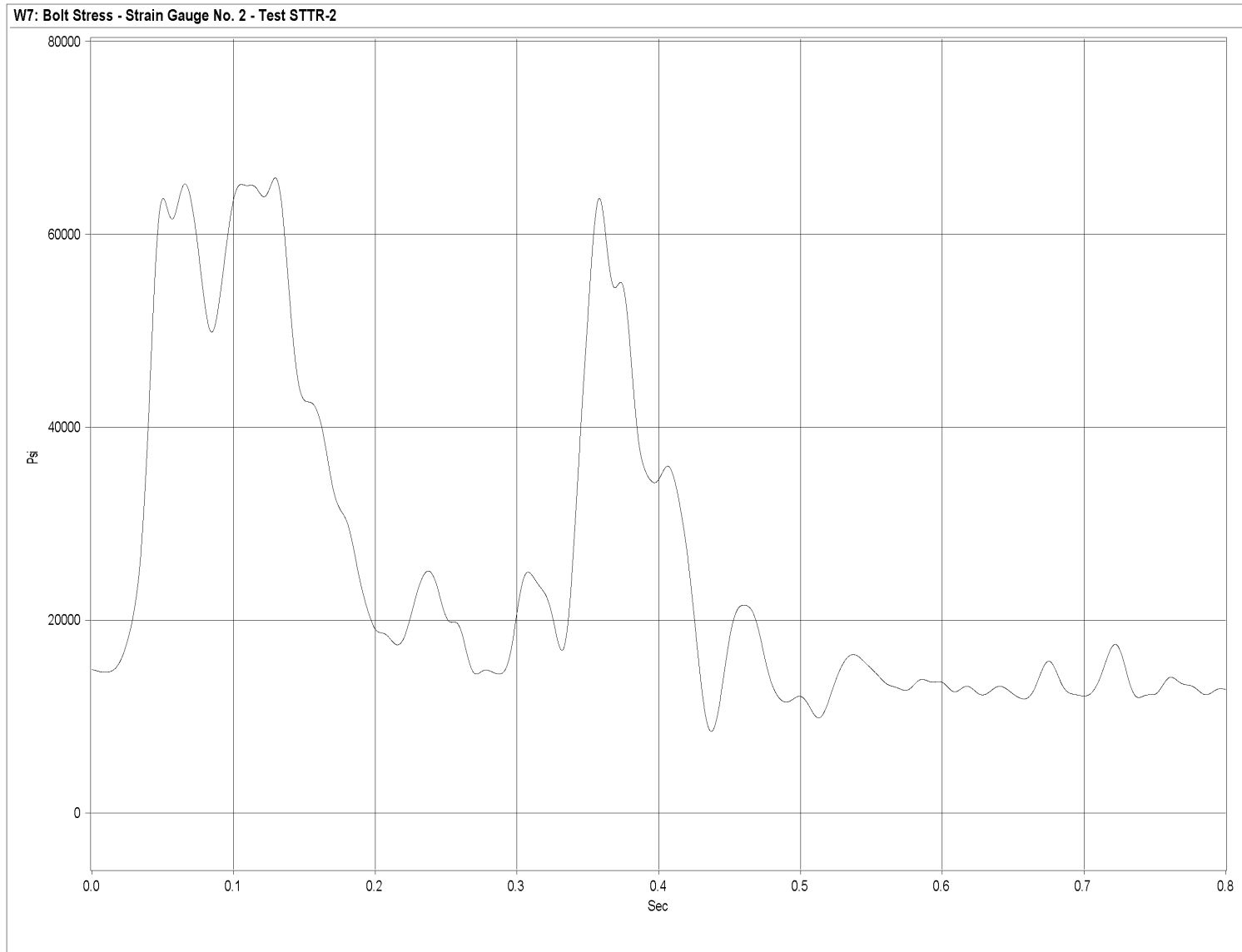


Figure U-4. Graph of Post No. 5 Downstream-Side Bolt Stress, Test STTR-2

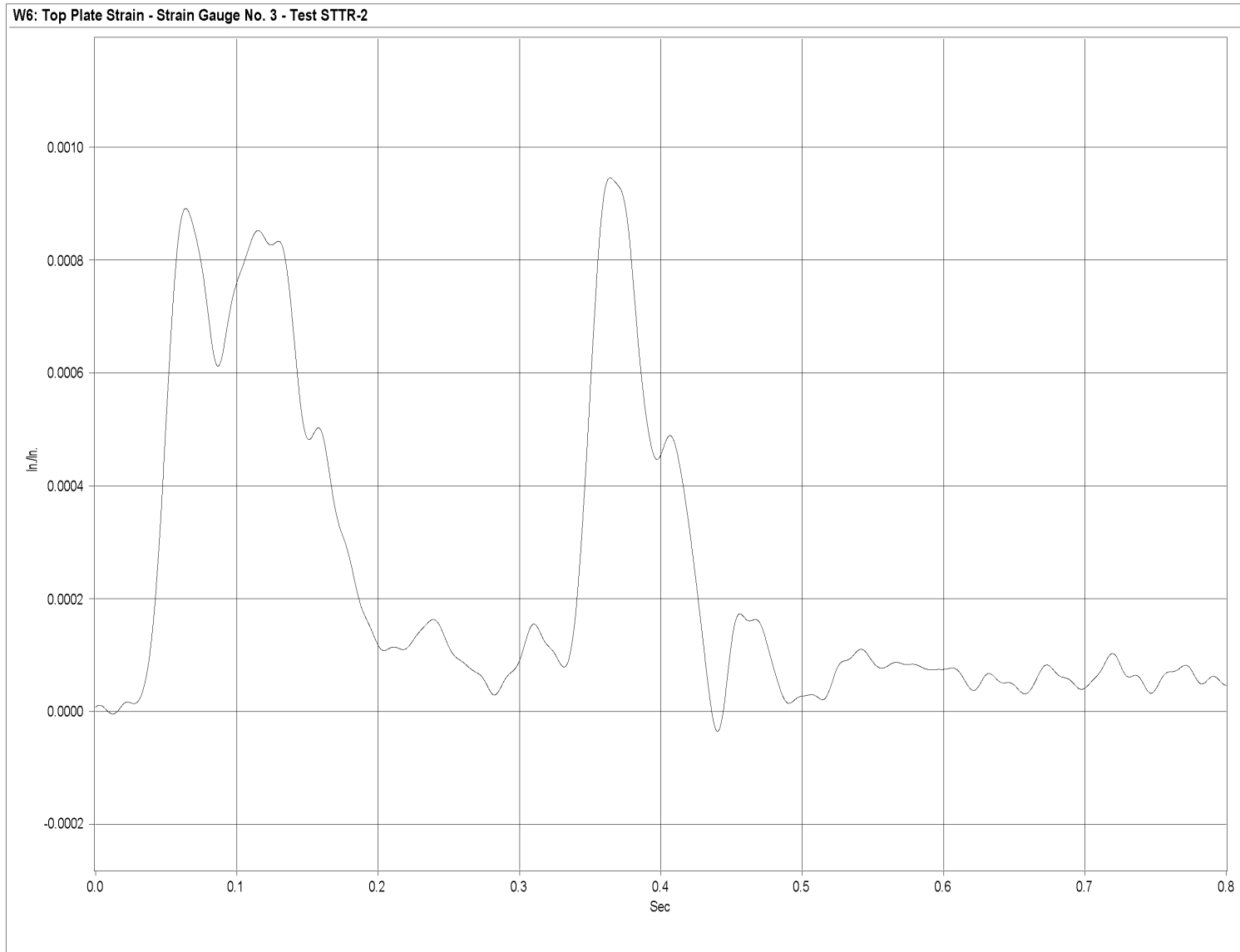


Figure U-5. Graph of Top Plate Post No. 5 - Middle and Perpendicular to Rail - Strain, Test STTR-2

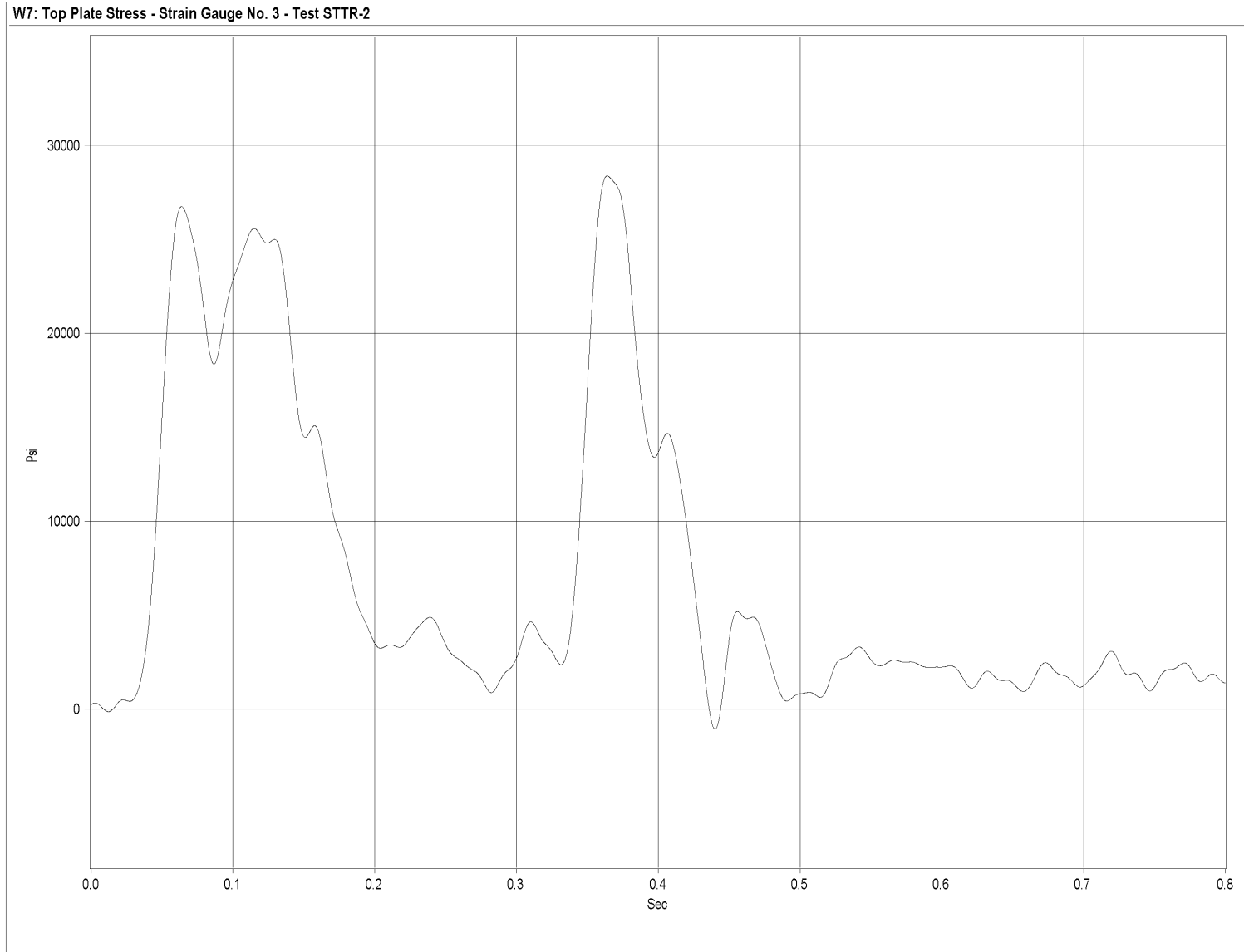


Figure U-6. Graph of Top Plate Post No. 5 - Middle and Perpendicular to Rail - Stress, Test STTR-2

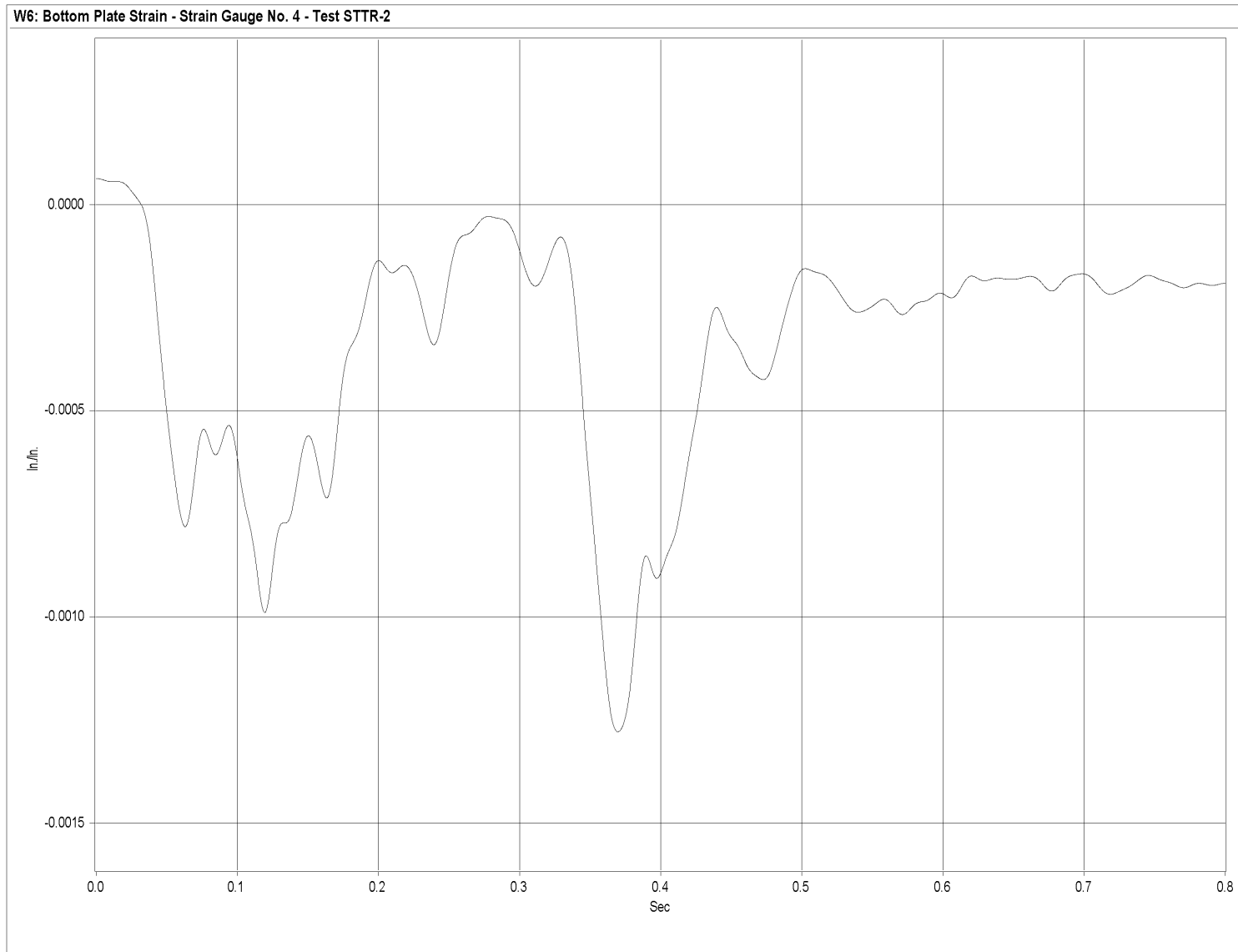


Figure U-7. Graph of Bottom Plate Post No. 5 - Middle and Perpendicular to Rail - Strain, Test STTR-2

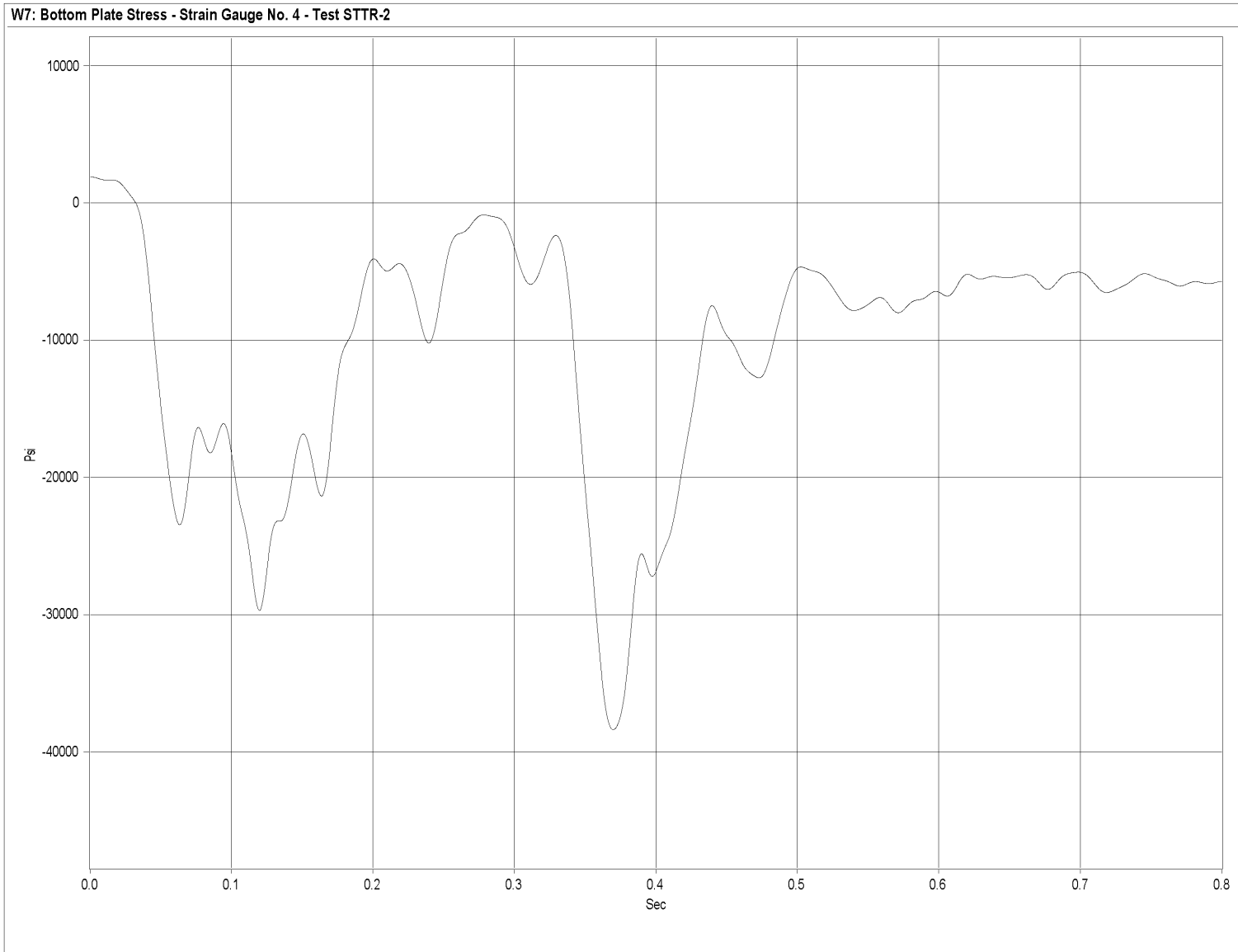


Figure U-8. Graph of Bottom Plate Post No. 5 - Middle and Perpendicular to Rail - Stress, Test STTR-2

450

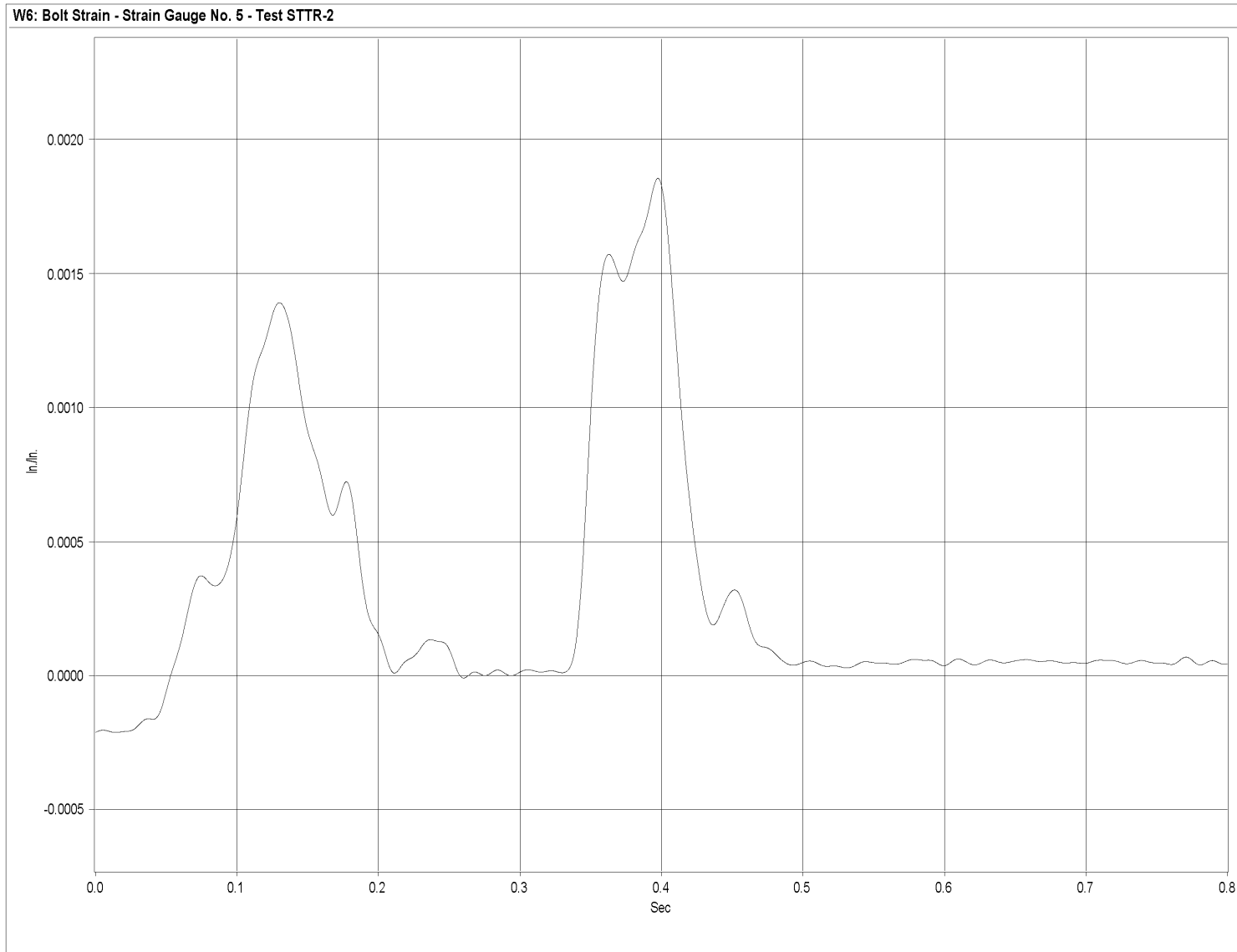


Figure U-9. Graph of Post No. 6 Upstream-Side Bolt Strain, Test STTR-2

451

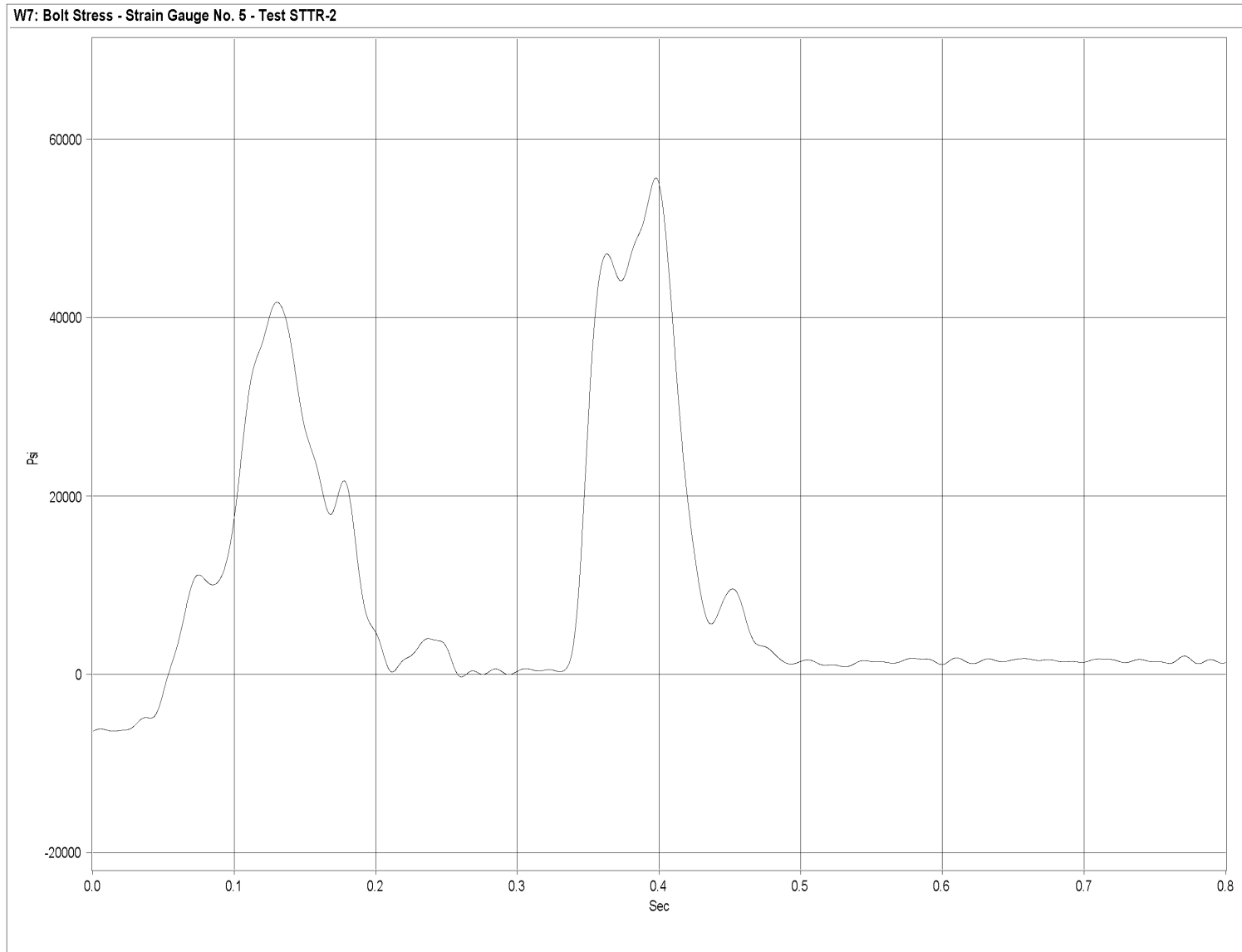


Figure U-10. Graph of Post No. 6 Upstream-Side Bolt Stress, Test STTR-2

452

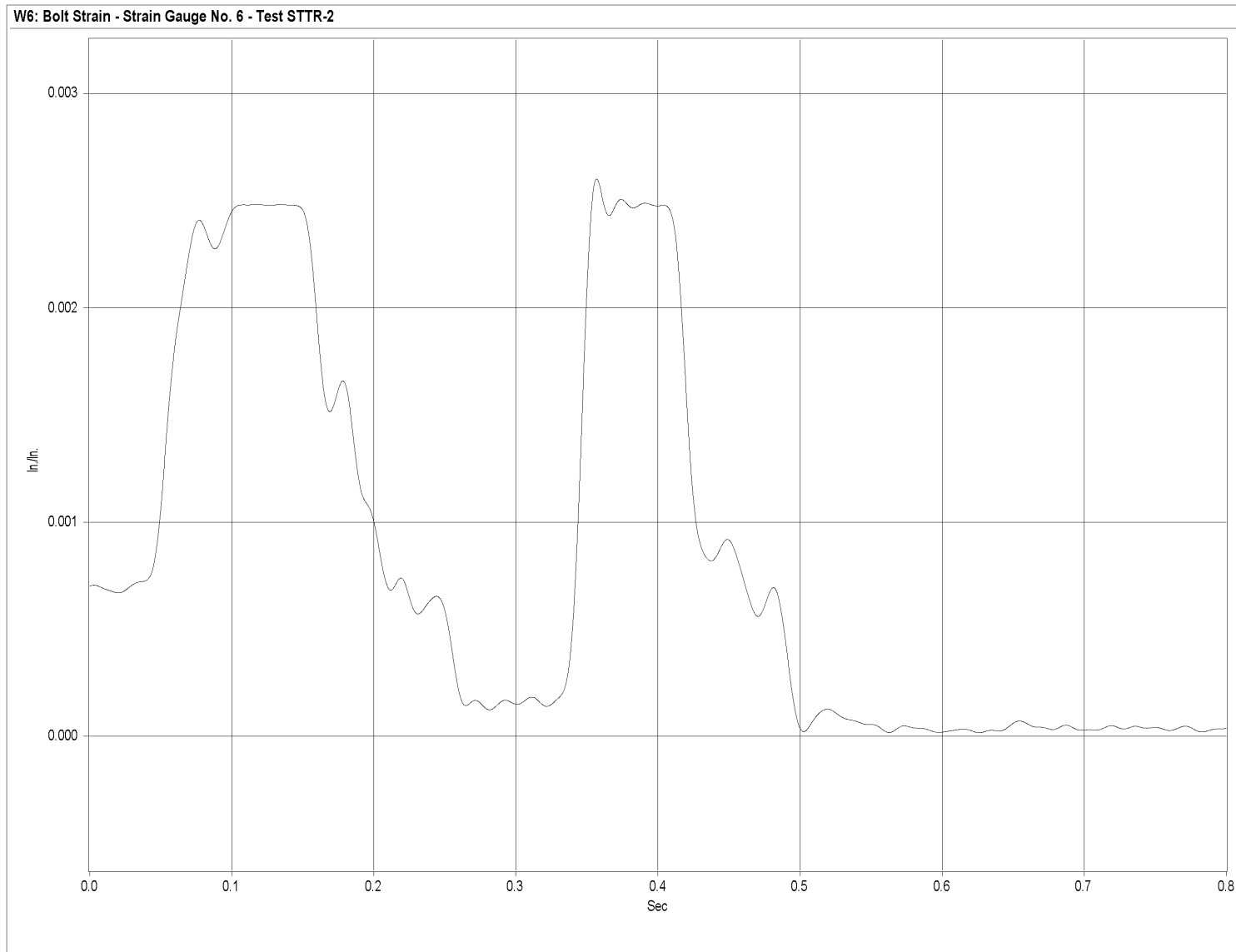


Figure U-11. Graph of Post No. 6 Downstream-Side Bolt Strain, Test STTR-2

453

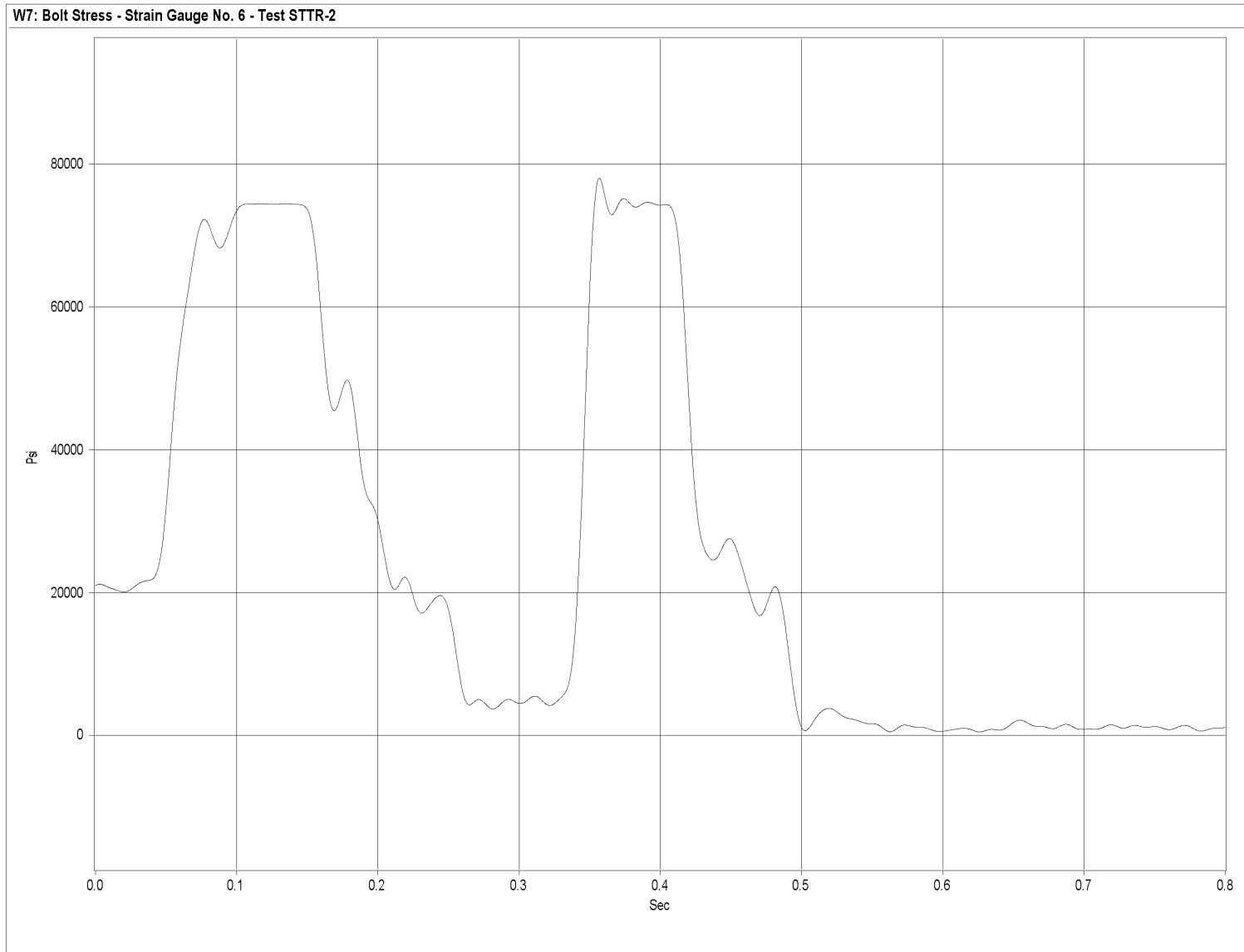


Figure U-12. Graph of Post No. 6 Downstream-Side Bolt Stress, Test STTR-2

454

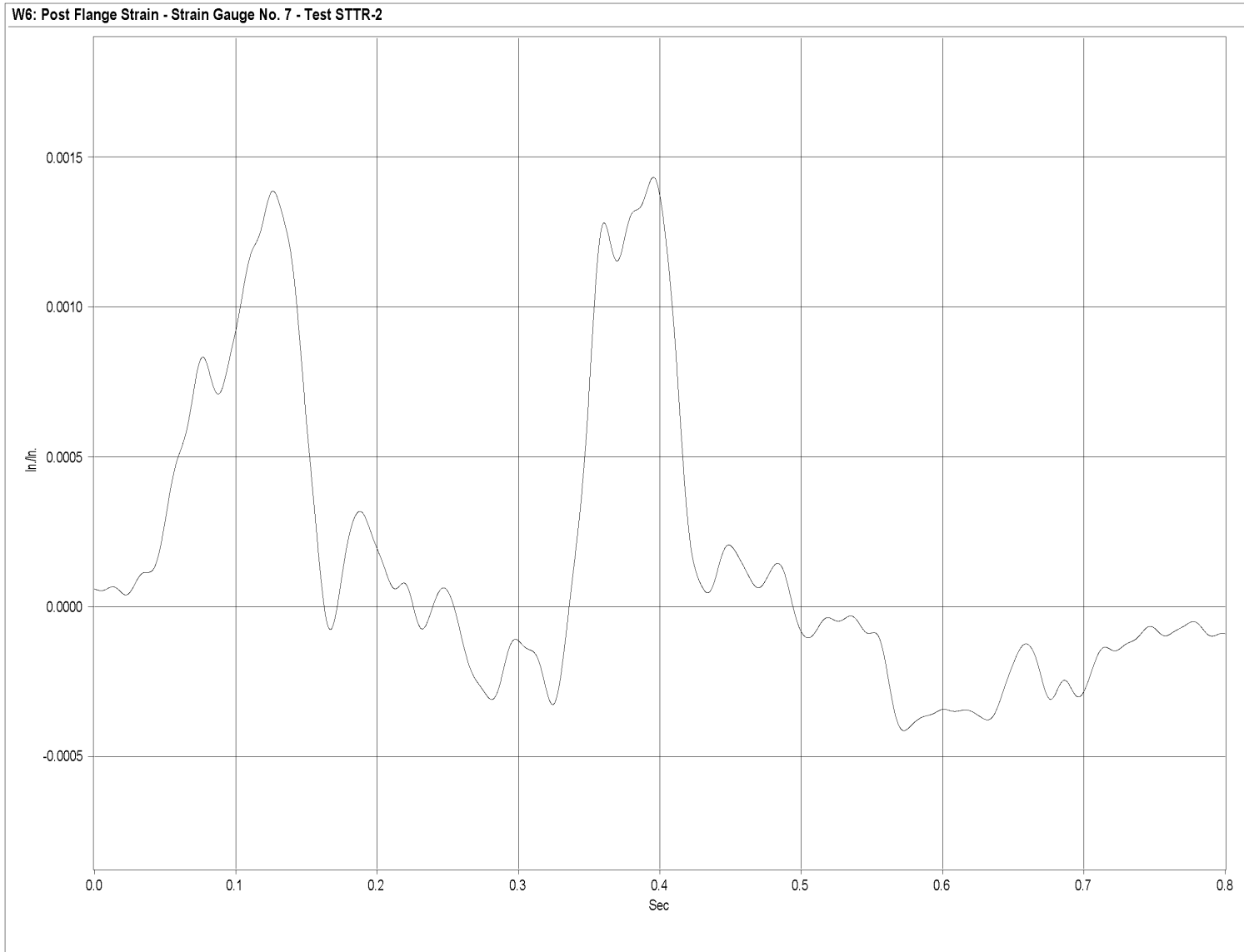


Figure U-13. Graph of Traffic-Side Flange Post No. 6 Strain, Test STTR-2

455

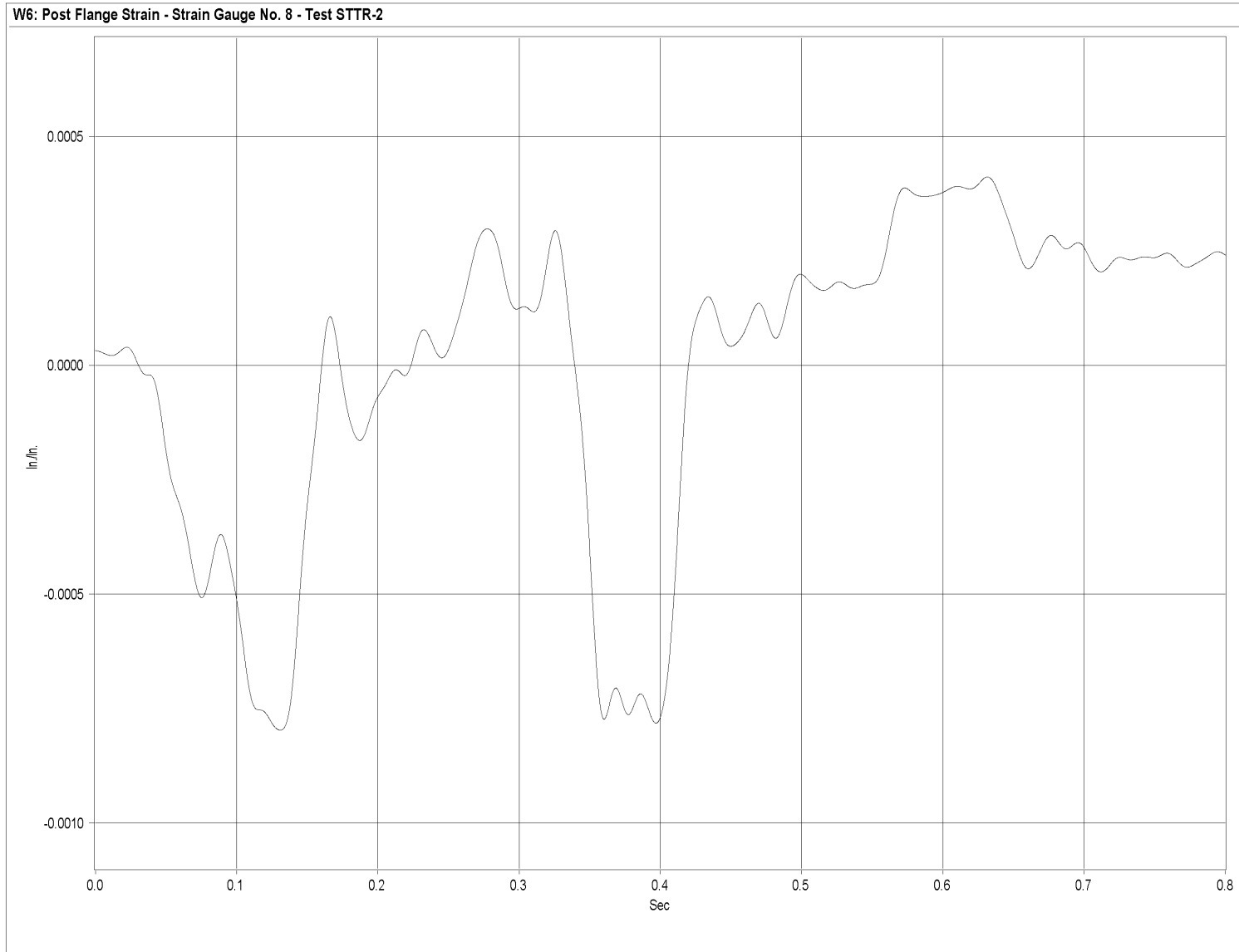


Figure U-14. Graph of Back-Side Flange Post No. 6 Strain, Test STTR-2

456

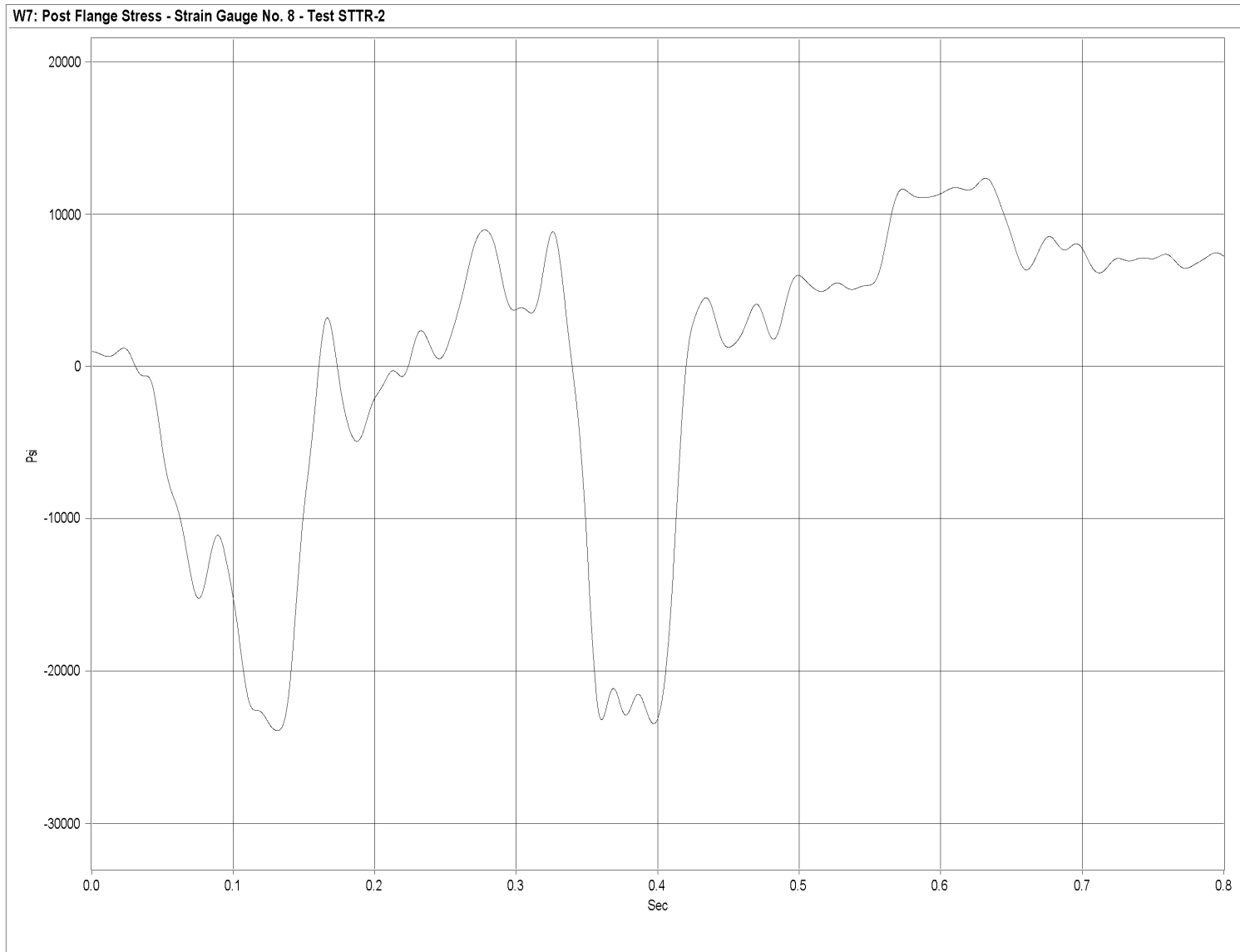


Figure U-15. Graph of Back-Side Flange Post No. 6 Stress, Test STTR-2

457

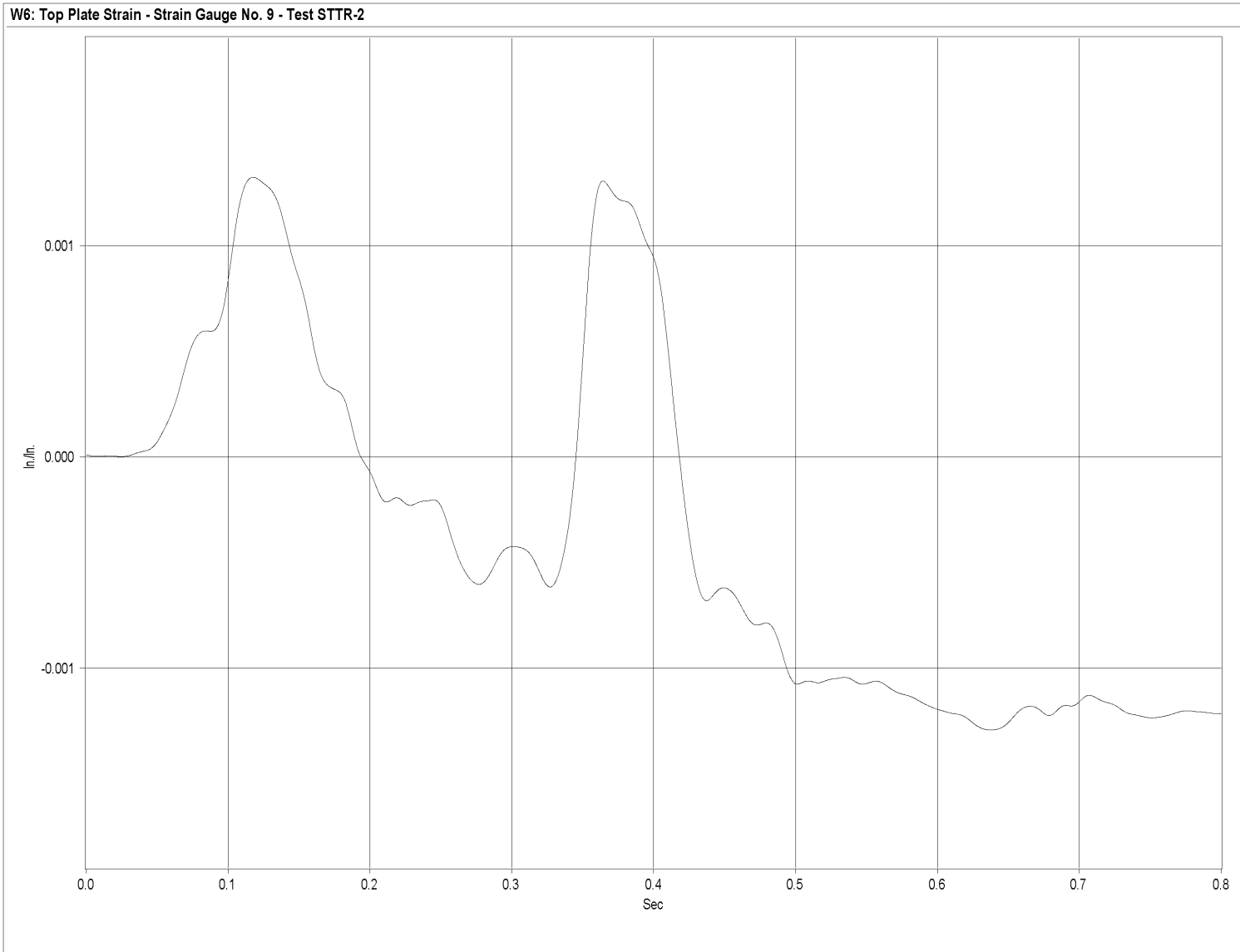


Figure U-16. Graph of Top Plate Post No. 6 - Middle and Perpendicular to Rail - Strain, Test STTR-2

458

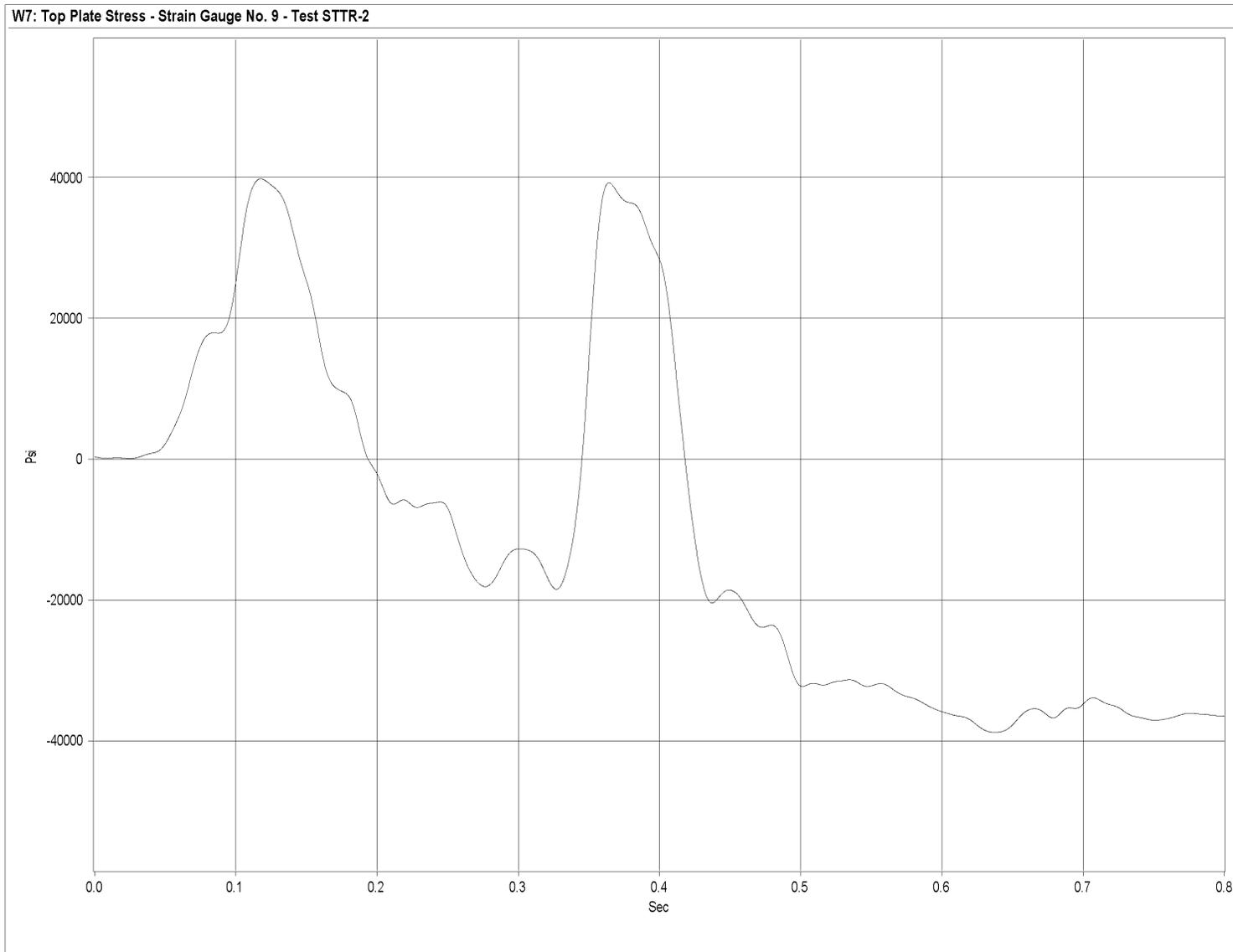


Figure U-17. Graph of Top Plate Post No. 6 - Middle and Perpendicular to Rail - Stress, Test STTR-2

459

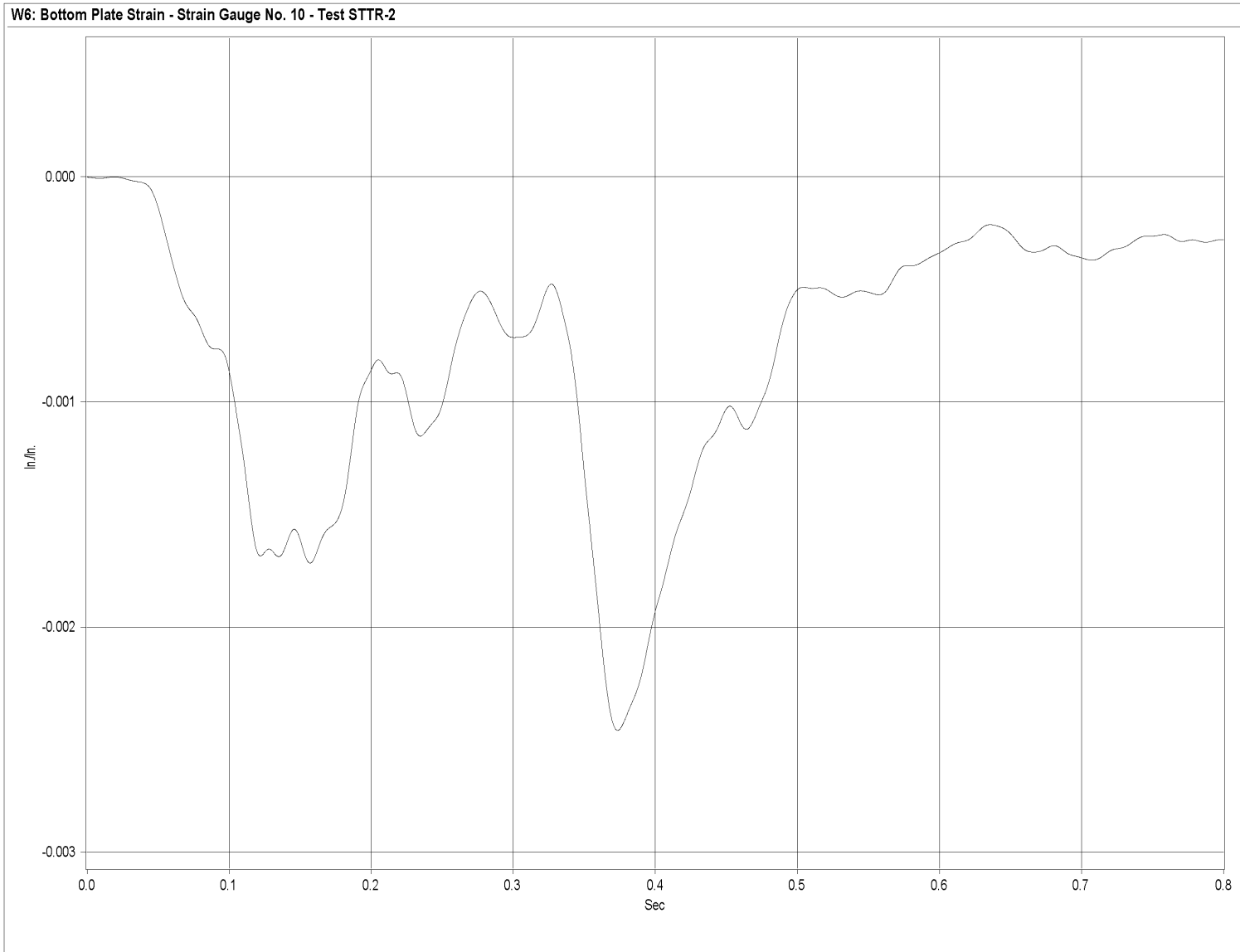


Figure U-18. Graph of Bottom Plate Post No. 6 - Middle and Perpendicular to Rail - Strain, Test STTR-2

460

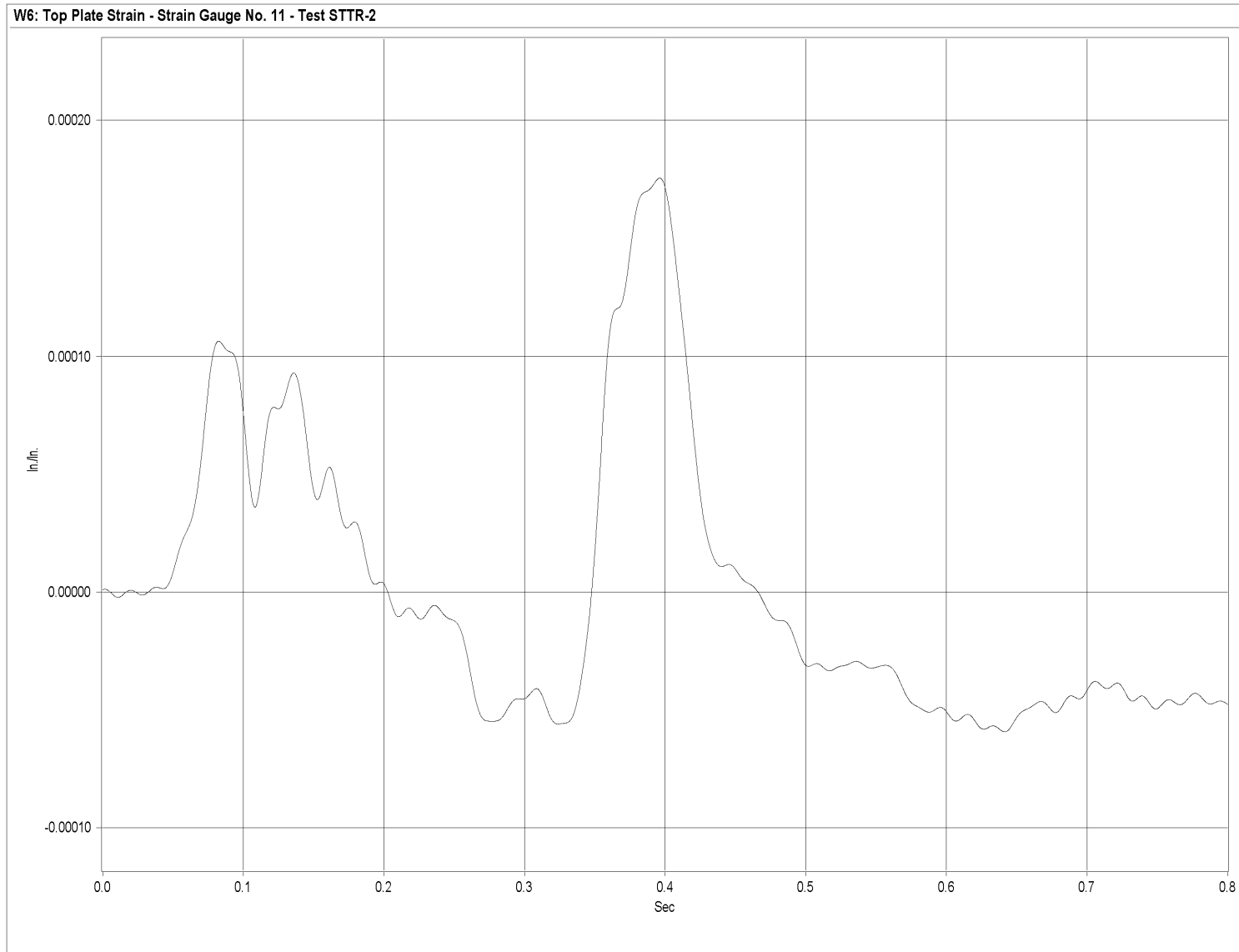


Figure U-19. Graph of Top Plate Post No. 6 - Upstream and Perpendicular to Rail - Strain, Test STTR-2

461

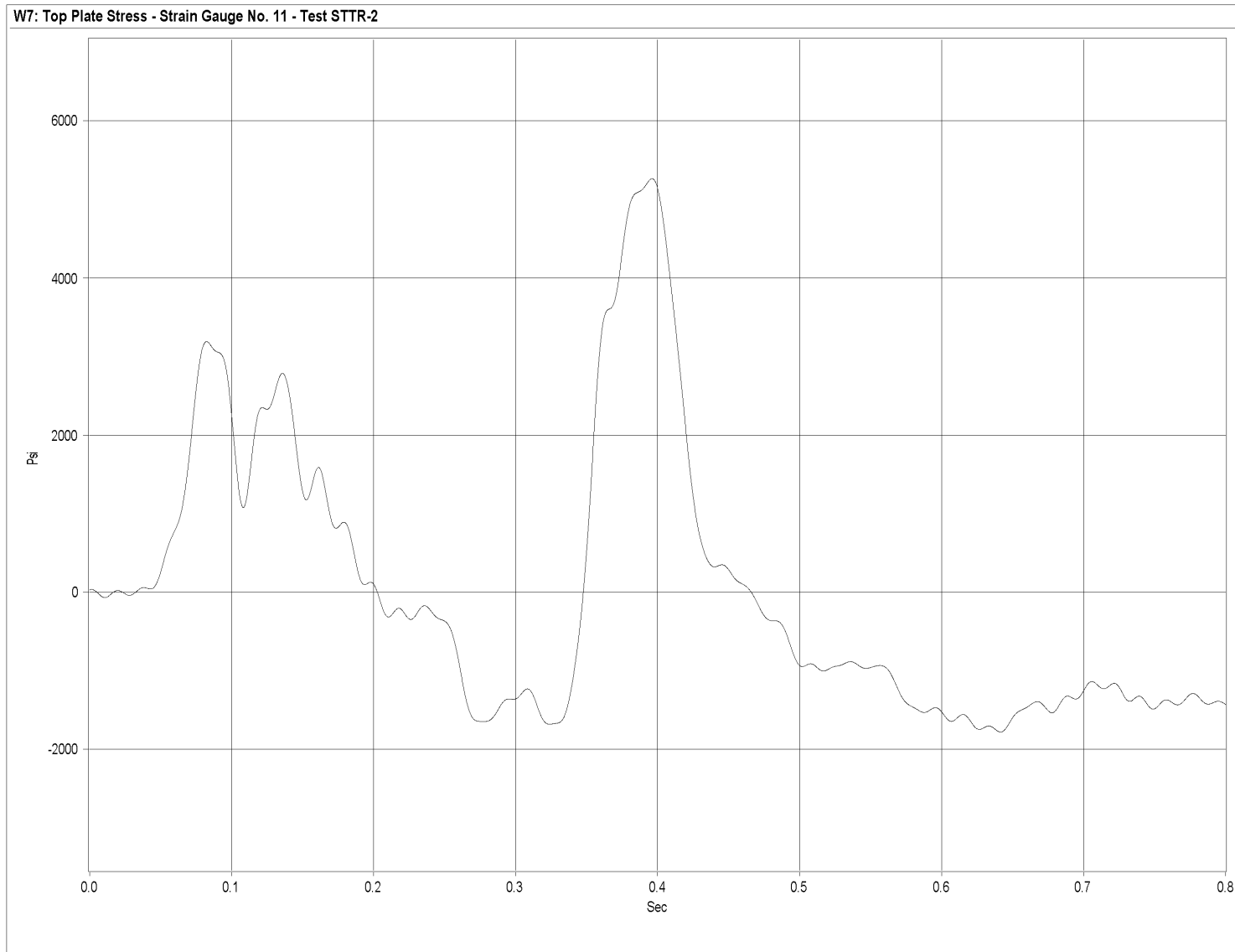


Figure U-20. Graph of Top Plate Post No. 6 - Upstream and Perpendicular to Rail - Stress, Test STTR-2

462

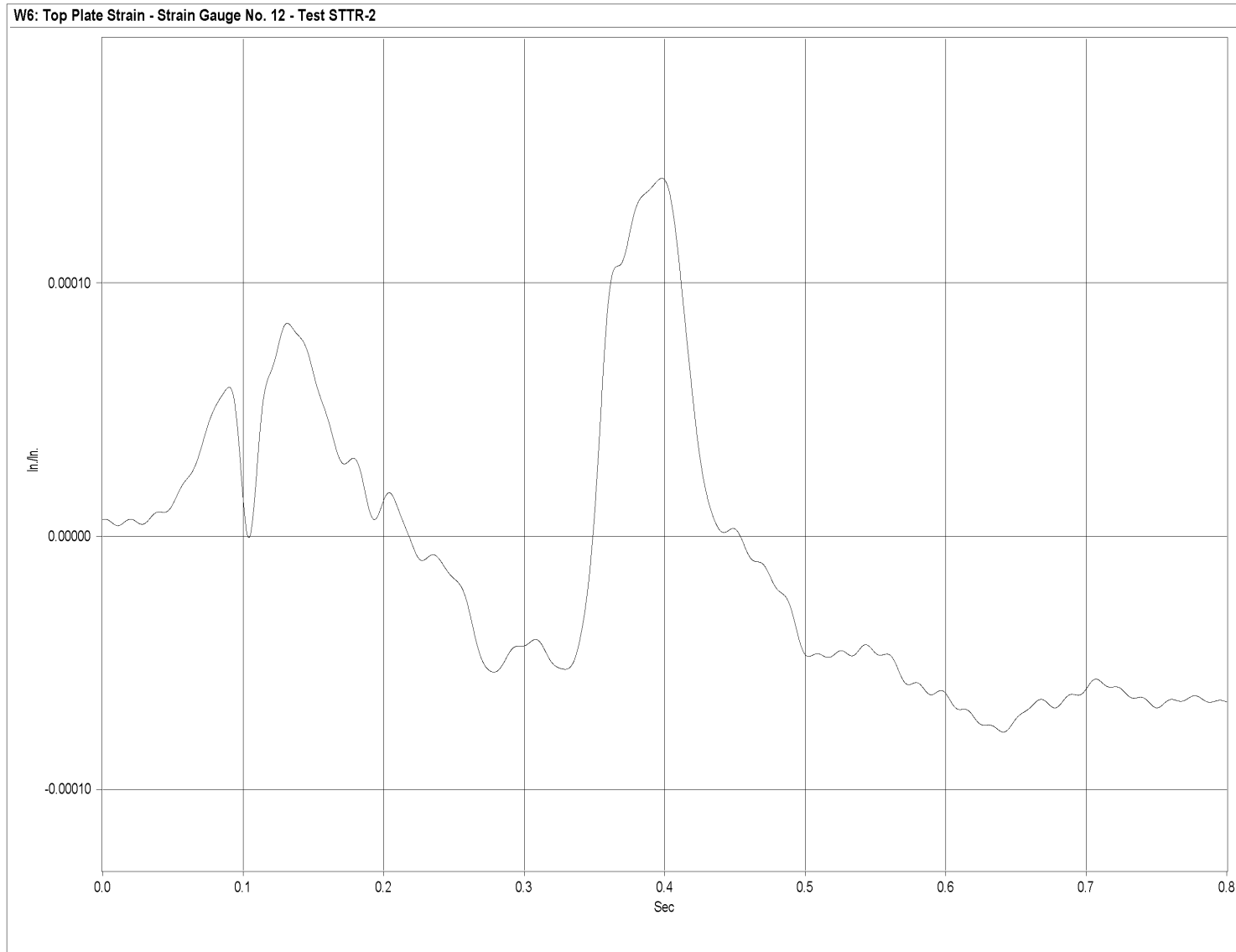


Figure U-21. Graph of Top Plate Post No. 6 - Downstream and Perpendicular to Rail - Strain, Test STTR-2

463

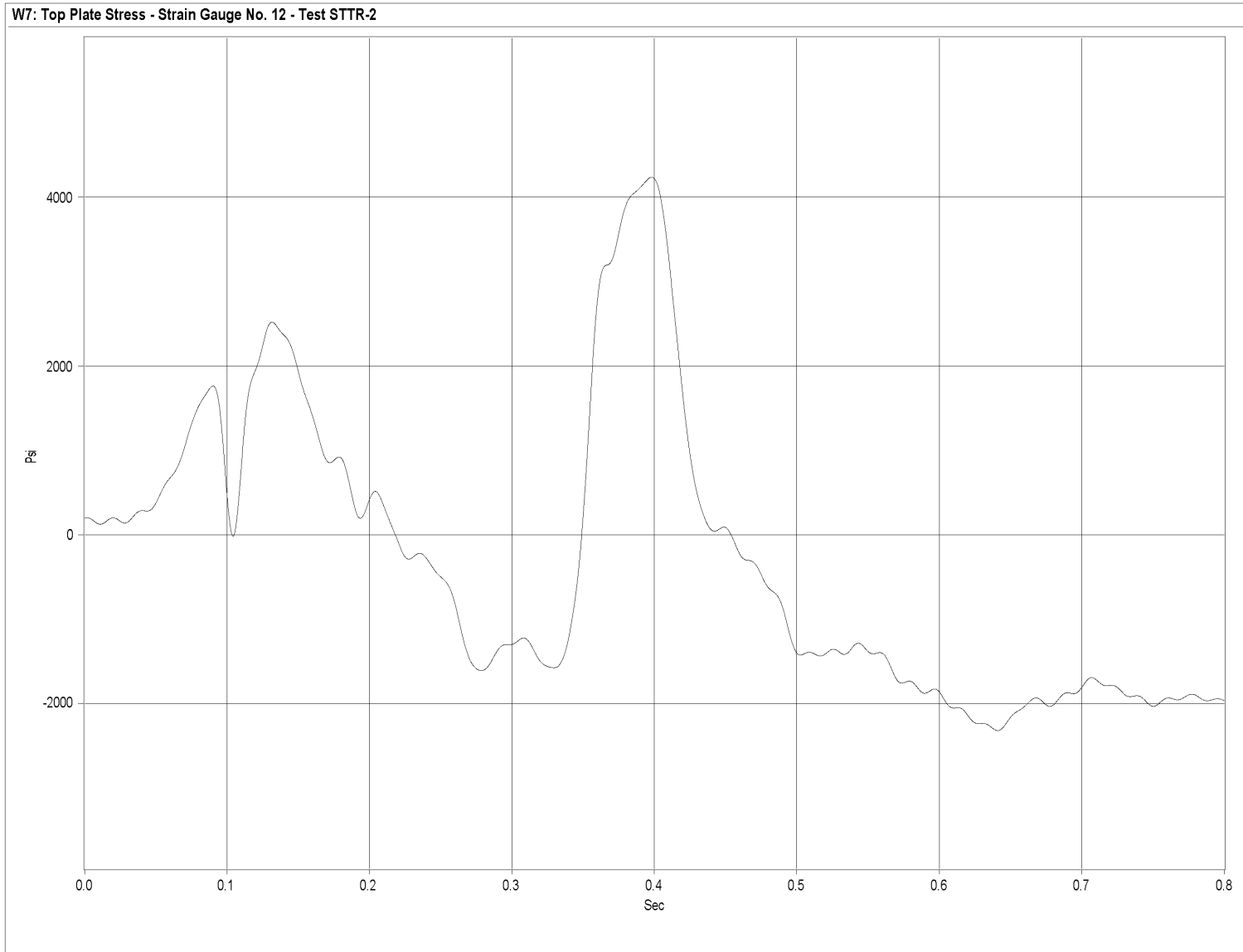


Figure U-22. Graph of Top Plate Post No. 6 - Downstream and Perpendicular to Rail - Stress, Test STTR-2

464

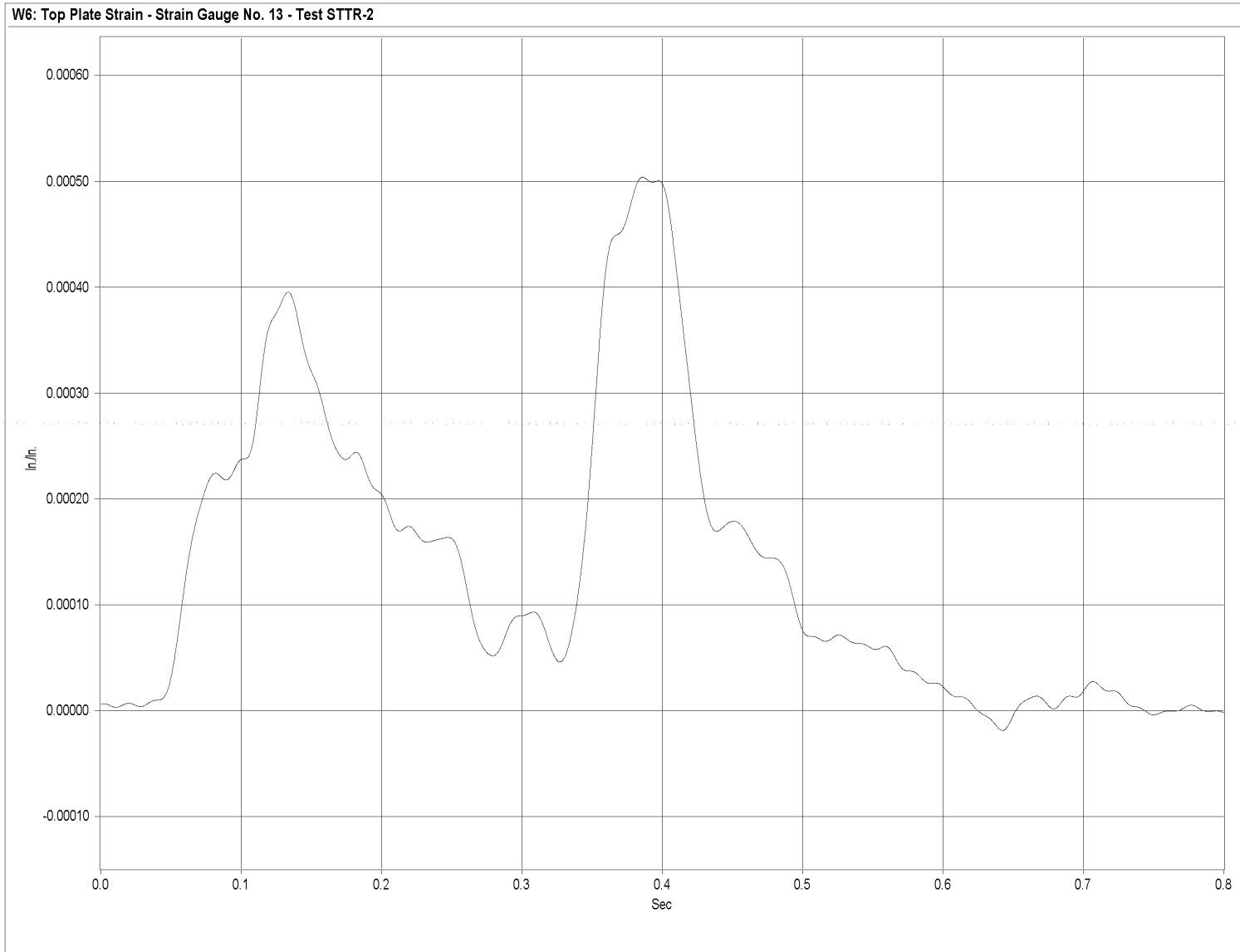


Figure U-23. Graph of Top Plate Post No. 6 - Middle Upstream and Perpendicular to Rail - Strain, Test STTR-2

465

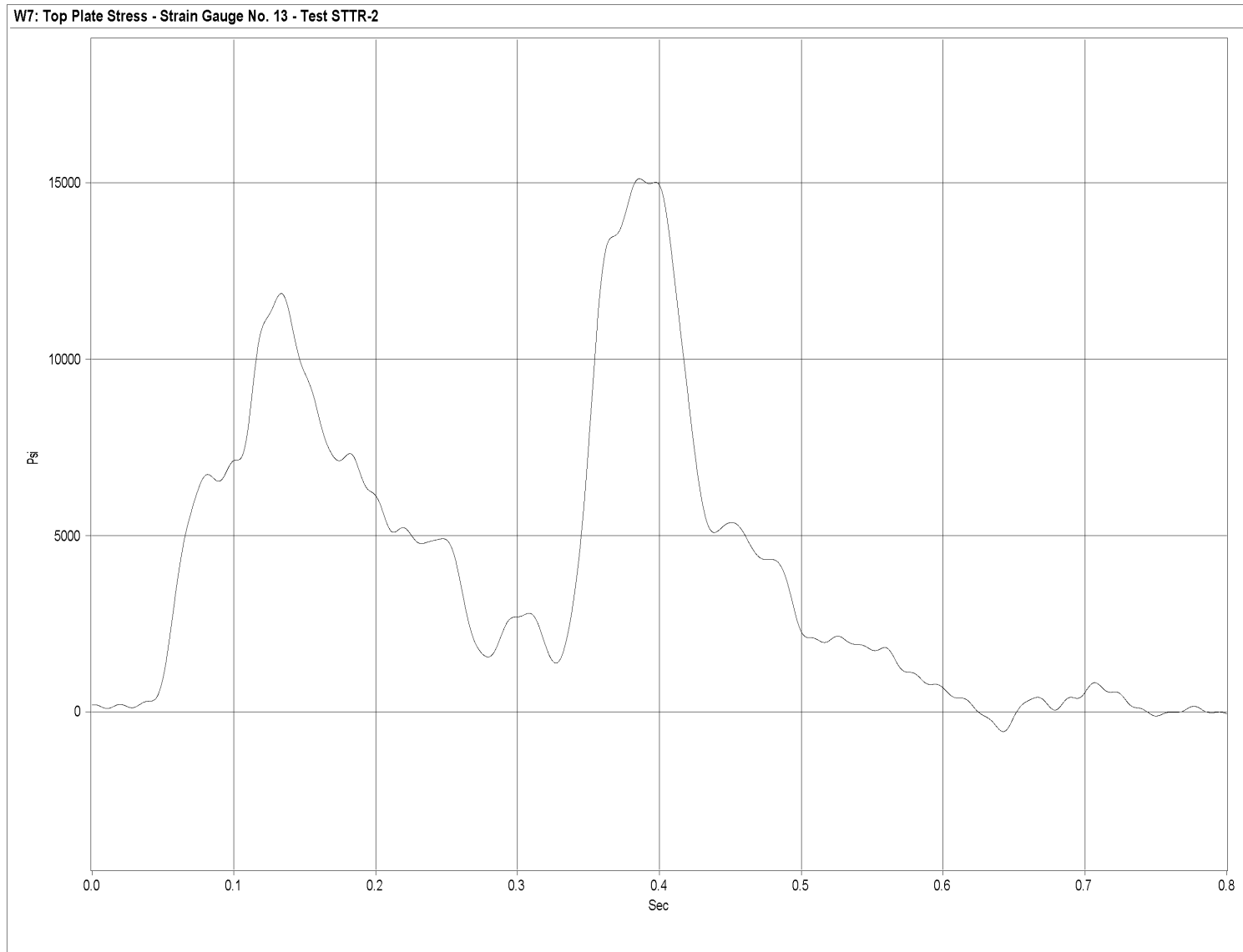


Figure U-24. Graph of Top Plate Post No. 6 - Middle Upstream and Perpendicular to Rail - Stress, Test STTR-2

466

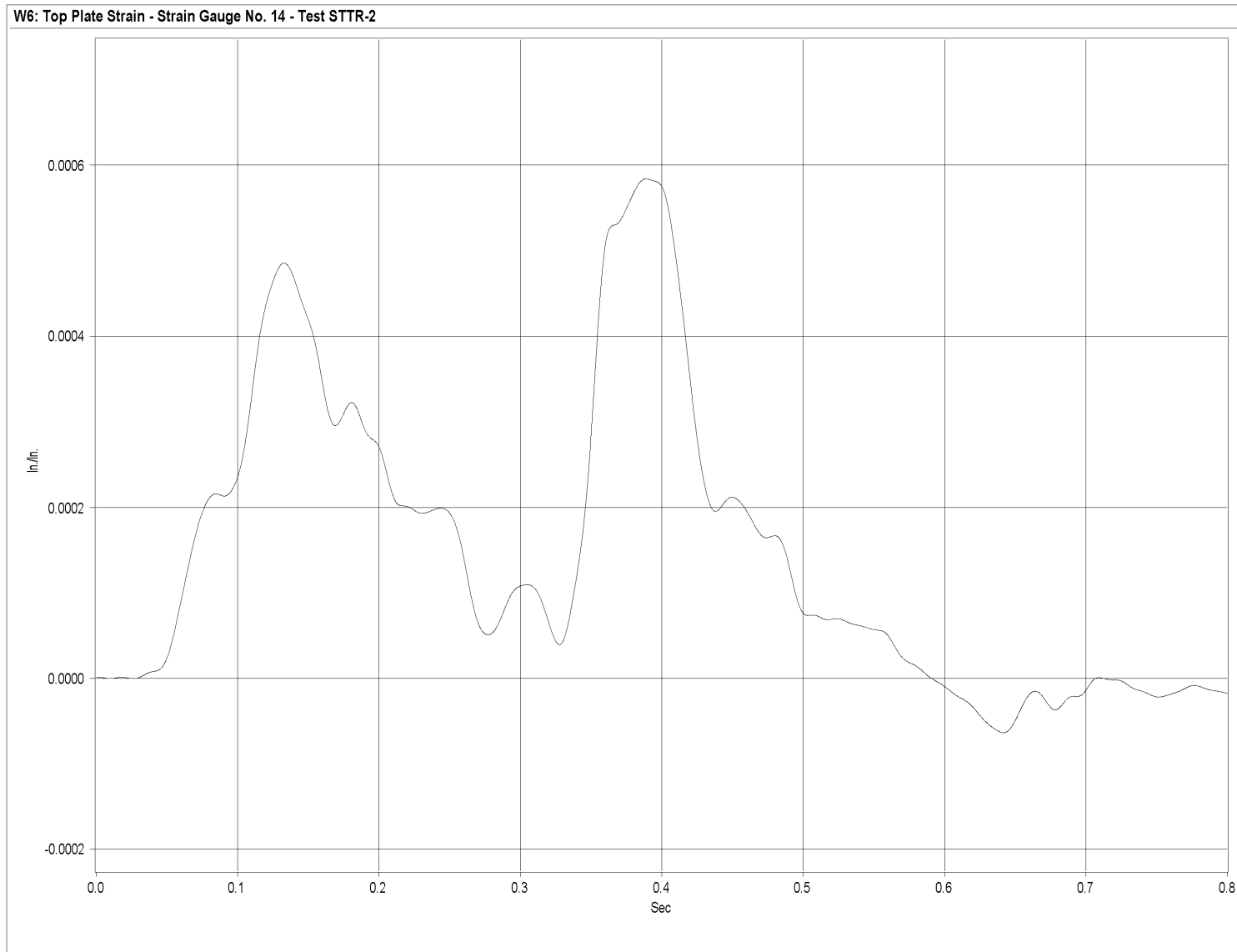


Figure U-25. Graph of Top Plate Post No. 6 - Middle Downstream and Perpendicular to Rail - Strain, Test STTR-2

467

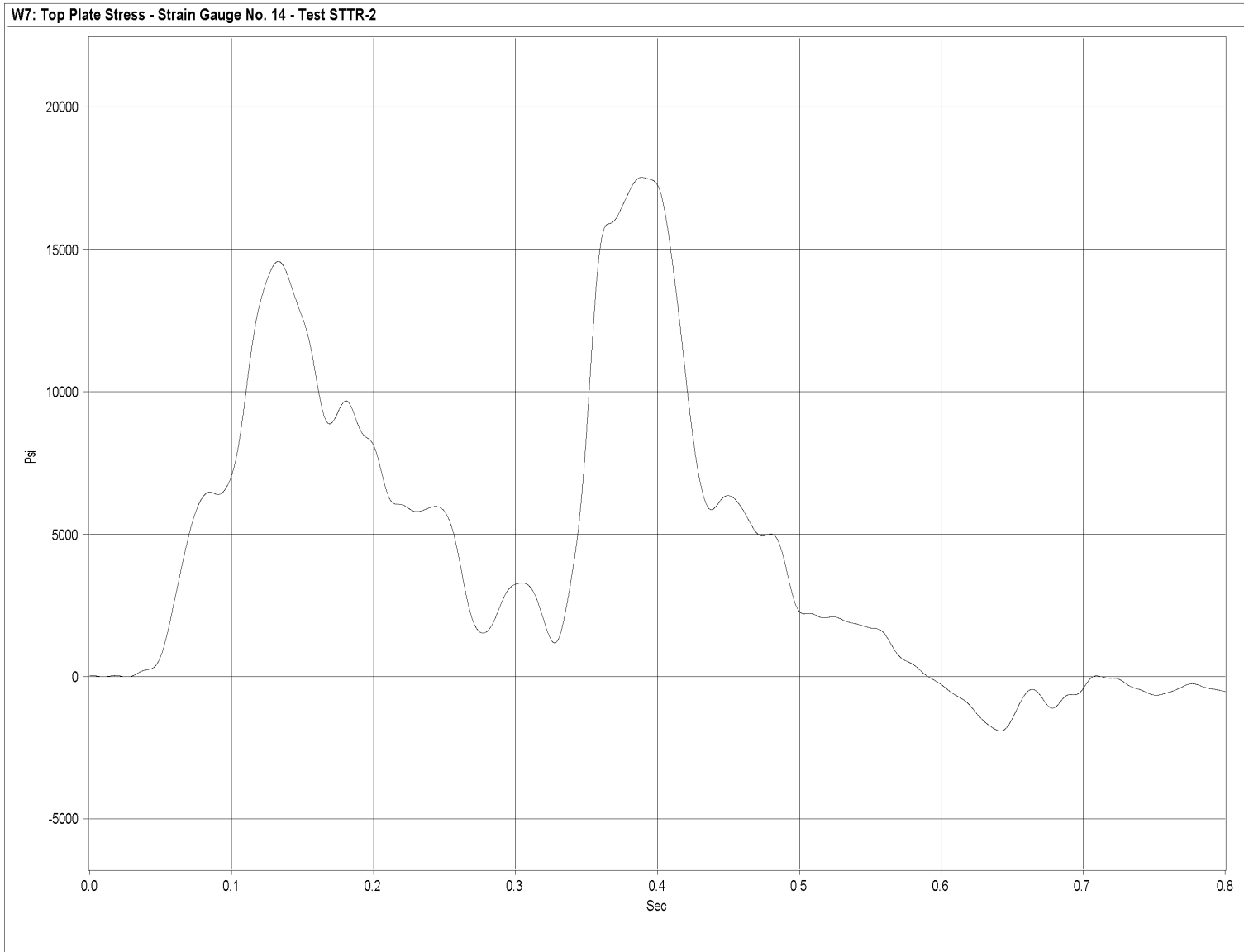


Figure U-26. Graph of Top Plate Post No. 6 - Middle Downstream and Perpendicular to Rail - Stress, Test STTR-2

468

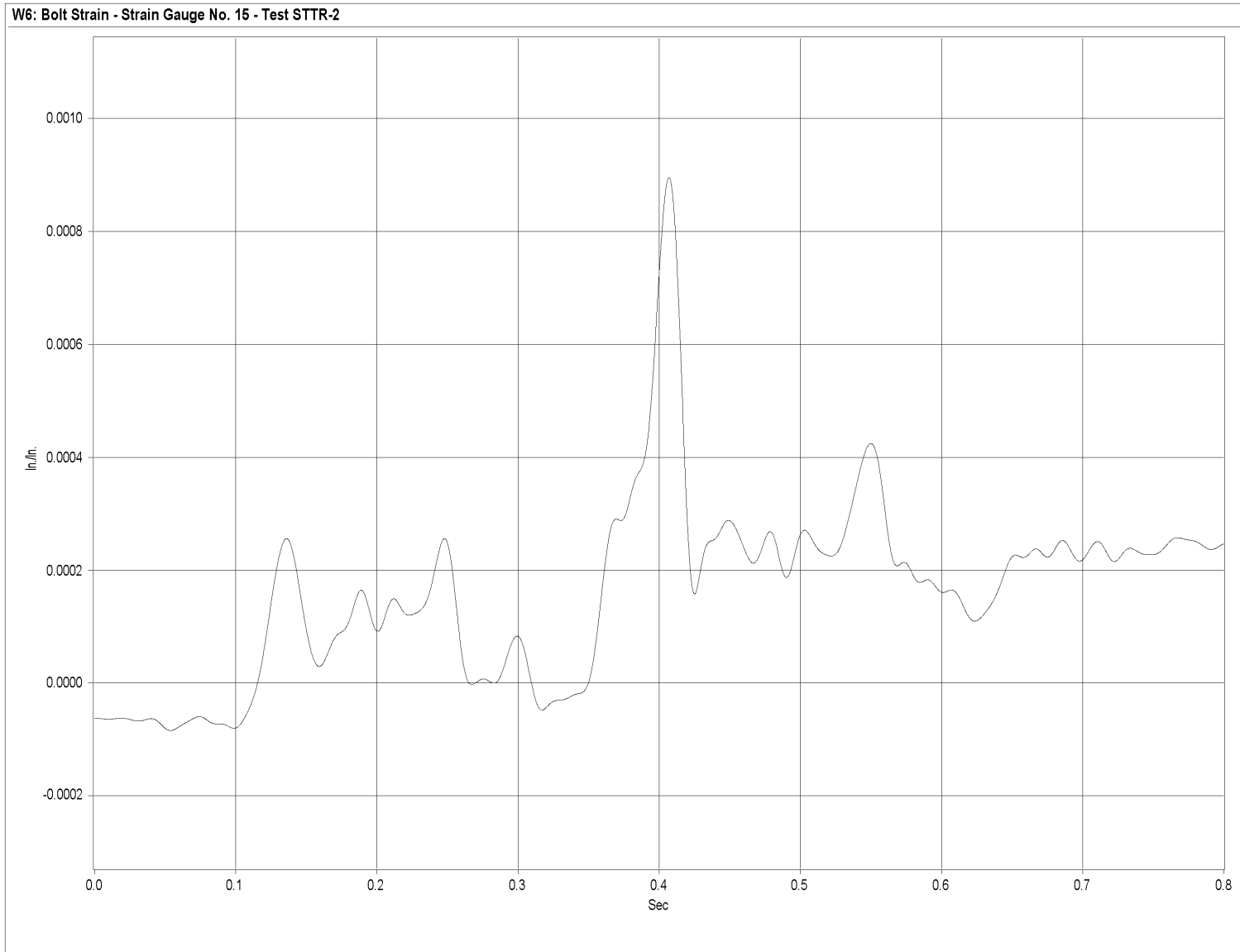


Figure U-27. Graph of Post No. 7 Upstream-Side Bolt Strain, Test STTR-2

469

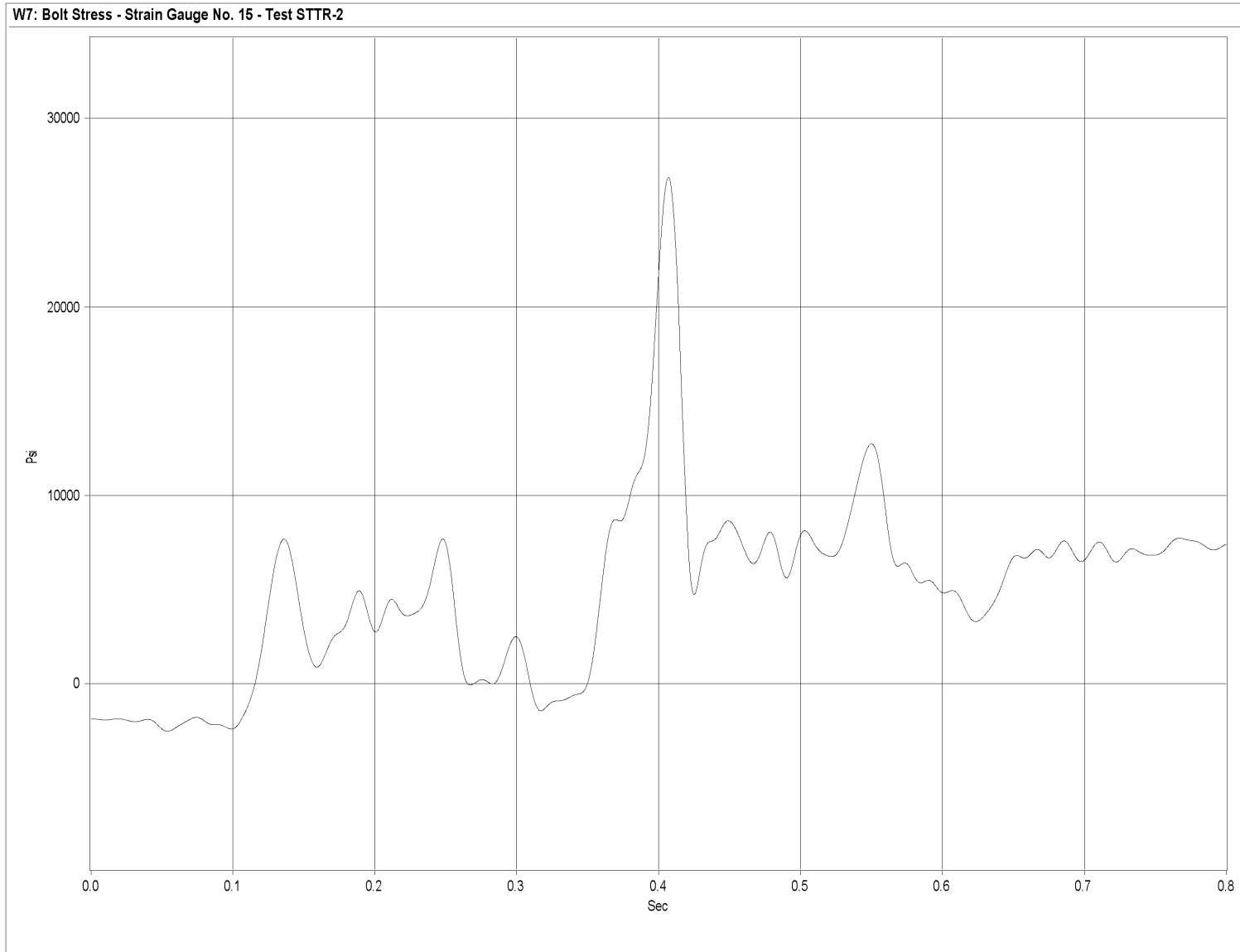


Figure U-28. Graph of Post No. 7 Upstream-Side Bolt Stress, Test STTR-2

470

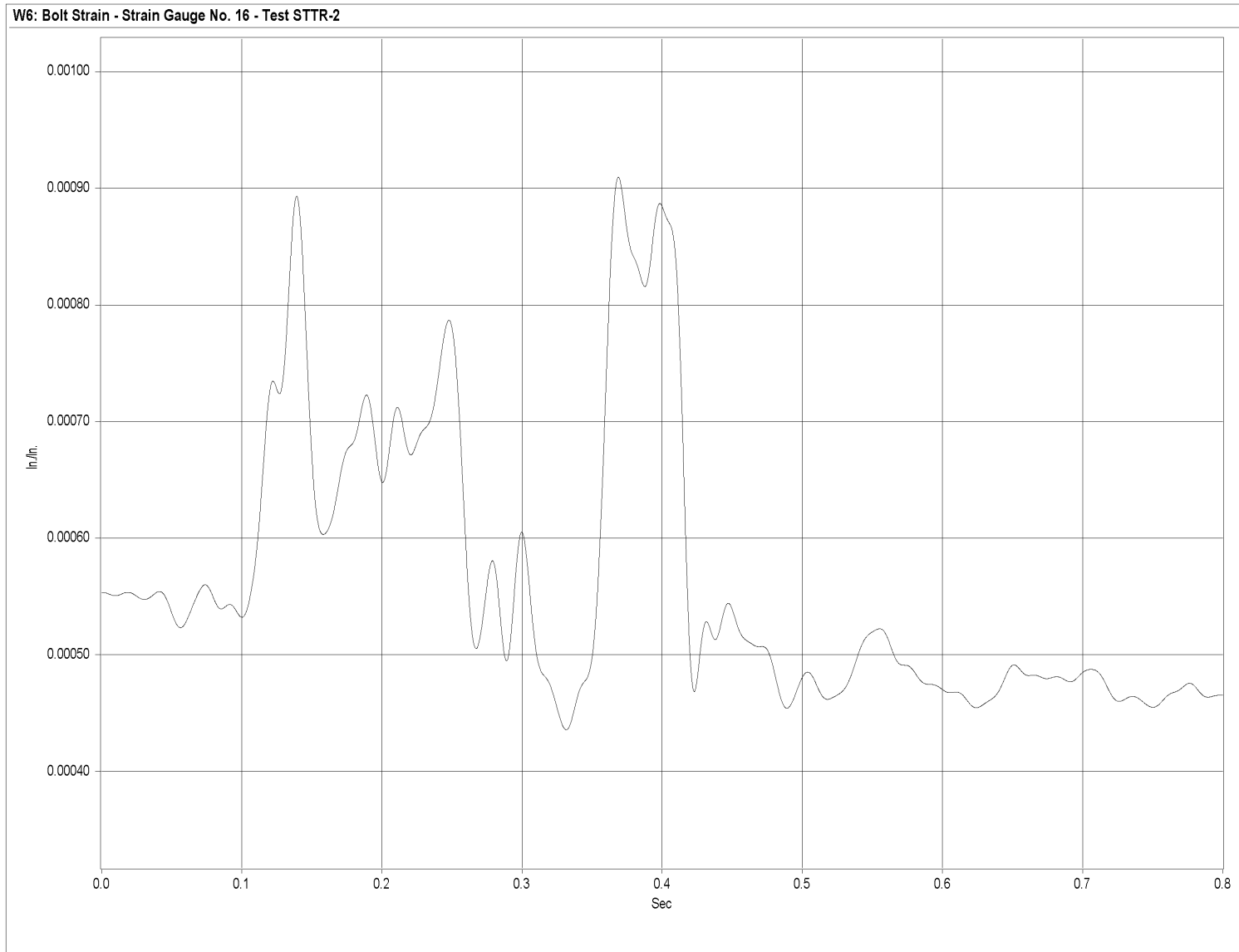


Figure U-29. Graph of Post No. 7 Downstream-Side Bolt Strain, Test STTR-2

471

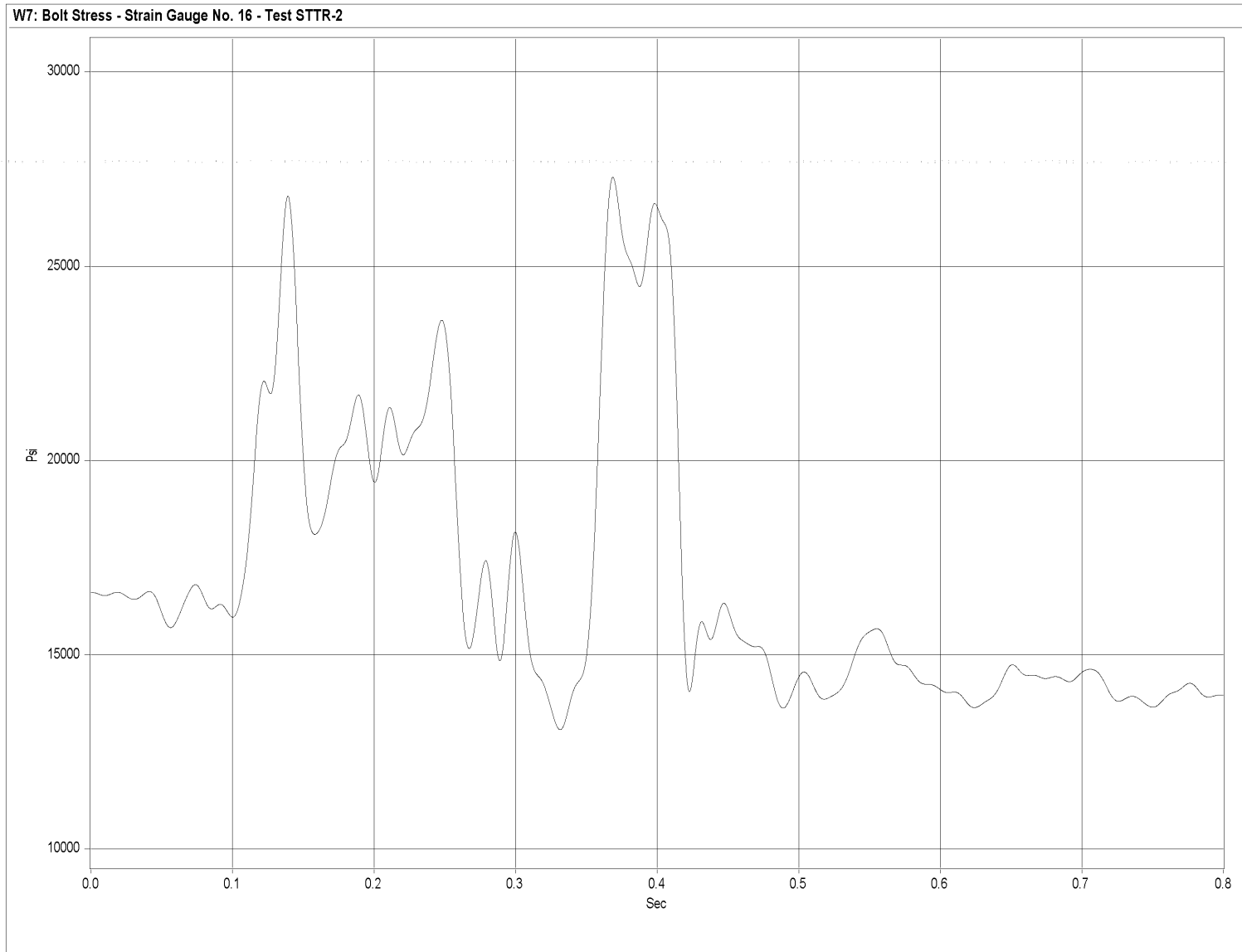


Figure U-30. Graph of Post No. 7 Downstream-Side Bolt Stress, Test STTR-2

472

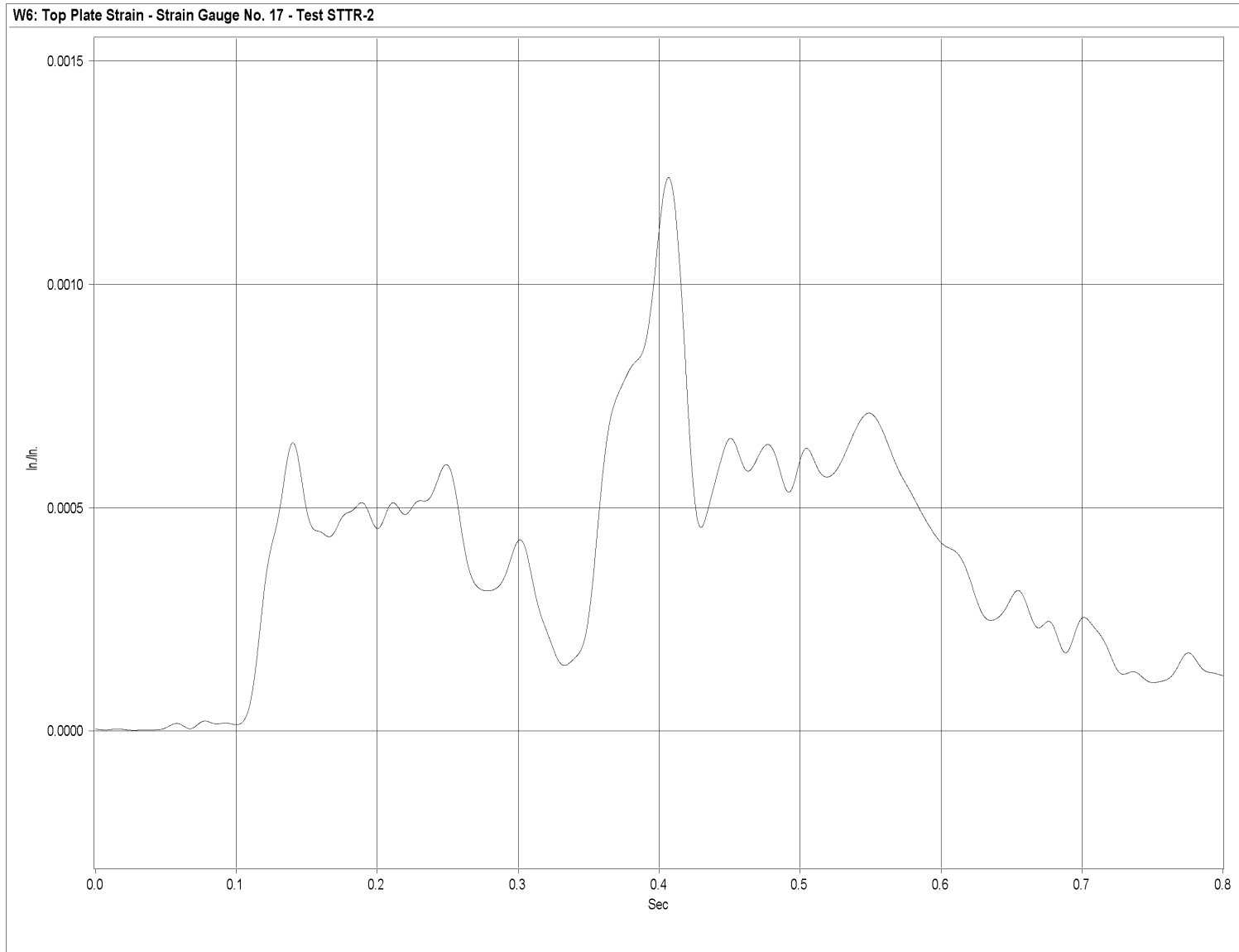


Figure U-31. Graph of Top Plate Post No. 7 - Middle and Perpendicular to Rail - Strain, Test STTR-2

473

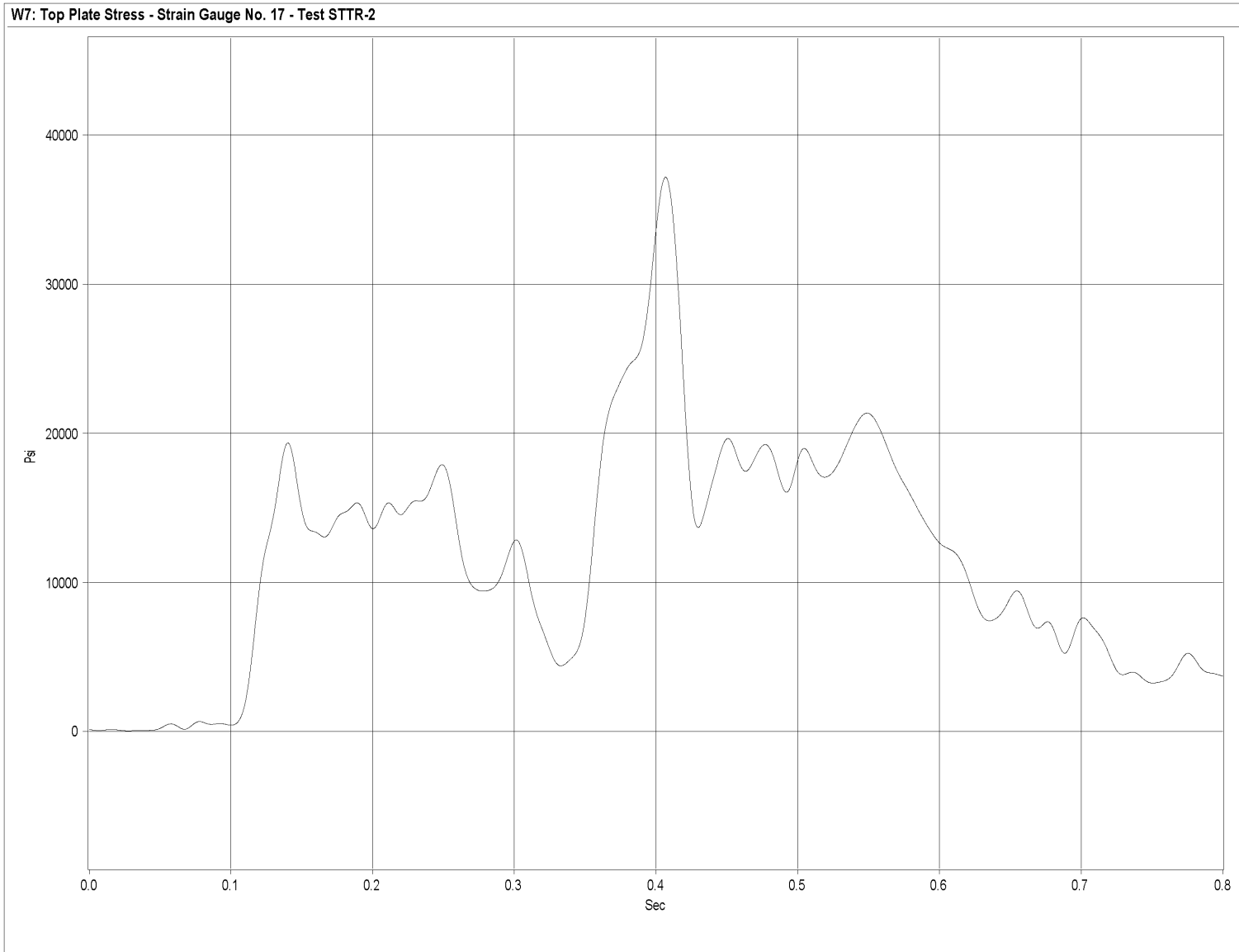


Figure U-32. Graph of Top Plate Post No. 7 - Middle and Perpendicular to Rail - Stress, Test STTR-2

474

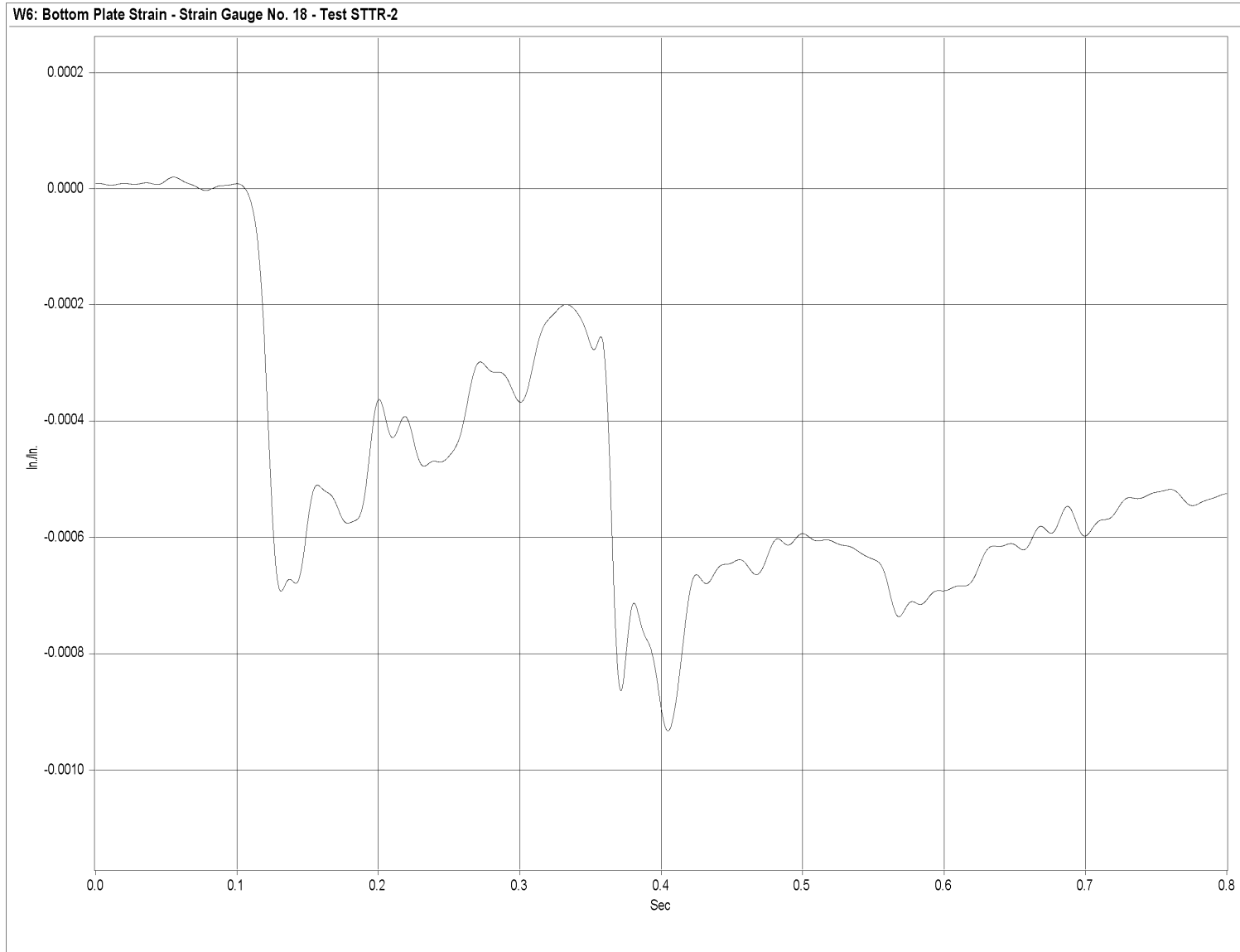


Figure U-33. Graph of Bottom Plate Post No. 7 - Middle and Perpendicular to Rail - Strain, Test STTR-2

475

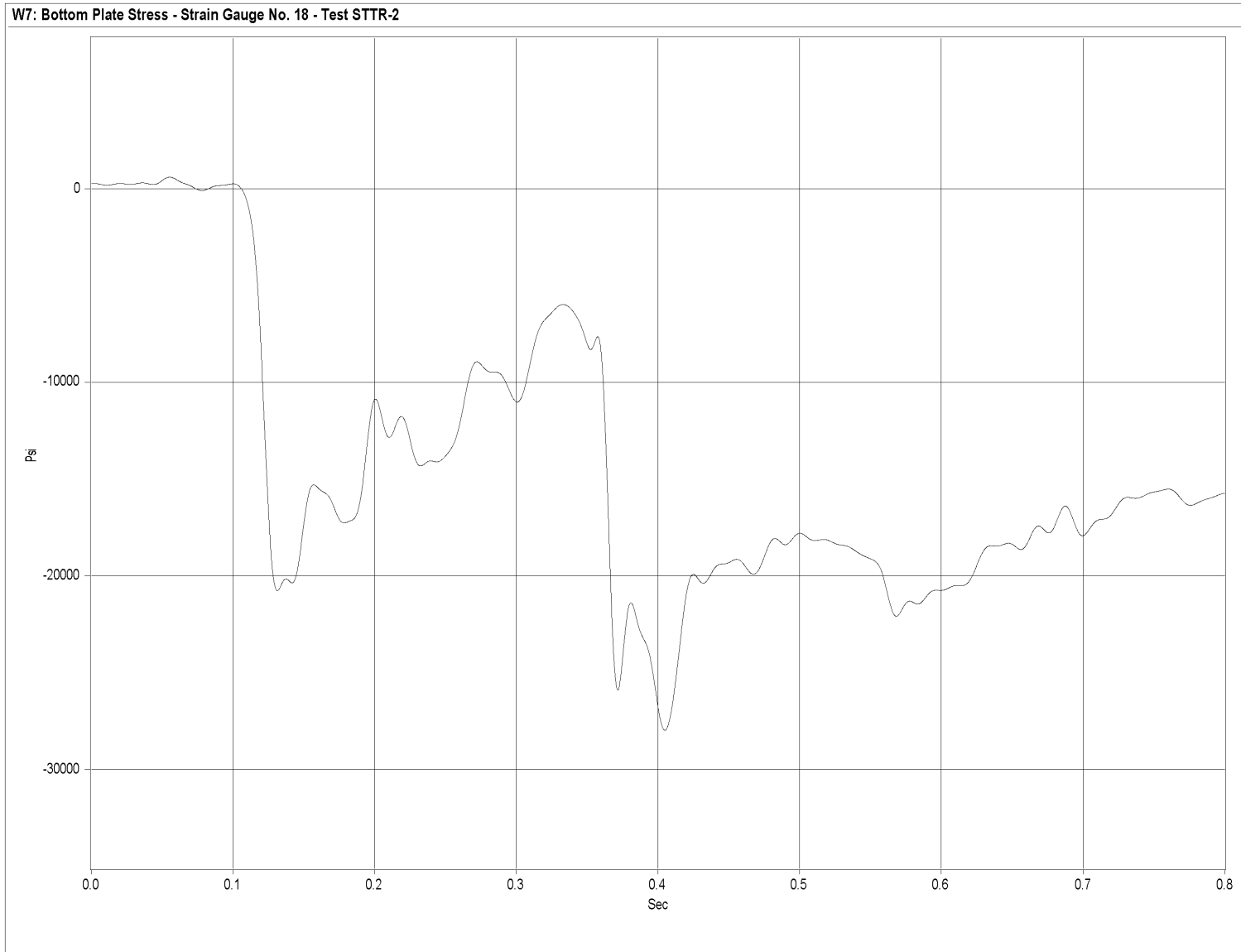


Figure U-34. Graph of Bottom Plate Post No. 7 - Middle and Perpendicular to Rail - Stress, Test STTR-2

476

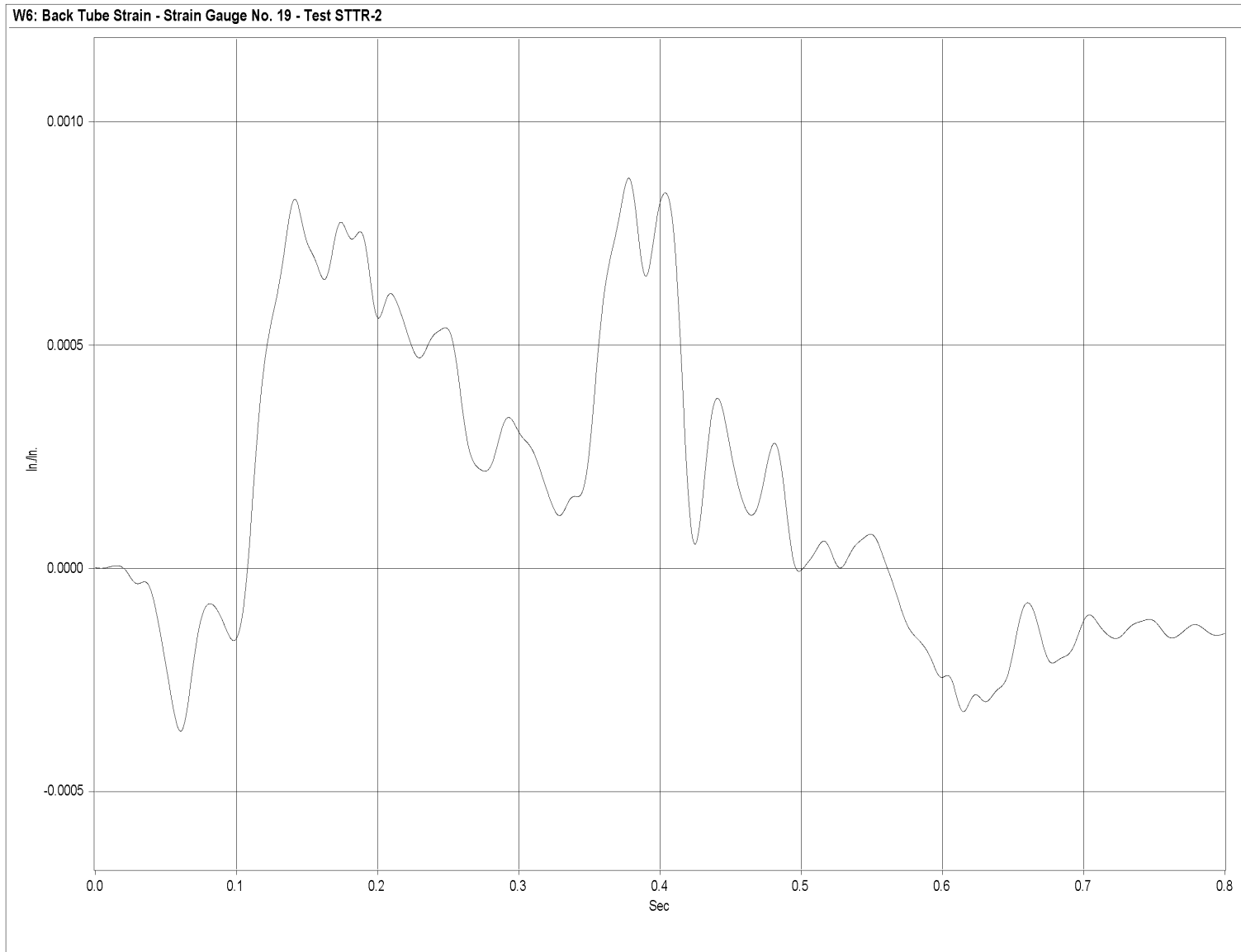


Figure U-35. Graph of Back-Side Steel Tube Rail at Midspan Between Post Nos. 6 and 7 Strain, Test STTR-2

477

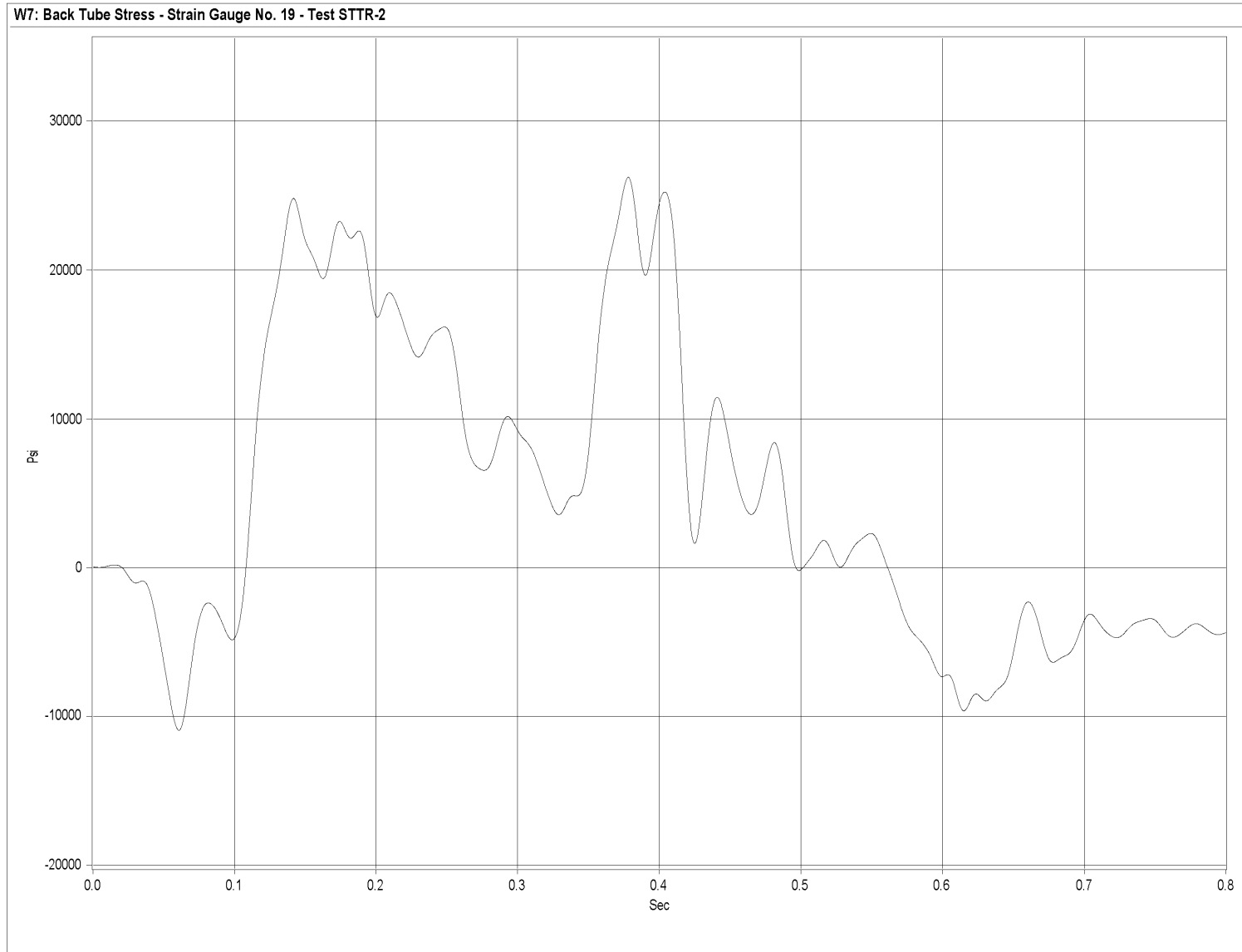


Figure U-36. Graph of Back-Side Steel Tube Rail at Midspan Between Post Nos. 6 and 7 Stress, Test STTR-2

478

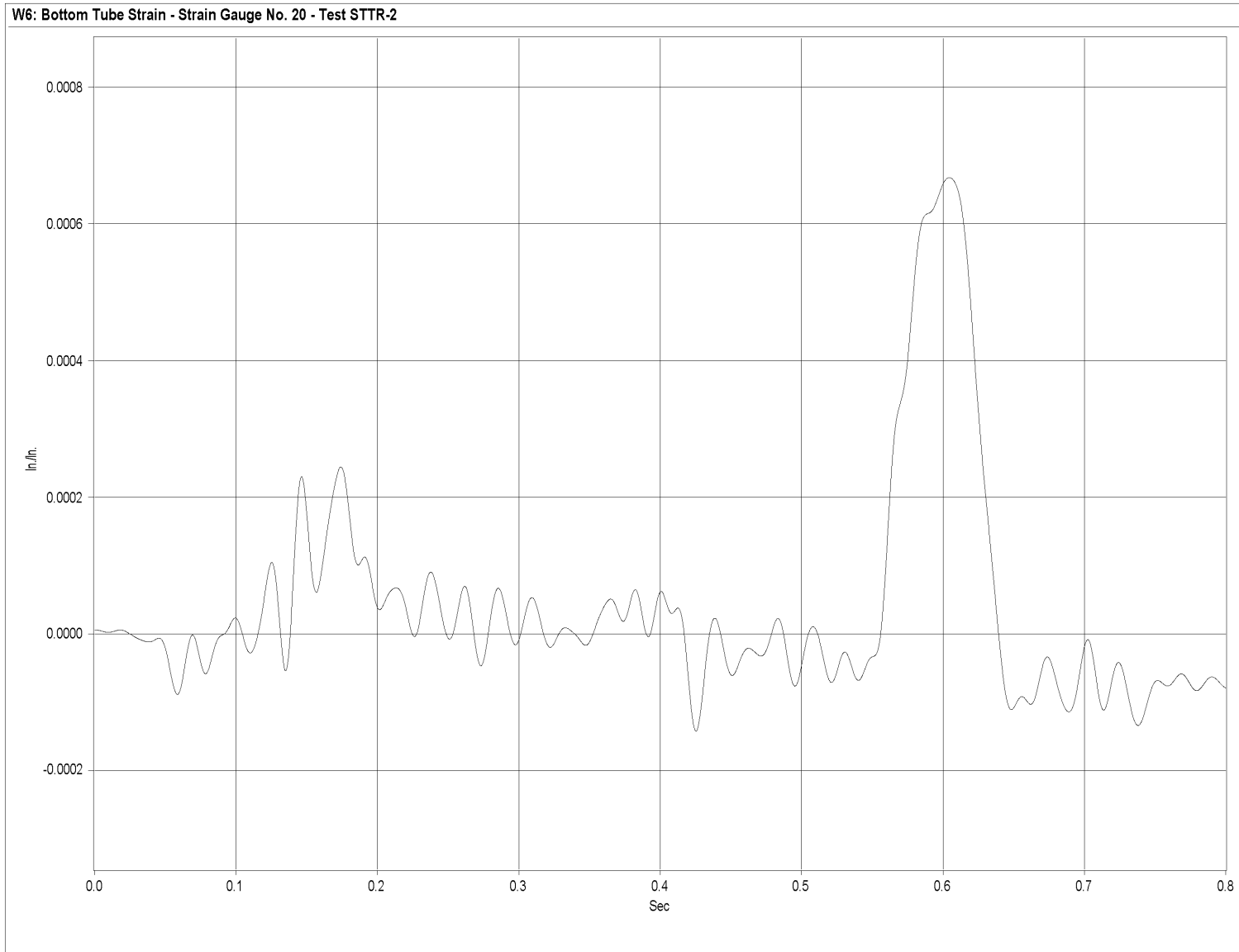


Figure U-37. Graph of Bottom-Side Steel Tube Rail at Midspan Between Post Nos. 6 and 7 Strain, Test STTR-2

479

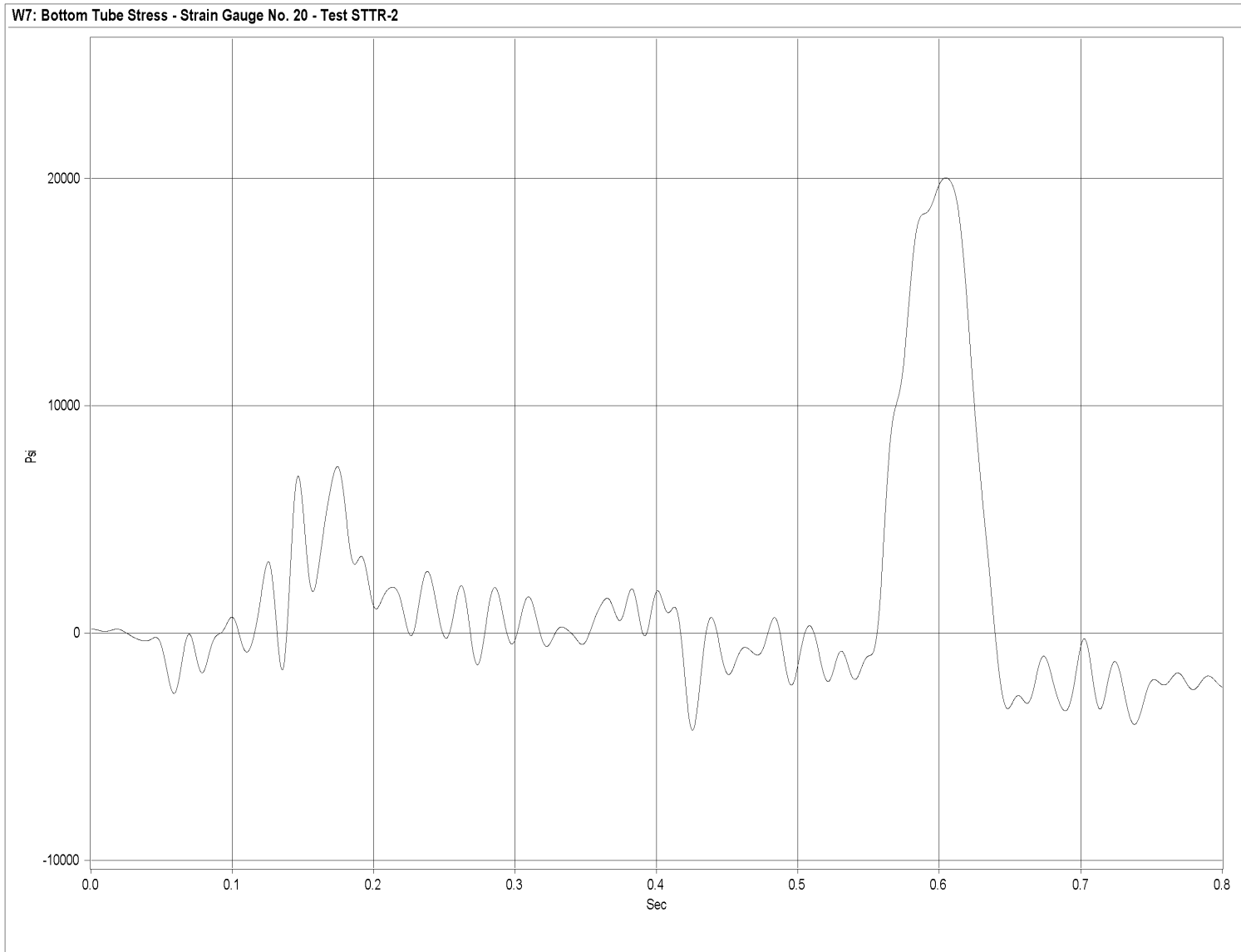


Figure U-38. Graph of Bottom-Side Steel Tube Rail at Midspan Between Post Nos. 6 and 7 Stress, Test STTR-2

APPENDIX V

Accelerometer Data Analysis - Test STTR-3

Figure V-1. Graph of Longitudinal Deceleration, Test STTR-3

Figure V-2. Graph of Longitudinal Occupant Impact Velocity, Test STTR-3

Figure V-3. Graph of Longitudinal Occupant Displacement, Test STTR-3

Figure V-4. Graph of Lateral Deceleration, Test STTR-3

Figure V-5. Graph of Lateral Occupant Impact Velocity, Test STTR-3

Figure V-6. Graph of Lateral Occupant Displacement, Test STTR-3

481

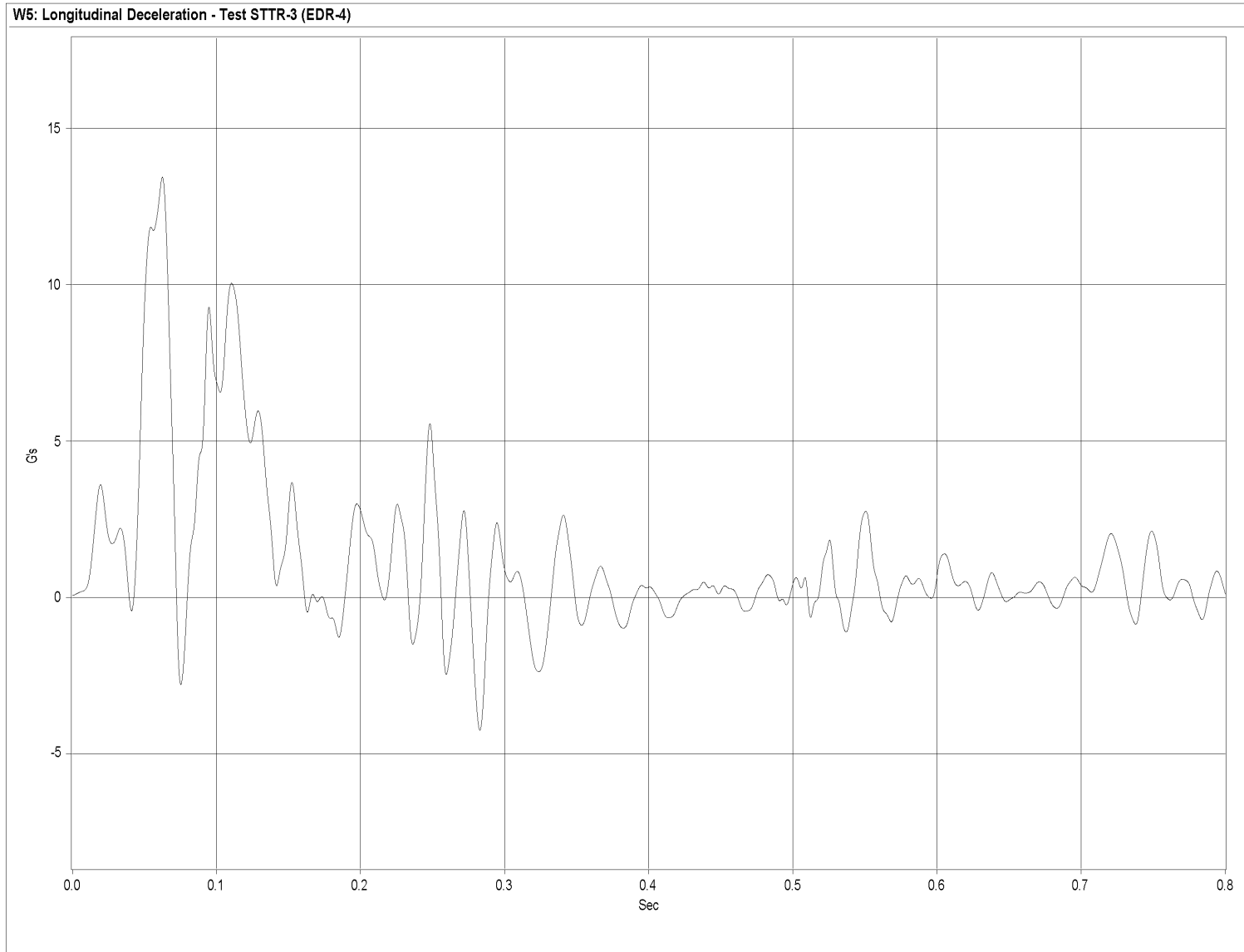


Figure V-1. Graph of Longitudinal Deceleration, Test STTR-3

482

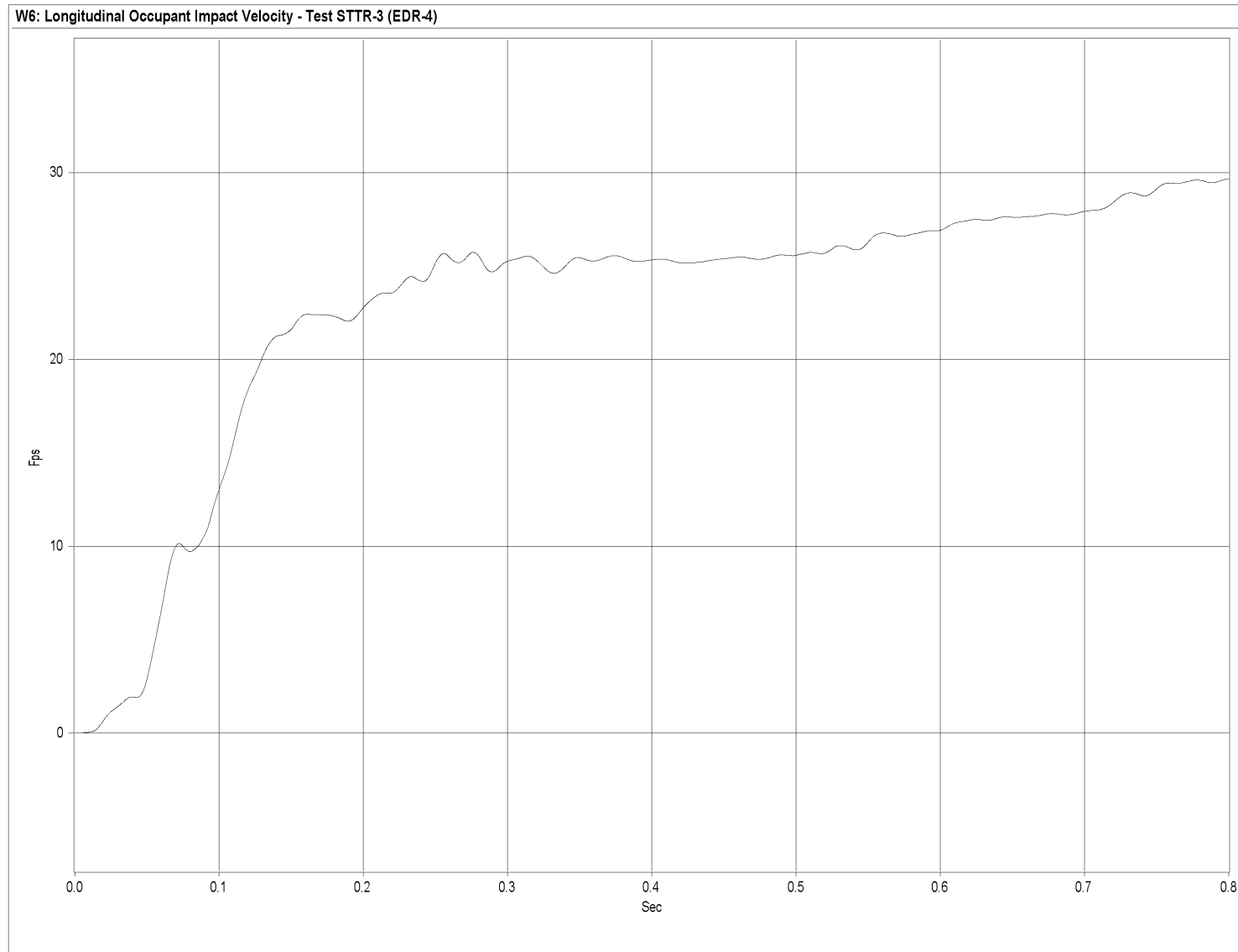


Figure V-2. Graph of Longitudinal Occupant Impact Velocity, Test STTR-3

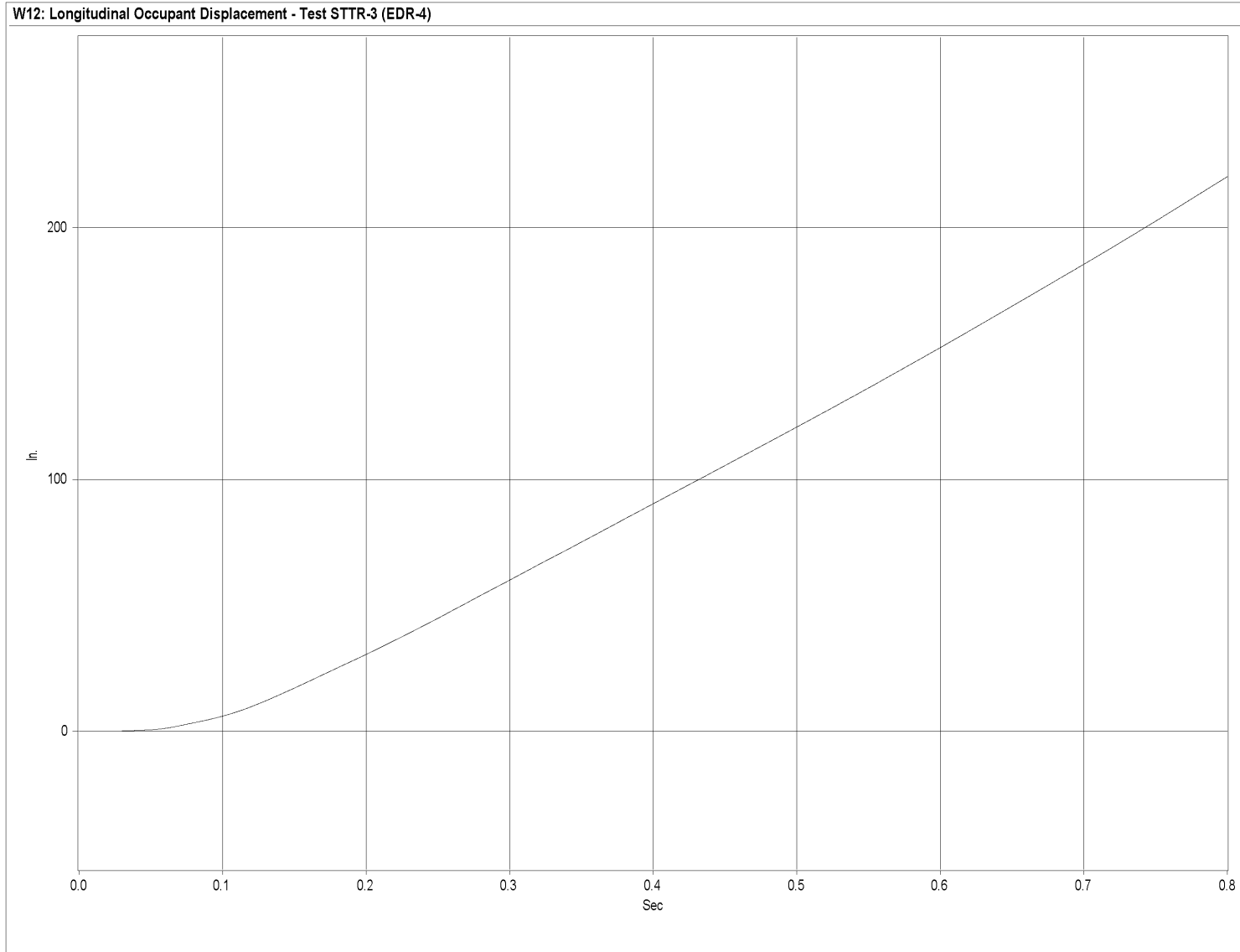


Figure V-3. Graph of Longitudinal Occupant Displacement, Test STTR-3

484

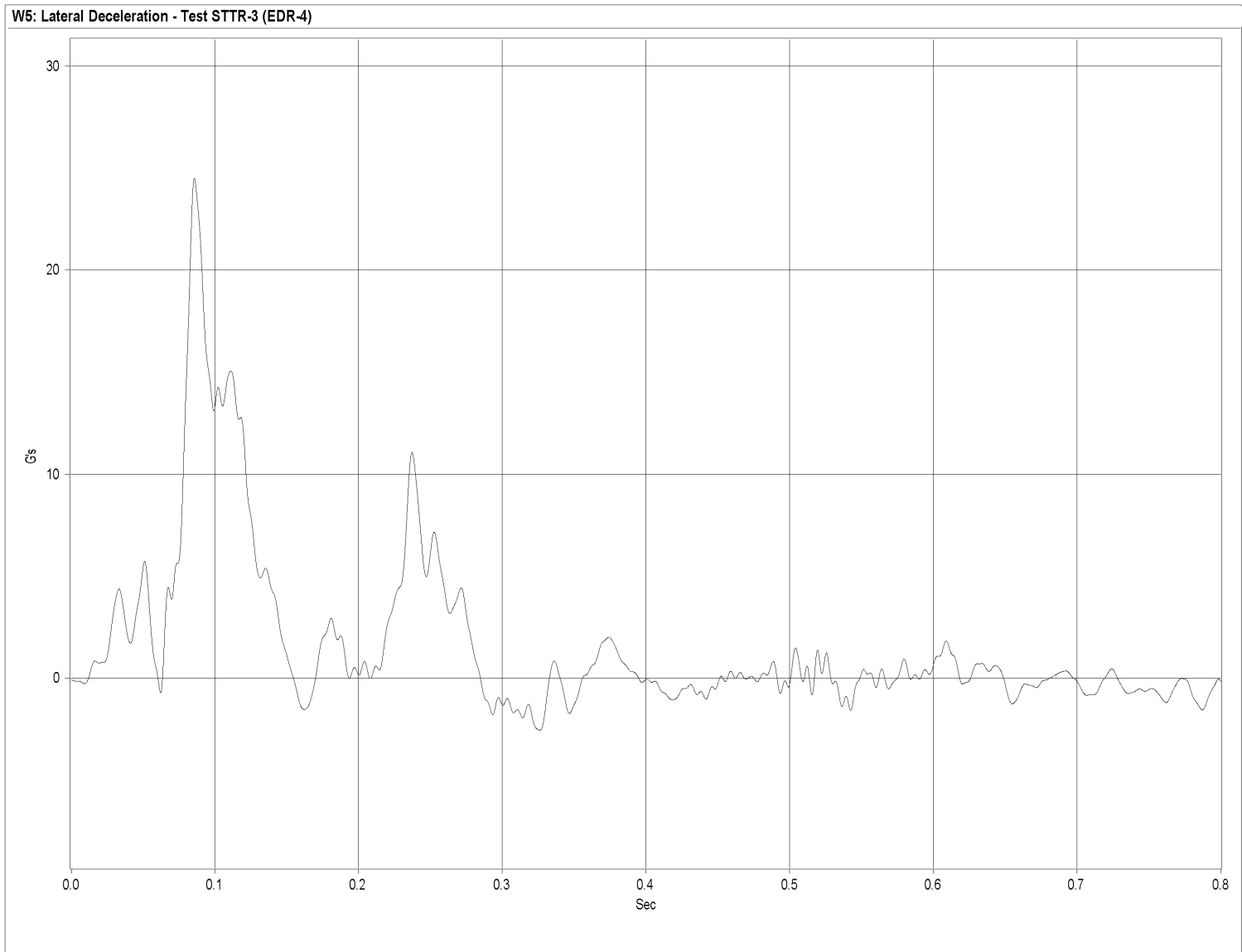


Figure V-4. Graph of Lateral Deceleration, Test STTR-3

485

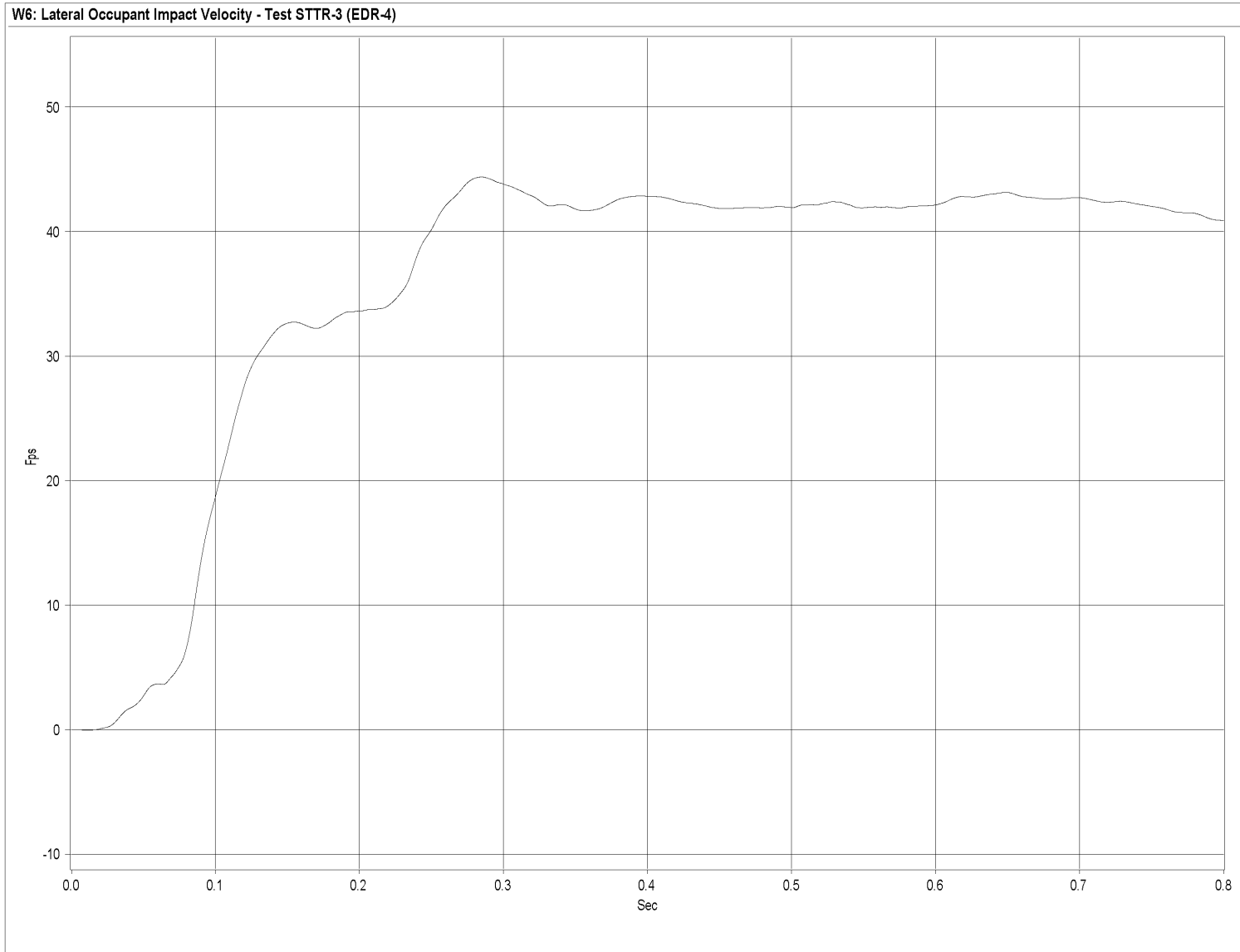


Figure V-5. Graph of Lateral Occupant Impact Velocity, Test STTR-3

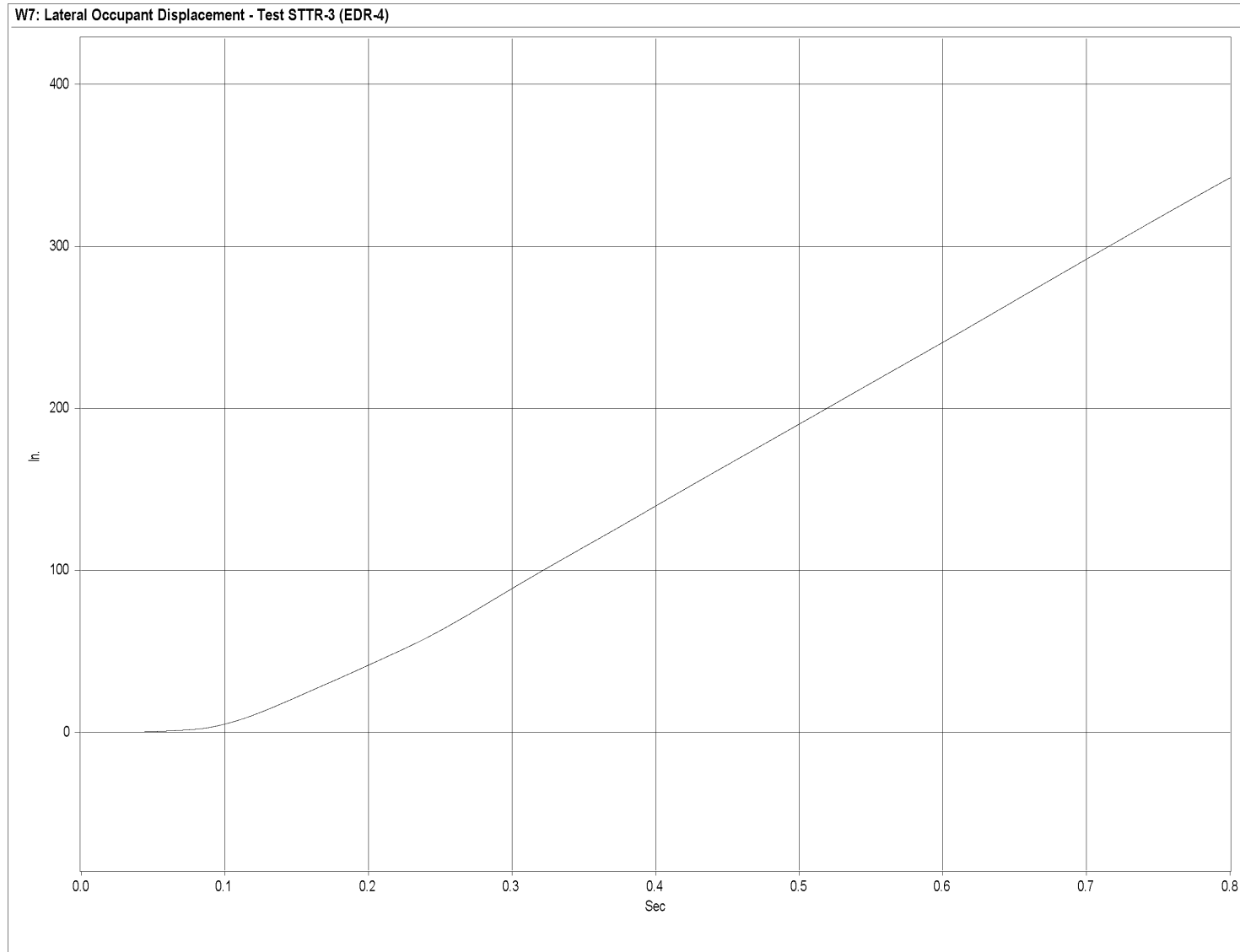


Figure V-6. Graph of Lateral Occupant Displacement, Test STTR-3

APPENDIX W

Rate Transducer Data Analysis - Test STTR-3

Figure W-1. Graph of Roll, Pitch, and Yaw Angular Displacements, Test STTR-3

488

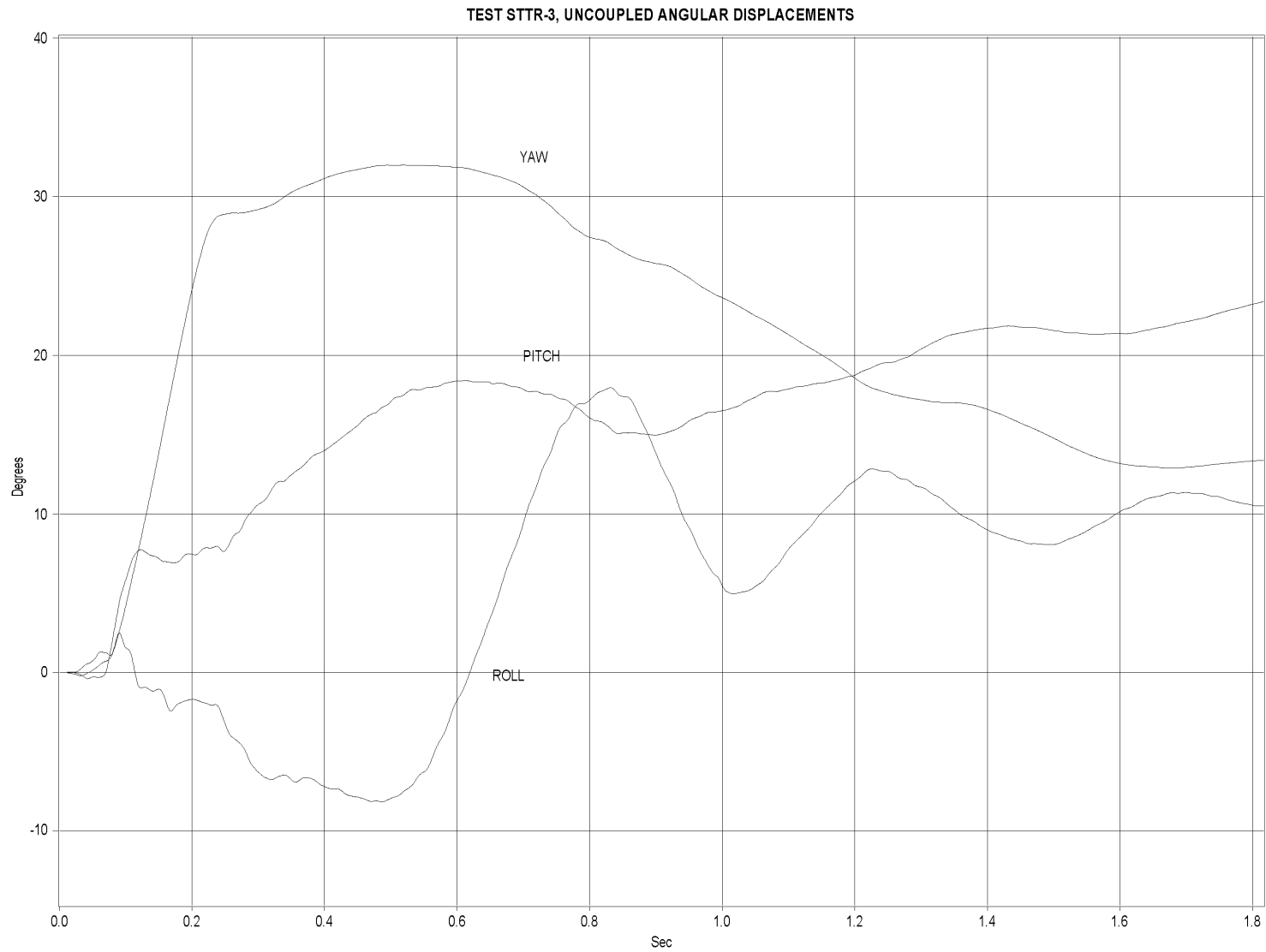


Figure W-1. Graph of Roll, Pitch, and Yaw Angular Displacements, Test STTR-3

APPENDIX X

Accelerometer Data Analysis - Test STTR-4

Figure X-1. Graph of Longitudinal Deceleration, Test STTR-4

Figure X-2. Graph of Longitudinal Occupant Impact Velocity, Test STTR-4

Figure X-3. Graph of Longitudinal Occupant Displacement, Test STTR-4

Figure X-4. Graph of Lateral Deceleration, Test STTR-4

Figure X-5. Graph of Lateral Occupant Impact Velocity, Test STTR-4

Figure X-6. Graph of Lateral Occupant Displacement, Test STTR-4

490

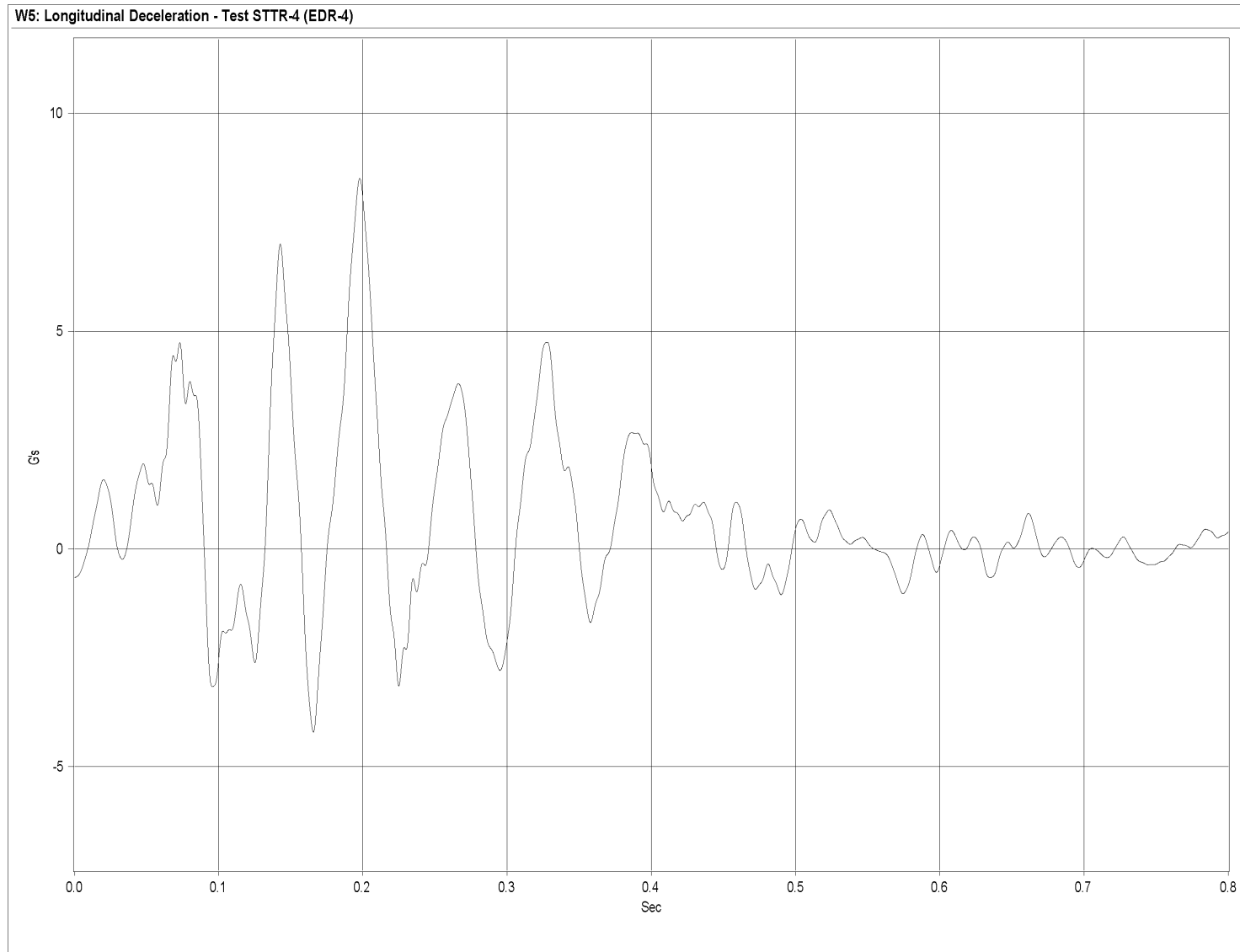


Figure X-1. Graph of Longitudinal Deceleration, Test STTR-4

491

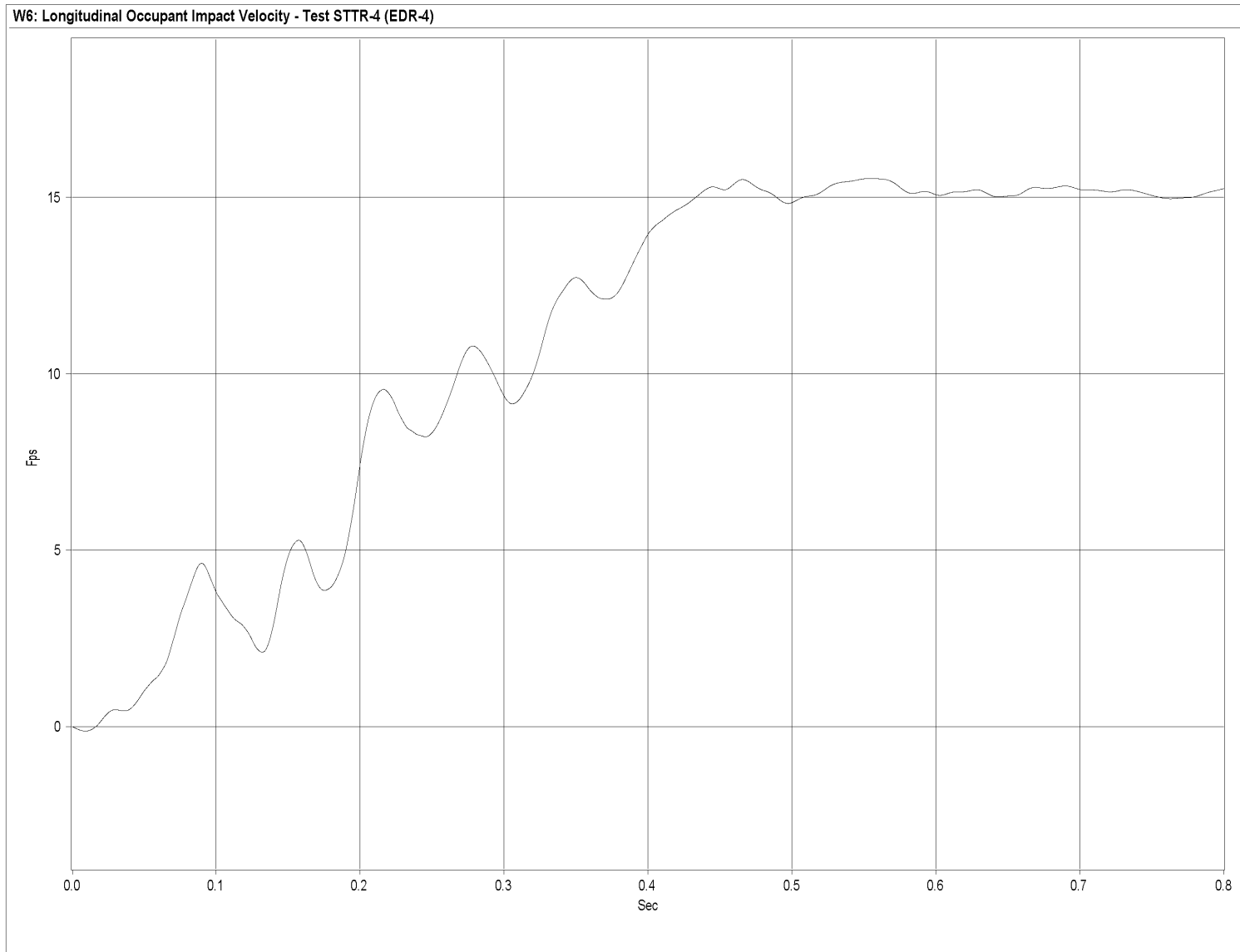


Figure X-2. Graph of Longitudinal Occupant Impact Velocity, Test STTR-4

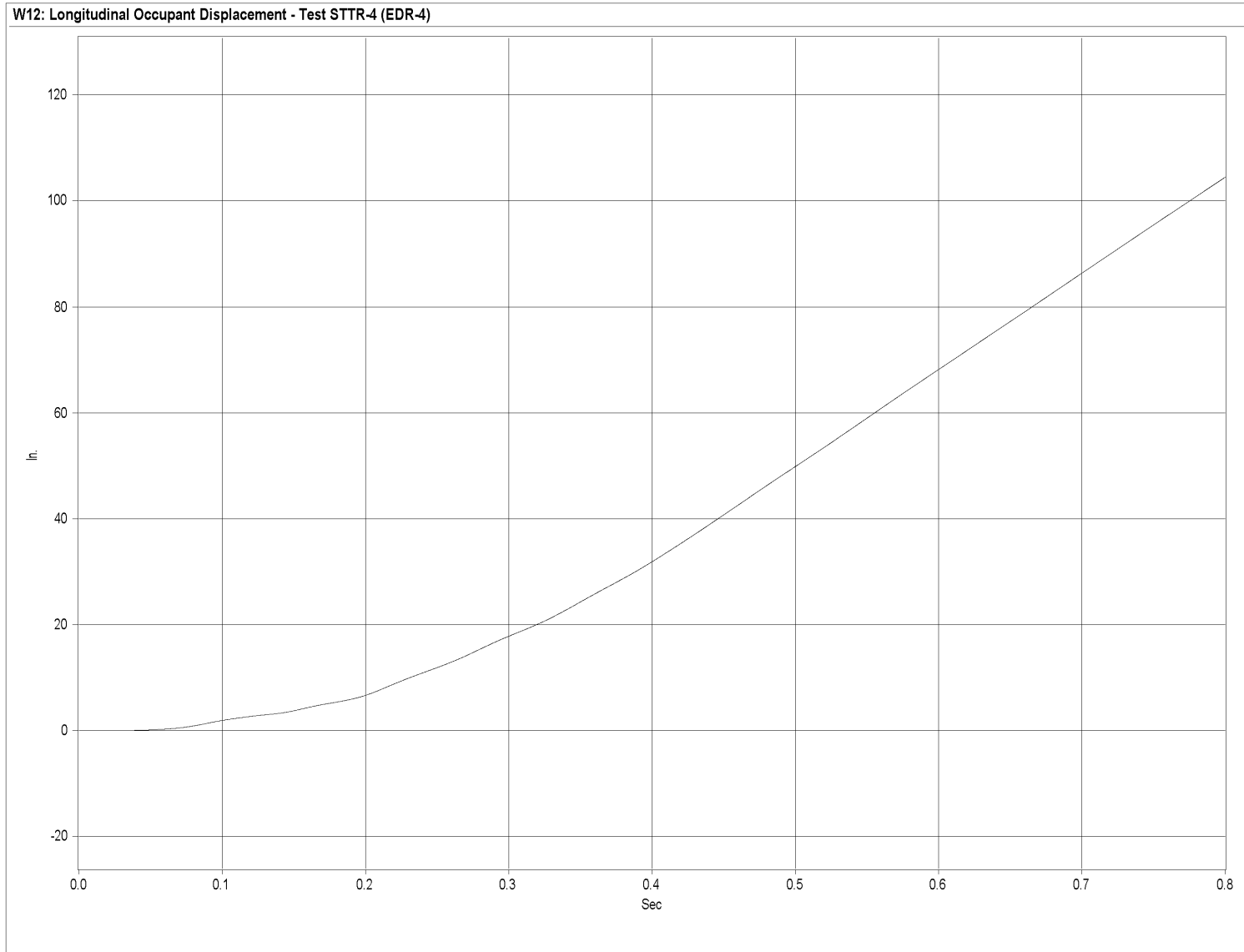


Figure X-3. Graph of Longitudinal Occupant Displacement, Test STTR-4

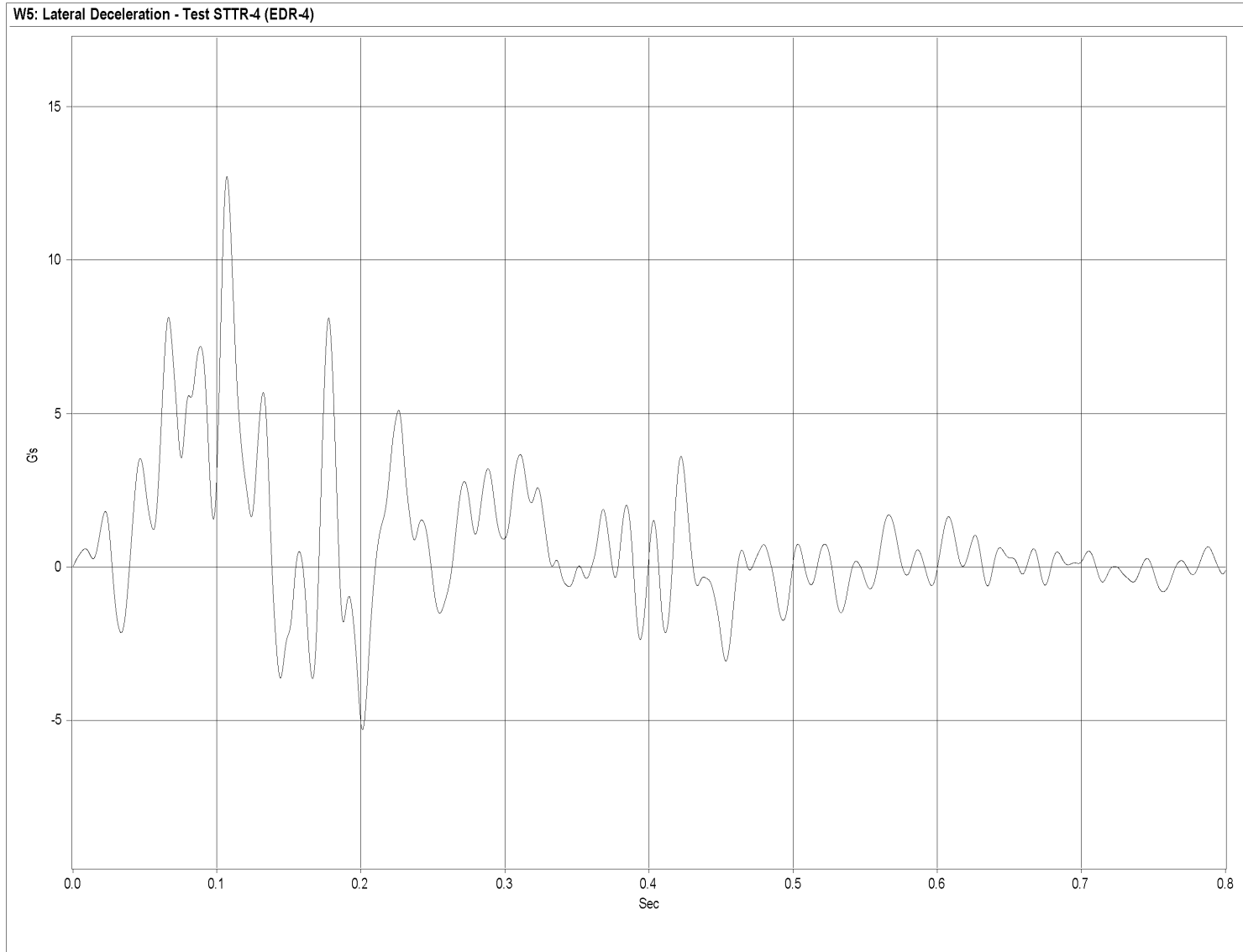


Figure X-4. Graph of Lateral Deceleration, Test STTR-4

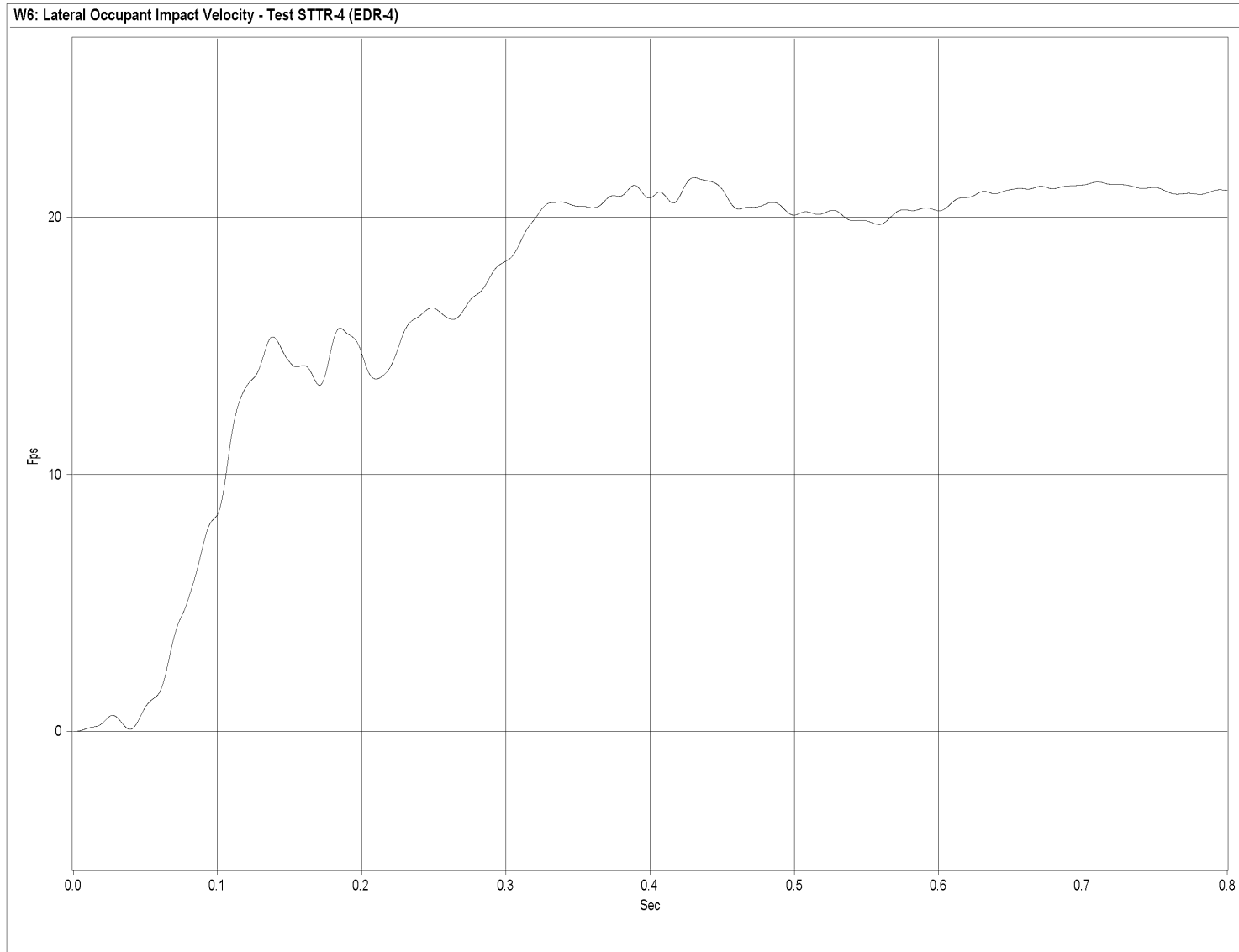


Figure X-5. Graph of Lateral Occupant Impact Velocity, Test STTR-4

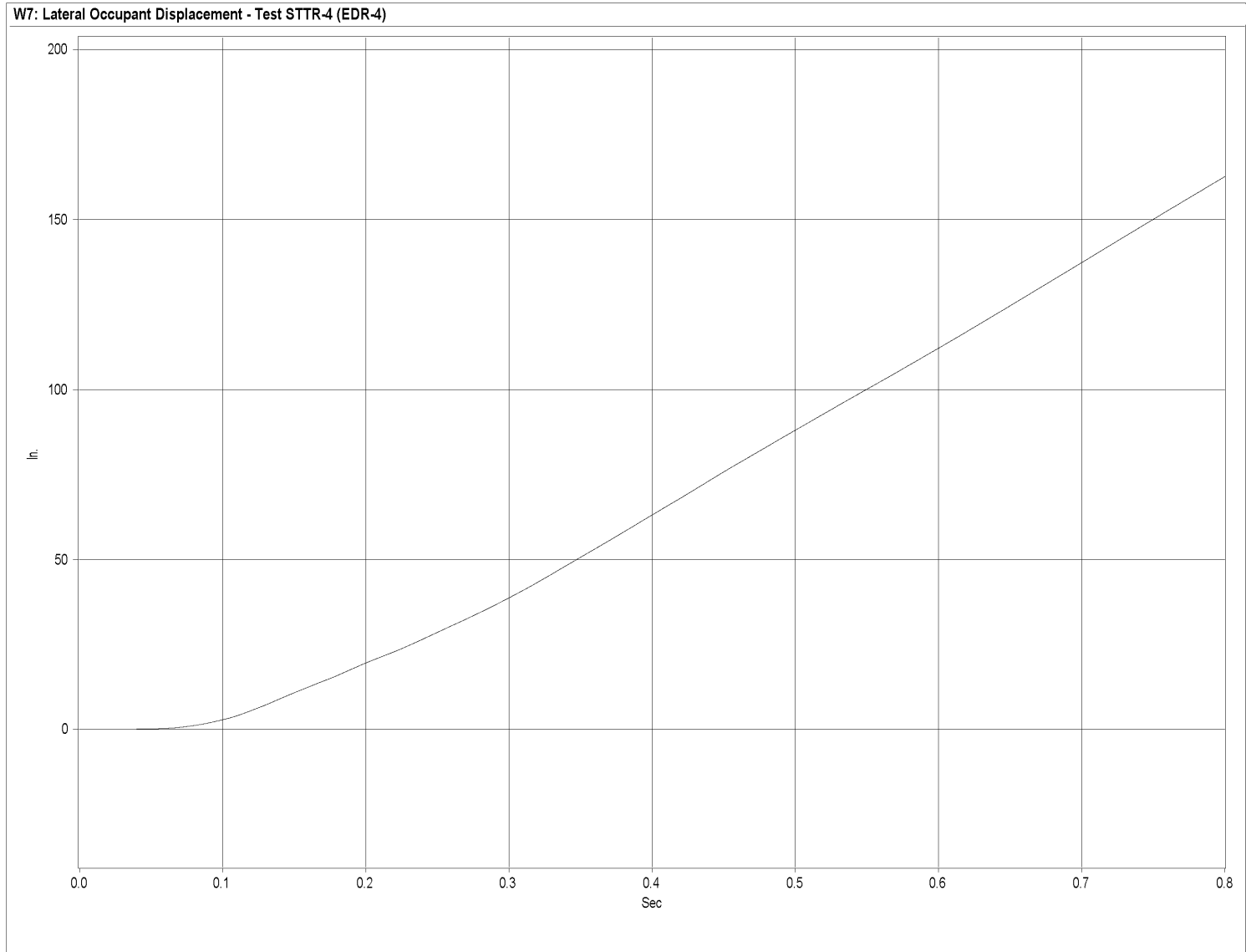


Figure X-6. Graph of Lateral Occupant Displacement, Test STTR-4

APPENDIX Y

Rate Transducer Data Analysis - Test STTR-4

Figure Y-1. Graph of Roll, Pitch, and Yaw Angular Displacements, Test STTR-4

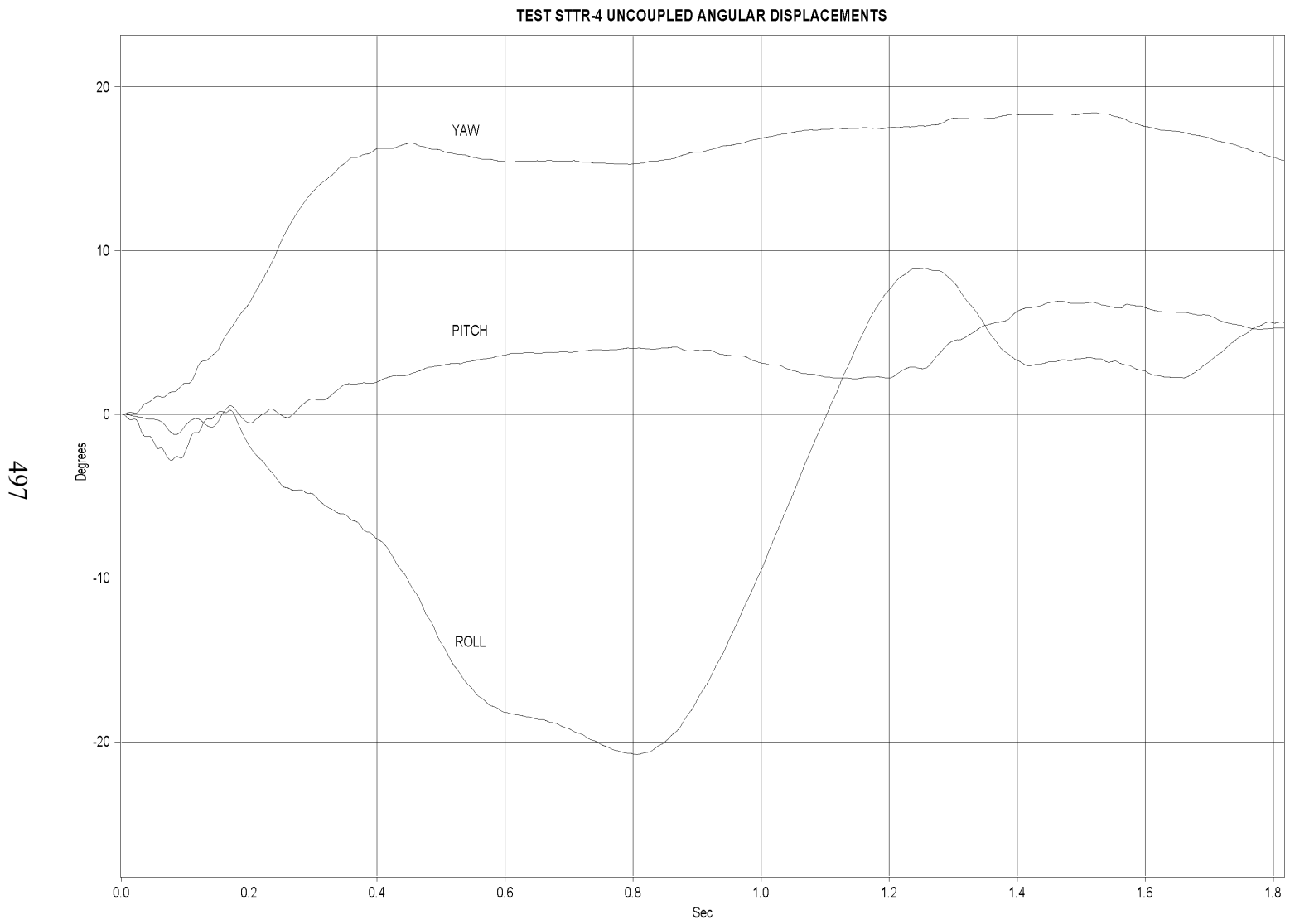


Figure Y-1. Graph of Roll, Pitch, and Yaw Angular Displacements, Test STTR-4